STEEP CAPILLARY WAVES ON GRAVITY WAVES

by

NILESH R POPAT

Thesis submitted for the degree of Doctor of Philosophy

School of Mathematics

University of Bristol

November 1989

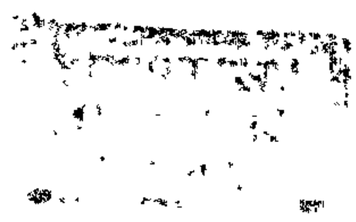

ACKNOWLEDGEMENTS

I would like to thank Prof. Howell Peregrine for his suggestion of the subject matter of this thesis and for his valued help and guidance throughout its preparation.

I would also like to thank Mr. Pete Shiarly for his help in the preparation of this text.

Financial assistance by the Science and Engineering Research Council is gratefully acknowledged.

MEMORANDUM

The work in this dissertation was carried out in the School of Mathematics, Bristol University, between October 1986 and November 1989 and has not been submitted for any other degree or diploma of any examining body. All the work discussed is the original work of the author except where acknowledged in the text.

Nilesh R Popat
November 1989

ABSTRACT

The frequent presence of ripples on the free surface of water on both thin film flows and ponds or lakes motivates this theoretical investigation into the propagation of ripples on gravity waves. These ripples are treated as "slowly-varying" waves in a reference frame where the gravity wave flow is steady. The methods used are those of the averaged Lagrangian (Whitham 1965, 1967, 1974) and the averaged equations of motion (Phillips 1966) which are shown to be equivalent. The capillary wave modulation is taken to be steady in the reference frame which brings the gravity wave, or gravity driven flow, to rest.

Firstly the motion over ponds or lakes is considered. Linear capillary-gravity waves are examined in order to set the scene. Crapper's (1957) exact finite-amplitude waves are examined next to show the actual behaviour of the flow field. The underlying gravity driven flow is that of pure gravity waves over an "infinite" depth liquid. These gravity waves are modelled with "numerically exact" solutions for periodic plane-waves. The initial studies are inviscid and show that steep gravity waves either "absorb" or "sweep-up" a range of capillary waves or, alternatively, cause them to break in the vicinity of gravity wave crests.

Improvements on the theory are made by including viscous dissipation of wave energy. This leads to a number of solutions approaching "stopping velocities" or the "stopped waves solution". In addition to these effects "higher-order dispersion" is introduced for weakly nonlinear waves near linear caustics. This clarifies aspects of the dissipation results and shows that wave reflection sometimes occurs.

Secondly, waves on thin film flows are considered. Linear capillary-gravity waves are again examined in order to set the scene. Kinnersley's (1957) exact finite-amplitude waves are examined next to show the actual behaviour of the flow field. The underlying gravity driven flow is given by shallow water gravity waves. No modelling of these is necessary simply because they are included within Whitham's or Phillips' equations ab initio. This study is inviscid and shows the unexpected presence of critical velocities at which pairs of solution branches originate.

CONTENTS

CHAPTER 1
INTRODUCTION

1.1 Our Aims: Waves on Thin Film Flows and the Infinite Depth "Exercise"

The flow of thin films exists in a variety of naturally occurring and important practical industrial situations. Consequently, there is great interest in the understanding of the behaviour of thin film flows which is reflected in a large volume of work related to thin film hydrodynamics. The phenomena of film flows that is of interest to us is the wavy region which occurs far downstream from a smooth surface flow upstream. The mainstream flow is usually gravity driven whilst the waves are usually surface tension driven.

A comprehensive review and discussion on methods used for wave modelling in thin film flows is given by Dukler (1972). He shows that all attempts to calculate the wave structure (amplitude, shape, velocity) follow one of five "policies" for solving the equations of motion. He also shows that none of these policies can provide a complete closed-form solution to the problem. That is, either the policy produces partial information about the waves, say only its amplitude, or it requires, as input data, some characteristic property of the waves such as velocity, amplitude or wavelength.

Moalem-Maron, Brauner and Dukler (1985) state that the situation to date has not changed substantially. An exception is the integral approach to the prediction of wave properties offered by Brauner and Moalem-Maron (1983). An experimental study of the transport characteristics of wavy thin films is also undertaken by Brauner and Moalem-Maron (1982). Examination of their results shows that the film flows usually have high Reynolds numbers ($R_e >> 1$). Thus, the effects of viscosity on individual waves is negligible. However, viscosity does act over longer time and space scales.

Our aim is to model the flow of pure capillary waves on thin films using an entirely different approach. Characteristic properties of both the mainstream flow (current distribution) and the waves are assumed to be "slowly-varying". That is, the time and length scales for variations of these properties are assumed to be very much larger than the period and wavelength of the individual waves.

There are two existing convenient descriptions of the behaviour of slowly-varying wavetrains both of which lead to conservation equations for the global properties of the motion. One possible approach is a direct averaging of the equations of motion as presented by Phillips (1966). The other possible approach is the averaged Lagrangian method of Whitham (1965, 1967) summarised in Whitham (1974).

The conservation equations arising from these two approaches simplify when the waves are either of infinitesimal amplitude or are propagating on liquid of infinite depth. The simplification occurs because for these two cases variations in the mainstream flow and the mean level of the liquid become independent of variations in wave properties. Therefore, the problem of short finite-amplitude capillary waves propagating on finite-amplitude deep water gravity waves is examined first as an preliminary "exercise" to aid in absorbing the general features of such approaches.

In fact, recent interest in remote sensing of the sea surface with satellite based radar has focused new attention on this "exercise". For example, Longuet-Higgins (1987) considers the case where the short waves are infinitesimal pure gravity waves rather than capillary waves. He uses accurate numerical solutions for steep pure gravity waves to find variations in the wavelength and steepness of these short waves. In the course of our investigation it turns out that this "exercise" contains a rich variety of interesting behaviour which deserve to be examined in their own right. Consequently, this case is dealt with extensively and waylays the thin films (finite depths) case in this thesis.

1.2 Wave-Current Interactions

When waves interact with slowly-varying currents wave energy density is not conserved as there is an interchange of energy between waves and mainstream flow. The appropriate conserved quantity is the wave-action density. For infinitesimal, or linear, waves on a uniform current Bretherton and Garrett (1968) show that wave-action density is equal to the wave energy density divided by the frequency of the waves relative to the liquid.

The interaction of gravity waves and currents was first analysed by Longuet-Higgins and Stewart in a number of papers culminating in a summary paper, Longuet-Higgins and Stewart (1964). That work is based on infinitesimal amplitude solutions for gravity waves.

Peregrine (1972) uses linear slowly-varying theory to consider the effect of currents in a river on gravity waves generated by a boat. A boat travelling upstream at a constant speed relative to the river produces (gravity) waves of constant amplitude. If these (gravity) waves propagate upstream into a region of stronger current they may experience considerable amplification. Also, the boat may generate waves that are "stopped" (that is, propagating upstream with a group velocity equal to the stream velocity). These waves, which appear to be moving since their phase velocity is upstream, persist until dissipated, which may take a surprisingly long time. Waves whose group velocity is equal to minus the stream velocity are said to be at their "stopping velocity".

Holliday (1973) considers the propagation of both linear and weakly-nonlinear gravity-capillary waves on a deep slowly-varying current. Infinitesimal gravity (capillary) waves are amplified and compressed - wavenumber increases (expanded - wavenumber decreases) as a negative (positive) current is encountered. At a particular current, namely the stopping velocity, these waves can progress no further and wave steepnesses become arbitrarily large.However, weakly-nonlinear waves are shown to propagate beyond the linear stopping velocity. A comparison results for weakly-nonlinear gravity and capillary waves shows that the effect of nonlinearity is much less pronounced for capillary waves than for gravity waves.

Gargett and Hughes (1972), in a analysis based on linear gravity waves, have concluded that the weak surface current induced by an internal wave can create a "barrier" (the stopping velocity) to surface waves. The results of Holliday (1973) show that nonlinear effects remove this "barrier" and reduce the amplitude enhancement considerably below that which would be predicted by linear slowly-varying theory.

Linear slowly-varying theory (linear ray theory) predicts infinite wave amplitudes at the envelopes, called caustics, of group velocity paths (or rays) as a finite flux of wave energy is squeezed through zero area. Infinite amplitudes are not consistent with linear theory and the crossing of group velocity paths (rays) implies rapid variation transverse to these paths (rays). The linear slowly-varying theory is clearly not valid in the region of the caustic as the wave amplitude is not slowly-varying and the waves may not be infinitesimal.

Peregrine and Smith (1979) discuss a weakly nonlinear theory for waves near caustics. Their main result for caustics is that nonlinearity produces caustics of two different types which they call "R-type" and "S-type" caustics. The R-type caustic is physically interpreted as a possible reflection of the waves whilst the S-type caustic is interpreted as possibly leading to wave breaking.

The singularities of linear caustics can be avoided by finding uniform solutions. Peregrine and Smith (1979) use an heuristic operator expansion method to derive a uniformly valid equation which incorporates the effects of weak nonlinearity. The solutions of the linearised equations involve Airy functions. The solutions of the weakly nonlinear equations involve the two Painlevé transcendents - one for each type of weakly nonlinear caustic. Their heuristic results agree with those of Smith (1976).

A noteworthy situation which involves caustics occurs off the South-East coast of South Africa. Here giant waves have caused extensive damage to shipping (Mallory 1974). The Agulhas current flows down the coast at 4 to 5 knots and is 90 to 165 km wide. Ships taking advantage of this current have encountered giant waves of the order 15 m when the wind produces waves propagating in opposition to the current. Smith (1976) studies this phenomenon. He considers a gravity wavetrain on deep liquid opposed by a steady irrotational current and reflected by a caustic. He derives a uniformly valid equation, a modified nonlinear Schrödinger equation, which describes the wave amplitude. He shows that the wave profile can be asymmetric and, thus, the wave peaks can have extremely steep leading edges which can pose a danger to shipping.

Numerically accurate solutions for pure gravity waves are now available. Schwartz (1974), Longuet-Higgins (1975) and Cokelet (1977) consider a perturbation expansion in wave steepness to calculate the properties of finite-amplitude plane progressive periodic deep water gravity waves. It is found that the mean properties of gravity waves, such as phase velocity and energy density, do not increase or decrease monotonically with wave steepness. Generally, flow properties attain their maxima or minima just before reaching the highest waves limit.

More recently, Teles da Silva and Peregrine (1988) use a boundary integral method to find such properties. They also include the effects of a vertical current shear. The properties of pure gravity waves can be used to study the refraction, reflection and breaking of finite-amplitude pure gravity waves in various situations using only the approximation that the nonlinear wavetrain and mainstream flow have slowly-varying properties.

Finite-amplitude gravity wave interactions with currents are studied by Crapper (1972). He uses an approximate finite-amplitude gravity wave Lagrangian proposed by Lighthill (1967) in Whitham's approach. A survey of work on gravity wave interactions with currents prior to 1976 is given in Peregrine (1976).

Peregrine and Thomas (1979) consider finite-amplitude gravity waves interacting with a mainstream flow on infinite depth liquid by using the tabulated properties to define an exact Lagrangian based on Lighthill's (1967) approximate Lagrangian. They consider two cases of mainstream flow. In one case a mainstream flow at 90° to the gravity wavetrain is considered. The gravity waves are refracted by the current gradient and if the wavetrain becomes parallel to the mainstream flow an R-type caustic arises giving wave reflection. In the other case a current either in the same direction as or opposite direction to the gravity wavetrain is considered. This case produces S-type caustics when the current opposes the wavetrain and represents wave breaking although if the wavetrain propagates to the stopping velocity with a small steepness reflection may occur.

Peregrine (1981) considers, in a similar manner to Peregrine and Thomas (1979), gravity waves approaching a circular caustic. An R-type caustic is found and "conjugate" solutions exist for sufficiently large value of his "caustic parameter C". This type of caustic usually indicates reflection of the wavetrain from the caustic unless the amplitude of the waves becomes too large in the approach to the caustic in which case wave breaking may occur. When reflection occurs from such a circular caustic a short-crested wave system is developed. However, the properties of short-crested waves (see, for example Marchant and Roberts 1988) can vary significantly from the progressive wave system used by Peregrine.

Ryrie and Peregrine (1982) and Peregrine and Ryrie (1983) also use similar techniques to Peregrine and Thomas (1979) to examine finite-amplitude gravity waves obliquely incident onto a gently sloping beach. An R-type caustic results and near the caustic singularity "conjugate" solutions exist. A wavetrain approaching a beach from infinite depths will steepen and be refracted to propagate normal to the

beach until it breaks as it leads up to the caustic singularity. However, solutions of higher amplitude correspond to a wavetrain which is refracted to propagate parallel to the beach. This behaviour is termed "anomalous" refraction.

Peregrine (1983) considers the possibility of wave jumps between "conjugate" solutions. For the example described above wave jumps can only occur for obliquely incident waves (see figure 3 of Peregrine and Ryrie 1982). Peregrine also considers the problem examined by Yue and Mei (1980), that of waves incident onto a wedge of small apex angle. Wave jumps can occur for this example and Peregrine presents an analysis for a single infinite depth gravity wavetrain incident upon a wedge. He finds that it is possible, where "conjugate" solutions exist, for one or more wave jumps to occur causing the wavefield to be significantly modified.

1.3 Surface Waves Dominated by Capillarity

Pure capillary waves are of primary consideration in this thesis. Small amplitude capillary waves form a well known part of the classical theory of hydrodynamics. For instance, Taylor (1959) analyses the small amplitude capillary waves which occur on a thin liquid sheet. Taylor observed that both symmetrical and antisymmetrical waves of such type exist and produced them experimentally on liquids as thin as 5-100 μm. Large amplitude capillary waves are not as well known.

Crapper (1957) presents an exact solution for progressive capillary waves of finite-amplitude on infinite depth liquid. He shows that pure capillary waves are very rounded at their crests and that the wave of maximum steepness (which is equal to wavenumber times amplitude) is reached when the surface of the wave bends back and touches itself enclosing a bubble of air in its trough. Thus, pure capillary waves have profiles that peak or "dimple" downward which is opposite to the case of pure gravity waves. This is illustrated in figure 1.1. Note that if any particular capillary wave steepness is taken as the liquid surface the lines below it are streamlines. The maximum steepness (2.29) is found to be over five times the maximum steepness (0.44) of pure gravity waves.

Schooley (1958) experimentally confirms Crapper's capillary wave solution by showing profiles of short-fetch wind-generated capillary waves that were photographed using a high-speed motion picture camera in a small water-wind tunnel. Crapper's prediction for maximum wave steepness is approached closely enough to give confidence in its correctness.

Kinnersley (1976) presents exact solutions for progressive capillary waves of finite-amplitude on finite depth liquid. He finds that Crapper's solution generalises into two finite-amplitude versions of Taylor's symmetrical and antisymmetrical sheet waves. The sectional shape and maximum steepness criterion for these two waves are similar to those for infinite depth. However, another form of singularity, that of zero sheet thickness, is possible and only occurs for symmetrical waves.

In a series of papers Hogan analyses the variations of mean wave properties with steepness and also examines wave profiles for both nonlinear pure capillary waves and nonlinear waves driven by surface tension and gravity on infinite depth liquid. Hogan (1979) analytically examines the case of nonlinear pure capillary waves. He finds that the potential energy density of such waves is greater than the kinetic energy density which is exactly the opposite behaviour to that of pure gravity waves. Also, the crest height above the mean level increases and then decreases whereas the trough depth below the mean level always increases with wave height for fixed wavelengths.

Hogan (1980) numerically examines nonlinear waves driven by both surface tension and gravity avoiding the case of Wilton's ripples. He finds that gravity waves have non-monotonic integral properties even when there is a small amount of surface tension present. However, as wavelengths decrease and the effects of surface tension become dominant the waves look and behave very much like pure capillary waves.

Hogan (1981) numerically examines the special case of Wilton's ripples. Wilton (1915) shows that when both gravity and surface tension are included for the case of collinear waves it is possible for two waves, one dominated by surface tension and the other by gravity, of wavenumbers k_1 and k_2 and frequencies σ_1 and σ_2, say, to interact and produce a composite wave whose wavenumber k_3 and frequency σ_3 are equal to $k_1 \pm k_2$ and $\sigma_1 \pm \sigma_2$ respectively. If the natural frequency of this composite wave is actually equal to σ_3 then this wave is excited at its frequency and resonance can occur. Hogan (1981) finds that one nonlinear wave is "capillary-like" whilst the other is "gravity-like" in its properties and profiles.

For pure capillary waves resonance is only possible if the two waves propagate at an angle to each other. McGoldrick (1965) shows that resonance of pure capillary waves is only possible if the angle between the waves is greater than 75° and less than approximately 80° - a very limited range.

Hogan (1984) analytically examines the particle trajectories in nonlinear pure capillary waves. He shows that particle orbits are neither circular nor closed. The bulk of liquid near the surface moves

considerably forward during the passage of a steep pure capillary wave. Also, the particles spend most of their time near wave crests. This contrasts with the behaviour of steep pure gravity waves.

Hogan (1985) numerically examines the particle trajectories of nonlinear waves driven by both surface tension and gravity. When surface tension is dominant particle trajectories are qualitatively the same as those of nonlinear pure capillary waves although a small influence of gravity dramatically reduces the scale of the results as compared to that of nonlinear pure capillary waves. When gravity is dominant particle trajectories are qualitative the same as those of nonlinear pure gravity waves. When the forces are equal waves with the same length and height, but belonging to different "families" of Wilton's ripples, have completely different particle trajectory properties.

Hogan (1986) analytically examines the highest waves, particle trajectories and phase speeds of both the symmetric and antisymmetric nonlinear pure capillary waves, given by Kinnersley (1976), on finite depths of liquid. He derives explicit criteria for the highest waves and finds expressions for the phase velocities for these two solutions in both of the classical frames of reference given by Stokes (1847). In the frame of reference in which the mean horizontal particle velocity is zero he finds that a decrease in sheet thickness results in a non-monotonic behaviour of global particle trajectory properties. In the frame of reference in which the mean horizontal velocity of the centre of mass in zero, i.e. no mass flux, he finds that the behaviour is monotonic.

1.4 Short Waves Propagating on Longer Waves

It is mentioned above that the problem of short finite-amplitude pure capillary waves propagating on long finite-amplitude pure gravity waves in infinite depth liquid is extensively studied in this thesis. Some past work on this problem is now examined. The simplest way to generate capillary waves is recorded in detail by Scott Russell (1945). On dragging a slender rod through water above some critical speed he observed waves of short length in front of the rod. It later emerged that the waves precede the rod because the velocity of energy propagation is greater than the velocity of crest, or trough, propagation.

Wind-generated waves of all wavelengths are present on the surfaces of ponds, lakes and the sea. When a wind is blowing it is observed that capillary waves are mostly seen on the front face of longer gravity waves. A photograph of such waves is shown in figure 1.2. Munk (1955) suggests that these capillary waves may be be due to some sort of unspecified disturbance near the gravity wave crests. Cox (1958) performed a series of experiments on 4.7 cm long plunger generated waves and found capillary waves on the front faces of gravity waves in the absence of wind.

Schooley (1958) experimentally shows wave profiles in the transition region from capillary to gravity waves. Examples are given which show that capillary waves of appropriate wavelength (so as to have the same velocity as the gravity waves, i.e. stationary capillary waves) often ride just in front of the start of the crests of the gravity waves.

Schooley (1960) also experimentally shows examples of "double-dimple" wave profiles (see his figure 1) in the region of 2.44 cm wavelengths as predicted by Wilton (1915). Additional experimental profiles are presented to suggest that the formation of double-dimple waves are the mechanism by which the phenomenon characterised by 3, 4, 5, etc., dimples of capillary waves of appropriate wavelength riding in front of the crests of gravity waves having the same velocity.

Inspired by Munk (1955), Longuet-Higgins (1963) suggests a possible mechanism to explain the observations of Cox (1958). As a progressive gravity waves reaches maximum steepness surface tension becomes important near the crest. This produces a travelling disturbance, in the form of a normal stress, which gives rise to a train of capillary waves which in turn must be present on the front face of the gravity waves. He shows the importance of capillary waves as regards the breaking of gravity waves. Through the action of radiation stress, energy is taken

from the gravity waves by the capillary waves. These capillary waves can dissipate this energy very quickly and efficiently and, thus, delay the breaking of gravity waves.

Crapper (1970) uses this idea of a travelling disturbance to also examine the problem. Capillary waves can have large steepnesses and he argues that since they are actually seen on the gravity waves they must be nonlinear. He considers the capillary waves to be stationary on a slowly-varying mainstream flow. He shows that the method produces very steep waves in front of the gravity wave crests when the mainstream flow, or surface velocity, is fast and that low steepness capillary waves are possible on the rear of the gravity waves.

McGoldrick (1972) observes non-stationary capillary waves in his experiments. His experiments also show that short gravity waves can be covered with capillary waves both in front of and behind crests. He proceeds to solve a time dependent model equation, using the method of multiple scales, neglecting the effects of viscosity. He concludes that the windless capillary waves are caused by nearly resonant harmonic nonlinear interactions.

Benney (1977) derives equations governing the resonant interaction of a weakly nonlinear, slowly-varying, capillary wavetrain and a small amplitude gravity wavetrain. He finds that when the group velocity of the capillary waves equals the phase velocity of the gravity waves the capillary wave envelope is steady with the capillary waves attaining maximum amplitude at gravity wave crests. The flow is not steady with individual capillary waves propagating slower than the gravity waves.

Ferguson, Saffman and Yuen (1978) provide further theoretical and experimental results on the subject. They derive a model wave equation which has several advantages over the one used by McGoldrick (1972). The model equation admits a similar dispersion relation to the full equation and Stokes-like pure gravity waves with highest waves enclosing a 120° angle. The numerical solution of this model equation is relatively straightforward. They find that on gravity waves of large amplitude either capillary waves can cover the entire gravity wave surface when the effects of viscosity are neglected or that capillary waves are a transient phenomena on the front crests of the basic gravity waves with magnitude and duration dependent on the choice of viscosity parameter.

Ferguson et al (1978) explain that their work has implications on all previous work. The solutions of Longuet-Higgins (1963) and Crapper (1970) can only be true for finite time. The error may perhaps lie in the neglect of viscosity in the generation process or back reaction. There is confirmation of Longuet-Higgins (1963) suggestion that the presence of capillary waves delays the onset of breaking of

gravity waves. Also the inviscid behaviour is consistent with that suggested by the weakly nonlinear analysis of McGoldrick (1972). Benney's solution is stable but dissipation would damp out the capillary waves unless an external source of energy, such as wind, existed. This is not considered by Benney. It must be noted that these conclusions all relate to the model equation derived by Ferguson et al. There is no guarantee that the full equations would give identical solutions and, thus, conclusions.

Chang, Wagner and Yuen (1978) conduct experiments intended to verify the theory of Longuet-Higgins (1963). Using laser optical slope gauges they obtain qualitative agreement particularly for the frequency and dissipation of capillary waves on the gravity waves flow. The agreement improves as the wavelength of the gravity waves increases but is rather poor when the capillary waves cover the gravity waves. The verification of Longuet-Higgins (1963) criterion for capillary wave steepness near the crests of the gravity waves is impossible by experiment. This is simply because this criterion is dependent on the curvature of the gravity waves in the absence of surface tension and, therefore, is impossible to measure.

1.5 An Outline of this Thesis

This thesis consists of two parts. The first part considers short capillary dominated waves either interacting with a gravity driven mainstream flow or propagating on the surface of long gravity waves on infinite depths of liquid and consist of four chapters. The second part considers the interaction of short capillary dominated waves with a gravity driven mainstream flow which, in the absence of waves, satisfies the shallow water equations. This part consists of two chapters.

Chapter 2 describes the general equations of motion as developed by Phillips (1966) and Whitham (1965, 1967, 1974) and also discusses a criteria for the presence of R and S-type near-linear caustics. The form and development of of the general equations in both finite and infinite depths of liquid are discussed separately.

Chapters 3 to 6 inclusive consist of the first part of this thesis. Chapter 3 considers the problem for the case where the short waves are infinitesimal-amplitude waves driven by both surface tension and gravity. An S-type surface tension dominated caustic is found. This chapter is designed to show the effects of gravity on surface tension dominated waves and, in some respects, justify the neglect of gravity for the short waves in subsequent chapters.

Chapter 4 considers the problem for the case where the short waves are finite-amplitude pure capillary waves as given by Crapper (1957). This is inviscid theory and illustrates the wide variety of possible solutions. A "parameter space" of gravity waves on which capillary waves do or do not break is developed. Some conclusions are reached which have implications on the breaking of gravity waves.

Chapter 5 also considers the problem for finite-amplitude pure capillary waves but includes the effects of dissipation due to viscosity. For some cases wave propagation is found to reach the stopping velocity. A weakly nonlinear uniform analysis is performed to find the actual behaviour of such propagations. It is found that partial reflection is possible as for some gravity waves cases.

Chapter 6 discusses the wide range of caustics possible when capillary waves with a two dimensional propagation space interact with a two dimension current distribution. The waves are taken to be infinitesimal amplitude pure capillary waves. All caustics present are found to be of S-type. This chapter concludes the first part of this thesis.

Chapter 7 adds the effects of wave energy dissipation and acceleration of the mainstream flow to the general equations of motion given in chapter 2. The idea here is to later be able to consider a vertically falling film of liquid. The "modified" consistency relations of Peregrine and Stiassnie (1979) are confirmed and developed further. A wave-action conservation equation is developed incorporating both the dissipation and acceleration effects. This equation shows that the linear result of Christoffersen and Jonsson (1980) is valid for nonlinear waves.

Chapter 8 discusses Kinnersley's (1976) symmetric and antisymmetric sheet waves. Slight corrections to Kinnersley's expressions are given where necessary. The symmetric wave case is examined in detail. Hogan's (1986) criterion for the highest waves is solved explicitly and wave profiles are given. Expressions for mean wave properties, such as kinetic and potential energy densities, are found. The variations of mean wave properties with wave steepness is shown for use in later chapters and for comparison with the results of Hogan (1979, 1980, 1981).

Chapters 9 and 10 consist of the second part of this thesis. Chapters 9 and 10 have similar motivations to those of chapters 3 and 4 respectively. Chapter 9 considers the simple case of infinitesimal amplitude waves driven by both surface tension and gravity but with the effects of surface tension dominating. Chapter 10 shows the variety of nonlinear solutions to the slowly-varying finite depth problem. All the solutions are inviscid. Many of the solutions have nonlinear singularities. The physical mechanisms underlying these singularities have yet to be clarified. Possible lines of future work are also discussed in this chapter. Specifically, the equations and solution method for the case of surface waves on a vertically falling film of liquid including dissipation are discussed. This case has been considered by the author but no results have been developed for lack of time.

Results to each chapter are discussed within each chapter so that no concluding chapter is given. However, an epilogue is given discussing the general outcome of this thesis.

CAPTIONS FOR FIGURES

Figure 1.1: Wave profiles for Crapper's waves for different values of steepness ak.

Figure 1.2: Capillary waves riding on the front faces of gravity waves. The capillary waves propagate from right to left on gravity waves propagating from left to right.

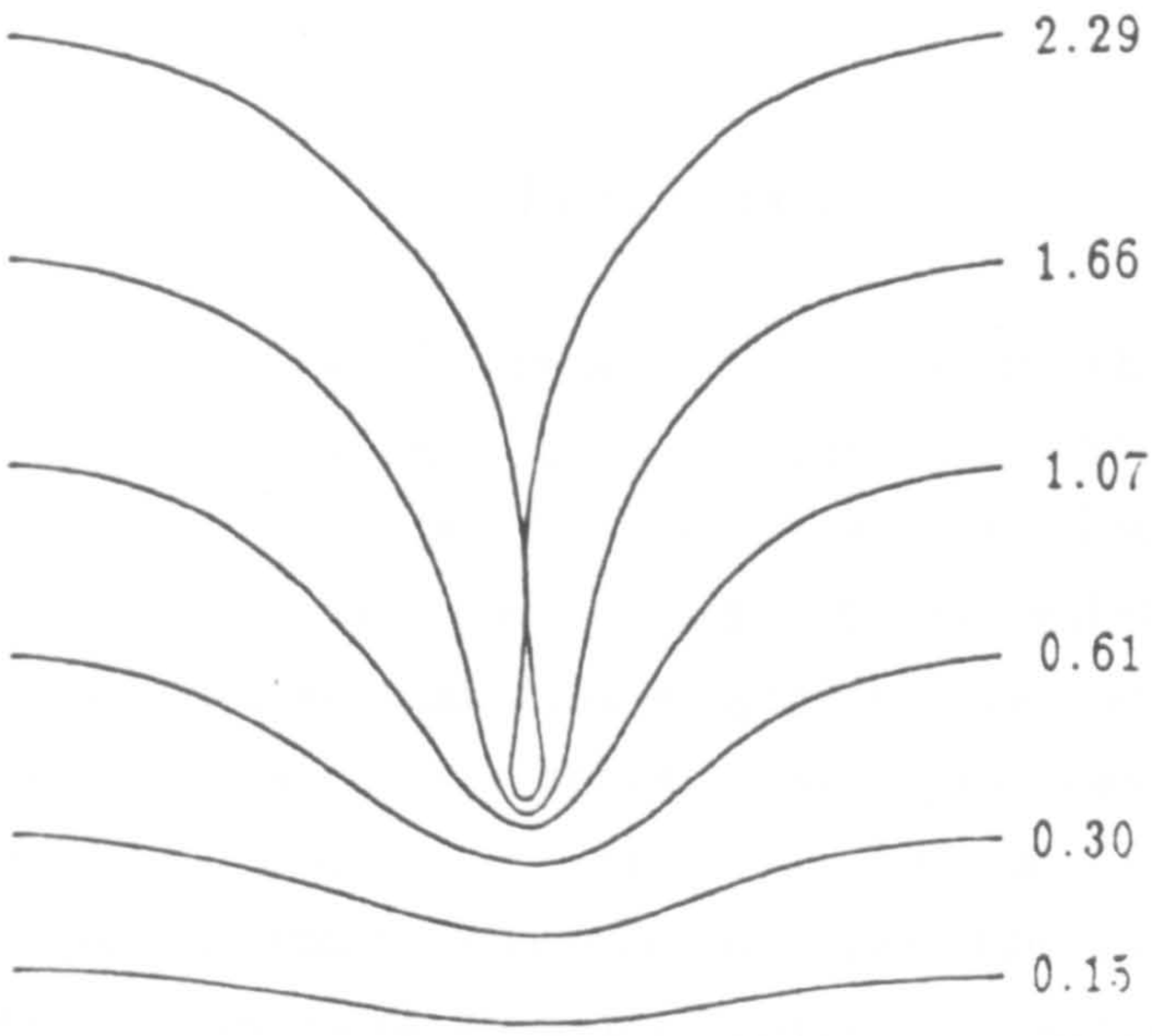

Figure 1.1: Wave profiles for Crapper's waves for different values of steepness ak.

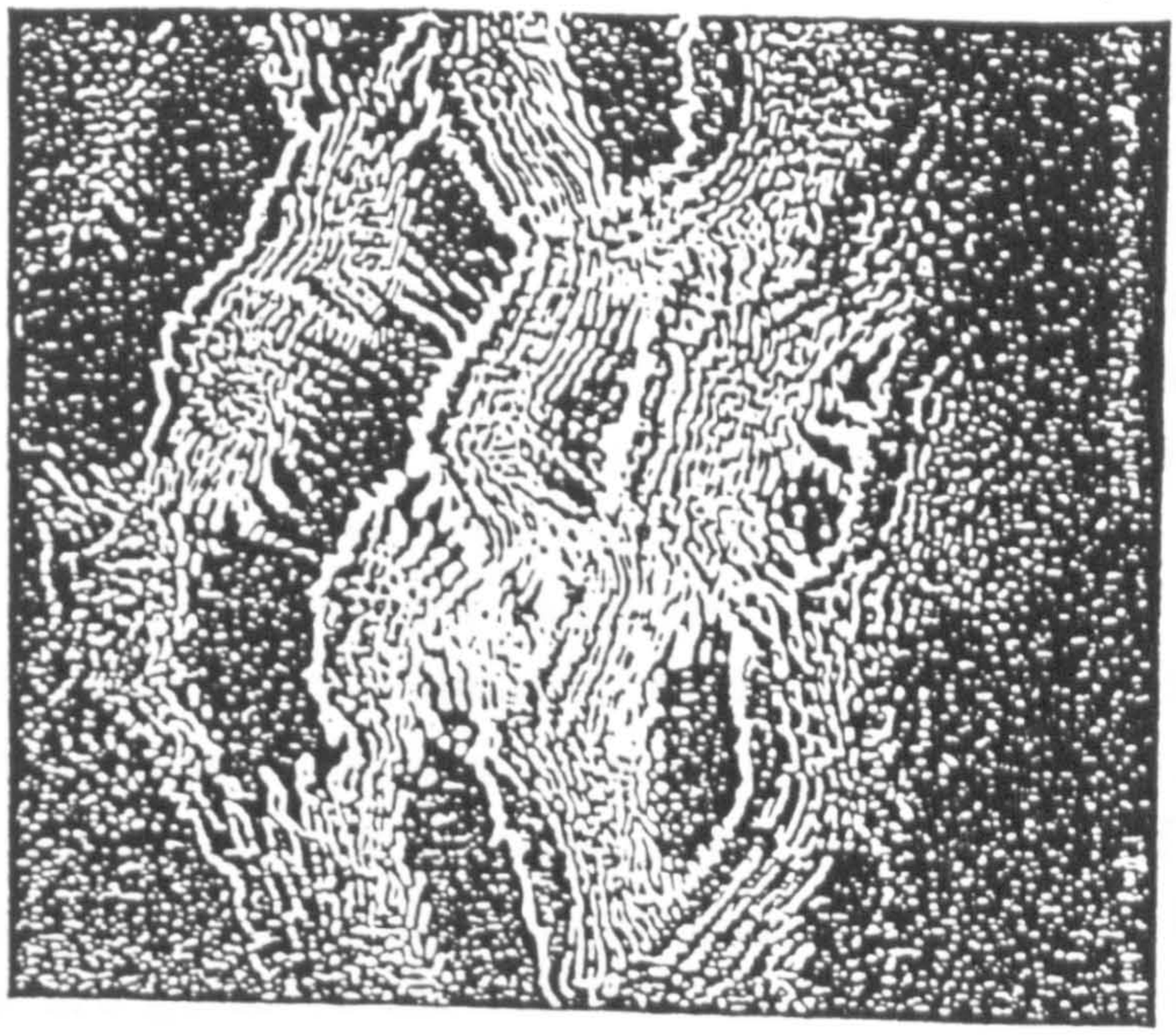

Figure 1.2: Capillary waves riding on the front faces of gravity waves.
Capilllary wave propagation direction.
←

CHAPTER 2
MATHEMATICAL FORMULATION

2.1 Introduction

In this chapter a brief summary is given of the present theory available for use in solving a general class of nonlinear problems of surface waves in liquids - those in which all the flow properties are assumed to be "slowly-varying". This is equivalent, as a first approximation, to assuming that flow properties are locally constant.

There are two available approaches to such problems. One is given by Phillips (1966, § 3.6) and the other by Whitham (1965, 1967, 1974, § 16.7). Phillips' approach directly averages the Euler equations of motion, to derive a system of equations called the averaged equations of motion, whilst Whitham's approach uses an averaged Lagrangian formulation. Since Whitham's equations lead to the introduction of wave-action and its conservation they are more attractive than the more general, but cumbersome, averaged equations of motion. However, the Lagrangian used by Whitham is only valid for irrotational flows. Crapper (1979) extends both systems of equations to include surface tension.

The general features of linear and near-linear, or weakly nonlinear, theory, as discussed by Peregrine and Smith (1979), are also summarised in this chapter. Linear theory shows that the amplitude of a slowly-varying wavetrain becomes particularly large near a linear caustic. The near-linear theory shows that there exist two types of near-linear caustics in which nonlinearity either tends to advance or retard the reflection of waves from the caustic.

In section 2.2 the averaged equations of motion are summarised. Section 2.3 discusses some kinematic relations usable with both the averaged equations and Whitham's equations of motion. Whitham's equations are summarised in section 2.4. Definitions of mean wave properties in terms of an averaged Lagrangian and relations between mean wave properties are given in section 2.5. The form of both the averaged equations and Whitham's equations for the case of infinite depths is discussed in detail in section 2.6. In section 2.7 the particular case of steady variation is considered. Section 2.8 discusses the general linear and near-linear features of such slowly-varying problems. Reference frames and dimensionless units are discussed in section 2.9.

2.2 The Averaged Equations of Motion

Define axes (x_i,z), where $i = 1,2$, with x_i oriented horizontally and z vertically upwards. The liquid is of depth $z = -h(x_i)$ and the free surface is at $z = \eta(x_i,t)$ with mean value $z = b(x_i,t)$. There is a mainstream flow, or current distribution, $(U_i(x_i,t),0)$ on which is superposed a wave motion with velocity field $(u_i(x_i,z,t),w(x_i,z,t))$. The functions $h(x_i)$, $U(x_i,t)$, $b(x_i,t)$ and the mean properties of the wave motion are assumed to be slowly-varying.

The definition of the wave motion is not unique. Stokes (1847) shows that there are an infinite number of ways in which to define the wave motion. He gives two preferred choices. The first is to require that the mean horizontal velocity below wave troughs be zero. The second is to require that the mean horizontal velocity of the centre of mass of the liquid be zero. The difference between the two definitions can be interpreted as a mass flux associated with the waves (Phillips, 1966, p 64). Here Stokes first definition is used.

Phillips (1966, § 3.6) uses the Euler equations of continuity, momentum and energy to derive the averaged equations of motion for the variations of wave parameters. The summation convention is used. There are differences in both notation and definition from that of Phillips (1966). The averaged equations of motion are:

the mass conservation equation

$$\rho \frac{\partial b}{\partial t} + \frac{\partial}{\partial x_i}(\rho d U_i + \mathcal{I}_i) = 0 \ , \qquad (2.2.1)$$

the momentum conservation equations

$$\frac{\partial}{\partial t}(\rho d U_i + \mathcal{I}_i) + \frac{\partial}{\partial x_j}\left[(\rho d U_i + \mathcal{I}_i)\left[\frac{\mathcal{I}_j}{\rho d} + U_j\right] + \frac{1}{2}\rho g d^2 \delta_{ij} + \mathcal{S}_{ij} - \frac{\mathcal{I}_i \mathcal{I}_j}{\rho d}\right]$$

$$- \rho g d \frac{\partial h}{\partial x_i} = 0 \ , \qquad (2.2.2)$$

and the energy conservation equation

$$\frac{\partial}{\partial t}\left[\frac{1}{2}\rho d U_i^2 + \frac{1}{2}\rho g b^2 + \mathcal{E} + U_i \mathcal{I}_i\right] + \frac{\partial}{\partial x_i}\left[U_i\left[\frac{1}{2}\rho d U_j^2 + \rho g d b + \mathcal{E} + U_j \mathcal{I}_j\right]\right.$$

$$\left. + \mathcal{F}_i + \mathcal{I}_i\left[g b + \frac{1}{2} U_j^2\right] + \mathcal{S}_{ij} U_j\right] = 0 \ , \qquad (2.2.3)$$

where

$$d(x_i,t) = b + h \qquad (2.2.4)$$

is the mean total depth, $\mathcal{I}_i$ is the wave momentum in the i-direction (equal to the mass flux in that direction due to the waves), $\mathcal{S}_{ij}$ is the radiation stress tensor, $\mathcal{E}$ is the energy density and $\mathcal{F}_i$ is the energy flux vector. Here ρ is the density of the liquid and g is the acceleration due to gravity.

Definitions of these mean properties, as well as the kinetic energy density T and potential energy density V, in terms of averaged integral expressions are given in appendix A. Note that the definition of the radiation stress $\mathcal{S}_{ij}$ differs from that of Phillips (1966, 3.6.12) but agrees with that of Longuet-Higgins (1975 expression 1.6) (for the component $\mathcal{S}_{11}$), Crapper (1979) and Stiassnie and Peregrine (1979).

There are many ways of writing these averaged equations of motion. The arrangement above is such that the first two terms of each are in conservation form and within each expression the terms are in the order: current, wave and interaction terms. One simplified way in which the momentum and energy conservation equations can be written is given here because it is the form in which the equations are used throughout the major part of this thesis. Subtracting U_i times the mass conservation equation (2.2.1) from the momentum conservation equations (2.2.2) gives

$$\frac{\partial \mathcal{I}_i}{\partial t} + \frac{\partial}{\partial x_j}(U_j \mathcal{I}_i + \mathcal{S}_{ij}) + \mathcal{I}_j \frac{\partial U_i}{\partial x_j}$$

$$+ \rho d\left[\frac{\partial U_i}{\partial t} + U_j \frac{\partial U_i}{\partial x_j} + g \frac{\partial b}{\partial x_i}\right] = 0 \ , \qquad (2.2.5)$$

as the momentum conservation equations. Also, subtracting $(gb - \frac{1}{2}U_i^2)$ times the mass conservation equation (2.2.1) and U_i times the momentum conservation equations (2.2.2) from the energy conservation equation (2.2.3) gives

$$\frac{\partial \mathcal{E}}{\partial t} + \frac{\partial}{\partial x_i}(U_i \mathcal{E} + \mathcal{F}_i) + \mathcal{S}_{ij} \frac{\partial U_j}{\partial x_i}$$

$$+ \mathcal{I}_i\left[\frac{\partial U_i}{\partial t} + U_j \frac{\partial U_i}{\partial x_j} + g \frac{\partial b}{\partial x_i}\right] = 0 \ , \qquad (2.2.6)$$

as the energy conservation equation for the wave motion. These are the same as those derived, from first principles, in Crapper (1979). This energy conservation equation represents an energy balance for the wave motion since if there are no waves present the left hand side of (2.2.6) is identically zero. An energy conservation equation for the mainstream motion is, thus, obtained by subtracting the energy conservation equation for the wave motion (2.2.6) from the energy conservation

equation (2.2.3). Then

$$\frac{\partial}{\partial t}\left[\frac{1}{2}\rho d U^2 + \frac{1}{2}\rho g b^2\right] + \frac{\partial}{\partial x_i}\left[U_i\left[\frac{1}{2}\rho d U_j^2 + \rho g d b\right] + \frac{1}{2}\mathcal{I}_i U_j^2\right]$$

$$+ U_i\left[\frac{\partial \mathcal{I}_i}{\partial t} + \frac{\partial}{\partial x_j}(\mathcal{I}_i U_j)\right] + g b \frac{\partial \mathcal{I}_i}{\partial x_i} + U_j \frac{\partial \mathcal{S}_{ij}}{\partial x_i} = 0 \qquad (2.2.7)$$

is the energy conservation equation for the mainstream motion.

2.3 Kinematic Relations

Suppose that the mainstream flow $(U_i,0)$ is uniform. If a wave is periodic in both space and time then the physical parameters describing the wave will be functions of the linear phase function $\chi = k_i x_i - \omega t$. Here ω is the frequency of the waves in axes (x_i,z) and k_i is the wavenumber vector.

In these axes the wave motion is superposed on the mainstream flow. If interest is focused on the wave motion alone then the waves are best viewed from a set of axes (x_i',z'), say, traversing with mainstream flow. A Galilean transformation gives $x_i' = x_i - U_i t$, $z' = z$ (with both set of axes coinciding at $t = 0$). Thus, if a wave property (e.g. a dispersion relation) on moving liquid is given by $f(k_i x_i - \omega t)$ then it is also given by $f(k_i x_i' + k_i U_i t - \omega t) = f(k_i x_i' - \sigma t)$ where $\sigma = \omega - k_i U_i$ is the frequency of the waves in the axes (x_i',z').

This relation between frequencies ω and σ is also assumed to hold if the mainstream flow is sufficiently slowly-varying. It follows that if a wave property is given on still liquid for a wave of frequency σ, the corresponding property for a wave on liquid in motion is given by the relation

$$\omega = \sigma + k_i U_i \ , \qquad (2.3.1)$$

known as the Doppler relation.

For slowly-varying wavetrains the appropriate form of the uniform plane-wave solution in terms of a phase function χ is still applicable locally but the phase function χ itself is not linear in x_i and t. The wavenumber k_i and the frequency ω are defined in terms of a generalised phase function $\chi(x_i,t)$ by

$$k_i = \frac{\partial \chi}{\partial x_i} \ , \quad \omega = -\frac{\partial \chi}{\partial t} \ . \qquad (2.3.2)$$

A pseudo-phase function $\psi(x_i,t)$ is also introduced to generalise the mainstream flow via the definitions

$$U_i = \frac{\partial \psi}{\partial x_i} , \quad \gamma = - \frac{\partial \psi}{\partial t} , \tag{2.3.3}$$

where γ is analogous to some Bernoulli "constant".

If the second derivatives of these phases exist and are continuous then four consistency relations arise:

$$\frac{\partial k_i}{\partial t} + \frac{\partial \omega}{\partial x_i} = 0 , \quad \frac{\partial k_j}{\partial x_i} = \frac{\partial k_i}{\partial x_j} , \tag{2.3.4}$$

$$\frac{\partial U_i}{\partial t} + \frac{\partial \gamma}{\partial x_i} = 0 , \quad \frac{\partial U_j}{\partial x_i} = \frac{\partial U_i}{\partial x_j} . \tag{2.3.5}$$

The first of each set of relations is in conservation form (relation 2.3.4 is sometimes called the equation for the conservation of wavenumber). The last of each set implies the distribution of the local wavenumber in space and the mainstream flow are irrotational or, in terms of tensor terminology, symmetric. This latter restriction on the mainstream flow can be greatly eased. This is discussed further in chapter 7.

2.4 Whitham's Equations and the Averaged Lagrangian

Whitham (1965, 1967, 1974) proposes that for slowly-varying wavetrains the equations for the wave parameters are found by use of an averaged Lagrangian $\mathcal{L}^w$ given by (appendix B)

$$\mathcal{L}^w = T - V \tag{2.4.1}$$

where w denotes that this is a property of the wave motion alone. Then

$$\mathcal{L}^w = \mathcal{L}^w(\sigma,k,a,d) \qquad \text{where} \qquad k^2 = k_i k_i \tag{2.4.2}$$

and a is the amplitude of the waves.

Whitham's equations (equations B18 - B19 of appendix B) in terms of this averaged Lagrangian $\mathcal{L}^w$ are:

the dispersion relation

$$\frac{\partial \mathcal{L}^w}{\partial a} = 0 , \tag{2.4.3}$$

an averaged Bernoulli equation which defines γ in terms of flow parameters

$$\rho\left[\gamma - \tfrac{1}{2}U_i^2 - gb\right] + \frac{\partial \mathcal{L}^w}{\partial d} = 0 \ , \qquad (2.4.4)$$

the mass conservation equation (compare with equation 2.2.1)

$$\frac{\partial}{\partial t}(\rho b) + \frac{\partial}{\partial x_i}\left[\rho d U_i + k_i \frac{\partial \mathcal{L}^w}{\partial \sigma}\right] = 0 \ , \qquad (2.4.5)$$

and the wave-action conservation equation

$$\frac{\partial}{\partial t}\left[\frac{\partial \mathcal{L}^w}{\partial \sigma}\right] + \frac{\partial}{\partial x_i}\left[U_i \frac{\partial \mathcal{L}^w}{\partial \sigma} - \frac{k_i}{k} \frac{\partial \mathcal{L}^w}{\partial k}\right] = 0 \ . \qquad (2.4.6)$$

The wave-action density $\mathcal{A}$ and wave-action flux vector $\mathcal{B}_i$ are defined by

$$\mathcal{A} = \frac{\partial \mathcal{L}^w}{\partial \sigma} \ , \qquad \mathcal{B}_i = - \frac{k_i}{k} \frac{\partial \mathcal{L}^w}{\partial k} \qquad (2.4.7)$$

so the wave-action conservation equation (2.4.6) becomes

$$\frac{\partial \mathcal{A}}{\partial t} + \frac{\partial}{\partial x_i}(U_i \mathcal{A} + \mathcal{B}_i) = 0 \ . \qquad (2.4.8)$$

Whitham's formulation gives the mass conservation equation (2.2.1); in place of the momentum conservation equations (2.2.2) or (2.2.5) there are the conservation equations in the consistency relations (2.3.5) and in place of the energy conservation equation (2.2.3) or (2.2.6) there is the wave-action conservation equation (2.4.8).

Note that equation (2.4.4) essentially defines γ in terms of other parameters of the liquid motion, i.e.

$$\gamma = \frac{1}{2} U_i^2 + gb - \frac{1}{\rho} \frac{\partial \mathcal{L}^w}{\partial d} \ . \qquad (2.4.9)$$

The validity of the variational principle used to derive Whitham's equations from an averaged Lagrangian can be shown to be correct using the two-timing principle as given in Whitham (1970).

2.5 Relations between Mean Wave Properties

All the mean properties of the wave motion are expressible in terms of the wave parameters σ and k_i and a minimum of four of the mean properties of the wave motion. Those mean properties most commonly used are the mean depth d, the mean kinetic energy density T, the mean potential energy density V and the mean bottom velocity squared given by

$$\overline{(u_k^2)_{-h}} \quad \text{or} \quad \overline{u_h^2} \tag{2.5.1}$$

where the subscript - h denotes evaluation at z = - h.

For consistency between the averaged equations of § 2.2 and Whitham's equations of § 2.4 (e.g. compare the mass conservation equations 2.2.1 and 2.4.5) the mean properties of the wave motion are defined, in terms of the averaged Lagrangian $\mathcal{L}^w$, in the following manner (Crapper 1979):

$$\mathcal{I}_i = k_i \frac{\partial \mathcal{L}^w}{\partial \sigma} , \quad \mathcal{S}_{ij} = \mathcal{L}^w \delta_{ij} - \frac{k_i k_j}{k^2} \frac{\partial \mathcal{L}^w}{\partial k} - d \frac{\partial \mathcal{L}^w}{\partial d} \delta_{ij} , \tag{2.5.2}$$

$$\mathcal{E} = \sigma \frac{\partial \mathcal{L}^w}{\partial \sigma} - \mathcal{L}^w , \quad \mathcal{F}_i = \frac{\sigma k_i}{k} \frac{\partial \mathcal{L}^w}{\partial k} - \frac{1}{\rho} \frac{\partial \mathcal{L}^w}{\partial d} \mathcal{I}_i . \tag{2.5.3}$$

Consistency between these two systems of equations also implies (Crapper 1979, relations 75)

$$\frac{\partial \mathcal{L}^w}{\partial \sigma} = 2 \frac{T}{\sigma} , \tag{2.5.4}$$

$$\frac{\partial \mathcal{L}^w}{\partial k} = - \frac{1}{k} \left[3T - 2V^{\varepsilon} + \frac{1}{2} \rho d \overline{u_h^2} \right] , \tag{2.5.5}$$

and

$$\frac{\partial \mathcal{L}^w}{\partial d} = - \frac{1}{2} \rho \overline{u_h^2} . \tag{2.5.6}$$

The first of these can be deduced using the expression (2A16) and definitions (2.4.1) and (2.5.4).

Expressions (2.5.5 - 2.5.7) and definitions (2.5.3, 4, 2.4.7) give the following expressions for mean wave properties:

$$\mathcal{I}_i = 2 \frac{T}{\sigma} k_i \ , \tag{2.5.7}$$

$$\mathcal{S}_{ij} = \left[3T - 2V^{\kappa} + \frac{1}{2} \rho \overline{du_h^2} \right] \frac{k_i k_j}{k^2} + \left[T - V + \frac{1}{2} \rho \overline{du_h^2} \right] \delta_{ij} \ , \tag{2.5.8}$$

$$\mathcal{E} = T + V \ , \tag{2.5.9}$$

$$\mathcal{F}_i = \left[3T - 2V^{\kappa} + \frac{1}{2} \rho \overline{du_h^2} \right] \frac{\sigma}{k^2} k_i + \frac{T}{\sigma} \overline{u_h^2} k_i \ , \tag{2.5.10}$$

$$\mathcal{A} = 2 \frac{T}{\sigma} \ , \tag{2.5.11}$$

$$\mathcal{B}_i = \left[3T - 2V^{\kappa} + \frac{1}{2} \rho \overline{du_h^2} \right] \frac{k_i}{k^2} \ . \tag{2.5.12}$$

2.6 The Case of Infinite Depth

When the depth of the liquid is infinite, i.e. $h \longrightarrow - \infty$, the continuity, momentum and energy equations can still be integrated from some level $z = - h$ below which there is no wave motion and which is taken to be constant. However, several different values of h could be chosen and the same averaged equations should be obtained. Thus, any term in the averaged equations in which h appears will have to vanish. In the momentum conservation equations (2.2.5) h appears, in d, multiplied by

$$\frac{\partial U_i}{\partial t} + U_j \frac{\partial U_i}{\partial x_j} + g \frac{\partial b}{\partial x_i} \ . \tag{2.6.1}$$

Consequently, these expressions must vanish. It follows that the mean level b varies only in relation to variations in the mainstream flow and does not depend on the waves. These terms occur again in the energy conservation equation (2.2.6) causing the last term of this equation to vanish. The implication here is that the current satisfies the shallow water equations even when waves are present. Note that for general finite depth flows the mainstream motion satisfies the shallow water equations in the absence of waves. That is wave energy and momentum

densities become negligible compared with those of the mean flow. Thus,

$$\frac{\partial b}{\partial t} + \frac{\partial}{\partial x_i}(dU_i) = 0 \ , \quad \frac{\partial U_i}{\partial t} + U_j \frac{\partial U_i}{\partial x_j} + g \frac{\partial b}{\partial x_i} = 0 \ . \tag{2.6.2}$$

The momentum conservation equations (2.2.5) become

$$\frac{\partial \mathcal{I}_i}{\partial t} + \frac{\partial}{\partial x_j}(U_j \mathcal{I}_i + \mathcal{S}_{ij}) + \mathcal{I}_j \frac{\partial U_i}{\partial x_j} = 0 \tag{2.6.3}$$

and the energy conservation equation (2.2.6) becomes

$$\frac{\partial \mathcal{E}}{\partial t} + \frac{\partial}{\partial x_i}(U_i \mathcal{E} + \mathcal{F}) + \mathcal{S}_{ij} \frac{\partial U_j}{\partial x_i} = 0 \ . \tag{2.6.4}$$

For infinite depths the Lagrangian $\mathcal{L}^w$ must be independent of mean depth d because the equations can not depend on depth h and because the mean level b does not depend on the wave motion. The expression (2.5.7) for the mean bottom velocity squared in terms of the averaged Lagrangian $\mathcal{L}^w$, thus, implies that

$$\overline{u_h^2} = 0 \tag{2.6.5}$$

which is actually the case for infinite depth flows. One implication of this is that, from definition (2.4.9) of γ,

$$\gamma = \frac{1}{2} U_j^2 + gb \tag{2.6.6}$$

is the definition for γ when the depth of the liquid is infinite. Other implications are that the mean wave properties, discussed in § 2.5, only require kinetic energy density T and the potential energy density V for evaluation.

Note that the two definitions of the wave motion as proposed by Stokes (1847) become identical for infinite depths simply because there is negligible wave motion at large depths even though the mass flux is still non-zero.

2.7 The Case of Steady Variations

Attention is now focused on the case when variations of the mainstream flow and the wave parameters, such as amplitude and wavelength, are steady, i.e.

$$\frac{\partial}{\partial t} = 0 \ . \tag{2.7.1}$$

When this is the case the majority of equations become purely algebraic. A list of these equations is given here for future reference.

The mass conservation equation (2.2.1), or (2.4.5), gives a constant value for the total mass flux:

$$\rho dU_i + \mathcal{I}_i = \text{constant}, - m_i \ . \tag{2.7.2}$$

The momentum conservation equations (2.2.2) and the energy conservation equation (2.2.3) do not become algebraic.

The consistency relations (2.3.4) and (2.3.5) give constant values for frequency ω and Bernoulli "constant" γ:

$$\omega = \text{constant} \ , \tag{2.7.3}$$

$$\gamma = \text{constant} \ . \tag{2.7.4}$$

The wave-action conservation equation gives a constant value for the total wave-action flux:

$$U_i \mathcal{A} + B_i = \text{constant}, \ b_i \ . \tag{2.7.5}$$

2.8 Linear and Near-Linear Caustics

A outline of results used in this thesis for the theory of linear and near-linear (weakly nonlinear) caustics, as given by Peregrine and Smith (1979), is presented in this section. These results are only applicable to infinite depth flows. The notation is slightly different. It is supposed that the amplitude of the waves is infinitesimal throughout the wave motion and that the mainstream motion $U_i(x_i,t)$ is given ab initio. It is also supposed that the waves are isotropic.

Define rays as lines in the flow field everywhere parallel to the total group velocity vector $C_{gi}(x_i,t)$. Solutions to linearised slowly-varying problems may be found by integrating in (x_i,t) along the rays from an initial point with given initial values of ω, k_i and a. This is called linear ray theory.

A caustic is defined to be an envelope of rays. In general if waves are propagating in three (two, one) dimensions a family of rays coalesce on a caustic surface (line, point). The position of the caustic varies with time. Here, however, attention is restricted to steady caustics in a steady wave field. It is assumed that variations of wave properties along the caustic are negligible compared to variations perpendicular to the caustic. This is a reasonable assumption since linear ray theory shows that the amplitude of a slowly-varying wavetrain varies greatest in this direction and is, in fact, singular at the caustic.

Suppose that the near-linear dispersion relation takes the form

$$G(\sigma,k) + H(k)\ a^2 = 0 \qquad (2.8.1)$$

where G and H are assumed to be slowly-varying functions of x_i. Only the first nonlinear effects are included and any dependence of H on σ is eliminated using the linear dispersion relation

$$G(\sigma,k) = 0\ . \qquad (2.8.2)$$

Let $x_1 = x$ be the coordinate perpendicular to the caustic with $x = 0$ being locally the position of the caustic. The $x_2 = y$ direction is then parallel to the caustic. Suppose that the waves approach the caustic from the - x half of the (x,y) plane. The above assumption means that all wave properties depend on x only. The consistency relations (2.3.4) and (2.3.5) immediately show that ω, $k_2 = m$ and $U_2 = V$ are constants so that the wavenumber component $k_1 = l$ and the amplitude a are the only dependent variables to be found with $U_1 = U$ being a given function of x.

It is easily shown that in the (x,l), or $(U(x),l)$, plane the tangent of the linear solution at the caustic is parallel to the l-axis.

The near-linear dispersion relation is given by (2.8.1) and so as long as H is everywhere non-zero the solution curves for near-linear theory will lie on one side of the linear curve G = 0. It is now supposed that H is always non-zero. In fact, solutions curves for near-linear theory must remain close to the lines

$$G = 0 \quad \text{and} \quad \frac{l}{k}\left[H\frac{\partial G}{\partial k} - \frac{1}{2}G\frac{\partial H}{\partial k}\right] - HU\frac{\partial G}{\partial \sigma} = 0 \qquad (2.8.3)$$

which represent the linear and the zero wave-action flux "stopped" waves solution curves respectively. These lines intersect at the linear caustic

$$G = U\frac{\partial G}{\partial \sigma} - \frac{l}{k}\frac{\partial G}{\partial k} = 0\ . \qquad (2.8.4)$$

Once the two lines given by equations (2.8.4) are found it is easy to sketch solution curves for near-linear theory since the sign of H in the near-linear dispersion relation (2.8.1) indicates which side of the linear solution G = 0 the near-linear solution curves lie. This is illustrated in figure 2.1.

Solutions may take one of two different forms, depending on the sign of

$$H\Big/\left[U^2\frac{\partial^2 G}{\partial \sigma^2} - 2U\frac{\partial^2 G}{\partial \sigma \partial l} + \frac{\partial^2 G}{\partial l^2}\right] \qquad (2.8.5)$$

at the caustic. The solutions are called R-type and S-type near-linear caustics for positive and negative values of (2.8.5) respectively.

For an R-type caustic the solution lines for the wavenumber lie on the concave side of the linear solution in the caustic region of the (x,l) or (U,l) plane. There are two branches of the near-linear solution corresponding to incident and reflected waves. Unlike the linear solution these do not meet at a caustic. However, each branch has a singularity in the slope of the amplitude before the position of the linear caustic is reached. This singularity implies a rapid variation of wavenumber and, hence, the slowly-varying assumption becomes invalid before the singularity is reached. The singularity occurs at a sufficiently small amplitude for the near-linear approximation to remain valid. It is concluded that the wave field of R-type caustics is regular, since wave steepnesses are not near their maximum, and that a reflection of waves may occur. Uniform solutions may be found and the

wave field has no singularity.

For an S-type caustic things are quite different. The solution for the wavenumber lies on the convex side of the linear solution in the caustic region of the (x,l) or (U,l) plane. As the linear solution approaches its singularity the near-linear solution diverges from it. There is no singularity in the wave solution. However, as the solution diverges from the linear solution the amplitude of the waves increases and the near-linear assumption breaks down. Fully nonlinear solutions (Peregrine and Thomas 1979) show waves can reach their maximum steepness. It is concluded that waves may break in the neighbourhood of S-type caustics.

2.9 Reference Frames and Dimensionless Units

The general problems considered in this thesis are of two types. One type is called the "wave-current interaction" problem, or just the "interaction" problem, and the other type the "wave propagation" problem, or just the "propagation" problem. In the interaction problem both the mainstream flow and the waves travel in a horizontal direction as a result of which interaction between the waves and mainstream flow occurs. In the propagation problem there is a gravity wavetrain present ab initio so that "small" waves propagate on the surface of the "long" gravity waves and do so in a direction parallel to the surface of the gravity waves. The mainstream flow, in this case, is a direct result of the gravity wave motion and is also in a direction parallel to the surface of the gravity waves.

Two reference frames are defined for use in both the wave-current interaction and wave propagation problems. The first is the ω reference frame with axes (x_1,z) in which the mean current, or mainstream flow, is $(U_1,0)$, e.g. frame fixed to an observer moving with the gravity waves. The second is the σ reference frame with axes (x_1',z') in which the mean current is zero (below wave troughs), i.e. frame moving with the mainstream flow $(U_1,0)$. These reference frames are called the ω-frame and σ-frame because the frequency of the waves in these frames is denoted by ω and σ respectively.

Two other frames are also defined for use specifically in the propagation problem. One frame (X_1,Z) is that which travels at the phase speed c of the gravity waves. The surface velocity of the gravity waves is defined to be $(U_1,0)$ in this frame which implies that this frame is also an ω-frame. The other frame is that frame given by Stokes first definition applied to the motion of the pure gravity waves alone,

i.e. frame in which the gravity waves have phase speed c. This frame is called the observer's-frame because it is the frame in which the propagation problem is physically observed.

For the interaction problem the ω-frame and σ-frame have x_1, x_1' horizontal and z, z' vertically upwards. However, for the propagation problem x_1, x_1' and z_1, z' are directed along and perpendicular (out of liquid) to the surface of the gravity waves where, in addition, coordinates (X,Z) are used with X horizontal and Z vertically upwards (figure 2.2). Note that if $U_1 = 0$ then $x_1 = x_1'$ and $z_1 = z'$.

For the purposes of the problems examined it is useful to work in one of three different systems of units. One is the standard system of S.I. units in which mass, length and time are measured in kilograms, meters and seconds respectively. These are denoted as "dimensional units".

The second is a dimensionless system in which density ρ, gravity g and wavenumber K of gravity waves take unit value. These units are denoted as "gravity" units and are represented by a subscript 0. If mass, length and time are denoted by M, L and T in dimensional units and by M_0, L_0 and T_0 in gravity units then

$$M = \frac{\rho}{K^3} M_0 \ , \quad L = \frac{1}{K} L_0 \ , \quad T = (gK)^{-\frac{1}{2}} T_0 \qquad (2.9.1)$$

define the dimensionless units.

The third is a dimensionless system in which density ρ, surface tension τ and the magnitude of frequency ω (non-zero) of the waves take unit value. These units are denoted as "capillary" units and are represented by a subscript 1. If mass, length and time are denoted by M, L and T in dimensional units and by M_1, L_1 and T_1 in capillary units then

$$M = \frac{\tau}{\omega^2} M_1 \ , \quad L = \left[\frac{S}{\omega^2}\right]^{\frac{1}{3}} L_1 \ , \quad T = \frac{1}{|\omega|} T_1 \qquad (2.9.2)$$

define the dimensionless units. One important feature is that given any expressions or equations in dimensional units the corresponding expression or equations in capillary units are most easily found by substituting $\rho = \tau = \omega^2 = 1$, $\omega = \omega_1 = \pm 1$ (+ 1 for $\omega > 0$ and - 1 for $\omega < 0$) and adding a subscript 1 to all the wave and mainstream flow parameters. This substitution method of non-dimensionalisation is employed throughout this thesis. Parameters such as wave-action flux b_1 and the mass flux m_1 are given in capillary units using (2.9.2).

CAPTIONS FOR FIGURES

Figure 2.1: Diagram illustrating the behaviour of near-linear waves in the neighbourhood of a linear caustic. Heavy lines represent the linear solution. Dashed lines represent the stopped waves solution given by $l(HG_k - \frac{1}{2}GH_k) - kHUG_\sigma = 0$. Thin continuous lines represent solutions of slowly varying near-linear theory; (a) R-type, and (b) S-type caustic.

Figure 2.2: Definition diagram for short waves on long gravity waves. Axes (X,Z) and (x,z) are ω-frames fixed to the gravity waves; axes (x_1,z_1) is a σ-frame locally fixed to the surface velocity distribution U of the gravity waves. $\mathfrak{C}$ is the phase speed of the gravity waves in the observers reference frame. c is the phase speed of the short waves in σ-frame (x_1,z_1). A and Λ are the amplitude and wavelength of the gravity waves.

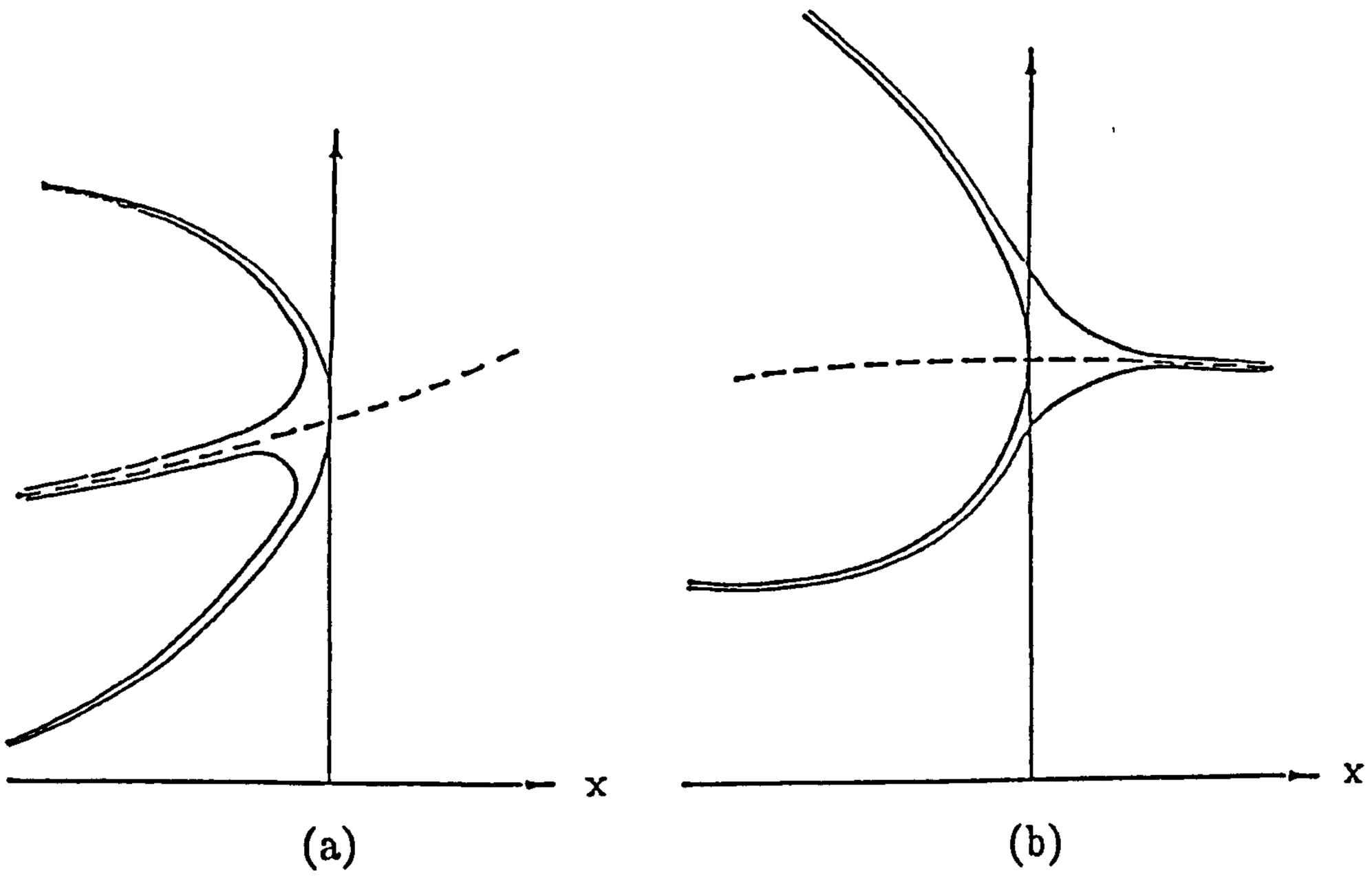

Figure 2.1: Diagram illustrating the behaviour of near-linear waves in the neighbourhood of a linear caustic. Heavy lines represent the linear solution. Dashed lines represent the stopped waves solution given by $1(HG_k - \frac{1}{2}GH_k) - k\Pi\dot{U}G_\sigma = 0$. Thin continuous lines represent solutions of slowly varying near-linear theory; (a) R-type, and (b) S-type caustic.

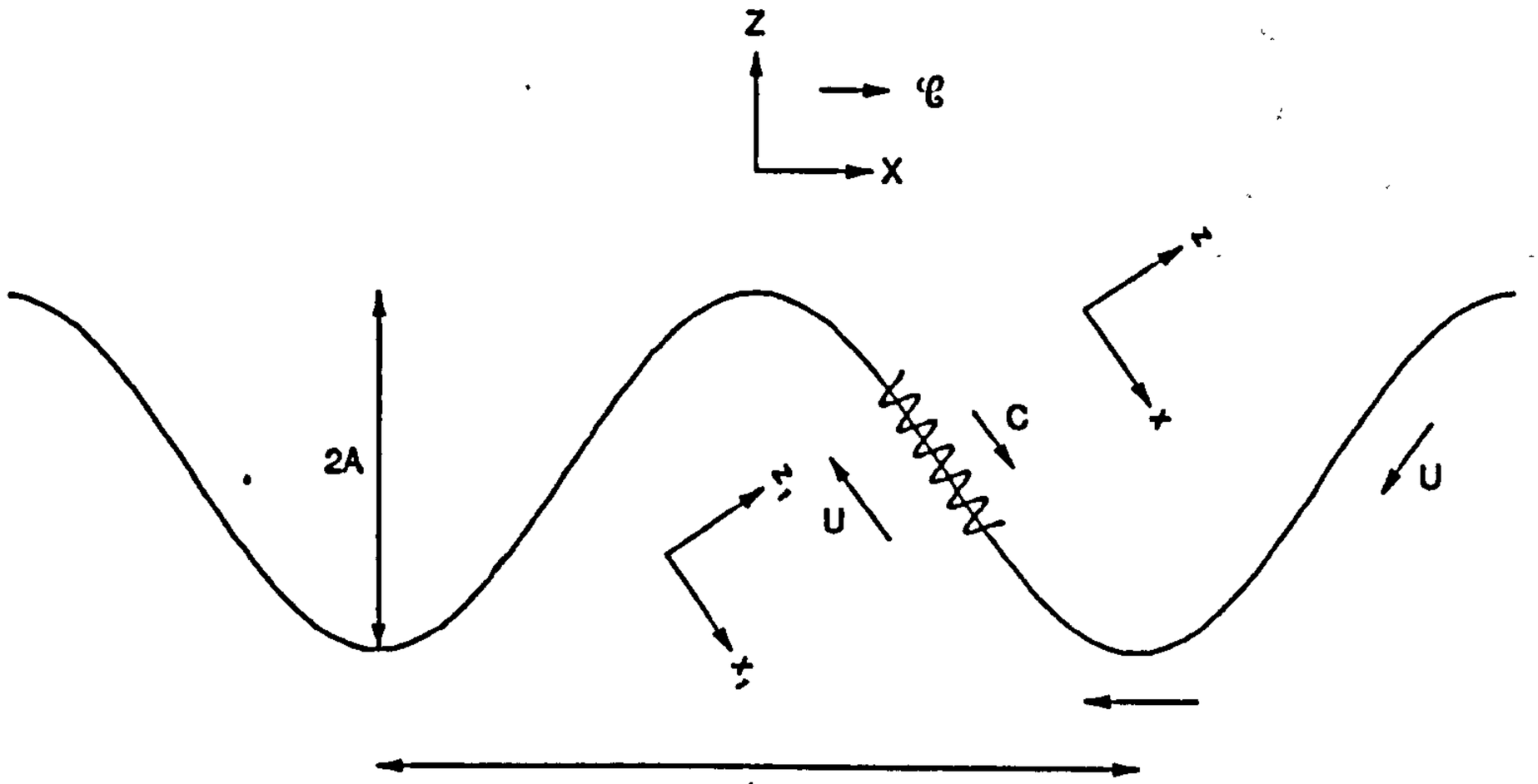

Figure 2.2: Definition diagram for short waves on long gravity waves. Axes (X,Z) and (x,z) are ω-frames fixed to the gravity waves; axes (x_1,z_1) is a σ-frame locally fixed to the surface velocity distribution U of the gravity waves. $\mathcal{C}$ is the phase speed of the gravity waves in the observers reference frame. c is the phase speed of the short waves in σ-frame (x_1,z_1). A and Λ are the amplitude and wavelength of the gravity waves.

CHAPTER 3
INFINITESIMAL AMPLITUDE CAPILLARY-GRAVITY WAVES ON INFINITE DEPTH LIQUID

3.1 Introduction

In this chapter both the wave-current interaction and the wave propagation problems are considered for the case of free irrotational infinitesimal plane-waves steadily travelling in the same or opposite sense either to a given steady current distribution (the interaction problem) or to the surface currents of a steady gravity wavetrain (the propagation problem) over an infinite depth of liquid. That is the case where $d = \infty$, $\partial/\partial t = 0$, $U_2 = 0$, $k_2 = 0$ and $U_1 = U$, $k_1 = k$, say. The waves are influenced by both surface tension and gravity.

Our aim is to find the variations of both wavenumber and wave steepness of the capillary-gravity waves for both problems. Whitham's equations are used to solve the problems. The equations for both the interaction and propagation problems are similar. Peregrine (1976, p64) shows that the propagation problem is solved in exactly the same way as the interaction problem except that gravity g and current U are everywhere replaced by effective gravity g^* and surface current U(X). For certain cases singularities in the wave field in the form of linear caustics are found. The behaviour in the neighbourhood of the linear caustic is found using the near-linear theory outlined in section 2.8.

In section 3.2 all the various wave solutions that can be encountered and some of their properties are considered. The equations solved numerically are developed in section 3.3. The cases of stationary and non-stationary waves are solved and discussed in sections 3.4 and 3.5 respectively. Section 3.6 discusses the type of near-linear caustic present and its consequences.

3.2 The Possible Waves

A uniform plane-wave of infinitesimal amplitude propagating over still liquid of infinite depth with vertical displacement and velocity potential

$$\eta = a \cos(kx - \sigma t) \ , \quad \phi = ace^{kz} \sin(kx - \sigma t) \qquad (3.2.1)$$

has dispersion relation and group velocity, the velocity of energy propagation,

$$\sigma^2 = gk + sk^3 \ , \quad c_g = \frac{d\sigma}{dk} = \frac{1}{2} c \left[\frac{g + 3sk^2}{g + sk^2}\right] \qquad (3.2.2)$$

where $s = \tau/\rho$ is the ratio of the surface tension to the density of the liquid. Variations of phase velocity and group velocity with wavenumber are shown in figure 3.1 together with the limiting cases of pure capillary waves and pure gravity waves.

If these waves are superposed onto a mainstream flow then the frequency of the waves is shifted by an amount kU as shown by the Doppler relation (2.3.1). The phase and group velocities of the waves are also shifted. The total phase and group velocities are denoted by C and C_g respectively where

$$C = U + c \quad \text{and} \quad C_g = U + c_g \ . \qquad (3.2.3)$$

Figure 3.2 shows the variation of frequency σ with wavenumber k as given by the dispersion relation (3.2.2) and the Doppler relation (2.3.1) for a constant mainstream flow U. The liquid is taken to be water with $\rho = 1000$ Kg m^{-3} and $\tau = 0.0742$ kg s^{-2}. If the wavenumber k is taken to be positive then sgn c = sgn c_g = sgn (σ), sgn C = sgn ω, and c_g and C_g may be identified by examination of the gradients of the curves and lines of figure 3.2: c_g is gradient of the tangent to the dispersion relation curves and C_g is this gradient minus the gradient of the Doppler relation line. Note that the effect of surface tension (gravity) is greatest on waves whose wavenumber k is large (small), i.e. small (large) wavelength.

In this section the Doppler relation (2.3.1) and the dispersion relation (3.2.2) are combined and all the possible waves, for a constant mainstream flow U, are discussed. The change is direction of their phase and group velocities, resulting from the presence of the mainstream flow U, are also discussed. A wave propagates in the direction of its (total) group velocity because this is the direction of propagation

of the energy of the wave: it is only the wave crests (and troughs) which propagate in the direction of the waves (total) phase speed. Figures in the vain of figure 3.2 are used for the specific cases $\omega = 0$, $\omega > 0$ and $\omega < 0$ in order to analyses the possible waves and their properties.

The analysis is similar to that given in Peregrine (1976) for the case of pure gravity waves. Firstly, consider the case of stationary waves where the frequency ω is zero (figure 3.3) so that the total phase speed C is zero. These waves are called stationary waves because the wave crests remain stationary. The Doppler relation (2.3.1) gives

$$kU = -\sigma \quad \Longrightarrow \quad U = -c \ . \tag{3.2.4}$$

Suppose $c \geq 0$ so that $U \leq 0$. Then, the dispersion relation (3.2.2) implies that there are either:

(a) two waves if $U \leq -c_{min}$ (figure 3.3). One wave, denoted CG, represents capillary-gravity waves whilst the other, denoted GC, represents gravity-capillary waves. Both these waves have c_g positive but only wave CG has C_g positive whilst wave GC has C_g negative. Consequently, before superposition onto the mainstream flow both waves travel in the + x direction but after superposition onto the mainstream flow only wave CG travels in the + x direction whereas wave GC travels in the - x direction.

(b) one wave if $U = -c_{min}$ (figure 3.3). This wave occurs when the CG and GC waves meet (if U is increased from a very large and negative value). It corresponds to the position of a caustic. This wave has c_g positive but has C_g zero. It follows that the mainstream flow U is such that $U = -c_g = -c_{min}$ and the energy of the wave remains stationary as well as the wave crests. It is seen from figure 3.1 that the group velocity curve passes through the position of minimum phase speed.

(b) no waves if $U \geq -c_{min}$ (figure 3.3).

For stationary waves, without loss of generality, k and U can be chosen to be positive in which case σ is negative, k and U can be chosen to be positive and negative respectively in which case σ is positive, etc., . Thus, the relative signs of k, U and σ are fixed. The sign convention chosen by us is that $k \geq 0$, $U \leq 0$ and $\sigma \geq 0$. Thus, the

mainstream motion, coming from the right, brings the waves, whose crests (and troughs) are coming from from the left, to rest.

By discussing the transition of the two stationary waves CG and GC as the magnitude of ω increases the general cases of $\omega > 0$ and $\omega < 0$ are interpreted. For $\omega \neq 0$ the conventions on signs becomes different. Without loss of generality two of ω, U, σ and k may be chosen to be of fixed sign. The signs of the other two parameters must be allowed to be positive and negative. The sign convention chosen by us is $k \geq 0$ and $U \leq 0$ since this proves best for interpreting the transition from the two stationary waves CG and GC. Suppose that $|\omega|$ is small (figures 3.4), i.e. long total period. Then:

(a) for U = 0 (figure 3.4) the Doppler relation gives $\sigma = \omega$. The waves CG and GC do not exist but two new waves appear. One, denoted G+, has $\omega > 0$ whilst the other, denoted G-, has $\omega < 0$. These waves have large wavelengths and are, thus, gravity waves. Wave G+ has c and c_g positive whilst wave G- has c and c_g negative. Note that, from definition (3.2.3) C = c and $C_g = c_g$. Consequently, wave G+ travels in the + x direction and wave G- travels in the - x direction.

(b) for $U \neq 0$ (figure 3.4) there are at most six waves: three with $\omega > 0$ and three with $\omega < 0$. Two correspond to waves G+ ($\omega > 0$) and G- ($\omega < 0$). The other four waves arise from the Doppler shifting of the stationary waves CG and GC: two waves arise form each of these waves, one with $\omega > 0$ and the other with $\omega < 0$. These are denoted by CG or GC followed by the corresponding sign of ω, i.e. CG-, GC-, CG+ and GC+.

The two waves arising from a transition of one stationary wave are distinct. Each stationary wave CG and GC is shifted a small amount by the Doppler relation but in opposite directions corresponding to $\omega > 0$ and $\omega < 0$. This in turn corresponds to the waves experiencing an increase or decrease in their phase velocity c. From the Doppler relation (2.3.1),

$$c = - U + \frac{\omega}{k} . \qquad (3.2.5)$$

Recalling that $U \leq 0$ and $k \geq 0$, it is seen that the CG- and GC- waves experience a decrease and the CG+ and GC+ waves experience an increase in phase velocity c.

Waves G+ and G- maintain the same signs of c, C and c_g, C_g for $U \neq 0$ as for U = 0 and, thus, experience no changes in

direction of propagation. Waves CG(+,-) and GC(+,-) all have c and c_g positive. Wave CG+ has C and C_g positive, wave CG- has C negative and C_g positive, wave GC+ has C positive and C_g negative and wave GC- has C and C_g negative. Thus, the directions of travel of waves CG(+,-) and waves GC(+,-) are the same as the stationary waves CG and GC respectively, i.e. in the - x and + x directions respectively. It is the direction of the phase speed C which is affected by the transition from stationary to non-stationary waves.

All these waves have a non-zero value for their total phase speed C so that their crests (and troughs) are in motion.

As the magnitude of ω increases the effect of surface tension on waves G+ and G- also increases whilst the relative importance of surface tension and gravity on waves CG(+,-) and GC(+,-) changes. Indeed, if $|\omega|$ is very large then waves G- can also be dominated by surface tension (waves G+ do not exist). This agrees with the classification of waves in terms of their frequencies as given by Kinsman (1965, § 1.2). All the other features remain unchanged including the notation, even for the two special cases $\tau \longrightarrow 0$ and $g \longrightarrow 0$ (discussed below). Thus, for $\omega \neq 0$ there are at most (least) six (two) waves.

A caustic occurs when the total group velocity C_g is zero, i.e. $c_g = - U$, so that the Doppler relation line is tangential to the dispersion relation curve and two waves coalesce. It follows that for the stationary waves case there is one possible caustic which occurs when the two waves CG and GC coalesce (figure 3.3), i.e. when $U = - c_{min}$ (figure 3.1). This is denoted as the CG/GC caustic.

For the non-stationary waves case there are, in general, three possible caustics. One occurs when waves GC+ and G+ coalesce and is denoted as the GC+/G+ caustic. The other two occur when waves CG- and GC-, or CG+ and GC+, coalesce and are denoted as the CG-/GC-, or CG+/GC+, caustics. These latter two caustics correspond to a transition of the CG/GC caustic of stationary wave theory. This can be seen by consideration of figures such as figure 3.4.

Two interesting special cases are those of pure gravity and pure capillary (figure 3.2) waves. For either of these cases there are at most four waves and only one possible caustic. For stationary pure gravity waves (Peregrine 1976) where $\tau \longrightarrow 0$ wave CG ceases to exist and no caustic is possible. For non-stationary pure gravity waves waves CG(+,-) cease to exist and the only possible caustic is the GC+/G+ caustic (a stopped gravity waves caustic).

For stationary pure capillary waves where $g \rightarrow 0$ wave GC ceases to exist and no caustic is possible. For non-stationary pure capillary waves waves G+ and GC+ cease to exist and the only possible caustic is the CG-/GC- caustic (a stopped capillary waves caustic). Note that this caustic does not require a minimum in phase velocity c as does the stationary wave CG/GC caustic. Also, wave G- still exists but is unphysical since wavelengths for this wave are large and, thus, it is bound to be affected by gravity.

ω	σ	c	C	c_g	C_g	b	notation
0	+	+	0	+	+	+	CG
0	+	+	0	+	-	-	GC
+	+	+	+	+	+	+	CG+
+	+	+	+	+	-	-	GC+
+	+	+	+	+	+	+	G+
-	+	+	-	+	+	+	CG-
-	+	+	-	+	-	-	GC-
-	-	-	-	-	-	+	G-

Table 3.1: Properties of the two possible stationary waves CG and GC and the six possible non-stationary waves CG(+,-), GC(+,-) and G(+,-) on a mainstream flow.

The properties of each possible type of wave are summarised in table 3.1. This table also gives the sign of a parameter b. This b is the value of the total wave-action flux $U\mathcal{A} + \mathcal{B}$ and is discussed below in § 3.3. Note that the sign of properties of stationary waves CG and GC are the same as those of non-stationary waves CG(+,-) and GC(+,-) except for frequency ω and total phase velocity C which are both zero. Also note that at a caustic the total group velocity C_g is zero for those waves which coalesce at the caustic.

For the major part of this thesis interest is focused on pure capillary waves. Thus, emphasis in this chapter is swayed towards waves CG(+,-) and GC- and towards the CG-/GC- caustic.

3.3 The Equations

To find expressions for the mean wave properties (§ 2.5, 6) the kinetic energy density T and potential energy density V are needed. Expressions for these can be found in any basic text on water waves or derived directly from the solution (3.2.1, 2) using the definitions in appendix A. These are given by

$$T = V = \frac{1}{4}\frac{\rho\sigma^2 a^2}{k} \ . \qquad (3.3.1)$$

The wave-current interaction problem is examined first. For a given value of current U wavenumber k of the waves is found by eliminating σ from the dispersion relation (3.2.2) using the Doppler relation (2.3.1). Thus,

$$sk^3 - U^2k^2 + (g + 2\omega U)k - \omega^2 = 0 \ . \qquad (3.3.2)$$

For a particular value of $|\omega|$ this equation is solved by varying U over a given range. Waves are only sought for $U \leq 0$ so that no waves are repeated. The actual waves found are then deduced using table 3.1.

The wave amplitude a is given by the wave-action conservation equation (2.7.5). From expressions (2.5.10 - 2.5.12) for $\mathcal{F}$, $\mathcal{A}$ and $\mathcal{B}$ in terms of mean wave properties and infinite depth mean property (2.6.5), which states that the mean bottom velocity squared is zero, the wave-action density $\mathcal{A}$ and wave-action flux $\mathcal{B}$ are given by

$$\mathcal{A} = \frac{\mathcal{E}}{\sigma} \ , \quad \mathcal{B} = \frac{\mathcal{F}}{\sigma} \ , \qquad (3.3.3)$$

but
$$c_g = \frac{\mathcal{F}}{\mathcal{E}} \quad \text{so} \quad \mathcal{B} = c_g \mathcal{A} \qquad (3.3.4)$$

so that
$$U\mathcal{A} + \mathcal{B} = \frac{U + c_g}{\sigma}\mathcal{E} = \frac{C_g}{\sigma}\mathcal{E} = b \ , \quad \text{say,} \qquad (3.3.5)$$

where b is the constant value of the total wave-action flux. This means that, since $\mathcal{E} \geq 0$, the sign of b is given by $\operatorname{sgn} b = \operatorname{sgn}(C_g\sigma)$ and is given in table 3.1 for each of the possible waves.

Now, since $\mathcal{E} = T + V$ is given using expressions (3.3.1), the amplitude of the waves is given by

$$a = \left[\frac{2k}{\rho\sigma C_g} b\right]^{\frac{1}{2}} \ . \qquad (3.3.6)$$

This equation shows that for linear waves the actual magnitude of b is qualitatively unimportant since it serves as a magnifying factor and nothing else. It is the sign of b which is important. This sign, and the sign of σ, are found using table 3.1. However, it is noted that $(b/\sigma C_g)$ is always positive. Once equation (3.3.2) is solved for wavenumber k, equation (3.3.6) is solved for amplitude a with σ and $C_g = U + c_g$ found using the Doppler relation (2.3.1) and expression (3.2.2) for c_g respectively. Wave steepness ak can then be deduced. Note that as the two waves which coalesce at the caustic approach the caustic the value of $C_g \longrightarrow 0$ for both waves and so the amplitude of these waves becomes singular.

The propagation problem is slightly more complicated. The waves now propagate on the surface of a gravity wave and not horizontally (figure 2.2). Suppose, for the moment, that there are no short waves so that only the motion of the gravity waves is considered. In the ω-frame the gravity waves are both steady and stationary so that their surface is a streamline of the gravity wave motion. Thus, the velocities of surface particles must be parallel to the surface and in the - X direction (figure 2.2). Note that the ω-frame must be used since U is unsteady in all other frames such as the observers frame. Also the surface is a surface of constant pressure so that the gradient of the pressure P^* is in a direction perpendicular to the surface. The effective gravity g^* (Peregrine 1976, p64) defined by

$$g^* = - \frac{\partial P^*}{\partial x} \qquad (3.3.7)$$

is in a direction perpendicular to the surface of the gravity waves.

Recall that for infinite depths of liquids the mainstream flow effects the waves but the waves have no effect on the mainstream flow (§ 2.6). Thus, in equations (3.3.2, 6) the current U now takes the value of the surface velocity, which is negative, of the gravity waves. Also gravity g is everywhere replaced by the effective gravity g^* (Peregrine 1976).

There is an easier method of solving the interaction problem only. This involves specifying the wavenumber k and solving for current U (as opposed to specifying U and solving for k) using

$$U = \frac{\omega}{k} \mp \left[\frac{g}{k} + sk\right]^{\frac{1}{2}} , \qquad (3.3.8)$$

derived from equation (3.3.2), where, for a specific value of $|\omega|$, the choice of sign is made from table 3.1 and waves are only sought

for $U \leq 0$ (if $\omega \geq 0$ then choose the minus sign and if $\omega < 0$ then both signs need to be considered). The corresponding amplitude variation is still found from equation (3.3.6).

This method is not plausible for the wave propagation problem since it is the current U, and the effective gravity g^*, which are given ab initio so that the wavenumber k must be sought and equation (3.3.2) must be used. Also, interpolation methods can not be used on the results of the interaction problem because this would not take account of variations arising as a result of the effective gravity g^*.

3.4 Stationary Waves

The simpler case of stationary waves is considered first. As $\omega = 0$ dimensional S.I. units are used. Throughout the rest of this thesis the values for density and surface tension are taken to be $\rho = 1000$ kg m^{-3}, $\tau = 0.0742$ kg s^{-2} which correspond to water. For the interaction problem equation (3.3.2) gives

$$sk^2 - U^2k + g = 0 \quad \text{or} \quad k = \frac{U^2 \pm (U^4 - 4sg)^{\frac{1}{2}}}{2s} . \qquad (3.4.1)$$

Thus, there are two waves: the plus (minus) sign represents wave CG (GC). The variation of wavenumber k with current U is plotted in figure 3.5a. This is exactly the same as the variation of k with - c given from figure 3.1 as is expected since U = - c. The one possible CG/GC caustic occurs when the solution curve in the (U,k)-plane has a vertical tangent and at this point the two waves coalesce so that

$$U = - c_{min} , \quad U^4 = 4sg \quad \text{and} \quad k = \frac{U^2}{2s} . \qquad (3.4.2)$$

The amplitude of the waves is given by equation (3.3.6) but since c = - U it follows that

$$a = \left[- \frac{2}{\rho U C_g} b \right]^{\frac{1}{2}} . \qquad (3.4.3)$$

At the caustic the group velocity c_g is equal to the phase velocity c (figure 3.1) so that the total group velocity C_g is zero ($C_g = C = 0$). Thus, from (3.4.3), the wave amplitude a is singular. The wave-action flux b is taken to be ± 1 with the appropriate sign chosen from table 3.1. The variation of steepness ak with current U is

plotted in figure 3.5b. It is noted that ak reaches seemingly unrealistic values of the order of 300. This is true of all figures in this chapter. A scaling of b in equation (3.4.3) or (3.3.6) would easily reduce (or increase) the values of ak - b is only qualitatively important. Solutions which depend quantitatively on b are considered in chapter 4 and these lead to reasonable values of ak.

Note that, from the expression (3.2.2) for c_g,

$$c_{gCG} + c_{gGC} = \frac{1}{2} c_{CG} \left[\frac{g + 3sk_{CG}^2}{g + sk_{CG}^2}\right] + \frac{1}{2} c_{GC} \left[\frac{g + 3sk_{GC}^2}{g + sk_{GC}^2}\right] \qquad (3.4.4)$$

but, from the Doppler relation (3.2.4) and equation (3.4.1),

$$\left.\begin{aligned} c_{CG} = c_{GC} \ , \ sk^2 = U^2k - g \ , \\ k_{CG} + k_{CG} = - U^2 \ , \ k_{CG}k_{GC} = g \end{aligned}\right\} \qquad (3.4.5)$$

so that $$c_{gCG} + c_{gGC} + 2U = 0 \quad \text{or} \quad C_{gCG} + C_{gGC} = 0 \qquad (3.4.6)$$

which implies that waves CG and GC have equal but opposite total group velocities C_g. Thus, from (3.4.3), it follows that the amplitude variation of both waves CG and GC is the same. However, the steepness variation of both waves differs because the wavenumber variation differs.

For pure capillary (gravity) waves where $g \longrightarrow 0$ ($\tau \longrightarrow 0$) the GC (CG) wave ceases to exist and no caustic exists. From (3.4.2) it is seen that the caustic is pushed to U = 0 and k = 0 (k = ∞) (see figures 3.5).

The propagation problem is solved using equations (3.4.1 - 3.4.5) but with U taking the value of the surface current distribution U(X) of the gravity waves and gravity g everywhere replaced by effective gravity g*(X). The surface properties of pure gravity waves are found using the program described by Teles da Silva and Peregrine (1988). This program works with gravity units described in § 2.9. Thus, the wavenumber K is needed to transform surface data to dimensional units. It is found, using (2.9.1), that

$$X = \frac{1}{K} X_o \ , \quad U = \left[\frac{g}{K}\right]^{\frac{1}{2}} U_o \ , \quad g^* = g\, g_o^* \ . \qquad (3.4.7)$$

In gravity units the surface properties are all functions of steepness AK only, whereas in dimensional units they are functions of both wavenumber K and steepness AK. Note that, in the ω-frame, gravity waves attain a maximum (minimum) in surface velocity at their crests

(troughs) and that this maximum (minimum) increases (decreases) as the steepness AK and wavenumber K of the gravity waves increases. An idea of the variations of wavenumber k and steepness ak is gained by examination of figures 3.5 over the range of surface velocities for particular gravity waves. This method is only exact for pure capillary waves because there is no effective gravity g* but serves as a rough guide here and aids interpretation.

Observations of water surfaces, such as those of ponds and lakes, suggest that wavelengths Λ = 0.1, 0.2 m are typical for the presence of capillary ripples on the surface of the gravity waves. Consequently, attention is focused on these values for wavelength with steepnesses AK = 0.3, 0.4 since these represent steep gravity waves.

Throughout this thesis figures for the propagation problem have troughs of gravity waves at the two ends and a crest at the centre unless otherwise stated. Results are plotted in figures 3.6 - 3.10. The variations of wavenumber k and steepness ak with distance X along the ω-frame (fixed to the gravity waves) are plotted. For Λ = 0.2 m a caustic exists when the gravity wave steepness AK is near its maximum (AK_{max} = 0.44) as illustrated in figure 3.6 where AK = 0.43. For instance, when AK = 0.4 or 0.3 both waves CG and GC exist over the whole length of the gravity waves so there is no caustic (figures 3.7, 8). Essentially, the velocity U(X) at the crest (the maximum of U(X)) is less than the velocity required for the existence of the caustic, given by expressions (3.4.2), so that, from figures 3.5, the caustic does not exist for this case. A decrease in wavelength Λ results in an increase in the crest value of U(X) so, from figures 3.5, the caustic may come into existence. For instance, for Λ = 0.1 m when AK = 0.4 the caustic exists (figure 3.9) but when AK = 0.3 the caustic does not exist (figure 3.10). When the caustic exists it is positioned symmetrically on either side of the crests of the gravity waves.

For gravity waves of length greater than approximately 0.47 m the caustic will never exist for any steepness AK not equal to the maximum steepness AK_{max} (the maximum steepness gravity wave has a stagnation point at the crest so that the velocity at that point, in the ω-frame, is always equal to zero). This is essentially because all these gravity waves have surface velocities U(X) at the crest which are less than the velocity required for the existence of the caustic, given by expression (3.4.2).

When the propagation problem is viewed from the observers reference frame in which the gravity waves are in motion it is easily seen that waves CG (GC) propagate in the + X (- X) direction towards the caustic, if it exists, situated on the backward (forward) faces of the gravity

waves. If no caustics exist then waves CG overtake the gravity waves whilst waves GC are overtaken by the gravity waves with either of the waves propagating over the whole of the gravity waves. If caustics exist then waves CG (GC) encounter caustic type behaviour as they propagate towards the backward (forward) faces of the gravity waves as the waves attempt to propagate over the crests.

For the case of pure capillary waves no caustic exists so that no caustic would be present for any values of Λ and AK. The only waves present would be waves CG and these would propagate over the whole length of the gravity waves. It is, therefore, seen from figures 3.7, 8 and 3.10 (3.6 and 3.9) that for the cases Λ = 0.2 m, AK = 0.3 , 0.4 and Λ = 0.1 m, AK = 0.3 (Λ = 0.2, AK = 0.43 and Λ = 0.1, AK = 0.4) the effects of gravity are qualitatively unimportant (important) on the propagation behaviour of waves CG. Thus, the effects of gravity are generally unimportant for propagations on gravity waves with "large" wavelengths and "small" steepnesses. This is further remarked on in chapter 4 where the case of pure capillary waves is considered.

3.5 The Doppler Shifted Waves

In general, the Doppler shifted waves are those waves which occur from the Doppler shifting of stationary waves. Such waves occur when the total frequency ω of the waves is non-zero so that these waves are non-stationary waves. Also, as ω is non-zero capillary units are used. Dimensionless equations are formally derived using expressions (2.9.2) which give

$$\sigma = |\omega|\ \sigma_1\ , \quad k = \left[\frac{\omega^2}{s}\right]^{\frac{1}{3}} k_1\ , \quad a = \left[\frac{s}{\omega^2}\right]^{\frac{1}{3}} a_1 \qquad (3.5.1)$$

$$U = (s|\omega|)^{\frac{1}{3}}\ U_1\ , \quad g = (s\omega^4)^{\frac{1}{3}}\ g_1\ , \quad C_g = (s|\omega|)^{\frac{1}{3}}\ C_{g1} \qquad (3.5.2)$$

but are most easily given by substituting $\rho = \tau = \omega^2 = 1$ and adding a subscript 1 to all other parameters, including ω, present in the general equations of § 3.3.

a The Wave-Current Interaction Problem

The interaction problem is examined first. The parameters for the problem are given by

$$\omega_1 = \frac{\omega}{|\omega|} = \pm 1 \quad \text{and} \quad b_1 = \left[\frac{\omega^2}{s}\right]^{\frac{1}{3}} \frac{1}{\tau}\ b \qquad (3.5.3)$$

which are the dimensionless values of ω and b. Note that $\omega_1 = +1$ and $\omega_1 = -1$ corresponds to $\omega > 0$ and $\omega < 0$ respectively. It is seen that the four parameter space of τ, s, ω and b is reduced to the three parameter space of ω_1, g_1 (or ρ, τ and $|\omega|$) and b_1. As already mentioned the magnitude of b_1 is unimportant for a linear waves analysis so that $b_1 = \pm 1$ is taken with the appropriate sign chosen from table 3.1.

Results are shown in figures 3.11, 12 for water where $|\omega| = 5$, 100 rad s^{-1} respectively. These give $g_1 = 27.30$ and 0.5030 respectively. The solution curves in the (U_1, k_1)-plane either have one or three vertical tangents confirming the possible existence of the three CG+/GC+, CG-/GC- and GC+/G+ caustics: all three caustics exist when ω is small, i.e. g_1 large, (figures 3.11) but only the CG-/GC- caustic exists for ω is large, i.e. g_1 small, (figures 3.12). This is readily seen from figures 3.2 - 3.4. As ω is increased from zero the CG+/GC+ and GC+/G+ caustics come into existence but as ω is further increased the values of U at which these caustics exist grow closer and closer and at some unique ω these two caustics coalesce and cease to exist. This explains

the transition from figure 3.11 to figure 3.12. As the two waves which coalesce at the caustic approach the caustic their amplitudes become singular. This is shown in the (U_1,ak) plots.

For pure capillary (gravity) waves where $g \longrightarrow 0$ ($\tau \longrightarrow 0$) the G+ and GC+ (CG(+,-)) waves cease to exist so that only one caustic exists.

b The Wave Propagation Problem

The propagation problem is now considered so $U = U(X)$ and g is replaced by $g^*(X)$. The parameter space must now include ρ, τ, Λ, AK and $|\omega|$, as well as ω_1 and b_1, since these are needed to define the gravity waves and transform X_o, $U_o(X_o)$ and g_o^* from gravity units to capillary units.

Results are shown in figures 3.13 - 3.15. These figures show the variation of either wavenumber k_1 or steepness ak with distance X_1 along the ω-frame fixed to the gravity waves. These are for gravity waves with wavelength $\Lambda = 0.1$ or 0.2 m and steepness AK = 0.4 and are typical of a strong interaction with steep gravity waves (AK is approximately 91 % of the maximum gravity wave steepness AK_{max}).

The cases with $\Lambda = 0.1$ m, $|\omega| = 8$ rad s^{-1} (figures 3.13) and $\Lambda = 0.2$ m, $|\omega| = 5$ rad s^{-1} (figures 3.14), which lie within the lower ranges of ω in table 3.2, illustrate the existence of either all three caustics or just the two GC+/G+ and CG-/GC- caustics respectively. All six waves are present at such low values of $|\omega|$ (figures 3.13, 14). Note that when $|\omega| = 8$ rad s^{-1} the scaled gravity $g_1 = 14.59$. The case $\Lambda = 0.2$ m, $|\omega| = 100$ rad s^{-1}, which lies within the higher ranges of ω in table 3.2, illustrates the existence of the CG-/GC- caustic only (figures 3.15). Only four of the six possible waves exist. The waves G+ and GC+ do not exist at such a high value of $|\omega|$.

The behaviour of all six waves is similar to stationary waves CG and GC. In general as $|\omega|$ is increased from zero all six waves exist firstly, then only four waves exist (no G+ and GC+ waves) and finally only two waves exist (no G- and CG- waves). Also, in general there may be either three, two (CG-/GC- and GC+/G+) or one caustic (CG-/GC-) only (see figures 3.13 - 3.15). When caustics exist they are again symmetrically situated about the crests of the gravity waves. It is known that waves CG(+,-) and G+ propagate in the + X direction and waves GC(+,-) and G- propagate in the - X direction. So, viewing the propagation from the observers frame, if the appropriate caustic exist then the appropriate waves encounter caustic type behaviour as they attempt to propagate over the gravity waves or if the appropriate caustic does not exist then the appropriate waves either overtake or are

overtaken by the gravity waves depending on the direction of traverse of the waves under consideration. This is similar to the stationary waves case.

Steepness AK	Wavelength Λ m	Approximate ranges of ω rad s^{-1} for which there exists a caustic lower rangs	higher ranges
0.3	0.20	$4.56 \leq \omega \leq 4.92$	$-685.89 \leq \omega \leq -70.75$
0.4	0.20	$4.39 \leq \omega \leq 7.20$	$-797.01 \leq \omega \leq -3.86$
0.3	0.10	$6.46 \leq \omega \leq 7.20$	$-228.66 \leq \omega \leq -12.17$
0.4	0.10	$0.00 < \omega \leq 10.18$	$-268.38 \leq \omega \leq 0.00$

Table 3.2: Ranges of ω over which caustics exist for linear capillary-gravity wave theory.

For fixed values of ρ, τ, Λ and AK the behaviour of the wave field as $|\omega|$ is varied is also investigated. The results are summarised in table 3.2. The table gives two ranges of ω over which caustics exist. However, there are a total of three possible caustics. This is resolved by examination of the stationary waves case. For the first three cases considered in table 3.2 there is no CG/GC caustic for the stationary waves case (§ 3.4). Thus, as ω is increased from zero the CG+/GC+ caustic will not exist for these cases. This is seen more clearer by examination of figure 3.2. Hence, for these cases the lower ranges of ω correspond to the GC+/G+ caustic only. Propagation plots for these lower ranges of ω are all qualitatively similar to figures 3.14. For all four cases the higher ranges of ω correspond to the CG-/GC- caustic. The propagation plots for these higher ranges are all qualitatively similar to figures 3.15.

For the fourth case the CG/GC caustic for the stationary waves case (§ 3.4) does exist. Thus, the lower ranges of ω correspond to both the CG+/GC+ and GC+/G+ caustics: the CG+/GC+ caustic exists throughout the lower range of ω whereas the GC+/G+ caustic exists for 6.21 rad $s^{-1} \leq \omega \leq$ 10.18 rad s^{-1}. As the value of ω is increased from zero the GC+/G+ caustic comes into existence at ω = 6.21 rad s^{-1}. Then as ω is further increased both caustics coalesce and cease to exist at the same value of $\omega \approx$ 10.19 rad s^{-1} and only the CG-/GC- caustic exists. This behaviour is as expected from the interaction problem

results. However, note that the value of ω at which the caustics coalesce will vary for different gravity waves, i.e. it is not unique. This is caused by gravity g being replaced by effective gravity g*: gravity is no longer constant and quantitative results of the interaction problem vary for different values of g in equation (3.3.2). The propagation plots for $6.21 \leq \omega \leq 10.18$ are qualitatively similar to figures 3.13. A typical example of propagation results for $0 \leq \omega \leq 6.21$ is not shown.

The general properties for any case, i.e. any AK and A, are similar to either the first three cases or the fourth case of table 3.2 depending on whether or not a CG/GC caustic exists for the corresponding stationary waves case.

For the case of pure capillary waves the waves GC+, G+ and the GC+/G+ caustic do not exist. Only waves CG(+,-), GC-, G- and the CG-/GC- caustic exist. This is, in fact, the case for all the higher ranges of ω in table 3.2 except for A = 0.1 m, AK = 0.4 where both caustics and all the waves exist for the lower ranges of ω in table 3.2. It is, therefore, seen from table 3.2 that for $|\omega| > 11$ rad s^{-1} all the propagation behaviour will be qualitatively the same as that of pure capillary waves for all four gravity waves considered. Moreover, for 71 rad $s^{-1} \leq |\omega| \leq 268$ rad s^{-1} the CG-/GC- caustic will be the only one existing for all four gravity waves considered so that the qualitative effects of gravity are negligible and all propagation figures are qualitatively the same as that in figure 3.15. Thus, the value $|\omega| = 100$ rad s^{-1} is typical for considering the qualitative characteristics of pure capillary waves and their CG-/GC- caustic.

Hogan (1980) investigates the properties of steep waves affected by both gravity and surface tension. He classifies waves according to values of the dimensionless parameter $\kappa = \tau k^2/\rho g$ and shows that $\kappa = 0.000075$ and 0.0075 represent gravity waves. Now, a wave of length 20 cm corresponds to $\kappa = 0.0075$. For this case Hogan shows that the maximum possible wave steepness AK is 0.3545. He points out that his criterion for maximum wave steepness, although only technical, does "have some relevance". If this is the case then the consideration of a gravity wave of length 20 cm and steepness 0.4 may be unrealistic. Nevertheless, such a wave is worth examining for a qualitative understanding of flow properties.

3.6 Near-Linear Caustics

The results of § 3.5 show that for a wide range of cases (table 3.2) linear caustics exist. Also caustics exist for some stationary wave cases discussed in § 3.4. The nature of the waves in the neighbourhood of the linear caustic is investigated here.

The wave field and linear caustics are steady and the X coordinate of the ω-frame fixed to the gravity waves is perpendicular to the caustic. The higher ranges of frequency ω in table 3.2 are the only ones considered since our interest lies in capillary dominated waves. Attention is, thus, focused on the CG-/GC- caustic. The results of Peregrine and Smith (1979), given in § 2.8, are used.

Wilton (1915) shows

$$\frac{\sigma^2}{k} - (g + sk^2) = \left[\frac{2s^2k^4 + sgk^2 + 8g^2}{8(g - 2sk^2)}\right] \alpha_1^2 + O(\alpha_1^4) \ . \qquad (3.6.1)$$

is the near-linear dispersion relation for plane-waves on still liquid. He is unclear about the specific nature of the constant α_1 (he says that α_1 is arbitrary and negative). In fact, by following a perturbation method similar to Isobe and Kraus (1983) and comparing with Wilton (1915), it is easily shown that α_1 can be taken as - ak.

For the propagation problem gravity g is replaced by effective gravity g^* so that, to order a^2, the near-linear dispersion relation is

$$\sigma^2 - (g^*k + sk^3) - \left[\frac{2s^2k^4 + sg^*k^2 + 8g^{*2}}{8(g^* - 2sk^2)}\right] k^3 a^2 = 0 \ . \qquad (3.6.2)$$

Thus
$$G = \sigma^2 - (g^*k + sk^3) \qquad (3.6.3)$$

and
$$H = - \left[\frac{2s^2k^4 + sg^*k^2 + 8g^{*2}}{8(g^* - 2sk^2)}\right] k^3 \ . \qquad (3.6.4)$$

Thus, since $g^* > 0$ and $2s^2k^4 + sg^*k^2 + 8g^{*2} > 0$, it follows that

$$\operatorname{sgn}\left[H \Big/ \left[U^2 \frac{\partial^2 G}{\partial \sigma^2} - 2U \frac{\partial^2 G}{\partial \sigma \partial k} + \frac{\partial^2 G}{\partial k^2}\right]\right] =$$

$$\operatorname{sgn}\ (g^* - 2sk^2)(3sk - U^2) \ . \qquad (3.6.5)$$

For all of the higher ranges of ω in table 3.2 equation (3.6.5) implies the existence of S-type near-linear caustics suggesting that the caustic represents a breaking type of singularity. Also for the case of pure capillary waves where $g = g^* = 0$ equation (3.6.5) implies that the existence of S-type near-linear caustics in the neighbourhood of the

CG-/GC- caustic.

The two factors in (3.6.5) cause two changes of sign relative to the gravity wave case of Peregrine and Smith (1979) and Peregrine and Thomas (1979). One, at $g^* = 2sk^2$, gives the wavenumber where the primary wave resonates with its second harmonic (Kinsman § 13.5). Our slowly-varying theory is inapplicable for such resonant interactions simply because only one wavetrain is present here (more than one wavetrain is required for resonance). No interpretation of the other change of sign, at $U^2 = 3sk$, has been found.

CAPTIONS FOR FIGURES

Figure 3.1: The variation of phase velocity c and group velocity c_g with wavenumber k. Dashed lines represent the limiting cases of pure capillary, i.e. $g \longrightarrow 0$, and pure gravity waves, i.e. $\tau \longrightarrow 0$.

Figure 3.2: The general variation of frequency σ with wavenumber k as given by the Doppler and dispersion relations. Dashed lines represent the limiting cases of pure capillary, i.e. $g \longrightarrow 0$, and pure gravity waves, i.e. $\tau \longrightarrow 0$.

Figure 3.3: Diagram illustrating the possible existence of stationary waves CG and GC.

Figure 3.4: Diagram illustrating the possible existence of Doppler shifted waves CG(+,-), GC(+,-) and G(+,-).

Figure 3.5: The variation of (a) wavenumber k and (b) steepness ak with current U for stationary waves.

Figure 3.6: The variation of (a) wavenumber k and (b) steepness ak with distance X for stationary waves where the gravity wave has A = 0.2 m, AK = 0.43.

Figure 3.7: The variation of (a) wavenumber k and (b) steepness ak with distance X for stationary waves where the gravity wave has A = 0.2 m, AK = 0.4.

Figure 3.8: The variation of (a) wavenumber k and (b) steepness ak with distance X for stationary waves where the gravity wave has A = 0.2 m, AK = 0.3.

Figure 3.9: The variation of (a) wavenumber k and (b) steepness ak with distance X for stationary waves where the gravity wave has A = 0.1 m, AK = 0.4.

Figure 3.10: The variation of (a) wavenumber k and (b) steepness ak with distance X for stationary waves where the gravity wave has A = 0.1 m, AK = 0.3.

Figure 3.11: The variation of (a) wavenumber k_1 and (b) steepness ak with current U_1 for $|\omega| = 5$ rad s^{-1}.

Figure 3.12: The variation of (a) wavenumber k_1 and (b) steepness ak with current U_1 for $|\omega| = 100$ rad s^{-1}.

Figure 3.13: The variation of (a) wavenumber k_1 and (b) steepness ak with distance X_1 for $|\omega| = 8$ rad s^{-1}, A = 0.1 m, AK = 0.4. Magnified figures are given in order to show the behaviour of all waves.

Figure 3.14: The variation of (a) wavenumber k_1 and (b) steepness ak with distance X_1 for $|\omega| = 5$ rad s^{-1}, A = 0.2 m, AK = 0.4. Magnified figures are given in order to show the behaviour of all waves.

Figure 3.15: The variation of (a) wavenumber k_1 and (b) steepness ak with distance X_1 for $|\omega| = 100$ rad s^{-1}, A = 0.2 m, AK = 0.4.

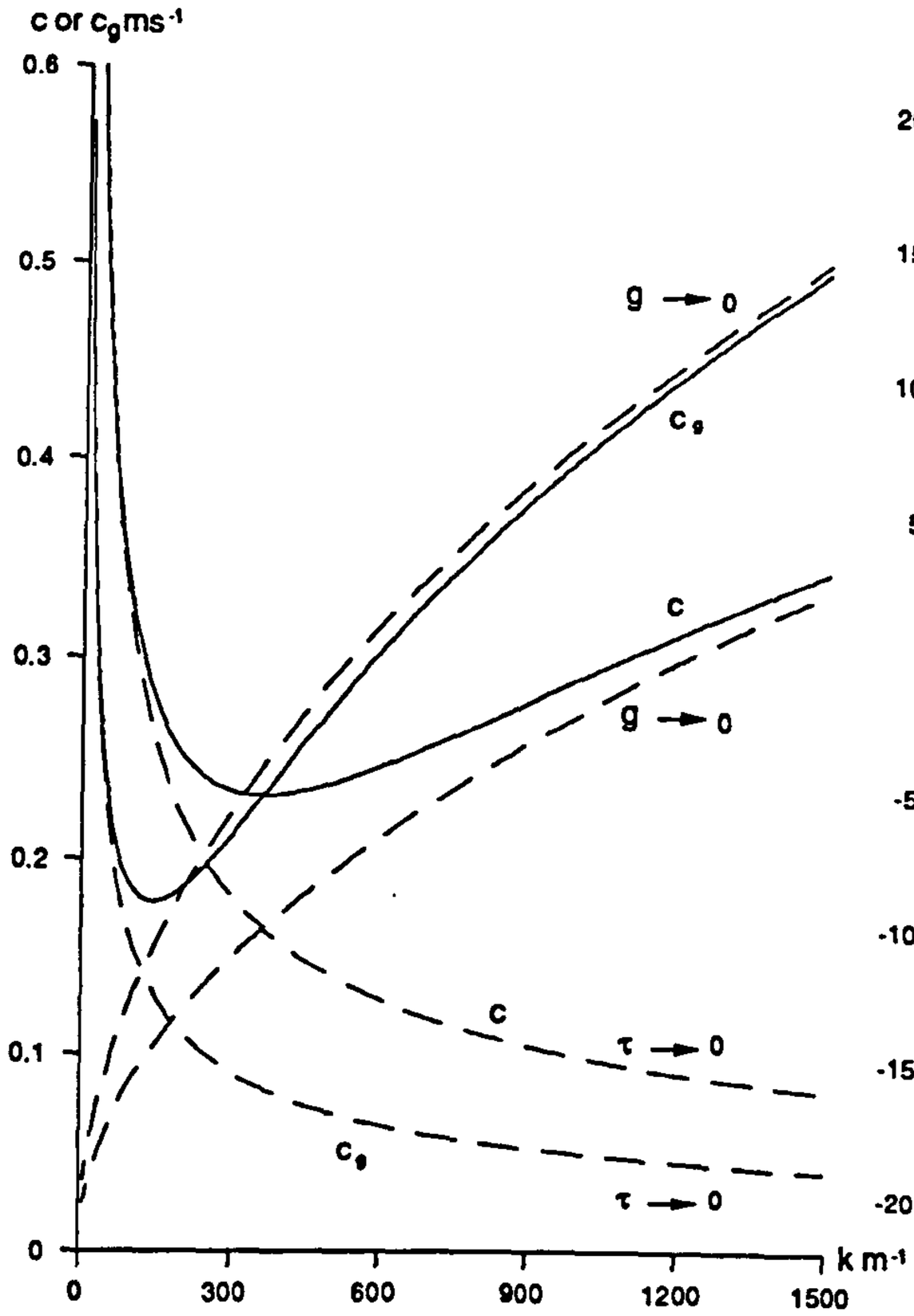

Figure 3.1

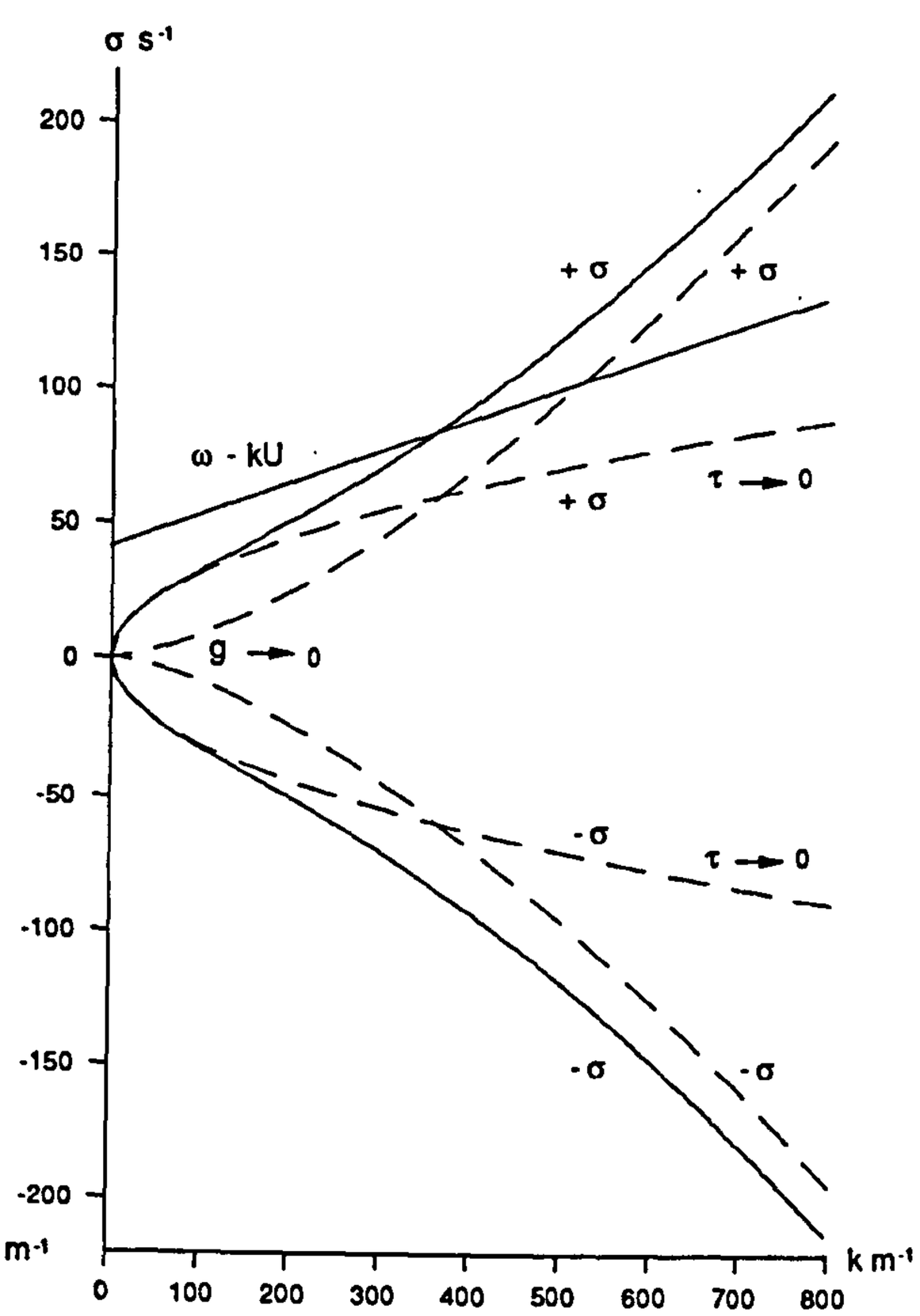

Figure 3.2

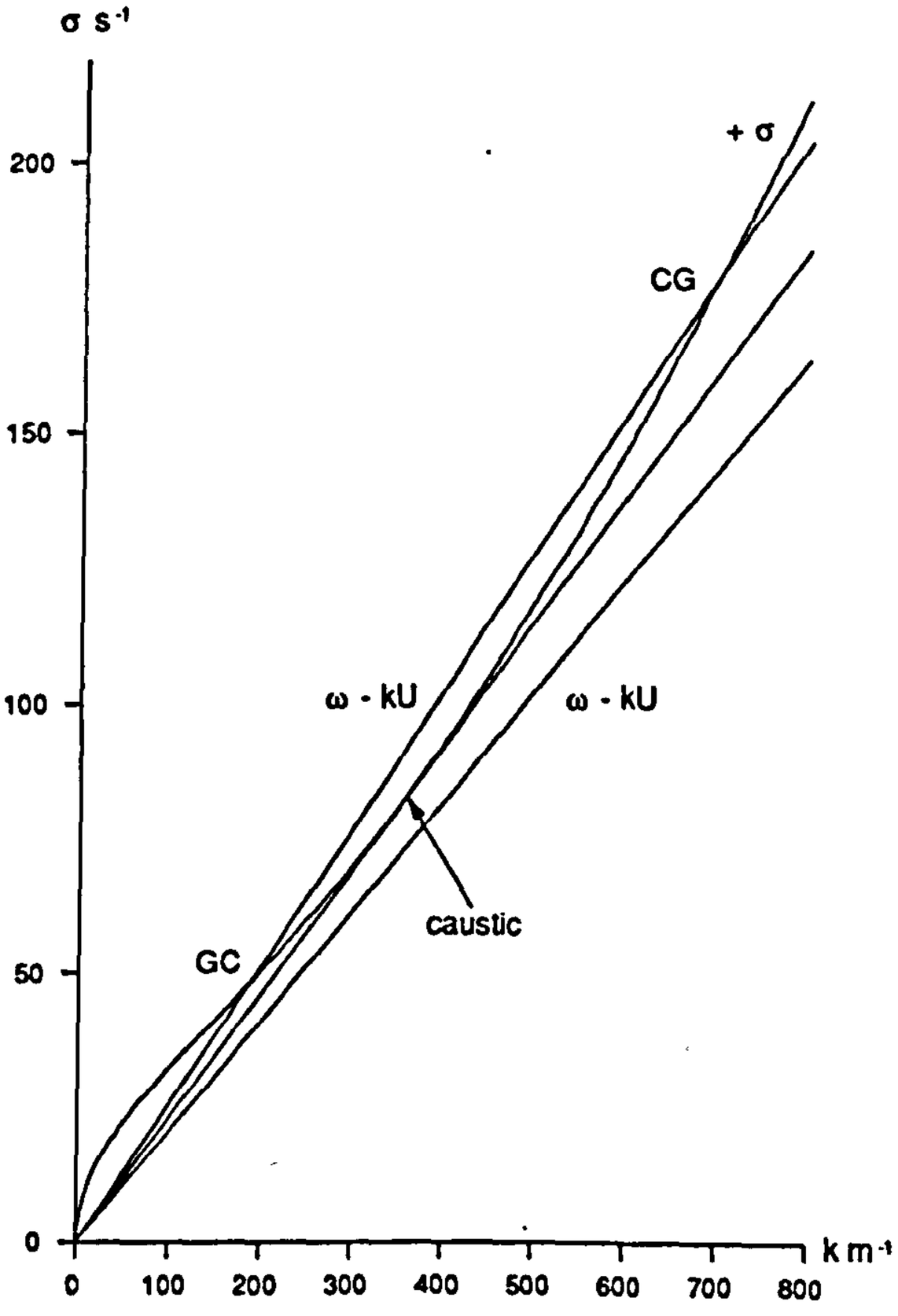

Figure 3.3

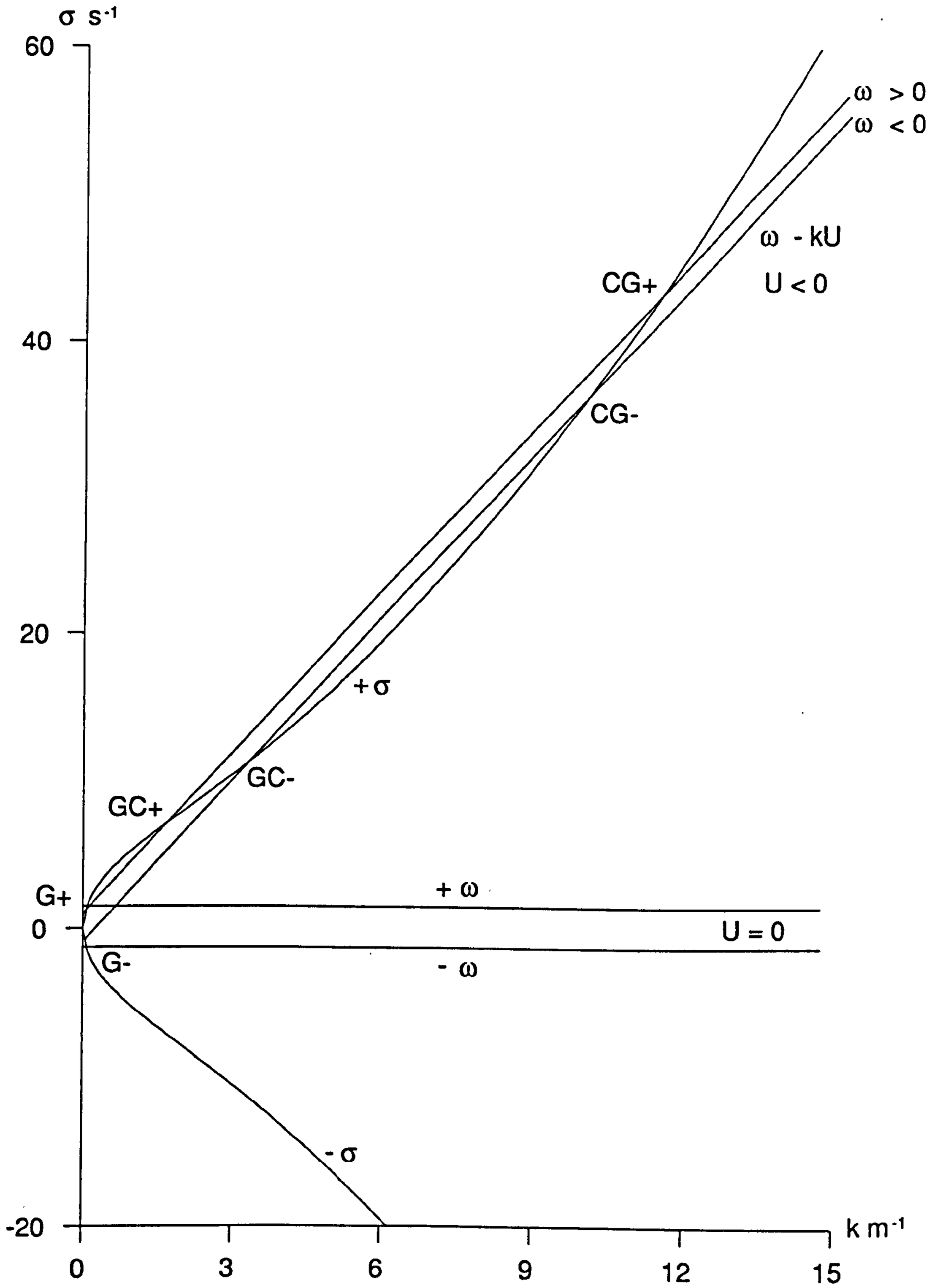

Figure 3.4

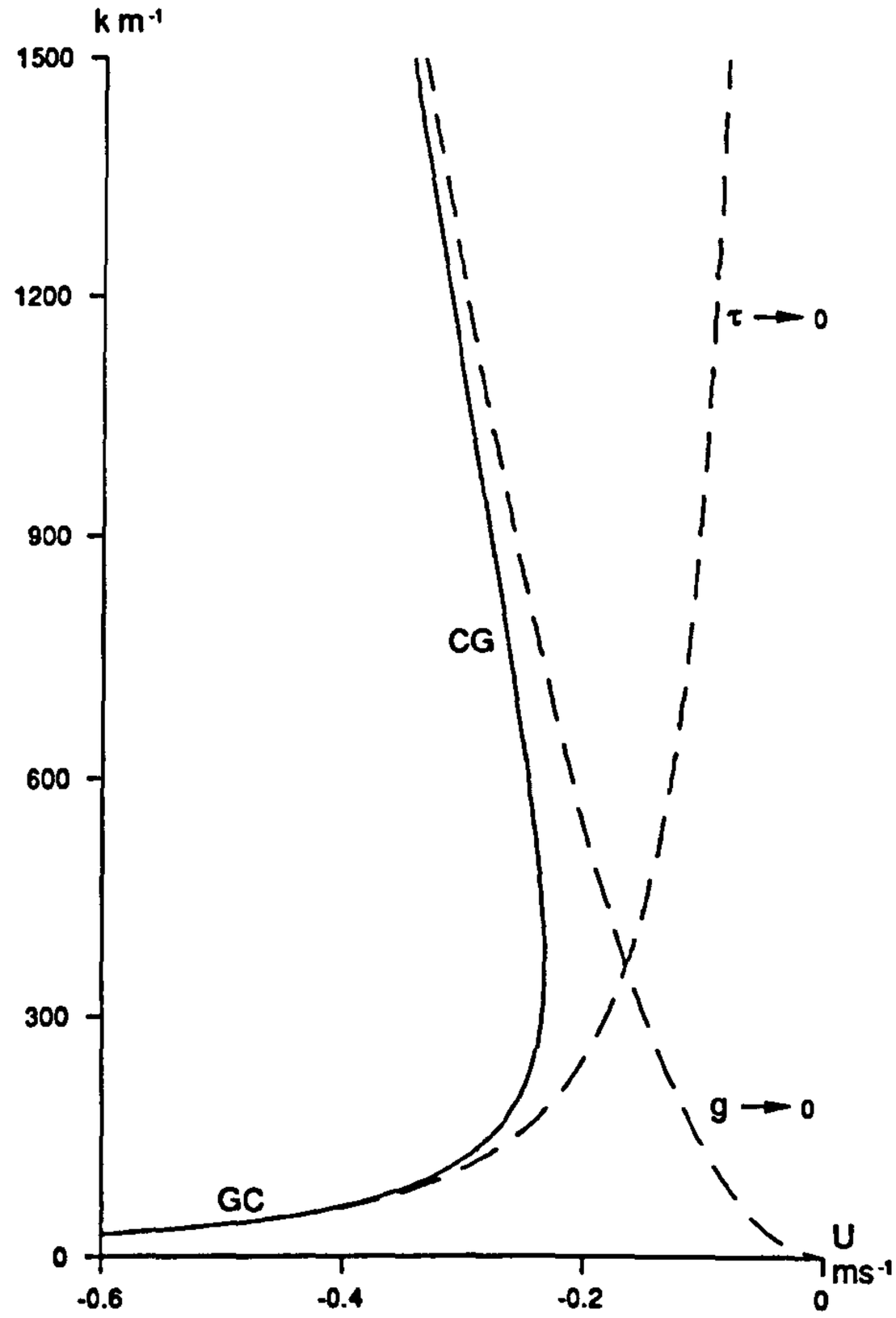

Figure 3.5a

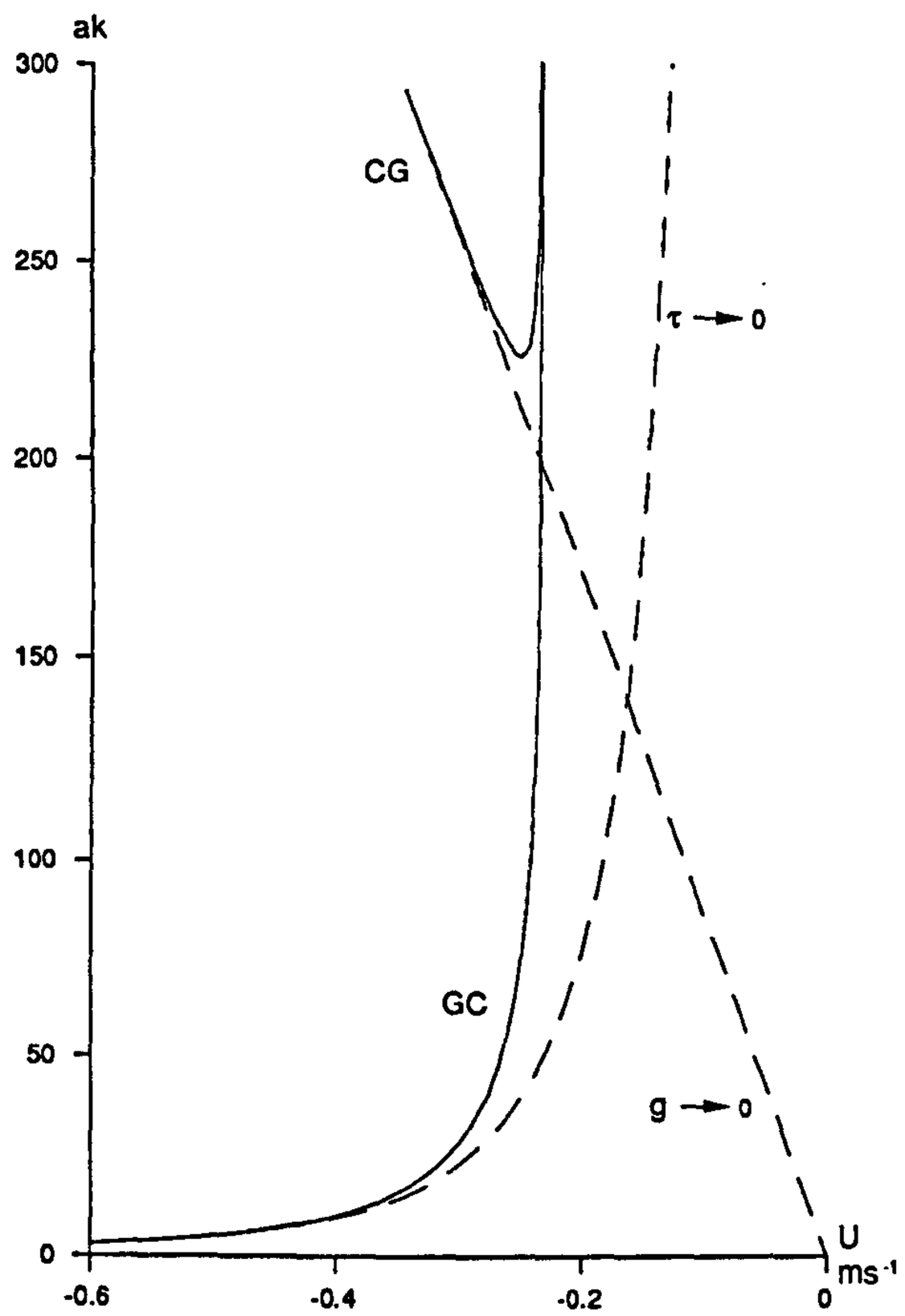

Figure 3.5b

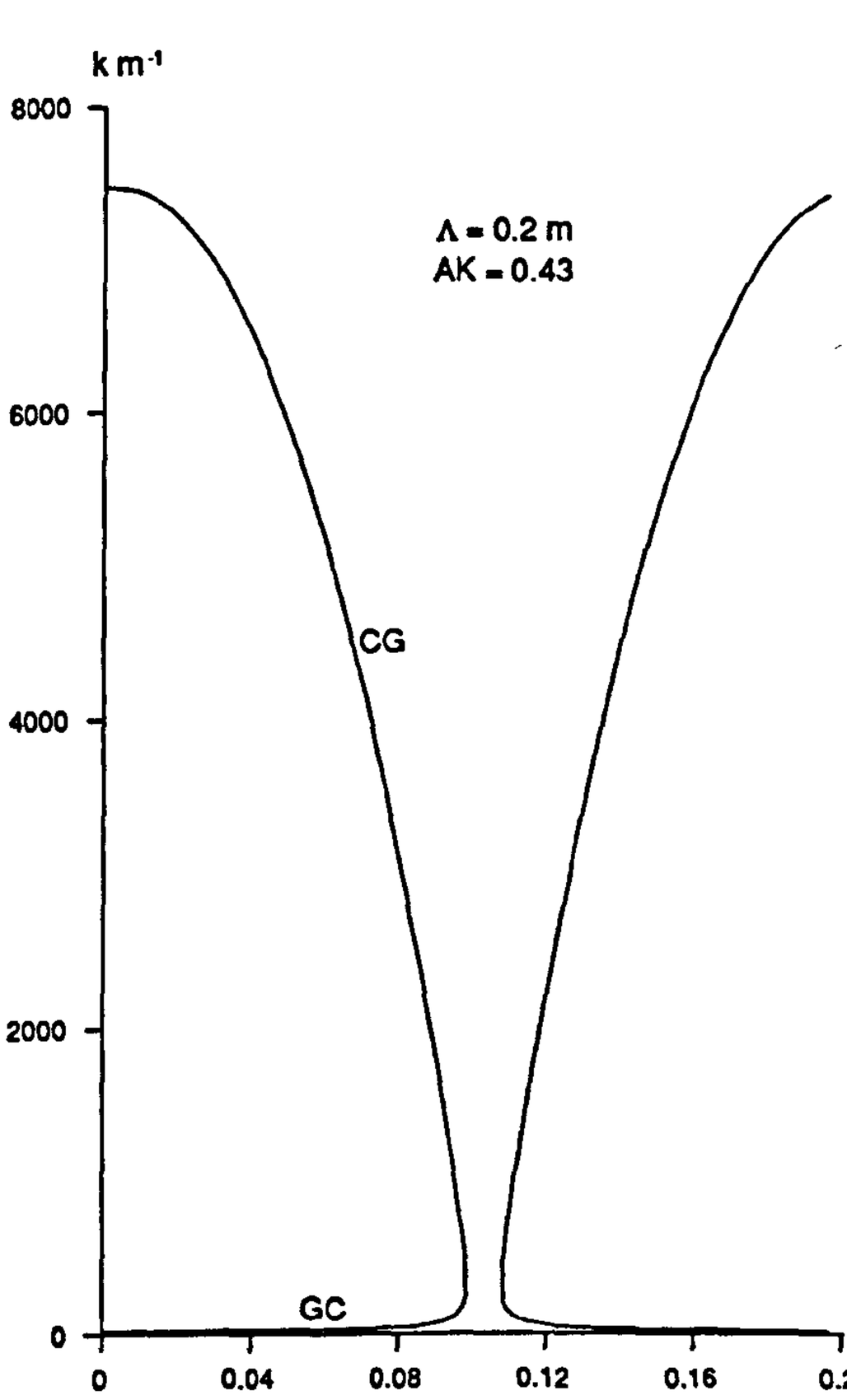

Figure 3.6a

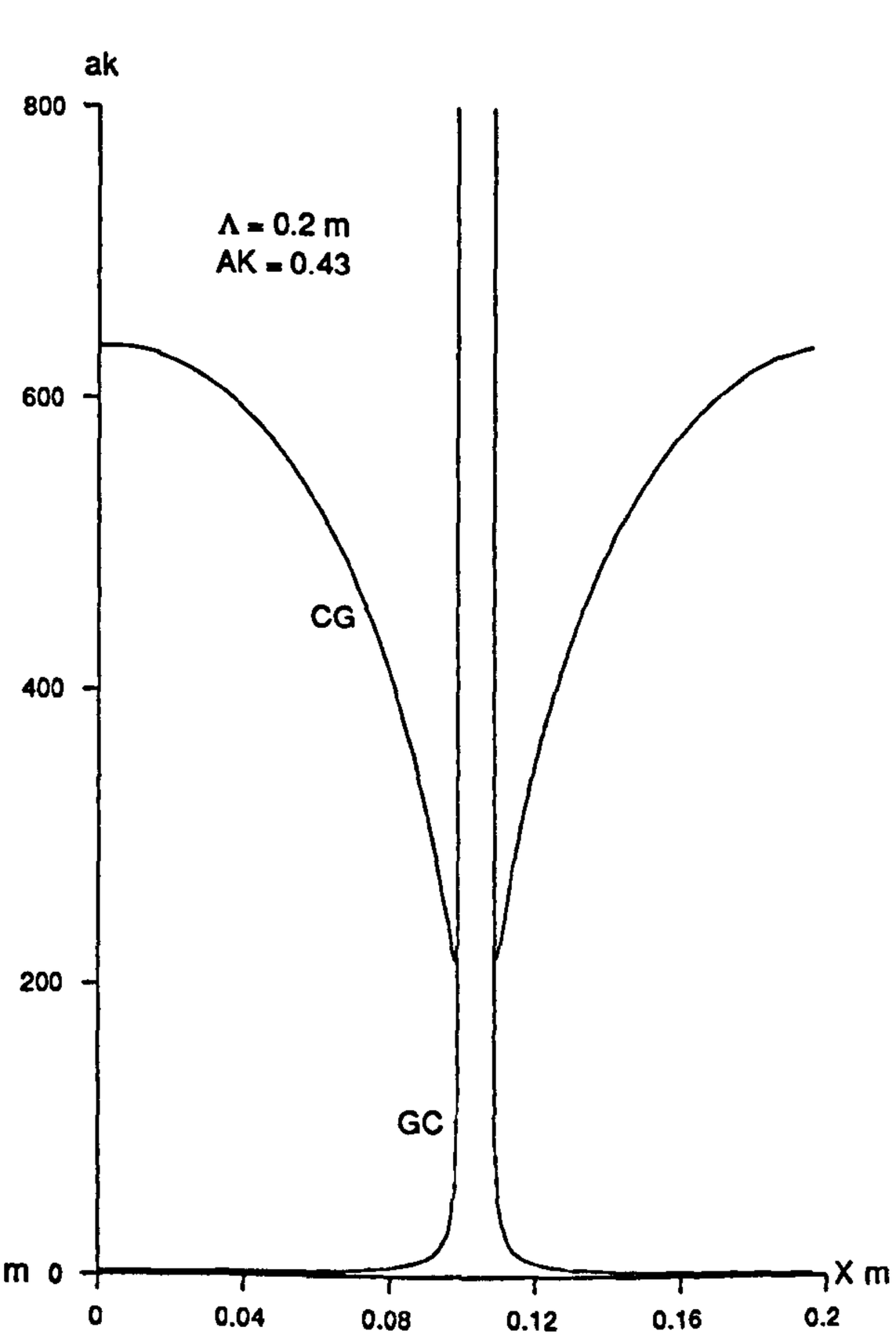

Figure 3.6b

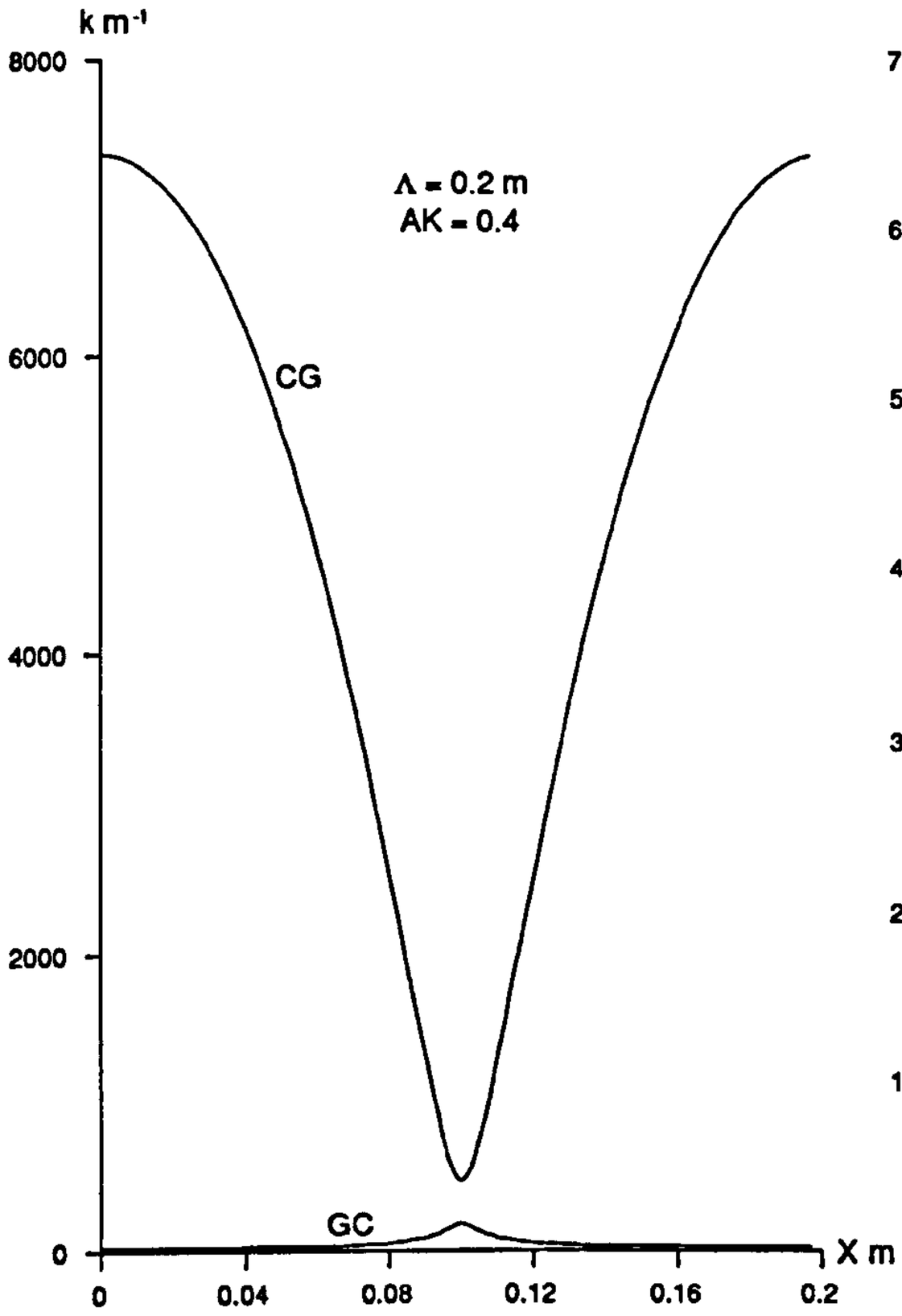

Figure 3.7a

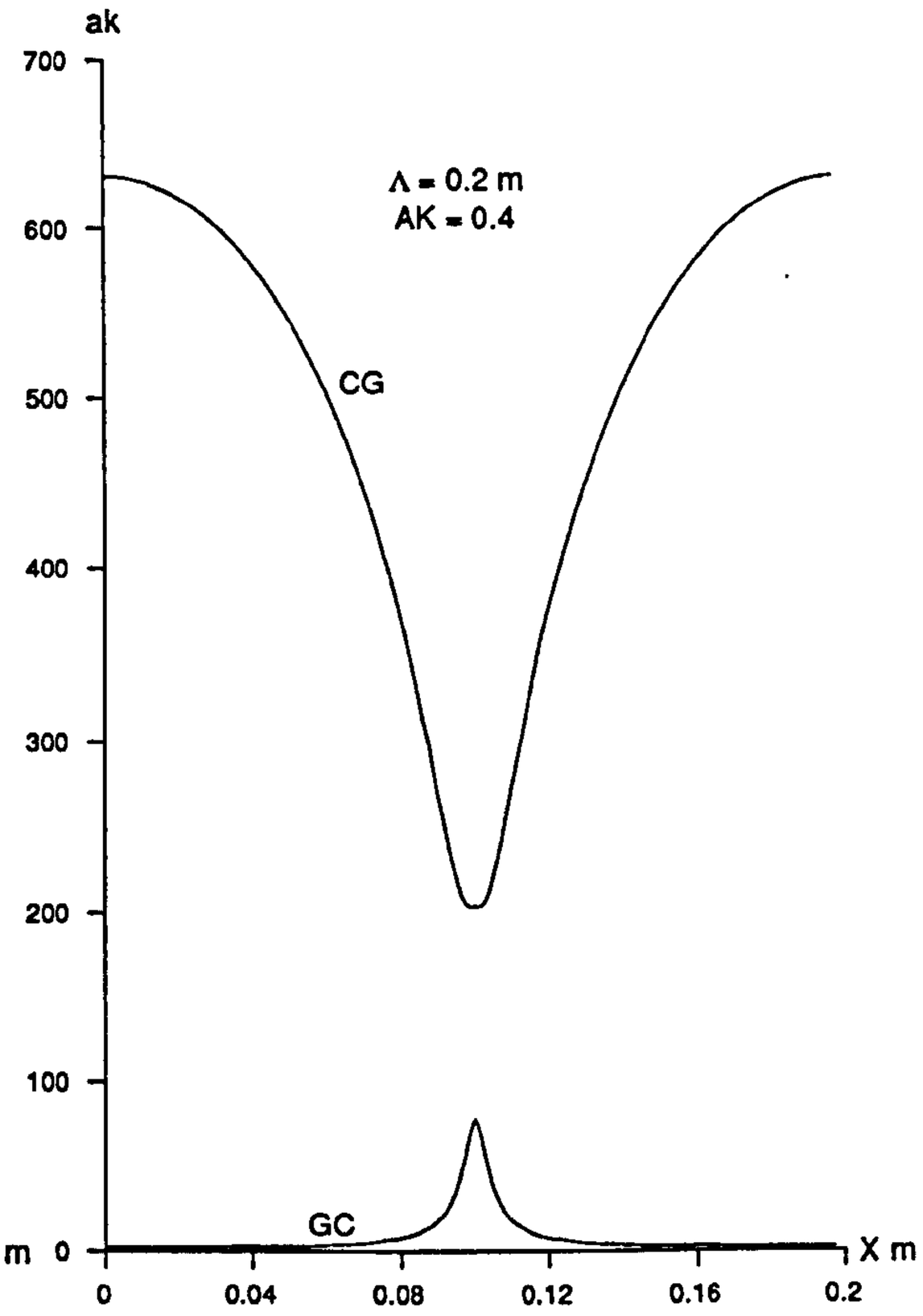

Figure 3.7b

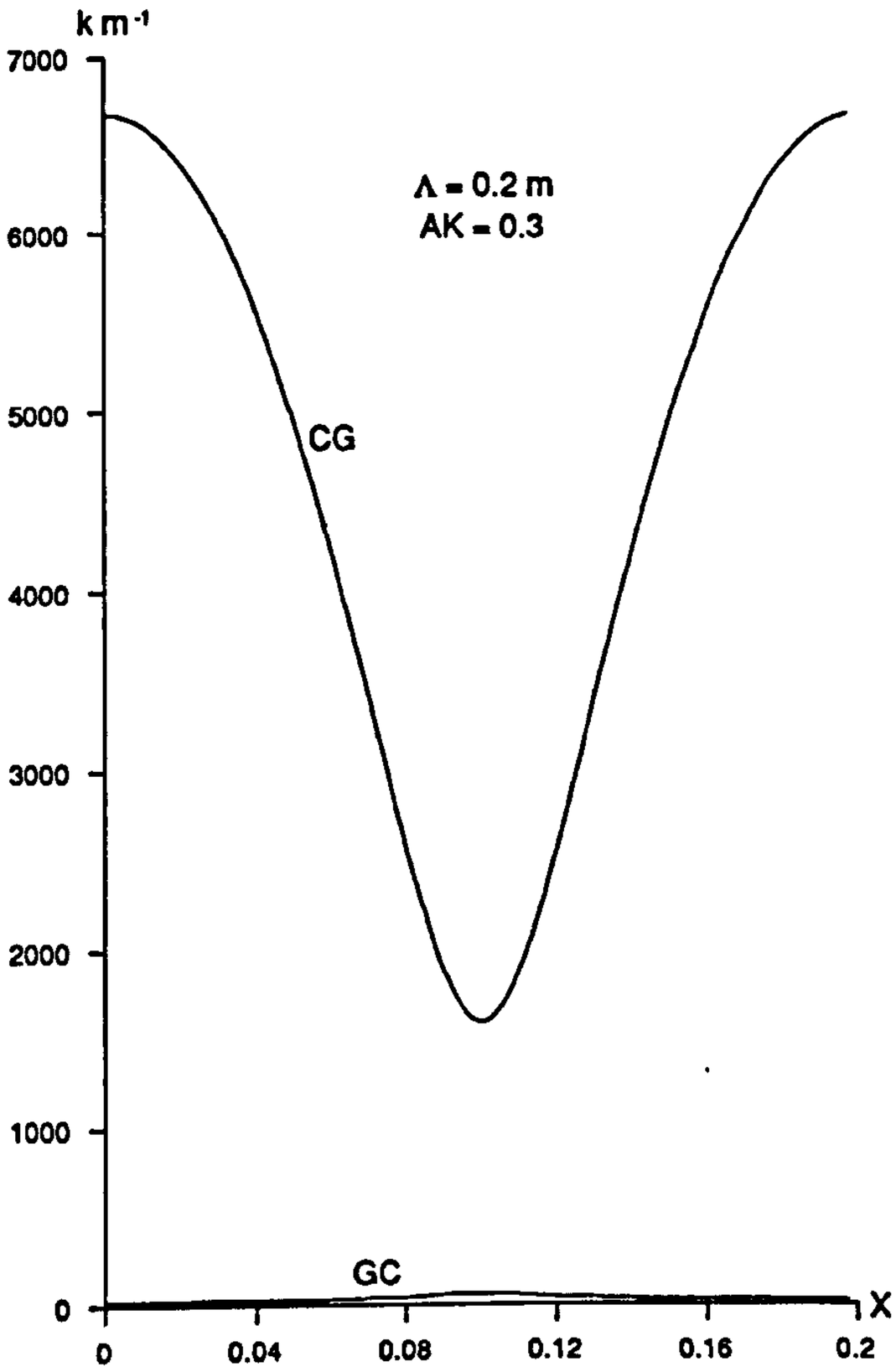

Figure 3.8a

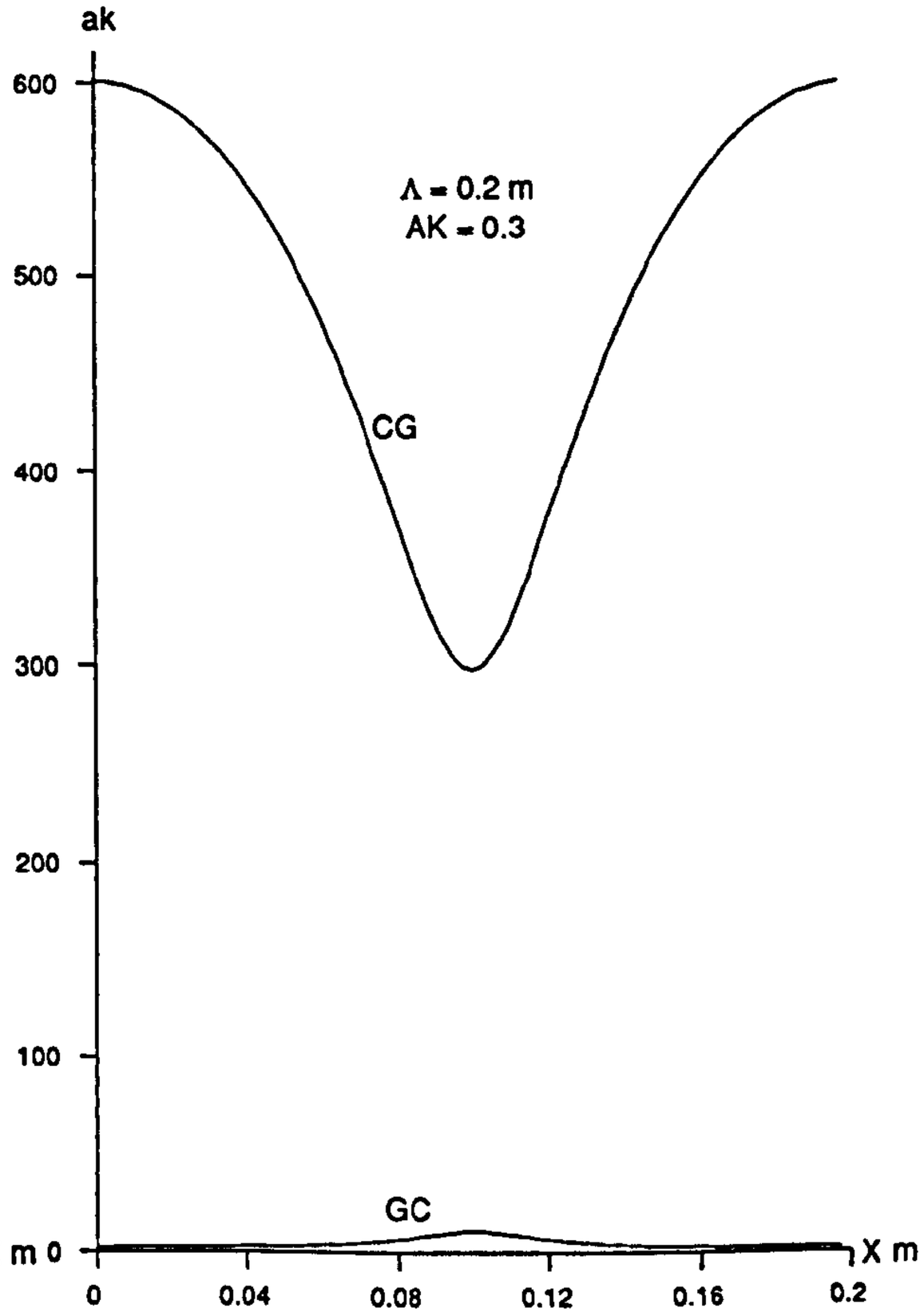

Figure 3.8b

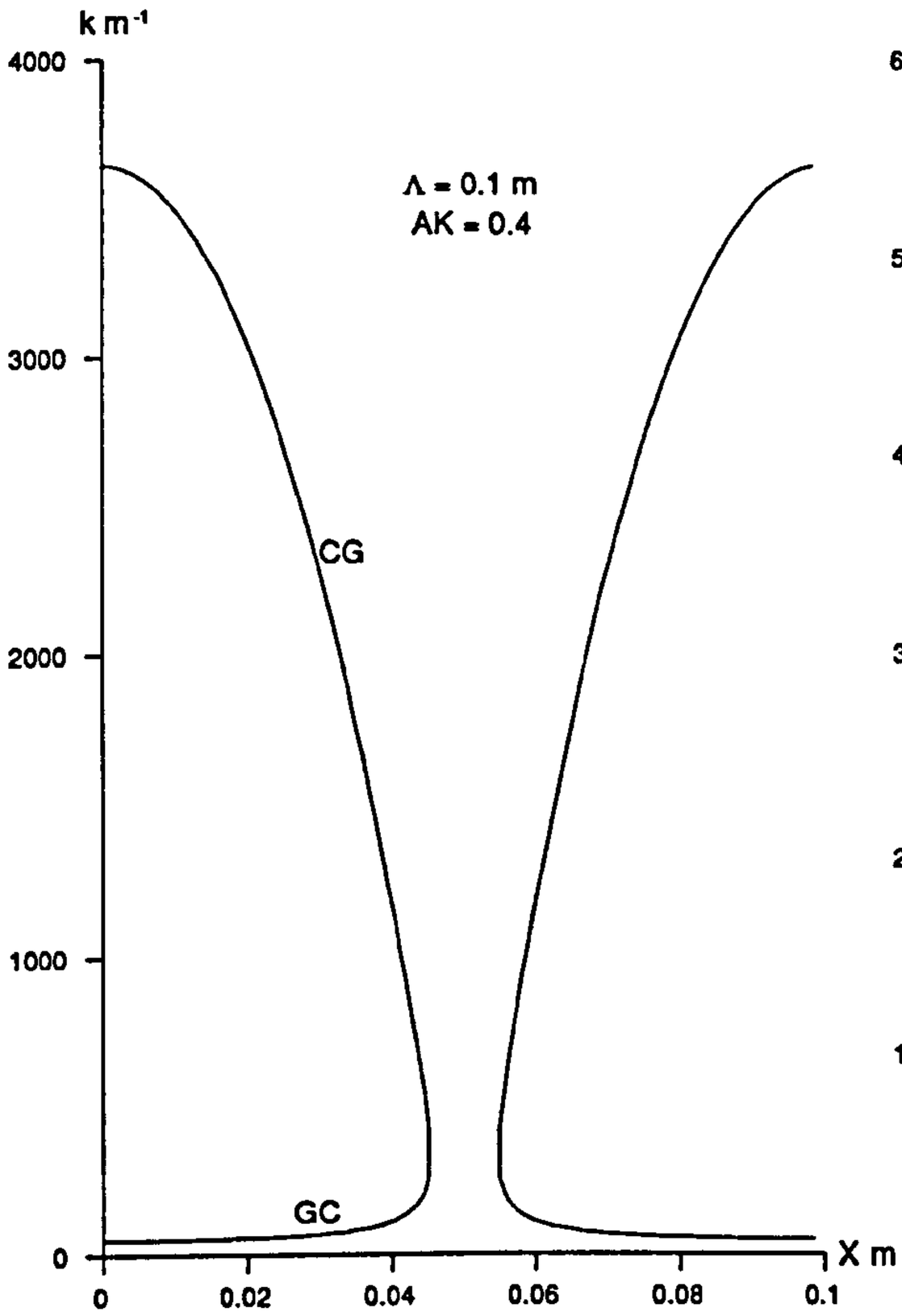

Figure 3.9a

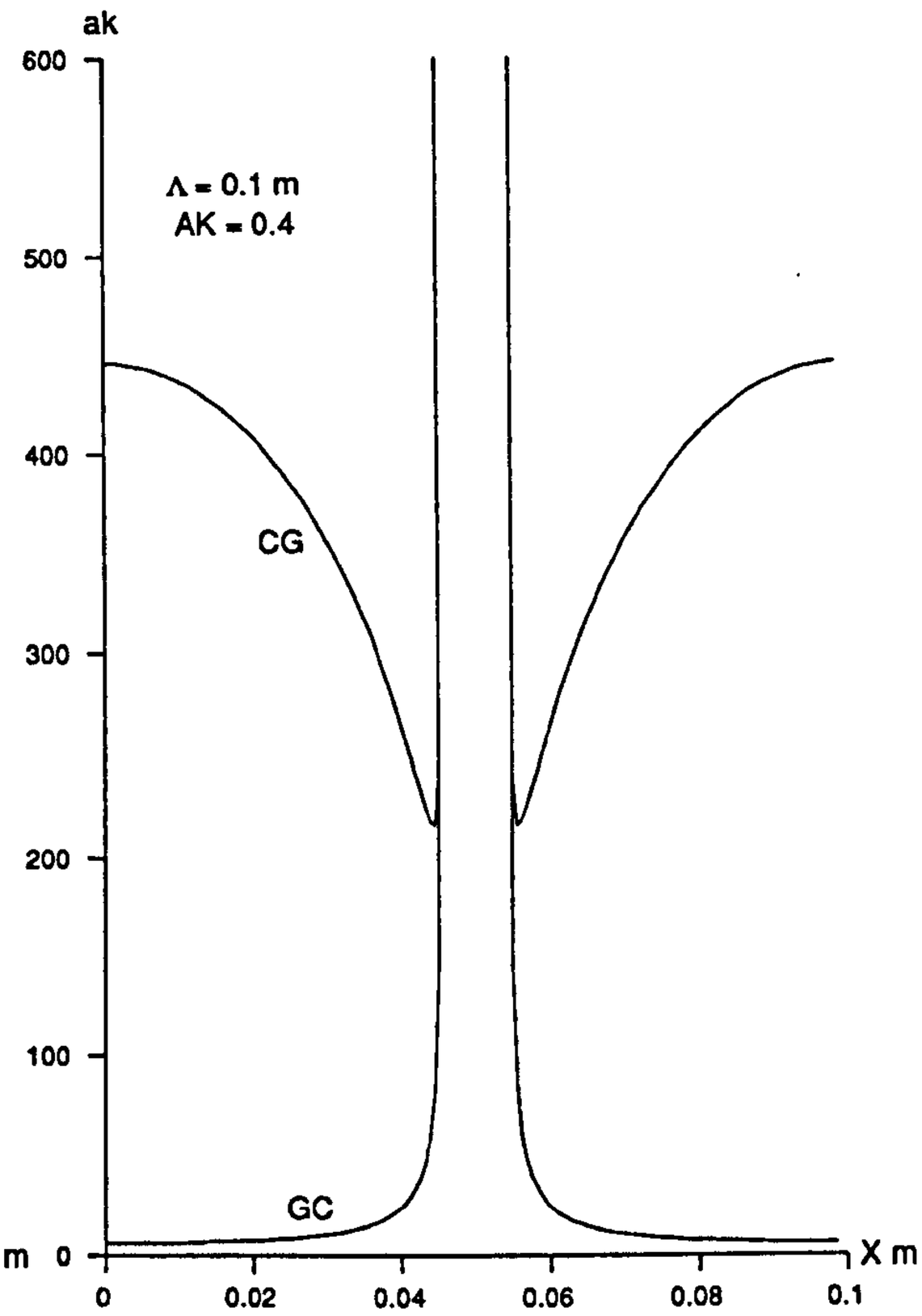

Fiugre 3.9b

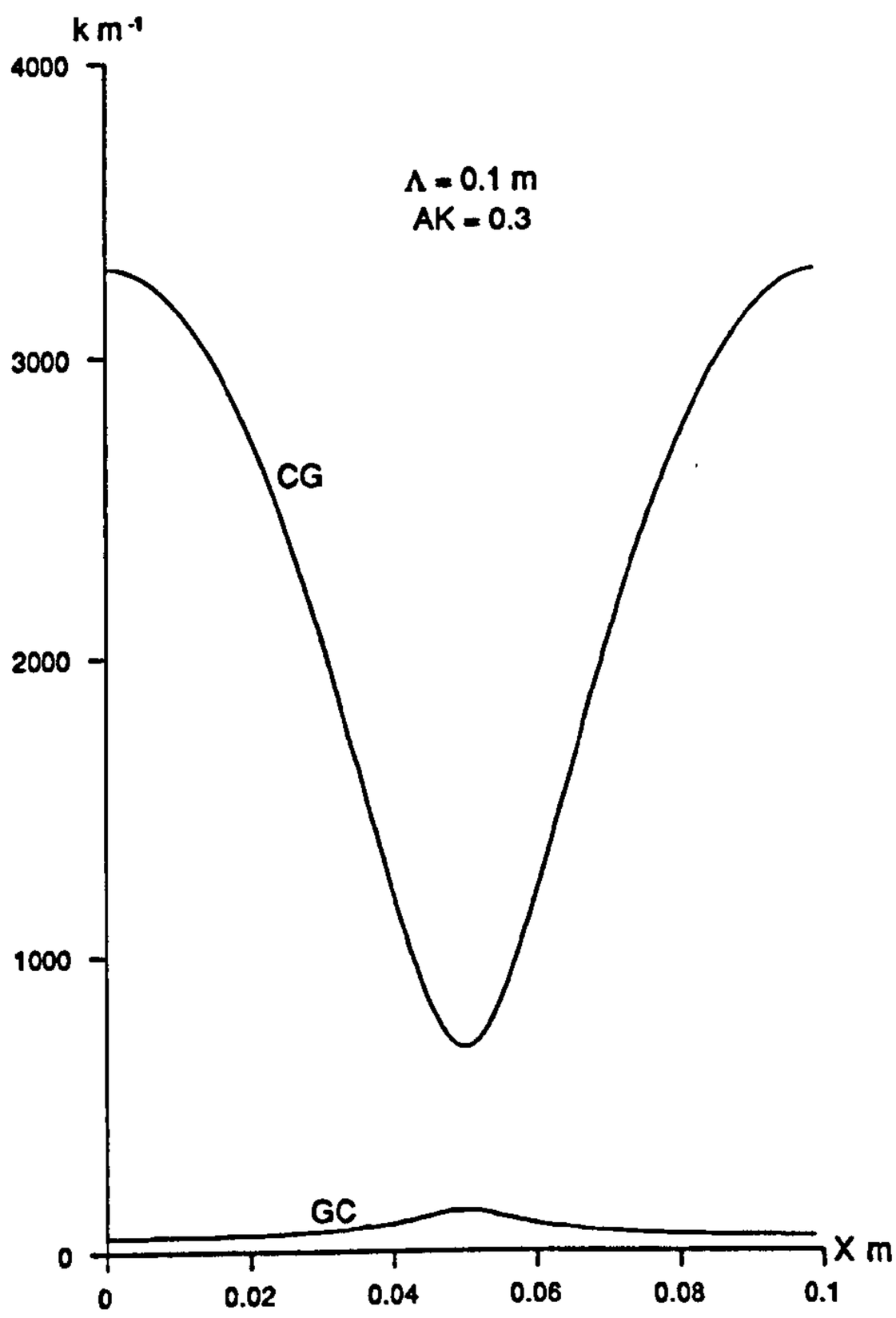

Figure 3.10a

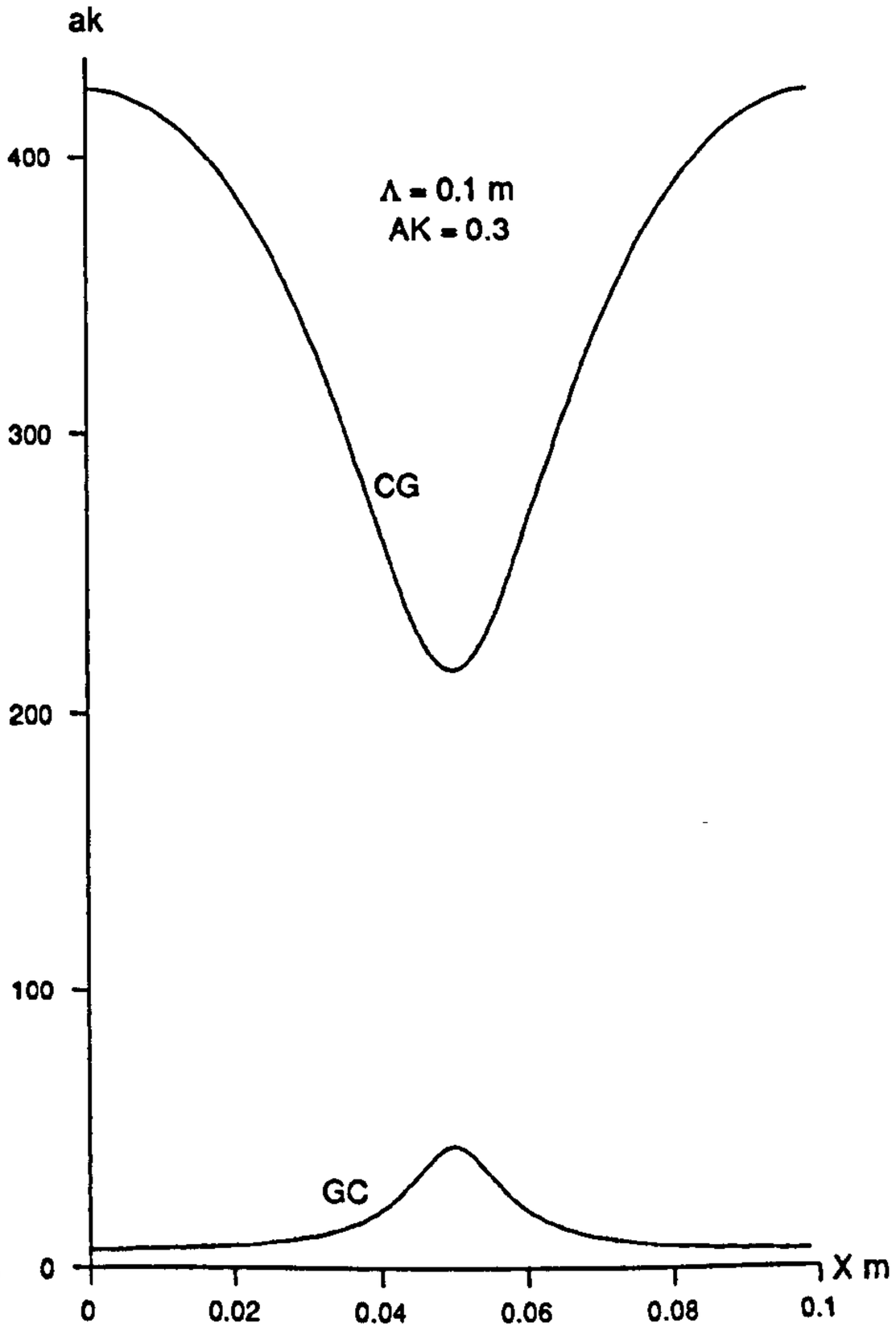

Figure 3.10b

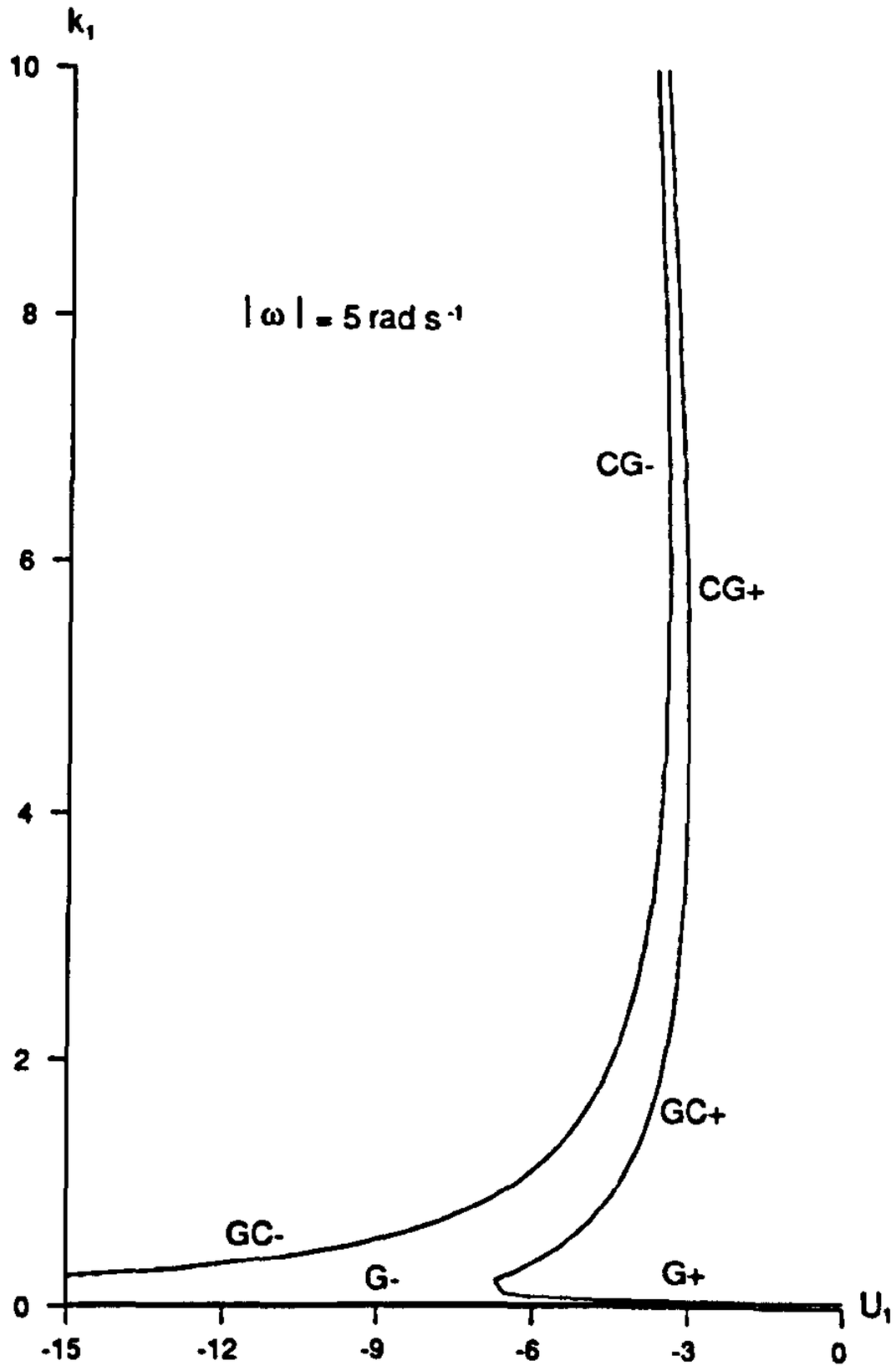

Figure 3.11a

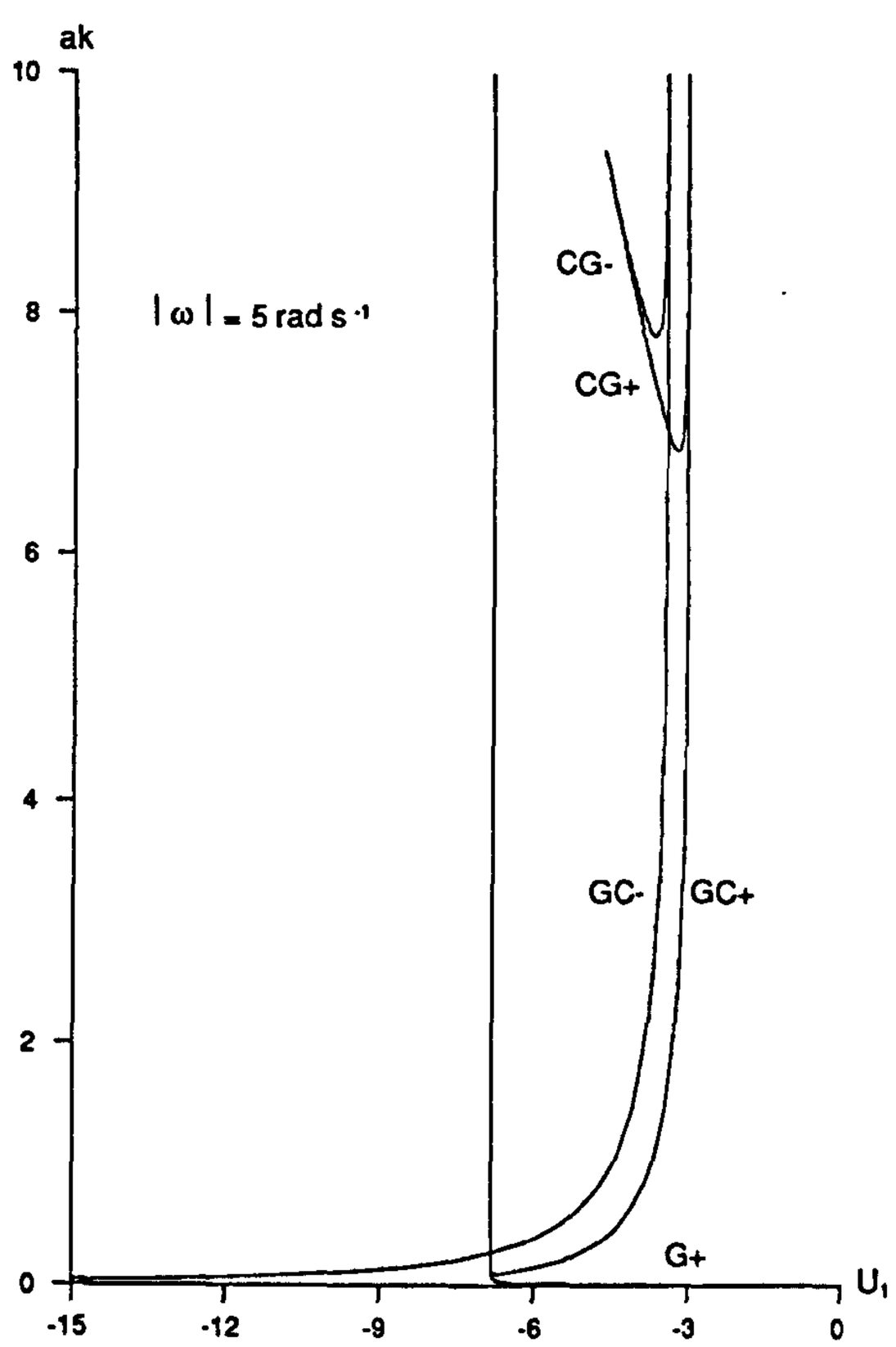

Figure 3.11b

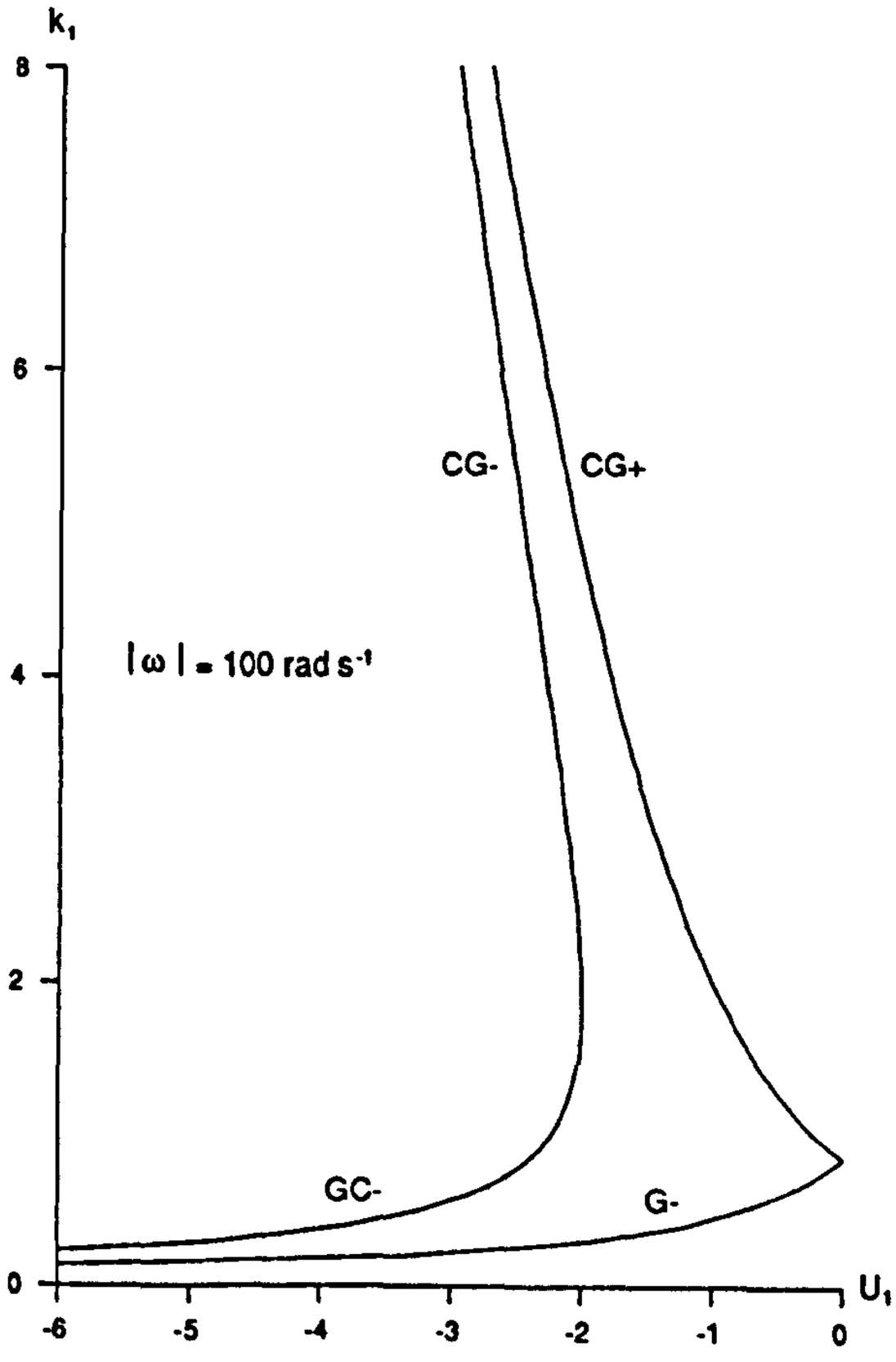

Figure 3.12a

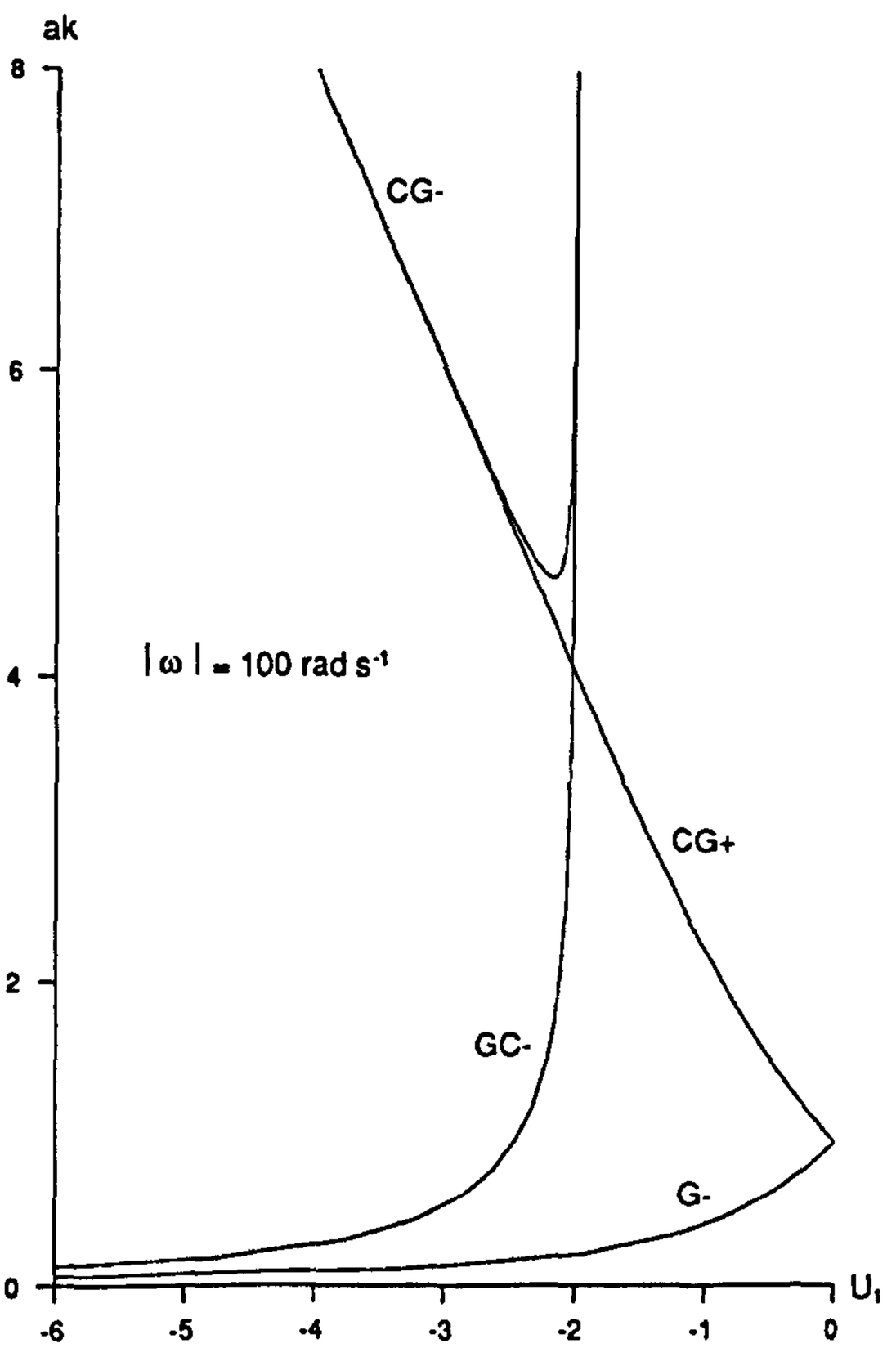

Figure 3.12b

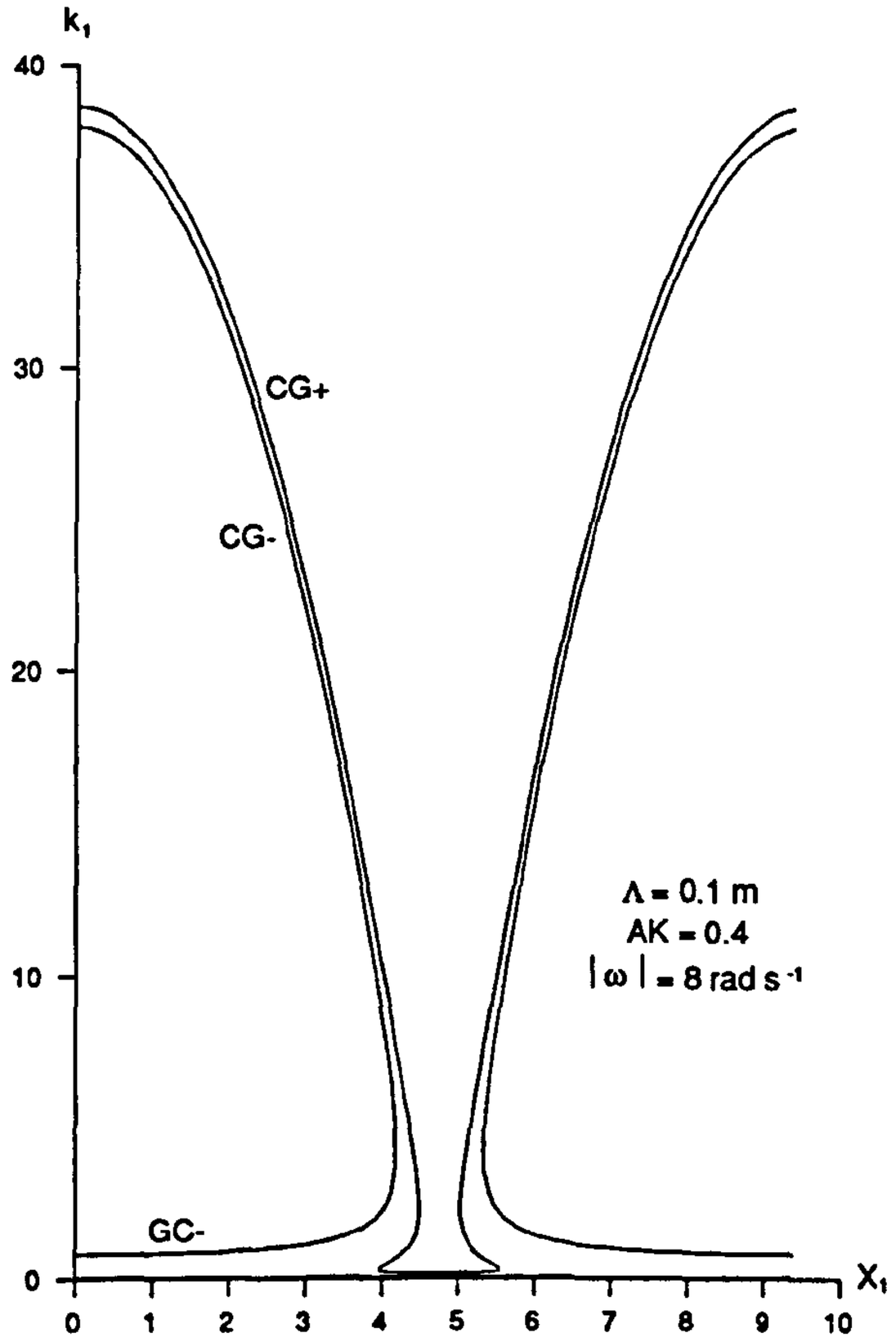

Figure 3.13a

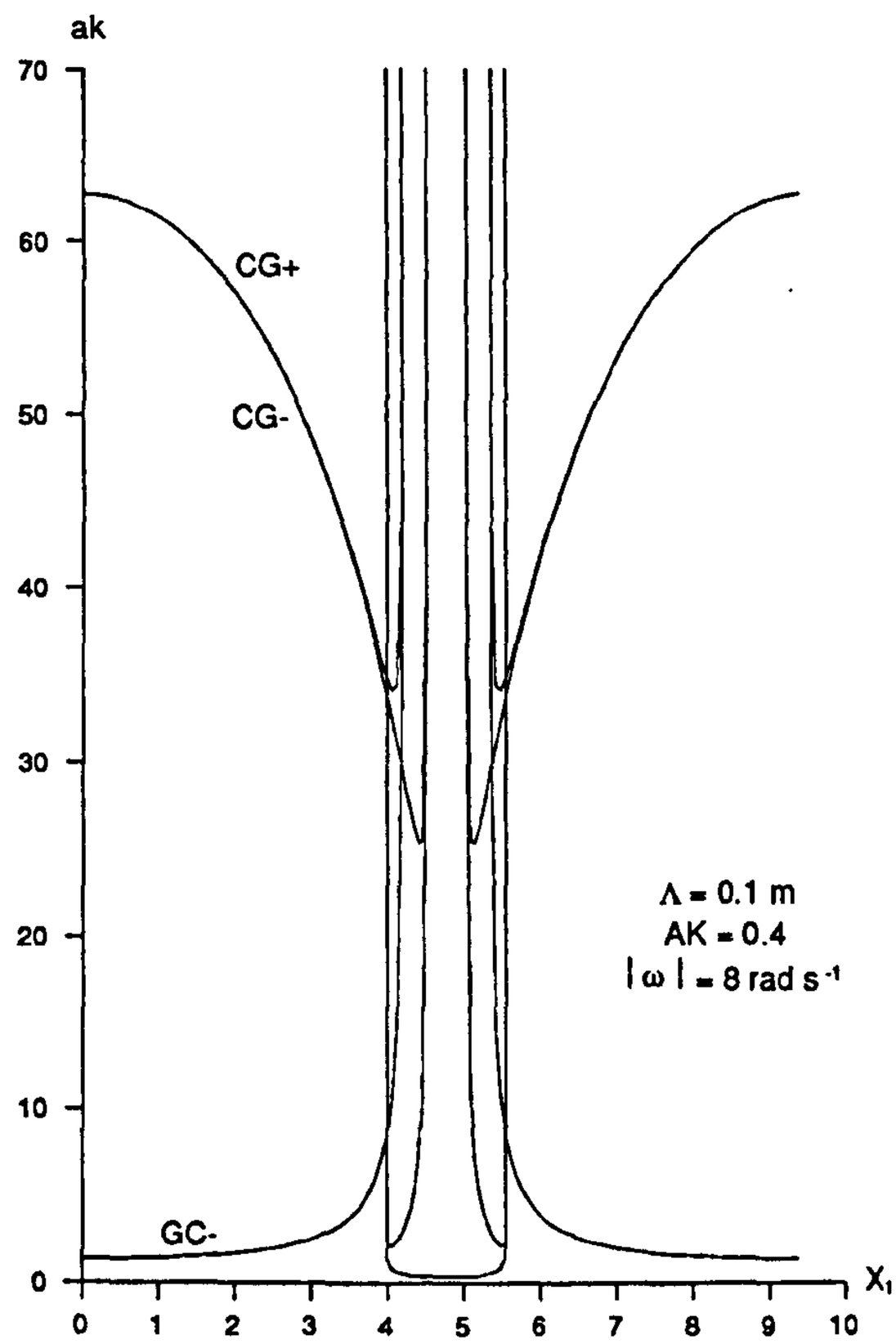

Figure 3.13b

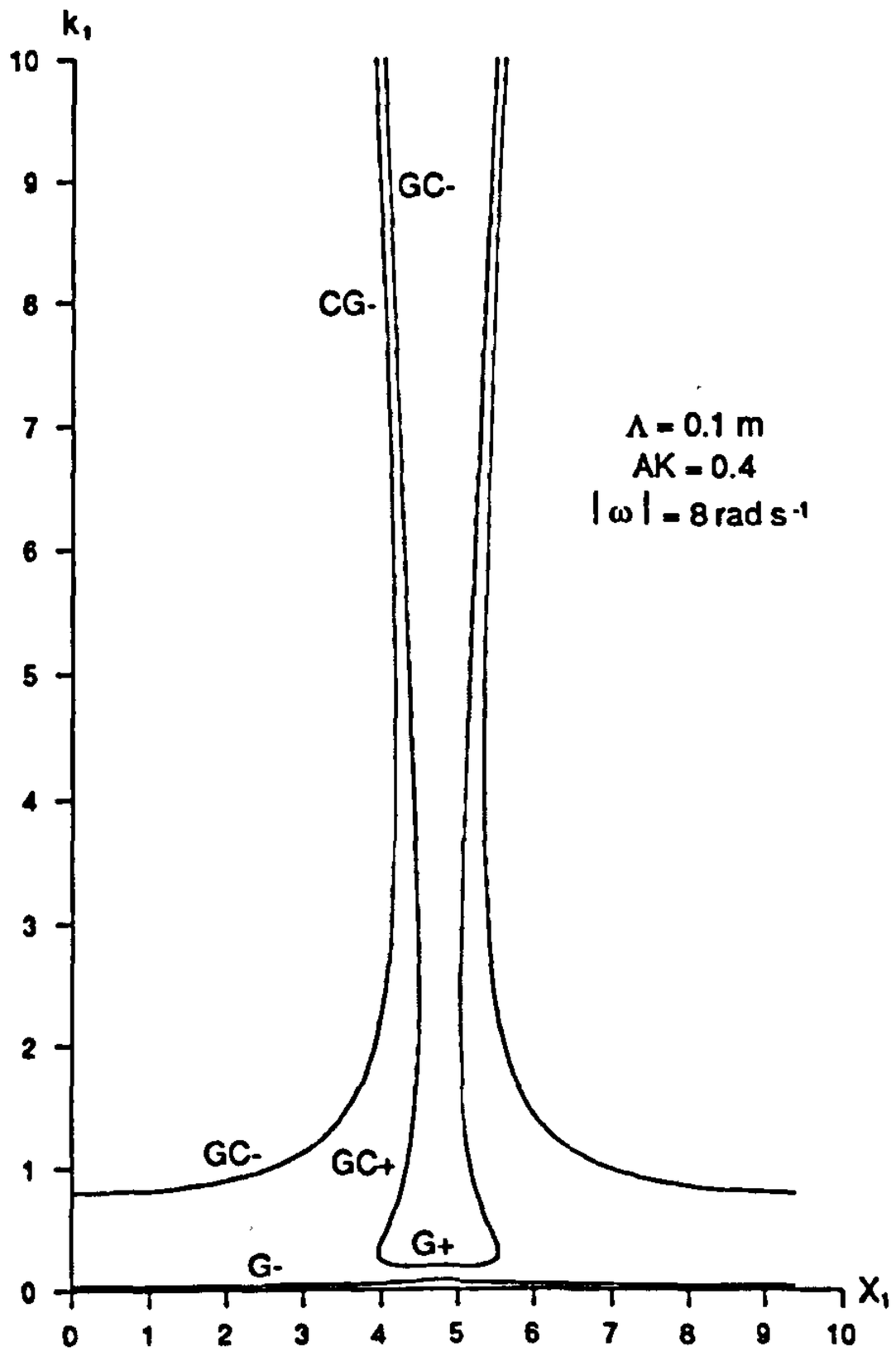

Figure 3.13a

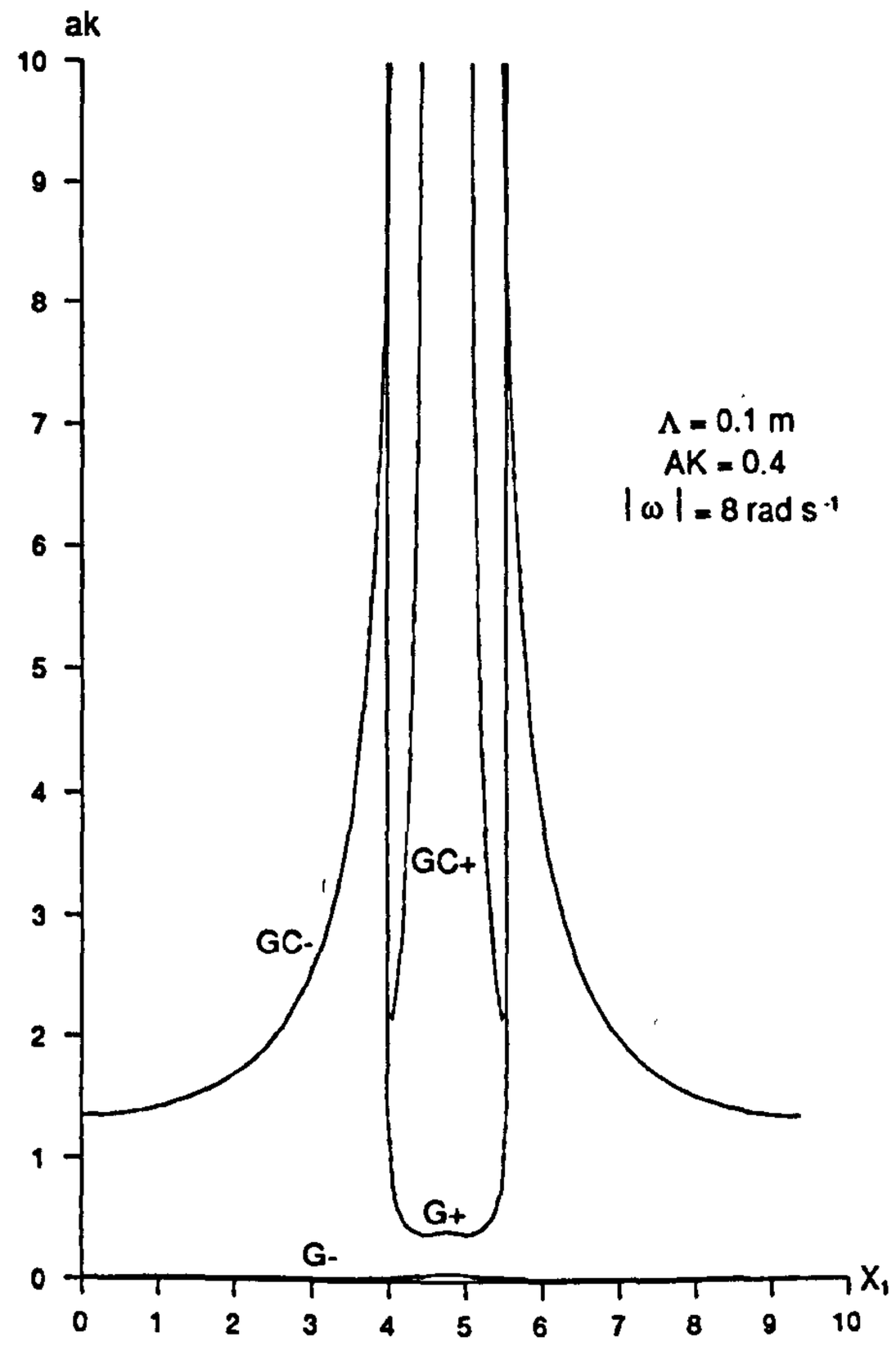

Figure 3.13b

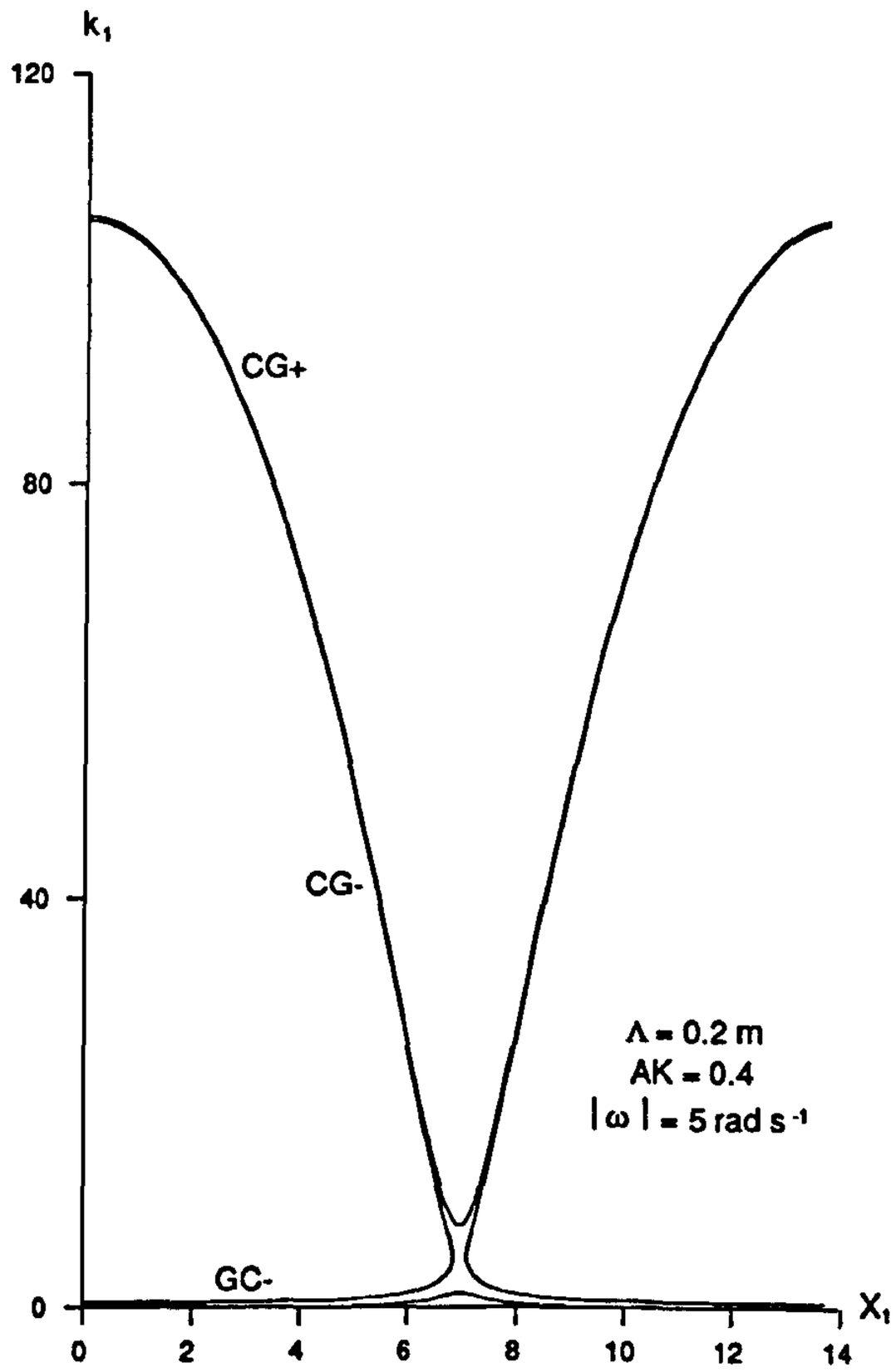

Figure 3.14a

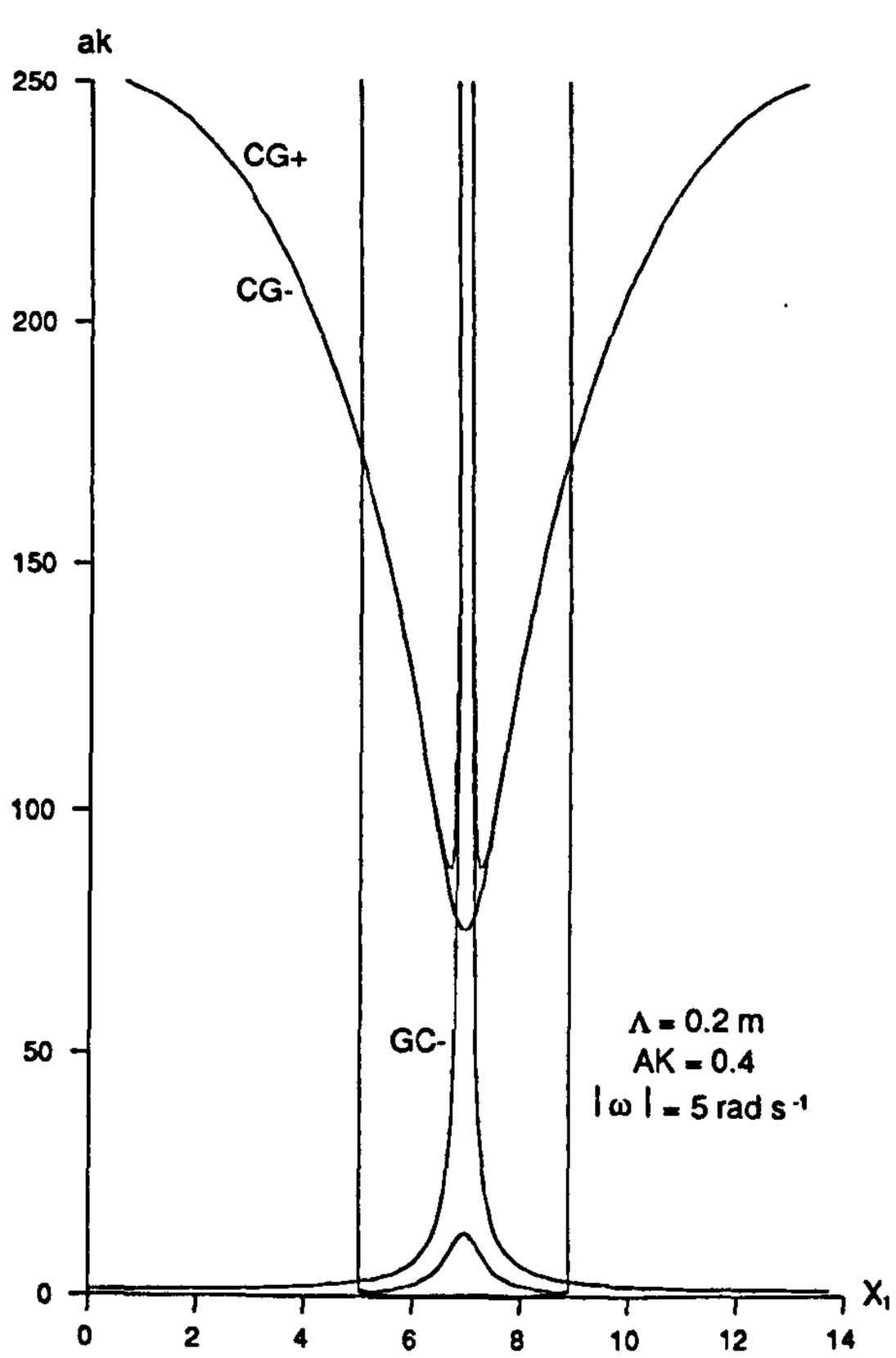

Figure 3.14b

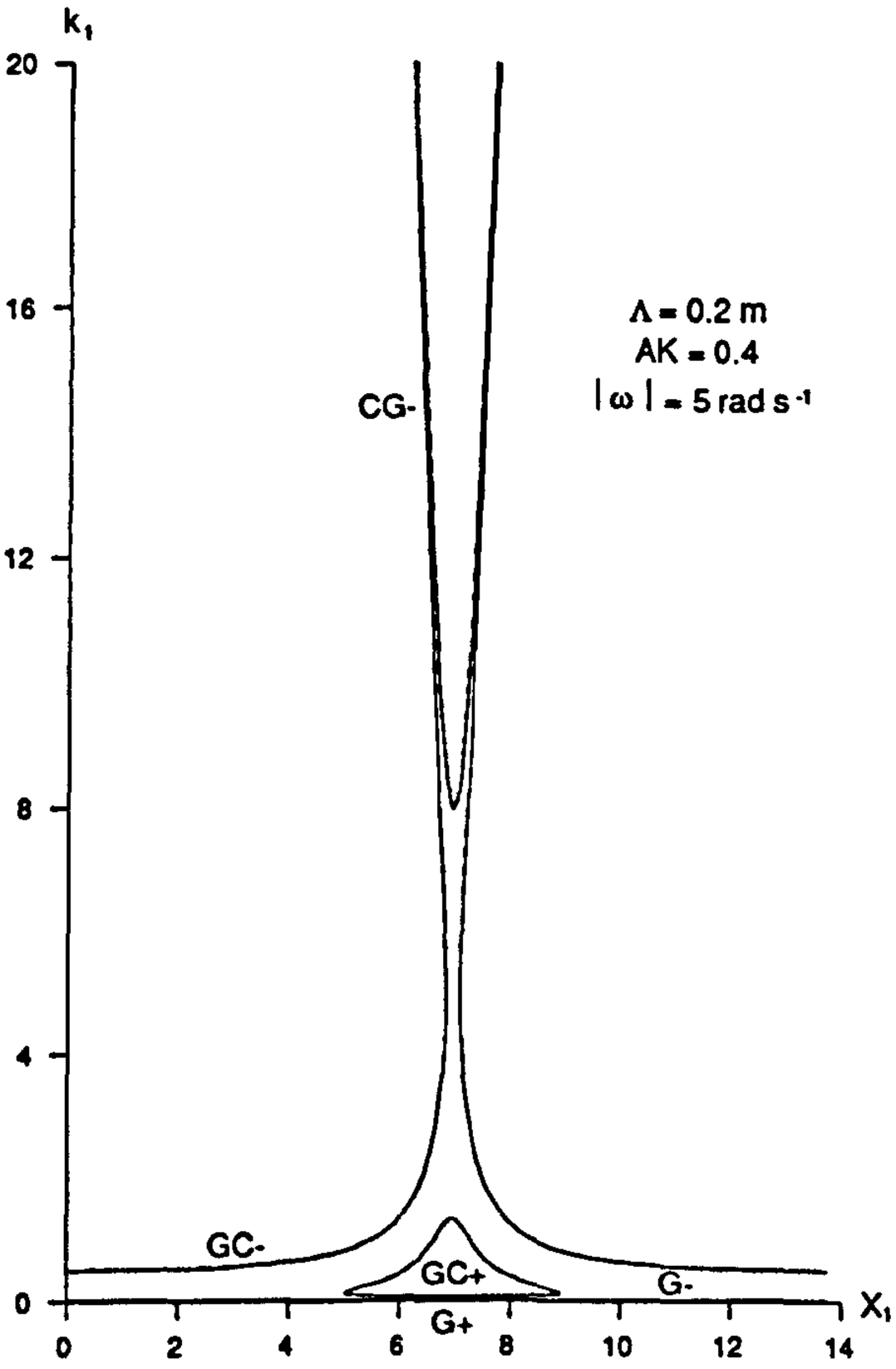

Figure 3.14a

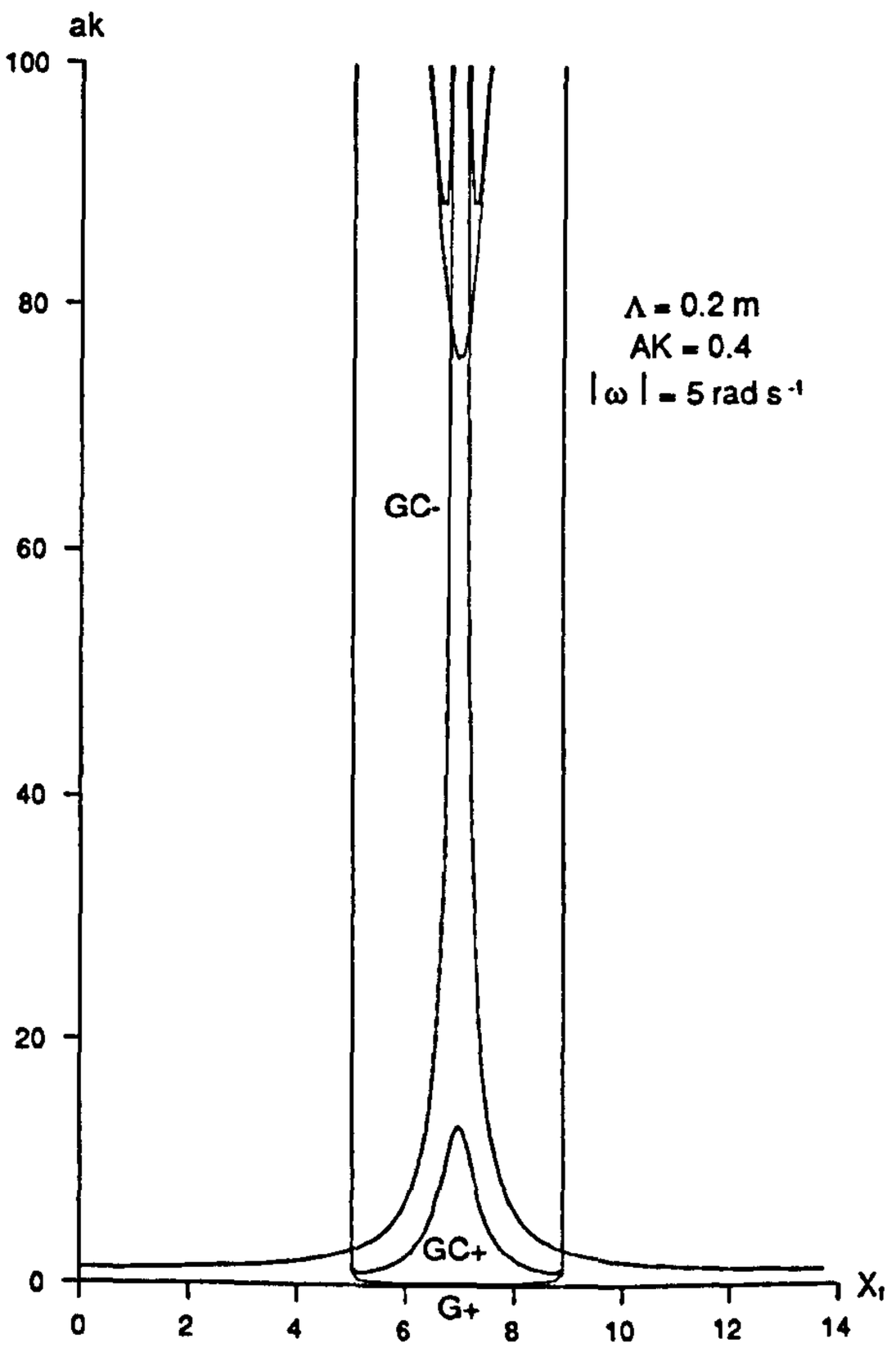

Figure 3.14b

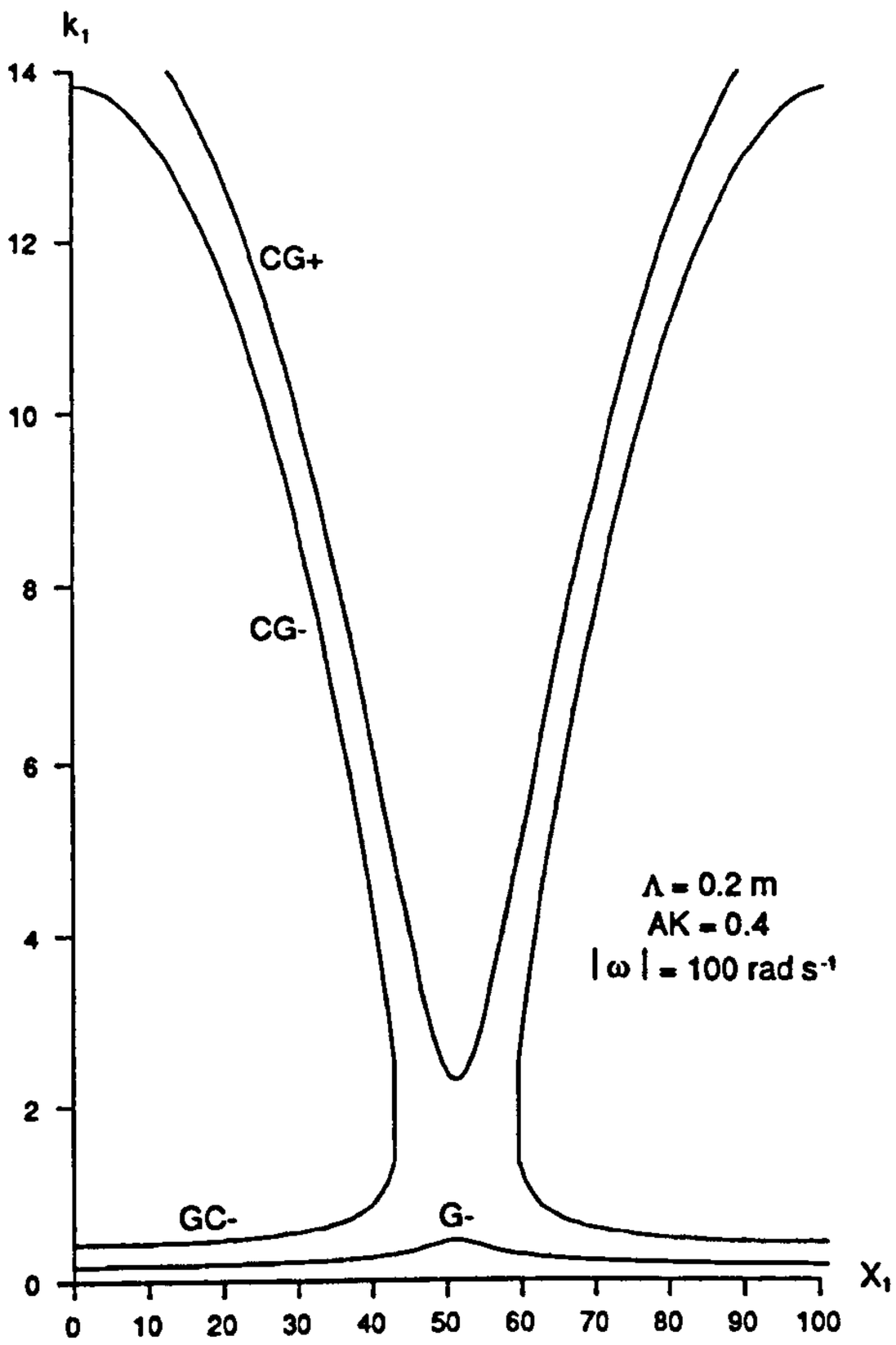

Figure 3.15a

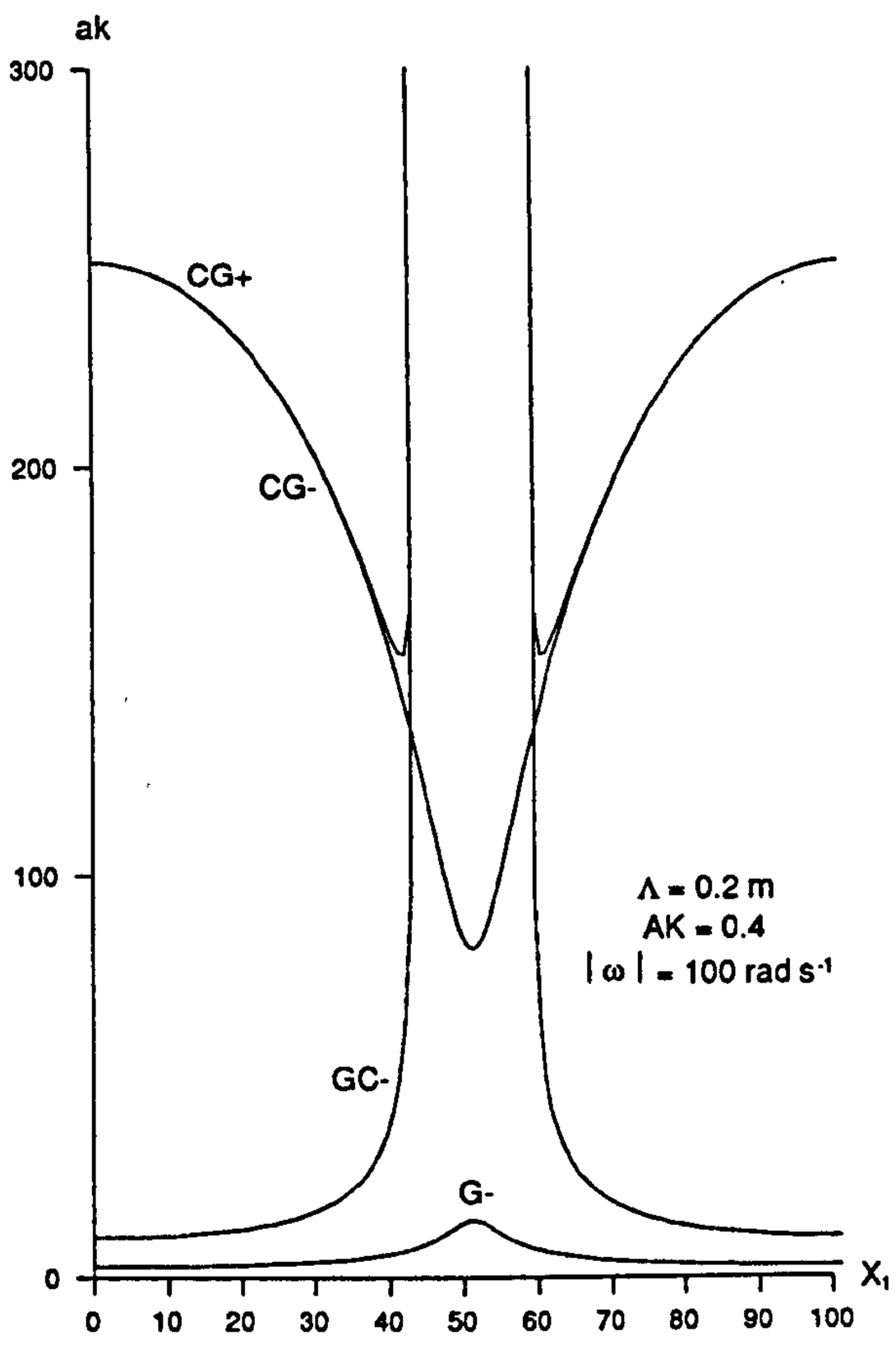

Figure 3.15b

CHAPTER 4
FINITE-AMPLITUDE PURE CAPILLARY WAVES ON INFINITE DEPTH LIQUID

4.1 Introduction

In this chapter the wave-current interaction and wave propagation problems are further examined for the case in which the "short" waves are of finite-amplitude. At present no exact analytical solution exists for finite-amplitude capillary-gravity waves (or pure gravity waves) over still liquid of infinite, or finite, depth. To consider this general case it would be necessary to either use an approximate theory or seek numerically exact solutions for such waves.

Our aim is to examine the train of waves seen on the forward faces of steep gravity waves near their crests. These waves have very small wavelengths so that they are capillary dominated and it is, thus, reasonable to neglect the effects of gravity. Longuet-Higgins (1963) examines this problem. He suggests that the capillary waves are generated by the travelling normal stress associated with the effect of surface tension near the crest of steep gravity waves, namely a pressure - $\tau\kappa$, where κ is the curvature of the gravity waves surface. The wavelength and amplitude of such capillary waves are then found as a linear perturbation on the nonlinear gravity waves. Other mechanisms of wave generation exist. For instance, it is readily observed that capillary waves are generated at the crests of small gravity waves as a result of small scale breaking of the gravity waves. Here we suppose that capillary waves already exist - the generation of capillary waves is not of primary interest.

For the case of finite-amplitude pure capillary waves an exact solution, found by Crapper (1957), is available. Lighthill (1965, equation 80) subsequently uses this exact solution to find the appropriate averaged Lagrangian. Crapper (1970) uses Lighthill's averaged Lagrangian to examine the interaction and propagation problems but restricts attention to the stationary waves case. Here, the results of Hogan (1979) are used to examine the interaction and propagation problems for both the cases of stationary and Doppler shifted finite-amplitude pure capillary waves. Hogan (1979) uses Crapper's exact solution to find expressions for mean wave properties such as the average kinetic energy density T and the averaged potential energy density V. It can easily be shown that T - V gives Lighthill's averaged Lagrangian.

Details of the exact solution found by Crapper (1957), together with some expressions derived from Hogan (1979), are given in section 4.2. The concept of generalised group velocity is examined in section 4.3. In section 4.4 the equations for both the interaction and propagation problem are developed using Whitham's equations as given in section 2.4. The cases of stationary and Doppler shifted waves are examined in sections 4.5 and 4.6 respectively. Section 4.7 find estimates for lower and upper bounds to wavenumbers as imposed by basic assumptions on the problems. The "critical gravity waves" curves for a given capillary wave solution are found and interpreted in section 4.8. The influence of the pure capillary waves on gravity wave breaking is discussed on section 4.9.

4.2 Crapper's Exact Solution

An exact solution for progressive pure capillary waves of arbitrary amplitude over infinite depth liquid has been found by Crapper (1957). The surface profile of pure capillary waves, in the σ-frame, is given by

$$\frac{x - ct}{\lambda} = \frac{2A \sin 2\pi\alpha}{\pi(1 + A^2 + 2A \cos 2\pi\alpha)} - \alpha \,, \qquad (4.2.1)$$

$$\frac{\eta}{\lambda} = \frac{2(1 + A \cos 2\pi\alpha)}{\pi(1 + A^2 + 2A \cos 2\pi\alpha)} - \frac{2(1 + A^2)}{\pi(1 - A^2)} \qquad (4.2.2)$$

where α varies from 0 to - 1 over one wavelength λ and η is such that $\bar{\eta} = 0$. The parameter A is a strictly increasing function of amplitude a for a given wavelength λ and is related to the wave steepness ak by

$$ak = \frac{4A}{1 - A^2} \quad \Longrightarrow \quad A = \frac{2}{ak}\left[\left[1 + \frac{(ak)^2}{4}\right]^{\frac{1}{2}} - 1\right] . \qquad (4.2.3)$$

From Crapper's (1957) analysis $0 \leq ak \leq 2.29$, so $0 \leq A \leq 0.455 = A_{max}$. The value A_{max} corresponds to the position where the surface profile is tangent to itself and, thus, encloses a bubble of air. This physical property of the exact solution is interpreted as the breaking point of the waves.

The dispersion relation for finite-amplitude pure capillary waves on still liquid is

$$\sigma^2 = sk^3D \qquad \text{where} \qquad D = \frac{1 - A^2}{1 + A^2} \tag{4.2.4}$$

so

$$D_{min} = 0.657 \leq D \leq 1 \ . \tag{4.2.5}$$

It proves to be easier to use the parameter D rather than A or ak. Certain expressions derived by Crapper (1957, 1970) and Hogan (1979) and used below are far more "pleasant" in terms of D. The only slight drawback is that this parameter D is a strictly decreasing function of amplitude a for a given wavelength λ.

From (4.2.3, 4) wave steepness ak in terms of D is

$$ak = \frac{2}{D}(1 - D)^{\frac{1}{2}}(1 + D)^{\frac{1}{2}} \ , \tag{4.2.6}$$

Expressions for the mean wave properties listed in § 2.5 are needed in order to derive equations for the wave-current interaction and wave propagation problems. Such expressions can be found once the mean kinetic energy density T and the mean potential energy density V are known (see § 2.6). Hogan (1979) derives expressions for these in terms of the parameter A. In terms of D these are

$$T = \left[\frac{1}{D} - D\right]\tau \ , \qquad V = 2\left[\frac{1}{D} - 1\right]\tau \ . \tag{4.2.7}$$

The possible waves theory of § 3.2 still applies because for a particular steepness ak, i.e. a particular value of D, plots of the dispersion relation (4.2.4) and the Doppler relation (2.3.1) are qualitatively similar to figure 3.2 (dispersion relation curve in the limit $g \rightarrow 0$). Thus, when finite-amplitude pure capillary waves interact with slowly-varying currents there is only one possible stationary wave CG and four possible Doppler shifted waves CG(+,-), GC- and G-. Also, there are no caustics possible for the stationary waves case and only one possible caustic CG-/GC- for the Doppler shifted waves case. Recall that waves G- will be strongly influenced by gravity and so, to all intent and purposes, are ignored.

4.3 Generalised Group Velocity

The concept of group velocity is very valuable in understanding and predicting the propagation of linear waves. Its extension to nonlinear waves presents difficulties since there are many possible definitions for the group velocity. Peregrine and Thomas (1979) analyse possible nonlinear group velocities for finite-amplitude deep-water pure gravity waves. A similar analysis is performed here for finite-amplitude pure capillary waves on infinite depth liquid.

A direct physical approach to the problem of wave propagation leads to a velocity for the propagation of some mean property J, say, of the waves. This velocity, denoted $(c_J)_i$, is defined as

$$(c_J)_i = \frac{(\text{flux of J})_i}{\text{density of J}} \ . \tag{4.3.1}$$

The most obvious properties J to consider are the energy density $\mathcal{E}$ and the wave-action density $\mathcal{A}$ with corresponding respective fluxes $\mathcal{F}_i$ and $\mathcal{B}_i$ so that

$$(c_E)_i = \frac{\mathcal{F}_i}{\mathcal{E}} \ , \qquad (c_A)_i = \frac{\mathcal{B}_i}{\mathcal{A}} \tag{4.3.2}$$

in the absence of any mainstream flow. In the presence of a mainstream flow U_i the total energy flux is $U_i\mathcal{E} + \mathcal{F}_i$ and the total wave-action flux is $U_i\mathcal{A} + \mathcal{B}_i$ so that

$$(C_E)_i = U_i + (c_E)_i \ , \qquad (C_A)_i = U_i + (c_A)_i \tag{4.3.3}$$

are the total generalised group velocities. For pure capillary waves on infinite depth liquid the mean properties $\mathcal{E}$, $\mathcal{F}_i$, $\mathcal{A}$ and $\mathcal{B}_i$ are given by the expressions in § 2.5 and the mean properties (4.2.7), $V^g = 0$ and (2.6.5) for the mean bottom velocity squared. Thus,

$$(c_E)_i = \frac{3T}{T + V}\, c_i \ , \qquad (c_A)_i = \frac{3}{2}\, c_i \ . \tag{4.3.4}$$

For linear pure capillary waves the group velocity $(c_g)_i$ is unique and is given by $(c_{glin})_i = 3c_i/2$. This linear group velocity is derived from definition (4.3.1) with mean property J as $\mathcal{E}$ and is, thus, the velocity of propagation of energy. It is seen that for nonlinear pure capillary waves $(c_A)_i$ gives the same as the linear waves case. In the linear-limit the kinetic and potential energy densities are equal, i.e. $T = V$, so that expressions (4.3.4) give $(c_E)_i = (c_A)_i = (c_{glin})_i$.

It is interesting to note (Peregrine and Thomas 1979) that it is not generally possible to define a propagation velocity in terms of the momentum density. For example, a generalised group velocity $(c_I)_i$ might be sought with

$$(c_I)_i \mathcal{I}_i = \mathcal{S}_{ij} \ , \tag{4.3.5}$$

where $\mathcal{I}_i$ and $\mathcal{S}_{ij}$ are given by expressions (2.5.7, 8), to which case there is no general solution for $(c_I)_i$.

Velocities defined in terms of (4.3.1) suffer from the disadvantage that they are based on the properties of a uniform wavetrain. Another relatively simple approach is to take the linear relation

$$(c_g)_i = \frac{\partial \sigma}{\partial k} \frac{k_i}{k} \tag{4.3.6}$$

and extend it to nonlinear waves. In general σ not only depends on k_i but also on some amplitude measure. Note that it is possible to choose different definitions for the amplitude measure (Hayes 1973) simply because the Whitham's analysis of § 2.4 and appendix B is independent of the amplitude measure chosen. It may be verified that the dispersion relation (2.4.3) and the values of the wave-action density $\mathcal{A}$ and wave-action flux $\mathcal{B}_i$ given by the definitions (2.4.7) are invariant with respect to a change in the definitions of the amplitude measure. On the other hand, the actual value of $(c_g)_i$, as defined by (4.3.6), does depend on which amplitude measure is actually kept constant. Lighthill (1965) suggests $\mathcal{L}^w/\sigma$ as a possible amplitude measure. This leads to a value of $(c_g)_i$ equivalent to $(c_E)_i$. Algebraic simplicity of the dispersion relation (4.2.4) suggests that the most natural amplitude measure is given by the parameter D. After a little algebra this leads to a value of $(c_g)_i$ equivalent to $(c_A)_i$.

The group velocities $(c_E)_i$ and $(c_A)_i$ are clearly not equal. The importance of wave-action density $\mathcal{A}$ in slowly-varying wave theory suggests that $(c_A)_i$ may be more significant. For example,

$$U + c_A = 0 \tag{4.3.7}$$

gives the "stopped" waves solution discussed below in § 4.6 and remarked upon in the introductory chapter.

Propagation velocities may also be obtained from the equations describing slowly-varying waves. Whitham (1967) and Lighthill (1967) first derived them for water waves but Hayes (1973) gives a more complete account. Hayes defines a "basic group velocity" $(c_B)_i$ and two

"basic signal velocities" $(c_\pm)_i$. The basic signal velocities are the velocities of characteristics of the partial differential equations describing linear modulations of both amplitude and wavenumber for a slowly-varying wavetrain. The basic group velocity is the average of the basic signal velocities.

Hayes chooses the wave-action density $\mathcal{A}$ as the amplitude measure, so that $\mathcal{L}^w = \mathcal{L}^w(\sigma,k,\mathcal{A})$, and uses the dispersion relation in the form

$$\frac{\partial \mathcal{L}^w}{\partial \mathcal{A}} = 0 \qquad (4.3.8)$$

to eliminate σ where necessary and defines a new function $\mathcal{X}^w(k,\mathcal{A})$ by

$$\mathcal{X}^w(k,\mathcal{A}) = \mathcal{A}\sigma - \mathcal{L}^w(\sigma,k,\mathcal{A}) \ . \qquad (4.3.9)$$

Hayes derives the basic group velocity as

$$(c_B)_i = \frac{\partial^2 \mathcal{X}^w}{\partial \mathcal{A} \partial k} \frac{k_i}{k} \ . \qquad (4.3.10)$$

Use of expressions (4.3.8, 9) and definitions (2.4.7) for $\mathcal{A}$ and $\mathcal{B}_i$ give

$$\sigma = \frac{\partial \mathcal{X}^w}{\partial \mathcal{A}} \quad \text{and} \quad \mathcal{B}_i = \frac{\partial \mathcal{X}^w}{\partial k} \frac{k_i}{k} \qquad (4.3.11)$$

so that

$$(c_B)_i = \frac{\partial \mathcal{B}_i}{\partial \mathcal{A}}\bigg|_k = \frac{\partial \sigma}{\partial k} \frac{k_i}{k}\bigg|_A \ . \qquad (4.3.12)$$

This means that the basic group velocity is that given by definition (4.3.6) with the amplitude measure as $\mathcal{A}$.

Hayes derives the basic signal velocities as

$$(c_\pm)_i = \left[\frac{\partial^2 \mathcal{X}^w}{\partial \mathcal{A} \partial k} \pm \left[\frac{\partial^2 \mathcal{X}^w}{\partial \mathcal{A}^2} \frac{\partial^2 \mathcal{X}^w}{\partial k^2}\right]^{\frac{1}{2}} \operatorname{sgn}(\cos \psi)\right] \frac{k_i}{k} \qquad (4.3.13)$$

where ψ is the angle between the normal to the perturbation (modulation) wavefronts, discussed by Hayes (1973), and the direction of propagation of the waves.

Note that, in general,

$$\frac{\partial^2 \mathcal{X}^w}{\partial \mathcal{A}^2} \frac{\partial^2 \mathcal{X}^w}{\partial k^2} \qquad (4.3.14)$$

may be either positive or negative and, thus, the velocities $(c_\pm)_i$ may be real or complex respectively. Complex values correspond to the equations describing these wave modulations as elliptic in which case an

initial value problem is illposed and a uniform wavetrain is unstable to linear modulations. This aspect is discussed by Lighthill (1965, 1967) and details of the instability are described by Benjamin (1967) and Lake et al (1977). Hayes gives the stability boundary based on this criterion for near-linear gravity waves in all depths of water. Peregrine and Thomas (1979) give the stability boundary for finite-amplitude deep water gravity waves as well as other work on stability.

Hogan (1985) examines the stability of a train of nonlinear gravity-capillary waves on the surface of an ideal liquid of infinite depth. He derives an evolution equation for the wave envelope correct to fourth order in wave steepness. The main difference from the third order evolution equation is, as far as stability is concerned, the introduction of a mean flow response. He proceeds to show that, in general, the mean flow effects for pure capillary waves are of opposite sign to those of pure gravity waves. For pure capillary waves this means that the "sidebands" of a resonant quartet transfer energy to the primary wave implying an instability in the primary wave - exactly the opposite behaviour to that of pure gravity waves.

Some more algebra shows that

$$(c_B)_i = 3\left[\frac{V - T + 2\tau}{2V - T + 4\tau}\right] c_i \ . \qquad (4.3.15)$$

Note that for the case of linear waves ($T = V = 0$) $(c_B)_i$ is equal to the linear group velocity $(c_{glin})_i$.

A little more algebra shows that

$$(c_\pm)_i = (c_B)_i \pm \left[-\frac{3T(V - 2T + 2\tau)}{2}\right]^{\frac{1}{2}} \frac{|c|}{(2V - T + 4\tau)} \operatorname{sgn}(\cos\psi) \frac{k_i}{k}$$

and since the expression in the square root is always negative the basic signal velocities $(c_\pm)_i$ are always complex. This means that finite-amplitude pure capillary wavetrains are unstable to all long modulations.

Figure 4.1 shows the variation of $|c_A|/|c|$, $|c_E|/|c|$ and $|c_B|/|c|$ with wave steepness ak for finite-amplitude pure capillary waves on infinite depth liquid. The definition most appropriate for our purposes is that given by $(c_A)_i$ essentially because wave-action density plays the greatest part in slowly-varying wave theory and it appears to be the most naturally derived group velocity from definition (4.3.6). In all other sections $(c_A)_i$ is denoted by $(c_g)_i$.

Such a clear definition is needed in order to decide the direction of propagation of the finite-amplitude capillary waves. This definition

(and all the other real valued definitions) imply that a finite-amplitude capillary wave propagates in the same direction as its linear counterpart. The direction of propagation is, thus, given by the direction of the total group velocity $(C_g)_i$. For the purposes of the waves CG(+,-), CG- and G- considered here this direction is given by the sign of C_g in table 3.1: if $C_g > 0$ ($C_g < 0$) then the waves propagate in the positive (negative) X direction. Thus, waves CG(+,-) propagate in the + X direction and waves GC- and G- propagate in the - X direction. It follows that all the properties of these waves, listed in table 3.1, are still applicable.

4.4 The Equations

Our aim is to find equations for the three unknowns k, σ and a. The derivation of such equations is simplified by the introduction of velocity variables P and Q defined by

$$P = \frac{\omega}{k} \quad \text{and} \quad Q = \frac{\sigma}{k} \tag{4.4.1}$$

equal to phase velocities C and c respectively. Then finding equations for the unknowns k and σ is equivalent to finding equations for the unknowns P and Q.

In these velocity variables the Doppler relation (2.3.1) and the dispersion relation (4.2.4) are

$$P = Q + U \quad \text{and} \quad D = \beta PQ^2 \tag{4.4.2}$$

where

$$s\omega\beta = 1 \ . \tag{4.4.3}$$

The velocity variable P is determined using the Doppler relation (4.4.2), the dispersion relation (4.4.2) and the wave-action conservation equation (2.7.5). Now, from the expressions (2.5.11, 12) for $\mathcal{A}$ and $\mathcal{B}$ and (2.8.5) for the mean bottom velocity squared, noting $V^g = 0$ for pure capillary waves, the wave-action density $\mathcal{A}$ and wave-action flux $\mathcal{B}$ are given by

$$\mathcal{A} = 2\frac{T}{\sigma} \ , \quad \mathcal{B} = 3\frac{T}{k} \ . \tag{4.4.4}$$

Thus, using the definitions (4.4.1) for P and Q, the Doppler and dispersion relation (4.4.2) and expression (4.2.7) for T the wave-action

conservation equation (2.7.5) gives

$$\tau s \left[\frac{1}{Q^3} - \beta^2 P^2 Q\right](2P + Q) = b \ . \qquad (4.4.5)$$

There are now two cases to consider, namely zero and non-zero total wave-action flux b. If $b = 0$ then, using the Doppler relation (4.4.2),

$$1 - \beta^2 P^2 (P - U)^4 = 0 \quad \text{or} \quad 3P - U = 0 \ . \qquad (4.4.6)$$

Using the dispersion relation (4.4.2) the first of these two equations gives $D = 1$ so this is the linear-limit of the nonlinear theory. Expanding this equation gives the sixth order polynomial

$$\beta^2 P^6 - 4\beta^2 P^5 U + 6\beta^2 P^4 U^2 - 4\beta^2 P^3 U^3 + \beta^2 P^2 U^4 - 1 = 0 \qquad (4.4.7)$$

for P in terms of β and U. This is equivalent to equation (3.3.2) with g set to zero.

The second of equations (4.4.6) implies that the total group velocity C_g is zero so that these waves have no direction of traverse. This equation represent nonlinear waves with zero total wave-action flux and so this is a "stopped" waves solution (see § 4.3 equation 4.3.7). Waves are stopped in the sense that their wave-action is stationary.

Note that our convention requires $U \leq 0$, $k \geq 0$ so that $P \leq 0$ which means that $\omega \leq 0$ for stopped waves. Thus, these waves have $C < 0$. However, stopped pure gravity waves have $C > 0$. This difference is due to the fact that for pure capillary waves $c < c_g$ so that $C = c + U < c_g + U = C_g = 0$ for stopped waves whereas for pure gravity waves $c > c_g$ (see Peregrine and Thomas 1979 for generalised c_g) so that $C > C_g = 0$ for stopped waves.

The second of equations (4.4.6) gives

$$P = \frac{U}{3} \ . \qquad (4.4.8)$$

If $b \neq 0$ then equation (4.4.5) gives rise to a seventh order polynomial for P in terms of β, b and U. Expanding (4.4.5), using the Doppler relation (4.4.2), gives

$$\begin{aligned} &3\beta^2 P^7 - 13\beta^2 U P^6 + 22\beta^2 U^2 P^5 - 18\beta^2 U^3 P^4 + (7\beta^2 U^4 + b^*)P^3 \\ &- (\beta^2 U^5 + 3b^* U)P^2 + (3b^* U^2 - 3)P + (U - b^* U^3) = 0 \qquad (4.4.9) \end{aligned}$$

where

$$\tau s b^* = b \ . \qquad (4.4.10)$$

For the case of stationary pure capillary waves the velocity variable P can no longer be used since $\omega = 0$ implies $P = 0$. A new variable R is defined where

$$R = \frac{1}{sk} \ . \qquad (4.4.11)$$

The definition of Q remains unchanged. The equations for the motion of such waves can then be derived using one of two methods. The first is to proceed as above and follow the analysis through using the new variable R. The other is to substitute

$$P = \frac{R}{\beta} \quad \text{or} \quad \beta P = R \qquad (4.4.12)$$

in the equations derived above and then take the limit $\omega \longrightarrow 0$ or, equivalently, $\beta \longrightarrow \infty$. The latter method is the more succinct method. However, all the equations derived below have been confirmed using both methods.

The Doppler relation (4.4.2) and the dispersion relation (4.4.2) become

$$0 = Q + U \ , \quad \text{and} \quad D = RQ^2 \ . \qquad (4.4.13)$$

The wave-action conservation equation (4.4.5) becomes

$$\tau s\left[\frac{1}{U^2} - R^2U^2\right] = b \ . \qquad (4.4.14)$$

For the case $b = 0$ equations (4.4.6) and (4.4.14) gives

$$R = \frac{1}{U^2} \qquad (4.4.15)$$

since $R > 0$ by our convention of $k > 0$. Note that there is no stopped waves solution. This is essentially because both the crests, or troughs, of the waves and the wave-action can not be simultaneously stationary.

For the case $b \neq 0$ equations (4.4.9) and (4.4.14) give

$$R = \frac{(1 - b^*U^2)^{\frac{1}{2}}}{U^2} \ . \qquad (4.4.16)$$

This equation leads to equation (5) in Crapper (1970) on substitution of k in favour of R.

Equations (4.4.8, 9, 9, 15, and 16) are solved for the unknown P or R, for a given wave-action flux b, by choosing a value of U and then finding the roots of the polynomials where appropriate using a standard solver (NAG LIB C02AEF). The unknown Q is then found using the Doppler relations (4.4.2, 13). These are then used to find the unknowns k and σ using definitions (4.4.1, 11). The wave amplitude a is found using the dispersion relations (4.4.2, 13) to find D and then using expression (4.2.6) which gives wave steepness ak in terms of D. Note that solutions within the steepness range given by (4.2.5) are the only ones allowed.

At the end of § 3.3 it is noted that, for the linear waves case, there exists a simpler method of solving the wave-current interaction problem. The same phenomenon exists for the nonlinear waves case presently under examination. The wavenumber k is determined using the Doppler relation (2.3.1), the dispersion relation (2.4.4) and the wave-action conservation equation (2.7.5). Using expression (4.4.4) for wave-action $\mathcal{A}$ and wave-action flux $\mathcal{B}$ the wave-action conservation equation (2.7.5) gives

$$T\left[2\,\frac{U}{\sigma} + \frac{3}{k}\right] = b \ . \qquad (4.4.17)$$

Again, there are two cases to consider, namely zero and non-zero total wave-action flux b. If $b = 0$ then either

$$T = 0 \qquad \text{or} \qquad 2Uk + 3\sigma = 0 \ . \qquad (4.4.18)$$

The first of these implies, from expression (4.2.7) for T, D = 1 so that this is the linear-limit of nonlinear theory. The Doppler relation (2.3.1) and the dispersion relation (4.2.4) give

$$sk^3 - U^2k^2 + 2\omega Uk - \omega^2 = 0 \qquad (4.4.19)$$

which is equation (3.3.2) with g = 0. This is solved, as in § 3.3, for k over a given range of U and using the same polynomial solver (NAG LIB C02AEF). Then σ is found using the Doppler relation (2.3.1) with a = 0 since ak = 0.

The second equation in (4.4.18) implies, with the use of the Doppler relation (2.3.1),

$$Uk = 3\omega \quad \text{or} \quad \sigma = -\,2\omega \ . \qquad (4.4.20)$$

The dispersion relation (4.2.4), thus, gives

$$k^3 = \frac{4\omega^2}{sD} \quad . \tag{4.4.21}$$

This equation is solved for k by varying D over its range (4.2.5). Then U and a are found using equation (4.4.20) and expression (4.2.6) for steepness ak in terms of D respectively. Note, from equations (4.4.20), that the frequency σ of these waves is constant and negative. These equations represent the "stopped" waves solution. Note that (4.4.20) implies that $\omega < 0$ for these waves as before.

If $b \neq 0$ then elimination of U, via the Doppler relation (2.3.1), in the wave-action conservation equation (4.4.17) gives

$$\frac{T}{k}\left[2\,\frac{\omega}{\sigma} + 1\right] = b \tag{4.4.22}$$

which, on use of the dispersion relation (4.2.4), gives

$$k^5 - 2\,\frac{T}{b}\,k^4 + \frac{T^2}{b^2}\,k^3 - \frac{4\omega^2T^2}{sDb^2} = 0 \quad . \tag{4.4.23}$$

This equation is solved, in the same manner as equation (4.4.21), for different values of the total wave-action flux b using a standard polynomial solver (NAG LIB C02AEF). Wave amplitude a is found using expression (4.2.6) for steepness ak in terms of D. Frequency σ is found using equation (4.4.22) (it could be found using the dispersion relation (4.2.4) but then table 3.1 would have to be used to find the appropriate sign of σ corresponding to particular waves). Current U is then deduced from the Doppler relation (2.3.1).

The solution to the propagation problem can, in fact, be solved using the equations derived above specifically for the interaction problem. However, interpolation methods must be used on results of the interaction problem to find the exact behaviour of the capillary waves as they propagate on the gravity waves since it is the surface current U(X) which is specified ab intio for the gravity waves. The use of interpolation methods takes considerable computational time. It proves quicker and easier to solve the propagation problem using the direct method involving the variables P and Q.

This interpolation method idea has one very important consequence. Knowledge of the range of surface velocities for given gravity waves can be used to gain both a qualitative and quantitative idea of the behaviour of capillary waves on gravity waves using the results of the

interaction problem as is suggested in § 3.4 and § 3.5. Thus, the results of the interaction problem prove to be very useful when interpreting the results of the propagation problem.

Both methods are actually used to solve both the interaction and propagation problems. The results obtained by both methods are exactly the same. A third method is also used to solve the propagation problem. This involves the solution of an ordinary differential equation and is given in chapter 5. This method also gives the same results.

Note that the interaction problem equations provide a quick and easy way to find the values of wave parameters when the capillary waves are at their breaking point (put $D = D_{min}$ in equation 4.3.22, 24) or, for that matter, at any specific steepness of interest. This is used below in § 4.7.

4.5 Stationary Waves

The case of stationary waves is considered first. Dimensional units are used. This case has already been considered by Crapper (1970). However, he aims to consider the effects energy dissipation and energy input and so adds terms representing these effects so that results defer. The validity of these terms and the problem of wave energy dissipation are addressed in detail in chapter 5. The equation describing the variation of wavenumber k with current U as derived from the equations of § 4.4 is the same as equation (5) of Crapper (1970). In fact, the equations derived in § 4.4 simplify considerably for this case.

Both the equations for the interaction and propagation problems lead to the same equations for this case. The general nonlinear equations (4.4.22, 16) give the equivalent pair of equations

$$k = \frac{T}{b} \quad \text{and} \quad k = \frac{\rho U^2}{(\tau^2 - \rho b U^2)^{\frac{1}{2}}} \,. \tag{4.5.1}$$

Either of these equations is solved to find the variation of k with U. Variations of σ and a are found using the general method described in § 4.4.

When $b = 0$ these equations lead to the those given by the linear equations (4.4.15, 19). It is seen that waves with $b > 0$ are the only ones which exist since $k > 0$ and $T > 0$. This agrees with the general properties of waves CG listed in table 3.1. It is also seen that waves

exist only when

$$U^2 < \frac{\tau^2}{\rho b} \tag{4.5.2}$$

so as b increases the range of U over which the waves exist decreases. This range for b agrees with that given in Crapper (1970). The stopped waves equations (4.4.20, 21) imply that the stopped waves solution branch tends to the single point U = k = 0 as $\omega \longrightarrow 0$, as does the caustic (§ 3.4), and ceases to exist.

Results for the interaction problem are shown in figures 4.2 for various values of the wave-action flux b. Essentially all the wave solution curves exhibit a "parabolic" (exactly for linear waves) type variation. The linear theory (dashed lines) shows no caustics. This is as is expected and is essentially due to the fact that there is no minimum in phase velocity (figure 3.1) for pure capillary waves. Wave solutions reach maximum steepness as the current U decreases from zero, say. At this position the waves have maximum wavenumber. Expressions (4.5.2) imply that waves exist for all b but since the maximum possible wavenumber decreases with increasing b those waves for "large" values of b will be strongly influenced by gravity. Indeed, waves for all b are influenced by gravity when wavenumbers k, or currents U, are "small".

Equations (4.5.2) are used to find solutions for the propagation problem as well as the interaction problem since they specify the wavenumber k as a function of U as does equation (4.4.16). For the cases considered, that is A = 0.2 and 0.1 m and AK = 0.3 and 0.4, it is found that for wave-action fluxes b not "close" to zero there are no solution curves for the capillary waves. This is as expected since waves with "large" b are strongly influenced by gravity. Essentially, this feature arises because the maximum velocity attained by the gravity waves is too low.

Results for the propagation problem are shown in figures 4.3 and 4.4 for A = 0.2 m and AK = 0.3 and 0.4 respectively. The linear-limit solution curves are shown (dashed lines) since these form a framework for the interpretation of the results. It is seen that the qualitative, and to some extent quantitative, characteristics of linear pure capillary wave propagations are the same as those of linear capillary-gravity wave propagations as shown in figures 3.8 and 3.7 respectively. Thus, these cases are worthwhile considering since the effects of gravity are qualitatively unimportant.

For both the cases the qualitative features of linear and nonlinear propagations are the same. An increase in the steepness of the gravity

waves does not change the qualitative behaviour of the waves. For very small b the waves propagate over the whole length of the gravity waves. For higher b the waves propagate over the gravity wave crests but break as they propagate rightward ($C_g > 0$) towards the gravity wave troughs. In the observers frame capillary waves with very small b will always overtake the gravity waves whereas capillary waves with larger b are absorbed on the forward faces of the gravity waves as they attempt to overtake the gravity waves. However, the feature of increasing steepness as the capillary waves propagate from the gravity wave crests to the gravity wave troughs is not realistic because wave energy dissipation would have a marked effect at such high wavenumbers (see § 4.7). This is shown to be the case in chapter 5.

4.6 The Doppler Shifted Waves

The case of Doppler shifted waves is now considered. The equations of § 4.4 are solved in capillary units.

a The Wave-Current Interaction Problem

The parameters for the problem are again ω_1 and b_1 as given by expressions (3.5.3). Note that now different solutions are obtained for different b_1 as for the stationary waves case above, i.e. b_1 effects the qualitative characteristics of variations of σ, k and a, whereas this is not the case for linear theory in chapter 3. It follows that the four parameter space τ, s, ω and b is reduced to the two parameter space of ω_1 and b_1 as for linear theory of § 3.5.

Results are shown in figures 4.5 and 4.6. Figures 4.5a and 4.6a show variations of wavenumber k_1 with current U_1 whilst figures 4.5b and 4.6b, c show corresponding variation of steepness ak with current U_1. For clarity of discussion attention is predominantly focused on figures 4.5a and 4.6a, i.e. on figures with wavenumber k_1 as the abscissa, with reference to other figures where necessary (steepness variation of waves on figures 4.5a or 4.6a can, ofcourse, be found from figures 4.5b, and 4.6b, c).

The zero total wave action flux case has five branches (dashed lines). Four of these correspond to linear theory; one, shown on figure 4.5a, is the linear-limit of waves CG+ and the other three shown on figure 4.6a are the linear-limits of waves CG-, GC- and G- (note that according to nonlinear theory the steepness of linear waves is zero). The fifth, shown on figure 4.6a, corresponds to the nonlinear stopped

waves solution.

The non-zero total wave action flux case has four branches corresponding to waves CG+ (figure 4.5a) and CG-, GC-, G- (figure 4.6a) (waves G- are not shown in any figures because, as already mentioned, the effects of gravity become important for these waves). Waves CG+ exist for $0 < b_1 < 2.26$, waves CG- exist for $0 < b_1 < 0.16$ and waves GC- exist for all $b_1 < 0$. Solution curves corresponding to waves CG- have a (local) minimum non-zero steepness whereas those for other waves do not (figures 4.5b, 4.6b, c). Waves CG- reach maximum steepness as U_1 both increases and decreases (figure 4.6b) but waves GC- reach maximum steepness as U_1 increases and zero steepness as U_1 decreases (figure 4.6c).

Waves CG+ have a finite non-zero steepness at $U_1 = 0$ and reach maximum steepness as U_1 decreases (note that waves CG+ can be regarded as an extension of waves G- with equal, but opposite, frequency ω and equal steepnesses when $U_1 = 0$ so that the existence of a finite non-zero steepness at $U_1 = 0$ is expected: a convention of $k > 0$ and $\omega > 0$ shows this more clearly). The qualitative characteristics of waves CG+ are the same as those of the stationary waves CG. This is easily seen from comparison of figures 4.2 and 4.5. However, waves CG- and GC- are, in no way, qualitatively, or quantitatively, similar to the stationary waves CG.

Suppose that waves are traversing in a direction such that the current U_1 is increasing, for example from $U_1 = -3$ towards $U_1 = 0$ say. Consider the waves CG- and GC- with reference to figures 4.6 because these waves are the ones which propagate past the linear caustic. Linear theory shows the existence of a linear caustic and as these linear waves traverse towards the caustic their steepness becomes singular and the slowly-varying assumption invalid as is shown in § 3.5.

Nonlinear theory suggests that as U_1 increases waves CG- and GC- can traverse past the linear caustic and break. However, the validity of the slowly-varying assumption must again be questioned. From figures 4.6b, c it is seen that solutions for "small" b_1 have the most rapidly varying steepness and that this rapid variation occurs in the neighbourhood of the linear caustic. Therefore, the validity of the slowly-varying assumption is most dubious for such solutions in this neighbourhood. In effect, it becomes increasingly difficult for a current to remain slowly-varying for all wave solutions as its velocity approaches the velocity at the caustic.

Whether or not the slowly-varying assumption is actually violated depends on the relative length scales for variations of the mainstream flow U(X) and the wavenumber k (or amplitude a). Flows with specific

current distributions U(X) are considered below where the propagation problem is examined. For such flows it may be possible, as suggested above, for the waves to traverse past the linear caustic and break or for waves to undergo reflection (CG- or GC- waves reflected onto CG- or CG- waves respectively with equal, but opposite, values of total wave-action flux). The actual behaviour is studied later, in chapter 5, using a uniform nonlinear approximation in the neighbourhood of the caustic.

Solution curves for waves CG- and GC- are close to the linear waves solution curves and stopped waves solution curve for small values of b_1 (figure 6a) and lie on their convex side of the linear solution curves. These correspond to near-linear theory and so S-type behaviour exists in the neighbourhood of linear caustic which confirms the results of § 3.7.

b The Wave Propagation Problem

The propagation problem is now considered. The parameter space now includes ρ, τ, A, AK and $|\omega|$ as well as ω_1 and b_1 as for linear theory of § 3.5. The qualitative and quantitative nature of propagations are seen from figures 4.5 and 4.6 for the interaction problem. Table 4.1 shows the range of velocity U_1 corresponding to four different gravity waves and two different values of $|\omega|$ which can be used to gain a feel for the behaviour of propagations. The liquid is, as usual, clean fresh water.

AK	A m	$\lvert\omega\rvert$ rad s^{-1}	U_{1max} U_{1crest}	U_{1min} $U_{1trough}$
0.3	0.1	100	- 1.26	- 2.56
0.3	0.1	500	- 0.74	- 1.50
0.3	0.2	100	- 1.79	- 3.62
0.3	0.2	500	- 1.04	- 2.12
0.4	0.1	100	- 0.79	- 2.69
0.4	0.1	500	- 0.46	- 1.57
0.4	0.2	100	- 1.12	- 3.80
0.4	0.2	500	- 0.66	- 2.22

Table 4.1: Surface velocity range in capillary units for several different gravity waves and corresponding $|\omega|$

The equations (4.4.1 - 4.4.10), involving the variables P and Q, are solved in capillary units. Note that equation (4.4.9) is an odd order polynomial so that there must be at least one solution for each sign of b_1 as expected from the possible waves analysis of § 3.2. Also note that waves CG+ have $P_1 > 0$ whereas the other three waves have $P_1 < 0$.

The wavelength $\Lambda = 0.2$ m is chosen because gravity waves of this length have a greater range of velocities U_1 (table 4.1) than gravity waves of length $\Lambda = 0.1$ m and, thus, show a wider range of behaviour. Figures 4.7 - 4.10 show the propagation of capillary waves with frequency $|\omega| = 100$ rad s^{-1} on gravity waves with $\Lambda = 0.2$ m, AK = 0.3 (figures 4.7 and 4.8) or 0.4 (figures 4.9 and 4.10). The linear-limit solution curves and the stopped waves solution curves are also shown (dashed lines) since these form a framework for the interpretation of the results. It is seen that the qualitative, and to some extent quantitative, characteristics of linear pure capillary wave propagations are the same as those of linear capillary-gravity wave propagations as shown, for example, in figures 3.15. Thus, these cases are worthwhile considering since the effects of gravity are qualitatively unimportant. Note that waves CG(+,-) traverse in the + X direction whereas wave GC- traverses in the - X direction.

Figures 4.7 and 4.8 show the behaviour of capillary waves on gravity waves with steepness (AK = 0.3) equal to approximately 68 % of the maximum steepness (AK = 0.44) of gravity waves on an infinite depth of water. Both waves CG+ and CG- always propagate over the crests of the gravity waves. Both also propagate over the troughs for "small" b_1 but break as they propagate towards the troughs for "large" b_1 (figures 4.7b and 4.8b).

Waves GC- also propagate over the crests for "small" $|b_1|$ but break as the crests are approached for "large" $|b_1|$ (figure 4.8c), e.g. when $b_1 \geq -1$ waves GC- propagate over the crests but for $b_1 \leq -2$ they break as the crest is approached. Waves GC- experience a decrease in steepness as they propagate towards the troughs of the gravity waves.

Figures 4.9 and 4.10 show the behaviour of capillary waves on gravity waves with steepness (AK = 0.4) equal to approximately 91 % of the maximum steepness (AK = 0.44) of gravity waves on an infinite depth of water. Waves CG+ behave qualitatively in the same manner on this gravity wavetrain as they do on the gravity wavetrain with AK = 0.3. This is seen by comparison of figures 4.7 and 4.9. This is expected since these waves exist at $U_1 = 0$ (figures 4.5) and are always qualitatively similar to stationary waves CG. This is seen from comparison of figures 4.4, 4.6 and 4.8.

Both waves CG- and GC- break as they approach the crests of the gravity waves (figures 4.10) no matter what the value of b_1. Thus, as the steepness of the gravity waves increases the capillary waves experience breaking as is expected. As both waves CG- and GC- propagate towards the troughs of the gravity waves the features of the propagation are qualitatively similar to those of AK = 0.3 case discussed above. This is seen by comparison of figures 4.8 and 4.10.

As mentioned for stationary waves CG the feature of increasing steepness as waves CG(+,-) propagate towards the gravity wave troughs (or crests) is not realistic because of the effects of wave energy dissipation (see § 4.7) as are discussed in chapter 5.

These propagations give a specific length scale for the variation of the mainstream flow and, thus, allow us to more closely examine the validity of the slowly-varying assumption. It is seen from figures 4.7 - 4.10 that as waves CG- and GC- approach the caustic the slowly-varying assumption definitely breaks down (the variation of wave steepness changes quickly in the neighbourhood of the caustic). This feature is further examined in chapter 5.

4.7 Lower and Upper Bounds for Wavenumbers

The above solutions assume that all the properties of the flow field are slowly-varying and that the effects of wave energy dissipation are negligible. However, these assumptions are not necessarily always valid. Upper and lower bounds for wavenumbers are easily calculated between which these assumptions can be assumed valid.

The lower bound k^1 for the wavenumber originates from the slowly-varying assumption for the current distribution U(X). Formally, the slowly-varying assumption may be stated as

$$k \gg \max \left| \frac{1}{U} \frac{dU}{dx} \right| . \qquad (4.7.1)$$

The curvature of the gravity waves also gives a length scale which will correspond to some lower bound since this has been ignored (x in 4.7.1 is the horizontal coordinate of the ω-frame for the interaction problem). Thus,

$$k \gg \max \kappa \qquad (4.7.2)$$

where κ is the curvature of the surface of the gravity waves. The

variation of the maximum curvature κ_{max}, i.e. the curvature at the crests, of pure gravity waves with steepness AK in gravity units is shown in figure 4.11.

Note that with θ defined from (figure 2.2)

$$\cos\theta = \frac{dX}{dx} \tag{4.7.3}$$

the x and X coordinates for the propagation problem are related. Thus, conditions (3.6.1) and (3.6.2) are found numerically using the known values of U, κ and θ. Note that in gravity units, denoted by a subscript 0, the wavelength of gravity waves is fixed to 2π. It is found that

$$\text{for} \quad AK = 0.3 \quad \max \left| \frac{1}{U_o} \frac{dU_o}{dx_o} \right| = 1.42 \ , \ \max \kappa_o = 0.78 \ ,$$

$$\text{for} \quad AK = 0.4 \quad \max \left| \frac{1}{U_o} \frac{dU_o}{dx_o} \right| = 0.48 \ , \ \max \kappa_o = 2.86 \ .$$

The maximum of these forms the basis of the lower bound k_o^l in gravity units. Thus,

$$\text{for } AK = 0.3 \quad k_o^l >> 1.42 \quad \text{and} \quad \text{for } AK = 0.4 \quad k_o^l >> 2.86 \ .$$

To convert these to dimensional and capillary units expressions (3.4.6) and (3.5.1) must be used so that specific values of ρ, τ, K and ω must be chosen. As usual, consider $\Lambda = 0.2$ m and 0.1 m with $|\omega| = 100$ rad s^{-1}. If the lower bound is chosen to be four times the number given above the lower bounds will be as shown in table 4.2.

Steepness	Wavelength	Values of lower and upper bounds for wavenumber k			
AK	Λ m	k^l m^{-1}	k_i^l	k^u m^{-1}	k_i^u
0.3	0.20	178	0.4	3940	8
0.4	0.20	359	0.7	3940	8
0.3	0.10	357	0.7	6260	12
0.4	0.10	718	1.4	6260	12

Table 4.2: Lower and upper bounds for wavenumbers k_i in capillary units.

The upper bound k^u is a result of the physical nature of capillary waves. Short capillary waves are quickly damped out by viscosity so that at high wavenumbers the results are irrelevant because of rapid viscous damping. Our criterion is to insist that the waves travel an appreciable fraction of the gravity wave before they decay because of viscosity. A time scale for the decay of free surface waves is found in Lamb (1932) as

$$T_d = \frac{1}{2\nu k^2} \tag{4.7.5}$$

where ν is the kinematic viscosity of the water. For pure capillary waves $c_g = 3c/2$ and $c^2 = sk$. So the length scale for the decay is

$$L_d = c_g T_d = \frac{3s^{\frac{1}{2}}}{4\nu} k^{-\frac{3}{2}} . \tag{4.7.6}$$

Suppose that the waves traverse a distance $\theta\Lambda$, for some fraction θ, before they decay. Then

$$L_d = \theta\Lambda = \frac{3s^{\frac{1}{2}}}{4\nu} (k^u)^{-\frac{3}{2}} \quad \text{so} \quad k^u = \left[\frac{3s^{\frac{1}{2}}}{4\nu\theta\Lambda} \right]^{\frac{2}{3}} . \tag{4.7.7}$$

Now, for water $\nu = 1.3 \times 10^{-6}$ m^2 s^{-1} so that

$$\Lambda = 0.2 \text{ m} \Longrightarrow k^u = 850\, \theta^{-\frac{3}{2}} \text{ m}^{-1} , \quad \Lambda = 0.1 \text{ m} \Longrightarrow k^u = 1350\, \theta^{-\frac{3}{2}} \text{ m}^{-1} .$$

$$\text{If } \theta = 0.1 \text{ then } \left\{ \begin{array}{lll} \Lambda = 0.2 \text{ m} & \Longrightarrow & k^u = 3940 \text{ m}^{-1} , \\ \Lambda = 0.1 \text{ m} & \Longrightarrow & k^u = 6260 \text{ m}^{-1} . \end{array} \right. \tag{4.7.8}$$

Converting to capillary units with $|\omega| = 100$ rad s^{-1} gives upper bound as in table 4.2. Note that this analysis is independent of the steepness of the gravity waves.

These lower and upper bounds can also be applied to the results of chapter 3. If the slowly-varying assumption is examined for the effective gravity $g^*(X)$, in the same manner as for $U(X)$, then it is found that the bounds are not changed. The most important effect of the lower bounds in chapter 3 is that the majority of solutions with the GC+/G+ caustic have the caustic occurring at wavenumbers lower than the lower bounds so that results regarding this caustic are dubious.

Examination of figures 4.3, 4, 7 - 10 shows that waves CG, CG+ and CG- (GC-) always have wavenumbers larger (smaller) than the lower (upper) bounds. The majority of solution curves for waves CG, CG+ and

CG- have wavenumbers larger than the upper bounds at some point so that waves CG, CG+ and CG- will be strongly affected by dissipation whilst waves GC- will hardly be affected. Only a few of the solution curves for waves GC- have wavenumbers smaller than the lower bounds and when this is the case the solution curves are in the trough regions of the gravity waves. However, this does not mean that the slowly-varying assumption is valid since it can also be violated by rapid rates of change of wavenumbers, steepness, etc., as is the case here.

4.8 Interpretation: Critical Gravity Waves

a Critical Gravity Waves

Define a breaking velocity U_B as that velocity U at which a capillary wavetrain reaches maximum steepness and so reaches breaking point. Then waves CG- have two breaking velocities (figures 4.6), waves GC-, CG+ and the stopped waves have one breaking velocity (figures 4.5 and 4.6). Again, waves G+ are not considered.

For given values of $|\omega|$, s and b_1, i.e. for a particular capillary wavetrain, the range of velocities of a gravity wavetrain may intersect the corresponding (U_1, k_1) solution curve in one of three following ways (figure 4.12):

Case 1. Intersection for the whole range of velocities. This implies the capillary wavetrain propagates over whole of the gravity wavetrain,

Case 2. Intersection for part of the range of velocities. This implies the capillary wavetrain either breaks or reaches zero steepness and, thus, ceases to exist somewhere on the gravity wavetrain, and

Case 3. No intersection with velocity range. This implies that this particular capillary wavetrain can not exist on this particular gravity wavetrain.

Of these case 2 is the most interesting for this is the only case which includes breaking. This case itself can be split in to two (figure 4.12). Case 2i (2ii) corresponds to breaking (either breaking or reaching zero steepness) as the waves propagate towards the crests (troughs). For waves CG- both cases 2i and 2ii represent breaking. For waves GC- and stopped waves cases 2i and 2ii represent breaking and reaching zero steepness respectively. Only case 2ii is

possible for waves CG+ and this represents breaking. Thus, waves CG-, GC- and stopped waves (waves CG- and CG+) are the only waves which can break whilst propagating towards the crests (troughs) of the gravity wavetrain.

Define a crest (trough) breaking velocity as the velocity required for breaking of the capillary wavetrain as it propagates towards the crests (troughs) of the gravity wavetrain. For waves CG- and CG+ the trough breaking velocities occur at a high wavenumber where dissipation is important (§ 4.7, table 4.2) and, hence, breaking is unlikely in practice. In chapter 5 this is shown to be the case. Thus, attention is confined to crest breaking velocities and, thus, to waves with $\omega < 0$. Note that the stopped waves come into this category.

For a particular value of b_1 waves CG-, GC- and stopped waves have unique crest breaking velocities U_{B1} in capillary units. For particular s and $|\omega|$ the dimensional value of this velocity is given by the expression in (3.5.2) for U in terms of U_1, i.e. $U_B = (s|\omega|)^{\frac{1}{3}} U_{B1}$.

Define the critical gravity waves for the chosen particular capillary wavetrain to be those gravity wavetrains whose surface velocity at the crest is equal to the crest breaking velocity U_B. The wavetrain will break whilst propagating over any steeper or shorter gravity waves where as it will propagate over any lower or longer gravity waves.

The surface velocity at the crest of a gravity wavetrain when expressed in gravity units is a function of steepness AK only and its value, U_{Co}, for the full range $0 < AK < 0.44$ is given in figure 4.13. For any chosen steepness AK and wavenumber K the surface velocity at the crest in dimensional units is given by an expression in (3.4.7) for U in terms of U_o, i.e. $U_C = (g/K)^{\frac{1}{2}} U_{Co}$. So wavenumbers of the critical gravity wavetrains for a particular capillary wavetrain are found by varying AK over its range, equating U_B to U_C and solving for K. This gives $K = g(s|\omega|)^{-\frac{2}{3}} U_{Co}^2/U_{B1}^2$.

b Results and Interpretation

The critical gravity waves for the stopped waves solution are shown in figure 4.14 for various values of $|\omega|$ with $s = 7.42 \times 10^{-5}$ m^3 s^{-2}, the value for water. Similar curves exist for all the CG- and GC- wave solutions shown in figures 4.6. Note that for a particular value of b_1 waves CG-, GC- and the stopped waves have wavenumbers k_{B1} and frequencies σ_{B1} associated with them. For given s and $|\omega|$ these wavenumbers and frequencies are expressed in dimensional units using expressions in (3.5.1, 2) for dimensional unit wave parameters in terms of capillary unit wave parameters. So associated with each curve in

figure 4.14 is a value of the dimensional quantities $|\omega|$, U_B, k_B and σ_B. These are given in table 4.3.

This table shows that for $|\omega| \geq 20$ rad s^{-1} the wavenumbers at the stopped waves breaking velocity corresponds to those of pure capillary waves ($k > 250$ m^{-1}). In chapter 3 it is deduced that the effects of gravity are qualitatively negligible for such values of ω. This is, therefore, reaffirmed here. Also, examination of table 4.2 shows that for 50 $s^{-1} \leq |\omega| \leq 1000$ s^{-1} the wavenumbers at the stopped wave breaking velocity lie within the lower and upper bound for all the four waves

$\lvert\omega\rvert$ rad s^{-1}	U_B m s^{-1}	k_B m^{-1}	σ_B rad s^{-1}
10	- 0.15	200	- 20
20	- 0.19	320	- 40
50	- 0.25	590	- 100
100	- 0.32	940	- 200
1000	- 0.69	4350	- 2000
2000	- 0.87	6900	- 4000
10000	- 1.49	20170	- 20000

Table 4.3: The dimensional values of breaking current, wavenumber and frequency corresponding to the stopped waves solution for different total frequencies $|\omega|$. These also correspond to the critical gravity wave curves for the stopped waves solution.

considered. Thus, a choice of $|\omega| = 100$ s^{-1} seems good since then wavenumbers for waves CG- will also have a chance of being within the ranges specified by the lower and upper bounds. This is shown to be the case in the figures above.

Recall that for a gravity wavetrain of fixed wavenumber K (steepness AK) the surface velocity at the crest U_c increases as steepness AK (wavenumber K) increases. By definition, a critical gravity wavetrain has surface velocity U_B at the crest. So a CG- or GC- (stopped) capillary wavetrain "just" propagates over (exists at) the crests of the critical gravity wavetrain ("just" in the sense that the steepness of the capillary waves is maximum at the crests of the gravity

waves) when observed from the ω-frame. Note that the stopped waves can not propagate over the crests of the critical gravity wavetrain because they do not propagate in any direction.

Also recall that if the surface velocity at the crest is greater than the breaking velocity then any CG- or GC- (stopped) capillary wavetrain breaks (does not exist) as it propagates towards (at) the crests of the gravity wavetrain. This will be so if for a fixed wavenumber K (steepness AK) the steepness AK (wavenumber K) of the gravity wavetrain is increased.

It is concluded that, for any gravity wavetrain with K and AK to the right (left) of the critical gravity wave curves of any CG- or GC- capillary wavetrain, those particular capillary waves will break (not break) as they propagate towards (over) the crests of the gravity wavetrain. Also, for any gravity wavetrain with K and AK to the right (left) of the critical gravity wave curves of the stopped waves (figure 4.14) the waves will not (will) exist at the crests of the gravity wavetrain.

Note that the crest breaking velocities of waves CG- and GC- are all less than the crest breaking velocity of the stopped waves solution branch (figure 6a). Thus, if a capillary wavetrain does not exist at the crests of gravity wavetrains for the stopped waves solution then it will definitely break as it propagates towards the crests for any CG- or GC- capillary wavetrains. However, if a capillary wavetrain does exist at the crests of gravity wavetrains for the stopped waves solution then it may, or may not, propagate over the crests for a CG- or GC- capillary wavetrain.

All the physical interpretation above is related to observations in the ω-frame of reference. However, when examining lakes or ponds, or any real liquid system, observations are usually made with respect to the observers frame defined in § 2.9. The above results are now given in this frame.

If, in the ω-frame, a CG- or GC- capillary wavetrain propagates over the crests of a gravity wavetrain then, in the observer's-frame, the gravity wavetrain either overtakes (waves GC-) or is overtaken by (waves CG-) the capillary wavetrain depending on the direction of propagation of the waves. Also, if, in the ω-frame, a CG- or GC- capillary wavetrain breaks as it is swept towards the crests of a gravity wavetrain then, in the observer's-frame, the gravity wavetrain either sweeps-up (waves GC-) or absorbs (waves CG-) the capillary wavetrain. Note that sweeping-up and absorbing are both due to the breaking of the capillary waves. Waves GC- are swept-up on the forward face of the gravity waves whilst the

waves CG- are absorbed on the rear face of the gravity waves because these waves propagate in the - X and + X direction respectively. Note that since, in the ω-frame, the stopped waves "packet" does not traverse then, in the observer's-frame, the stopped waves "packet" is carried along by the gravity wavetrain at the phase speed c of the gravity wavetrain.

Thus, for any gravity wavetrain with K or AK to the right (left) of the critical gravity wave curves for a GC- or CG- capillary wavetrain, that gravity wavetrain will either sweep-up (overtake) or absorb (be overtaken by) that capillary wavetrain. Also, for any gravity wavetrain with K or AK to the right (left) of the critical gravity wave curves for the stopped waves wavetrain, that gravity wavetrain will carry along the waves with breaking (no breaking) occurring at some point on the gravity wavetrain.

Relating this to figure 4.14 it follows that if a gravity wavetrain does not have waves existing at its crests for the stopped waves solution then it will definitely sweep-up any GC- or absorb CG- capillary wavetrains. However, if a gravity wavetrain does have waves existing at its crests for the stopped waves then it may, or may not, overtake or be overtaken by a GC- or CG- capillary wavetrain.

Note that the likelihood of waves CG- either overtaking or being absorbed by a gravity wavetrain is very small since these waves will be quickly damped out by energy dissipation as the majority of wave solutions for these waves reach wavenumbers greater than the upper bounds given in table 4.4. Waves GC- are the ones which are either overtaken by or swept-up by a gravity wavetrain.

4.9 The Breaking of Gravity Waves

Suppose that a train of capillary waves is propagating up the forward face of a gravity wave (figure 2.2). These will be either the stopped waves or waves GC-. Examining the capillary waves motion it is seen that the the liquid under the capillary waves propagates rightward relative to their profiles (figure 4.15). When the capillary waves are at their breaking point they form a bubble ABCDE (figure 4.15). There is then a shear at AE where the surface of the liquid touches itself. Also, the vorticity generated by the bubble ABCDE is directed anti-clockwise. Longuet-Higgins (1988) shows that the transient effects of breaking of these capillary waves may result in a net drift current directed leftward.

Banner and Phillips (1974) point out that the incipient breaking of a steady gravity wavetrain is characterised by the occurrence of stagnation points at gravity wave crests. As previously mentioned the motion of liquid under a gravity wavetrain when viewed from a reference frame fixed to the gravity waves, i.e. the ω-frame, is leftward. The possible transient leftward net drift due to capillary waves breaking would increase the magnitude of the surface velocity of gravity waves and, thus, further remove it from the stagnation value. Consequently, the breaking of either the stopped waves or waves GC- on the forward faces of steep gravity wavetrains could have a stabilising influence on the gravity waves. On the other hand, the unsteady disturbance from capillary wave breaking may precipitate breaking of the gravity waves.

It is also possible for capillary wave propagation to have a destabilising effect on the gravity wave motion. Capillary waves CG, CG+ and CG- propagate down the forward faces of gravity waves. If the effects of wave energy dissipation are accounted for (see chapter 5) then these waves rapidly dissipate their energy. This results in a momentum transfer to the surface current. A surface drift current develops whose direction of motion is rightward. Thus, a net decrease in the magnitude of the surface velocity for gravity waves would result so that the stagnation value is approached giving the destabilising effect.

These interactions between breaking or dissipating waves and the mean flow have yet to be effectively modelled. In the following chapter we are only able to account for the effects of dissipation on the capillary waves.

CAPTIONS FOR FIGURES

Figure 4.1: The variation of generalised group velocity ratios $|c_A|/|c|$, $|c_E|/|c|$ and $|c_B|/|c|$ with steepness ak for finite-amplitude pure capillary waves.

Figure 4.2: The variation of (a) wavenumber k and (b) steepness ak with current U for stationary waves; various wave-action fluxes b as shown.

Figure 4.3: The variation of (a) wavenumber k and (b) steepness ak with distance X for stationary waves where the gravity wave has Λ = 0.2 m, AK = 0.3; various wave-action fluxes b as shown.

Figure 4.4: The variation of (a) wavenumber k and (b) steepness ak with distance X for stationary waves where the gravity wave has Λ = 0.2 m, AK = 0.4; various wave-action fluxes b as shown.

Figure 4.5: The variation of (a) wavenumber k_1 and (b) steepness ak with current U_1 for Doppler shifted waves CG+; various wave-action fluxes b_1 as shown.

Figure 4.6: The variation of (a) wavenumber k_1 and (b,c) steepness ak with current U_1 for Doppler shifted waves CG- and GC-; various wave-action fluxes b_1 as shown.

Figure 4.7: The variation of (a) wavenumber k_1 and (b) steepness ak with distance X_1 for waves CG+ with $|\omega|$ = 100 rad s^{-1} where the gravity wave has Λ = 0.2 m, AK = 0.3; various wave-action fluxes b_1 as shown.

Figure 4.8: The variation of (a) wavenumber k_1 and (b,c) steepness ak with distance X_1 for waves CG- and GC- with $|\omega|$ = 100 rad s^{-1} where the gravity wave has Λ = 0.2 m, AK = 0.3; various wave-action fluxes b_1 as shown.

Figure 4.9: The variation of (a) wavenumber k_1 and (b) steepness ak with distance X_1 for waves CG+ with $|\omega|$ = 100 rad s^{-1} where the gravity wave has Λ = 0.2 m, AK = 0.4; various wave-action fluxes b_1 as shown.

Figure 4.10: The variation of (a) wavenumber k_1 and (b,c) steepness ak with distance X_1 for waves CG- and GC- with $|\omega|$ = 100 rad s^{-1} where the gravity wave has Λ = 0.2 m, AK = 0.4; various wave-action fluxes b_1 as shown.

Figure 4.11: The variation of curvature κ_{co} at the crest with steepness AK for gravity waves.

Figure 4.12: Diagram illustrating the possible ways in which the velocity range of a gravity wavetrain can intersect a capillary wave solution curve of the type given shown in figures 4.2, 5, 6.

Figure 4.13: The variation of surface velocity U_{co} at the crest with steepness AK for gravity waves.

Figure 4.14: Critical gravity waves curves for the stopped waves solution; various frequencies ω as shown. Corresponding wavenumbers k_1, etc., at the crest breaking velocity are given in table 4.3.

Figure 4.15: Diagram illustrating the motion of liquid under a breaking capillary wave: ABCDE shows the enclosed bubble singularity with the surface touching itself at AE.

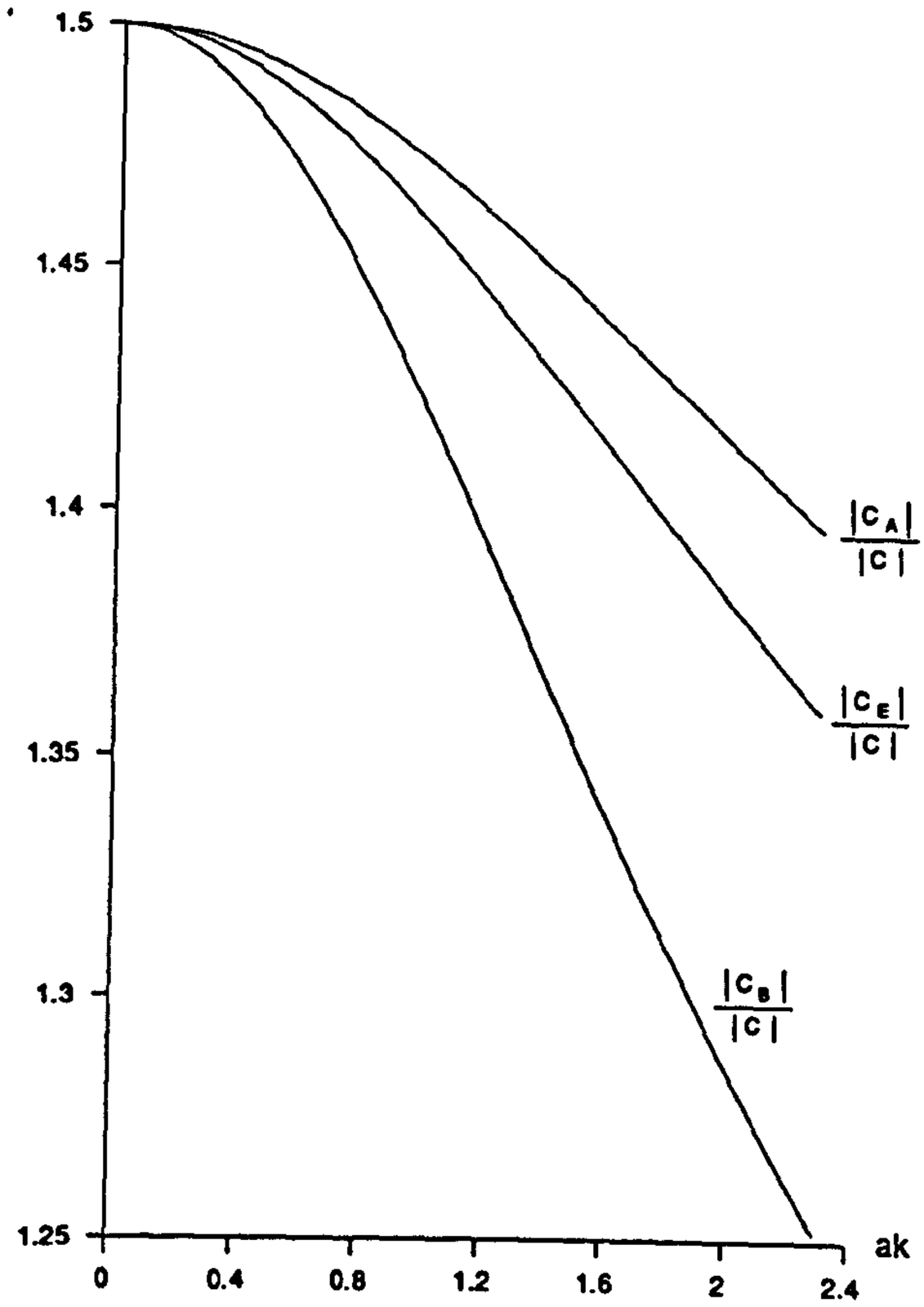

Figure 4.1

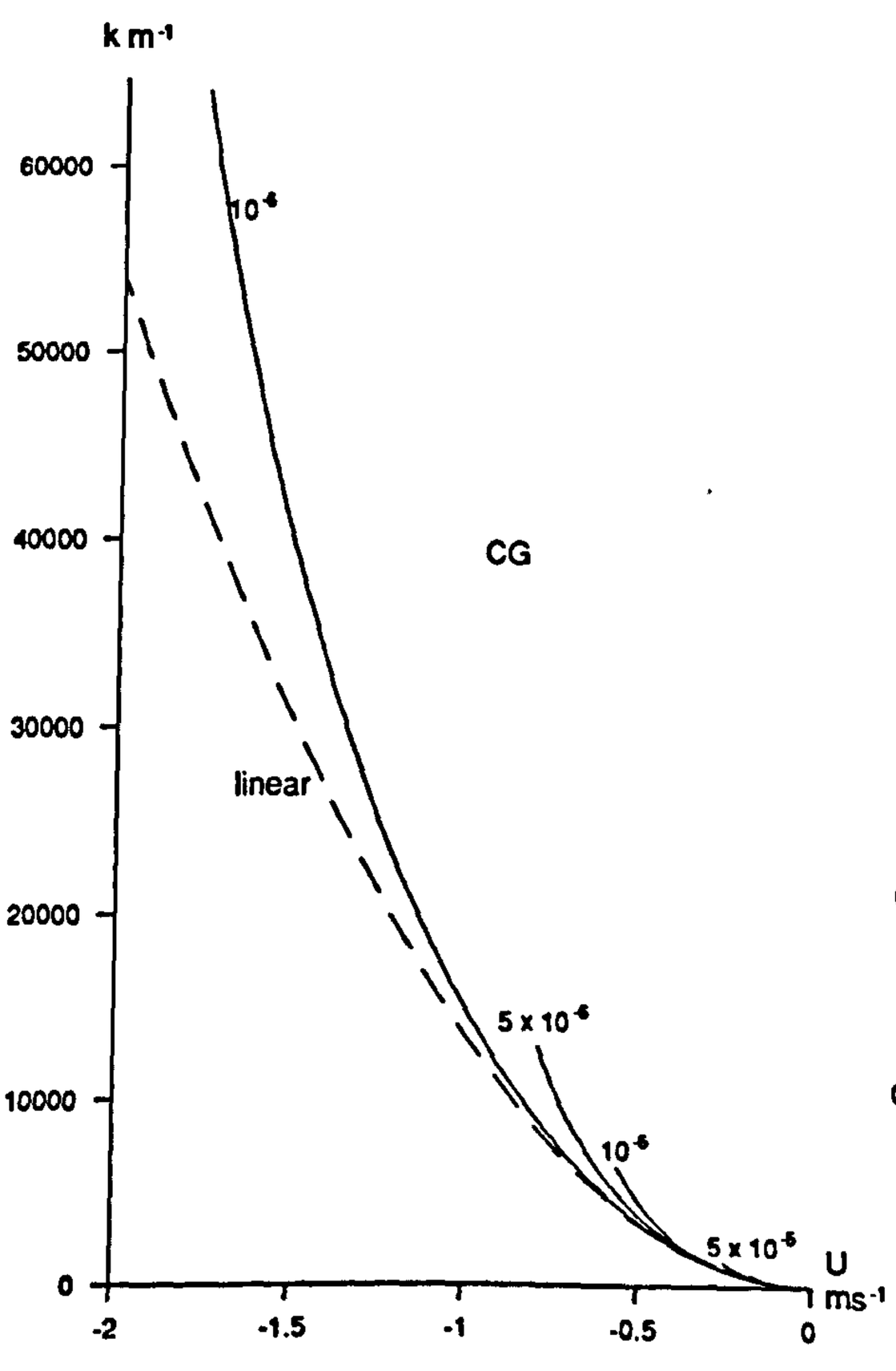

Figure 4.2a

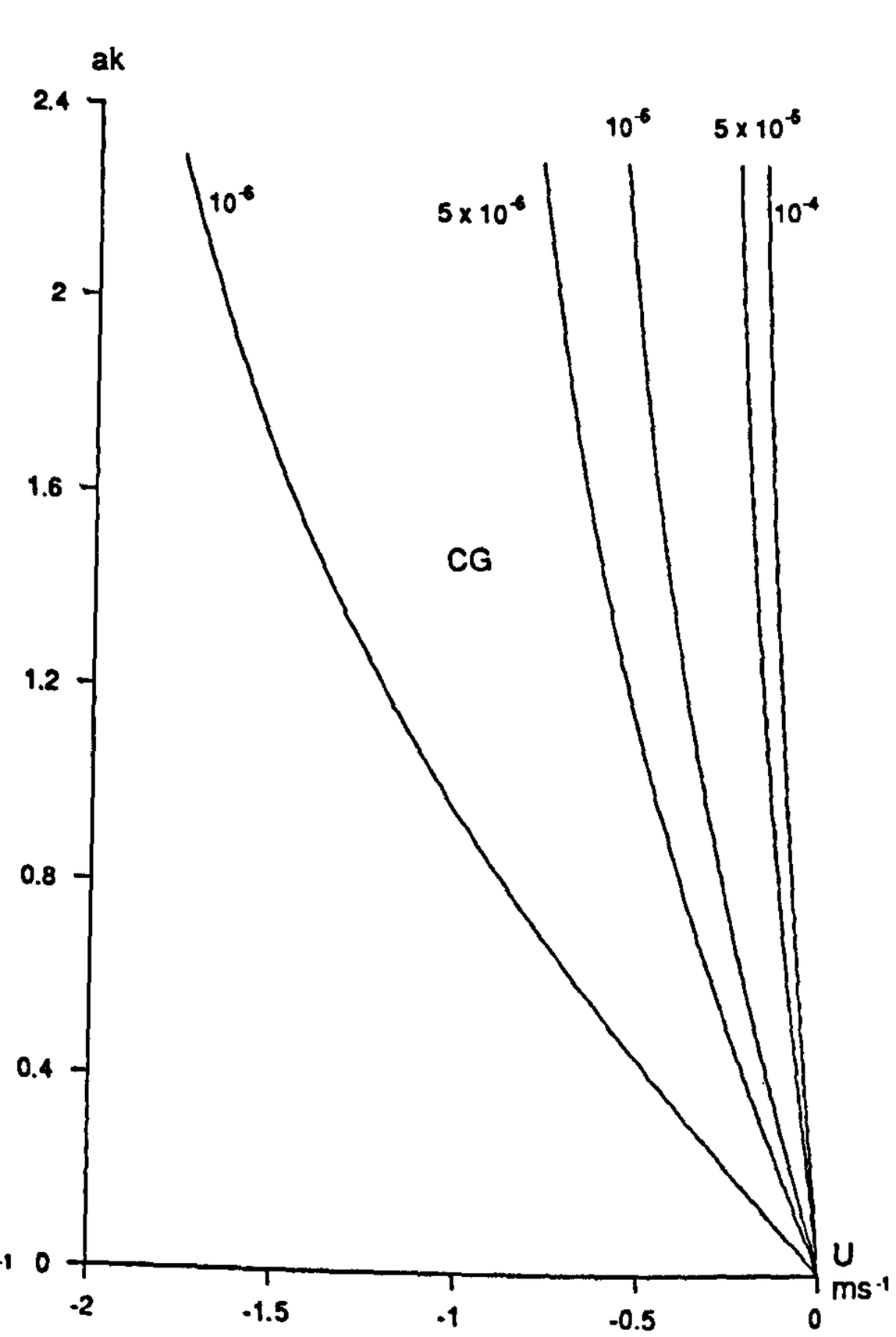

Figure 4.2b

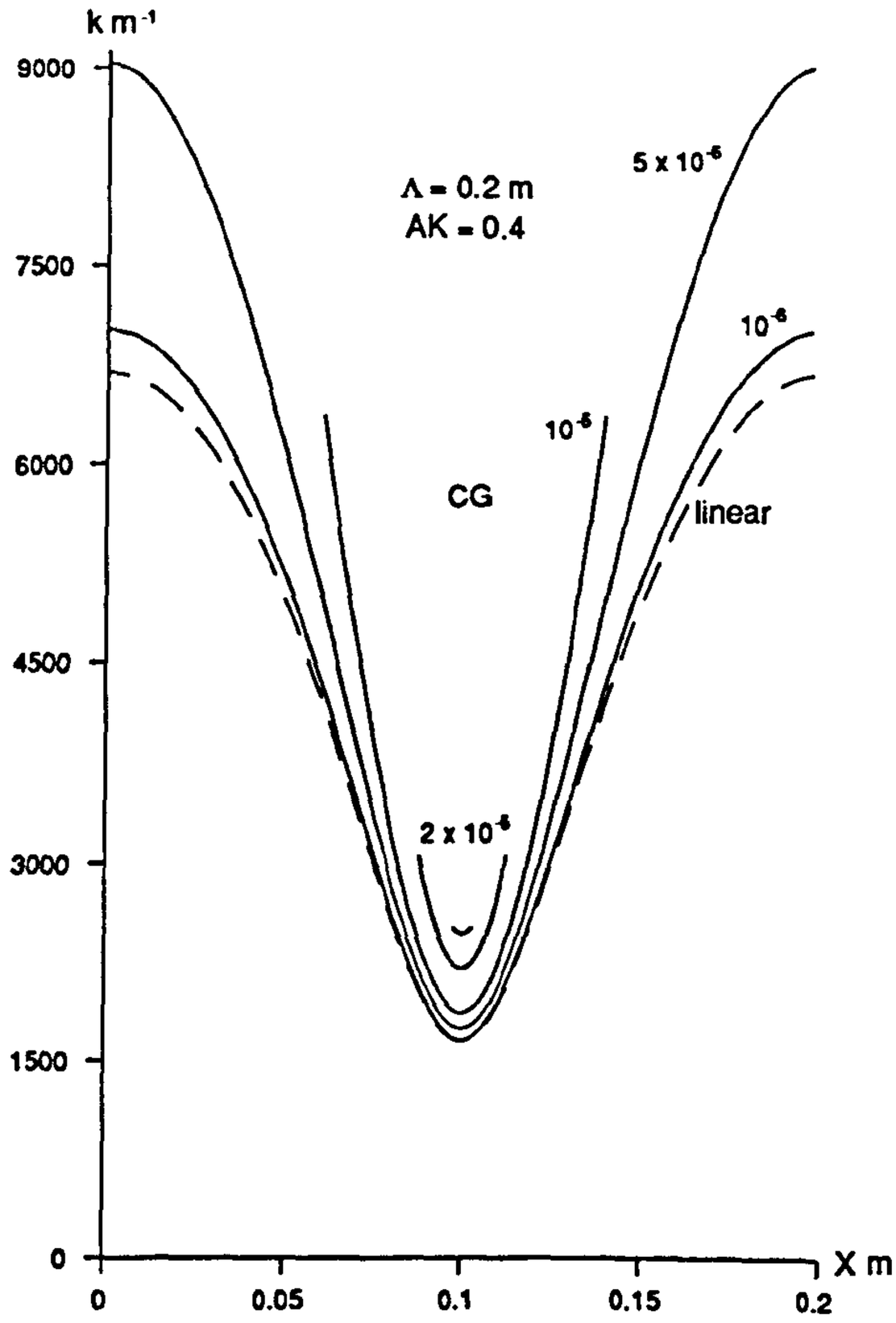

Figure 4.3a

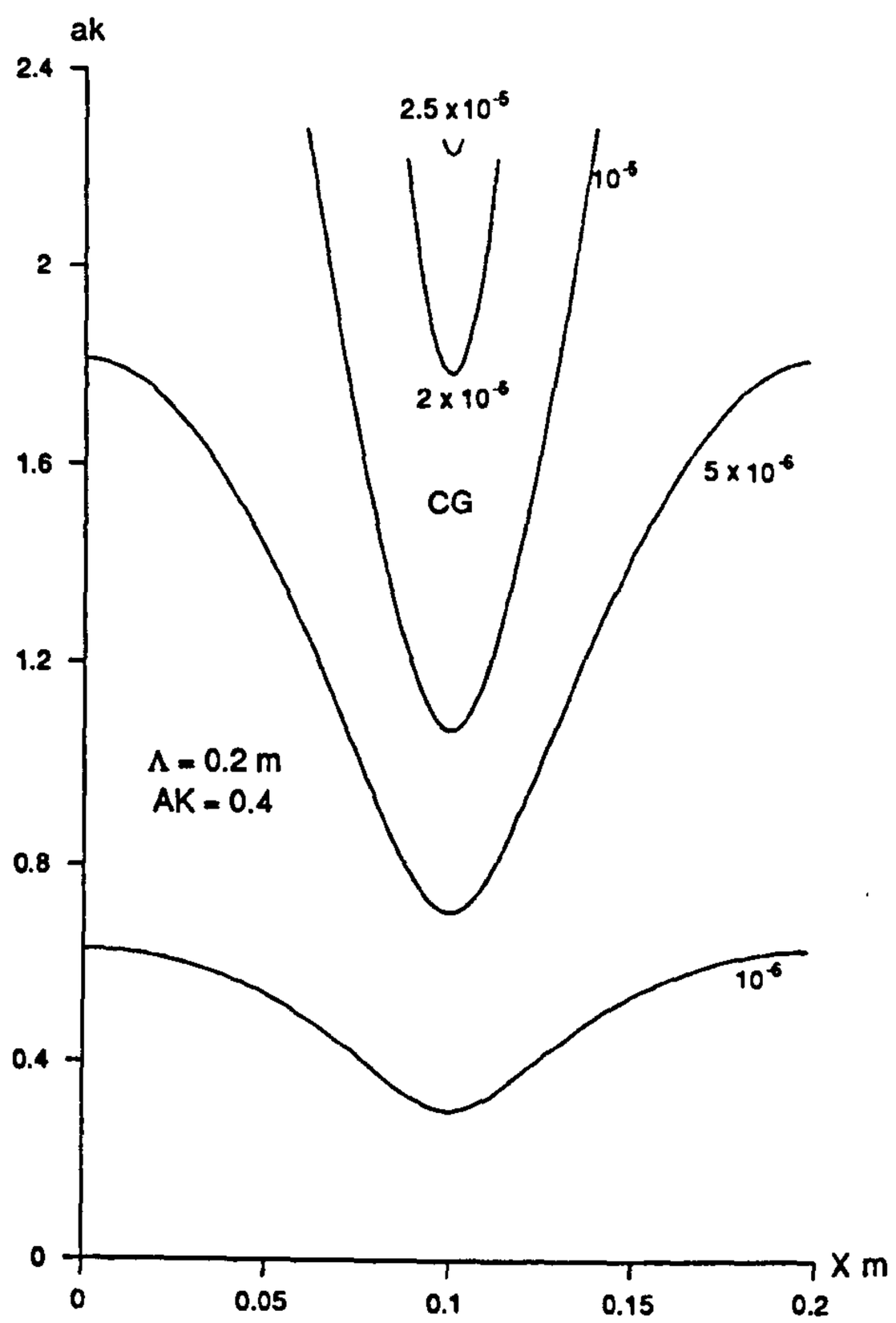

Figure 4.3b

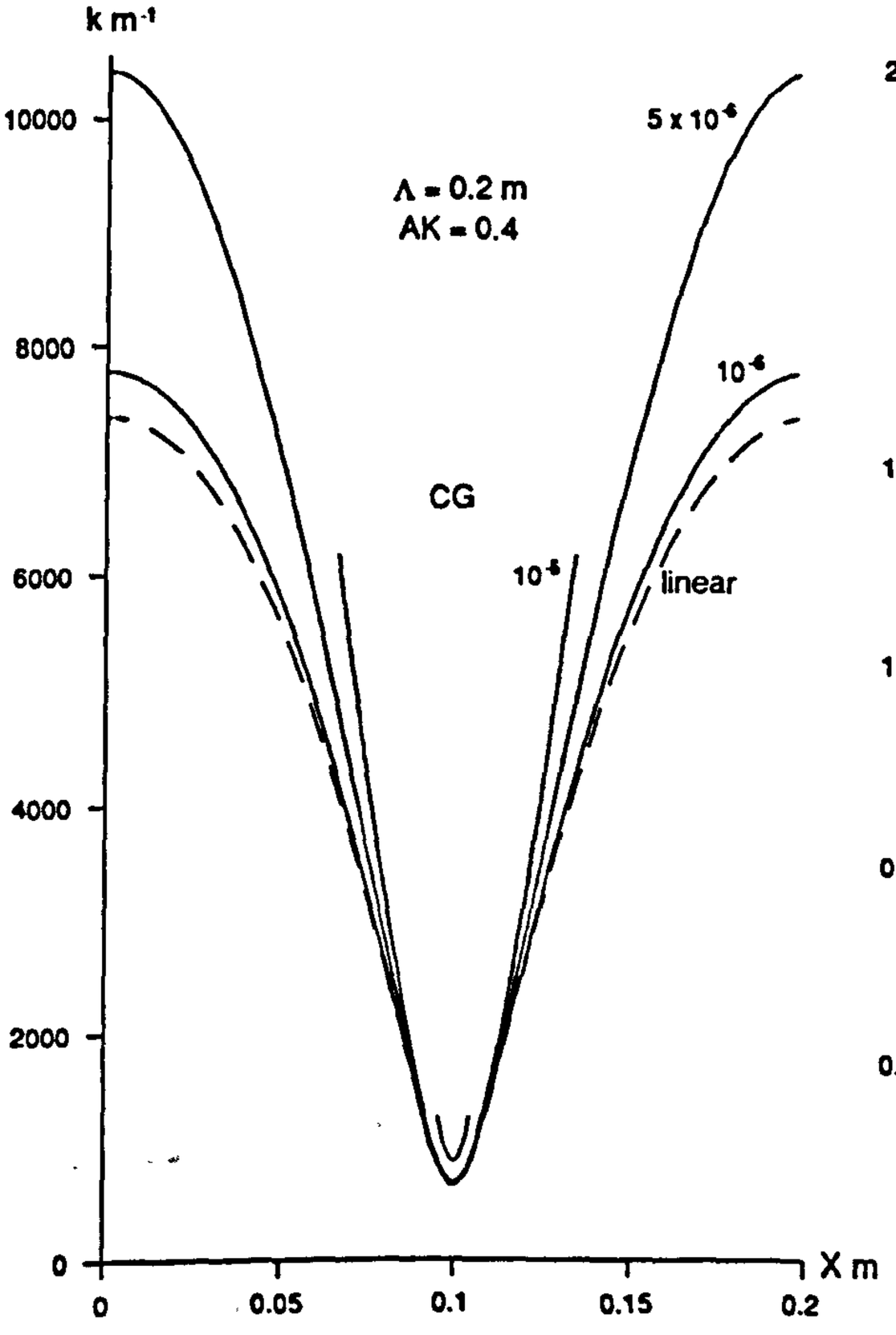

Figure 4.4a

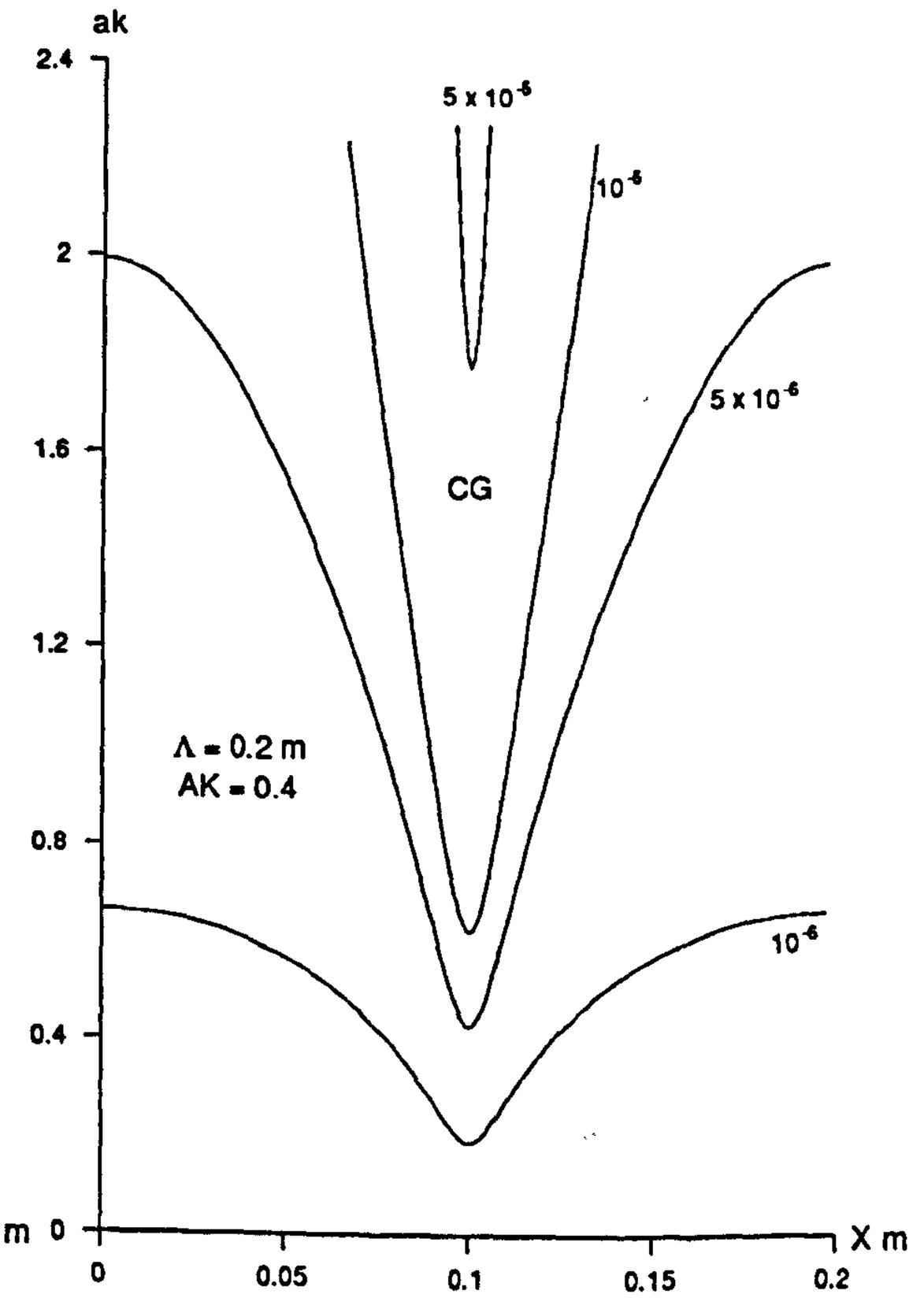

Figure 4.4b

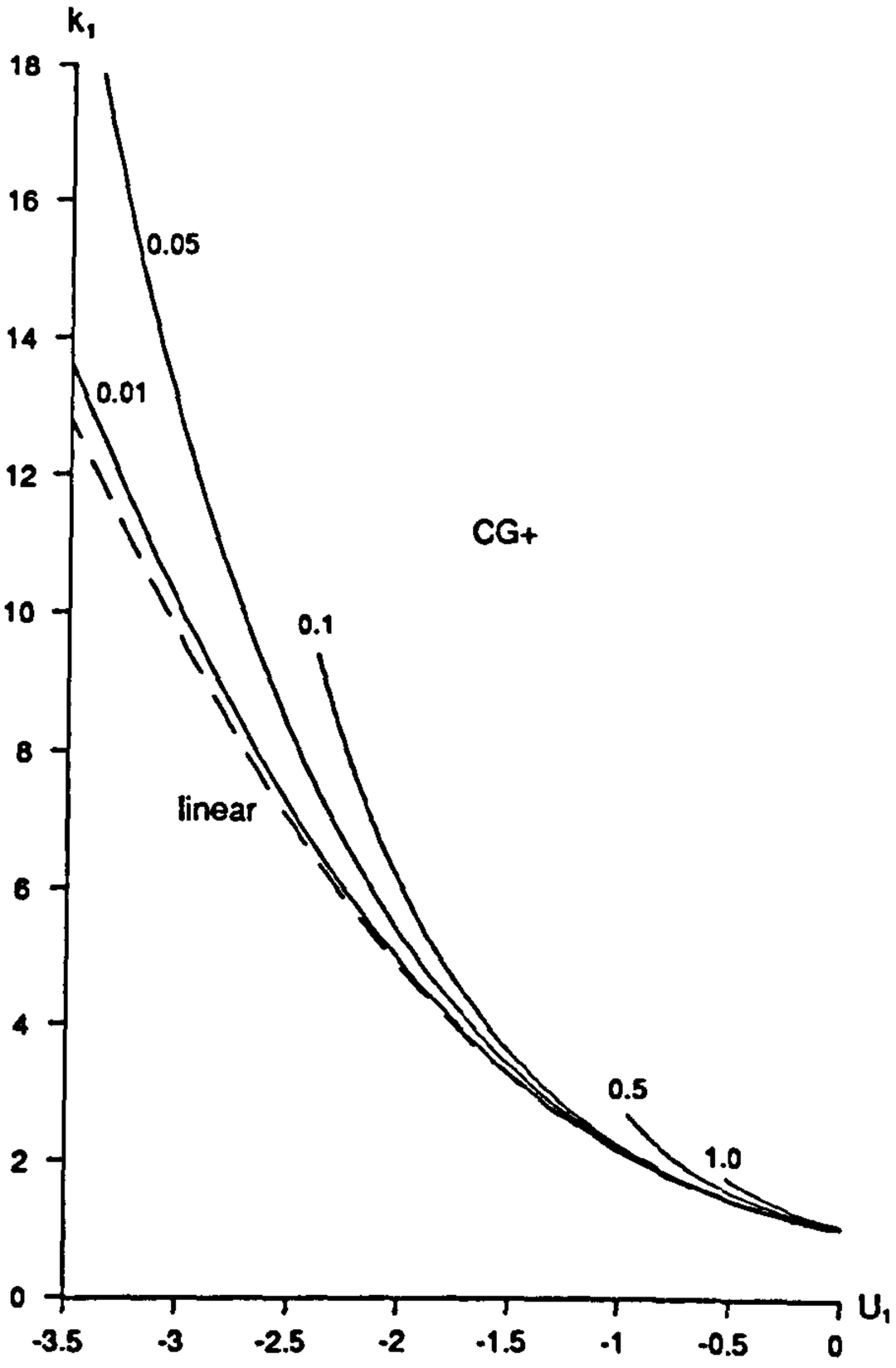

Figure 4.5a

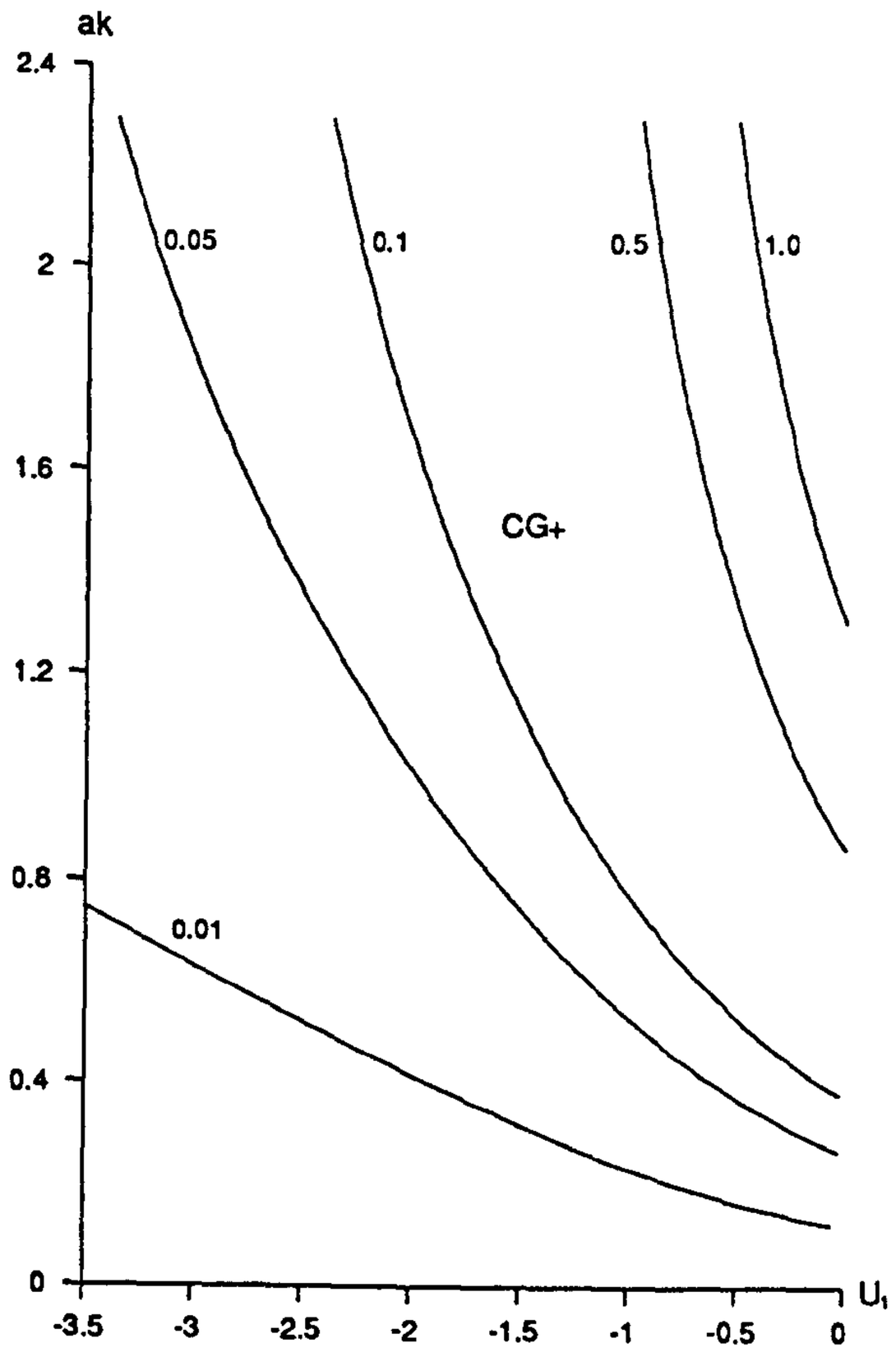

Figure 4.5b

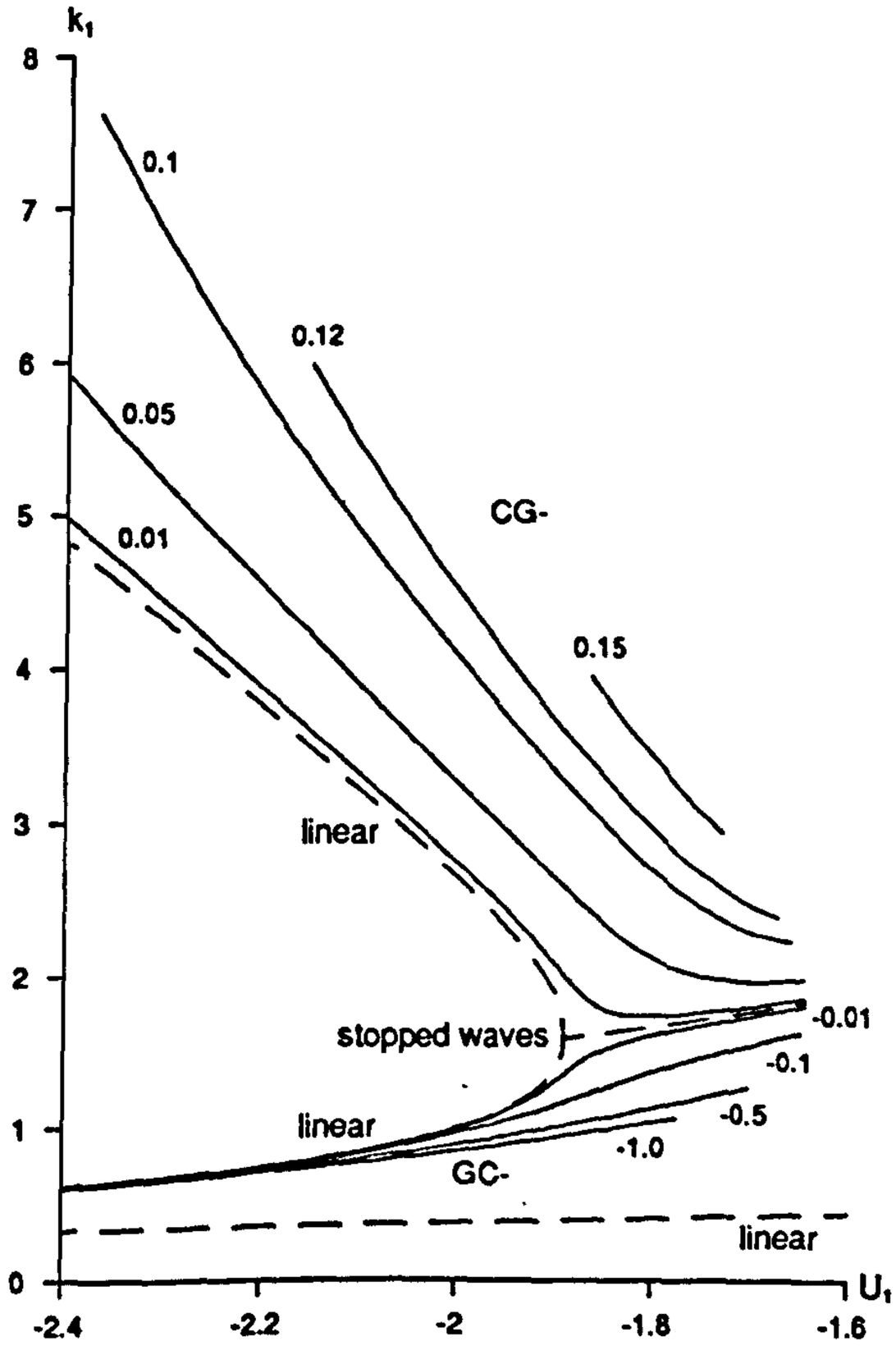

Figure 4.6a

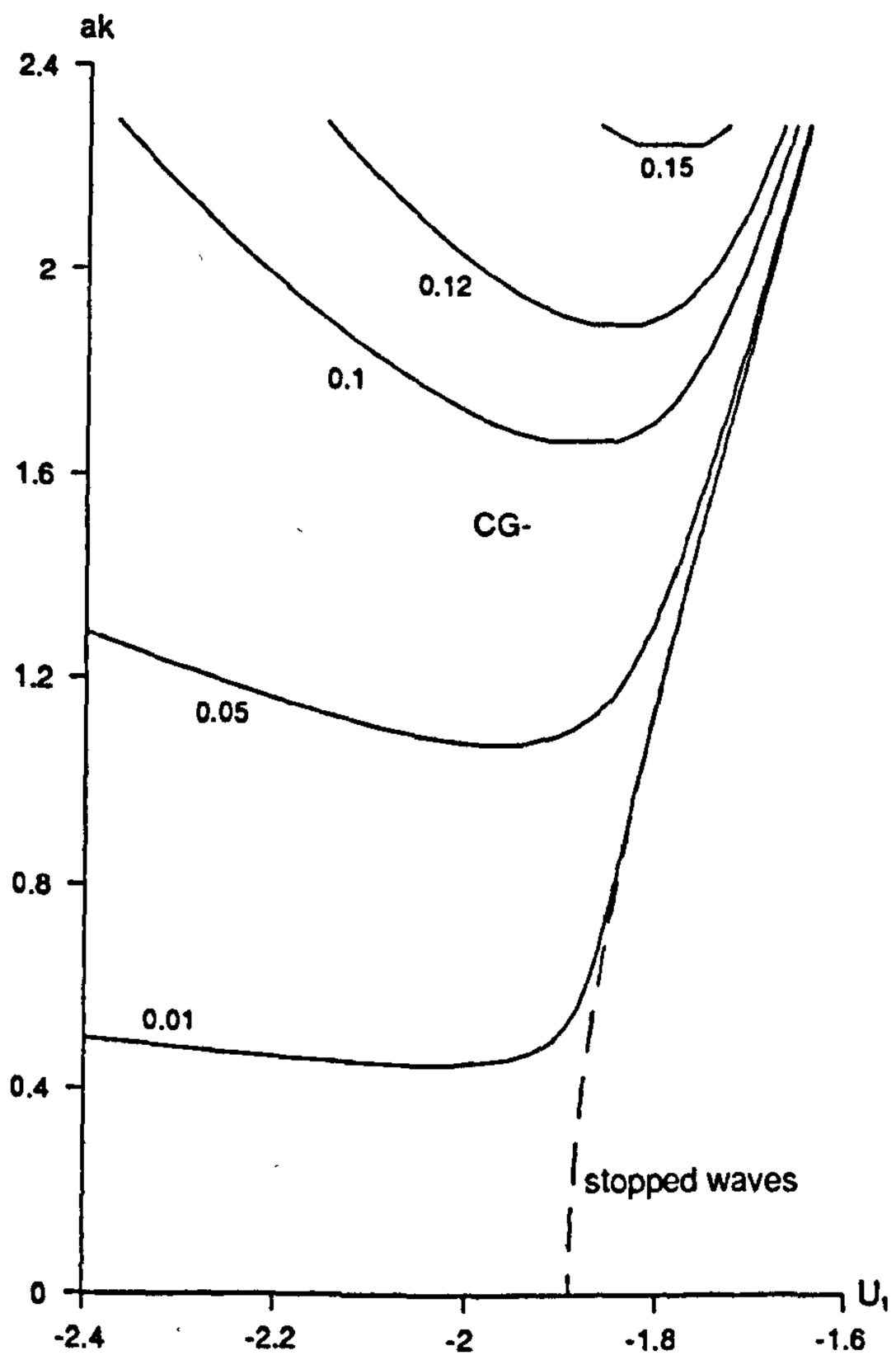

Figure 4.6b

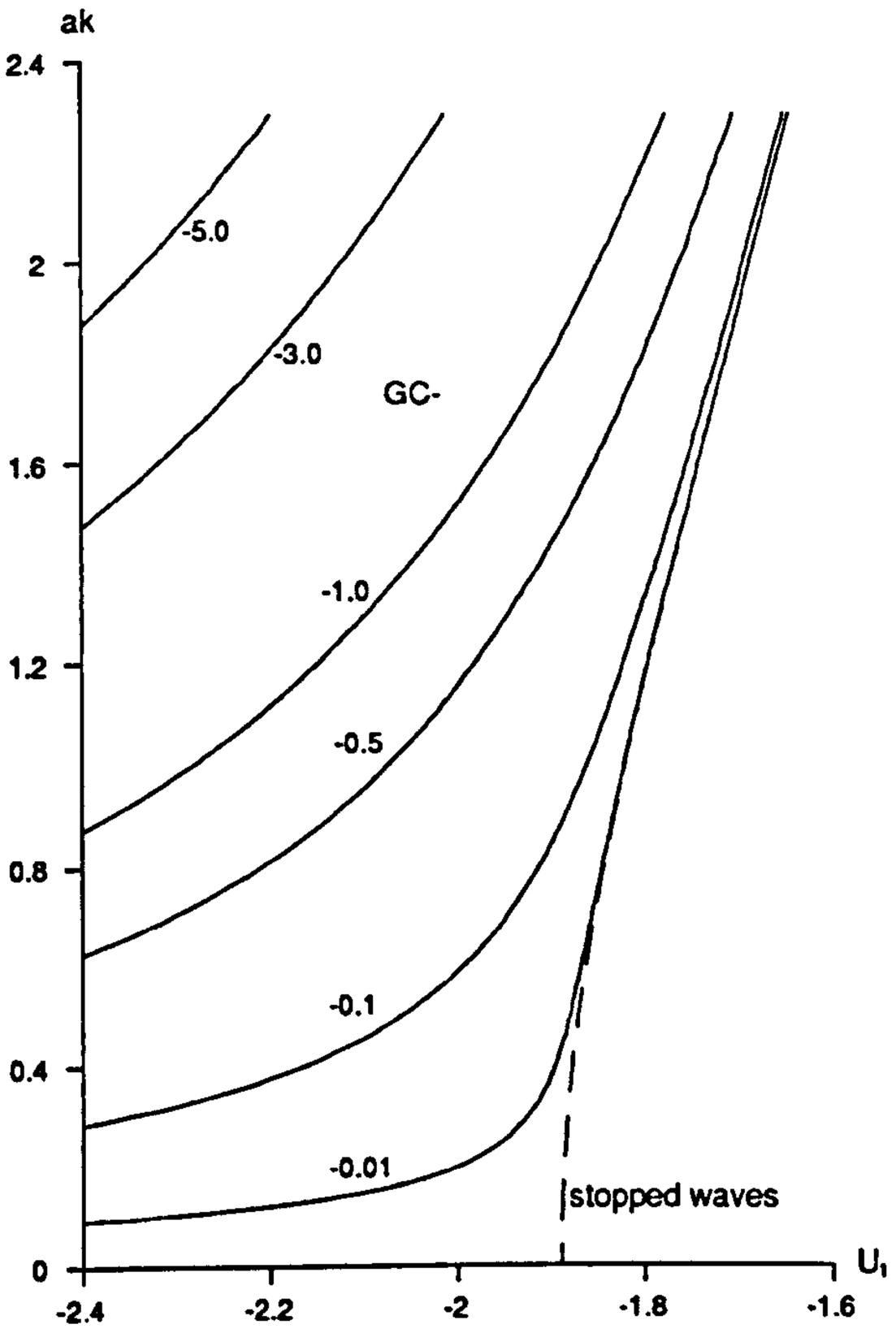

Figure 4.6c

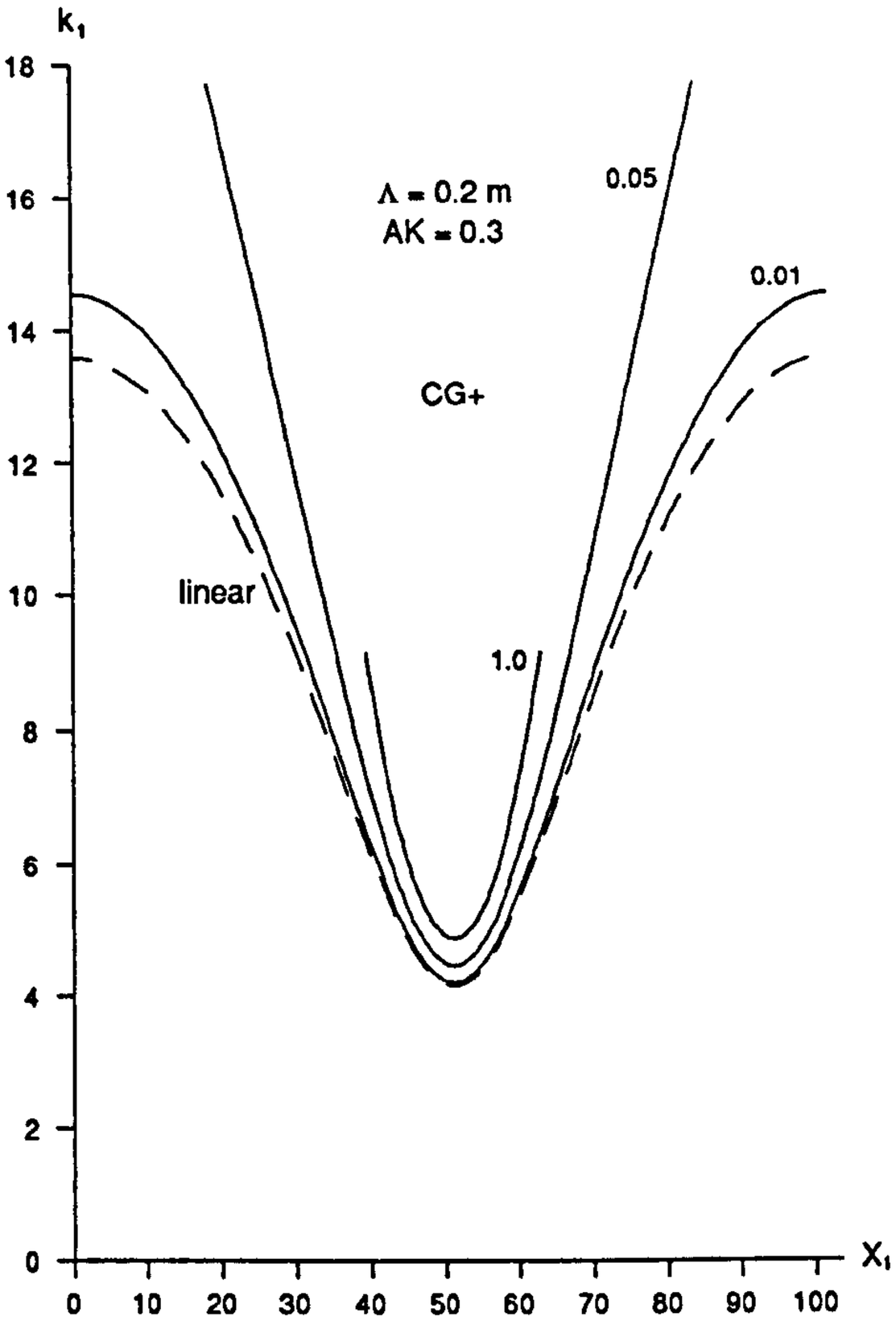

Figure 4.7a

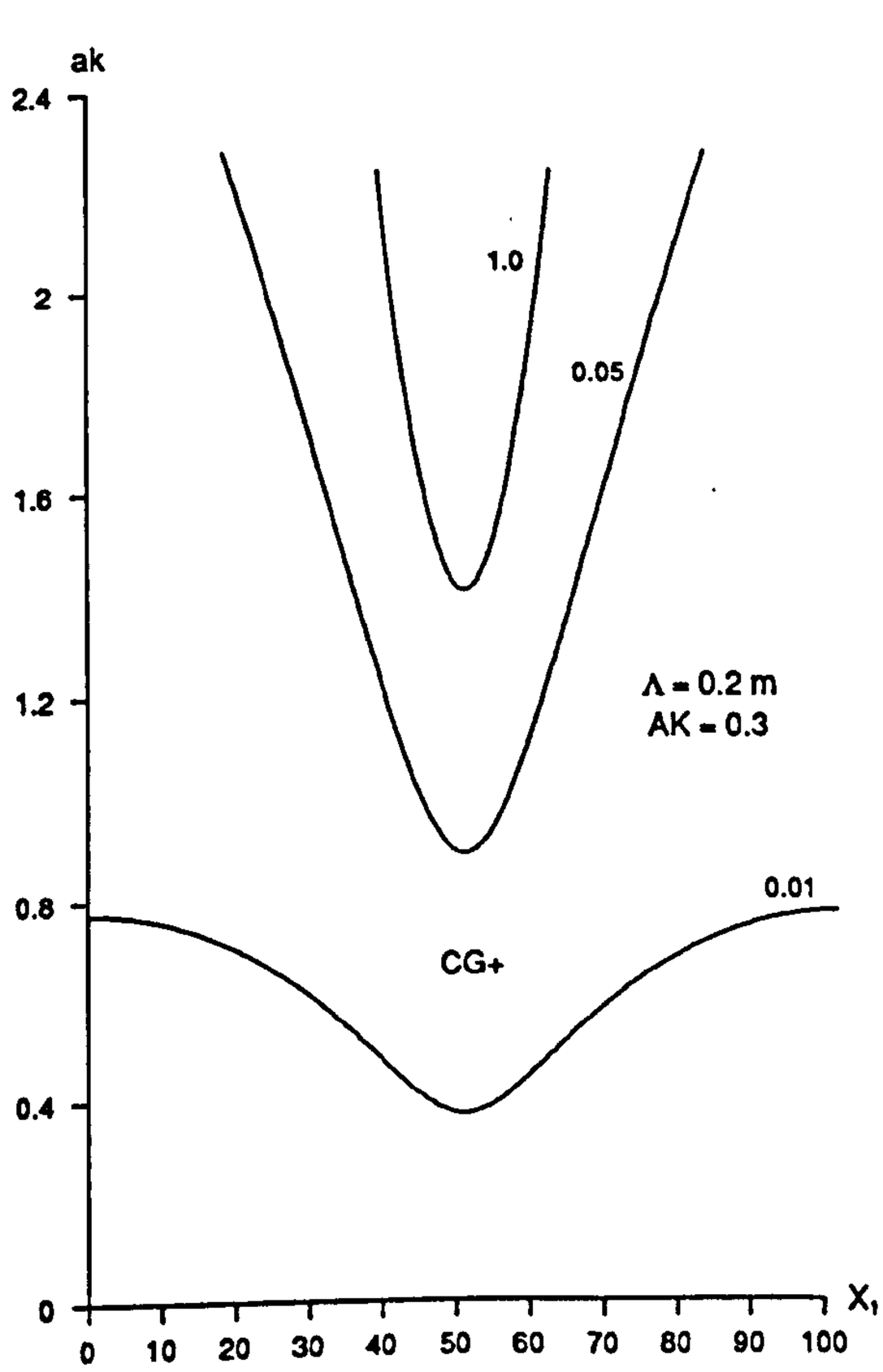

Figure 4.7b

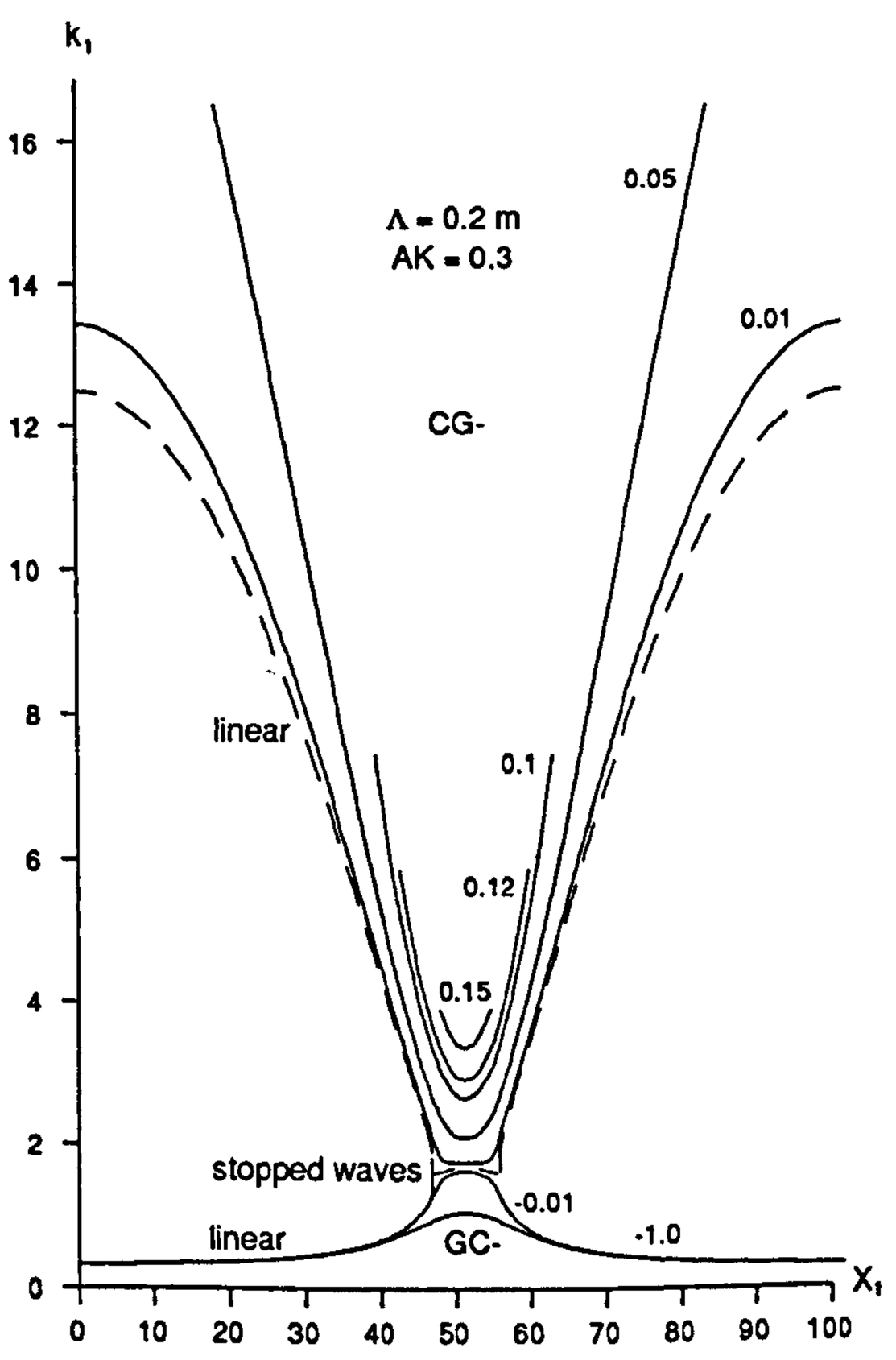

Figure 4.8a

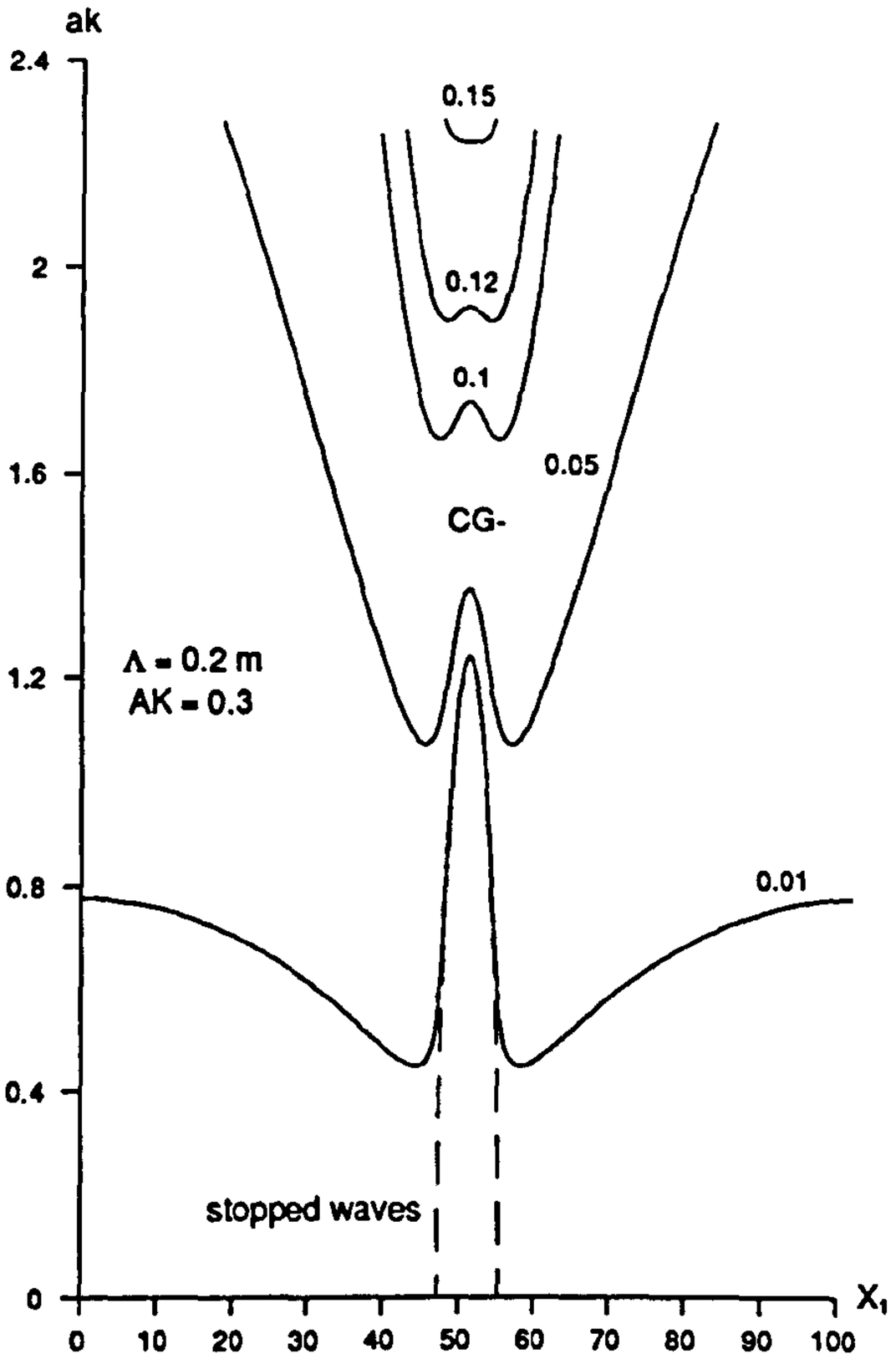

Figure 4.8b

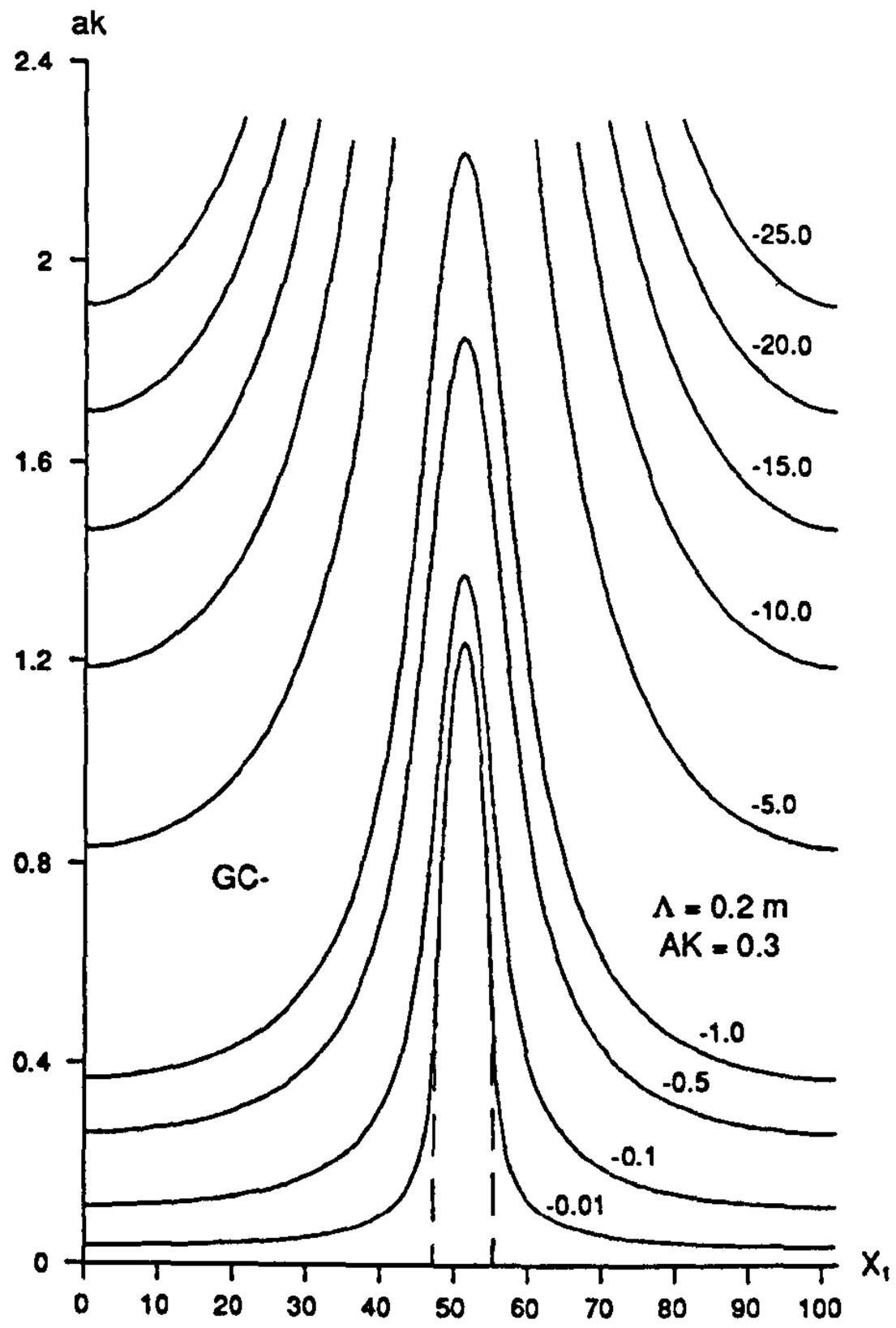

Figure 4.8c

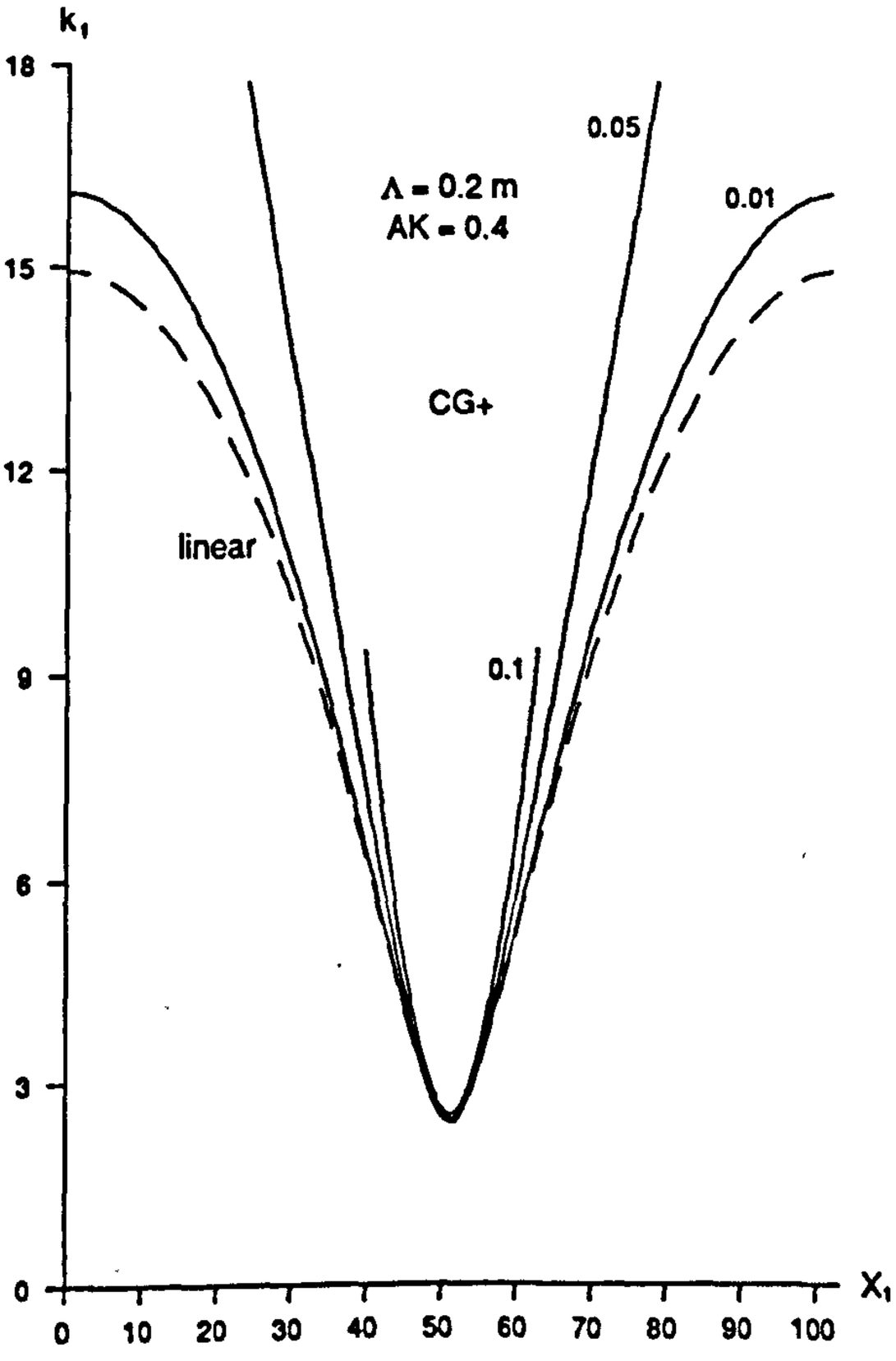

Figure 4.9a

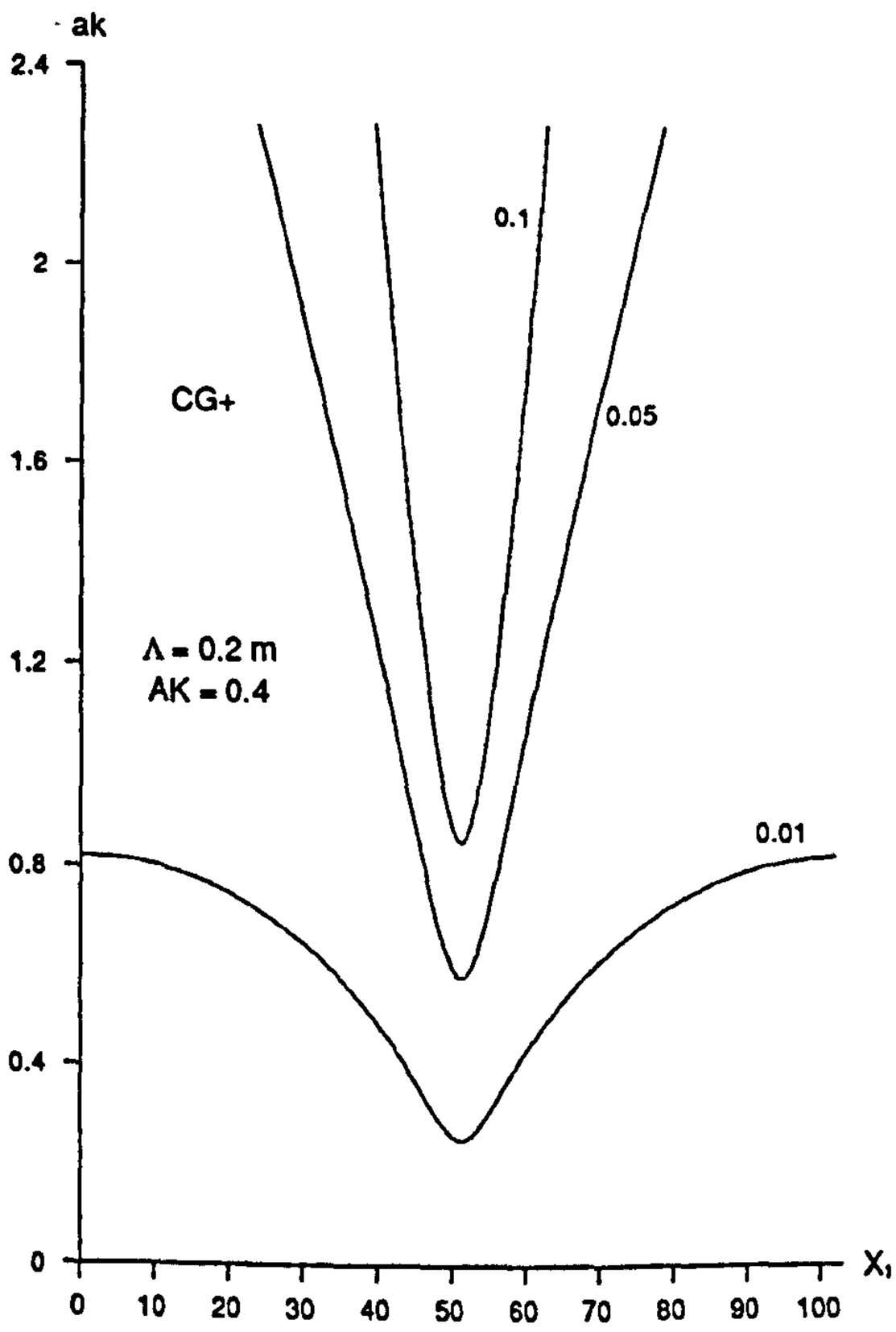

Figure 4.9b

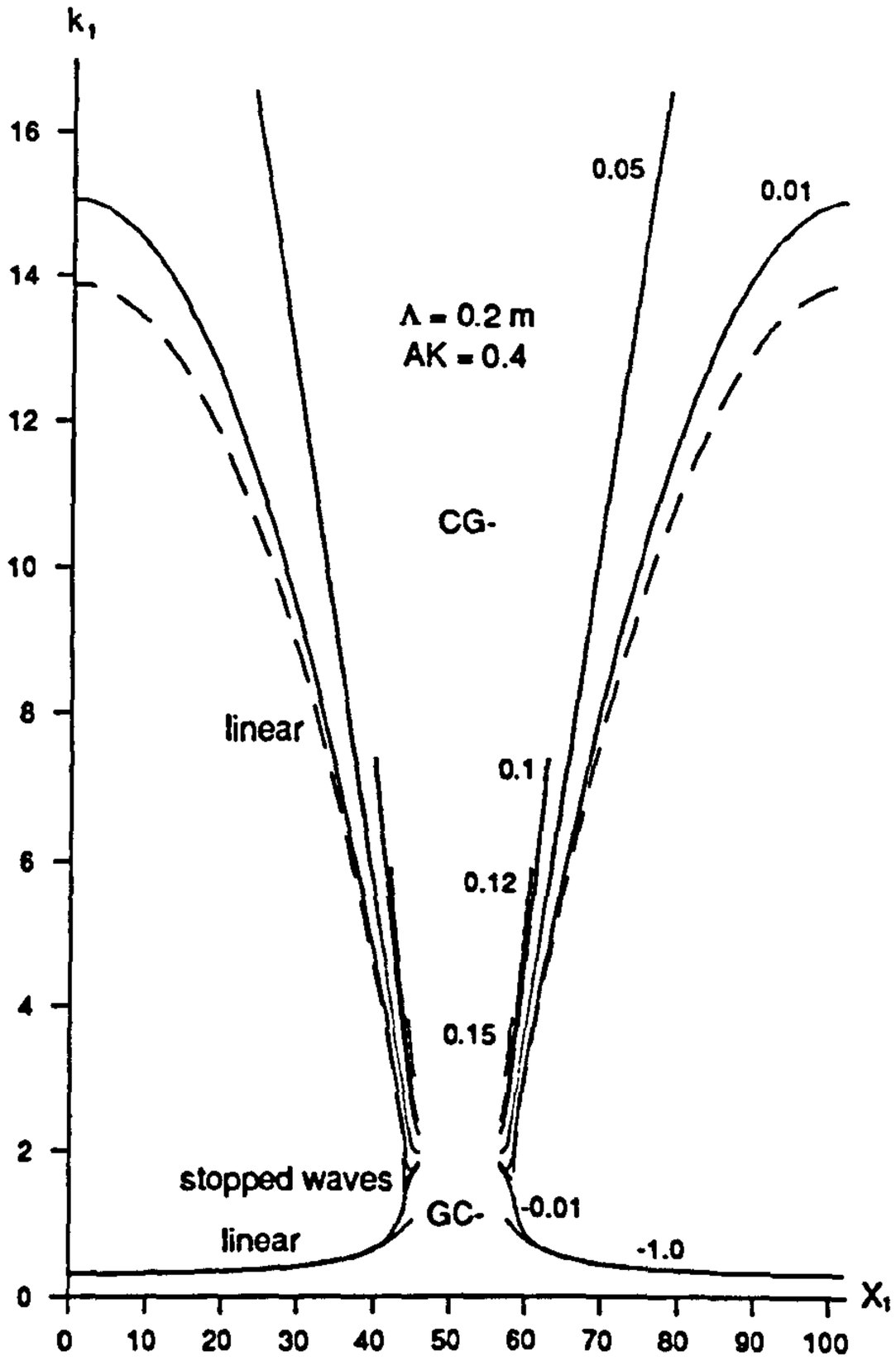

Figure 4.10a

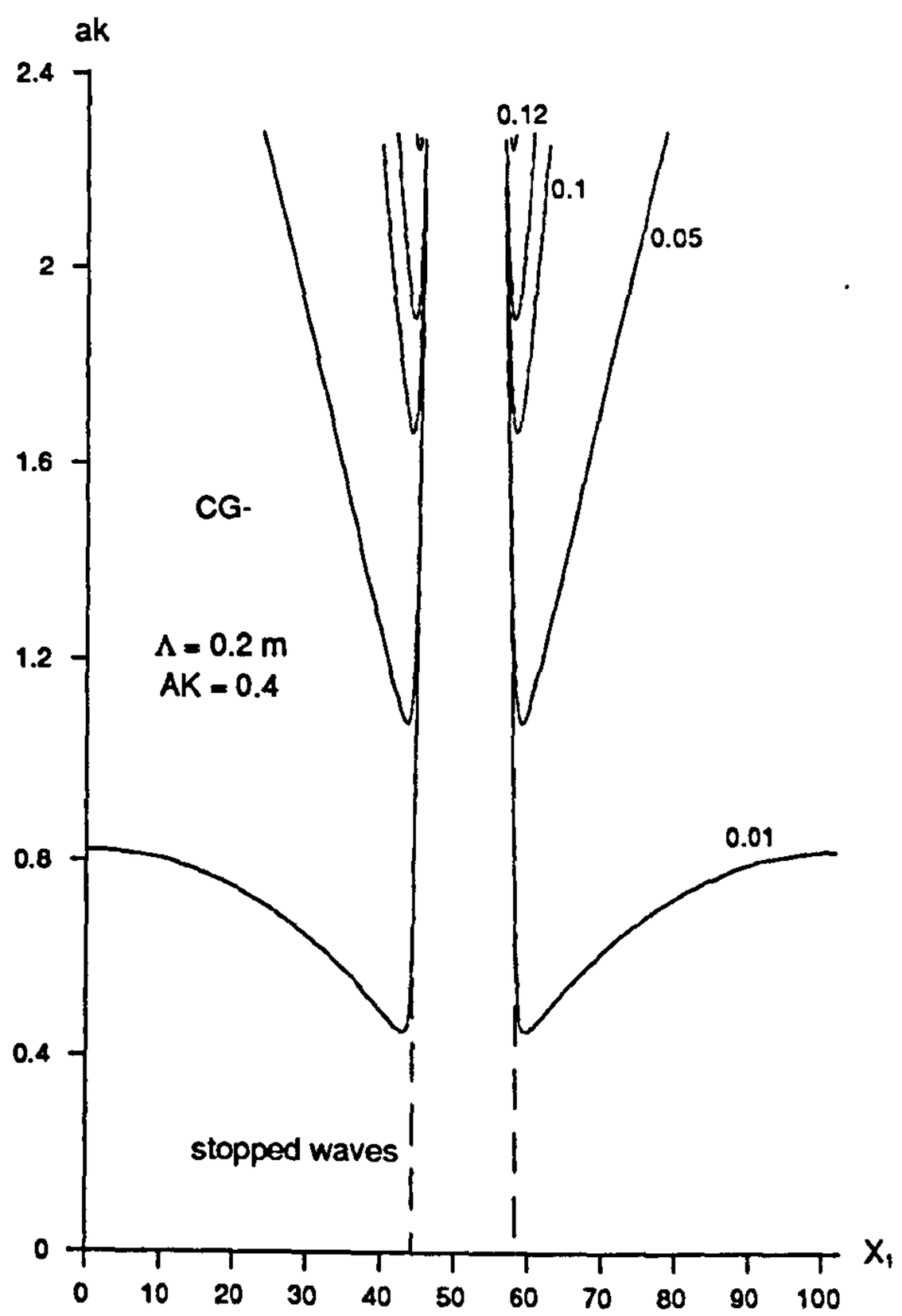

Figure 4.10b

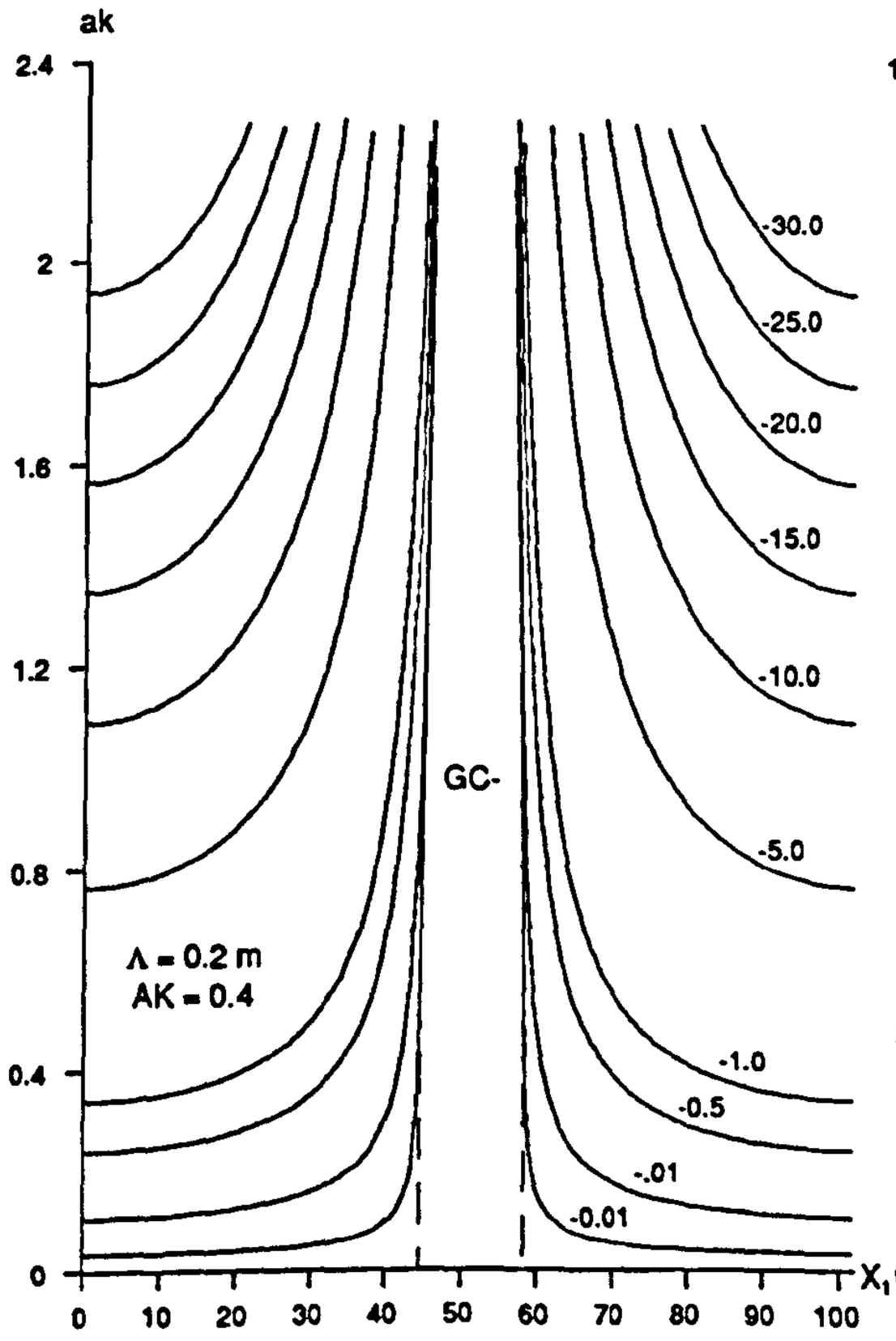

Figure 4.10c

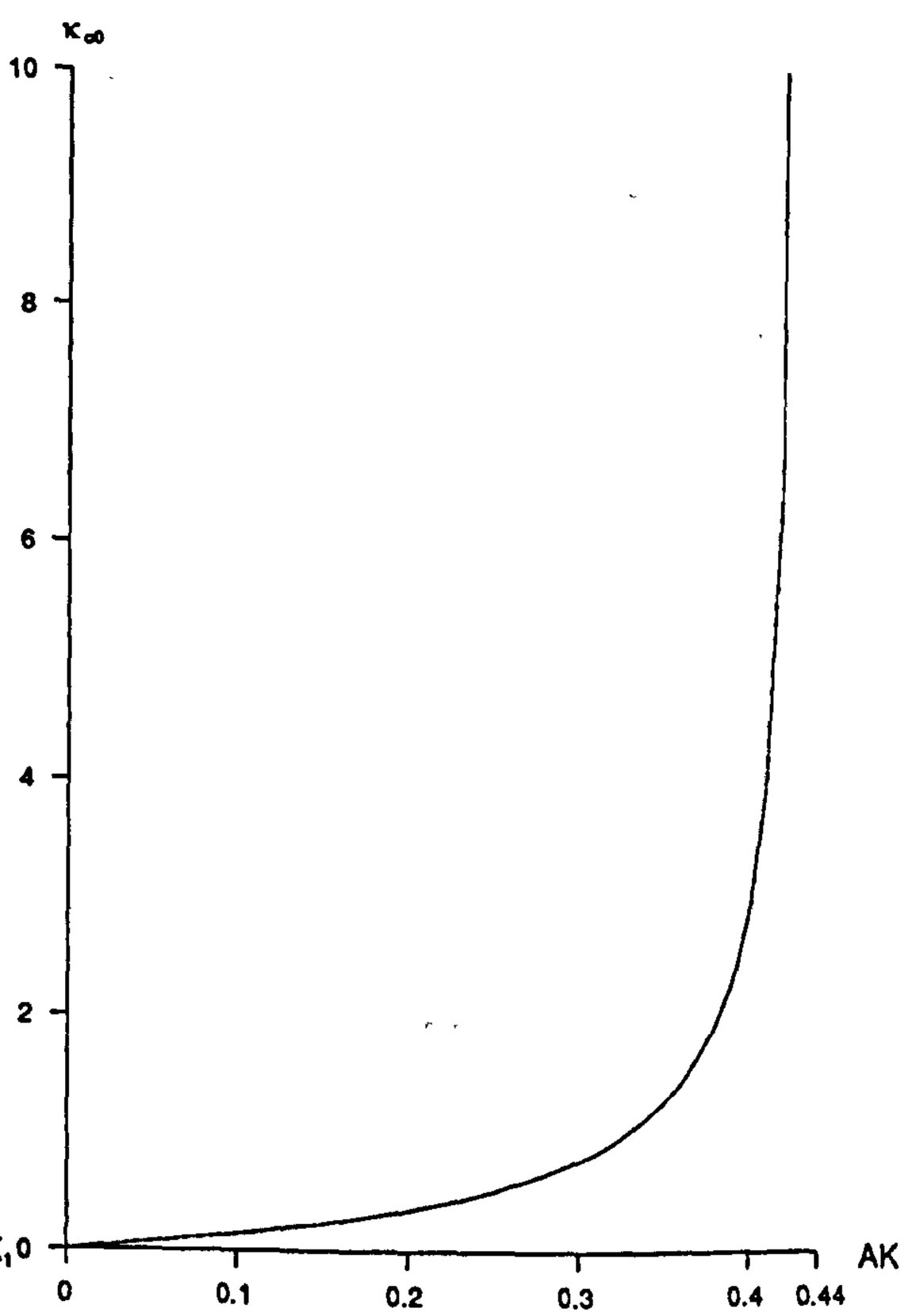

Figure 4.11

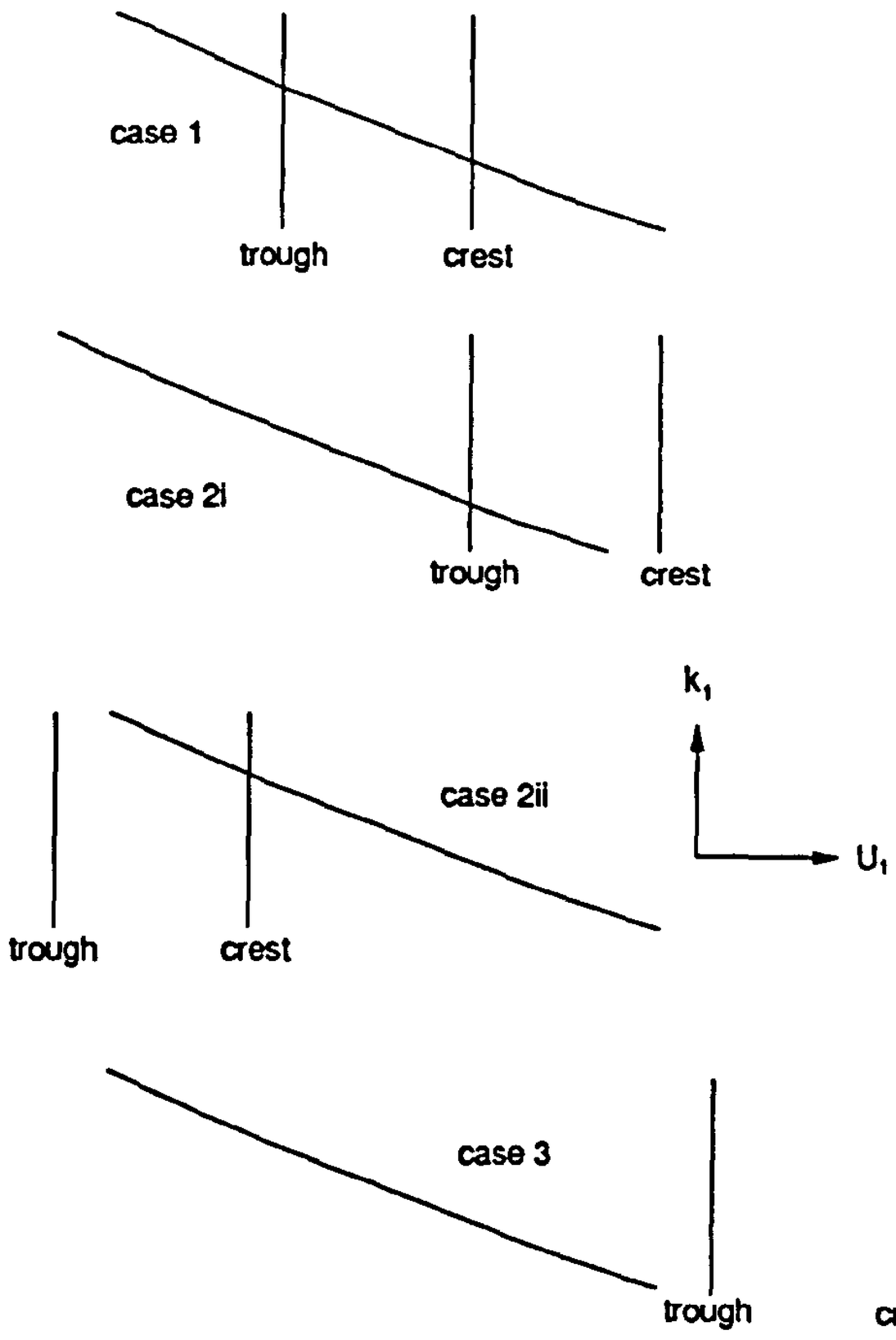

Figure 4.12

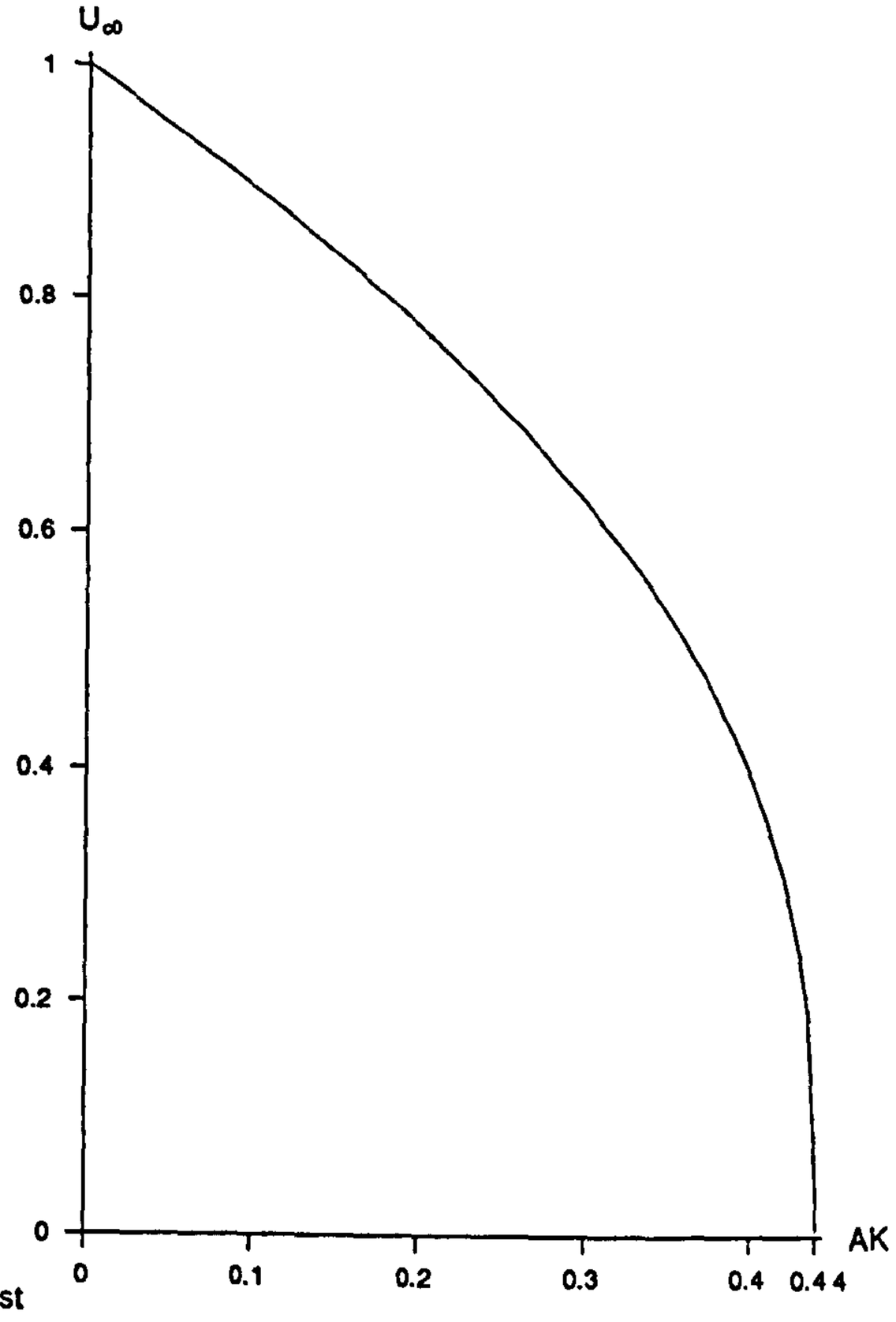

Figure 4.13

Figure 4.14

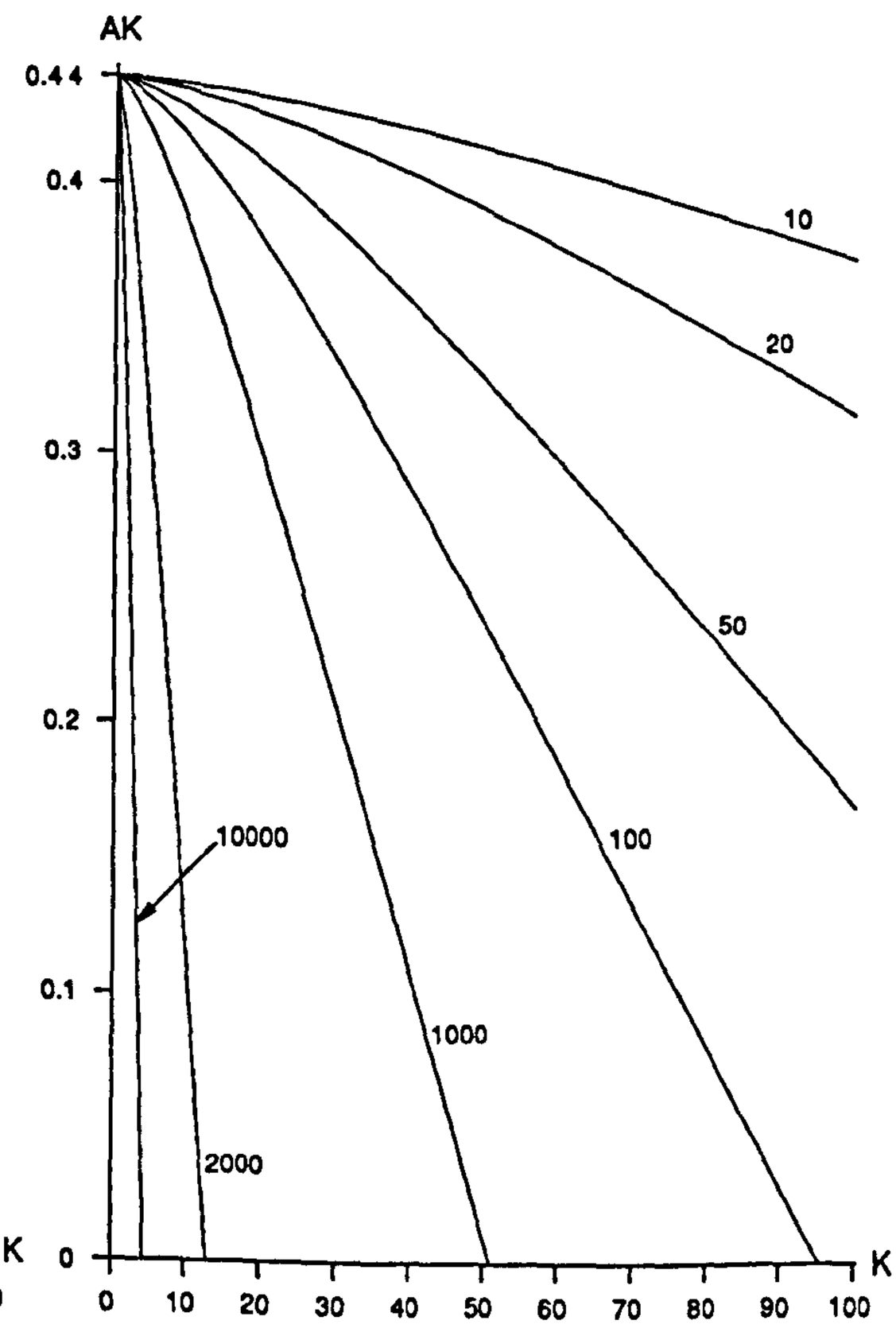

Figure 4.14

Figure 4.15

CHAPTER 5
FINITE-AMPLITUDE PURE CAPILLARY WAVES WITH DISSIPATION AND THE UNIFORM APPROXIMATION THEORY

5.1 Introduction

Chapters 3 and 4 consider the linear and nonlinear interaction and propagation problems respectively. In both these chapters the effects of viscosity are assumed to be negligible. However, from observation it is seen that capillary waves are quickly damped out by viscosity. In this chapter the effects of energy dissipation on nonlinear capillary waves are considered. A dissipation term is added to the averaged energy conservation equation and the subsequent equation derived is solved.

Crapper (1970) includes both energy input and dissipation terms in the averaged energy conservation equation for the case of stationary waves. His energy input term is derived from Longuet-Higgins (1963) hypothesis for the generation of capillary waves near the crests of the gravity waves. Our problem does not address the generation of capillary waves so that no such energy input term is considered. Moreover, the observation that capillary waves may, in fact, be generated at the crest of gravity waves as a result of small scale breaking of the gravity waves would sometimes make the addition of such a term dubious.

As remarked upon in previous chapters the results of slowly-varying theory are most dubious in the neighbourhood of the linear caustic. It is found that similar features exist for the slowly-varying dissipative problem. Consequently, a uniform near-linear Schrödinger approximation in the neighbourhood of the linear caustic is used in order to examine the validity of the slowly-varying results. A nonlinear Schrödinger equation (NLS equation) is derived which includes the effects of linear (first order) dissipation. Peregrine and Smith (1979) outline the heuristic development of such an NLS equation and Rosales (1978) gives details of the standard method of solution employed. This aids in forming an overall view of the behaviour of the wave field and, thus, concluding the infinite depth propagation problem.

In section 5.2 the general form of the dissipative averaged energy conservation equation is discussed and a dissipation term is added to this equation. It is shown in section 5.3 that the averaged energy conservation equation and the wave-action conservation equation are analytically equivalent when dissipation is negligible. In section 5.4 the numerically solved equation is derived and the generation of initial

conditions is discussed. The special case of no gravity waves, i.e. U = 0, is considered analytically in section 5.5. The cases of stationary and Doppler shifted waves are considered in section 5.6 and 5.7 respectively. The uniform NLS equation is derived and discussed in section 5.8 with subsequent results given in section 5.9. In section 5.10 a general discussion of the overall wave field is undertaken and certain conclusions are made relating to actual observations.

5.2 The Dissipative Averaged Energy Equation

When waves in a slowly-varying wave field are dissipating energy the total wave-action flux $U\mathcal{A} + \mathcal{B}$ is no longer constant. The effects of dissipation on the wave-action conservation equation (2.4.9) are not immediately clear. This question is examined further in § 5.3 and fully answered later in chapter 7. In order to consider such effects the averaged energy conservation equation (2.6.4) for the wave motion, with a term added for dissipation, must be used. This states

$$\frac{d}{dx}\left(U\mathcal{E} + \mathcal{F}\right) + \mathcal{S}\frac{dU}{dx} = -\mathcal{D} \qquad (5.2.1)$$

where $\mathcal{D}$ is mean rate of energy dissipation and $\mathcal{S} = \mathcal{S}_{11}$ is the "11"-component of the radiation stress. The validity of this form of the averaged energy conservation equation is shown later in chapter 7 but is intuitively obvious. Note that the addition of dissipative effects means that the wave-current interaction problem can no longer be considered since the distance coordinate x is present in the equations ab initio. Consequently, only the wave propagation problem is considered.

As the propagation problem is in consideration the velocity variables P and Q, defined by (4.4.1), are used. The left hand side of equation (5.2.1) is considered first. Expressions for $\mathcal{E}$, $\mathcal{F}$ and $\mathcal{S}$ are found using the expressions (2.5.8 - 2.5.10) for these parameters in terms of the four "basic" mean wave properties. Note that V^E and the mean bottom velocity squared are both zero. Use of expression (4.2.7) for T, the dispersion relation (4.4.2) for D in terms of P and Q and noting $V = V^T$ it follows that

$$\mathcal{E} = \frac{\tau}{\beta PQ^2}\left(1 - \beta PQ^2\right)\left(3 + \beta PQ^2\right), \quad \mathcal{F} = 3\frac{\tau}{\beta PQ}\left(1 - \beta^2P^2Q^4\right) \qquad (5.2.2)$$

$$\mathcal{S} = 2\frac{\tau}{\beta PQ^2}\left(1 - \beta PQ^2\right)\left(1 + 2\beta PQ^2\right). \qquad (5.2.3)$$

Then, using the Doppler relation (4.4.2) to eliminate U, the averaged energy conservation equation (5.2.1) gives

$$\frac{d}{dx}\left[\tau\,\frac{(1-\beta PQ^2)}{\beta Q^2}\,[3+\beta Q^2(P+2Q)]\right]$$

$$+\,2\,\frac{\tau}{\beta PQ^2}\,(1-\beta PQ^2)(1+2\beta PQ^2)\left[\frac{dP}{dx}-\frac{dQ}{dx}\right]=-\,\mathcal{D}\,. \qquad (5.2.4)$$

The right hand side of equation (5.2.1) is now considered. An expression for the dissipation term $\mathcal{D}$ is found using a result quoted in both Batchelor (1967, § 5.14) and Lamb (1932, § 329). They show that for an irrotational liquid motion

$$\mathcal{D}=\frac{\mu}{\lambda}\int_0^{\lambda}\frac{\partial}{\partial x_i}(q^2)\;n_i\;ds \qquad (5.2.5)$$

where μ is the viscosity of the liquid, q is the velocity at the surface of the waves, n_i is a unit vector directed outward and normal to the plane of the surface and ds is a length element along the surface of the waves. The expression (5.2.5) can also be used to derive a finite depth dissipative term as is done later.

Crapper (1970) finds the expression for the dissipation term $\mathcal{D}$ corresponding to finite-amplitude pure capillary waves on a liquid of infinite depth using the solution given in § 4.2. In our notation

$$\mathcal{D}=\frac{4\mu}{s\beta^5}\,\frac{1}{P^5Q^5}\,(1-\beta^2P^2Q^4)(3-\beta^2P^2Q^4)\;. \qquad (5.2.6)$$

This expression has been verified by the author.

Linearisation of both $\mathcal{D}$, in terms of Crapper's parameter A, and expression (4.2.3), for the parameter A in terms of wave steepness ak, leads to

$$\mathcal{D}_{lin}=2\mu sk^4a^2+O(a^4k^4) \qquad (5.2.7)$$

which agrees with the expression in Lamb (1932, § 348). It follows that

$$\frac{\mathcal{D}}{\mathcal{D}_{lin}}=\frac{1}{8D^3}\,(1+D^2)(3-D^2)\;. \qquad (5.2.8)$$

Figure 5.1 shows the variation of $\mathcal{D}/\mathcal{D}_{lin}$ with wave steepness ak. It is seen that $\mathcal{D}/\mathcal{D}_{lin}$ is a monotonic increasing function of steepness ak, i.e. as the steepness of the waves increases the rate of dissipation of energy also increases, as would be expected. It is also seen that the rate of change of $\mathcal{D}/\mathcal{D}_{lin}$ increases as steepness ak increases.

5.3 A Wave-Action Conservation Equation with Dissipation

Our aim in this section is to derive a wave-action conservation equation with terms added to account for the effects of dissipation. From the expression (2.5.11) for the wave-action density $\mathcal{A}$ in term of the kinetic energy density T it is seen that the difference between energy type terms and wave-action type terms is a factor of σ. Thus, dividing the energy conservation equation by σ should give a wave-action conservation type equation. Now, using definitions (4.4.1) for P and Q,

$$\sigma = \frac{Q}{s\beta P} \tag{5.3.1}$$

so that, on division by σ, the energy conservation equation (5.2.4) gives

$$\frac{\tau s P}{Q}\frac{d}{dx}\left[\frac{3}{Q^2} + \beta\, 2(Q-P) - \beta^2\, PQ^2(P+2Q)\right]$$

$$+ \tau s\left[\frac{2}{Q^3} + \beta\, 2\,\frac{P}{Q} - \beta^2\, 4P^2Q\right]\left[\frac{dP}{dx} - \frac{dQ}{dx}\right] = -\,\beta\,\frac{s\mathcal{D}P}{Q}\,. \tag{5.3.2}$$

The expression (4.4.5) for the total wave-action flux $U\mathcal{A} + B$ suggests that if a wave-action conservation type equation is to be derived then terms of order β^0 and β^2 should collect together but terms of order β should cancel. Collecting terms of similar order in β gives

$$\beta^0 \qquad \frac{P}{Q}\frac{d}{dx}\left[\frac{3}{Q^2}\right] + \frac{2}{Q^3}\left[\frac{dP}{dx} - \frac{dQ}{dx}\right] = \frac{d}{dx}\left[\frac{2P+Q}{Q^3}\right]\,, \tag{5.3.3}$$

$$\beta^1 \qquad 2\,\frac{P}{Q}\frac{d}{dx}(Q-P) + 2\,\frac{P}{Q}\left[\frac{dP}{dx} - \frac{dQ}{dx}\right] = 0\,, \tag{5.3.4}$$

$$\beta^2 \qquad \frac{P}{Q}\frac{d}{dx}\left[-\,PQ^2(P+2Q)\right] - 4P^2Q\left[\frac{dP}{dx} - \frac{dQ}{dx}\right]$$

$$= -\,\frac{d}{dx}\left[P^2Q(2P+Q)\right] \tag{5.3.5}$$

as is required. Thus, it immediately follows that

$$\frac{d}{dx}(U\mathcal{A} + B) = -\,\frac{\mathcal{D}}{\sigma}\,. \tag{5.3.6}$$

Therefore, when the viscosity μ of the liquid is zero, i.e. $\mathcal{D} = 0$, the energy conservation equation (5.2.1) and the wave-action conservation equation (5.3.6) must give the same results. Note that this is proof only for the special case of two dimensional finite-amplitude pure

capillary waves on infinite depth liquid. A general approach for any slowly-varying wave system is undertaken later in chapter 7. It follows that the energy conservation equation (5.2.1) and the wave-action conservation equation (5.3.6) are interchangeable.

5.4 The Numerically Integrated Equation and "Windows"

The behaviour of $\mathcal{E}$, $\mathcal{F}$, $\mathcal{S}$, described in Hogan (1979), and $\mathcal{D}$ with steepness ak (figure 5.1) suggest that the equation (5.2.4) will not be stiff. Thus, a numerical integrating package (NAG LIB D02CBF) for non-stiff systems is used. This package uses a variable-order variable-step Adams method. This requires the equation to be solved, in our case the energy conservation equation, to be written in the form

$$\frac{dP}{dx} = f(x,P) \quad . \tag{5.4.1}$$

After a little algebra the energy conservation equation (5.2.4) gives

$$\frac{dP}{dx} = \frac{M + N}{W} \quad . \tag{5.4.2}$$

where $M = \frac{4\mu}{\tau S \beta^4} \frac{1}{P^4(P - U)^3} [1 - \beta^2 P^2 (P - U)^4][3 - \beta^2 P^2 (P - U)^4]$,

$$N = 2[4P - U + \beta^2 P^2 (P - U)^4 (2P - U)] \frac{dU}{dx}$$

and $$W = 6P + 2\beta^2 P (P - U)^4 [(3P - U)^2 - 3P^2] \quad .$$

In equation (5.4.2) x is a curvilinear coordinate on the surface of the gravity waves (figure 2.2) but the surface data for the gravity waves is known in terms of the horizontal coordinate X. Consequently, equation (5.4.2) needs to be expressed in terms of X. Now, it is seen that $dX = \cos\theta \, dx$, where θ is the angle between the horizontal and the surface of the gravity waves, so

$$\frac{dU}{dx} = \cos\theta \frac{dU}{dX} \tag{5.4.3}$$

and

$$\frac{dP}{dX} = \frac{M + N}{W \cos\theta} \cdot \tag{5.4.4}$$

This equation is integrated numerically to find the variation of P or k with X. Then frequency σ is found using Doppler relation (2.3.1) and wave steepness ak is found using dispersion relation (4.4.2) for D and

expression (4.2.6) for wave steepness ak in terms of D. Note that θ is part of the surface data of gravity waves which is known ab initio. The results of the integration should give a constant total wave-action flux $U\mathcal{A} + \mathcal{B}$ when the viscosity of the liquid is zero. This is used to check the accuracy of the numerical integrating scheme.

The integrating routine requires a direction of integration, i.e. + X or - X or, equivalently, + x or - x, and an initial value for X and P or k. Capillary waves are attenuated by energy dissipation and this is found to be the case when integration is performed in the direction of the total group velocity C_g as may be expected since waves propagate in this direction. Integrating in the opposite direction results in the solution of a final value problem (a feature made use of later in § 5.8, 9). In terms of P and Q the total group velocity C_g is given by

$$C_g = \frac{1}{2}\,(2P + Q) \qquad (5.4.5)$$

Now, from table 3.1, waves CG and CG(+,-) have $C_g > 0$ whilst waves GC- and G- have $C_g < 0$ so that waves CG, CG(+,-) propagate in the + X direction and waves GC- and G- in the - X direction as is briefly remarked upon in § 4.3.

The initial values of X and P are chosen in the following manner. Firstly choose a value for β or, equivalently, values for s and ω. Then choose a particular gravity wavetrain together with a position on the gravity wave at which capillary wave propagation commences. This is usually chosen to be at a crest or trough of the gravity wavetrain. The initial values of both X and U are then fixed. The initial value of P or k is given by the Doppler relation (4.4.2) or (2.3.1) and the dispersion relation (4.4.2) or (4.2.4), i.e.

$$D = \beta P(P - U)^2 \quad \text{or} \quad sk^3D = (\omega - kU)^2\ . \qquad (5.4.6)$$

As D is varied over its range (4.2.5) this equation gives at most four ranges for P or k corresponding to the four possible waves CG(+,-), GC- and G-. Thus, these four possible ranges give four possible "windows" from which propagation can commence. In essence taking D = 1, D_{min} gives the curves which bound each window

$$U = P \mp \left[\frac{D}{\beta P}\right]^{\frac{1}{2}} \quad \text{or} \quad U = \frac{\omega}{k} \mp (skD)^{\frac{1}{2}} \qquad (5.4.7)_{\mp}$$

in the (U,P) or (U,k)-plane. The latter are shown in figures 5.2a, b

for $\omega = 0$ and $\omega \neq 0$ respectively. This feature of windows exists whether or not dissipation is present in a problem. This explains why in § 4.5 and § 4.6 the solution curves corresponding to the stationary wave CG or waves CG(+,-), GC- (and G-) merge from distinct regions.

5.5 The Special Case U = 0

The accuracy and efficiency of the numerical integrating routine for equation (5.4.4) is checked using the exact solution for the case U = 0 as well as solutions for the case $\mu = 0$. From the general analysis of § 3.2 and the window analysis above it is seen that when U = 0 waves will only exist if $\omega \neq 0$ and that the only waves which exist are waves CG+ and G-. Now, since U = 0 these waves have equal magnitudes of k, σ, c, c_g and b for a particular $|\omega|$ but opposite signs of σ, c and c_g. Note that these waves will be realistic only when $|\omega|$ is "large" because the effects of gravity decrease as $|\omega|$ increases. It follows that these two waves actually represent the one single wave when U = 0 whose direction of traverse is given by the sign of ω, that is + X (- X) direction if ω is positive (negative).

Putting U = 0 in the wave-action conservation equation (5.3.6) gives

$$\frac{dB}{dx} = - \frac{\mathcal{D}}{\omega} \qquad (5.5.1)$$

or, equivalently, $$\frac{dP}{dx} = \frac{2\mu}{3\beta^4 \tau s} \frac{(1 - \beta^2 P^6)(3 - \beta^2 P^6)}{P^8 (1 + 2\beta^2 P^6)} \; . \qquad (5.5.2)$$

This equation is easily integrated using standard methods to give

$$\frac{2\mu x}{\beta \tau s} = 2\beta P^3 - \frac{3}{4} \ln \left| \frac{1 - \beta P^3}{1 + \beta P^3} \right| + \frac{21}{4\sqrt{3}} \ln \left| \frac{\sqrt{3} - \beta P^3}{\sqrt{3} + \beta P^3} \right| + \text{constant} \; . \qquad (5.5.3)$$

Note that the dispersion relation (4.4.2) states $D = \beta P^3$ when U = 0 so that equation (5.5.2) could be expressed directly in terms of D and then integration performed. This is done as a check for the solution (5.5.3). The value of the constant is determined by the choice of initial values for x and P or D. The numerical routine integrates equation (5.4.4) or (5.5.2) for this special case to give exactly the same solution as given by expression (5.5.3). The solution (5.5.3) shows that the capillary wave steepness diminishes rapidly with increasing (decreasing) X for wave CG+ (G-) as would be expected in the absence of a mainstream flow.

5.6 Stationary Waves

As mentioned in § 4.4 the velocity variable P defined by (4.4.1) is only suitable when the frequency ω of the waves is non-zero and a variable R, defined by (4.4.11), must be used. The equations for the motion of stationary waves can then be derived using one of the two methods outlined in § 4.4, i.e. the direct method or substitution method. Both methods have been used to confirm the equations derived below.

The energy conservation equation (5.2.4) becomes

$$\frac{d}{dx}\left[2\tau Q(1 - RQ^2)\right] - \frac{2\tau}{RQ^2}(1 - RQ^2)(1 + 2RQ^2)\frac{dQ}{dx} = -\mathcal{D} \quad (5.6.1)$$

where $$\mathcal{D} = 4\frac{\mu}{S}\frac{1}{R^5Q^6}(1 - R^2Q^4)(3 - R^2Q^4) \ . \quad (5.6.2)$$

The corresponding numerically integrated equation is still given by the ordinary differential equation (5.4.4) but with

$$M = -\frac{4\mu}{\tau S}\frac{1}{R^4U^3}(1 - R^2U^4)(3 - R^2U^4) \ , \ N = -2U(1 + R^2U^4)\frac{dU}{dx}$$

and $$W = 2RU^6 \ .$$

For this case there is only one possible window given by

$$D = RU^2 \quad \text{or} \quad skD = U^2 \ . \quad (5.6.3)$$

As usual dimensional units are used for this case. The differential equation (5.4.4) is integrated in the + X direction because $C_g > 0$ for waves CG. Initial values of P are found using equation (5.6.3). Once the variation of P or k with X and, thus, U is found σ and a are found using the general method described in § 5.4.

Results are shown in figures 5.3, 4 for $\mu = 1.304 \times 10^{-3}$ kg m^{-1} s^{-1} - the value for water. The gravity waves have wavelength $\Lambda = 0.2$ m and steepness AK = 0.3. As shown in chapters 3 and 4 the effects of gravity on waves CG propagating on gravity waves with $\Lambda = 0.2$ m and AK = 0.3, 0.4 are qualitatively unimportant. The propagation of capillary waves can be initialised from any position on the gravity waves. However, all the general features are shown when propagations are commenced from either the troughs (figure 5.3) or the crests (figure 5.4) of the gravity waves. Each solution curve is denoted by the

appropriate initial wavenumber k with the corresponding value of b and

initial position given in table 5.1. The linear solution curves (dashed lines) are also shown since they provide an interpretive framework. This is an inviscid solution curve and provides a "limit" of the parameter space for wavenumber k and steepness ak.

k m^{-1}	b kg m^3 s^{-2}	Position	k m^{-1}	b kg m^3 s^{-2}	Position
7000	9.46×10^{-7}	trough	1700	2.89×10^{-6}	crest
8500	4.21×10^{-6}	trough	2000	1.46×10^{-5}	crest
10000	6.12×10^{-6}	trough	2500	2.56×10^{-5}	crest

Table 5.1: Initial wavenumbers k, wave-action fluxes b and positions of propagation.

Figures 4.3 shows the qualitative characteristics of non-dissipative propagations. Table 5.2 gives initial wavenumbers of dissipative wave propagations and values of b for the qualitatively corresponding non-dissipative wave propagations of figures 4.3 so that comparison can easily be made.

Initial k m^{-1}	Corresponding b kg m^3 s^{-2}	Initial k m^{-1}	Corresponding b kg m^3 s^{-2}
7000	10^{-6}	1700	10^{-6}
8500	5×10^{-6}	2000	10^{-5}
10000	5×10^{-6}	2500	2.5×10^{-5}

Table 5.2: Initial wavenumbers k for dissipative wave propagations and values of b for qualitatively corresponding non-dissipative wave propagations of figures 4.3.

There is a marked contrast between dissipative and non-dissipative propagations. Comparing figures 5.4 and 4.3 it is seen that that waves actually experience a rapid decrease in steepness as they propagate from gravity wave crests towards gravity wave troughs. The increasing steepness effects of non-dissipative theory has been over shadowed by

the decreasing steepness effect of wave energy dissipation. However, comparing figures 5.3 and 4.3 it is seen that when propagations commence from gravity wave troughs both dissipative and non-dissipative theory give decreasing steepness effects. Thus, waves CG dissipate in a shorter distance when propagating from gravity wave troughs than they do when propagating from gravity wave crests.

When propagations commence from the gravity wave crests waves CG become invisible to the eye after propagating 4 cm where as when propagations commence from the gravity wave troughs waves CG become invisible to the eye after propagating only 1 cm. Thus, waves CG remain visible to the eye for longer distances when on the forward faces of gravity waves. This explains why stationary capillary waves are most often observed on the forward faces of gravity waves.

The steepness of waves CG decreases rapidly when the initial steepness is large - greater than 0.8, say. Examination of the variation of dissipation ratio $\mathcal{D}/\mathcal{D}_{lin}$, given by expression (5.2.12), with wave steepness ak, as shown in figure 5.1, shows that the rate of change of $\mathcal{D}/\mathcal{D}_{lin}$ is greatest when ak is large so that this behaviour is to be expected.

If the steepness of the gravity waves is increased, to AK = 0.4 say, it is found that results are qualitatively the same as for the case AK = 0.3 considered here.

These waves have stationary crests and troughs but as a packet they propagate in the + X direction. Thus, in the observers frame the wave packet would be seen attempting to overtake the gravity waves but would very quickly dissipate and cease to exist.

The integrating routine gives results which agree exactly with those previously derived in chapter 4 for the case of zero viscosity and the total wave-action flux is found to remain constant as required. This is the third method mentioned in § 4.4 for finding inviscid solutions and has been tested for both stationary and Doppler shifted waves. Note that this requires a large number of points (order 10^3) on one gravity wavelength with routine NAG LIB D02CBF in order to force the routine to take small step lengths and thereby maintain a high level of accuracy.

5.7 The Doppler Shifted Waves

The case of Doppler shifted waves is now considered so that the equations of § 5.4 are solved in capillary units. The parameters for the problem are ω_1 and μ_1 where μ_1 is the dimensionless viscosity and is given by

$$\mu_1 = \frac{(s\omega)^{\frac{1}{3}}}{\tau}\mu \ . \qquad (5.7.1)$$

Results are given for water with μ taking the values $\mu = 0$, where necessary, and $\mu = 1.304 \times 10^{-3}$ kg m^{-1} s^{-1} so that comparison between inviscid and dissipative results can easily be made. Also, tables of the form of table 5.2 are given so that the results of this chapter are easily related to those of chapter 4. The gravity waves have wavelength $\Lambda = 0.2$ m and steepness $AK = 0.3$. The capillary waves have frequency $|\omega| = 100$ rad s^{-1} so that $\mu_1 = 3.428 \times 10^{-3}$. These parameter values are chosen because the effects of gravity on Doppler shifted waves are negligible for such a case. As usual, attention is confined to waves CG(+,-) and GC- since waves G- are strongly affected by gravity in any real situation. The propagation of the capillary waves can be initialised from any position on the gravity waves. However, all the general features of solutions are shown when propagations are commenced at either the trough or the crest.

The results are shown in figures 5.5 - 5.13. Figures 5.9, 5.11 and 5.13 have $\mu = 0$ whilst the others have $\mu \neq 0$. Also figures 5.4, 5.7, 5.12 and 5.13 have propagations commencing at the gravity wave troughs, and so have a crest at the centre, whilst figures 5.5, 5.8 - 5.11 have propagations commencing at the gravity wave crests, and so have a trough at the centre. In any case, the initial position for waves CG(+,-) is $X_1 = 0$ whilst that for waves GC- is $X_1 \simeq 102$. Each solution curve is denoted by the appropriate initial wavenumber k_1 with the corresponding wave notation, initial value of b_1 and initial position given in table 5.3. The linear solution curves and the stopped waves curves (dashed lines) are also shown since these provide an interpretive framework. These are inviscid solution curves and provide the "limits" of the parameter space for wavenumber k and steepness ak.

Figures 4.7 and 4.8 show the qualitative characteristics of non-dissipative propagations for waves CG(+,-) and GC-. Table 5.4 gives initial wavenumbers of dissipative wave propagations and values of b_1 for the qualitatively corresponding non-dissipative wave propagations of figures 4.7 and 4.8 so that comparison can be easily made.

k_1	Wave	b_1	Position	k_1	Wave	b_1	Position
14	CG+	0.006	trough	1.85	CG-	0.03	crest
17	CG+	0.03	trough	2.6	CG-	0.1	crest
20	CG+	0.04	trough	3.4	CG-	0.15	crest
4.2	CG+	0.01	crest	1.04	GC-	- 1.1	crest
5.0	CG+	0.1	crest	1.48	GC-	- 0.05	crest
5.8	CG+	0.2	crest	1.52	GC-	- 0.04	crest
13	CG-	0.006	trough	0.317	GC-	- 34	trough
16	CG-	0.03	trough	0.328	GC-	- 1.7	trough
19	CG	0.04	trough	0.3289	GC-	- 0.03	trough

Table 5.3: Initial wavenumbers k_1, wave-action fluxes b_1 and positions of propagation for waves GC(+,-) and GC-.

Initial k_1 and wave		Corresponding b_1	Initial k_1 and wave		Corresponding b_1
14	CG+	0.01	1.85	CG-	0.01
17	CG+	0.01	2.6	CG-	0.1
20	CG+	0.01	3.4	CG-	0.15
4.2	CG+	0.01	1.04	GC-	- 1.0
5.0	CG+	0.05	1.48	GC-	- 0.01
5.8	CG+	1.0	1.52	GC-	- 0.01
13	CG-	0.01	0.317	GC-	- 25.0
16	CG-	0.01	0.328	GC-	- 5.0
19	CG-	0.01	0.3289	GC-	- 0.1

Table 5.4: Initial wavenumbers k_1 for dissipative wave propagations and values of b_1 for qualitatively corresponding non-dissipative wave propagations of figures 4.7, 8.

Figures 5.5 and 5.6 show the propagation behaviour of waves CG+ with viscosity $\mu \neq 0$. Waves CG+ have positive C_g and, thus, propagate in the + X_1 direction. As for stationary waves CG the dissipative behaviour of these waves is markedly different to the non-dissipative behaviour shown in figures 4.7. The characteristic behaviour of waves CG+ is the same as that of stationary waves CG for both dissipative and non-dissipative theory. Waves CG+ are rapidly damped out. Also, if propagation commences form the crest of the gravity waves then waves CG+ remain visible to the eye four times the distance if propagation commences from the trough. This is seen by comparison of figures 5.5 and 5.6. However, the feature of rapid dissipation implies that the slowly-varying assumption may be violated by such propagations.

Figures 5.7 and 5.8 (5.9) show the propagation of waves CG- with viscosity $\mu \neq 0$ ($\mu = 0$). Propagations with $\mu = 0$ corresponding to figures 5.7 are all qualitative similar to those with $b = 0.01$ in figures 4.8a, b. Those corresponding to figures 5.8 are shown in figures 5.9. Waves CG- have positive C_g and, thus, propagate in the + X direction. Waves CG- also show marked differences between dissipative and non-dissipative behaviour. They also rapidly dissipate and cease to exist. They never increase in steepness and, thus, never propagate towards breaking.

Figures 5.10 and 5.12 (5.11 and 5.13) show the propagation of waves GC- with viscosity $\mu \neq 0$ ($\mu = 0$). Those of figures 5.10 (5.12) can be compared with figures 4.7a, c and 5.11 (5.13). Waves GC- have negative C_g and, thus, propagate in the - X_1 direction. Dissipation still affects the waves but not to the same degree as for waves CG-. The steepness of the waves is attenuated, in comparison to non-dissipative results, as expected.

One striking feature is dominant on the propagation of waves GC-. The majority of solutions propagate and eventually reach the stopped waves solution where the total group velocity C_g is zero (figures 5.10 initial $k_1 = 1.52, 1.49, 1.04$ and figures 5.12 initial $k_1 = 0.3289$) but have non-zero non-maximum amplitude when this occurs. If the equations are integrated further in the - X_1 direction the total group velocity C_g of the waves immediately becomes positive and the waves steepness rapidly increases. Both of these features confirm that the solution is mathematically and physically unrealistic beyond the point at which total group velocity C_g is zero. Also, solutions commencing at this point, where $C_g = 0$, and integrated in the + X_1 direction, i.e. CG- wave solutions, have a negative total group velocity C_g after a remarkably short distance and also rapidly increase in steepness. Again, both of these features confirm that propagation in the + X_1 direction is also

unrealistic. This suggests that waves GC- can not be reflected into waves CG-. The question of the behaviour of these solutions from this point onwards is at present unknown.

This type of behaviour also exists for waves CG- (figures 5.8 initial $k_1 = 1.86$) but not so often. This could be due to the basic assumption of the theory, namely, the slowly-varying assumption since wave properties in the neighbourhood of the stopped waves curves do vary quickly and the slowly-varying assumption does break down. This quickly varying feature commences in the neighbourhood of the caustic and, thus, firstly breaks down there. This is further investigated below in § 5.8 where a uniform theory is applied to study the behaviour in the neighbourhood of the caustic. Note that the solutions with initial $k_1 = 1.04$ (figures 5.10) and 0.328 (figures 5.12) propagates over the whole of the gravity wave shown but end with a lower steepness and a lower total wave-action flux. When these solutions are allowed to propagate further they will eventually reach the stopped waves solution.

Waves GC- can still break but it is found that they propagate further before breaking (figures 5.12 and 5.13 initial $k_1 = 0.317$). Also there exist waves which break as they approach the crests of the gravity waves for $\mu = 0$ but propagate over the crests when $\mu \neq 0$ (figures 5.12 and 5.13 initial $k_1 = 0.328$). There are no solutions which reach zero steepness no matter how small the value of the initial steepness of the waves (figures 5.10 initial $k_1 = 1.48$, 1.04). If propagation is commenced with a small initial steepness and, thus, a small initial total wave-action flux, then the steepness of the waves remains small but non-zero and proceeds to increase as the gravity wave crests are approached. This is because when the steepness of waves GC- is small their wavenumbers are also small so that dissipation effects become negligible. In fact, under these circumstances the solution curves eventually hit the stopped waves curve (figures 5.10 initial $k_1 = 1.48$).

It is generally deduced that the increasing steepness effect of non-dissipative theory experienced by waves CG, CG(+,-) is over shadowed by the decreasing steepness effect of wave energy dissipation. This can be attributed to the small wavelengths of these waves. It is concluded that for waves CG and CG(+,-) the majority of propagations result in rapid and complete dissipation of the waves. Some propagations for waves CG-, which commence close to the stopped waves solution and with a low value of total wave-action flux, reach the stopped wave solution.

For waves GC- the majority of propagations result in an overall decrease of steepness and total wave-action flux with solutions eventually reaching the stopped waves solution where the total group velocity C_g is zero but with finite-amplitude. Some propagations

commencing with a high value of steepness and total wave-action flux may (e.g. figures 5.12 initial k_i = 0.317) or may not (e.g. figures 5.10 initial k_i = 1.04) break.

In the observers frame waves CG(+,-) behave in a similar fashion to stationary wave CG. They attempt to overtake the gravity wave crests and troughs but quickly dissipate and cease to exist. As the steepness of waves GC- is attenuated there will be cases where the inviscid theory of chapter 4 predicts that the capillary waves are swept-up by the gravity waves on the forward faces of the gravity waves but dissipation allows the capillary waves to be overtaken by the gravity waves so that no breaking occurs. The general translation of propagations from the ω-frame to the observers frame should, by now, be familiar to the reader so that greater detail is not given.

The case A = 0.2 m, AK = 0.4 is not considered here because of the following reason. The surface velocity at the crests of the gravity waves is less than all the crest breaking velocities. Consequently, no windows exist at the crests and it would not be possible to show all the features of possible solutions as shown above. Propagations which commence at the troughs of the gravity waves have similar features to those for the case AK = 0.3 with the added restriction, seen from the stopped waves solutions curves of figures 4.8, that no waves can propagate over the crests. Thus, as waves CG- approach the crests they will dissipate and reach zero steepness or, on a rare occasion, reach the stopped waves solution and as waves GC- approach the crests they will either break, after propagating slightly further, or reach the stopped waves solution.

Note that the fact that the stopped waves curves separate the two regimes of the CG- and the GC- waves further suggests that the correct definition for the group velocity has been made for the problem considered here.

It is found that all wave propagation commencing in the neighbourhood of the stopped waves solution are "attracted" towards the stopped waves solution and that there is no propagation away from the stopped waves solution. Thus, positions on the stopped waves solution are propagation solution points which can not experience changes in wave parameters, such as steepness. How can this be possible, especially when wave energy dissipation is present ?

It is easy to investigate the time it takes for wave modulations to reach the stopped waves curve according to slowly-varying theory using an analysis local to the zero total group velocity position. Numerical investigations show that total group velocity of such wave solutions

becomes zero linearly. That is,

$$\frac{dX}{dt} = C_g \sim - X \quad \text{or} \quad t \sim - \ln |X| \qquad (5.7.2)$$

local to the zero total group velocity positions now transformed to X = 0. This means that wave solutions take an infinitely long period of time to reach zero total group velocity, i.e. the zero total group velocity position can never be reached by slowly-varying wave modulations.

Simple consideration of the (X,t)-plane shows that any wave modulation of finite length in X will experience a continuous decrease in length as time increases. Thus, as the zero total group velocity position is approached the slowly-varying assumption for the wave modulation will be violated. The only possible way in which the slowly-varying assumption could remain valid is for the wave modulation to be of infinite length, i.e. a uniform wavetrain. Thus, the zero total group velocity positions can only be sustained by uniform wavetrains approaching the zero total group velocity positions from "infinity" - in our case the trough, say. The uniform wavetrain is a source of wave-action flux and balances the dissipative effects at positions on the stopped waves curve.

It remains to investigate the behaviour of the waves CG- and GC-, especially those wave solutions which hit the stopped waves curves, in the neighbourhood of the caustic where the slowly-varying assumption breaks down. One possibility, pursued below, is to use a near-linear Schrödinger equation type of analysis as outlined, for instance, in Peregrine and Smith (1979).

5.8 Uniform Near-Linear Schrödinger Approximation in the Neighbourhood of the Caustic

Throughout all the analysis so far it has been assumed that both the mainstream flow and the wave parameters are slowly-varying. It is explained in chapter 4 that for the wave-current interaction problem this assumption is most dubious for waves with "small" b_1 in the vicinity of the linear caustic. Also, for the wave propagation problem this assumption definitely breaks down in this vicinity. Peregrine and Smith (1979) give, using a heuristic Taylor expansion in the neighbourhood of a linear caustic, a near-linear Schrödinger equation (NLS equation) which represents a uniform approximation in the neighbourhood of a linear caustic. This heuristic derivation is continued and an appropriate first order dissipation term is derived and added to the (steady-state) NLS equation. This equations is then solved in order to investigate the validity of results for slowly-varying theory.

From Peregrine and Smith (1979) the time-dependent NLS equation, valid in the neighbourhood of a caustic is,

$$i \frac{\partial \mathcal{G}}{\partial \omega} \frac{\partial a}{\partial t} - \frac{1}{2} \frac{\partial^2 \mathcal{G}}{\partial k^2} \frac{\partial^2 a}{\partial x^2} + x \frac{\partial \mathcal{G}}{\partial x} a + H |a|^2 a = 0 \qquad (5.8.1)$$

where $$\mathcal{G} = \mathcal{G}(\omega, k, a;\ U(x), x, t) = \mathcal{G}(\sigma - kU, k, a) = G(\sigma, k, a) \qquad (5.8.2)$$

using the notation of § 2.8 with the coefficients all evaluated at the linear caustic $k = k_c$, $U = U_c$ situated at $x = 0$. This equation describes both an incident and a reflected wave solution. It requires that waves be incident from the - x direction. Here a is the complex amplitude of the first approximation, although, as may be seen, the equation includes cubic terms.

Attention is focused on waves CG- and GC- only since these are the only waves which exist in the neighbourhood of the linear caustic. Note that no such analysis can be performed for the stationary waves CG since for this case there is no caustic point. Note that the wavenumber k_{c1}, frequency σ_{c1} and current U_{c1} at the caustic are given by

$$k_{c1} = 2^{\frac{2}{3}}, \quad \sigma_{c1} = 2 \quad \text{and} \quad U_{c1} = -\ 3 \times 2^{-\frac{2}{3}} . \qquad (5.8.3)$$

The idea is to use the linear dissipation term $\mathcal{D}_{lin}$ given by expression (5.2.7) to find the appropriate first order dissipation term. The heuristic derivation in Peregrine and Smith (1979) involves a Taylor

expansion about the caustic. In the neighbourhood of the caustic the total linear energy density $\mathcal{E}$ and the linear dissipation D_{lin} are given by

$$\mathcal{E} = \frac{\tau}{2} k_c^2 |a|^2 \quad \text{and} \quad \mathcal{D}_{lin} = 2\mu s k_c^4 |a|^2 \tag{5.8.4}$$

where a subscript c denotes values at the caustic. $\mathcal{D}_{lin}$ is an energy term so it is required that the time-dependent NLS equation (5.8.1) must be manipulated to the form of an energy conservation equation. Thus, the expression (5.8.4) for $\mathcal{E}$ implies that equation (5.8.1) must be manipulated to include a term of the form

$$\frac{\partial \mathcal{E}}{\partial t} = \frac{\tau}{2} k_c^2 \frac{\partial}{\partial t} |a|^2 \ . \tag{5.8.5}$$

Taking a*(5.8.1) - a(5.8.1)*, where * denotes complex conjugation, gives

$$\frac{\tau}{2} k_c^2 \frac{\partial}{\partial t} |a|^2 + i \frac{\tau}{4} \left[\frac{\partial^2 \mathcal{G}}{\partial k^2} \Big/ \frac{\partial \mathcal{G}}{\partial \omega}\right] k_c^2 \left[a^* \frac{\partial^2 a}{\partial x^2} - a \frac{\partial^2 a^*}{\partial x^2}\right] = 0 \ . \tag{5.8.6}$$

Note that the $x\ \partial\mathcal{G}/\partial x$ and H terms present in the time-dependent NLS equation (5.8.1) are no longer present. To add the first order effects of dissipation simply replace the right hand side of this energy conservation equation by - $\mathcal{D}_{lin}$, with $\mathcal{D}_{lin}$ given by expression (5.8.4), so that

$$\frac{\partial}{\partial t} |a|^2 + i \frac{1}{2} \left[\frac{\partial^2 \mathcal{G}}{\partial k^2} \Big/ \frac{\partial \mathcal{G}}{\partial \omega}\right] \left[a^* \frac{\partial^2 a}{\partial x^2} - a \frac{\partial^2 a^*}{\partial x^2}\right] = - \frac{4\mu s}{\tau} k_c^2 a^* a \ . \tag{5.8.7}$$

This energy equation must now be manipulated to give those terms present in the time-dependent NLS equation (5.8.1). The simplest method of doing this is reverse the manipulations involved in deriving the energy equation (5.8.7). In doing this those terms which have cancelled during the formation of (5.8.7), i.e. the terms involving $x\ \partial\mathcal{G}/\partial x$ and H in the time-dependent NLS equation (5.8.1), are added back simply because one of our criteria for the equation derived is that this equation must reduce to the time-dependent NLS equation when the viscosity μ is zero. It is easily found that

$$i \frac{\partial \mathcal{G}}{\partial \omega} \frac{\partial a}{\partial t} - \frac{1}{2} \frac{\partial^2 \mathcal{G}}{\partial k^2} \frac{d^2 a}{dx^2} + x \frac{\partial \mathcal{G}}{\partial x} a + H |a|^2 a = - i \frac{2\mu s}{\tau} \frac{\partial \mathcal{G}}{\partial \omega} k_c^2 a \ . \tag{5.8.8}$$

Thus, the steady-state dissipative NLS equation takes the form

$$\text{so} \qquad \frac{d^2a}{dx^2} - mx\,a - n\,|a|^2a - ip\,a = 0 \qquad (5.8.9)$$

$$\text{where} \qquad m = 2\,\frac{\partial \mathcal{G}}{\partial x}\Big/\frac{\partial^2 \mathcal{G}}{\partial k^2}\,,\quad n = 2H\Big/\frac{\partial^2 \mathcal{G}}{\partial k^2}\,,\quad p = \frac{4\mu s}{\tau}\,k_c^2\,\frac{\partial \mathcal{G}}{\partial \omega}\Big/\frac{\partial^2 \mathcal{G}}{\partial k^2}\,. \qquad (5.8.10)$$

The coefficient m represents the effects of the linear dispersion, n the effects of the higher order dispersion (S-type near-linear caustics imply that $n < 0$ whereas R-type near-linear caustics imply $n > 0$) and p the first order effects of dissipation.

The results, present in chapter 4 and above, for the slowly-varying propagation problem show that the X-axis of the ω-frame is directed perpendicular to both the caustics occurring symmetrically on either side of the gravity waves crests or troughs. However, neither of the caustics is situated at $X = 0$. Moreover, only one caustic has waves incident from the - X direction - the caustic occurring to the left of gravity wave crests. These restrictions are easily removed: a simple translation of X places the caustic at $X = 0$ and, if necessary, a simple reflection $X \longrightarrow -X$ ensures that waves are incident from the - X direction. Thus, both the caustics can be examined with either of waves CG- or GC- as the incident waves and the other as the reflected waves. Note that a simple reflection $x \longrightarrow -x$ does not change the form of the steady-state NLS equation which is clearly seen from examination of equation (5.8.8). Consequently take $x \longrightarrow X$ in the steady-state NLS equation (5.8.9) so that the equation under consideration is

$$\frac{d^2a}{dX^2} - 2\left[\frac{\partial \mathcal{G}}{\partial X}\Big/\frac{\partial^2 \mathcal{G}}{\partial k^2}\right] Xa - 2H\Big/\frac{\partial^2 \mathcal{G}}{\partial k^2}\,|a|^2a - i\,\frac{4\mu s}{\tau}\left[\frac{\partial \mathcal{G}}{\partial \omega}\Big/\frac{\partial^2 \mathcal{G}}{\partial k^2}\right]k_c^2\,a = 0\,. \qquad (5.8.11)$$

This equation is scaled to capillary units after which Ince (1944, p 328) is followed. Thus, define

$$w = \left[\mp\,\frac{1}{8}\,n_1^3 m_1^2\right]^{\frac{1}{6}}\,a_1\,, \qquad z = (m_1)^{\frac{1}{3}}\,X_1 \qquad (5.8.12)$$

$$\text{where} \qquad n_1 = \left[-\,\frac{k_1^5}{8(3k_1 - U_1^2)}\right]_c\,, \qquad m_1 = \left[\frac{2\sigma_1 k_1}{3k_1 - U_1^2}\,\frac{dU_1}{dX_1}\right]_c\,. \qquad (5.8.13)$$

The choice of sign for the w expression depends on the sign of n_1 and this in turn depends on the type of near-linear caustic present. It is shown in chapter 3 that the CG-/GC- caustic is of S-type so that $n_1 < 0$ and the upper sign must be chosen.

The fact that waves must be incident from the - X direction means that dU/dX must be positive at the caustic so that $m_1 > 0$. Thus, waves are always incident from the - z direction when either of the caustics on a gravity wave is considered. Therefore, the equation to consider for either of the caustics is

$$\frac{d^2w}{dz^2} - zw + 2|w|^2w - iB\,w = 0 \qquad (5.8.14)$$

where

$$B = \left[\frac{16s|\omega|k_1^4\sigma_1}{3k_1 - U_1^2}\left[\frac{dU_1}{dX_1}\right]^{-2}\right]^{\frac{1}{3}}\frac{\mu}{\tau}\,. \qquad (5.8.15)$$

This equation is a generalised Painlevé equation. It can be written in the form

$$\frac{d^2w}{dz^2} - (z + iB)\,w + 2|w|^2w = 0\,. \qquad (5.8.16)$$

For B = 0 Miles (1978, 1980) gives

$$w \sim A_1\,\frac{1}{2}\,\pi^{-\frac{1}{2}}\,z^{-\frac{1}{4}}\exp\left[-\frac{2}{3}\,z^{\frac{3}{2}}\right] \qquad \text{as } z \longrightarrow +\infty$$

and Peregrine and Smith (1979) give

$$w \sim A_2\,\pi^{-\frac{1}{2}}\,(-z)^{-\frac{1}{4}}\sin\left[\frac{2}{3}\,(-z)^{\frac{3}{2}} + \frac{\pi}{4}\right] \qquad \text{as } z \longrightarrow -\infty$$

where A_1 and A_2 can be complex. This means that for B = 0 the near-linear (cubic) term in the generalised Painlevé equation (5.8.14) is asymptotically small so that the asymptotic form of the Airy function applies. The question is: Do these expansions still remain valid for $B \neq 0$? If the near-linear term is omitted then the generalised Painlevé equation is

$$\frac{d^2w}{dz^2} - (z + iB)\,w = 0 \qquad (5.8.17)$$

for which asymptotic limits are easily given by transformation ($z \longrightarrow z + iB$) of those above for the Airy function. Essentially, these asymptotic expansions are valid as $z \longrightarrow \pm\infty$ for the generalised Painlevé equation if $|w|^2w$ is small compared to w'' and $(z + iB)\,w$ and the w'' and $(z + iB)\,w$ terms balance each other. This is, in fact, the case

as $z \longrightarrow + \infty$ but not as $z \longrightarrow - \infty$. Thus,

$$w \sim A_1 \, Ai(z + iB) \longrightarrow A_1 \, \frac{1}{2} \, \pi^{-\frac{1}{2}} \, z^{-\frac{1}{4}} \exp\left[- \frac{2}{3} \, z^{\frac{3}{2}} - iB \, z^{\frac{1}{2}} \right] \quad (5.8.18)$$

as $z \longrightarrow + \infty$.

The generalised Painlevé equation (5.8.14) is integrated in the - z direction with use of the asymptotic condition (5.8.18) to generate initial conditions. A standard integrating routine (NAG LIB D02CBF) is used. This requires a system of first order coupled "real" equations. The substitution $w = re^{i\theta}$ is used to generate such equations. The accuracy of the integrating routine is checked with the results of Rosales (1978) and Miles (1978, 1980) who examine the case of B = 0 in great detail. Our results agree qualitatively (maxima and minima occur at approximately the same values of z but take slightly different values of w) with those of Rosales (1978) and Miles (1978, 1980). Their methods are more accurate than those used here because they include extra terms in the asymptotic expansion of the Airy function (the first ten terms to be precise).

To examine particular cases considered above and in the slowly-varying theory of chapter 4 specific values of B and A_1 are required. The value of B is easily found from definition (5.8.15) once specific values of Λ, AK and ω are chosen since then, for any slowly-varying solution of chapter 4 ($\mu = 0$) or § 5.6, 7 ($\mu \neq 0$), the value of dU_1/dX_1 at both the caustics is fixed by the value U_{c1} of the current at the caustics. Note that for particular Λ, AK and ω the positions X_{c1} of the caustics are unique so that the value of U_1 at the caustic positions X_{c1} is equal to U_{c1} and is, thus, the same for all slowly-varying solutions whether linear or nonlinear. The values of k_1 and σ_1 differ from k_{c1} and σ_{c1} respectively for the nonlinear solutions (see, for example, figures 4.5 or 4.7).

Various values of A_1 are used. The modulus $|w|$ of the solution of the generalised Painlevé equation for a particular A is separated into the constitutive incident and reflected parts. This is only taken to a first approximation assuming that the incident and reflected waves behave in a linear fashion, i.e. $w = a_i e^{i(kx-\omega t)} + a_r e^{-i(kx-\omega t)}$, except in the immediate neighbourhood of the caustic. The values of a_{i1} and a_{r1} of the incident and reflected waves are then calculated using expression (5.8.12). The value of X_1 is not needed but can be calculated also using expression (5.8.12).

Formally, a uniform solution must be matched (as $z \longrightarrow -\infty$) with a slowly-varying solution (as $z \longrightarrow 0$). Thus, the values of a_{i1} and a_{r1} as $z \longrightarrow -\infty$ must be equal to the amplitudes, at the caustic positions X_{c1}, of (two) slowly-varying solutions (since $z = 0$ is the position of the caustic for the slowly-varying theory). This matching requires analytic solutions so since only numerical solutions are available a patching method is used. The values of a_{i1} and a_{r1} are found at $z = -10$ and these are taken to be the values as $z \longrightarrow -\infty$.

The slowly-varying solutions, with these amplitudes at the caustic positions X_{c1}, are found using the method of § 5.4 but integrating in the opposite direction to the actual direction of propagation, i.e. solving a final value problem. This requires values of k_1 corresponding to amplitudes a_{i1} and a_{r1} and these are easily found using the value U_{c1} of the current at the caustics, the Doppler relation (2.3.1), the dispersion equation (4.2.4) and expression (4.2.6) which gives wave steepness ak in terms of the parameter D. These give

$$(1 - k_1 U_{c1})^2 = k_1^3 D \quad \text{and} \quad k_1 = \frac{2}{a_1 D}(1 + D)^{\frac{1}{2}}(1 - D)^{\frac{1}{2}} , \quad (5.8.19)$$

where $a_1 = a_{i1}$ or a_{r1}, which gives two equations for the two unknowns D and k_1. These will give k_{i1} or k_{r1}. Equations (5.8.19) are transcendental equations and are solved using a standard solver (NAG LIB C05NBF) for such equations. Note that these equations have a maximum of four possible solutions corresponding to the four possible waves CG(+,-), GC- and G-. Only the two solutions for waves CG- and GC- are sought. Thus, there will be two solutions for incident waves and two solutions for reflected waves - one each for waves CG- and GC-.

5.9 Results for Uniform NLS Theory

Consider, as usual, the typical case where A = 0.2 m, AK = 0.3 and $|\omega|$ = 100 rad s^{-1}. For such a gravity wave it is found that the magnitude of the derivative $(dU_1/dX_1)_c$, needed to calculate the dissipation parameter B in the generalised Painlevé equation, is 4.452×10^{-2}. Then expressions (5.8.3, 15) give B = 0 for $\mu = 0$ and B = 0.151 for $\mu \neq 0$. The value of A_1 is taken to be 0.15 since it is found that this value corresponds to near-linear steepnesses for the pure capillary waves.

Figures 5.14a and 5.15a show the variations of $|w_1|$ with z_1 for solutions of the generalised Painlevé equation corresponding to A = 0.15 and B = 0 and 0.151 respectively. These figures also show the corresponding variations of incident and reflected wave amplitudes w_{i1} and w_{r1}. These latter curves are used to find the values of incident and reflected wave amplitudes a_{i1} and a_{r1} at z = - 10. Using expression (5.8.11) it is found that

$$a_{i1} = a_{r1} = 0.0908 \qquad \mu = 0 \ ;$$

$$a_{i1} = 0.146 \quad \text{and} \quad a_{r1} = 0.0561 \qquad \mu \neq 0 \ .$$

Substitution of these amplitudes and U_{c1}, given from (5.8.3), into equations (5.8.19) gives values of wavenumber k_1 and steepness ak corresponding to the incident and reflected waves. These are respectively given by

$$a_{i1} = a_{r1} = 0.0908 \implies k_1 = 1.69, \ ak = 0.153$$

$$\text{and} \quad k_1 = 1.50, \ ak = 0.136 \ ,$$

$$a_{i1} = 0.146 \implies k_1 = 1.77, \ ak = 0.258 \quad \text{and} \quad k_1 = 1.46, \ ak = 0.224 \ ,$$
$$a_{r1} = 0.0561 \implies k_1 = 1.65, \ ak = 0.0924 \quad \text{and} \quad k_1 = 1.53, \ ak = 0.0859 \ .$$

The maximum steepness of finite-amplitude pure capillary waves is 2.29 so that the steepnesses corresponding to this uniform NLS solution are all near-linear. Note that the uniform solutions shown in figures 5.14a and 5.15a correspond to both the caustics on a gravity waves and, thus, to both cases of waves CG- and GC- incident on the caustics situated to the left and right of gravity wave crests with waves GC- and CG- reflected respectively.

All that remains is to find slowly-varying wave solutions, corresponding to both the incident and reflected waves, with these amplitudes and wavenumbers at the caustic positions. Those for the incident waves are found, as described above, by integrating in the direction opposite to that of wave propagation. Recall that waves CG- (GC-) travel in the + X (- X) direction so integration is performed in the - X (+ X) direction to find the incident wave behaviour. Integration is commenced at the caustic positions, given by $X_1 = 47.1$ for waves CG- and $X_1 = 55.4$ for waves GC-, with (incident) initial wavenumbers as above. Those for the reflected waves are found by integrating forwards in the usual way but with propagation commencing from the caustic positions with (reflected) initial wavenumbers as above.

The slowly-varying solutions are shown in figures 5.14b, c and 5.15b, c for $\mu = 0$ and $\mu \neq 0$ respectively. These figures also show the linear and stopped waves propagation curves (dashed lines) to aid understanding. Both figures show the incident waves CG- (GC-) propagating towards the caustic situated to the left (right) of gravity wave crests and the corresponding reflected waves GC- (CG-) propagating away from this caustic. The incident and reflected wave values of a_{c1}, k_{c1}, $(ak)_c$ and b_{c1} are shown in table 5.5. Note that both the incident waves CG- and GC- for $\mu \neq 0$ reach a position where their zero total group velocity is zero, i.e. they coincide with the stopped waves curve.

It is also noted that for $\mu = 0$ both incident waves CG- and GC- can be regarded as commencing propagation from wave troughs but for $\mu \neq 0$ the incident waves GC- are the only such one. In this case waves CG- can be regarded as commencing propagation at $X_1 = 37.2$ with $k_1 = 8.63$ and wave steepness at its maximum.

a_{i1}	k_{i1}	$(ak)_{i1}$	b_{i1}	a_{r1}	k_{r1}	$(ak)_{r1}$	b_{r1}
0.0976	1.69	0.153	0.0003	0.0976	1.50	0.136	- 0.0003
0.0976	1.50	0.136	- 0.0003	0.0976	1.69	0.153	0.0003
0.146	1.76	0.258	0.0013	0.056	1.53	0.0859	- 0.00007
0.146	1.45	0.224	- 0.0013	0.056	1.65	0.0924	0.0000006

Table 5.5: Cases considered for evaluation of solutions to the uniform NLS theory in the neighbourhood of the caustic; values given are those at the caustic.

5.10 Discussion

In the neighbourhood of the caustic position the uniform theory is a more accurate model than the slowly-varying theory so long as wave steepnesses in this region are near-linear. For the specific example chosen this is clearly the case. In fact, any propagation with a value of A_1 between zero and approximately 0.3 will correspond to linear or near-linear slowly-varying propagations. Moreover, the qualitative characteristics of these propagations will be similar to the particular case considered above. Consequently, these results serve as a model example of the behaviour of the flow field.

Figures 5.14a shows that for $\mu = 0$ the qualitative characteristics of the uniform NLS solution are similar to its linear counterpart, i.e. the near-linear term in the generalised Painlevé equation (5.8.14) has no strong qualitative effects. This figure and figures 5.14b, c show that waves CG- (GC-), incident from the $- X_1$ ($+ X_1$) direction, will be reflected as waves GC- (CG-), propagating in the $- X_1$ ($+ X_1$) direction, with equal but opposite (constant) total wave-action flux b.

Figures 5.15a show that for $\mu \neq 0$ the qualitative characteristics of the uniform NLS solution are very different from those of its linear counterpart. Again this figure and figures 5.15b, c show that the waves are reflected but for this case the magnitude of the total wave-action flux b (at the caustic positions) of the reflected waves is much reduced compared to that of the incident waves. The signs of wave-action flux will, as before, be changed. The marked differences between the incident and reflected wave amplitude curves in figure 5.15a can be interpreted to mean that incident waves spend a considerable time in the neighbourhood of the caustic with dissipation acting. This is obviously related to the infinite time it takes for wave propagations to reach the stopped waves curves.

Thus, this uniform theory shows that wave reflection, for waves CG- and GC- only, definitely occurs at the caustic position if wave steepnesses are near-linear. Any waves which do not have near-linear steepnesses in the neighbourhood of the caustic may, or may not, behave in the manner suggested by the slowly-varying solution. This is because the slowly-varying assumption is clearly violated by those waves whose propagations come near the stopped waves solution whereas it may, or may not, hold for other wave propagations (figures 5.5 - 5.13). The question of the validity of slowly-varying solutions for such cases is still open.

These features modify the general propagation behaviour of waves as discussed in § 4.7. Some general conclusions are now made about the propagation behaviour of the stationary waves CG and the three Doppler shifted waves CG(+,-) and GC- as seen in either the ω-frame or the observers frame of reference.

The ω-frame is dealt with first. Slowly-varying solutions suggest that stationary waves CG and waves CG+ dissipate and cease to exist, whilst propagating towards the leftward faces of the gravity waves, after propagating approximately a quarter of the wavelength of the gravity waves (as seen by the naked eye). This is the expected behaviour of waves with such large wavelengths so that the slowly-varying approximation appears to be a good one.

Waves CG- dissipate in a similar fashion to waves CG+ for the majority of propagations. The behaviour of these waves differs in that a small proportion of all the possible slowly-varying propagations reach a position where their total group velocity is zero. This position is called a "stopping velocity position" since $C_g = U + 3c/2 = 0$ so that $U = - 3c/2$ which is the "stopping velocity". Such propagations do not propagate near the caustic position (figures 5.8, initial $k_i = 1.86$). Also, the slowly-varying approximation does not appear to be violated because neither wavenumber nor steepness vary rapidly. It must, therefore, be concluded that such waves, in fact, attempt to reach a stopping velocity position whilst taking an infinitely long time to do so. Exactly how this type of behaviour is sustained is unclear since the strong dissipative effects will not allow a uniform wavetrain at infinity, say the trough.

According to slowly-varying solutions waves GC- can exhibit one of three types of behaviour. One is to break as they propagate towards the rightward faces of gravity waves (figures 5.12, initial $k_i = 0.317$). Such propagations do not violate the slowly-varying approximation so that the solution is valid. Breaking of this type is sometimes observed on pond or lakes.

A second is to propagate over the crests and down the leftward faces of gravity waves (figure 5.10 initial $k_i = 1.04$ and figures 5.12 initial $k_i = 0.328$). Such propagations experience quite rapid changes in steepness as they propagate past the caustics and over the crests so that the validity of the slowly-varying approximation is dubious. The uniform theory is no use for such propagations since they always have a nonlinear steepness at the caustic. Thus, if the slowly-varying approximation is not violated, the waves propagate over the whole length of the gravity waves and have their steepness attenuated.

The third is to propagate to a stopping velocity position (figures 5.10 initial k_1 = 1.48, 1.52 and figures 5.12 initial k_1 = 0.3289). The steepnesses of this third type of propagation are not necessarily near-linear when at the caustic position. However, any propagations with near-linear steepnesses at the caustic position always reach a stopping velocity position. From the "time" analysis of § 5.7 and the uniform analysis of § 5.8, 9 it follows that there are two possible type of behaviour for such wavetrains.

One possibility is partial reflection of the waves at the caustic position. Thus, waves GC- are partially reflected to waves CG-, which would rapidly dissipate, after spending a considerably long time near the caustic position. The second possibility is that the waves attempt to reach a stopping velocity position whilst taking an infinitely long period of time to do so. Moreover, the virtually constant values of wavenumber and steepness in the region near troughs (figures 5.10 initial k_1 = 1.48 and figures 5.12 initial k_1 = 0.3289) suggest the presence of a uniform wavetrain at the troughs which could sustain this type of behaviour. Thus, waves GC- would appear to "sit" on the forward faces of gravity waves for long periods of time. A combination of these two effects is also possible. A capillary wavetrain maybe partially reflected and partially "transmitted" at a caustic near the crests of gravity wavetrains.

Note that, according to slowly-varying theory, any waves GC- which propagate over the whole length of the gravity waves will have their steepness attenuated by dissipative effects. These waves will never reach zero steepness (see § 5.7 or figures 5.10) and so, after propagating several wavelengths, will reach a stopping velocity position. This is the characteristic of the third type of general behaviour for waves GC-. Also note that waves GC- reach positions, near the troughs, where their wavelengths are quite large and so might possibly be affected by gravity. However, this is qualitatively unimportant since such waves will not be greatly affected by dissipation and so will propagate past the troughs towards the crests of the gravity waves where wavelengths are small again.

Attention is now focused onto the observers frame. Stationary waves CG and waves CG+ rapidly dissipate and cease to exist whilst attempting to overtake the gravity waves. Waves CG- also rapidly dissipate in the same manner as waves CG or CG+ for the majority of propagations. A small proportion of propagations for waves CG- take an infinitely long time to try and reach a stopping velocity position whilst attempting to overtake the gravity waves. The mechanism for the sustenance of such behaviour is unclear.

Waves GC- exhibit one of four types of behaviour. One is to be swept-up on the forward faces of gravity waves whilst the gravity waves attempt to overtake them. A second is to actually be overtaken by the gravity waves but have their steepness attenuated after, say, one wavelength of the gravity waves has passed. A third is to take an infinitely long time to try and reach a stopping velocity position and, thus, sit on the gravity wave fronts whilst the gravity waves attempt to overtake them. The fourth is to be partially reflected, at the caustic position, to waves CG- whilst the gravity waves attempt to overtake them. These reflected waves rapidly dissipate and cease to exist whilst attempting to overtake the gravity waves. A combination of the latter two behaviours is also possible. Note that any waves GC- which exhibit the second type of behaviour eventually reach a stopping velocity position and, thus, exhibit either the third or fourth types of behaviour or, ofcourse, a combination of these.

The general behaviours of the capillary waves in any frame of reference are now summarised. Considering some general distribution of capillary waves generated by a puff of wind it will be found that the waves either:

i) rapidly dissipate and cease to exist (stationary waves GC, waves CG+ or CG-);

ii) exhibit breaking on the forward faces of gravity waves (waves GC-);

iii) take an infinitely long time to try and reach a stopping velocity position (waves CG- or GC-);

iv) are eventually partially reflect on the forward faces of gravity waves (waves GC-) to waves (CG-) which rapidly dissipate and cease to exist; or

v) experience a combination of the latter two behaviours (waves GC-).

CAPTIONS FOR FIGURES

Figure 5.1: The variation of dissipation ratio $\mathcal{D}/\mathcal{D}_{lin}$ with steepness ak for finite-amplitude pure capillary waves.

Figure 5.2: Diagram illustrating the existence of windows for (a) stationary waves, and (b) Doppler shifted waves.

Figure 5.3: The variation of (a) wavenumber k and (b) steepness ak with distance X for stationary waves with $\mu \neq 0$ where the gravity wave has A = 0.2 m, AK = 0.3 and crest at centre; various initial wavenumbers k as shown.

Figure 5.4: The variation of (a) wavenumber k and (b) steepness ak with distance X for stationary waves with $\mu \neq 0$ where the gravity wave has A = 0.2 m, AK = 0.3 and trough at centre; various initial wavenumbers k as shown.

Figure 5.5: The variation of (a) wavenumber k_1 and (b) steepness ak with distance X_1 for waves CG+ with $\mu \neq 0$, $|\omega|$ = 100 rad s^{-1} where the gravity wave has A = 0.2 m, AK = 0.3 and crest at centre; various initial wavenumbers k_1 as shown.

Figure 5.6: The variation of (a) wavenumber k_1 and (b) steepness ak with distance X_1 for waves CG+ with $\mu \neq 0$, $|\omega|$ = 100 rad s^{-1} where the gravity wave has A = 0.2 m, AK = 0.3 and trough at centre; various initial wavenumbers k_1 as shown.

Figure 5.7: The variation of (a) wavenumber k_1 and (b) steepness ak with distance X_1 for waves CG- with $\mu \neq 0$, $|\omega|$ = 100 rad s^{-1} where the gravity wave has A = 0.2 m, AK = 0.3 and crest at centre; various initial wavenumbers k_1 as shown.

Figure 5.8: The variation of (a) wavenumber k_1 and (b) steepness ak with distance X_1 for waves CG- with $\mu \neq 0$, $|\omega|$ = 100 rad s^{-1} where the gravity wave has A = 0.2 m, AK = 0.3 and trough at centre; various initial wavenumbers k_1 as shown.

Figure 5.9: The variation of (a) wavenumber k_1 and (b) steepness ak with distance X_1 for waves CG- with $\mu = 0$, $|\omega|$ = 100 rad s^{-1} where the gravity wave has A = 0.2 m, AK = 0.3 and trough at centre; various initial wavenumbers k_1 as shown.

Figure 5.10: The variation of (a) wavenumber k_1 and (b) steepness ak with distance X_1 for waves GC- with $\mu \neq 0$, $|\omega|$ = 100 rad s^{-1} where the gravity wave has A = 0.2 m, AK = 0.3 and trough at centre; various initial wavenumbers k_1 as shown.

Figure 5.11: The variation of (a) wavenumber k_1 and (b) steepness ak with distance X_1 for waves GC- with $\mu = 0$, $|\omega|$ = 100 rad s^{-1} where the gravity wave has A = 0.2 m, AK = 0.3 and trough at centre; various initial wavenumbers k_1 as shown.

Figure 5.12: The variation of (a) wavenumber k_1 and (b) steepness ak with distance X_1 for waves GC- with $\mu \neq 0$, $|\omega|$ = 100 rad s^{-1} where the gravity wave has A = 0.2 m, AK = 0.3 and crest at centre; various initial wavenumbers k_1 as shown.

Figure 5.13: The variation of (a) wavenumber k_1 and (b) steepness ak with distance X_1 for waves GC- with $\mu = 0$, $|\omega|$ = 100 rad s^{-1} where the gravity wave has A = 0.2 m, AK = 0.3 and crest at centre; various initial wavenumbers k_1 as shown.

Figure 5.14: (a) The variation of amplitude $|w_1|$ with distance z_1 as given by the generalised Painlevé equation for asymptotic parameter A = 0.15 and viscosity parameter B = 0 ($\mu = 0$) with the corresponding variations of the constitutive incident and reflected wave amplitudes w_{1i} and w_{1r}; (b,c) The corresponding incident and reflected slowly varying solutions [(b) wavenumber k_1 and (c) steepness ak verses distance X_1] for waves CG- and GC-. The gravity wave has A = 0.2 m, AK = 0.3 and crest at centre.

Figure 5.15: (a) The variation of amplitude $|w_1|$ with distance z_1 as given by the generalised Painlevé equation for asymptotic parameter A = 0.15 and viscosity parameter B = 151 ($\mu \neq 0$) with the corresponding variations of the constitutive incident and reflected wave amplitudes w_{1i} and w_{1r}; (b,c) The corresponding incident and reflected slowly varying solutions [(a) wavenumber k_1 and (b) steepness ak verses distance X_1] for waves CG- and GC-. The gravity wave has A = 0.2 m, AK = 0.3 and crest at centre.

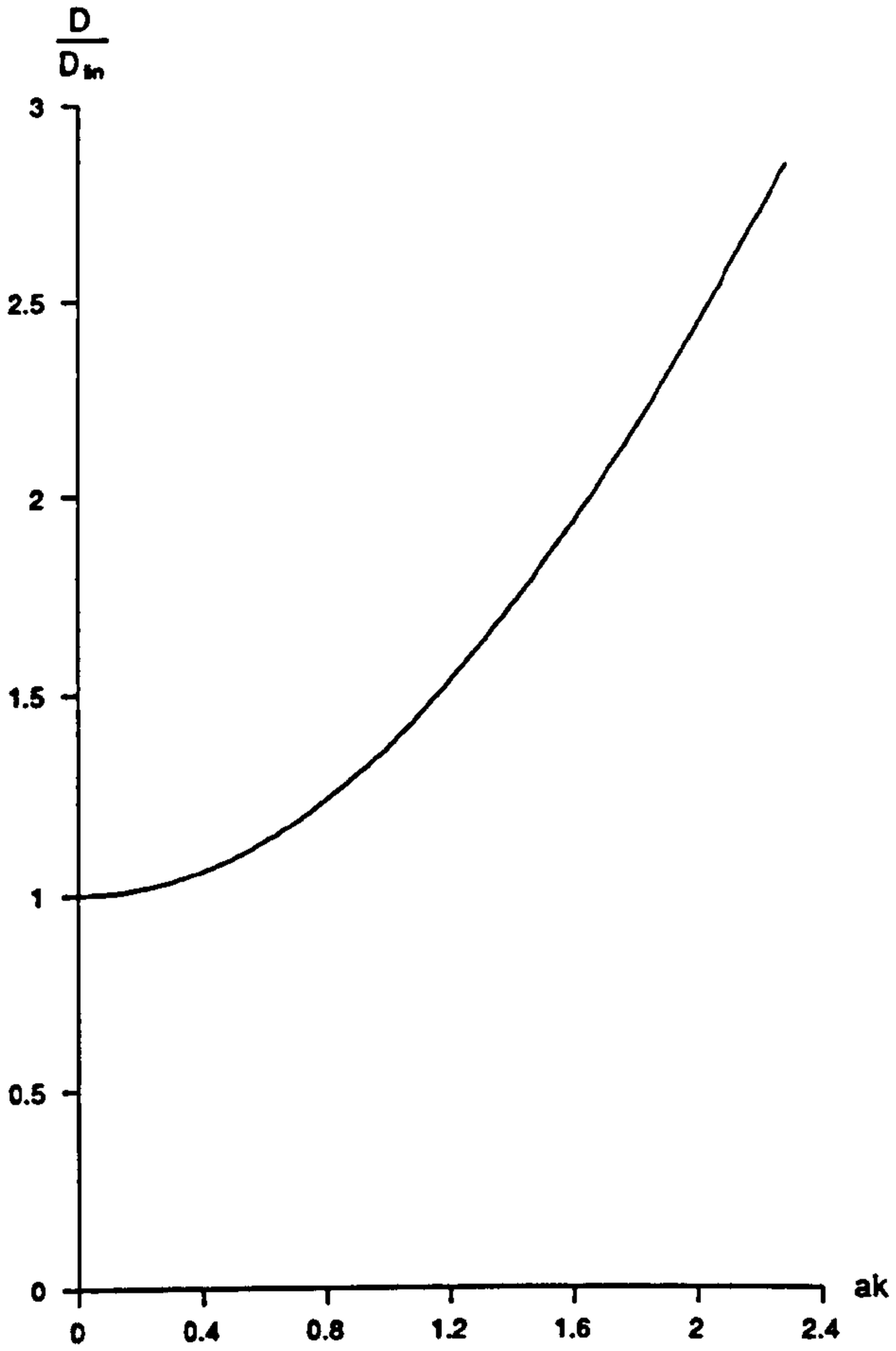

Figure 5.1

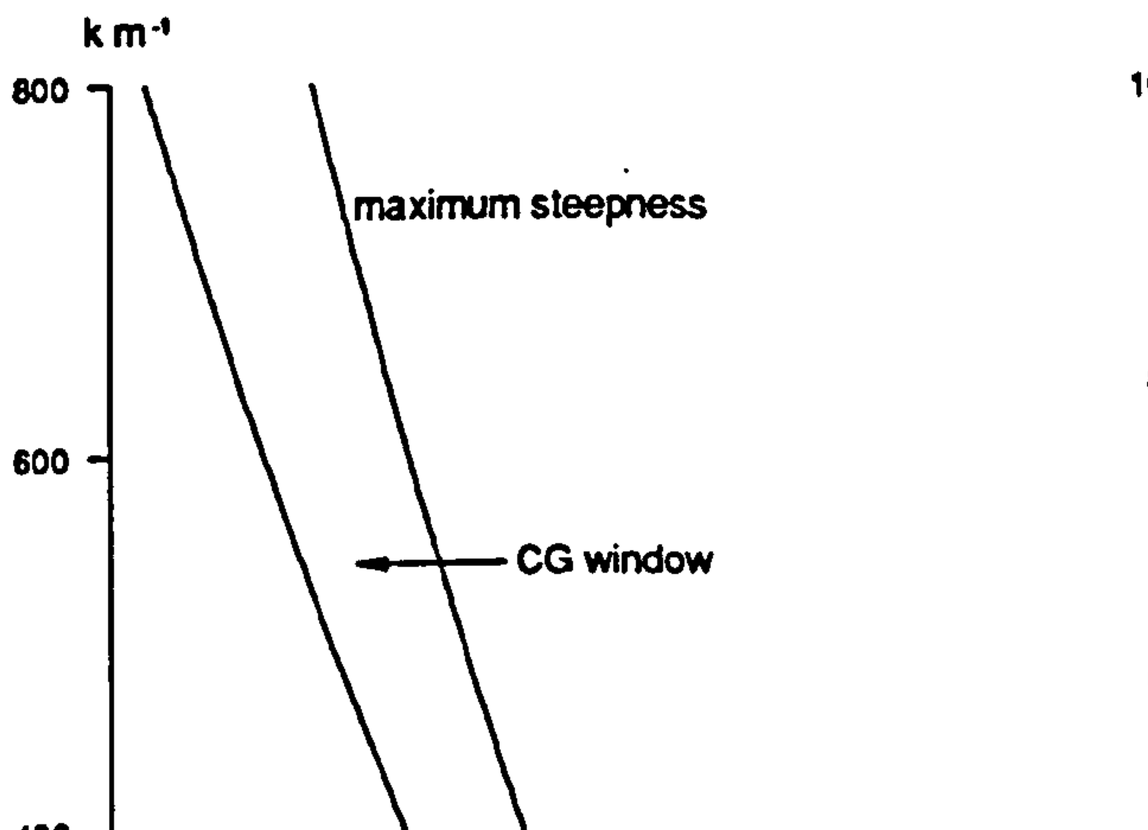

Figure 5.2a

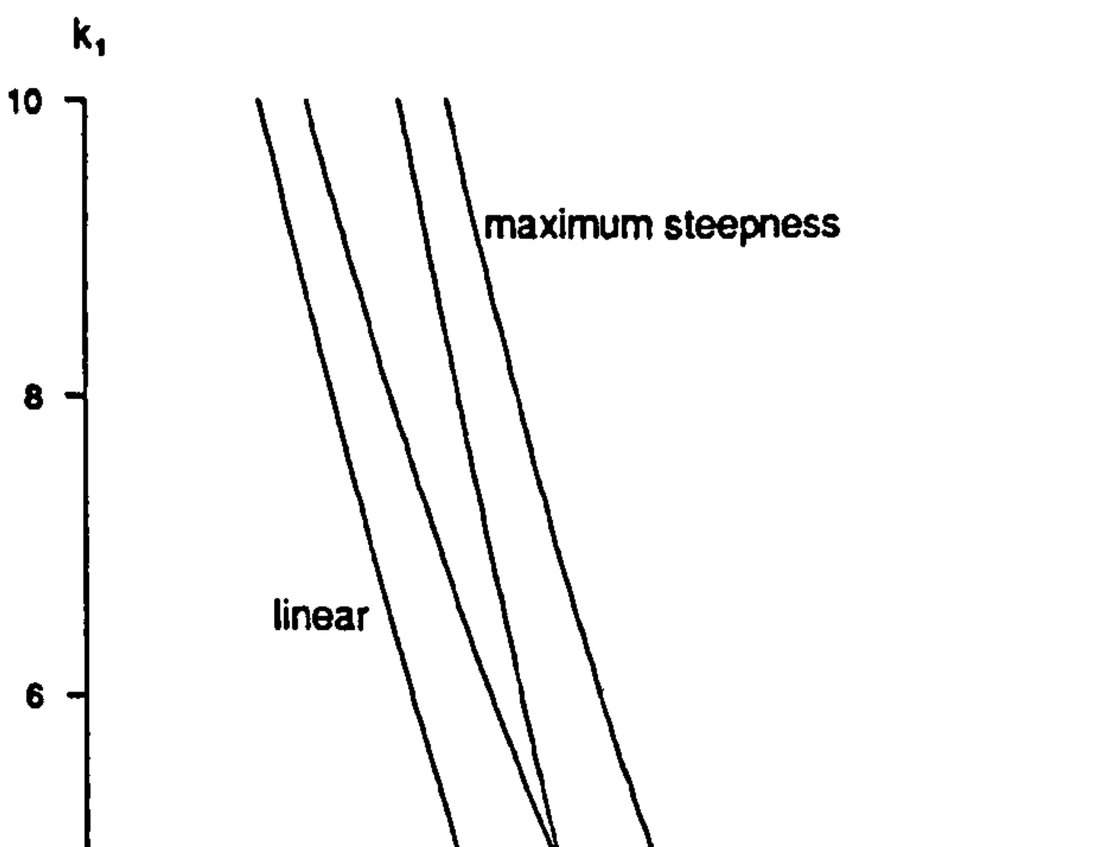

Figure 5.2b

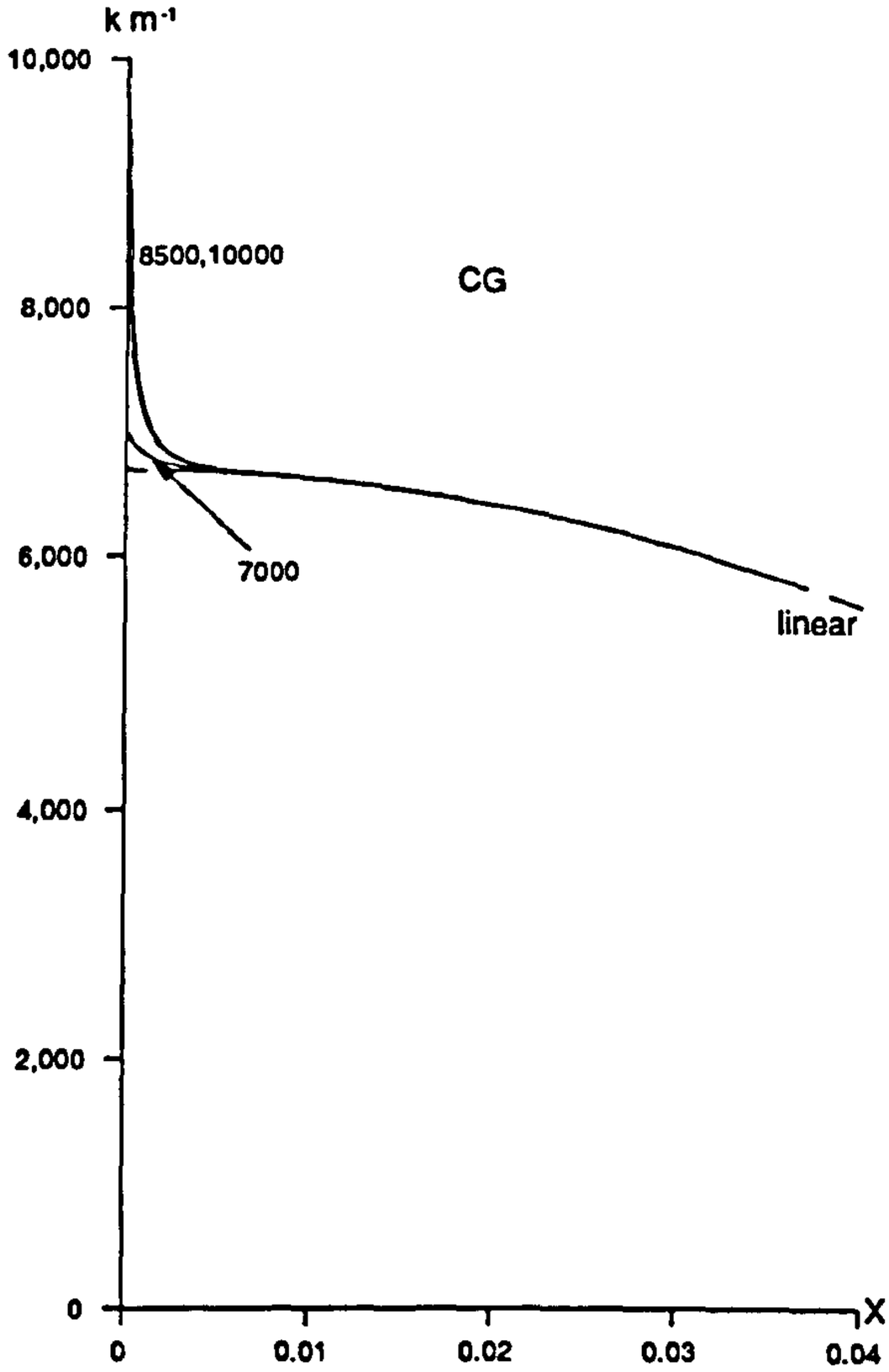

Figure 5.3a

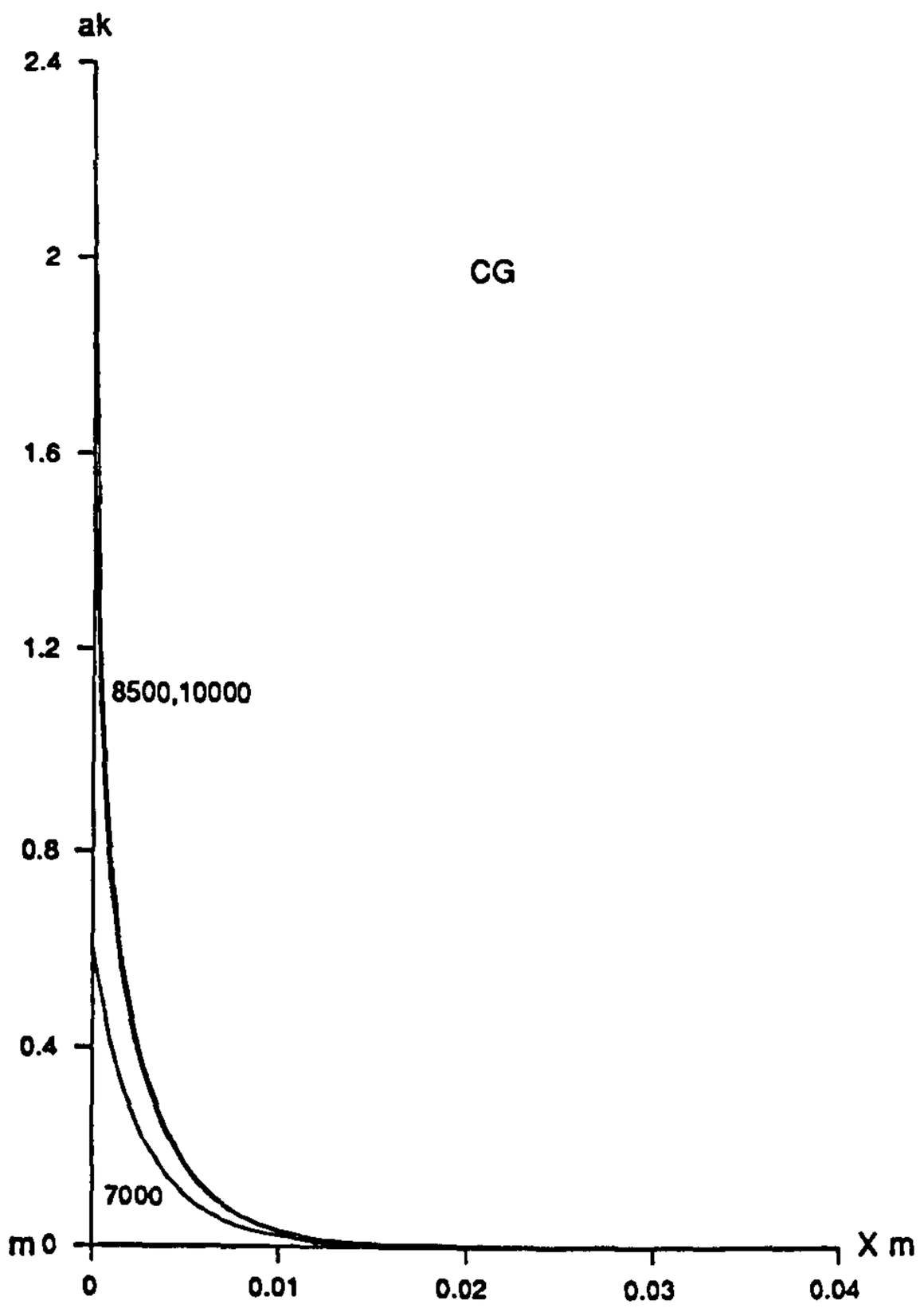

Figure 5.3b

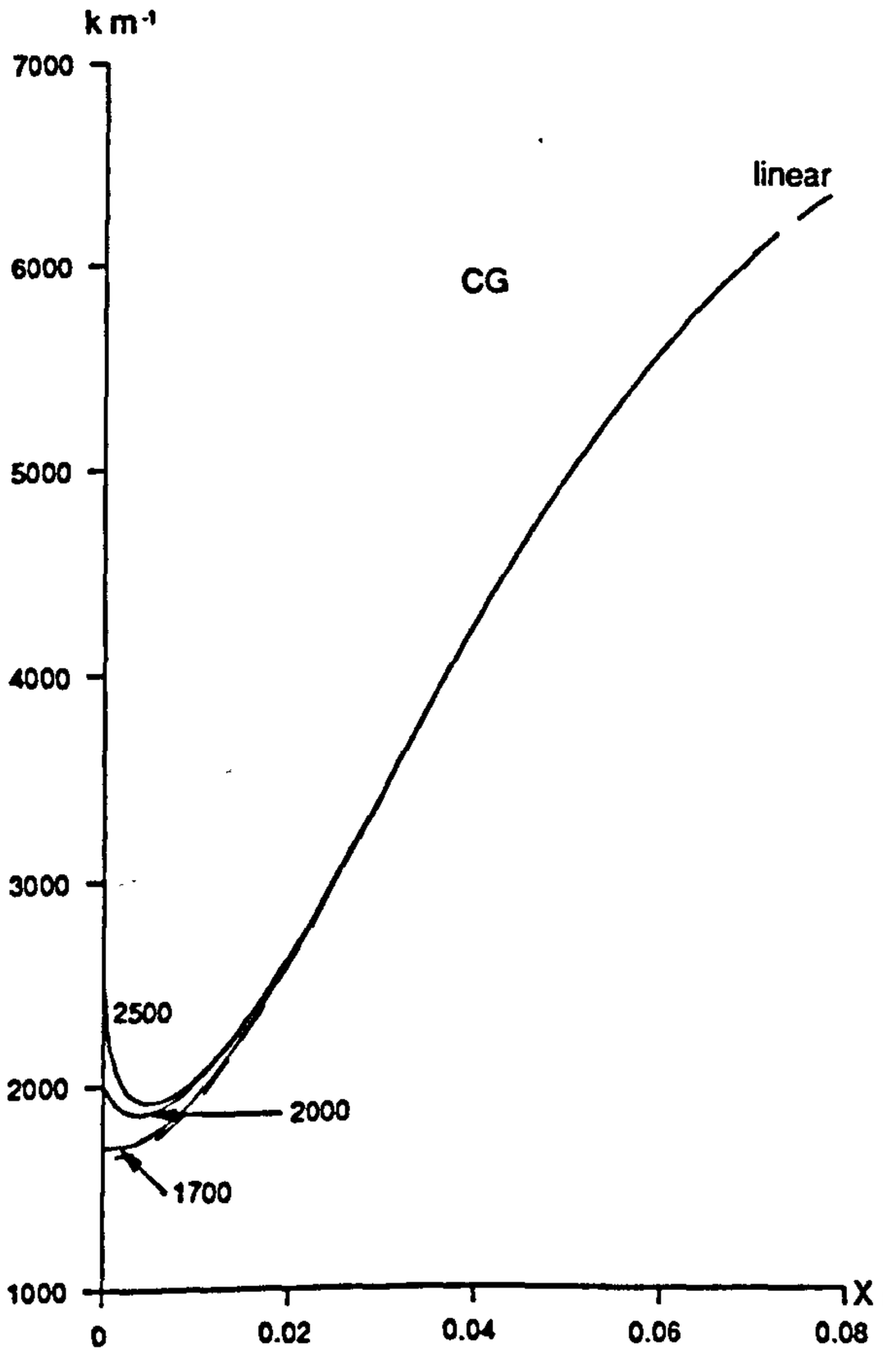

Figure 5.4a

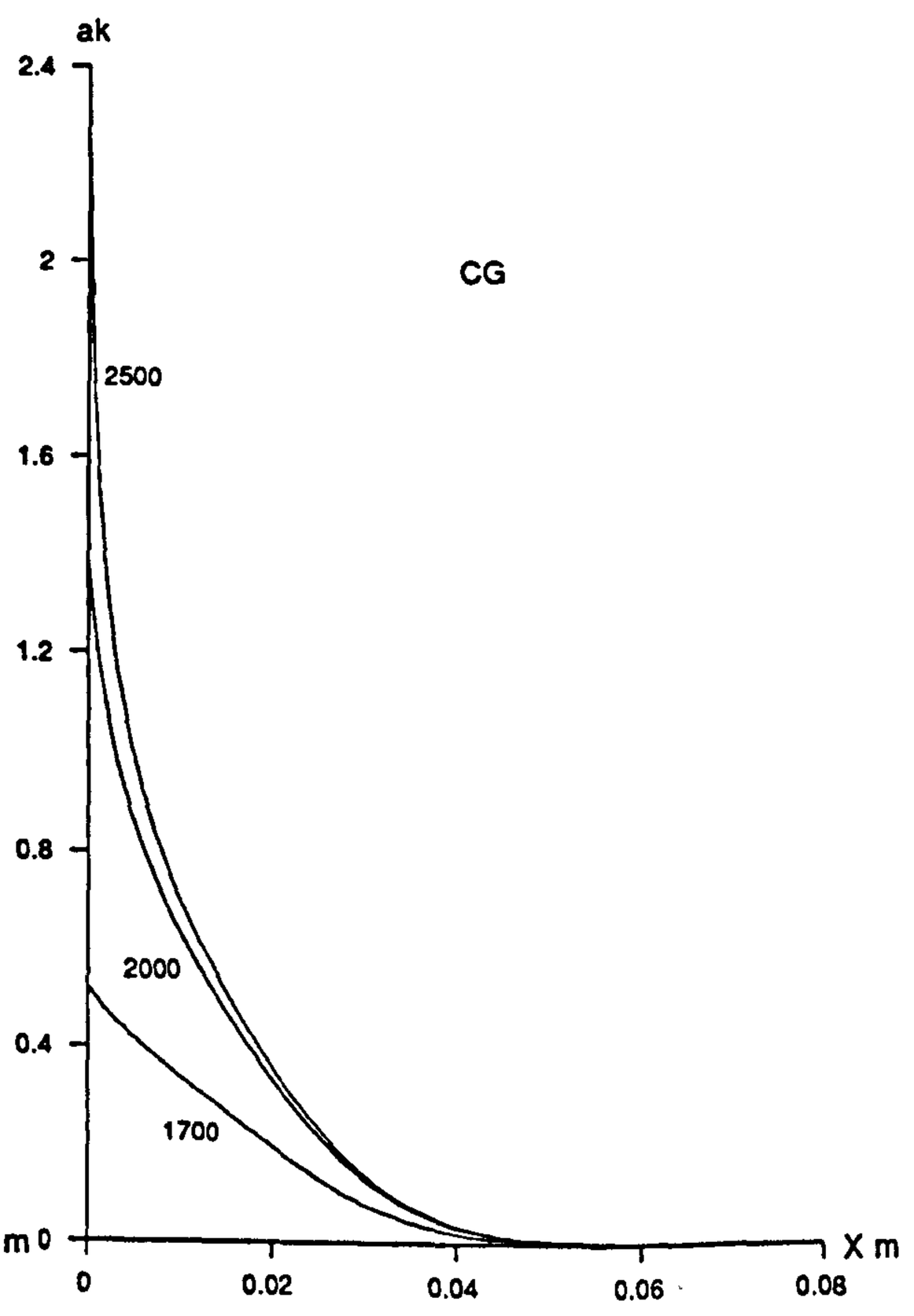

Figure 5.4b

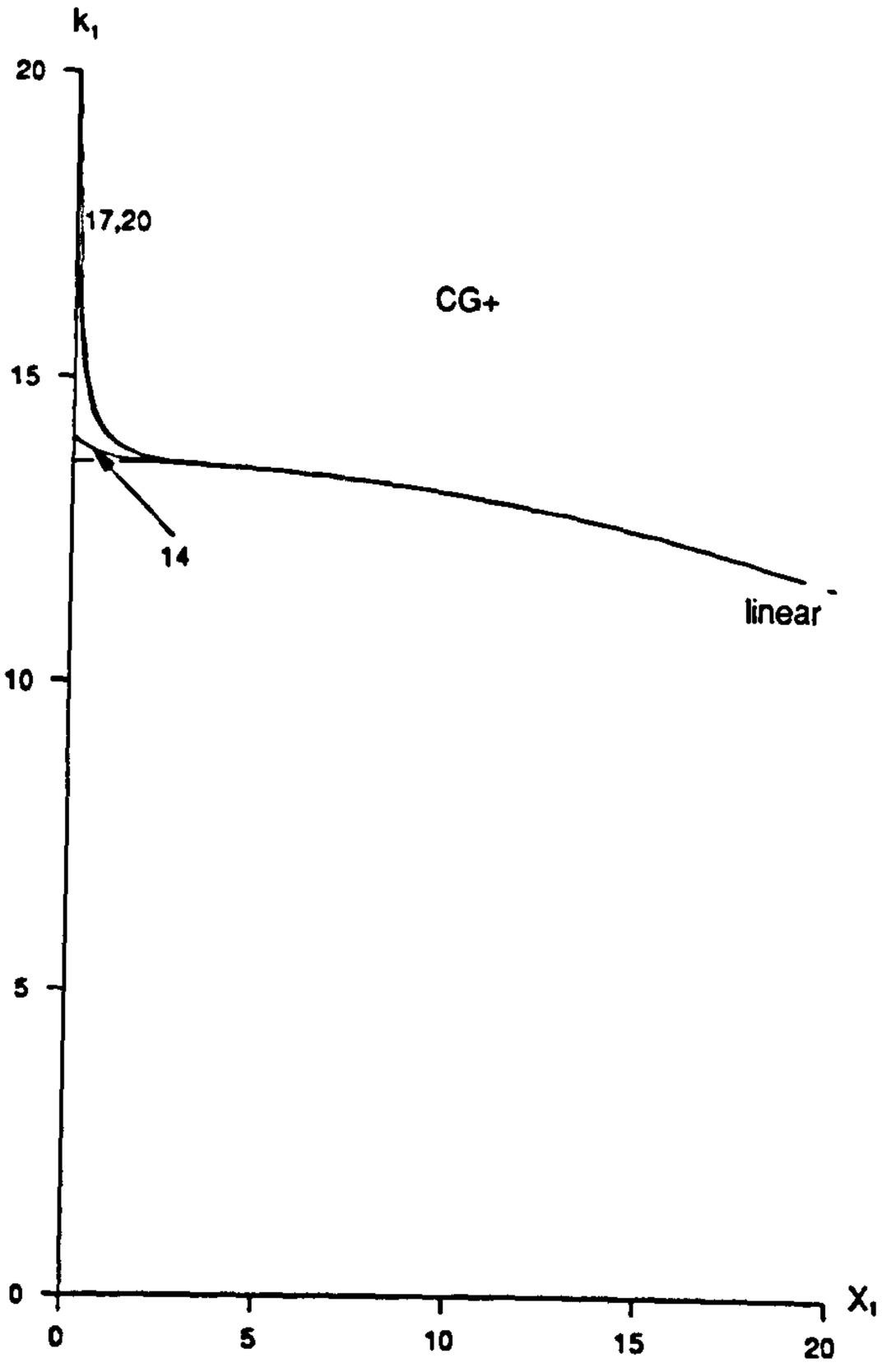

Figure 5.5a

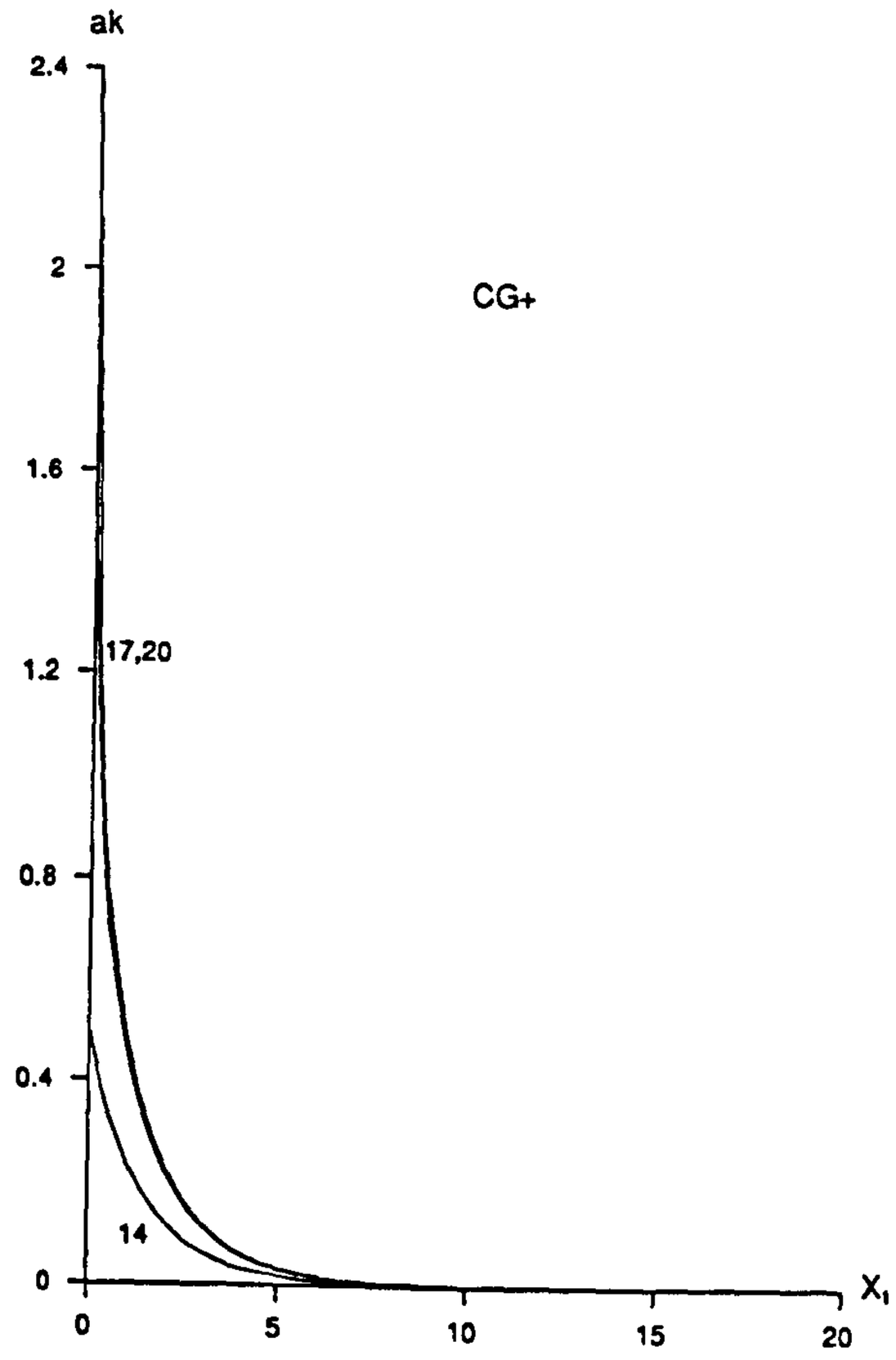

Figure 5.5b

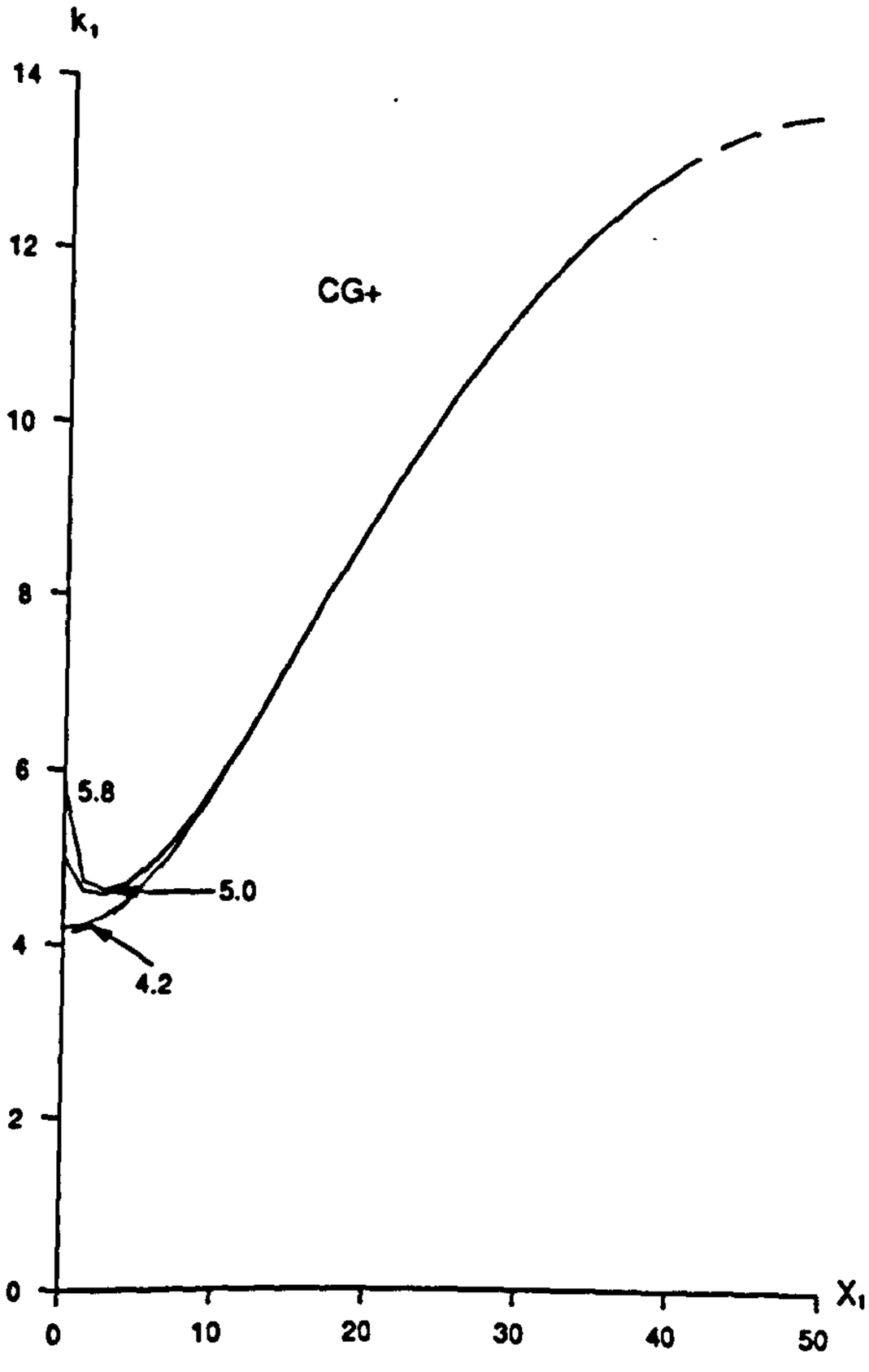

Figure 5.6a

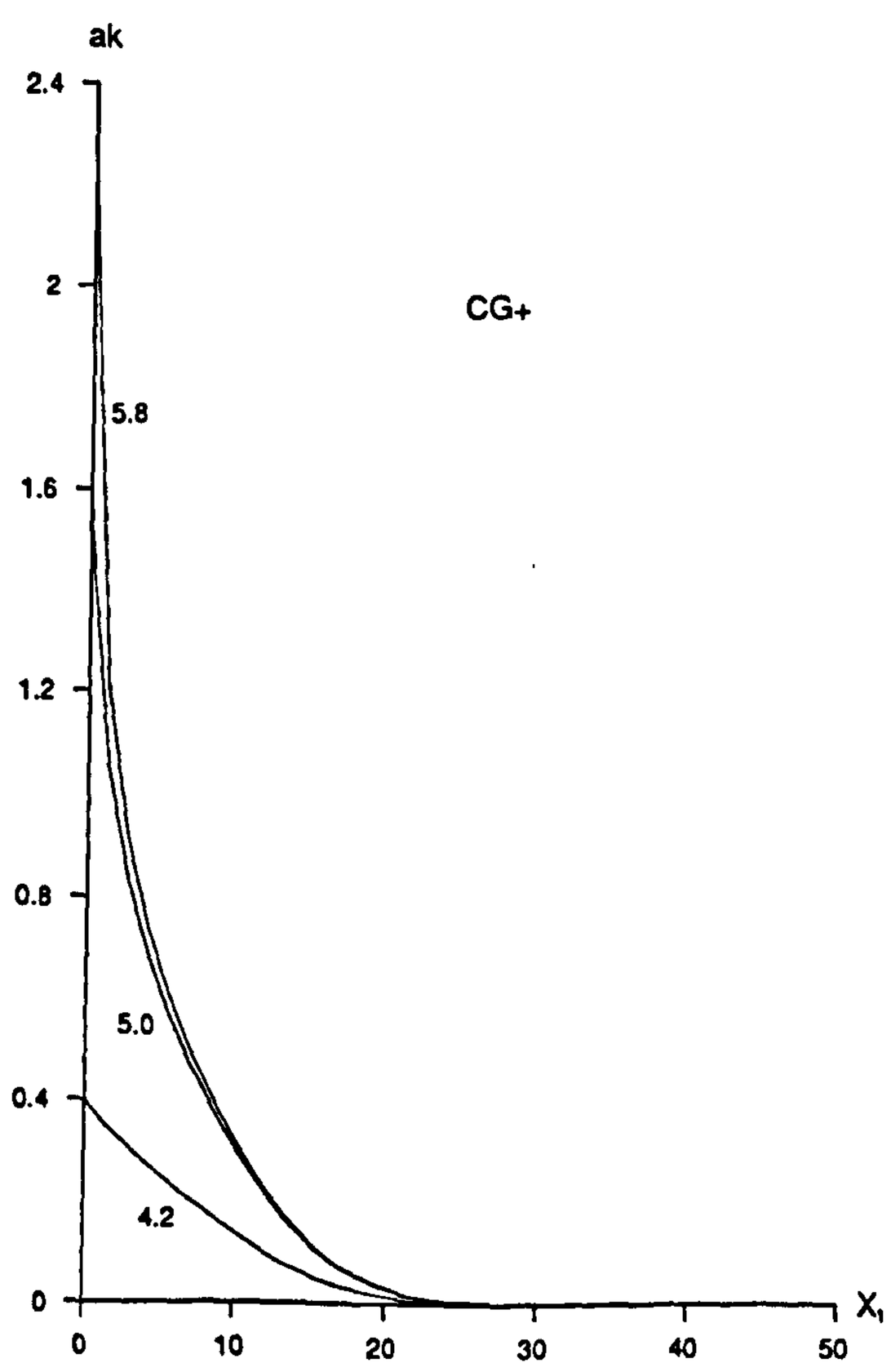

Figure 5.6b

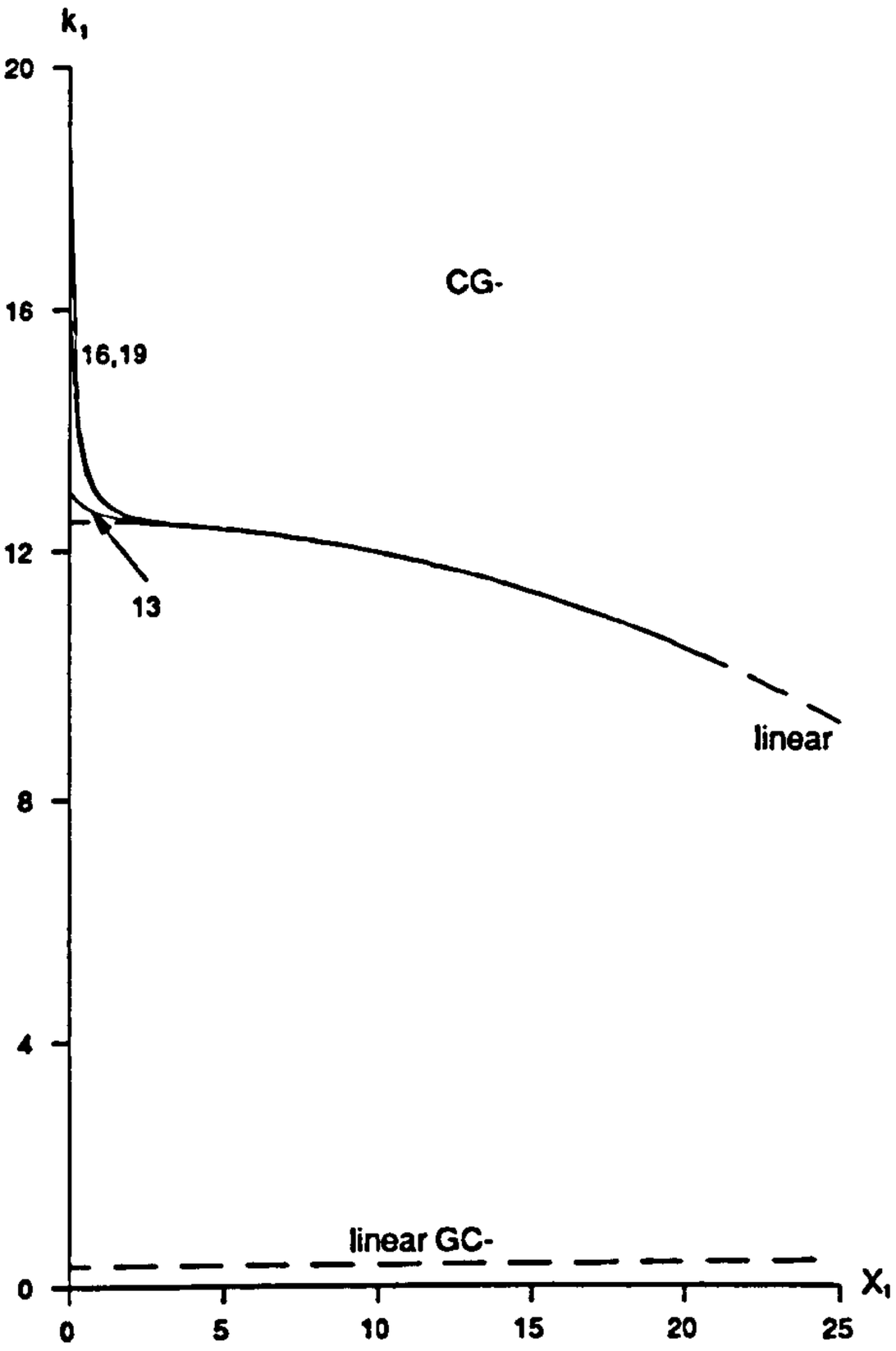

Figure 5.7a

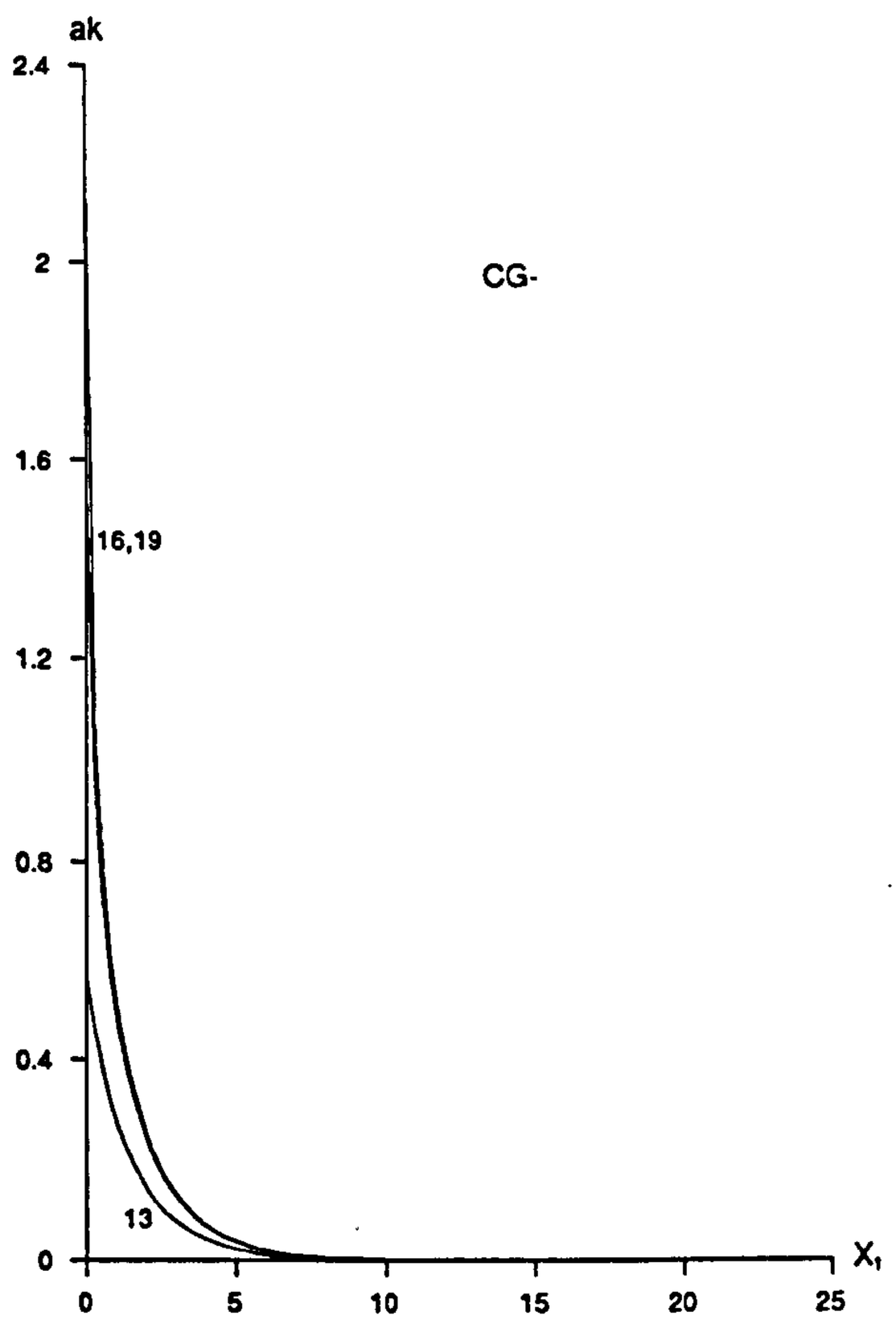

Figure 5.7b

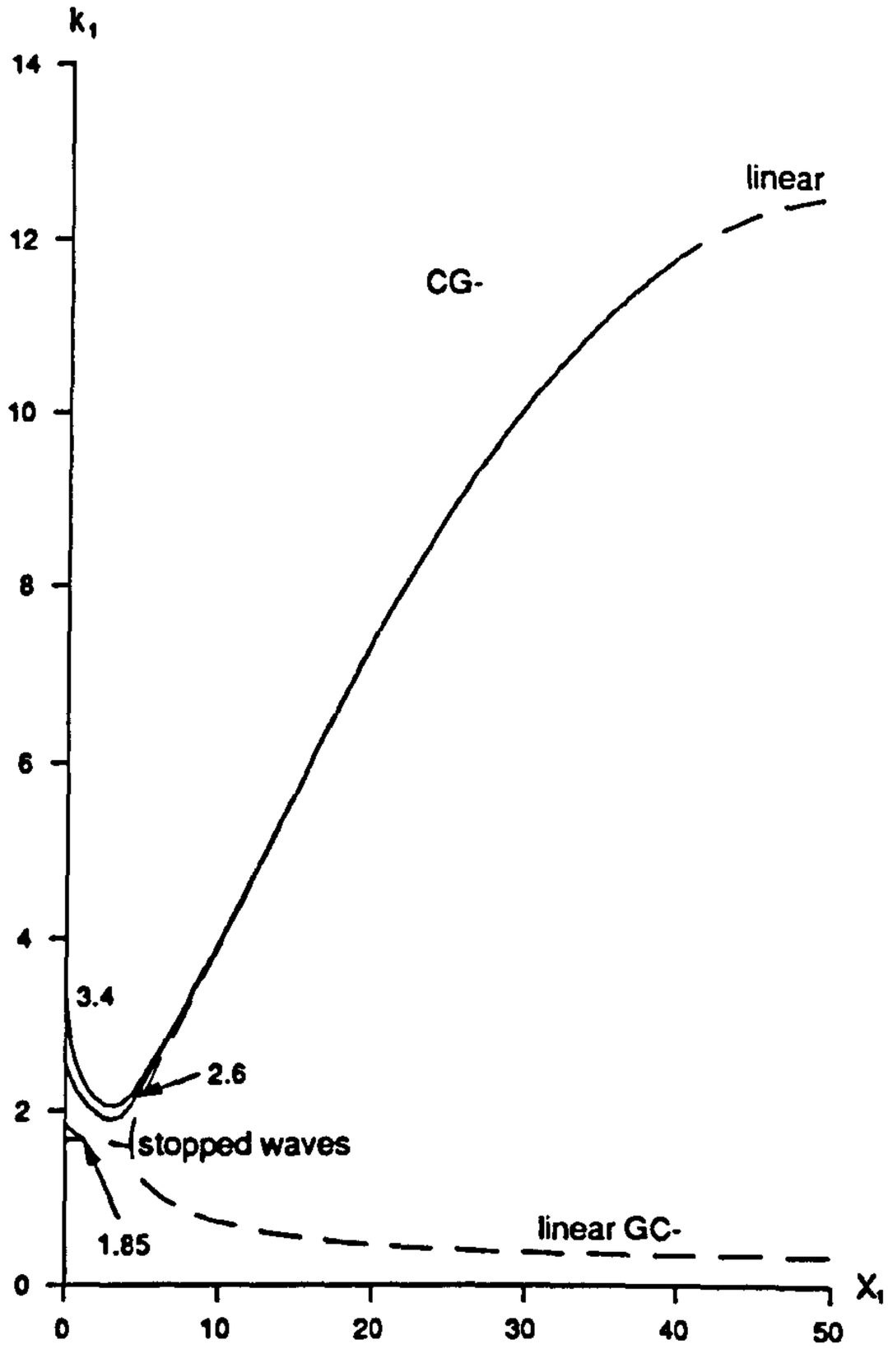

Figure 5.8a

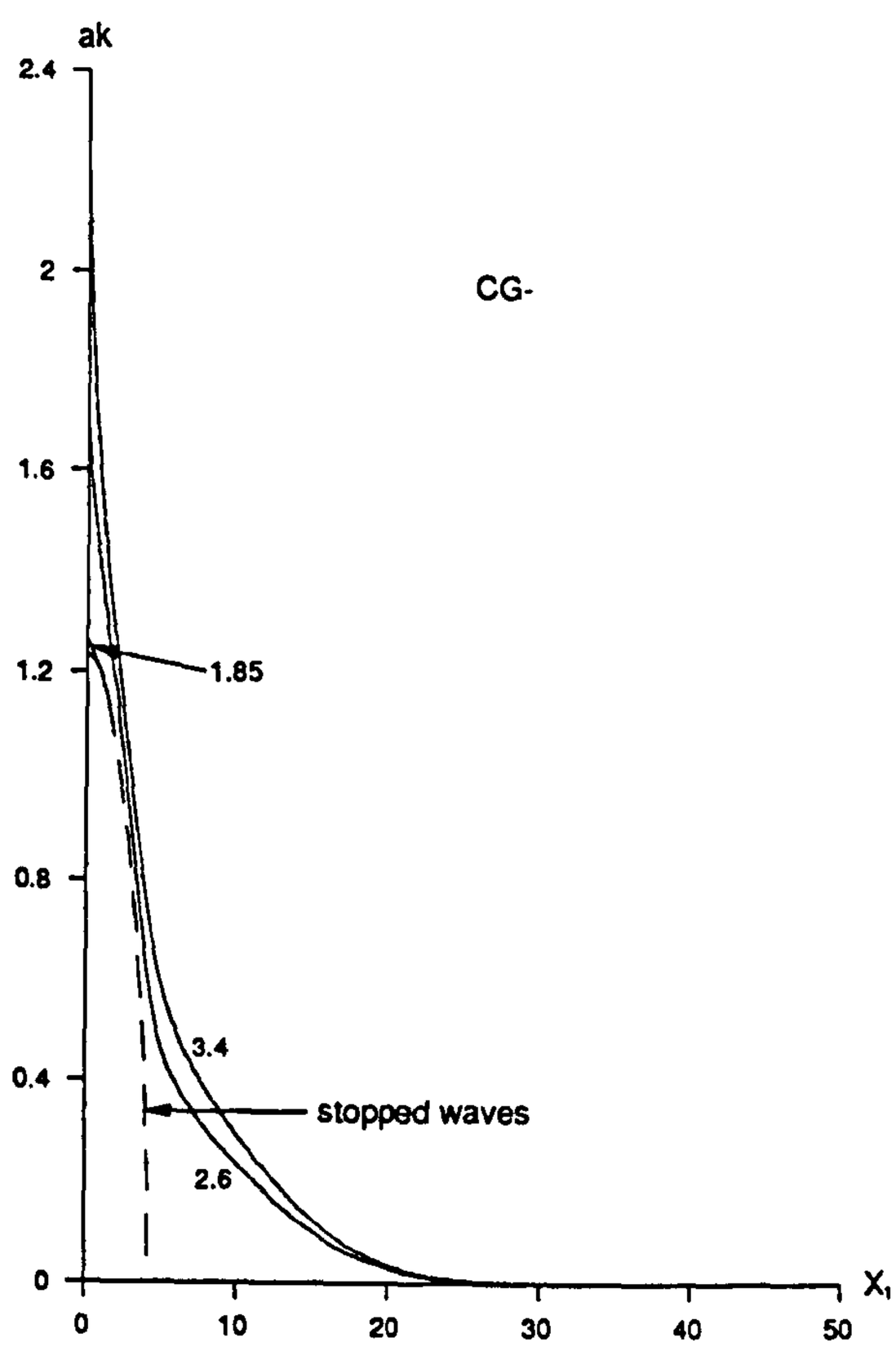

Figure 5.8b

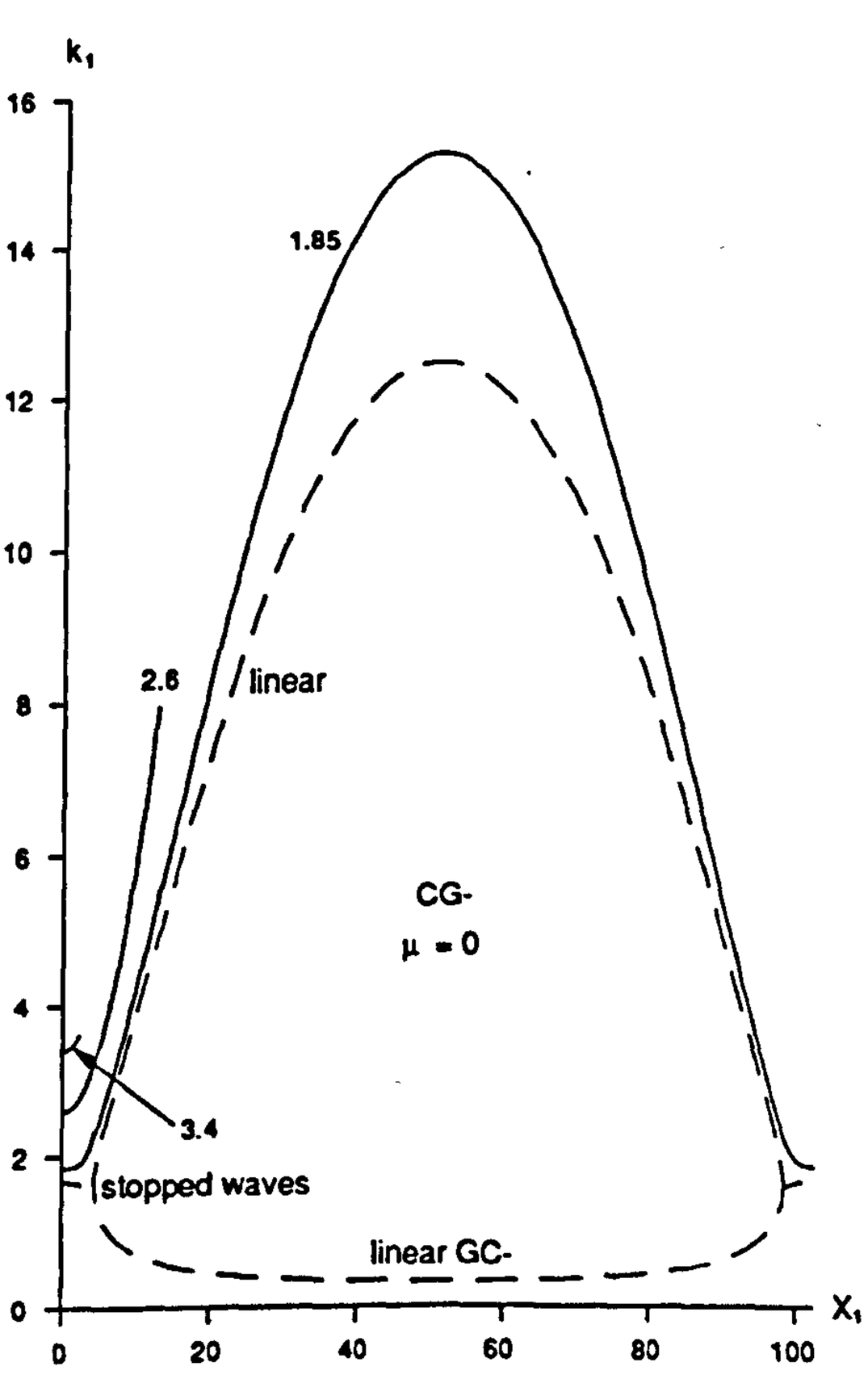

Figure 5.9a

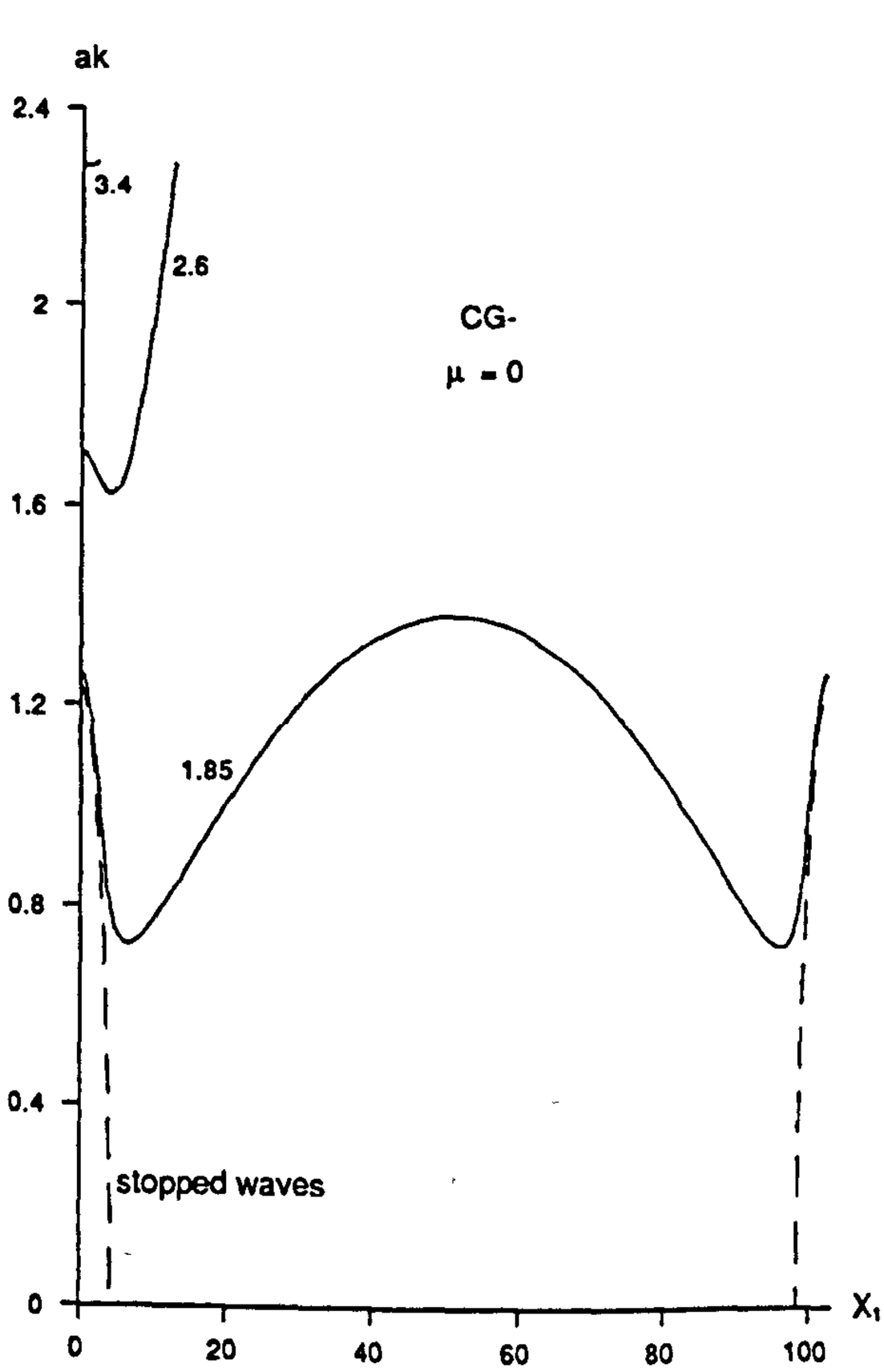

Figure 5.9b

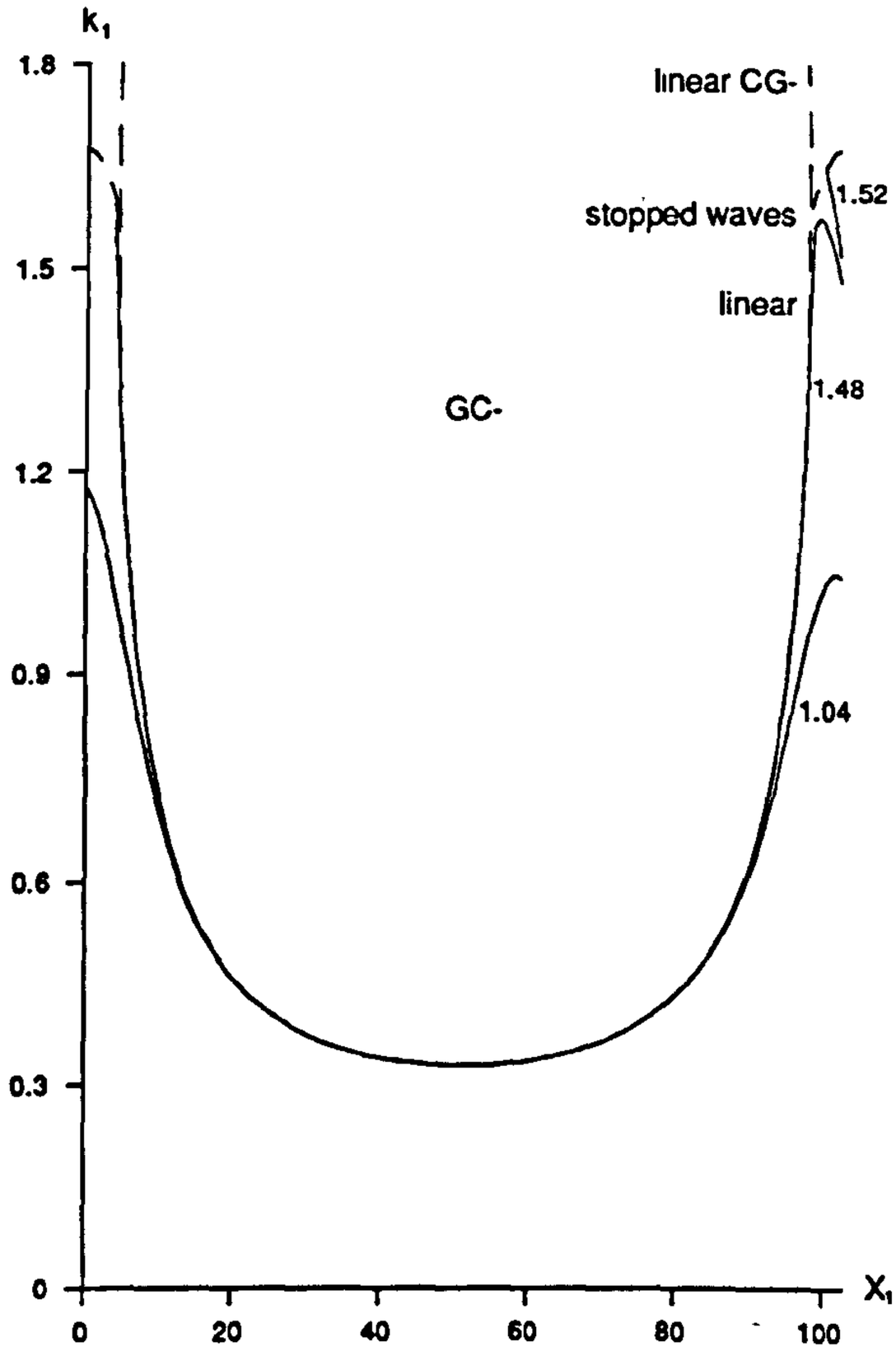

Figure 5.10a

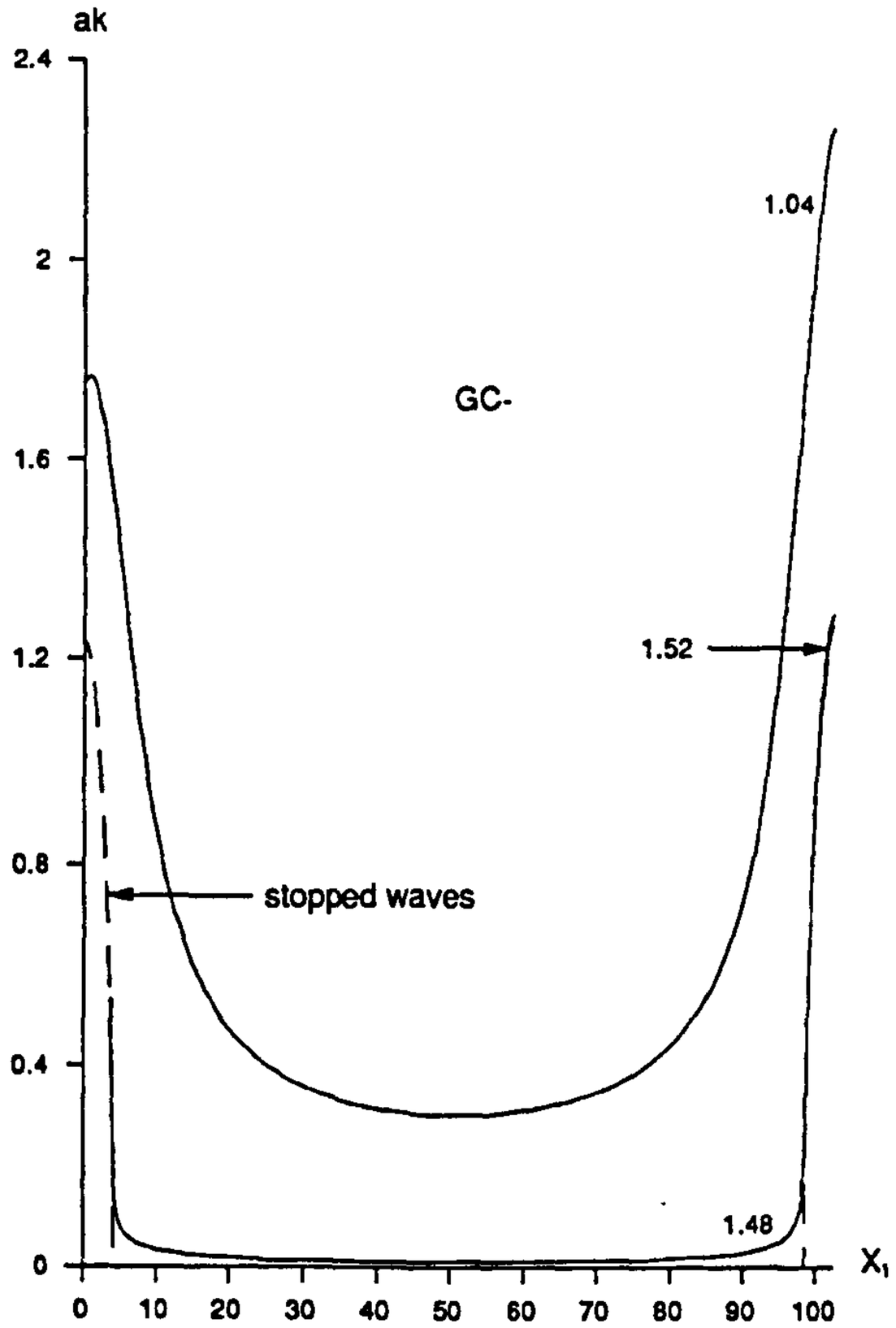

Figure 5.10b

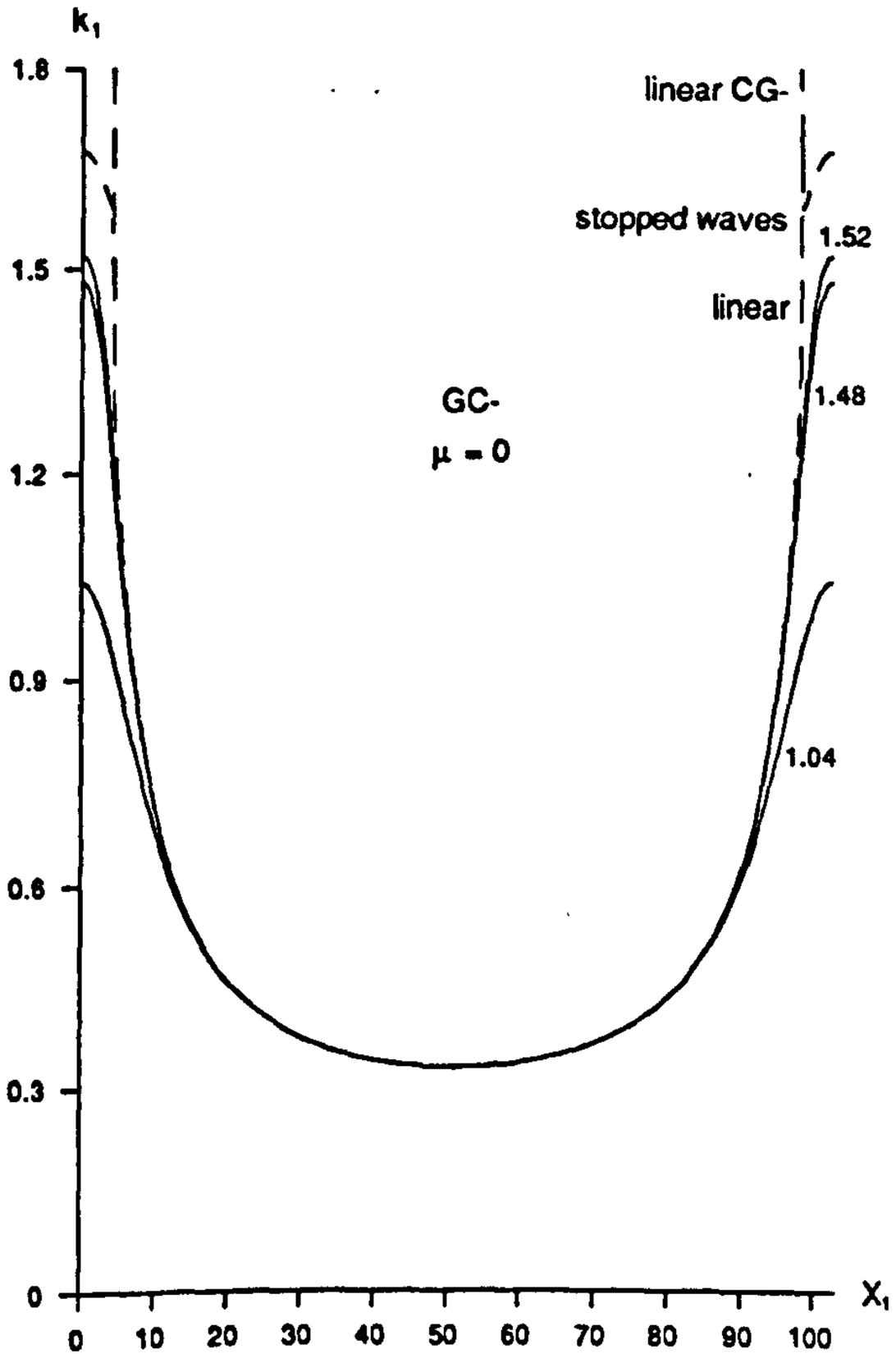

Figure 5.11a

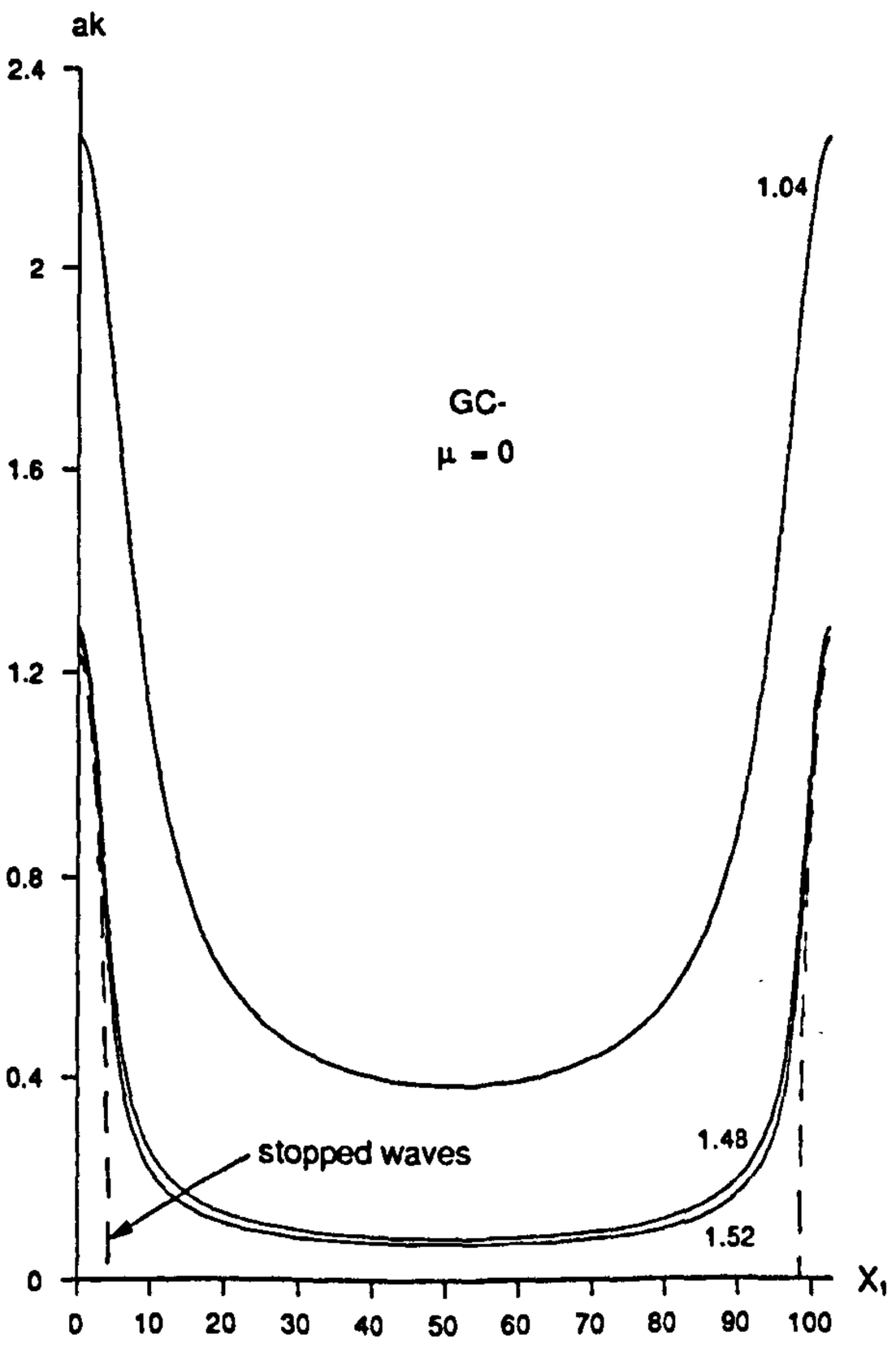

Figure 5.11b

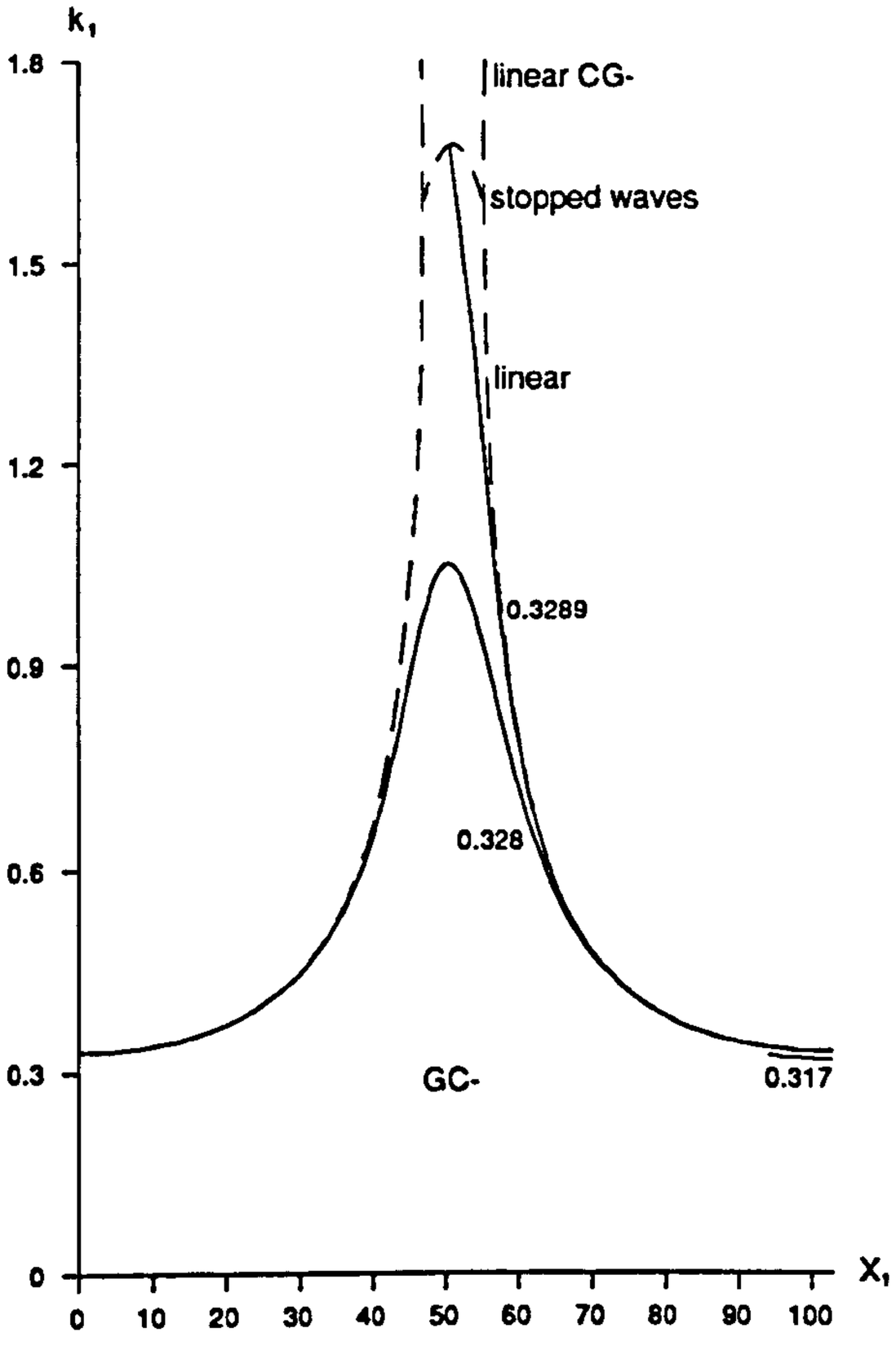

Figure 5.12a

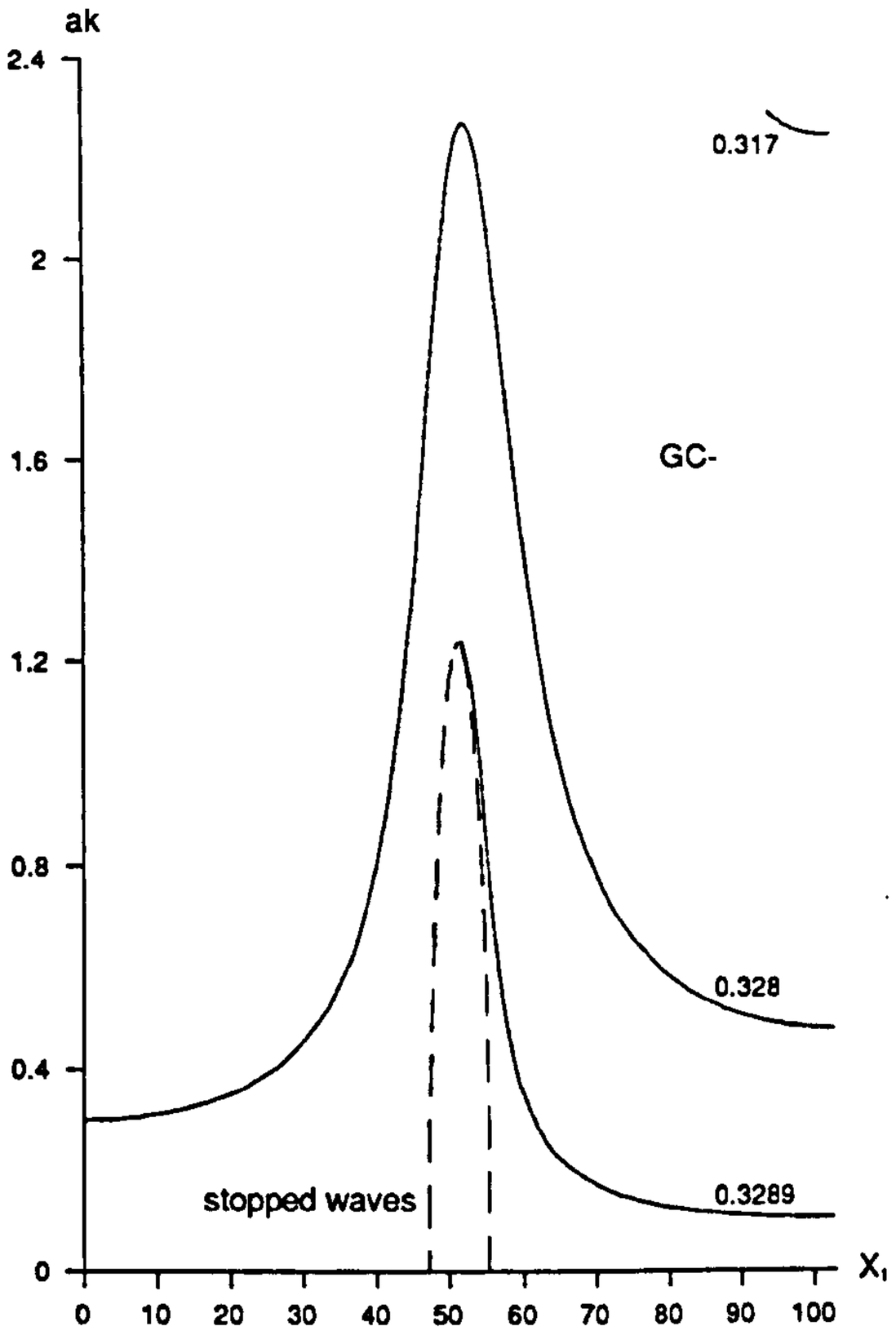

Figure 5.12b

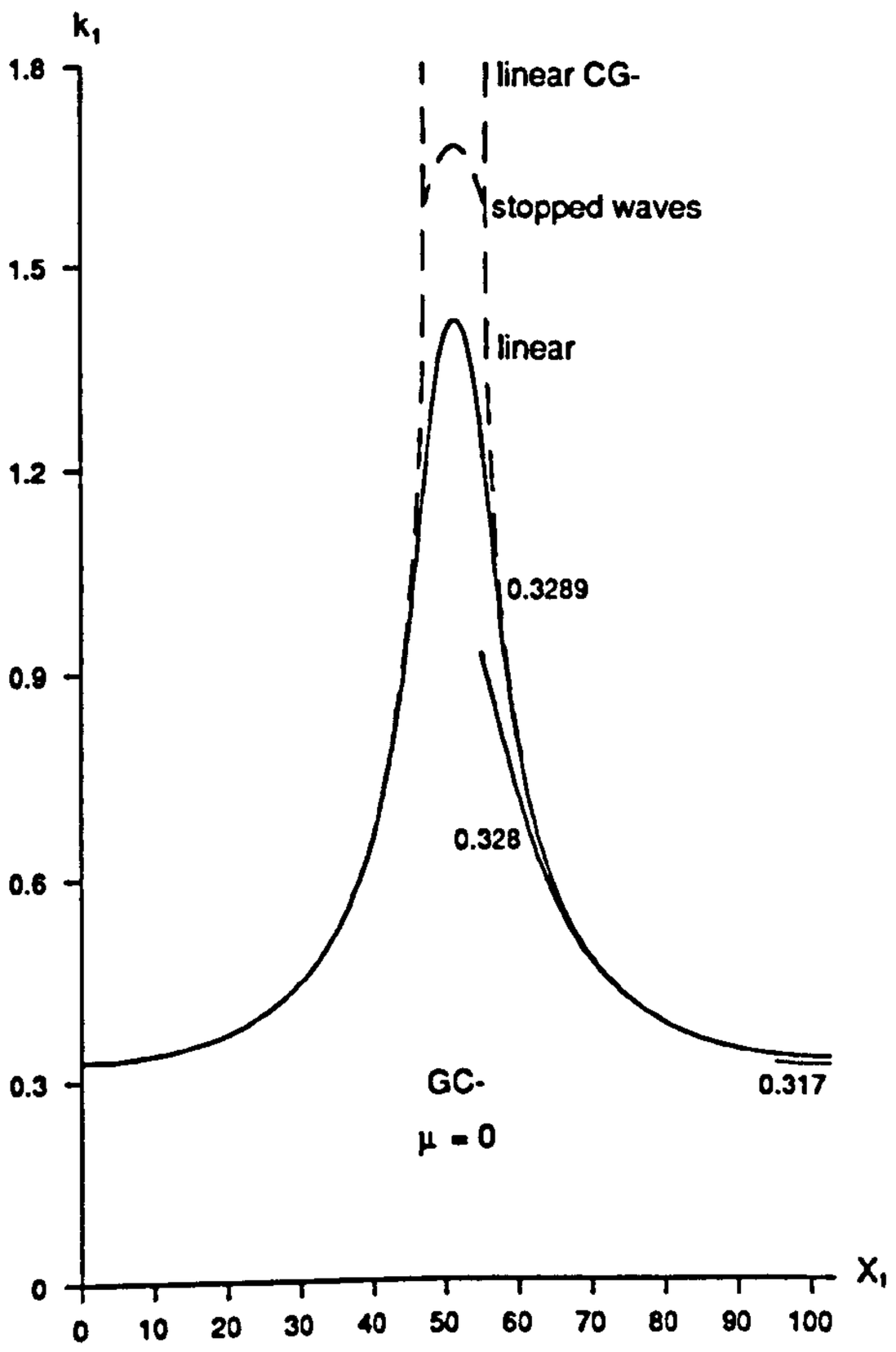

Figure 5.13a

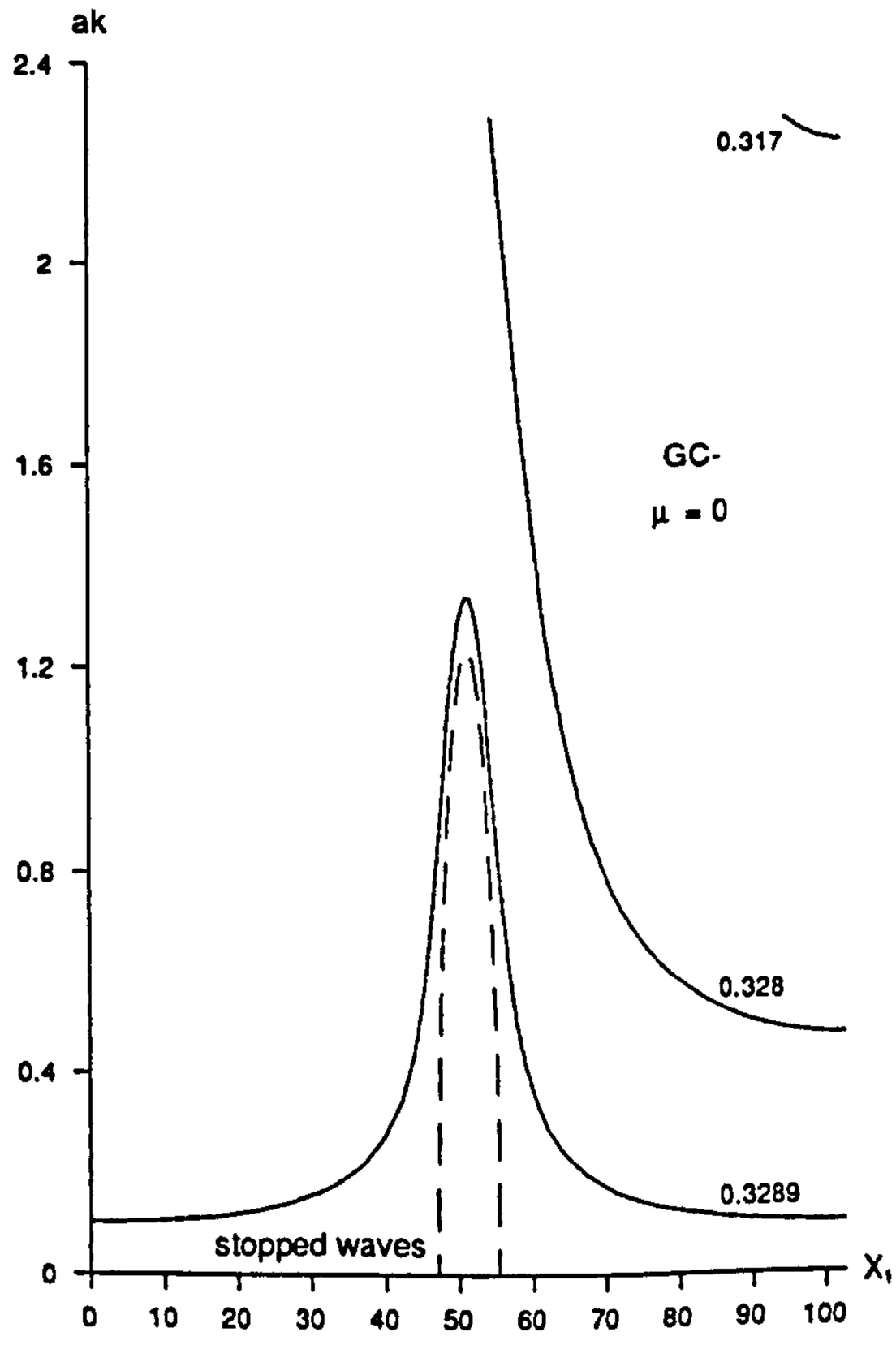

Figure 5.13b

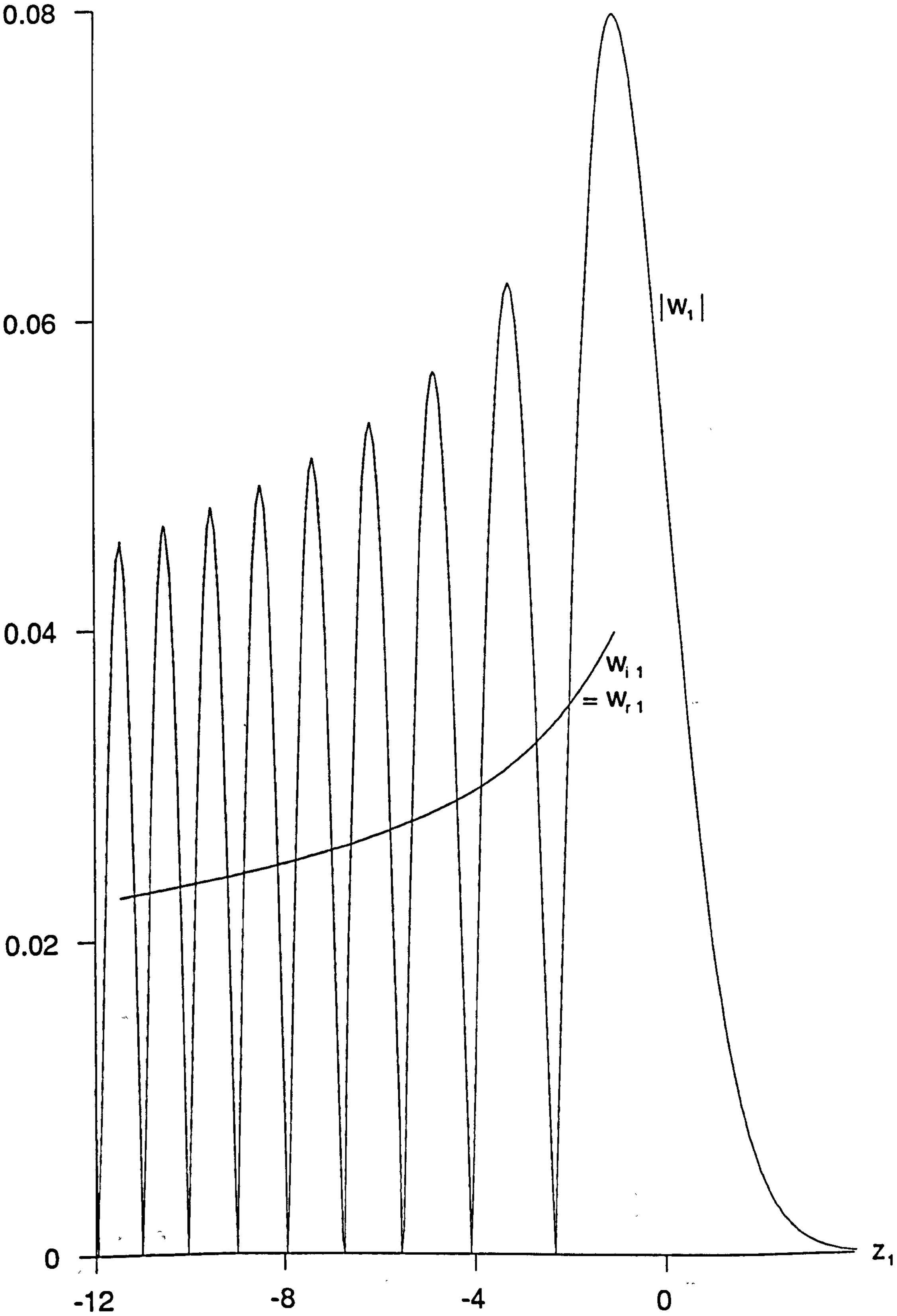

Figure 5.14a

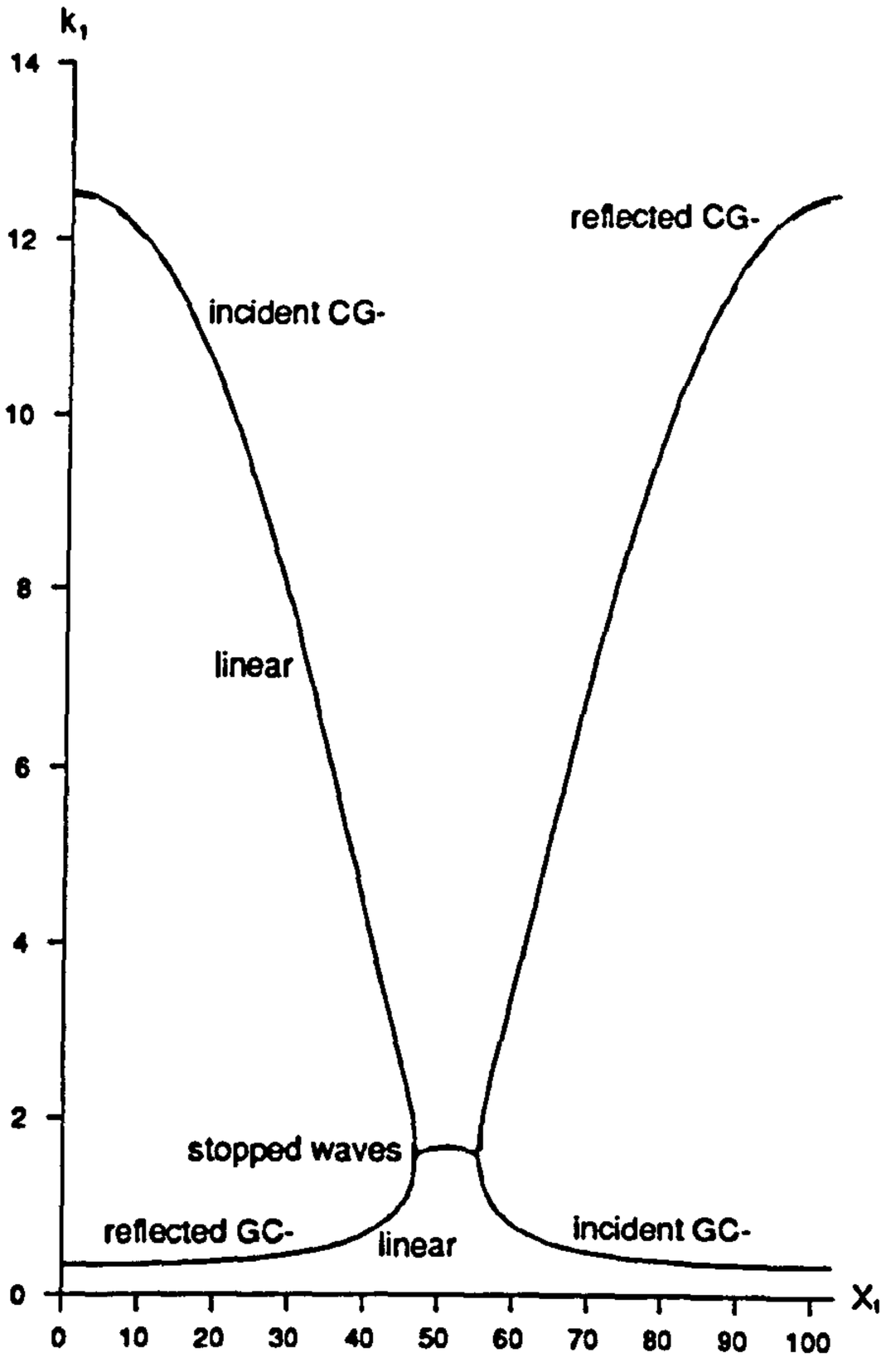

Figure 5.14b

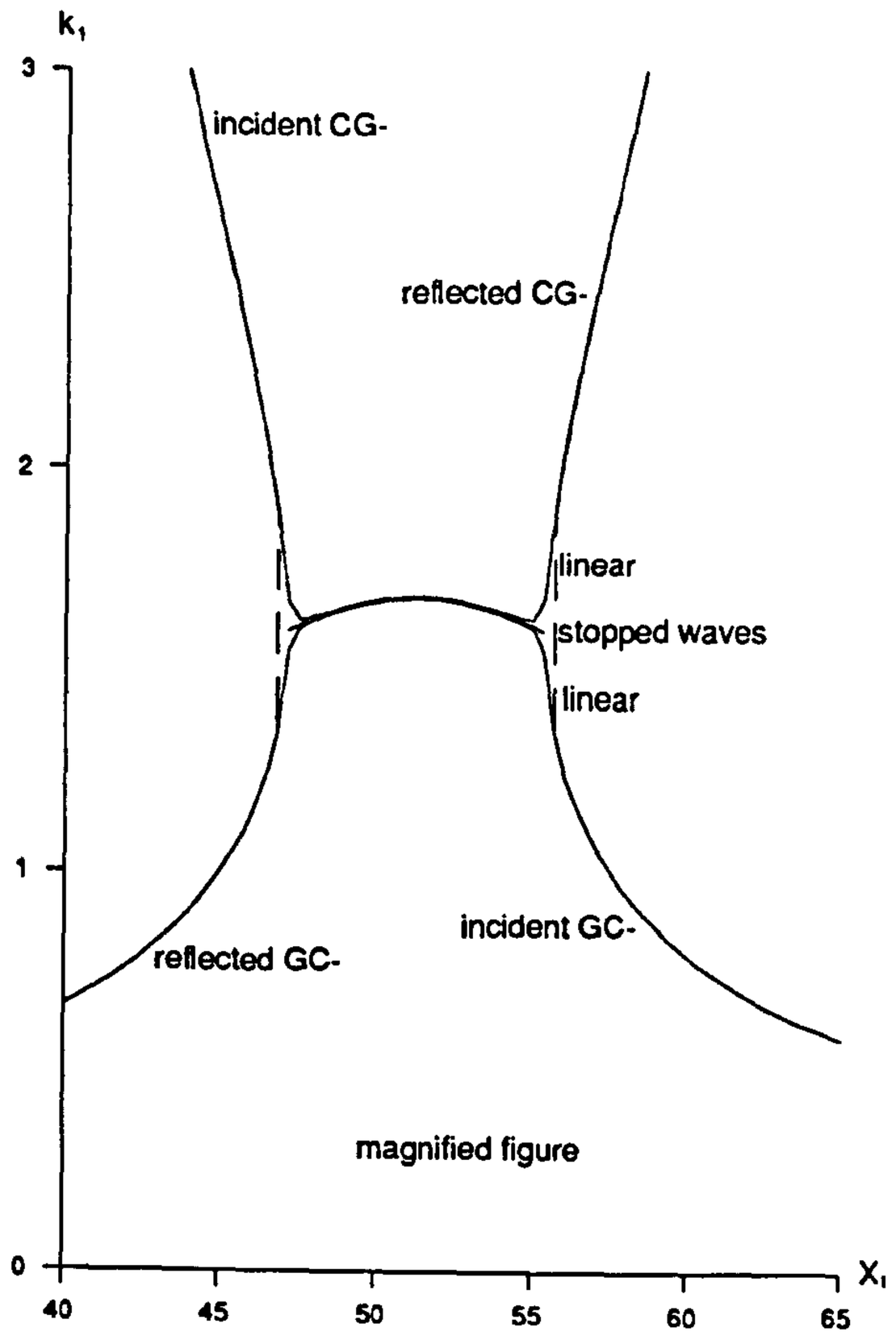

Figure 5.14b

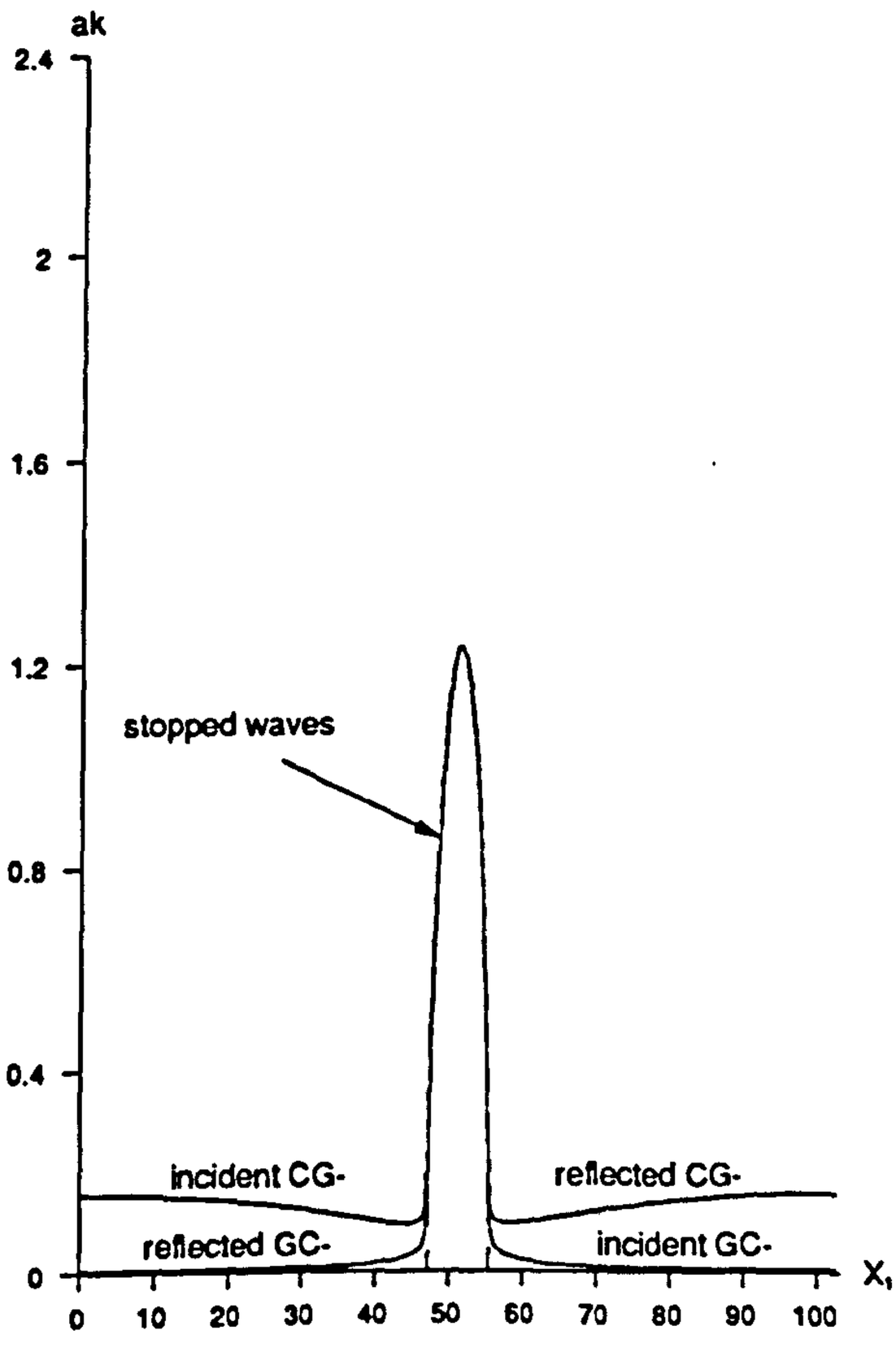

Figure 5.14c

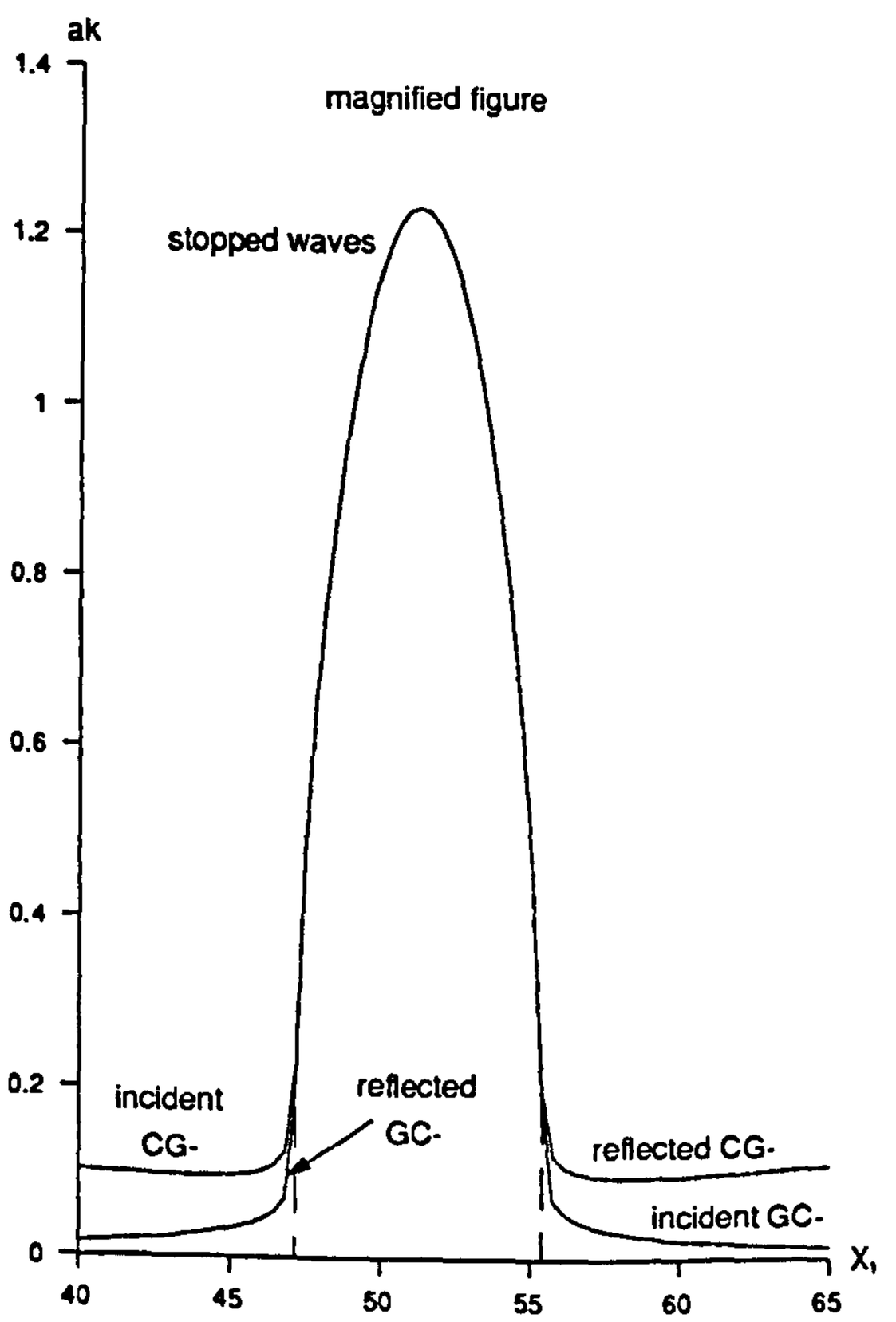

Figure 5.14c

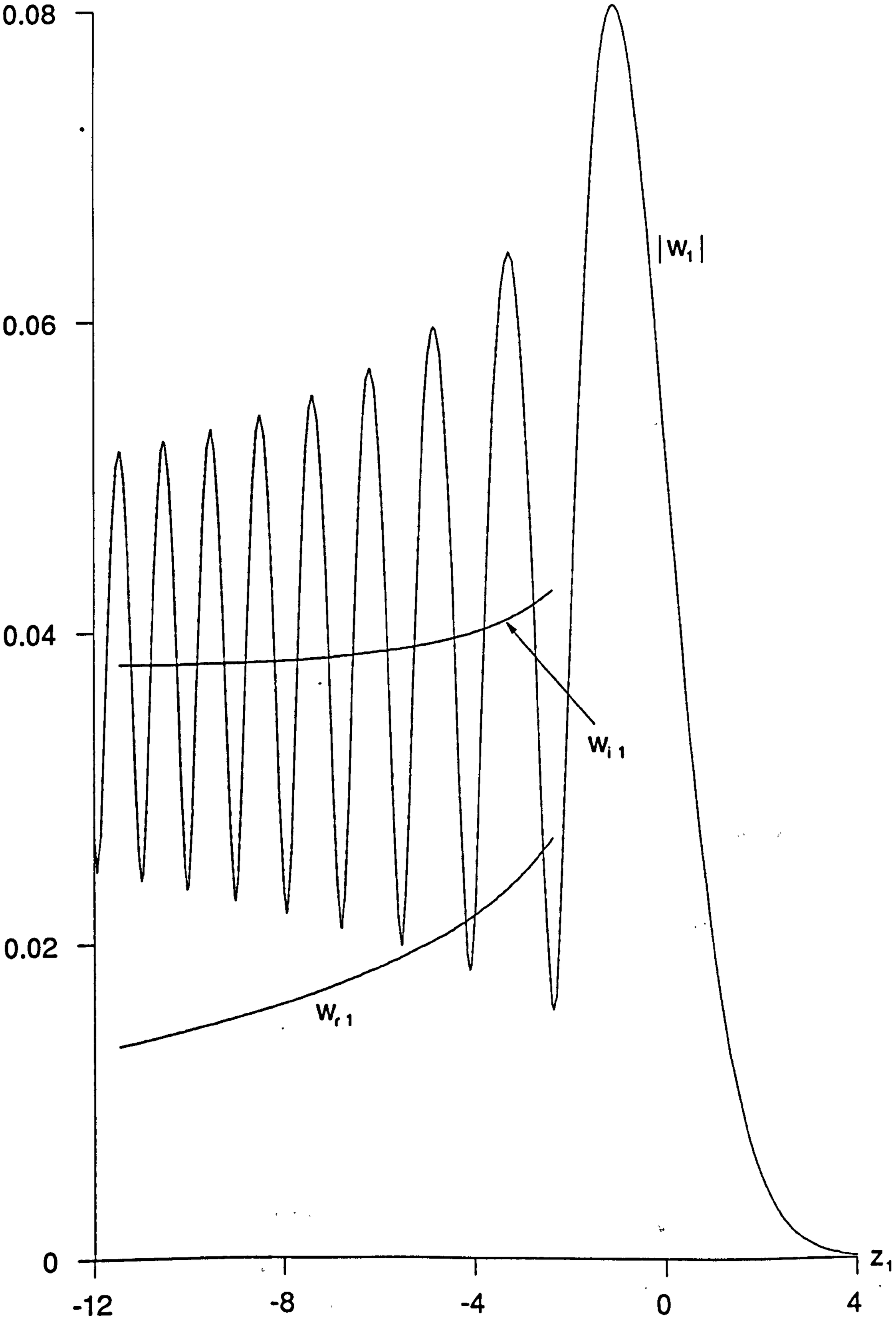

Figure 5.15a

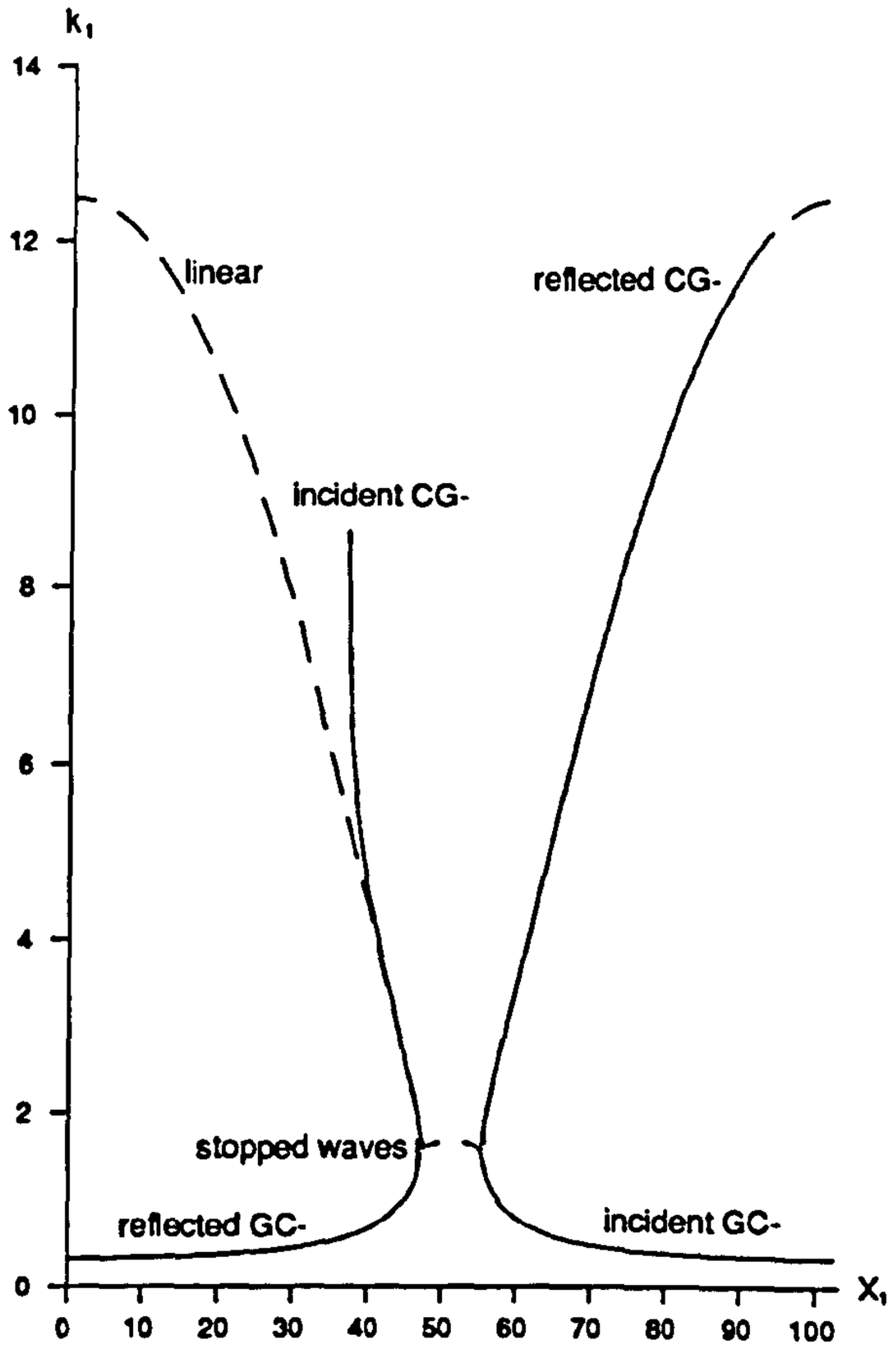

Figure 5.15b

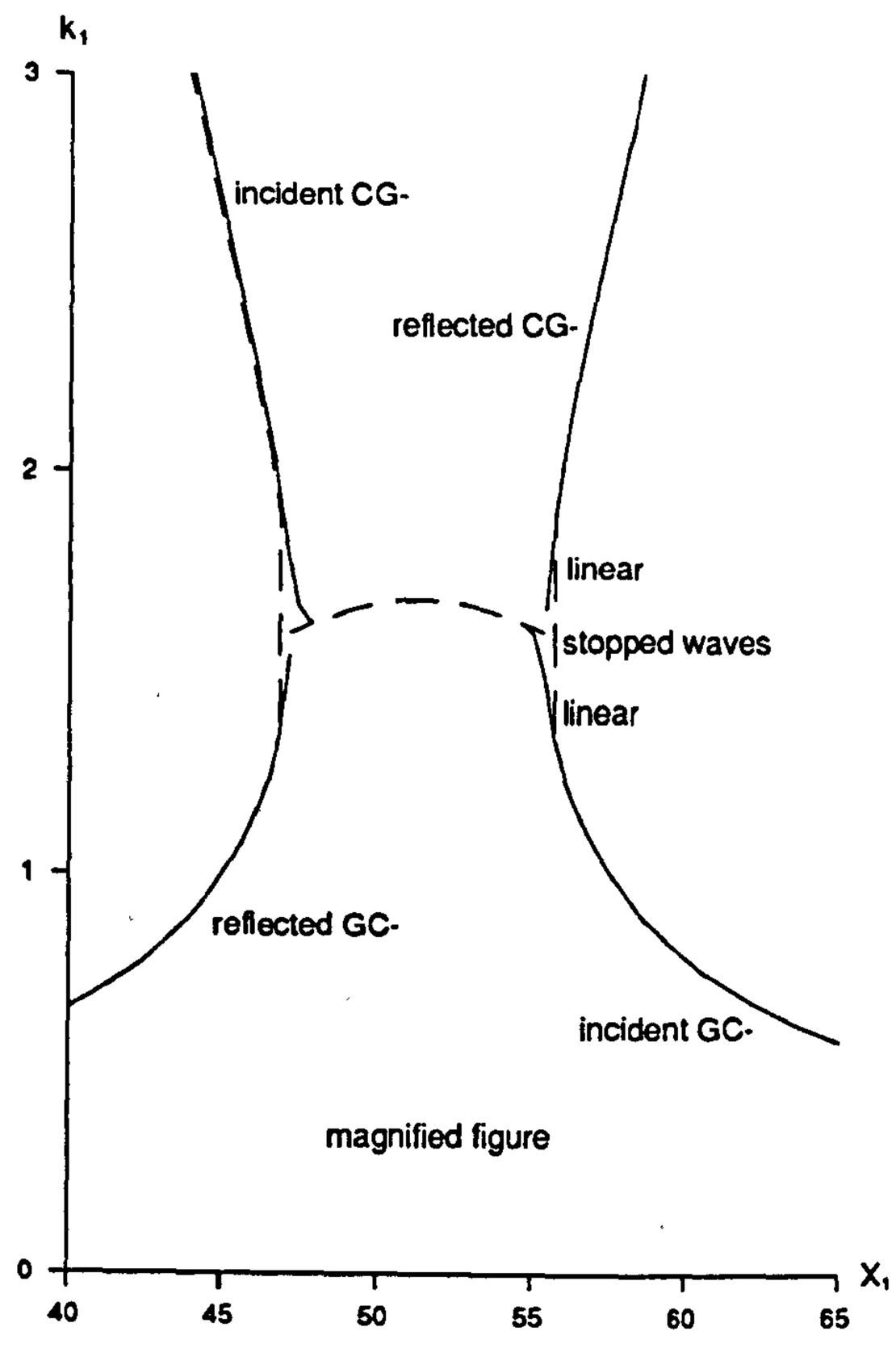

Figure 5.15b

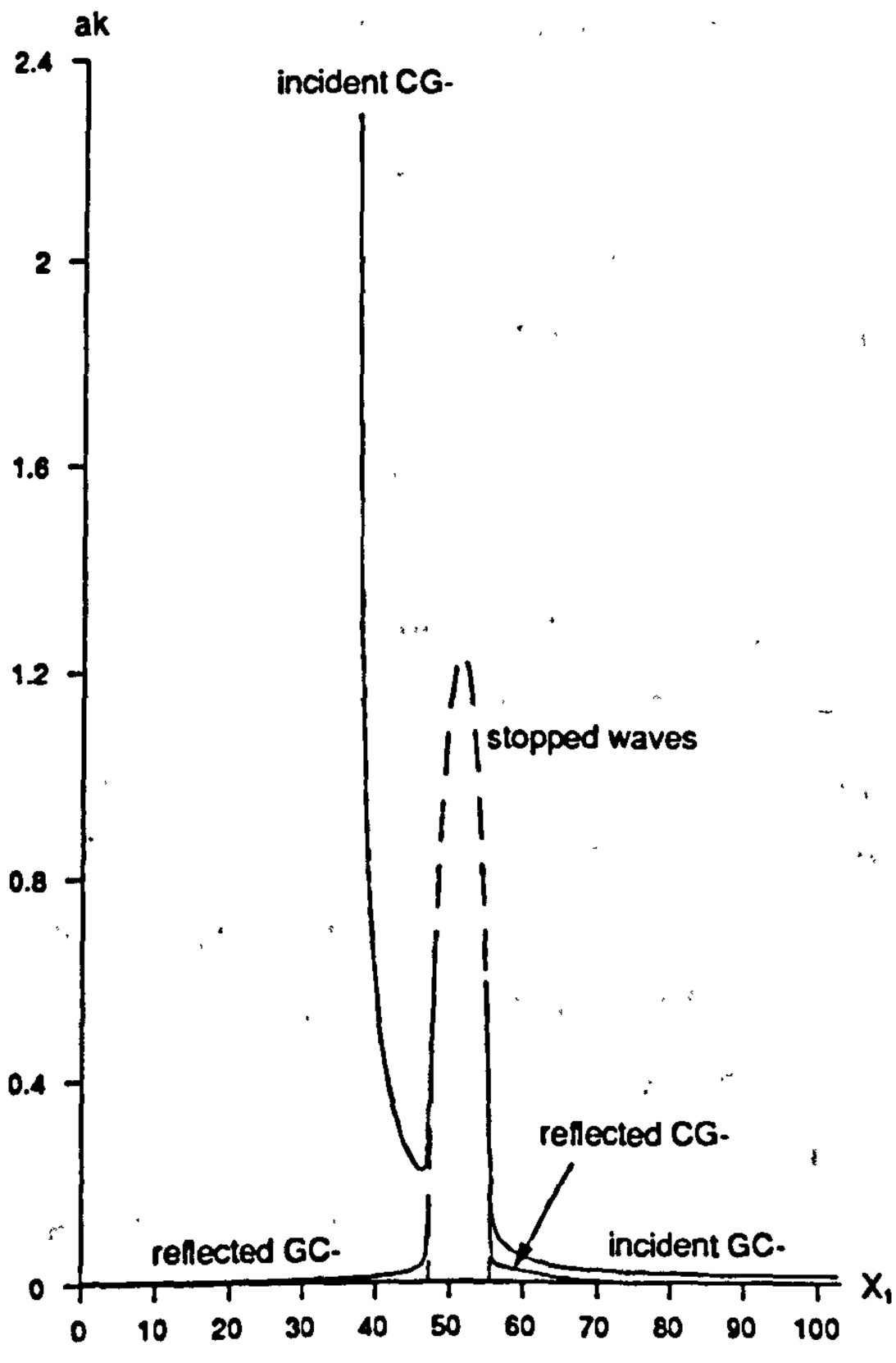

Figure 5.15c

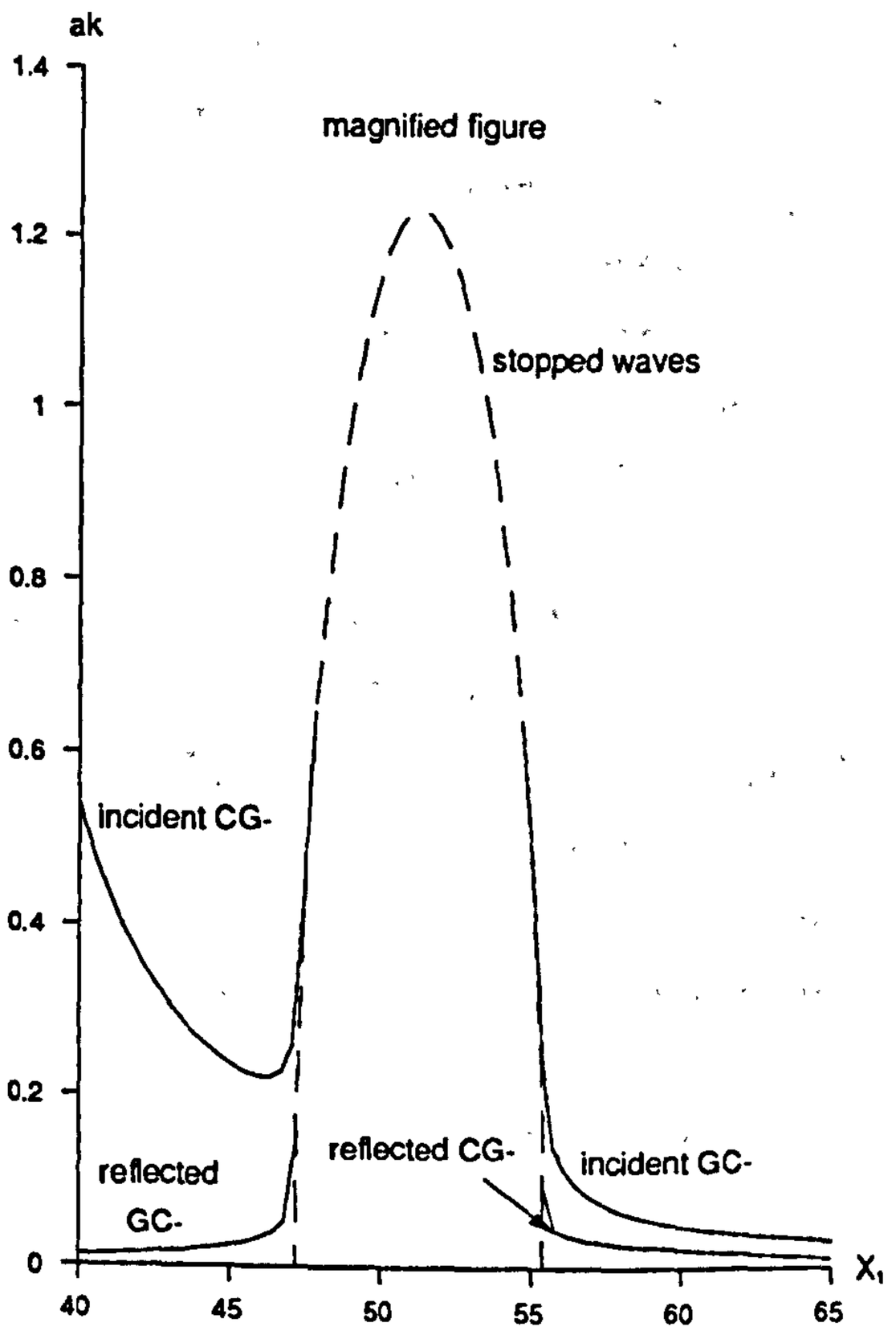

Figure 5.15c

CHAPTER 6
LINEAR THREE DIMENSIONAL PURE CAPILLARY WAVE-CURRENT INTERACTIONS ON INFINITE DEPTH LIQUID

6.1 Introduction

Peregrine and Smith (1979) examine the specific physical example of linear three dimensional pure gravity waves on three dimensional deep water currents. They determine those currents upon which caustics can occur and the type of near-linear caustics present. At that stage they state that "similar results can be expected to arise for other dispersive waves in a moving medium". Here this remark is shown to be true for linear pure capillary waves. The analysis of Peregrine and Smith (1979) section 5 is followed. The equations for the linear caustics are developed and subsequent results are discussed in section 6.2. The nature of near-linear caustics are discussed in section 6.3.

6.2 The Equations

The general theory of § 2.8 is used for studying caustics. As usual, only steady straight caustics in a steady wave field are considered. It is supposed that the caustic is situated at $x = 0$, where $x_i = (x,y)$, with the x-axis perpendicular to the caustic. It is also supposed that waves are incoming from the - x half of the (x,y)-plane. Variations in the wave parameters are in the x direction only since variations of parameters along the caustic are negligible. The notation of § 2.8 is used.

It is supposed that both the waves and the mainstream flow are three dimensional. Therefore, both waves and mainstream flow propagate in two dimensions so that $k_i = (l,m)$ and $U_i = (U,V)$ with l, m, U and V generally non-zero. As the caustics and the wave field are steady and there are no variations in the y direction the consistency relations (2.3.4) imply that the total frequency ω and the wavenumber vector component m are constant.

For pure capillary waves the linear dispersion relation on still liquid is given by

$$G(\sigma,k) = \sigma^2 - sk^3 = 0 \qquad (6.2.1)$$

where $k^2 = k_i k_i = l^2 + m^2$. At a caustic caused by the mainstream flow the condition (2.8.4) for the presence of a caustic gives

$$U \frac{dG}{d\sigma} - \frac{1}{k} \frac{dG}{dk} = 2U\sigma + 3sk l = 0 \ . \qquad (6.2.2)$$

Suppose that ω, m and U(x) are given. Then equations (6.2.1, 2) can be solved to find the values l_o and V_o, of the two unknowns l and V, at the caustic. However, it is more interesting to examine these equations from another direction. The equations are used to find all possible currents on which caustics can occur. This is done by fixing m and eliminating l between equations (6.2.1, 2) to yield a relation between U and V. Equation (6.2.2) gives

$$4U^2\sigma^2 = 9s^2k^2 l^2 \qquad (6.2.3)$$

which, on using the dispersion relation (6.2.1), gives

$$4U^2k = 9s l^2 \qquad \text{since } k \neq 0 \ . \qquad (6.2.4)$$

Squaring this equation, substituting for $k^2 = l^2 + m^2$ and solving gives

$$l = \pm \frac{2|U|}{9s} \left[2U^2 + (4U^4 + 81s^2m^2)^{\frac{1}{2}}\right]^{\frac{1}{2}} \qquad \text{since } l^2 > 0 \ . \qquad (6.2.5)$$

This solution for the wavenumber component l at caustics is used to eliminate l from equations (6.2.1, 2) and find the desired relation between U and V for a fixed m. Two cases, namely $m = 0$ and $m \neq 0$, arise. For the first of these expression (6.2.5) gives

$$l = \pm \frac{4U^2}{9s} \ . \qquad (6.2.6)$$

Then, since $k = |l|$ equation (6.2.2) implies

$$U = 0 \quad \text{or} \quad 27s\omega \mp 4U^3 = 0 \ . \qquad (6.2.7)$$

using the Doppler relation (2.3.1). Now if U = 0 then (6.2.6) gives k = 0 which is unphysical. Thus, the solutions for this case are, using expression (6.2.6) for l,

$$U = \pm 3.4^{-\frac{1}{3}} (s\omega)^{\frac{1}{3}} \ , \ l = \pm \left[\frac{4\omega^2}{s}\right]^{\frac{1}{3}} \ . \qquad (6.2.8)$$

Note that because $m = 0$ makes equations (6.2.1, 2) independent of V caustics occur at these values of U for all V.

The second case, namely $m \neq 0$, itself is split up into two cases. These are U = 0 and U ≠ 0. For U = 0 expression (6.2.5) implies $l = 0$, so that at the caustic waves propagate along it. It follows that $k = |m|$ so that caustics occur on flows with

$$V = \frac{\omega \pm s^{\frac{1}{2}}|m|^{\frac{3}{2}}}{m} \quad . \tag{6.2.9}$$

using the Doppler relation (2.3.1) and the dispersion relation (6.2.1).

For the U ≠ 0 it is expected that the solution for wavenumber component l at the caustic should pass through the whole range of real numbers as U goes from - ∞ to + ∞ (with $l = 0$ when U = 0). This is only possible if

$$l = \pm \frac{2U}{9s}\left[2U^2 + (4U^4 + 81s^2m^2)^{\frac{1}{2}}\right]^{\frac{1}{2}} \tag{6.2.10}$$

for any U. Then caustics occur on flows with V given, from equation (6.2.2), by

$$V = \frac{2U(\omega - lU) + 3skl}{2mU} \quad . \tag{6.2.11}$$

using the Doppler relation (2.3.1). These are solved by fixing m and varying U to find the value of l and, thus, k using expression (6.2.10) and then substituting these into expression (6.2.11) to find V.

It follows that for a given fixed value of m there is a line of points in the (U,V) plane at which caustics can occur. These are found using equation (6.2.8) for $m = 0$, equation (6.2.9) for $m \neq 0$ and U = 0, and equations (6.2.10, 11) for $m \neq 0$ and U ≠ 0. The equations show that each line of caustic points, other than $m = 0$, has two symmetrical branches. The lines of symmetry are U = 0 and $V = \omega/m$. This feature of symmetry is exactly the same as for the pure gravity waves case studied by Peregrine and Smith (1979) and is to be expected from the isotropy of the dispersion relation.

The way in which caustics arise is clarified by considering two specific simple currents:

i U ≠ 0, V = 0, and
ii U = 0, V ≠ 0.

Case i corresponds to currents flowing with or against the waves. This is the familiar case already examined in chapter 3 for $m = 0$ with gravity g non-zero. Case ii corresponds to a shearing current which bends rays around until they are parallel to the current and form a caustic if the current increases sufficiently with x.

In general, the variation of wavenumber component l with current U or V, for fixed V or U respectively, is sought. Use of the Doppler relation (2.3.1) and the dispersion relation (6.2.1) gives

$$U = \frac{1}{l} \left[\omega - mV \mp (sk^3)^{\frac{1}{2}}\right] , \qquad (6.2.12)$$

or

$$V = \frac{1}{m} \left[\omega - lU \mp (sk^3)^{\frac{1}{2}}\right] \qquad (6.2.13)$$

which respectively give the required variations. The variations for cases i and ii are given by substituting $V = 0$ and $U = 0$ in expressions (6.2.12, 13) respectively. Caustics occur at positions where the solution curves of these equations have vertical tangents in the (U, l) or (V, l)-planes.

Note that for the case $m \neq 0$, $U = 0$ and $l = 0$, with V given by expression (6.2.9), there exists a caustic point according to the conditions (6.2.1, 2). However, on closer examination it is seen that this caustic exists only when U is fixed to zero and V varied. This caustic does not exist when V is fixed to one of the two values given by expression (6.2.9) and U varied through zero. The dispersion relation (6.2.1), in the form of expressions (6.2.12, 13), must be examined for this case. The derivatives of these with respect to l are found since a caustic exists where these derivatives are zero. Use of L'Hopital's rule leads to

$$\frac{dU}{dl} \longrightarrow \mp \frac{3}{4} \left[\frac{s}{|m|}\right]^{\frac{1}{2}} \qquad \text{as } l \longrightarrow 0 \qquad (6.2.14)$$

and since this is non-zero for all values of m there is no caustic at $U = 0$ and $l = 0$ when U is varied. Also,

$$\frac{dV}{dl} = \mp \frac{3l}{2m} \frac{s^{\frac{1}{2}}}{(l^2 + m^2)^{\frac{1}{4}}} \qquad (6.2.15)$$

which is zero when l is zero so that there is a caustic point at $U = 0$ and $l = 0$ when V is varied.

Throughout the previous chapters, where $V = m = 0$, a convention of $U < 0$ and $l > 0$ with ω taking any sign is adhered to. Other conventions, such as $\omega > 0$ and $l > 0$ with U taking any sign, are possible. This latter convention takes the CG-/GC- caustic point into the regime $U > 0$, $k > 0$. The versatility of conventions is basically due to the simple form of the Doppler relation (2.3.1) for this case. When $V \neq 0$ no convention can be imposed on U. The only possible convention is to take $\omega > 0$ and $m > 0$ with U, V and l taking any sign (solutions for $\omega < 0$, or $m < 0$, are found by the transformation $U \rightarrow -U$, $V \rightarrow -V$, or $V \rightarrow -V$).

The cases of stationary and Doppler shifted linear pure capillary waves are considered separately. For stationary waves dimensional units are used. The currents at which caustics occur are shown in figure 6.1. The lines are all symmetrical about $U = 0$ and $V = 0$ as expected. There are no higher order singularities, such as a triple-root caustic, of the type discussed by Peregrine and Smith (1979), i.e caustics are either of R-type or S-type. The case studied in previous chapters, i.e. $m = V = 0$, suggests that caustics will be S-type.

For Doppler shifted waves dimensionless capillary units are used. As mentioned in § 2.9 equations in these units are most easily given by substituting $\rho = \tau = \omega^2 = 1$, and adding a suffix 1 to all dimensional quantities, including ω, to give the corresponding quantity in capillary units. However, since the convention for this chapter has $\omega > 0$ the parameter $\omega_1 = +1$ so that substituting $\rho = \tau = \omega = 1$ is all that is necessary to find the appropriate equations in capillary units. The currents at which caustics occur are shown in figure 6.2. The lines are all symmetrical about $U_1 = 0$ and $V_1 = 1/m_1$ as expected. As for the stationary waves case there are no higher order singularities.

Figures 6.3, 4 show the solutions of the dispersion relation (6.2.1), as given by expressions (6.2.12, 13), for the two cases i and ii described above respectively. For both cases it is seen that two different caustics arise for one value of m ($m > 1$ for case i and all m for case ii). These two caustics would involve quite different wavetrains.

Figures 6.5, 6 show solutions for $V_1 = 3$ and $U_1 = 3$ with varying m_1 whilst figures 6.7, 8 show solutions for varying V_1 and U_1 for a single m_1, namely $m_1 = 3$. These four figures show the richness of caustics present in a three dimensional problem. All the caustics which arise are different although there may be qualitative similarities which allow them to be split into sets.

6.3 Near-Linear Caustics

The results above show that for a wide range of cases linear caustics exist. The nature of the waves in the neighbourhood of the linear caustic is now investigated. Wilton (1915) shows that

$$\frac{\sigma^2}{k} - sk^2 = -\frac{1}{8} sk^2 \alpha_1^2 + O(\alpha_1^4) \quad . \tag{6.3.1}$$

is the near-linear dispersion relation for plane waves on still liquid. As stated in § 3.7 α_1 is found to be equal to - ak. It follows that the near-linear dispersion relation is

$$\sigma^2 - sk^3 + \frac{1}{8} sk^5 a^2 = 0 \tag{6.3.2}$$

so $$H \Big/ \left[U^2 \frac{\partial^2 G}{\partial \sigma^2} - 2U \frac{\partial^2 G}{\partial \sigma \partial k} + \frac{\partial^2 G}{\partial k^2}\right] = \frac{sk^6}{8[2U^2 k - 3s(2l^2 + m^2)]} \quad . \tag{6.3.3}$$

Thus, $$\operatorname{sgn}\left[H \Big/ \left[U^2 \frac{\partial^2 G}{\partial \sigma^2} - 2U \frac{\partial^2 G}{\partial \sigma \partial k} + \frac{\partial^2 G}{\partial k^2}\right]\right] =$$

$$\operatorname{sgn}\,[2U^2 k - 3s(2l^2 + m^2)] \quad . \tag{6.3.4}$$

Note that this is independent of the velocity component V so that for a particular value of U, l and m a particular type of caustic exists for all possible V. Substitution of either expressions (6.2.8) or (6.2.10) into expression (6.3.4) shows, after a little algebra, that all near-linear caustics are of S-type. This implies that waves will usually travel past a linear caustic and eventually break.

CAPTIONS FOR FIGURES

Figure 6.1: The currents (U,V) at which caustics occur for stationary waves; various wavenumber component values m as shown.

Figure 6.2: The currents (U_1,V_1) at which caustics occur for Doppler shifted waves; various wavenumber component values m_1 as shown.

Figure 6.3: The variation of wavenumber component l_1 with current component U_1 for case $V_1 = 0$; various wavenumber component values m_1 as shown.

Figure 6.4: The variation of wavenumber component l_1 with current component V_1 for case $U_1 = 0$; various wavenumber component values m_1 as shown.

Figure 6.5: The variation of wavenumber component l_1 with current component U_1 for case $V_1 = 3$; various wavenumber component values m_1 as shown.

Figure 6.6: The variation of wavenumber component l_1 with current component V_1 for case $U_1 = 3$; various wavenumber component values m_1 as shown.

Figure 6.7: The variation of wavenumber component l_1 with current component U_1 for case $m_1 = 0$; various current component values V_1 as shown.

Figure 6.8: The variation of wavenumber component l_1 with current component V_1 for case $m_1 = 0$; various current component values U_1 as shown.

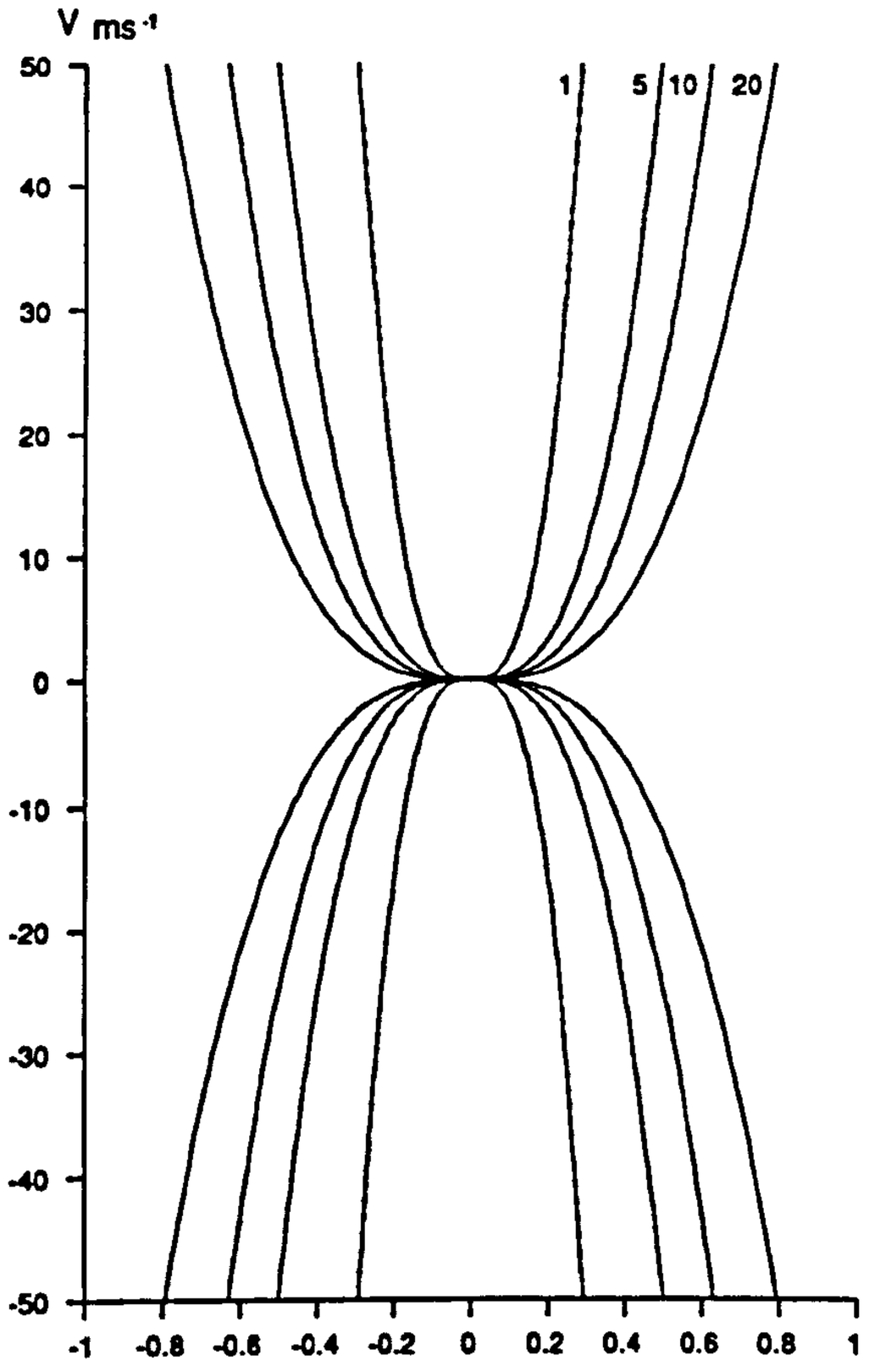

Figure 6.1

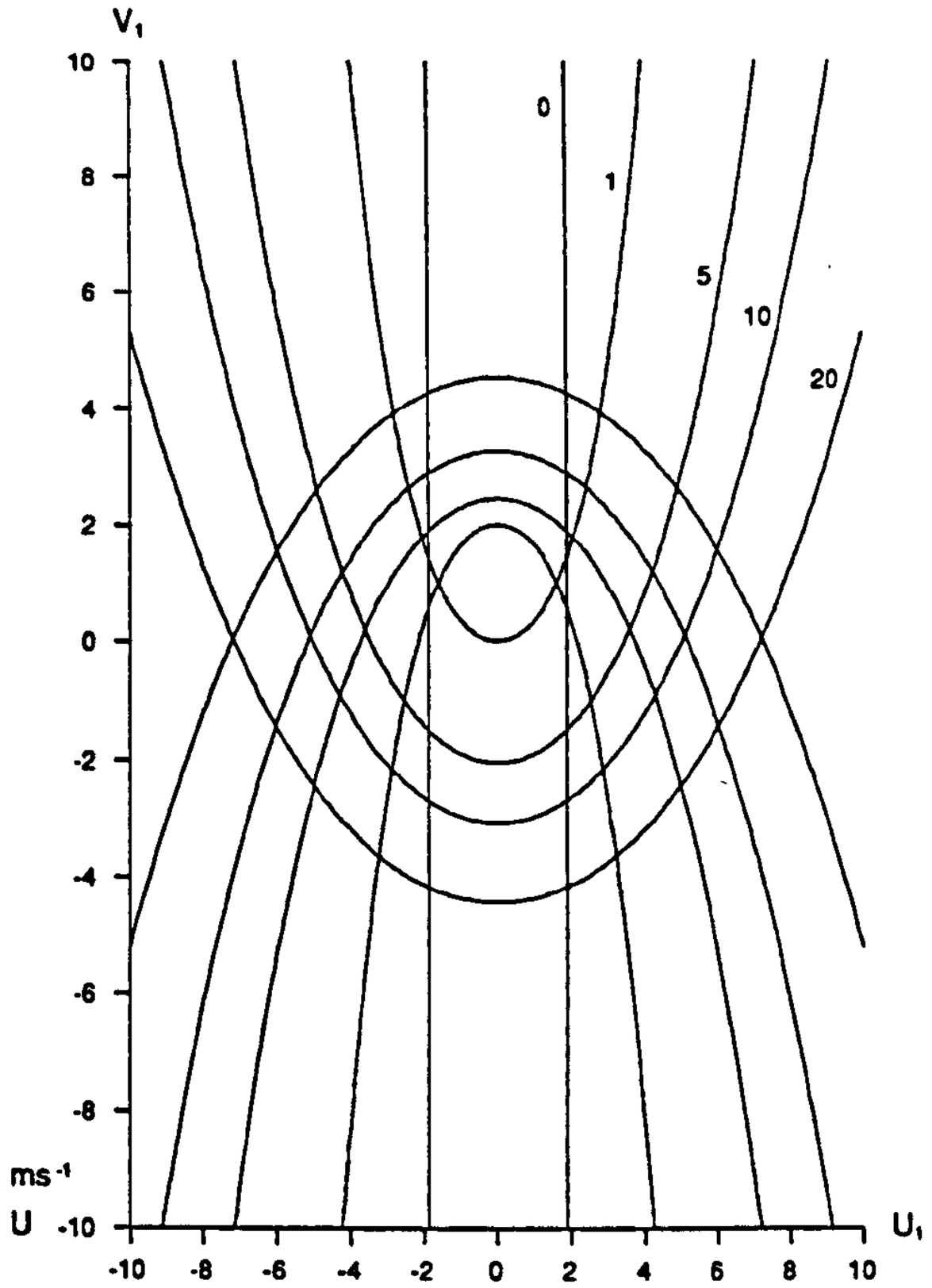

Figure 6.2

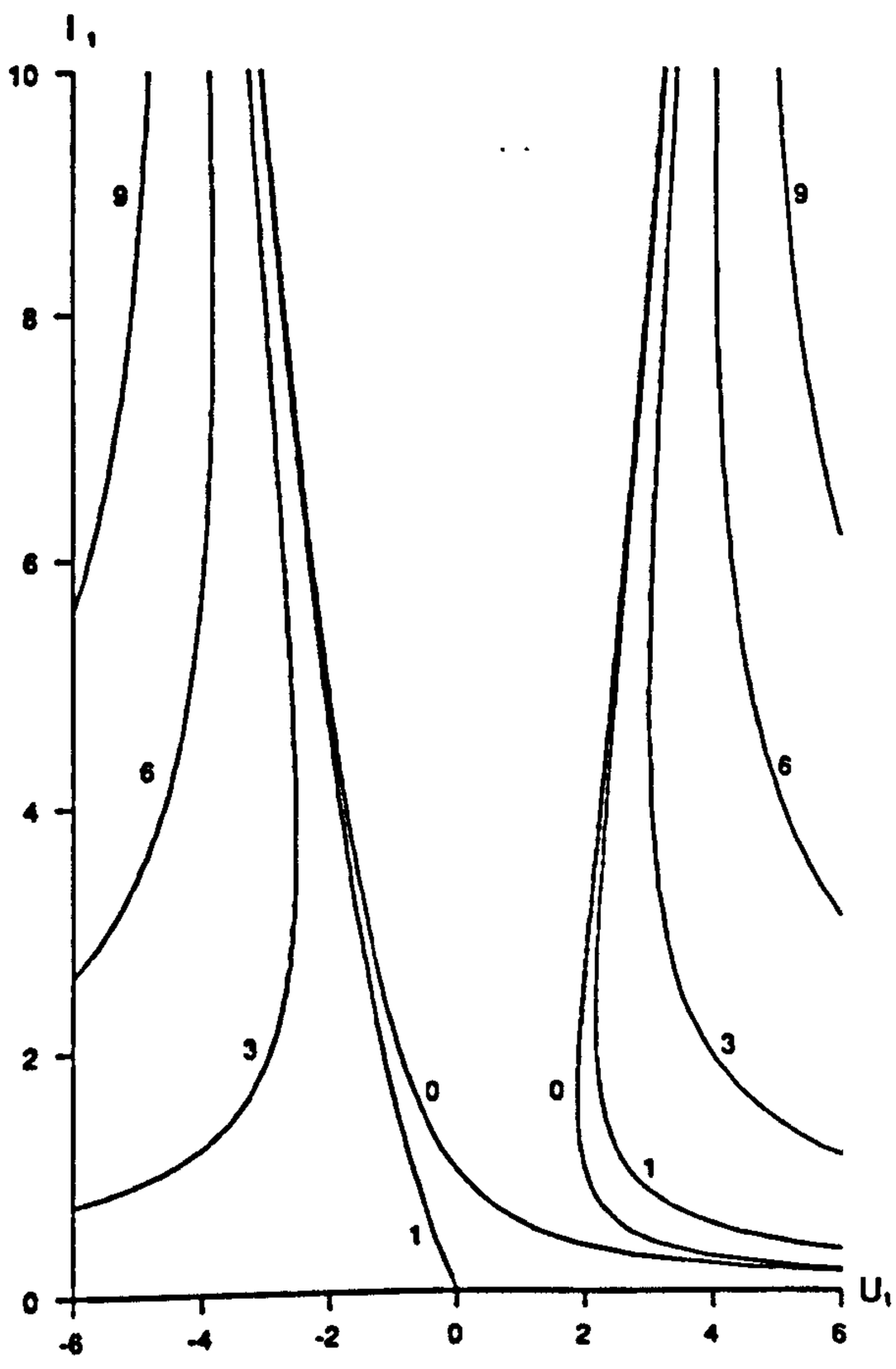

Figure 6.3

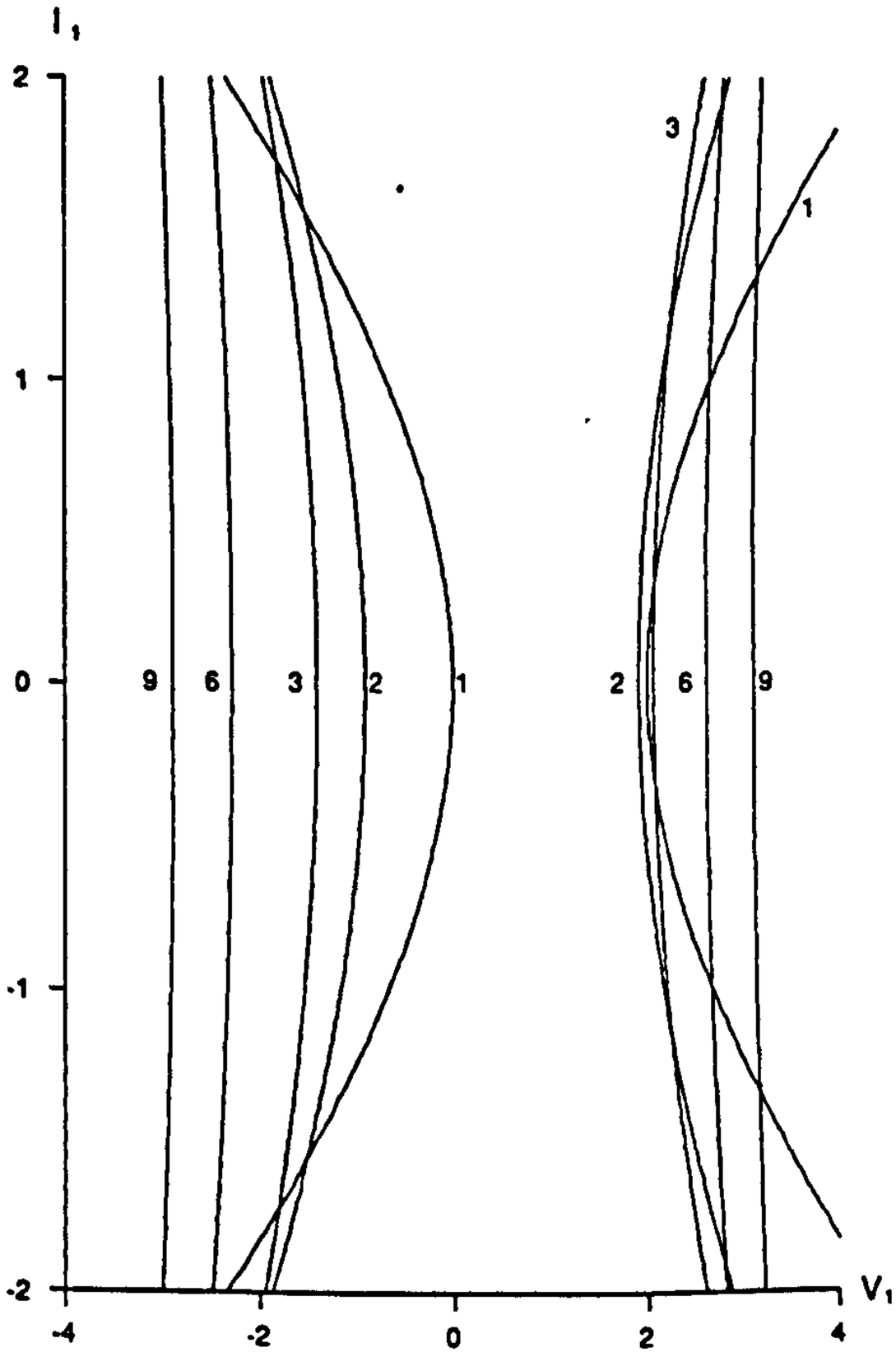

Figure 6.4

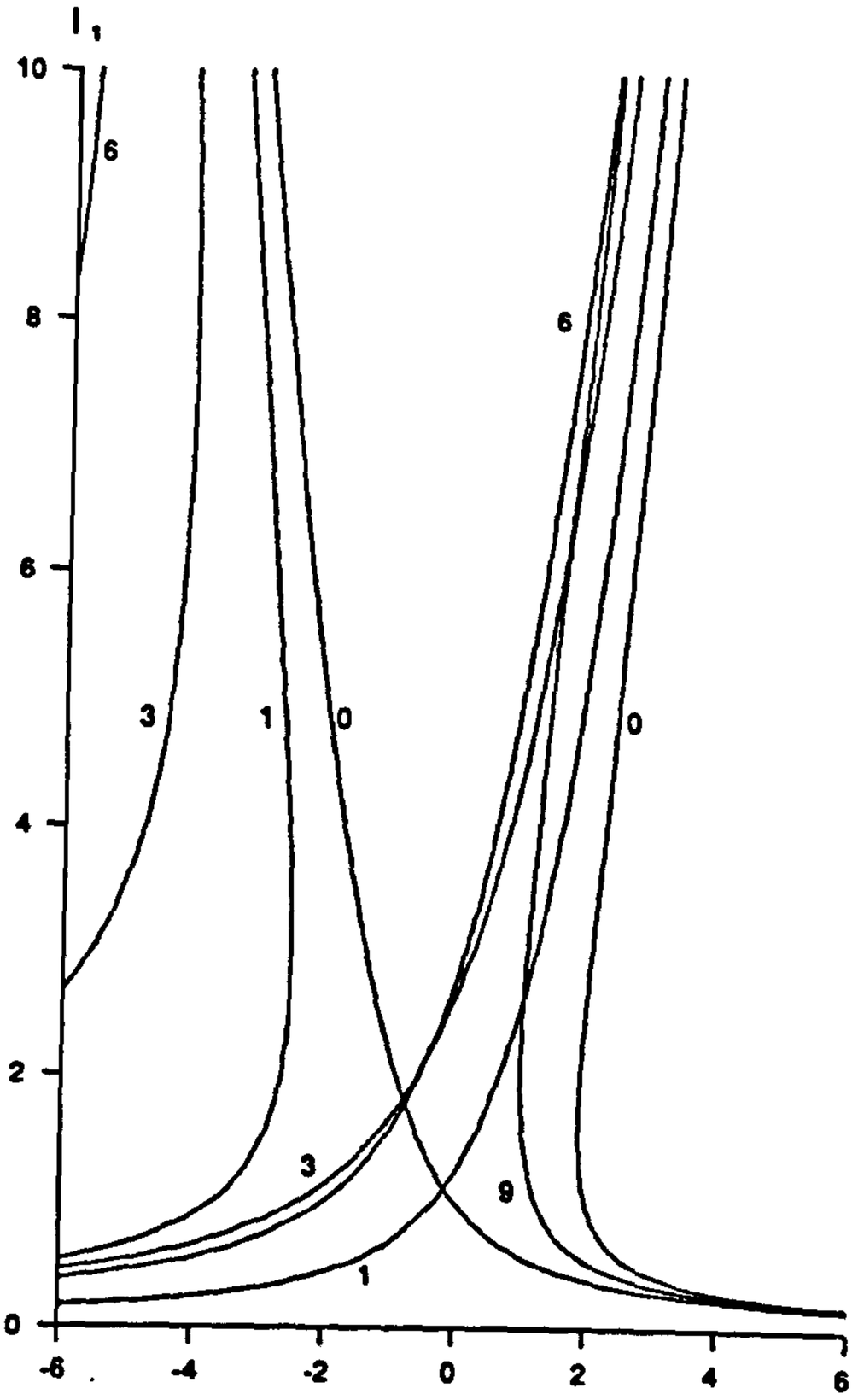

Figure 6.5

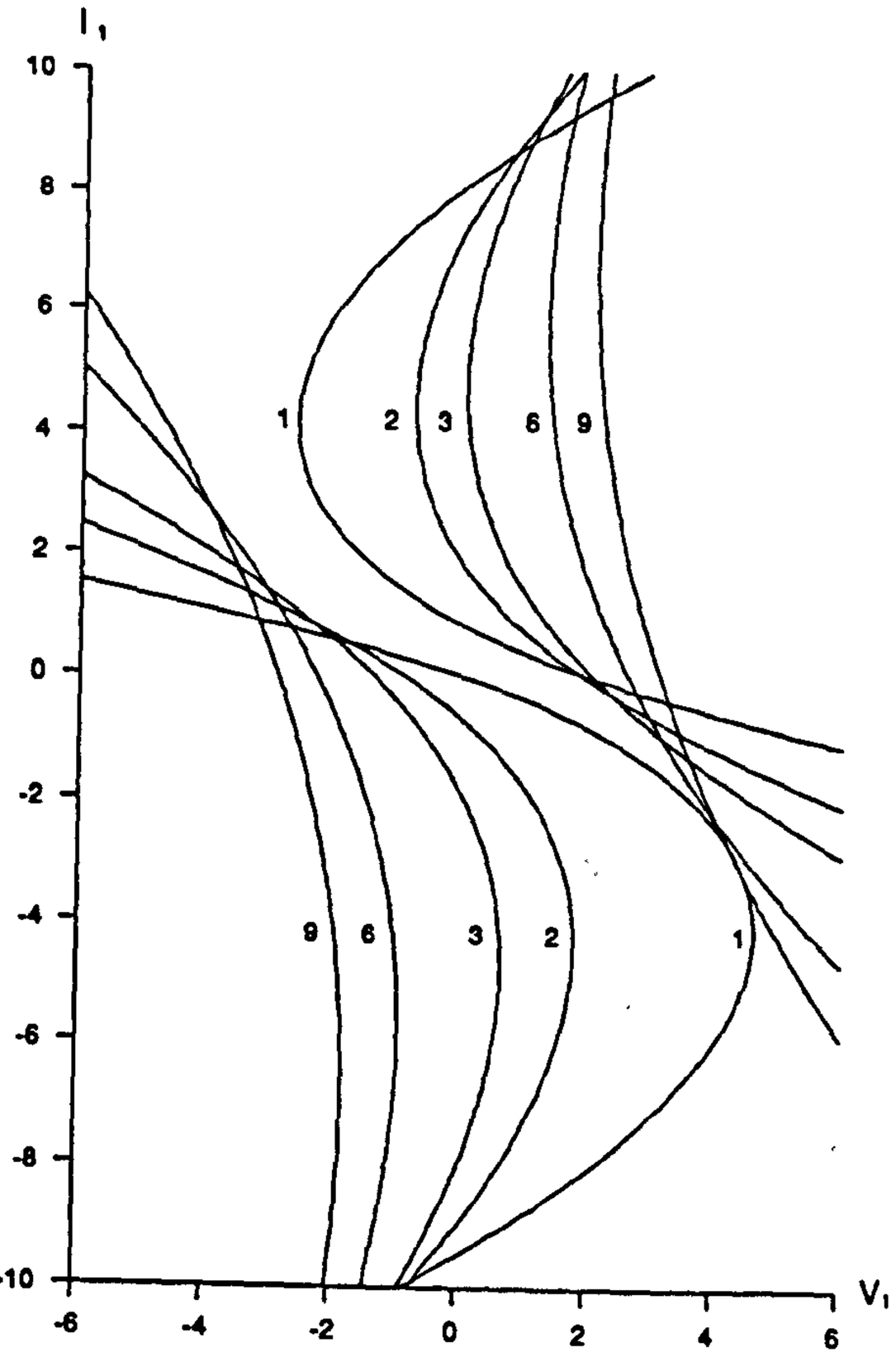

Figure 6.6

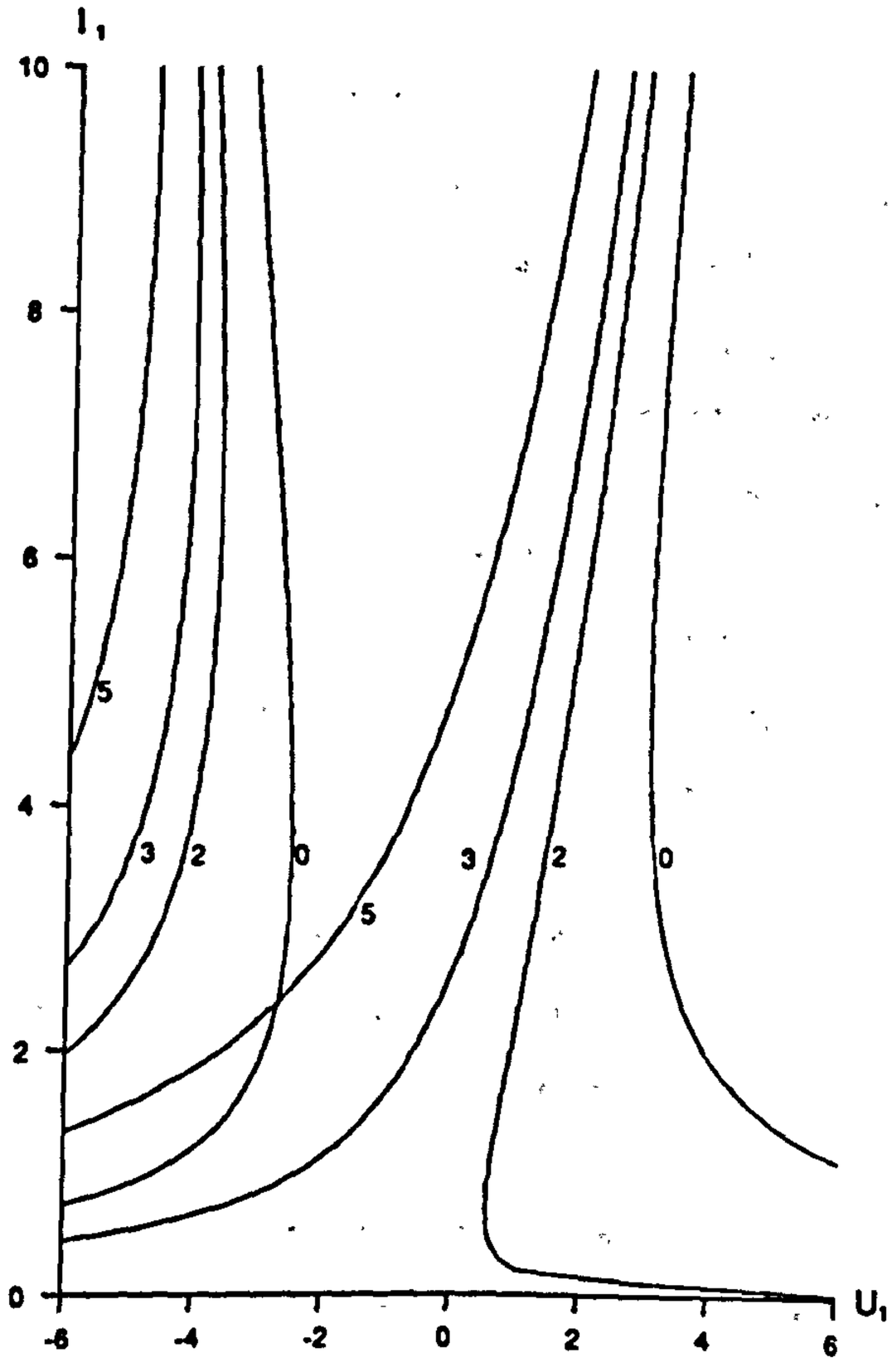

Figure 6.7

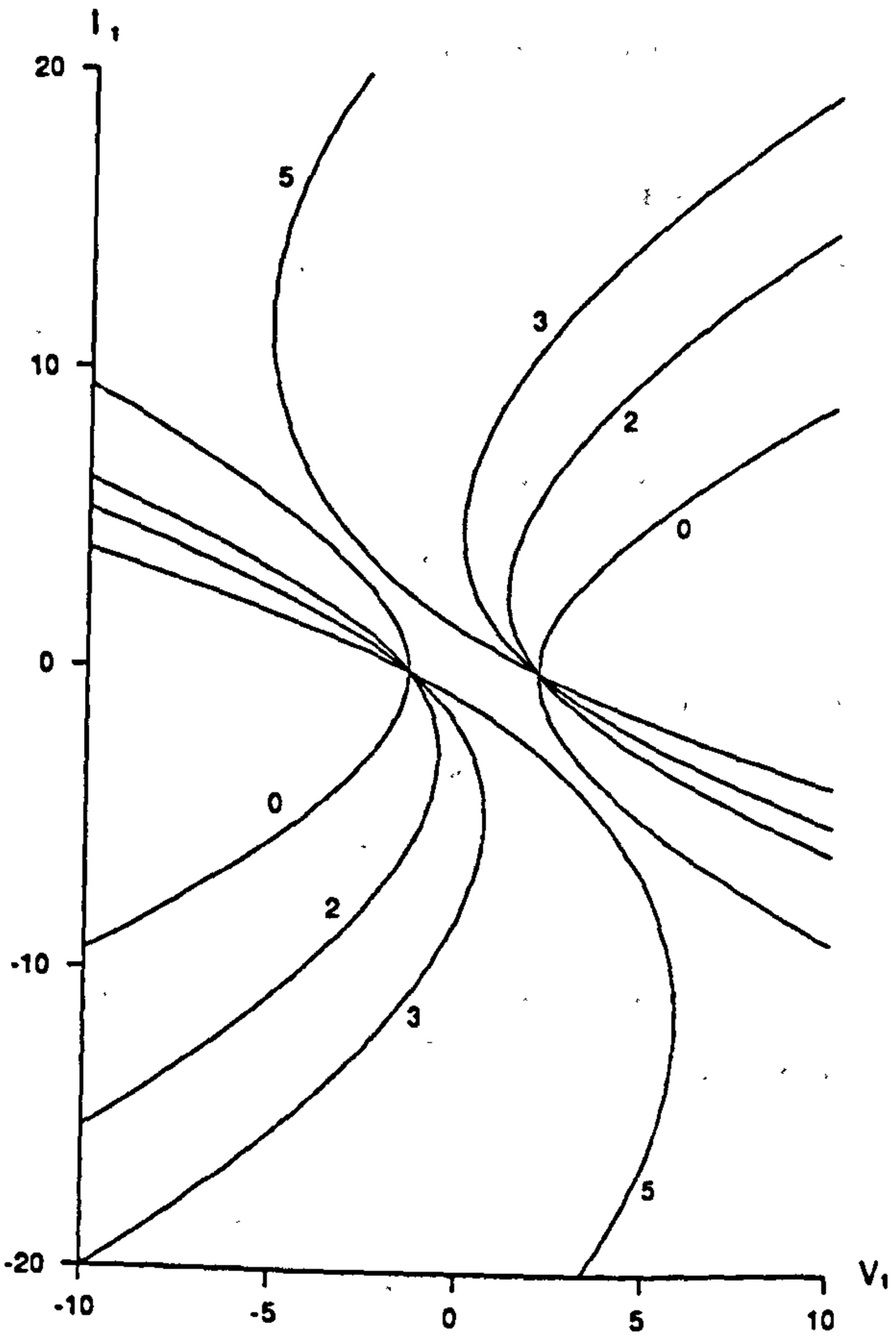

Figure 6.8

CHAPTER 7
EQUIVALENCE OF SYSTEMS OF EQUATIONS

7.1 Introduction

The behaviour of slowly-varying wavetrains is usually studied by using either the averaged equations (§ 2.2) or Whitham's equations (§ 2.4). These two systems are always used interchangeably without question. In chapter 5 it is shown, for the case of free irrotational pure capillary waves on liquid of infinite depth, that the energy conservation equation (2.2.6) is, indeed, equivalent to the wave-action conservation equation (2.4.6, 8).

It is our aim to show that the the two systems are generally equivalent for waves on both finite and infinite depth liquid. Also the effects of dissipation of wave energy due to the viscosity of the liquid and of a "parallel acceleration" (this term is explained below in section 7.4) of the mainstream flow are added to the averaged equations of motion. Subsequently, these are used to aid in the development of a modified wave-action conservation equation which includes such dissipation and acceleration effects.

Crapper (1979) shows that Whitham's equations can be manipulated into the averaged equations provided the consistency relations (2.3.5) for the mainstream flow are true. However, this means that it is necessary to assume that the flow field is globally irrotational, i.e. curl $U_i = 0$. Stiassnie and Peregrine (1979) examine the two systems of equation from an irrotationality point of view. They point out the fact that the averaged equations only require the flow field to be locally irrotational, i.e. curl $u_i = 0$, whilst Whitham's equations require the flow field to be globally irrotational. This is essentially because the averaged equations are derived from Euler's equations which only require local irrotationality whilst Whitham's equations are derived by averaging a Lagrangian for a globally irrotational flow. Stiassnie and Peregrine (1979) go on to derive modified consistency relations, replacing the consistency relations (2.3.5), which generalise Whitham's equations to non-globally irrotational flows. They do this by manipulating the averaged equations into forms similar to Whitham's equations.

It is, therefore, implied that there must exist necessary and sufficient conditions, known here as "equivalence relations", for the two systems of equations to be equivalent. Also these equivalence relations must be the same as the modified consistency relations derived

by Stiassnie and Peregrine (1979). Here this is shown to be the case so that the modified consistency relations of Stiassnie and Peregrine are confirmed. The method used here differs from that of Stiassnie and Peregrine (1979).

In sections 7.2, 3 the two systems are shown to be equivalent and the equivalence relations are derived for the cases of finite and infinite depth liquids respectively. The effects of wave energy dissipation and a "parallel acceleration" of the mainstream flow are added to the averaged equations in section 7.4. General expressions for dissipation terms are also derived in section 7.4 which give the first-order dissipation effects when no (real) bed is present. The modified wave-action conservation equation and modified equivalence relations are subsequently derived in section 7.5.

7.2 The Equivalence Relations

In this section our aim is to show that the two systems of equations are equivalent and thereby derive the equivalence relations. Formally, this requires us to show that the momentum conservation equation (2.2.2, 5) and energy conservation equation (2.2.3, 6) are equivalent to the wave-action conservation equation (2.4.6, 8). This is because the mass conservation equation (2.2.1, 2.4.5) is common to both systems and the Bernoulli equation (2.4.4) is regarded as defining the parameter γ in terms of other flow parameters. This is done by deriving general equations relating terms present in the averaged equations and Whitham's equations from first principles via manipulations of the averaged Lagrangian $\mathcal{L}^w$. These equivalence relations show that the consistency relations (2.3.5) are sufficient, but not necessary, for the averaged equations and Whitham's equations to be equivalent.

To simplify the presentation of equations in this chapter a symbolic notation is used. The following table gives all the symbolic names. Each name corresponds to terms on the left hand side of an equation or relation given in chapter 2 but not to the equation or relation itself - this aspect is very important. The relevant equation number, together with a description of the corresponding equation, is given in the table 7.1. Note that MCE, FECE, ECE, WACE and IECE are scalar terms, FMMCE, MMCE, CCR and IMMCE are vector terms and ICR is a tensor term - all of these are terms not equations.

symbolic name	equation number	description
MCE	(2.2.1, 2.4.5)	mass conservation equation
FMMCE	(2.2.2)	full momentum conservation equation
FECE	(2.2.3)	full energy conservation equation
MMCE	(2.2.5)	momentum conservation equation
ECE	(2.2.6)	energy conservation equation
CCR	(2.3.5)	consistency conservation relation
ICR	(2.3.5)	irrotationality consistency relation
WACE	(2.4.6, 8)	wave-action conservation equation
IMMCE	(2.6.3)	infinite depth momentum conservation equation
IECE	(2.6.4)	infinite depth energy conservation equation

Table 7.1: Symbolic names for equations and the corresponding descriptions

Equations needed here and for comparison with Stiassnie and Peregrine (1979) and Crapper (1979) are derived in appendix C. The two important equations are C10 and C21. These state

$$\frac{\partial I_i}{\partial t} + \frac{\partial}{\partial x_j}(U_j I_i + S_{ij}) + I_j \frac{\partial U_i}{\partial x_j} + d \frac{\partial}{\partial x_i}\frac{\partial \mathcal{L}^w}{\partial d} = k_i \left[\frac{\partial \mathcal{A}}{\partial t} + \frac{\partial}{\partial x_j}(U_j \mathcal{A} + B_j)\right] + I_j \left[\frac{\partial U_i}{\partial x_j} - \frac{\partial U_j}{\partial x_i}\right] , \tag{7.2.1}$$

$$\frac{\partial \mathcal{E}}{\partial t} + \frac{\partial}{\partial x_i}(U_i \mathcal{E} + \mathcal{F}_i) + S_{ij} \frac{\partial U_j}{\partial x_i} + \frac{1}{\rho} I_i \frac{\partial}{\partial x_i}\frac{\partial \mathcal{L}^w}{\partial d} = \frac{1}{2} \overline{u_h^2} \left[\rho \frac{\partial b}{\partial t} + \frac{\partial}{\partial x_i}(\rho d U_i + I_i)\right] + \sigma \left[\frac{\partial \mathcal{A}}{\partial t} \frac{\partial}{\partial x_i}(U_i \mathcal{A} + B_i)\right] . \tag{7.2.2}$$

These equations do not assume the validity of any equations or relations in § 2.2, § 2.3 or § 2.4 except the Doppler relation (2.3.1), consistency relations (2.3.4) involving the wavenumber vector k_i and the total wave frequency ω, and the dispersion relation in the basic Whitham form (2.4.3) involving the Lagrangian $\mathcal{L}^w$. The equations (7.2.1, 2) are, thus, purely algebraic relations between terms present in either the averaged equations or Whitham's equations of motion. This is also the case for any other equations in this chapter unless otherwise stated. It is important to keep this in mind when further reading this chapter.

These two equations can be compared to equations (48) and (53) respectively of Crapper (1979) - derived using the same methods as those used in appendix C. His equations state that the left hand sides of equations (7.2.1, 2) are equal to zero. This is because he assumes that the mass conservation equation (2.2.1), the wave-action conservation equation (2.4.6) and the irrotationality consistency relation (2.3.5) are true, i.e. MCE = 0, WACE = 0 and ICR = 0, so that the right hand sides of equations (7.2.1, 2) are set to zero. He has all the apparatus to derive the equivalence relations but does not do so. He instead goes on to show that the consistency relations (2.3.5) are sufficient conditions for the equivalence of the two systems of equations.

From Whitham's equation (2.4.4), which effectively defines γ in terms of mean wave properties,

$$\frac{\partial \mathcal{L}^w}{\partial d} = - \rho\left[\gamma - \frac{1}{2} U_j^2 - gb\right] \tag{7.2.3}$$

so

$$\frac{\partial}{\partial x_i}\frac{\partial \mathcal{L}^w}{\partial d} = \rho\left[\frac{\partial U_i}{\partial t} + U_j \frac{\partial U_i}{\partial x_j} + g \frac{\partial b}{\partial x_i}\right]$$

$$- \rho\left[\frac{\partial U_i}{\partial t} + \frac{\partial \gamma}{\partial x_i} + U_j\left[\frac{\partial U_i}{\partial x_j} - \frac{\partial U_j}{\partial x_i}\right]\right] . \tag{7.2.4}$$

Substituting this into equations (7.2.1, 2) gives the equations

$$\frac{\partial I_i}{\partial t} + \frac{\partial}{\partial x_j}(U_j I_i + S_{ij}) + I_j \frac{\partial U_i}{\partial x_j} + \rho d\left[\frac{\partial U_i}{\partial t} + U_j \frac{\partial U_i}{\partial x_j} + g \frac{\partial b}{\partial x_i}\right] =$$

$$\delta_i\left[\frac{\partial \mathcal{A}}{\partial t} + \frac{\partial}{\partial x_j}(U_j \mathcal{A} + B_j)\right]$$

$$+ \rho d\left[\frac{\partial U_i}{\partial t} + \frac{\partial \gamma}{\partial x_i}\right] + (\rho d U_j + I_j)\left[\frac{\partial U_i}{\partial x_j} - \frac{\partial U_j}{\partial x_i}\right] \tag{7.2.5}$$

or

$$\text{MMCE} = k_i \text{ WACE} + \rho d \text{ CCR} + (\rho d U_j + I_j) \text{ ICR} , \tag{7.2.6}$$

$$\frac{\partial \mathcal{E}}{\partial t} + \frac{\partial}{\partial x_i}(U_i \mathcal{E} + \mathcal{F}_i) + S_{ij} \frac{\partial U_j}{\partial x_i} + I_i\left[\frac{\partial U_i}{\partial t} + U_j \frac{\partial U_i}{\partial x_j} + g \frac{\partial b}{\partial x_i}\right] =$$

$$\frac{1}{2}\overline{u_h^2}\left[\rho \frac{\partial b}{\partial t} + \frac{\partial}{\partial x_i}(\rho d U_i + I_i)\right] + \sigma\left[\frac{\partial \mathcal{A}}{\partial t} + \frac{\partial}{\partial x_i}(U_i \mathcal{A} + B_i)\right]$$

$$+ I_i\left[\frac{\partial U_i}{\partial t} + \frac{\partial \gamma}{\partial x_i} + U_j\left[\frac{\partial U_i}{\partial x_j} - \frac{\partial U_j}{\partial x_i}\right]\right] \tag{7.2.7}$$

or

$$\text{ECE} = \tfrac{1}{2}\overline{u_h^2} \text{ MCE} + \sigma \text{ WACE} + I_i \text{ (CCR} + U_j \text{ ICR)} . \tag{7.2.8}$$

Note that equation (7.2.7) is identically zero if no waves are present.

These provide equations which relate the left hand sides of the averaged momentum and energy conservation equation (2.2.5, 6) and Whitham's wave-action conservation equation (2.4.6). Recall that in both systems the mass conservation equations are identical simply because the wave momentum vector $\mathcal{I}_i$ is defined in terms of $\mathcal{L}^w$ by (2.5.2).

Stiassnie and Peregrine (1979) use the averaged momentum and energy conservation equations in their "complete" form (2.2.2, 3). Equations relating these averaged equations and Whitham's equations are derived by reversing the manipulations, outlined at the end of § 2.2, needed to derive the averaged equations in the form (2.2.5, 6) from the form (2.2.2, 3). Thus, adding U_i times the mass conservation equation (2.2.1) to equation (7.2.5) gives

$$\frac{\partial}{\partial t}\,(\rho d U_i + \mathcal{I}_i) + \frac{\partial}{\partial x_j}\left[(\rho d U_i + \mathcal{I}_i)\left[\frac{\mathcal{I}_j}{\rho d} + U_j\right] + \frac{1}{2}\,\rho g d^2\,\delta_{ij} + \mathcal{S}_{ij} - \frac{\mathcal{I}_i \mathcal{I}_j}{\rho d}\right]$$

$$- \rho g d\,\frac{\partial h}{\partial x_i} = U_i\left[\rho\,\frac{\partial b}{\partial t} + \frac{\partial}{\partial x_j}(\rho d U_j + \mathcal{I}_j)\right] + k_i\left[\frac{\partial \mathcal{A}}{\partial t} + \frac{\partial}{\partial x_j}(U_j \mathcal{A} + B_j)\right]$$

$$+ \rho d\left[\frac{\partial U_i}{\partial t} + \frac{\partial \gamma}{\partial x_i}\right] + (\rho d U_j + \mathcal{I}_j)\left[\frac{\partial U_i}{\partial x_j} - \frac{\partial U_j}{\partial x_i}\right] \qquad (7.2.9)$$

or $$\mathrm{FMMCE} = U_i\ \mathrm{MCE} + k_i\ \mathrm{WACE} + \rho d\ \mathrm{CCR} + (\rho d U_j + \mathcal{I}_j)\ \mathrm{ICR} \qquad (7.2.10)$$

and adding $(gb - \frac{1}{2}U_i^2)$ times the mass conservation equation (2.2.1) and U_i times equation (7.2.9) to equation (7.2.7) gives

$$\frac{\partial}{\partial t}\left[\frac{1}{2}\,\rho d U_i^2 + \frac{1}{2}\,\rho g b^2 + \mathcal{E} + U_i \mathcal{I}_i\right] + \frac{\partial}{\partial x_i}\left[U_i\left[\frac{1}{2}\,\rho d U_j^2 + \rho g d b + \mathcal{E} + U_j \mathcal{I}_j\right]\right.$$

$$\left. + \mathcal{F}_i + \mathcal{I}_i\left[gb + \frac{1}{2}\,U_j^2\right] + \mathcal{S}_{ij} U_j\right] = \gamma\left[\rho\,\frac{\partial b}{\partial t} + \frac{\partial}{\partial x_i}(\rho d U_i + \mathcal{I}_i)\right]$$

$$+ \omega\left[\frac{\partial \mathcal{A}}{\partial t} + \frac{\partial}{\partial x_i}(U_i \mathcal{A} + B_i)\right] + (\rho d U_i + \mathcal{I}_i)\left[\frac{\partial U_i}{\partial t} + \frac{\partial \gamma}{\partial x_i}\right] \qquad (7.2.11)$$

or $$\mathrm{FECE} = \gamma\ \mathrm{MCE} + \omega\ \mathrm{WACE} + (\rho d U_i + \mathcal{I}_i)\ \mathrm{CCR}\ , \qquad (7.2.12)$$

since $$(\mathcal{I}_i U_j + \mathcal{I}_j U_i)\left[\frac{\partial U_i}{\partial x_j} - \frac{\partial U_j}{\partial x_i}\right] = 0\ , \quad U_i U_j\left[\frac{\partial U_i}{\partial x_j} - \frac{\partial U_j}{\partial x_i}\right] = 0\ . \qquad (7.2.13)$$

The derivation of equation (7.2.12) requires use of the Doppler relation (2.3.1), the definition of γ as given by Whitham's equation (2.4.4) or (7.2.3) and expression (2.5.6) for the mean bottom velocity squared in terms of $\mathcal{L}^w$.

The mass conservation equation (2.2.1) or (2.4.5), i.e. MCE = 0, is given by both systems of equations. Substitution of this into these equations gives equations (11) and (10) respectively of Stiassnie and

Peregrine (1979). Note that Stiassnie and Peregrine (1979) take the averaged equations and manipulate these equations to give their equations (11) and (10). As stated above, the method used here does not assume the validity of either the averaged equations or Whitham's equations of motion. It derives purely algebraic relations between the left hand sides of the two sets of equations.

From the equations (7.2.9, 11) it follows that the equivalence relations are

$$\rho d\left[\frac{\partial U_i}{\partial t} + \frac{\partial \gamma}{\partial x_i}\right] + (\rho dU_j + \mathcal{I}_j)\left[\frac{\partial U_i}{\partial x_j} - \frac{\partial U_j}{\partial x_i}\right] = 0 \qquad (7.2.14)$$

or

$$\rho d\ CCR + (\rho dU_j + \mathcal{I}_j)\ ICR = 0\ , \qquad (7.2.15)$$

$$(\rho dU_i + \mathcal{I}_i)\left[\frac{\partial U_i}{\partial t} + \frac{\partial \gamma}{\partial x_i}\right] = 0 \qquad (7.2.16)$$

or

$$(\rho dU_i + \mathcal{I}_i)\ CCR = 0\ , \qquad (7.2.17)$$

which are conditions (13) and (12) respectively of Stiassnie and Peregrine (1979).

The equivalence relations (7.2.14, 16) are also easily derived from equations (7.2.5, 7). Equation (7.2.5) gives the equivalence relation (7.2.14) whilst equation (7.2.7) gives the a third equivalence relation

$$\mathcal{I}_i\left[\frac{\partial U_i}{\partial t} + \frac{\partial \gamma}{\partial x_i} + U_j\left[\frac{\partial U_i}{\partial x_j} - \frac{\partial U_j}{\partial x_i}\right]\right] = 0 \qquad (7.2.18)$$

or

$$\mathcal{I}_i\ (CCR + U_j\ ICR) = 0\ . \qquad (7.2.19)$$

Note that unlike the equivalence relations (7.2.14, 16) this relation is identically zero if no waves are present. Adding U_i times equivalence relations (7.2.14) to relation (7.2.18) gives the equivalence relation (7.2.16) after using the expressions (7.2.13).

Now, the equivalence relation (7.2.16) can be derived from relations (7.2.14) by taking the scalar product with $(\rho dU_i + \mathcal{I}_i)$. Thus, the three equivalence relations (7.2.14, 16, 18) are all related and the only independent ones are the vector relations (7.2.14).

Equivalence relations (7.2.14) can be rewritten (Stiassnie and Peregrine 1979) to show the influence of the waves on the currents more directly by eliminating γ using the defining expression (2.4.4) or (7.2.3) and expression (2.5.6) for the mean bottom velocity squared

in terms of $\mathcal{L}^w$:

$$\frac{\partial U_i}{\partial t} + U_j \frac{\partial U_i}{\partial x_j} + g \frac{\partial b}{\partial x_i}$$

$$+ \frac{\mathcal{I}_i}{\rho d} \left[\frac{\partial U_i}{\partial x_j} - \frac{\partial U_j}{\partial x_i}\right] + \frac{1}{2} \frac{\partial}{\partial x_i} \overline{u_h^2} = 0 \ . \qquad (7.2.20)$$

Note that the last two terms are negligible if the depth of the liquid is infinite (§ 2.6) and exactly zero if there are no waves. This shows, again, that the mainstream flow satisfies the shallow water equations (2.6.2) if the depth of liquid is infinite or if there is no wave motion.

The equivalence relations (7.2.14) replace consistency relations (2.3.5) in order to make the averaged equations and Whitham's equations fully equivalent. Note that these show that the mainstream flow need not necessarily be irrotational for Whitham's equations to hold which is the motivation for Stiassnie and Peregrine (1979).

7.3 The Case of Infinite Depth

Taking the limit $d \to 0$ in the finite depth equivalence relations (7.2.14) gives (divide relation 7.2.14 by ρd and take the limit)

$$\frac{\partial U_i}{\partial t} + \frac{\partial \gamma}{\partial x_i} + U_j \left[\frac{\partial U_i}{\partial x_j} - \frac{\partial U_j}{\partial x_i}\right] = 0 \qquad (7.3.1)$$

or

$$CCR + U_j \ ICR = 0 \ . \qquad (7.3.2)$$

Another method of deriving this is by noting that for infinite depths the averaged Lagrangian $\mathcal{L}^w$ is independent of d (§ 2.6). Then the derivative expression (7.2.4) gives

$$\frac{\partial U_i}{\partial t} + U_j \frac{\partial U_i}{\partial x_j} + g \frac{\partial b}{\partial x_i} = \frac{\partial U_i}{\partial t} + \frac{\partial \gamma}{\partial x_i} + U_j \left[\frac{\partial U_i}{\partial x_j} - \frac{\partial U_j}{\partial x_i}\right] \qquad (7.3.3)$$

which, using the shallow water equations (2.6.2), gives relation (7.3.1).

The fact that $\mathcal{L}^w$ is independent of d is enough to give simplified versions of equations (7.2.1, 2) valid for infinite depth liquids. This is most easily seen by following the algebra of appendix C

with $\mathcal{L}^w = \mathcal{L}^w(\sigma,k,a)$ only. The equations (7.2.1, 2) simplify to

$$\frac{\partial \mathcal{I}_i}{\partial t} + \frac{\partial}{\partial x_j}(U_j \mathcal{I}_i + \mathcal{S}_{ij}) + \mathcal{I}_j \frac{\partial U_i}{\partial x_j} = k_i \left[\frac{\partial \mathcal{A}}{\partial t} + \frac{\partial}{\partial x_j}(U_j \mathcal{A} + B_j)\right] + \mathcal{I}_j \left[\frac{\partial U_i}{\partial x_j} - \frac{\partial U_j}{\partial x_i}\right] \tag{7.3.4}$$

or
$$\text{IMMCE} = k_i \ \text{WACE} + \mathcal{I}_j \ \text{ICR} \ , \tag{7.3.5}$$

$$\frac{\partial \mathcal{E}}{\partial t} + \frac{\partial}{\partial x_i}(U_i \mathcal{E} + \mathcal{F}_i) + \mathcal{S}_{ij} \frac{\partial U_j}{\partial x_i} = \sigma \left[\frac{\partial \mathcal{A}}{\partial t} + \frac{\partial}{\partial x_i}(U_i \mathcal{A} + B_i)\right] \tag{7.3.6}$$

or
$$\text{IECE} = \sigma \ \text{WACE} \ . \tag{7.3.7}$$

The dependence of the mainstream flow on the shallow water equations results in the inapplicability of the mass conservation equation (2.2.1) or (2.4.5). Note that the mass conservation equation does not appear in equation (7.3.6) even though it does appear in equation (7.2.2).

Consequently, equations (7.3.4, 6) imply that the equivalence relations for infinite depths can be given by the single set of relations

$$\mathcal{I}_j \left[\frac{\partial U_i}{\partial x_j} - \frac{\partial U_j}{\partial x_i}\right] = 0 \tag{7.3.8}$$

or
$$\mathcal{I}_j \ \text{ICR} = 0 \ . \tag{7.3.9}$$

Note that multiplying relation (7.3.1) by $\mathcal{I}_i$ and using relation (7.3.8) gives

$$\mathcal{I}_i \left[\frac{\partial U_i}{\partial t} + \frac{\partial \gamma}{\partial x_i}\right] = 0 \tag{7.3.10}$$

or
$$\mathcal{I}_i \ \text{CCR} = 0 \ . \tag{7.3.11}$$

Thus, it is concluded that the equivalence relations for a liquid of infinite depth are given by (7.3.8) with the limiting relations (7.3.1) of the finite depth equivalence relations and (7.3.10) as restrictions imposed by the shallow water equations (2.6.2). However, the shallow water approximation for the mainstream flow when the depth of the liquid is infinite is inappropriate and further analysis is needed. This type of analysis has been considered to some extent by Peregrine (1976, § IIF) or, using a rather different approach, by Hasselmann (1971). From § 2.7 it is deduced that this would mean that the wave motion would have to affect the mainstream flow.

7.4 Wave Energy Dissipation and "Parallel Acceleration"

Our aim is to be derive equations which model flows of liquids incorporating two extra features. One feature is the effect of dissipation of wave energy due to viscosity. The second feature is to consider flows in which the mainstream motion is in a non-horizontal direction. There exist naturally occurring flows which incorporate either one or both of these features. For example, the wind-generated infinite depth waves considered in previous chapters include the effects of wave energy dissipation. Also, the flow of a vertically falling sheet of liquid is accelerated by gravity and sometimes has waves dissipating energy present on the sheet.

For finite depth flows the primary effects of energy dissipation arise from the boundary layer set up at the bed. The modelling of such dissipative effects requires a completely new approach to the problem and is not pursued here. Instead, attention is restricted to those flows in which either the depth of liquid is infinite, as in chapter 5, or in which the liquid is bounded by two free surfaces so that the dominant dissipative effects are in the body of the liquid. Such a sheet flow occurs, for example, when water flows over a sharp edged weir. The two free surface problem is supposed to be symmetrical about the centreline and so the "bed" is thought of as being a pseudo-bed at the centreline. This is the case in the vertically falling film problem.

Therefore, in this section terms corresponding to the effects of wave energy dissipation are added to the averaged equations. Also terms corresponding to an acceleration of the mainstream flow parallel to the bed, henceforth called the "parallel acceleration", are also added to the averaged equations.

a The Effects of Wave Energy Dissipation

The effects of wave energy dissipation are to modify the momentum conservation equations (2.2.2) by the addition of a dissipation term Σ_i to the right hand side and modify the energy conservation equation (2.2.3) by the addition of $U_i\Sigma_i - \mathcal{D}$ to the right hand side. Thus, Σ_i is the mean momentum transfer (from waves to mainstream flow) and $\mathcal{D}$ is the mean rate of energy dissipation of the waves (compare these additions with Phillips, 1966, p 65). The mass conservation equation (2.2.1) is unaffected.

The dissipation terms Σ_i and $\mathcal{D}$ are defined by

$$\Sigma_i = \overline{\int_{-h}^{\eta} \mu \left[\frac{\partial^2}{\partial x_j^2} + \frac{\partial^2}{\partial z^2}\right] u_i \, dz} \, , \qquad (7.4.1)$$

$$\mathcal{D} = - \overline{\int_{-h}^{\eta} \mu \, u_i \left[\frac{\partial^2}{\partial x_j^2} + \frac{\partial^2}{\partial z^2}\right] u_i + w \left[\frac{\partial^2}{\partial x_j^2} + \frac{\partial^2}{\partial z^2}\right] w \, dz} \, , \qquad (7.4.2)$$

and are derived by integrating and averaging over the waves those terms with viscosity present in the Navier-Stokes equations of motion. These terms are neglected when the averaged equations of § 2.2 are derived (see, for example, Crapper 1979). Thus, Σ_i is the term found by integrating the Navier-Stokes equations over the total depth and averaging, and $U_i\Sigma_i - \mathcal{D}$ is the term found by multiplying the Navier-Stokes equations by $(U_i + u_i, w)$, integrating over the total depth and averaging.

Following the manipulations at the end of § 2.2 it is seen that the effect of dissipation on the averaged momentum and energy conservation equation in the form given by equations (2.2.5, 6) is to add Σ_i on the right hand side of the momentum conservation equation (2.2.5), as before, but simply add $-\mathcal{D}$ to the right hand side of the energy conservation equation (2.2.6). Thus, the use of the energy conservation equation in chapter 5 with $\mathcal{D}$ alone is validified.

The expressions (7.4.1) and (7.4.2) for the wave energy dissipation terms Σ_i and $\mathcal{D}$ are examined more closely in order to see how the expression (5.14.8) in Batchelor (1967) for $\mathcal{D}$, used in chapter 5 and later in chapter 10, is derived. These dissipation terms are a property of the wave motion only and the effects of the mainstream flow is purely one of convecting the term Σ_i in the energy conservation equation (2.2.3). Thus, for the present analysis U_i is taken to be zero.

Letting $u_3 = w$ and $x_3 = z$ and using the summation convention over $i = 1$, 2 and 3 (previously summation convention is over $i = 1$, 2 only) gives the integrand of (7.4.2) as

$$\mu \, u_i \frac{\partial^2 u_i}{\partial x_j^2} = 2\mu \, u_i \frac{\partial e_{ij}}{\partial x_j} \quad \text{where} \quad e_{ij} = \frac{1}{2}\left[\frac{\partial u_i}{\partial x_j} + \frac{\partial u_j}{\partial x_i}\right] \qquad (7.4.3)$$

denotes the rate-of-strain tensor (Batchelor 1967 expression 3.3.16). Then

$$\mu \, u_i \frac{\partial^2 u_i}{\partial x_j^2} = \frac{\partial}{\partial x_j}(u_i \, 2\mu \, e_{ij}) - 2\mu \, e_{ij} \frac{\partial u_i}{\partial x_j} \, . \qquad (7.4.4)$$

Integrating over the total depth and averaging over the waves is the same as integrating over a volume element, with unit span, of the liquid. Consequently, it is possible to use the divergence theorem on the first of the two terms in (7.4.4) to give

$$\overline{\int_{-h}^{\eta} \frac{\partial}{\partial x_j}(u_i \, 2\mu \, e_{ij}) \, dz} = \int_S 2\mu \, e_{ij} \, u_i n_j \, dS \qquad (7.4.5)$$

where S represents the boundaries of the liquid and n_i is the unit outward normal to the surface. The boundaries of the liquid consist of the free surface, the bed (at infinity) or pseudo-bed (centreline) and two surfaces periodically situated normal to the bed or pseudo bed.

Now, n_i is oppositely oriented on the two periodically situated surfaces so that these two parts of the surface integral (7.4.5) cancel each other. To consider the surface integral (7.4.5) on the other surfaces, i.e. the free surface and the bed (at infinity) or pseudo-bed (centreline), it is noted that the rate-of-strain tensor e_{ij} is related to the stress tensor σ_{ij} and pressure p by

$$2\mu \, e_{ij} = \sigma_{ij} + p \, \delta_{ij} \qquad (7.4.6)$$

so
$$\int_S 2\mu \, e_{ij} \, u_i n_j \, dS = \int_S \sigma_{ij} u_i n_j \, dS + \int_S p u_i n_i \, dS \; . \qquad (7.4.7)$$

On the free surface $\sigma_{ij} n_j = p_o n_i$, where $p = p_o$ is the constant surface pressure, so that

$$\int_S 2\mu \, e_{ij} \, u_i n_j \, dS = 2p_o \int_S u_i n_i \, dS \; . \qquad (7.4.8)$$

On the the bed at infinity $u_i = 0$ and the surface integral (7.4.5) vanishes. On the pseudo-bed (centreline) $\sigma_{ij} n_j = (\tau_b)_i = p_b n_i$ where $(\tau_b)_i$ is the bed shear stress and p_b is the variable bed pressure so that

$$\int_S 2\mu \, e_{ij} \, u_i n_j \, dS = 2 \int_S p_b \, u_i n_i \, dS \; . \qquad (7.4.9)$$

On the pseudo-bed (centreline) $u_i n_i$ is identically zero which is also the case on the free surface when viewed from a reference frame moving with the waves (no mass flow through the free surface). Thus, the integrals (7.4.8, 9) are equal to zero and so the integral (7.4.5) is zero.

The second of the two terms in (7.4.4) gives the expression

$$\mathcal{D} = \overline{\int_{-h}^{\eta} \mu \, e_{ij} e_{ij} \, dz} \qquad (7.4.10)$$

which is the origin of Batchelor's expression. Our usual summation convention is now re-established.

The dissipation term Σ_i simplifies when the waves are two dimensional. Thus, suppose that there are no variations in the x_2 direction. Then $u = u_1$, $x = x_1$ and $\Sigma = \Sigma_1$, say, so

$$\Sigma = \mu \overline{\int_{-h}^{\eta} \left[\frac{\partial^2 u}{\partial x^2} + \frac{\partial^2 u}{\partial z^2}\right] dz} \; . \qquad (7.4.11)$$

The Cauchy-Reimann equations for a two dimensional locally irrotational incompressible flow give

$$\frac{\partial u}{\partial x} = - \frac{\partial w}{\partial z} \qquad (7.4.12)$$

so that

$$\Sigma = \mu \overline{\left[\frac{\partial u}{\partial z} - \frac{\partial w}{\partial x}\right]_{-h}^{\eta}} \; . \qquad (7.4.13)$$

b The Effects of Parallel Acceleration

The effects of parallel acceleration, g_{pi}, of the mainstream flow on the averaged momentum and energy conservation equations (2.2.2, 3) are found in a similar manner to the derivation of the wave energy dissipation terms Σ_i and $\mathcal{D}$. The gravity term g in the averaged equations must be replaced by g_v where g_v represents an acceleration term for the mainstream flow directed perpendicular to the bed (at infinity) or pseudo-bed (centreline) and into the liquid, i.e. in the - z direction.

The addition of a parallel acceleration term to the Euler, or the Navier-Stokes, momentum equations is simply given by adding a term ρg_{pi}. Integrating over the total depth and averaging results in modification of the momentum conservation equations (2.2.2) by the addition of $\rho d g_{pi}$ to the right hand side. Similarly, multiplying the Euler momentum equations, with the additional ρg_{pi} term, by $(U_i + u_i, w)$, integrating over the total depth and averaging results in modification of the energy conservation equation (2.2.3) by the addition of $(\rho d U_i + \mathcal{I}_i) g_{pi}$ to the right hand side. The mass conservation equation (2.2.1) is, again, unaffected.

Following the manipulations at the end of § 2.2 it is seen that the effect of a parallel acceleration, g_{pi}, of the mainstream flow on the averaged momentum and energy conservation equations (2.2.5, 6) is to add ρdg_{pi} to the right hand side of the momentum conservation equation (2.2.5), as before, but simply add $g_{pi}\mathcal{I}_i$ to the right hand side of the energy conservation equation (2.2.6).

7.5 The Modified Wave-Action Conservation Equation

The wave-action conservation equation (2.4.6) and the equivalence relations (7.2.14, 16) must be modified by the addition of new terms when the effects of wave energy dissipation and parallel acceleration are considered. In this section it is our aim to derive the modified wave-action conservation equation and modified equivalence relations. The work of chapter 5 suggests that the appropriate term to add to the wave-action conservation equation for dissipation effects is $-\mathcal{D}/\sigma$. Christoffersen and Jonsson (1980) prove this to generally be the case for infinitesimal amplitude wave motions.

Adding appropriate terms to both sides of equation (7.2.8) gives

$$\frac{\partial \mathcal{E}}{\partial t} + \frac{\partial}{\partial x_i}(U_i\mathcal{E} + \mathcal{F}_i) + \mathcal{S}_{ij}\frac{\partial U_j}{\partial x_i} + \mathcal{I}_i\left[\frac{\partial U_i}{\partial t} + U_j\frac{\partial U_i}{\partial x_j} + g_v\frac{\partial b}{\partial x_i}\right]$$

$$- (g_{pi}\mathcal{I}_i - \mathcal{D}) = \frac{1}{2}\overline{u_h^2}\left[\rho\frac{\partial b}{\partial t} + \frac{\partial}{\partial x_i}(\rho d U_i + \mathcal{I}_i)\right]$$

$$+ \sigma\left[\frac{\partial \mathcal{A}}{\partial t} + \frac{\partial}{\partial x_i}(U_i\mathcal{A} + \mathcal{B}_i)\right] + \mathcal{I}_i\left[\frac{\partial U_i}{\partial t} + \frac{\partial \gamma}{\partial x_i} + U_j\left[\frac{\partial U_i}{\partial x_j} - \frac{\partial U_j}{\partial x_i}\right]\right]$$

$$- (g_{pi}\mathcal{I}_i - \mathcal{D}) \qquad (7.5.1)$$

or

$$\text{ECE} - (\mathcal{I}_i g_{pi} - \mathcal{D}) = \tfrac{1}{2}\overline{u_h^2}\,\text{MCE} + \sigma\,\text{WACE} + \mathcal{I}_i\,(\text{CCR} + U_j\,\text{ICR}) + (g_{pi}\mathcal{I}_i - \mathcal{D})\ . \qquad (7.5.2)$$

The wave-action conservation equation (2.4.7) replaces the averaged energy conservation equation (2.2.3, 6) in Whitham's formulation of the equations of motion. Also, the wave-action conservation equation is identically zero when no waves are present as is the averaged energy conservation in the form (2.2.6). This is also true of equation (7.5.1). Physically, terms involving wave energy dissipation and parallel acceleration must be involved in the modified wave-action conservation equation. Thus, the specific form of the modified wave-action conservation equation is easily seen from equation (7.5.1). It must take

the form

$$\frac{\partial \mathcal{A}}{\partial t} + \frac{\partial}{\partial x_i}(U_i \mathcal{A} + B_i) = \frac{1}{\sigma}\,(g_{pi} \mathcal{I}_i - \mathcal{D}) \qquad (7.5.3)$$

or

$$\text{WACE} = \frac{1}{\sigma}\,(g_{pi} \mathcal{I}_i - \mathcal{D})\ . \qquad (7.5.4)$$

The form of the equivalence relations when wave energy dissipation and parallel acceleration of the mainstream flow are added are derived by use of the equations (7.2.9, 11). Terms must be added to these equations which are such that the right hand side of the modified equations subsequently derived contain terms involving the wave-action conservation equation in the form (7.5.3) rather than the form (2.4.6). Adding appropriate terms to both sides gives

$$\begin{aligned}
&\frac{\partial}{\partial t}\,(\rho d U_i + \mathcal{I}_i) + \frac{\partial}{\partial x_j}\left[(\rho d U_i + \mathcal{I}_i)\left[\frac{\mathcal{I}_j}{\rho d} + U_j\right] + \frac{1}{2}\,\rho g_v d^2\,\delta_{ij} + \mathcal{S}_{ij} - \frac{\mathcal{I}_i \mathcal{I}_j}{\rho d}\right] \\
&\quad - \rho g_v d\,\frac{\partial h}{\partial x_i} - (\Sigma_i + \rho d g_{pi}) = U_i\left[\rho\,\frac{\partial b}{\partial t} + \frac{\partial}{\partial x_j}(\rho d U_j + \mathcal{I}_j)\right] \\
&\quad + k_i\left[\frac{\partial \mathcal{A}}{\partial t} + \frac{\partial}{\partial x_j}(U_j \mathcal{A} + B_j) - \frac{1}{\sigma}\,(g_{pj} \mathcal{I}_j - \mathcal{D})\right] \\
&\quad + \rho d\left[\frac{\partial U_i}{\partial t} + \frac{\partial \gamma}{\partial x_i}\right] + (\rho d U_j + \mathcal{I}_j)\left[\frac{\partial U_i}{\partial x_j} - \frac{\partial U_j}{\partial x_i}\right] \\
&\quad - (\Sigma_i + \rho d g_{pi}) + \frac{k_i}{\sigma}\,(g_{pj} \mathcal{I}_j - \mathcal{D}) \qquad (7.5.5)
\end{aligned}$$

or

$$\begin{aligned}
&[\text{FMMCE} - (\Sigma_i + \rho d g_{pi})] = U_i\ \text{MCE} + k_i\left[\text{WACE} - \frac{1}{\sigma}\,(g_{pj} \mathcal{I}_j - \mathcal{D})\right] \\
&\quad + \rho d\ \text{CCR} + (\rho d U_j + \mathcal{I}_j)\ \text{ICR} - (\Sigma_i + \rho d g_{pi}) + \frac{k_i}{\sigma}\,(g_{pj} \mathcal{I}_j - \mathcal{D}) \qquad (7.5.6)
\end{aligned}$$

and $\frac{\partial}{\partial t}\left[\frac{1}{2}\rho d U_i^2 + \frac{1}{2}\rho g_v b^2 + \mathcal{E} + U_i \mathcal{I}_i\right] + \frac{\partial}{\partial x_i}\left[U_i\left[\frac{1}{2}\rho d U_j^2 + \rho g_v d b + \mathcal{E} + U_j \mathcal{I}_j\right] + \mathcal{F}_i + \mathcal{I}_i\left[g_v b + \frac{1}{2} U_j^2\right] + \mathcal{S}_{ij} U_j\right] - (U_i \Sigma_i - \mathcal{D})$

$- (\rho d U_i + \mathcal{I}_i) g_{pi} = \gamma\left[\rho \frac{\partial b}{\partial t} + \frac{\partial}{\partial x_i}(\rho d U_i + \mathcal{I}_i)\right] + \omega\left[\frac{\partial \mathcal{A}}{\partial t} + \frac{\partial}{\partial x_i}(U_i \mathcal{A} + B_i) - \frac{1}{\sigma}(g_{pi}\mathcal{I}_i - \mathcal{D})\right] + (\rho d U_i + \mathcal{I}_i)\left[\frac{\partial U_i}{\partial t} + \frac{\partial \gamma}{\partial x_i}\right]$

$- (U_i \Sigma_i - \mathcal{D}) - (\rho d U_i + \mathcal{I}_i) g_{pi} + \frac{\omega}{\sigma}(g_{pi}\mathcal{I}_i - \mathcal{D})$ (7.5.7)

or $[\text{FECE} - (U_i \Sigma_i - \mathcal{D}) - (\rho d U_i + \mathcal{I}_i) g_{pi}] = \gamma\ \text{MCE} + \omega\left[\text{WACE} - \frac{1}{\sigma}(g_{pi}\mathcal{I}_i - \mathcal{D})\right] + (\rho d U_i + \mathcal{I}_i)\ \text{CCR}$

$- (U_i \Sigma_i - \mathcal{D}) - (\rho d U_i + \mathcal{I}_i) g_{pi} + \frac{\omega}{\sigma}(g_{pi}\mathcal{I}_i - \mathcal{D})$. (7.5.8)

In equations (7.5.6, 8) the terms in the square brackets represent the modified momentum and energy conservation equations respectively. It, therefore, follows that the modified equivalence relations are

$\rho d\left[\frac{\partial U_i}{\partial t} + \frac{\partial \gamma}{\partial x_i}\right] + (\rho d U_j + \mathcal{I}_j)\left[\frac{\partial U_i}{\partial x_j} - \frac{\partial U_j}{\partial x_i}\right]$

$- (\Sigma_i + \rho d g_{pi}) + \frac{k_i}{\sigma}(g_{pj}\mathcal{I}_j - \mathcal{D}) = 0$ (7.5.9)

or $\rho d\ \text{CCR} + (\rho d U_j + \mathcal{I}_j)\ \text{ICR}$

$- (\Sigma_i + \rho d g_{pi}) + \frac{k_i}{\sigma}(g_{pj}\mathcal{I}_j - \mathcal{D}) = 0$ (7.7.10)

and $(\rho d U_i + \mathcal{I}_i)\left[\frac{\partial U_i}{\partial t} + \frac{\partial \gamma}{\partial x_i}\right]$

$- U_i(\Sigma_i + \rho d g_{pi}) + \frac{k_j U_j}{\sigma}(g_{pi}\mathcal{I}_i - \mathcal{D}) = 0$ (7.5.11)

or $(\rho d U_i + \mathcal{I}_i)\ \text{CCR}$

$- U_i(\Sigma_i + \rho d g_{pi}) + \frac{k_j U_j}{\sigma}(g_{pi}\mathcal{I}_i - \mathcal{D}) = 0$ (7.5.12)

where the Doppler relation is used to derive the modified equivalence relation (7.5.11) from equation (7.5.7).

Subtracting U_i times equivalence relations (7.5.9) from relation (7.5.11) gives the relation (7.2.18) after using expressions (7.2.13). Alternatively, the relation (7.2.18) is immediately deducible from expression (7.5.1) on use of the modified

wave-action conservation equation (7.5.3). Thus, the equivalence relation (7.2.18) does not change when dissipation and parallel acceleration are added to the system.

The modified equivalence relation (7.5.11) can not be derived from the equivalence relations (7.5.9) by, for example, taking the scalar product with ($\rho dU_i + \mathcal{I}_i$). Therefore, the vector relations (7.5.9) and one of the scalar relations (7.5.11, 7.2.18) are independent.

The equivalence relations (7.5.9), together with the definition of γ given by expression (2.4.9), replace the modified momentum conservation equations in order to make the modified averaged equations and the modified Whitham's equations fully equivalent.

Throughout this thesis the case of an irrotational mainstream flow is always considered. Also it is supposed that the consistency relations (2.3.5) are satisfied so that Whitham's replacement of the momentum conservation equations is, as previously mentioned, given by the former of these consistency relations. This can only be the situation if there is no wave energy dissipation or parallel acceleration of the mainstream flow. However, when either one or both of these effects are considered the above form of the equivalence relations must replace the momentum conservation equations. Note that the mainstream flow can still be supposed (globally) irrotational.

CHAPTER 8
FINITE-AMPLITUDE PURE CAPILLARY WAVES ON FINITE DEPTH LIQUID

8.1 Introduction

Taylor (1959) analyses the possible infinitesimal amplitude pure capillary waves which occur on a thin liquid sheet. He shows that two types of waves are produced. One type is symmetrical and the other antisymmetrical with respect to the centreline of the sheet. He experimentally confirmed the existence of such waves using liquid sheets as thin as 5-100 μm.

Finite-amplitude pure capillary waves were first analysed by Crapper (1957). He shows that there exists an exact solution for large amplitude pure capillary waves on liquid of infinite depth and that this solution is expressible in terms of elementary functions (§ 4.2). At that time he made the following remark: "there is also an exact solution if the liquid has finite uniform depth. The analysis is, however, rather complicated, involving elliptic functions, and the solution is not considered worth evaluating in detail."

This statement remained untested for almost twenty years. Kinnersley (1976) examines this point and shows that there two generalisations of Crapper's (1957) solution. These are shown to be finite-amplitude versions of Taylor's symmetrical and antisymmetrical sheet waves. The analysis presented in Kinnersley's paper is a generalisation of Crapper's approach.

Hogan (1986) examines these two finite-amplitude solutions. He extends Kinnersley's work to give an exact criterion for highest waves and also shows that Kinnersley's parameter c is not equivalent to either definition of the phase speed given by Stokes (1847).

In section 8.2 the wave solutions of Kinnersley (1976) are described with slight corrections and alterations where necessary. Attention is then focused on the symmetrical waves solution. In section 8.3 the highest waves criterion of Hogan (1986) is explicitly solved for these symmetrical waves. In section 8.4 expressions for the mean level of the liquid, the mean kinetic energy density, the mean potential energy density and the mean bottom velocity squared are found. The variation of these and other mean quantities are discussed in section 8.5.

8.2 Kinnersley's Exact Solution

Kinnersley (1976) considers steady, symmetric, periodic nonlinear pure capillary waves which propagate on a sheet of incompressible inviscid liquid of finite thickness. The motion in the liquid is two-dimensional and irrotational and the wave is moving to the right. By considering the motion in a frame of reference fixed to the waves the flow is reduced to a steady state. Kinnersley's results are given in such a frame but with his Cartesian axis $\hat{x}_K$ measured horizontally to the left (downstream) and axis z_K measured vertically downwards. The subscript K denotes that these are Kinnersley's axes and a hat denotes variables in a frame fixed to the waves. The axes used in our work are chosen with $\hat{x}$ measured horizontally to the right (upstream) and z measured vertically upwards. Consequently, Kinnersley's results need slight modification owing to these differences. Essentially, all that is required is a transformation $\hat{x}_K = -\hat{x}$ and $z_K = -z$. Elsewhere Kinnersley's notation is used throughout including the convention that the modulus of elliptic functions is omitted, since all functions of velocity function ϕ have modulus κ and all functions of the stream function ψ have modulus κ' where $\kappa^2 + \kappa'^2 = 1$ and $0 \leq \kappa \leq 1$. Note that this velocity potential and stream function are dimensionless. Excellent references for both elliptic functions and elliptic integrals are Byrd and Friedman (1971) and Abramowitz and Stegun (1965). The centreline of the sheet is given by $\psi = 0$ and the free surfaces by $\psi = \pm B$.

For symmetric waves (case Ib of Kinnersley) the wave profile, relative to axes moving with speed c, is given by

$$\hat{x} = -\frac{S}{c^2 A \kappa'^2}\left[2E(\phi) - \kappa'^2\phi - 2\kappa^2 \mathrm{sn}\ \phi\ \mathrm{cd}\ \phi + \frac{2\kappa\kappa'^2 \mathrm{sd}\ \phi\ \mathrm{nd}\ \phi}{\mathrm{dn}\ \psi - \kappa\ \mathrm{cd}\ \phi}\right] \quad (8.2.1)$$

$$z = -\frac{S}{c^2 A \kappa'^2}\left[(1 + \kappa^2)\psi - 2E(\psi) + \frac{2\kappa'^2 \mathrm{sn}\ \psi\ \mathrm{cn}\ \psi}{\mathrm{dn}\ \psi - \kappa\ \mathrm{cd}\ \phi}\right] \quad (8.2.2)$$

where $E(\phi)$ is the incomplete elliptic integral of the second kind. Thus, expressions (8.2.1, 2) are in the form $\hat{x} = \hat{x}(\phi,\psi)$ and $z = z(\phi,\psi)$ respectively with velocity potential ϕ and stream function ψ as the independent variables. The parameter A is generally not related to Crapper's parameter A described in § 4.2.

Now, sn and cn range between ± 1 with period 4K (K no longer represents the wavenumber of a gravity wavetrain), where $K(\kappa)$ is the complete elliptic integral of the first kind, whilst dn ranges between 1 and κ' with period 2K. It follows that $\phi = 0, \pm 4K$, etc., at wave crests and $\phi = \pm 2K, \pm 6K$, etc., at wave troughs.

The parameter A is related to the free surface $\psi = + B$ by

$$1 = - A\kappa'^2 \text{sn } B \text{ cd } B \ . \qquad (8.2.3)$$

Choosing B to lie in the first quadrant, i.e. $0 \leq B \leq K$, A must be negative. This implies (see Kinnersley 1976) ϕ and ψ increase to the right and upwards, i.e. in the directions of our axes.

The crest-to-crest wavelength λ is given by

$$\lambda = \hat{x}(4K,\psi) - \hat{x}(0,\psi) \ , \qquad (8.2.4)$$

so

$$\lambda = - \frac{4s}{c^2 A\kappa'^2} (2E - \kappa'^2 K) \qquad (8.2.5)$$

where $E(\kappa)$ is the complete elliptic integral of the second kind.

The amplitude a of the waves is given by

$$a = \frac{1}{2} [z(0,+ B) - z(2K,+ B)] \ , \qquad (8.2.6)$$

so

$$a = - \frac{2s\kappa}{c^2 A\kappa'^2} \text{ sc } B \qquad (8.2.7)$$

The trough depth t, measured from the centreline to a trough on the surface, is given by

$$t = z(2K,+ B) \qquad (8.2.8)$$

so

$$t = - \frac{s}{c^2 A\kappa'^2} [(1 + \kappa^2)B - 2E(B) + 2 \text{ sc } B(\text{dn } B - \kappa)] \ . \qquad (8.2.9)$$

The phase speed c_p, defined by Stokes (1847) first definition, is given by

$$c_p = \frac{\kappa'^2 K}{2E - \kappa'^2 K} c \ . \qquad (8.2.10)$$

The expressions (8.2.5, 7, 9) differ from those of Kinnersley by a negative sign. Those in his paper give negative values for λ, a and t.

These symmetric waves can be regarded as either occurring on a liquid of finite depth, with a fixed bottom at $\psi = 0$, or as a nonlinear version of Taylor's symmetrical waves on a liquid sheet. For the latter case the lower boundary occurs on $\psi = - B$ and the trough depth t represents the sheets minimum semi-thickness.

For antisymmetric waves (case IIb of Kinnersley) the wave profile is given by

$$\hat{x} = - \frac{S}{c^2 A} \left[2E(\phi) - \phi + \frac{2\kappa \, sn \, \phi \, dn \, \phi}{dn \, \psi - \kappa \, cn \, \phi} \right] \qquad (8.2.11)$$

$$z = - \frac{S}{c^2 A} \left[- 2E(\psi) + \psi - 2 \, dn \, \psi \, cs \, \psi + \frac{2 \, ns \, \psi \, cs \, \psi}{ds \, \psi - \kappa \, cn \, \phi} \right] \qquad (8.2.12)$$

where the parameter A is related to B by

$$1 = - A \, cs \, B \, nd \, B \, , \qquad (8.2.13)$$

which means that A is negative, and λ, a and t are given by

$$\lambda = - \frac{4S}{c^2 A} (2E - K) \, , \qquad (8.2.14)$$

$$a = - \frac{2S\kappa}{c^2 A} \, nc \, B \, , \qquad (8.2.15)$$

$$t = - \frac{S}{c^2 A} [B - 2E(B) + 2 \, sn \, B \, dc \, B - 2\kappa(nc \, B - 1)] \qquad (8.2.16)$$

This solution is the finite-amplitude version of Taylor's antisymmetric sheet waves.

The phase speed c_p is given by

$$c_p = \frac{(4\kappa^2 - 1)K + 4(1 - 2\kappa^2)E}{3(2E - K)} \, c \qquad (8.2.17)$$

Both the phase speeds (8.2.10, 17) are derived by Hogan (1986) and show that, in general, $c_p \neq c$ so that c is not the phase speed of the waves. Hogan (1986) also shows that c is not equal to the second definition of phase speed given by Stokes (1847) for either the symmetric or antisymmetric waves.

Crapper's (1957) solution (case III of Kinnersley) is given, in this notation, by

$$\hat{x} = - \frac{S}{c^2 A} \left[\phi + \frac{2 \sin \phi}{\cosh \psi - \cos \phi} \right] \qquad (8.2.18)$$

$$z = - \frac{S}{c^2 A} \left[\psi - \frac{2 \sinh \psi}{\cosh \psi - \cos \phi} \right] \qquad (8.2.19)$$

where the parameter A is related to B by

$$1 = A \tanh B \ , \tag{8.2.20}$$

which means that A is positive, and λ and a are given by

$$\lambda = \frac{2\pi S}{c^2 A} = \frac{2\pi S}{c^2} \tanh B \ , \tag{8.2.21}$$

$$a = \frac{2S}{c^2 A} \operatorname{cosech} B = \frac{2S}{c^2} \operatorname{sech} B \ . \tag{8.2.22}$$

The parameter A is not identical to Crapper's parameter A described in § 4.2 but they are simply related. For this case the phase speed defined by Stokes (1847) first definition is equal to c.

Generally the parameters κ, B and c are interpreted as depth, amplitude and velocity (or frequency) parameters although other interpretations are possible as is revealed by limiting cases such as the linear-limit $\kappa \longrightarrow 0$. The parameter A can then be interpreted as a wavelength parameter. Note that the limit $\kappa \longrightarrow 0$ represents the infinitesimal amplitude limit of these solutions and the limit $B \longrightarrow 0$ represents capillary waves on a liquid sheet which is very thin. Also as $\kappa \longrightarrow 1$ the trough depth, or sheet minimum semi-thickness, $t \longrightarrow 0$.

Crapper's solution is obtained from both the symmetric and antisymmetric solutions by taking the limit $\kappa \longrightarrow 0$ after the transformation

$$\psi \longrightarrow \psi - K(\kappa') \ , \ z \longrightarrow \frac{S\beta}{c^2 \kappa'^2} [(1 + \kappa^2)K(\kappa') - 2E(\kappa') - z] \ . \tag{8.2.23}$$

which essentially shifts the position of the origin. This transformation takes Kinnersley's Ib and IIb solutions and transforms them to the Ia and IIa solutions respectively. The Ia and Ib, or IIa and IIb, solutions are exactly the same in a physical context but differ analytically in the directions of ϕ and ψ and, thus, in the labelling of streamlines. Also, this transformation does not effect the phase speeds of the waves and it is easily seen that both expressions (8.2.10, 17) for c_p tend to c in the limit $\kappa \longrightarrow 0$.

8.3 Highest Waves

Crapper (1957) shows that finite-amplitude capillary waves on liquid of infinite depth have maximum steepness when the free surface touches itself to enclose a bubble in the trough (see § 4.2 and figure 1.1). The qualitative characteristics of free surfaces of Kinnersley's waves and Crapper's waves are the same. It, therefore, follows that the criterion for the maximum steepness is given by requiring a vertical tangent at $\hat{x} = \frac{1}{2}\lambda$.

For the symmetric (case Ib) waves Hogan (1986) shows that the criterion is explicitly given by requiring

$$L^2 - 2(1 + \kappa^2) = 2L \text{ cn } \phi \text{ ds } \phi \qquad (8.3.1)$$

where
$$L(\phi) = 4E - 2E(\phi) + \kappa'^2\phi - 2\kappa'^2K \ . \qquad (8.3.2)$$

The criterion is solved by fixing κ and solving equation (8.3.1) for ϕ. The value of $B = B_{max}$ corresponding to the maximum steepness wave is then given from

$$\text{dn } B_{max} = \frac{\kappa(L \text{ cd } \phi + 2 \text{ sn } \phi)}{L + 2\kappa^2 \text{ sn } \phi \text{ cd } \phi} \ . \qquad (8.3.3)$$

Expressions (8.3.1 - 8.3.3) have been verified from first principles.

Similarly, for the antisymmetric (case IIb) waves, fix κ and solve for ϕ from

$$I^2 \text{ sn } \phi \text{ dn } \phi = 2(2 \text{ dn}^2\phi - 1)(I \text{ cn } \phi + \text{sn } \phi \text{ dn } \phi) \qquad (8.3.4)$$

where
$$I(\phi) = 4E - 2E(\phi) + \phi - 2K \qquad (8.3.5)$$

with the maximum value of $B = B_{max}$ then found from

$$\text{ds } B_{max} = \frac{\kappa(I \text{ cn } \phi + 2 \text{ sn } \phi \text{ dn } \phi)}{I} \ . \qquad (8.3.6)$$

If $B > B_{max}$ then the free surface of the waves intersects itself. This is interpreted as wave breaking, as it is for the infinite depth case, so that $B = B_{max}$ represents the breaking point of the waves. Note that the criterion for the highest waves is independent of the velocity variable c.

Also note that Hogan (1986) requires a vertical tangent at $\hat{x}_K = \frac{1}{2}\lambda$ for $\phi \neq 2K$ (which correspond to a wave trough). The condition $\phi \neq 2K$ is not required above simply because $\phi = 2K$ is not a possible solution. The position $\phi = 2K$ corresponds to a wave trough where a vertical tangent can not occur. In fact, there is a horizontal tangent at a trough. The requirement of $\hat{x}_K = \frac{1}{2}\lambda$ rather than $x_K = \frac{1}{2}\lambda$ clearly makes no difference to the exact form of the criterion. This has been analytically confirmed by the author.

Attention is focused on the symmetric (case Ib) waves. The equations (8.3.1) is solved numerically using a standard transcendental equation solver (NAG LIB C05PBF). The solver requires an initial guess for ϕ. It is found that the routine always converges to the solution when the initial value of ϕ is unity. Many other initial guesses will also always converge. The value of B_{max} is then found using the definition

$$dn^{-1}(\phi) = \int_{\phi}^{1} \frac{1}{(1 - t^2)(t^2 - \kappa'^2)}\, dt \qquad (8.3.7)$$

which is calculated using a standard integrating routine (NAG LIB D01AHF).

This method is employed for all κ with $0 \leq \kappa < 1$. For $\kappa = 1$ the complete elliptic integral of the first kind $K(\kappa) \longrightarrow \infty$ and a rather different approach has to be undertaken to find B_{max}. Kinnersley (1976) considers this limiting case in more detail and finds that $B_{max} = \pi/4$. This is, in fact, the limiting solution of (8.2.1, 3) as $\kappa \longrightarrow 1$. The variation of B_{max} with κ is shown in figure 8.1. It is seen that $B_{max} \longrightarrow \infty$ as $\kappa \longrightarrow 0$. Typical wave profiles for the symmetric (case Ib) waves are shown in figures 8.2, 3 and discussed in § 8.6. Typical wave profiles for the antisymmetric (case IIb) waves are given in Hogan (1986).

8.4 The Four "Basic" Mean Wave Properties

In § 2.5 expressions for all the mean properties of the wave motion are given in terms of four "basic" mean wave properties: the mean kinetic energy density, the mean potential energy density, the mean bottom velocity squared and the mean depth of the waves. In this section expressions for these four mean properties are found for the symmetric (case Ib) waves. Hogan (1979) performs the same calculations for Crapper's waves.

Substituting $\psi = + B$ into the solution (8.2.1, 2) gives the surface profile as

$$\hat{x} = \frac{s\beta}{c^2\kappa'^2}\left[2E(\phi) - \kappa'^2\phi - 2\kappa^2 \mathrm{sn}\ \phi\ \mathrm{cd}\ \phi + \frac{2\alpha\kappa'^2 \mathrm{sd}\ \phi\ \mathrm{nd}\ \phi}{1 - \alpha\ \mathrm{cd}\ \phi}\right] \qquad (8.4.1)$$

$$\eta = \frac{s\beta}{c^2\kappa'^2}\left[\epsilon + \frac{2\beta}{1 - \alpha\ \mathrm{cd}\ \phi}\right] \qquad (8.4.2)$$

where $$\alpha = \kappa\ \mathrm{nd}\ B\ ,\ \beta = \kappa'^2\ \mathrm{sn}\ B\ \mathrm{cd}\ B \qquad (8.4.3)$$

and $$\epsilon = (1 + \kappa^2)B - 2E(B)\ . \qquad (8.4.4)$$

Note that $$\beta = -\frac{1}{A}\ . \qquad (8.4.5)$$

Also let $$\theta = 2E - \kappa'^2 K\ . \qquad (8.4.6)$$

It is seen that the surface profile is a function of three parameters, namely κ, B and c. Therefore, expression for mean wave properties are sought in terms of these three parameters.

The integral definitions of the mean properties required are given in the σ-frame in which the waves move at their phase speed c_p. The surface profile in the σ-frame is given by the Galilean transformation

$$\hat{x} = x - c_p t \qquad (8.4.7)$$

where x is the horizontal axis in the σ-frame. The z-axis remains unchanged.

The calculation of these mean properties requires the evaluation of

$$\frac{dx}{d\phi} = \frac{d\hat{x}}{d\phi} \quad \text{and} \quad \frac{d\eta}{d\phi} \qquad (8.4.8)$$

so these are examined first. Detailed algebra is shown in appendix D. It

is found that

$$\frac{d\hat{x}}{d\phi} = \frac{s\beta}{c^2} \frac{1}{(1 - \alpha\ cd\ \phi)^2} [(1 + 2\kappa^2 sd^2\phi) - \alpha^2(cd^2\phi + 2sd^2\phi)] \qquad (8.4.9)$$

$$\frac{d\eta}{d\phi} = \frac{s\beta}{c^2} \frac{1}{(1 - \alpha\ cd\ \phi)^2} [-\ 2\alpha\beta\ sd\ \phi\ nd\ \phi] \ . \qquad (8.4.10)$$

Extensive use of Byrd and Friedman (1971) is made in deriving these expressions and the expressions below.

At this stage five integrals, for use in the expressions for the mean wave properties, are defined:

$$I_1(B,k) = \int_0^{4K} \frac{1}{1 - \alpha\ cd\ \phi}\, d\phi \ , \quad I_2(B,k) = \int_0^{4K} \frac{sd^2\phi}{(1 - \alpha\ cd\ \phi)^2}\, d\phi$$

$$I_3(B,k) = \int_0^{4k} \frac{(1 + 2\kappa^2 sd^2\phi) - \alpha^2(cd^2\phi + 2\ sd^2\phi)}{(1 - \alpha\ cd\ \phi)^3}\, d\phi$$

$$I_4(B,k) = \int_0^{4k} \frac{1}{dn^4\phi(1 + \kappa\ cd\ \phi)^4} \frac{(1 + 2\kappa^2 sd^2\phi) - \alpha^2(cd^2\phi + 2\ sd^2\phi)}{(1 - \alpha\ cd\ \phi)^2}\, d\phi$$

$$I_5(B,k) = \int_0^{4k} \frac{1}{dn^2\phi(1 + \kappa\ cd\ \phi)^2} \frac{(1 + 2\kappa^2 sd^2\phi) - \alpha^2(cd^2\phi + 2\ sd^2\phi)}{(1 - \alpha\ cd\ \phi)^2}\, d\phi$$

Note that the only dependence on B in these integrals is through α. Also, all the integrals defined for this and proceeding work are all functions of the surface parameter B and the modulus κ only; there is no dependence on the velocity variable c.

a. The Mean Level b

The mean level b is given by

$$\bar{\eta} = b = \frac{1}{\lambda} \int_0^{\lambda} \eta\ dx \qquad (8.4.11)$$

which, on substitution of expression (8.4.2) for η, gives

$$b = \frac{s\beta}{c^2\kappa'^2} \left[\epsilon + \frac{2\beta}{\lambda} \int_0^{4K} \frac{1}{1 - \alpha\ cd\ \phi} \frac{dx}{d\phi}\, d\phi\right] \qquad (8.4.12)$$

so, using expression (8.2.5) for λ and expression (8.4.9), it follows that

$$b = \frac{s\beta}{2c^2\kappa'^2\theta} (2\theta\epsilon + \kappa'^2\beta I_3) \ . \qquad (8.4.13)$$

Therefore, b is a function of κ, B and c.

The bed has $\psi = 0$ and so $z = 0$. Therefore, in the notation introduced in chapter 2 depth $h = 0$ and mean depth $d = b$. However, if the origin is transformed, in the z direction, so that depth $h \neq 0$ then expression (8.4.13) would not give the mean level b but would only give the mean depth d.

b. The Mean Kinetic Energy Density T

Longuet-Higgins (1975) takes the expression (A11) for the mean kinetic energy density T and shows that

$$T = \frac{\rho c_p}{2\lambda} \int \eta \, d\Phi \qquad (8.4.14)$$

where Φ is the velocity potential of the wave motion in the σ-frame and the integral limits range over one period of Φ. Now, the velocity potential ϕ is a dimensionless quantity derived from a dimensional velocity potential $\hat{\Phi}_K$ in Kinnersley (1976). The relation between $\hat{\Phi}_K$ and ϕ is, from Kinnersley (1976),

$$\hat{\Phi}_K = \frac{S}{CA} \phi = - \frac{S\beta}{C} \phi \qquad (8.4.15)$$

using formula (8.4.5) for A. Also, since $\hat{\Phi}_K$ is the velocity potential in the frame fixed to the waves (regardless of the orientation of the axes, i.e. $\hat{\Phi}_K = \hat{\Phi}$), the relation between $d\hat{\Phi}_K$ and $d\Phi$ is

$$d\hat{\Phi}_K = d\Phi - c_p \, dx \qquad (8.4.16)$$

which is found using the relation (8.4.7) between $\hat{x}$ and x.

Substitution of expressions (8.4.15, 16) into expression (8.4.14) gives

$$T = \frac{\rho c_p}{2\lambda} \left[- \frac{S\beta}{C} \int_0^{4K} \eta \, d\phi + c_p \int_0^{\lambda} \eta \, dx \right] . \qquad (8.4.17)$$

The first of the two integrals give

$$\int_0^{4K} \eta \, d\phi = \frac{S\beta}{C^2 \kappa'^2} \int_0^{4K} \left[\epsilon + \frac{2\beta}{1 - \alpha \, \mathrm{cd} \, \phi} \right] d\phi \qquad (8.4.18)$$

so

$$\int_0^{4K} \eta \, d\phi = \frac{S\beta}{C^2 \kappa'^2} (4K\epsilon + 2\beta I_1) . \qquad (8.4.19)$$

The second of the two integrals is related to the mean level of the liquid and so, from expressions (8.4.11, 13), gives

$$\int_0^\lambda \eta \, dx = \frac{2s^2\beta^2}{c^4\kappa'^4} (2\theta\epsilon + \kappa'^2\beta I_3) \qquad (8.4.20)$$

It follows that

$$T = \frac{\tau\kappa'^2 K\beta^2}{4\theta^3} (\kappa'^2 K I_3 - \theta I_1) \; . \qquad (8.4.21)$$

Therefore, T is a function of κ and B only; no dependence on c.

c. The Mean Potential Energy Density V

The mean potential energy density V is given, from definition (A13), by

$$V = \frac{\tau}{\lambda} \int_0^\lambda \left\{ \left[1 + \left[\frac{d\eta}{dx} \right]^2 \right]^{\frac{1}{2}} - 1 \right\} dx \qquad (8.4.22)$$

so

$$V = \frac{\tau}{\lambda} \int_0^{4K} \left\{ \left[\left[\frac{d\hat{x}}{d\phi} \right]^2 + \left[\frac{d\eta}{d\phi} \right]^2 \right]^{\frac{1}{2}} - \frac{d\hat{x}}{d\phi} \right\} d\phi \; . \qquad (8.4.23)$$

Note that the positive square root must be taken in these expressions for V simply because a negative square root would imply a non-zero potential energy density contribution of -2τ in the presence of no waves, i.e. $\eta = 0$.

It is shown in appendix D that

$$\left[\left[\frac{d\hat{x}}{d\phi} \right]^2 + \left[\frac{d\eta}{d\phi} \right]^2 \right]^{\frac{1}{2}} = \frac{s\beta}{c^2} \frac{(1 - \alpha^2 cd^2\phi)}{(1 - \alpha \, cd \, \phi)^2} \; . \qquad (8.4.24)$$

It follows, from expressions (8.4.9, 24), that

$$\left[\left[\frac{d\hat{x}}{d\phi} \right]^2 + \left[\frac{d\eta}{d\phi} \right]^2 \right]^{\frac{1}{2}} - \frac{d\hat{x}}{d\phi} = \frac{s\beta}{c^2} \frac{2(\alpha^2 - \kappa^2) sd^2\phi}{(1 - \alpha \, cd \, \phi)^2} \qquad (8.4.25)$$

So, using expression (8.2.5) for λ and expression (8.4.22) for V,

$$V = \frac{\tau\kappa'^2}{2\theta} (\alpha^2 - \kappa^2) I_2 \qquad (8.4.26)$$

Note that V is is function of κ and B only as is T.

d. The Mean Bottom Velocity Squared $\overline{u_h^2}$

The horizontal component u of the velocity of the liquid particles in the σ-frame is given using the equation

$$\hat{u}_K = - \hat{u} = - u + c_p \qquad (8.4.27)$$

derived using $\hat{x}_K = - \hat{x}$ and the relation (8.4.7) between $\hat{x}$ and x. This gives

$$\overline{u_h^2} = c_p^2 + \frac{1}{\lambda} \int_o^{4K} (\hat{u}_K^2 - 2c_p \hat{u}_K)_h \frac{d\hat{x}}{d\phi} \, d\phi \ . \qquad (8.4.28)$$

The velocity component $\hat{u}_K$ is found using equation (27) in Kinnersley (1976). Note that this equation is given incorrectly by a negative sign. The corrected equation gives

$$\hat{u}_K = \frac{\kappa'^2 (cd^2\psi - \kappa^2 sd^2\psi \, sn^2\phi)}{(dn \, \phi + \kappa \, nd \, \psi \, cn \, \phi)^2} \, c. \qquad (8.4.29)$$

On the bed $\psi = 0$ so that $sn \, \psi = 0$ and $cn \, \psi = dn \, \psi = 1$. Therefore,

$$\hat{u}_{Kh} = \frac{\kappa'^2}{(dn \, \phi + \kappa \, cn \, \phi)^2} \, c \qquad (8.4.30)$$

so, using expressions (8.2,5, 10) for λ and c_p and also expressions (8.4.9, 28, 30), it follows that

$$\overline{u_h^2} = \left[\frac{\kappa'^4 K^2}{\theta^2} + \frac{\kappa'^6}{4\theta^2} (\theta I_4 - 2K I_5) \right] c^2 \ . \qquad (8.4.31)$$

Note that this is a function of B because the integrals I_4 and I_5 are function of B. This is due, mathematically, from the change of variables of the integrals, as prescribed in expression (8.4.28), from x to ϕ. Physically, it is expected that the mean bottom velocity squared will be a function of wavelength and since wavelength is a function of B this feature of dependence on B follows. This is also to be expected since waves of different amplitudes and depths would have different values of the mean bottom velocity squared. It is seen from expression (8.4.34) that the mean bottom velocity squared is a function of all three variables κ, B and c.

It is, therefore, seen that expressions for the mean properties of the wave motion are expressed generally in terms of κ, B and c except for certain special cases where the variables κ and B are enough.

However, all the expressions involve one or more of the integrals I_1 - I_5. These definite integrals can be worked out in terms of complete elliptic integrals of the first, second and third kind. For instance, the simplest of the integrals I_1 is given by

$$I_1 = \int_0^{4K} \frac{1}{1 - \alpha\ \mathrm{cd}\ \phi}\, d\phi = \int_0^{4K} \frac{\mathrm{dn}\ \phi(\mathrm{dn}\ \phi + \alpha\ \mathrm{cn}\ \phi)}{\mathrm{dn}^2\phi - \alpha^2\mathrm{cn}^2\phi}\, d\phi \qquad (8.4.32)$$

so
$$I_1 = \frac{1}{1 - \alpha^2}\left[\int_0^{4K} \frac{\mathrm{dn}^2\phi}{1 - \alpha_1^2\mathrm{sn}^2\phi}\, d\phi + \alpha \int_0^{4K} \frac{\mathrm{cn}\ \phi\ \mathrm{dn}\ \phi}{1 - \alpha_1^2\mathrm{sn}^2\phi}\, d\phi \right. \qquad (8.4.33)$$

where
$$\alpha_1^2 = \frac{\kappa^2 - \alpha^2}{1 - \alpha^2}\ . \qquad (8.4.34)$$

The first of the two integrals in expression (8.4.32) is given by formula (339.01) in Byrd and Friedman (1971). The second of the two integrals is zero because $\mathrm{cn}(\phi + 2K) = -\ \mathrm{cn}(\phi)$. It follows that

$$I_1 = \frac{1}{\kappa^2 - \alpha^2}\left[4\kappa^2 K - \frac{\kappa'^2\alpha^2}{1 - \alpha^2}\,\Pi(4K, \alpha_1^2)\right] \qquad (8.4.35)$$

where $\Pi(\phi, \alpha_1^2)$ is the incomplete elliptic integral of the third kind. Again the modulus κ is omitted from notation for the elliptic integral.

Now
$$\Pi(4K, \alpha_1^2) = \int_0^{4K} \frac{du}{1 - \alpha_1^2\mathrm{sn}^2 u} = 2\Pi(\alpha_1^2) + 2\int_0^{K} \frac{du}{1 - \alpha_1^2\mathrm{cd}^2 u} \qquad (8.4.36)$$

where $\Pi(\alpha^2)$ is the complete elliptic integral of the third kind. Since the second of the integrals in expression (8.4.33) is zero it is seen, from expression (8.4.32), that the integral in expression (8.4.36) is the same as I_1 but with limits 0 and K rather than 0 and 4K and with α replaced by α_1. It follows that

$$\Pi(4K, \alpha_1^2) = 2\Pi(\alpha_1^2) + \frac{2}{\kappa^2 - \alpha_1^2}\left[\kappa^2 K - \frac{\kappa'^2\alpha_1^2}{1 - \alpha_1^2}\,\Pi(K, \alpha_2^2)\right] \qquad (8.4.37)$$

where
$$\alpha_2^2 = \frac{\kappa^2 - \alpha^2}{1 - \alpha_1^2}\ . \qquad (8.4.38)$$

So
$$I_1 = \frac{2}{\kappa^2 - \alpha^2}\left[\left[2 - \frac{\kappa'^2\alpha^2}{(1 - \alpha^2)(\kappa^2 - \alpha_1^2)}\right]\kappa^2 K \right.$$
$$\left. - \frac{\kappa'^2\alpha^2}{1 - \alpha^2}\left[\Pi(\alpha_1^2) - \frac{\kappa'^2\alpha_1^2}{1 - \alpha_1^2}\,\Pi(K, \alpha_2^2)\right]\right]\ . \qquad (8.4.39)$$

Similar expressions can be derived of I_2 - I_5. The expression for I_2 is simpler in form than (8.4.39) whereas those for I_3 - I_5 are more complex. Substitution of these expressions into those derived above for mean wave properties would lead to long expressions in terms of various elliptic functions and integrals. The evaluation of any elliptic functions or integrals requires the formation of complex numerical routines. Such routines are prone to many errors. It proves simpler and, in some ways, more efficient to evaluate the integrals I_1 - I_5 themselves using using a standard integrating routine (NAG LIB D01AHF).

The algebra in this section involves complicated expressions and formulae for elliptic functions and so is prone to many possible errors. The simplest method of checking the general expressions for the mean wave properties and, thus, the algebraic manipulations used is to show that the linear-limit of the expressions gives the correct results. This is shown to be the case in appendix E.

8.5. Variations of Mean Wave Properties

The variations of mean wave properties are given in units with density ρ and surface tension τ taking unit value and the length λ of the waves equal to 2π. Such units are chosen for comparison with the results of Hogan (1979, 1980, 1981). The variation of all the mean properties considered by Hogan are given. For example, the variation of (c_p^2/c_o^2) is given where $c_o^2 = \tanh B$ is the linear phase velocity. The specification of the velocity parameter c, in terms of κ and B, is given from the expression (8.2.5) for $\lambda = 2\pi$ as

$$c^2 = \frac{2\beta}{\pi\kappa'^2} (2E - \kappa'^2 K) . \qquad (8.5.1)$$

Expressions for all the mean wave properties of the wave motion are given in § 2.5. It is seen that since wavenumber k = 1 in these units

$$\bar{I} = \frac{2Tk}{\sigma} = \frac{2T}{\sigma} = \lambda . \qquad (8.5.2)$$

In § 8.3 the domain for the variables κ and B is found. It is shown explicitly in figure 8.1. It is most logical to show the variation of mean wave properties along sections through this domain. Four general sections are considered. These are $\kappa = 0.25$, 0.75 with $0 \leq B \leq B_{max}$, $B = 0.7$ with $0 < \kappa < 1$ and $B = 2.0$ with $0 < \kappa < \kappa_{max}$. The evaluations of the elliptic functions $sn(\phi,\kappa)$, $cn(\phi,\kappa)$ and $dn(\phi,\kappa)$ and the elliptic

integrals $K(\kappa)$, $E(\kappa)$ and $E(\phi,\kappa)$ are carried out using rigorously tested routines supplied by Prof. P. Drazin of Bristol University, England.

The profiles of waves along these sections are shown in figure 8.2, 3 respectively. For the sections κ = 0.25, 0.75 and B = 2.0 capillary waves reach their maximum steepness where they enclose. a bubble of air in troughs. However, for the section B = 0.7 capillary waves never reach the maximum steepness "enclosed bubble" shape. This is simply because $B_{max} \geq \pi/4$ for all values of κ. In this case the capillary waves become singular when κ = 1 and the bed is touched by wave troughs.

Variations of mean wave properties are shown in figures 8.4 - 8.7 for the four sections. It is seen that as $B \longrightarrow 0$ all mean wave parameters shown, except (c_p^2/c_o^2), also tend to zero. Marked differences in variations are shown for the cases κ = 0.75 (figure 8.5) and B = 0.7 (figures 8.6). Many mean wave properties have local maxima which is not the case for infinite depth Crapper waves. Also, it is possible for the radiation stress component S_{zz} to take positive values. This differs from the infinite depth Crapper waves.

From the classical theory of infinitesimal water waves (see any basic text on the subject) it is known that waves in general are uninfluenced by the presence of a bed when $kd > \pi$. Here k = 1 so kd = d = b. However, it is possible for trough depth t to be "small" even when the mean depth d is "large". For example, the maximum wave for κ = 0.75 (figures 8.2, 5) and the wave touching the bed for B = 0.7 (figure 8.3, 6) have "large" mean depth d but "small" trough depth t. Under such circumstances the bed would be expected to have an influence on the waves. Moreover, for infinitesimal waves (see appendix E) d = t. Thus, it seems more appropriate to take the condition $kt = t < \pi$ as a criterion for waves influenced by the bed. If thin film flows are of interest then the criterion would be kt < 0.3, say, or more generally kt "small".

From § 8.2 it is seen that expressions for wave steepness ak and the parameter kt are independent of the parameter c. This allows for calculation of the variations of ak or kt with either κ or B as given by the highest waves (κ,B)-curve. The variations of ak and kt with κ are also shown in figure 8.1. Now, for fixed κ (B) steepness ak always increases as B (κ) increases. Thus, the variation of ak shown in figure 8.1 gives the maximum steepness. Also, for fixed κ (B) parameter kt increases (decreases) as B (κ) increases. Thus, the variation of kt shown in figure 8.1 gives its maximum possible value. Note that if the variation of kt with B, as given by the highest wave

curve, is considered then the curve given would represent the minimum value of kt.

It is, thus, seen from figure 8.1 that $kt < \pi$ if either $\kappa > 0.02$ or $B < 4.5$. These give bounds for waves whose motion is generally influenced by the bed. A "small" subcatogory of this range comes under thin film flows. It is seen that $kt < 0.3$ if either $\kappa > 0.45$ or $B < 1.45$.

CAPTIONS FOR FIGURES

Figure 8.1: The variation of B_{max} with κ for the Kinnersley's symmetric waves.

Figure 8.2: Wave profiles for Kinnersley's symmetric waves with (a) $\kappa = 0.25$ and (b) $\kappa = 0.75$ where B ranges from zero to B_{max}.

Figure 8.3: Wave profiles for Kinnersley's symmetric waves with (a) $B = 0.07$ and (b) $B = 2.0$ where κ ranges from zero to κ_{max} ($\kappa_{max} = 1$ for $B = 0.07$).

Figure 8.4: The variation of mean wave properties with steepness ak for $\kappa = 0.25$ (B varies); units with $\rho = \tau = 1$ and $\lambda = 2\pi$ are used.

Figure 8.5: The variation of mean wave properties with steepness ak for $\kappa = 0.75$ (B varies); units with $\rho = \tau = 1$ and $\lambda = 2\pi$ are used.

Figure 8.6: The variation of mean wave properties with steepness ak for $B = 0.07$ (κ varies); units with $\rho = \tau = 1$ and $\lambda = 2\pi$ are used.

Figure 8.7: The variation of mean wave properties with steepness ak for $B = 2.0$ (κ varies); units with $\rho = \tau = 1$ and $\lambda = 2\pi$ are used.

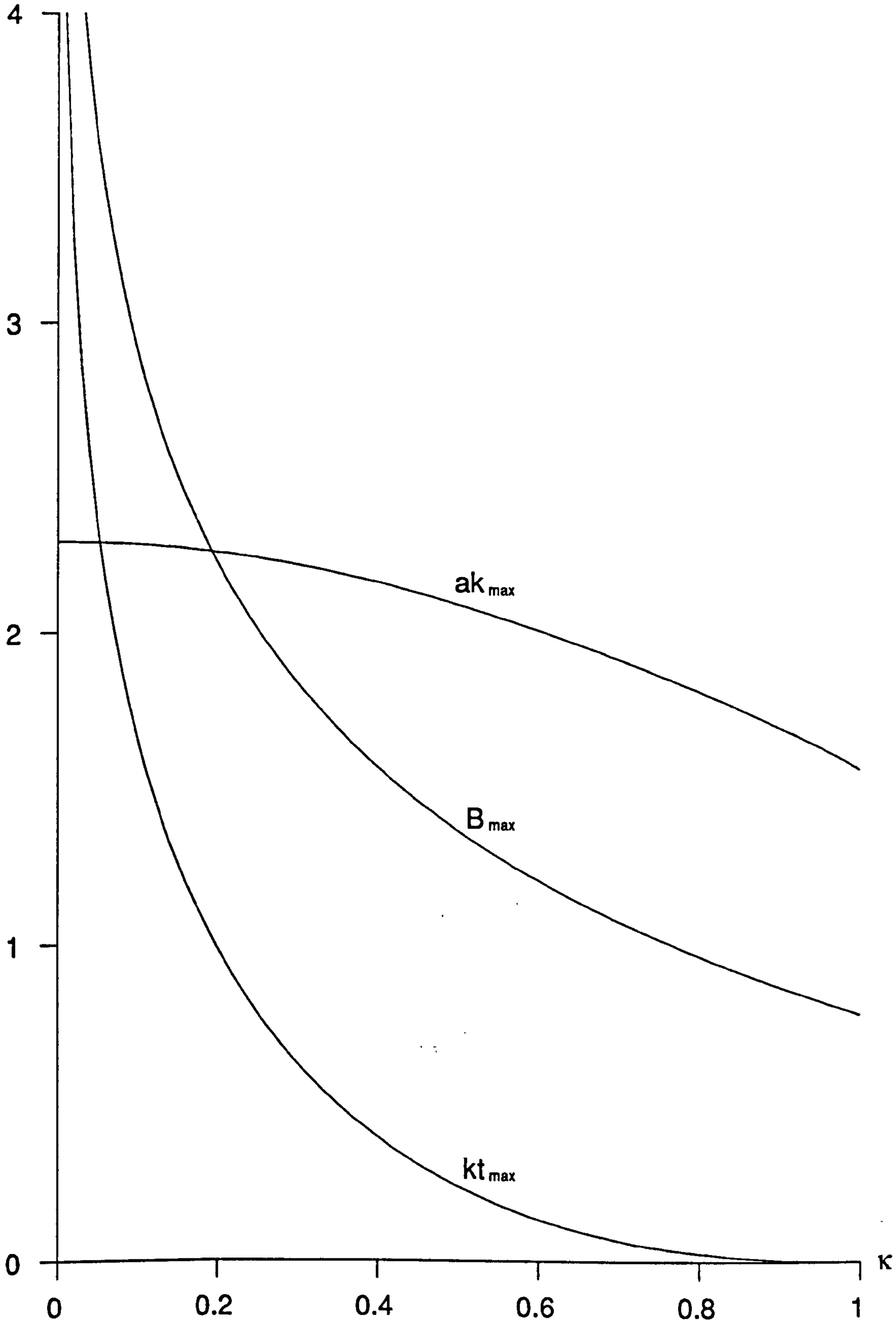

Figure 8.1

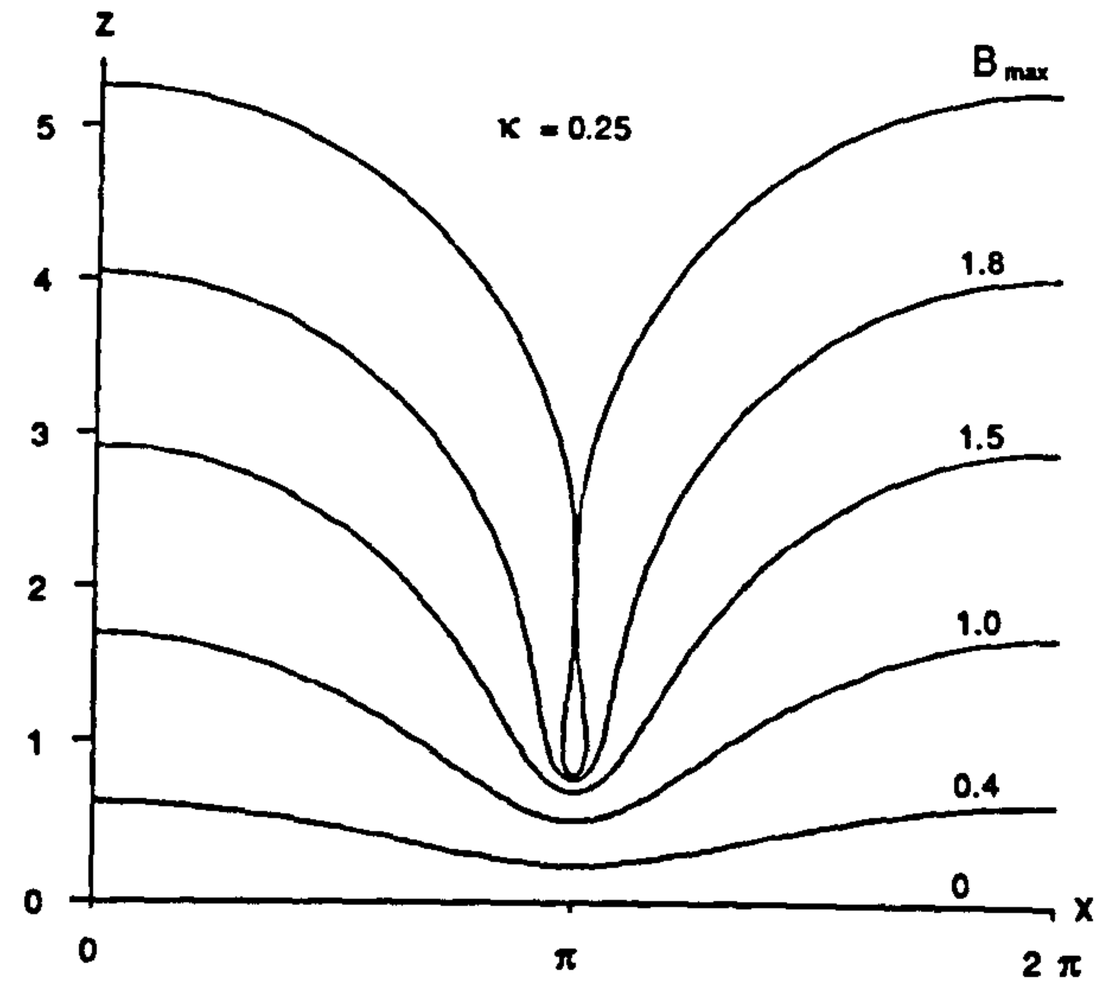

Figure 8.2a

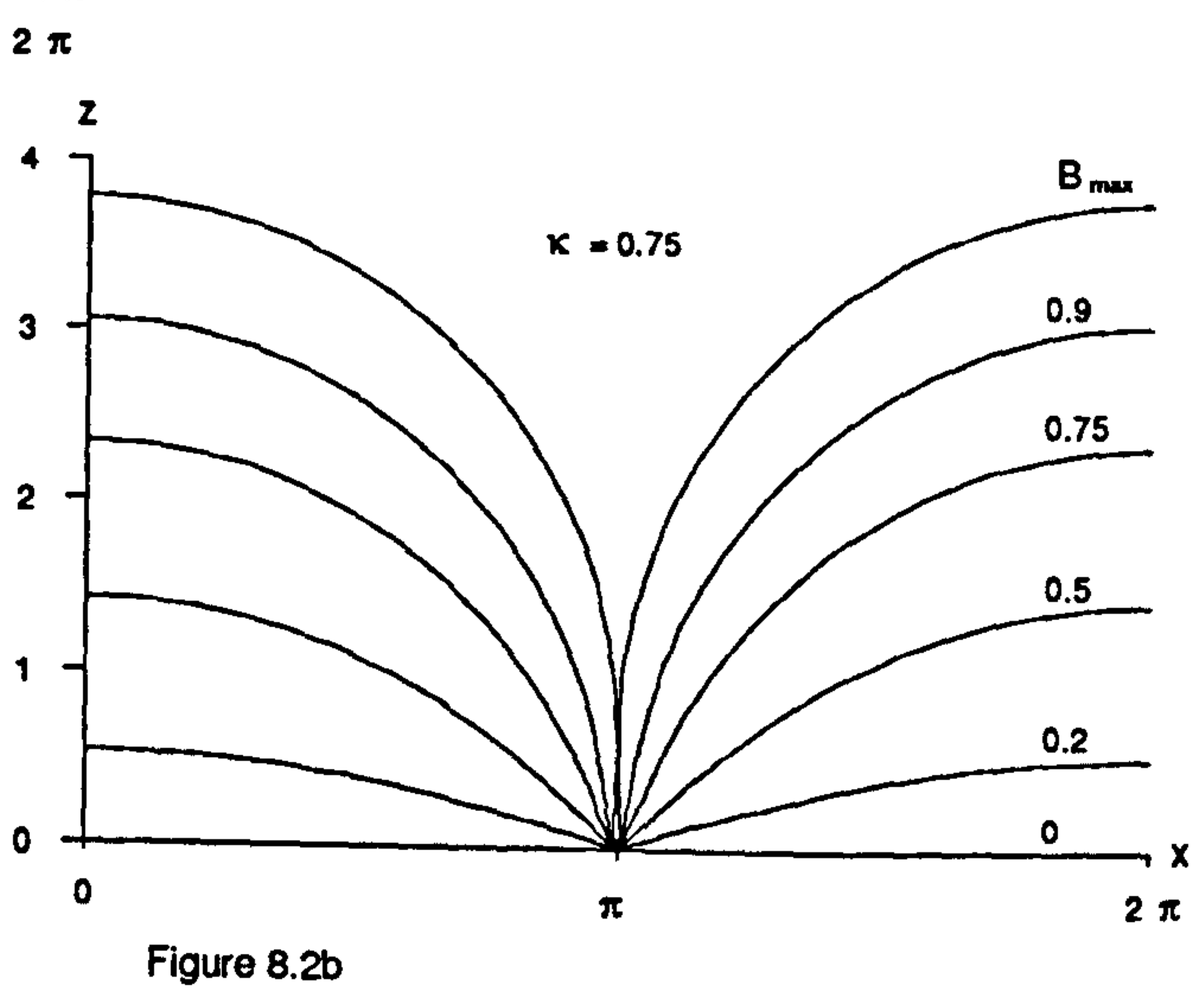

Figure 8.2b

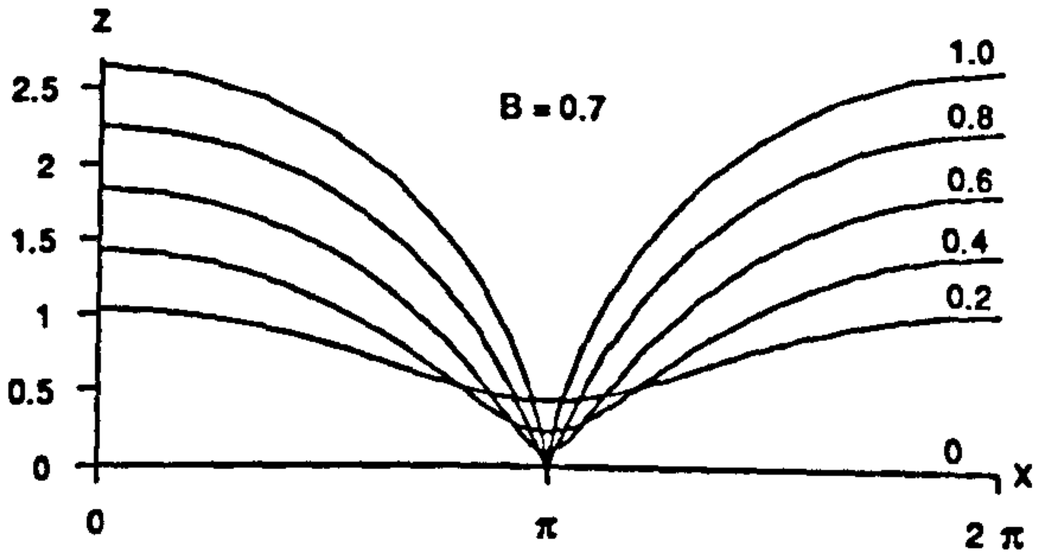

Figure 8.3a

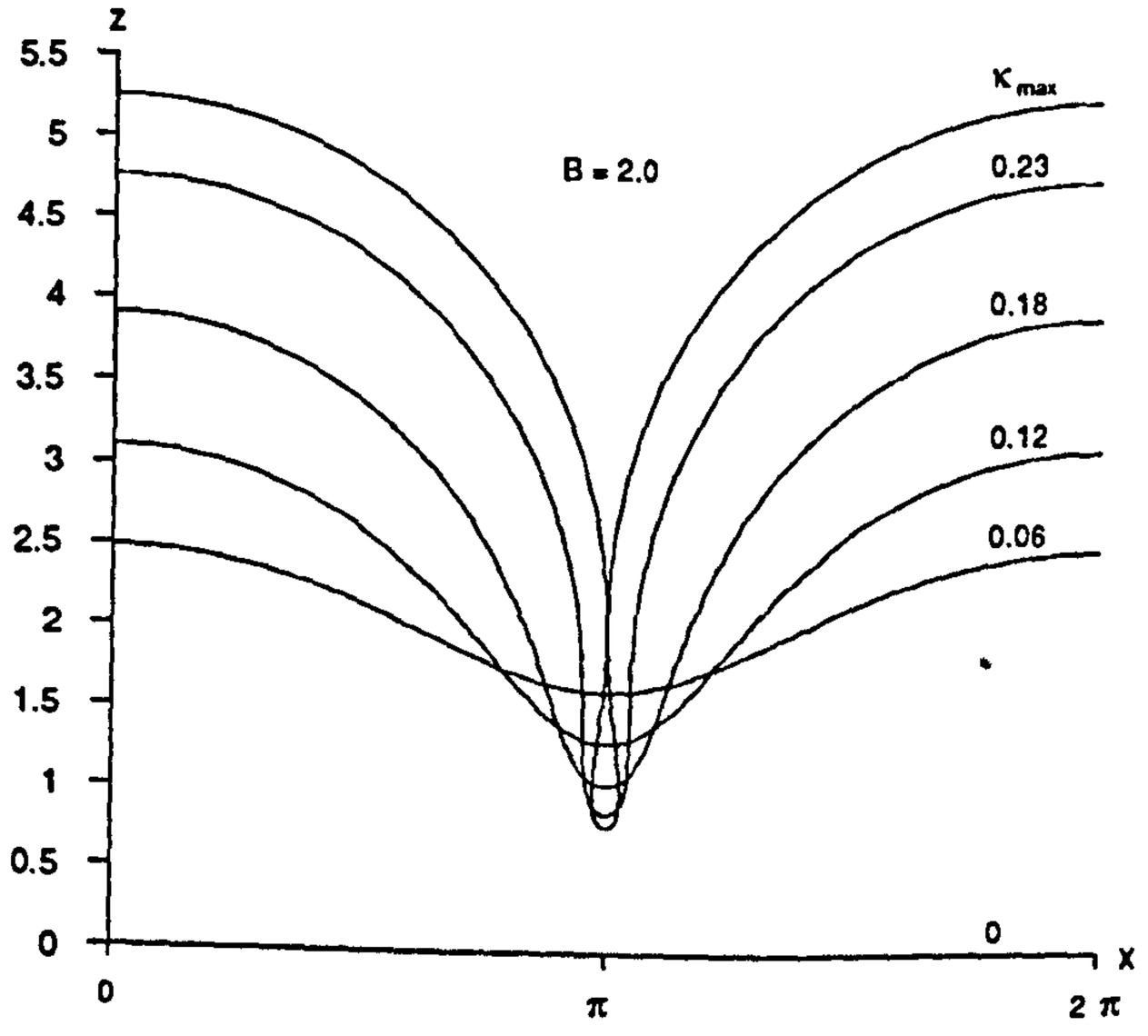

Figure 8.3b

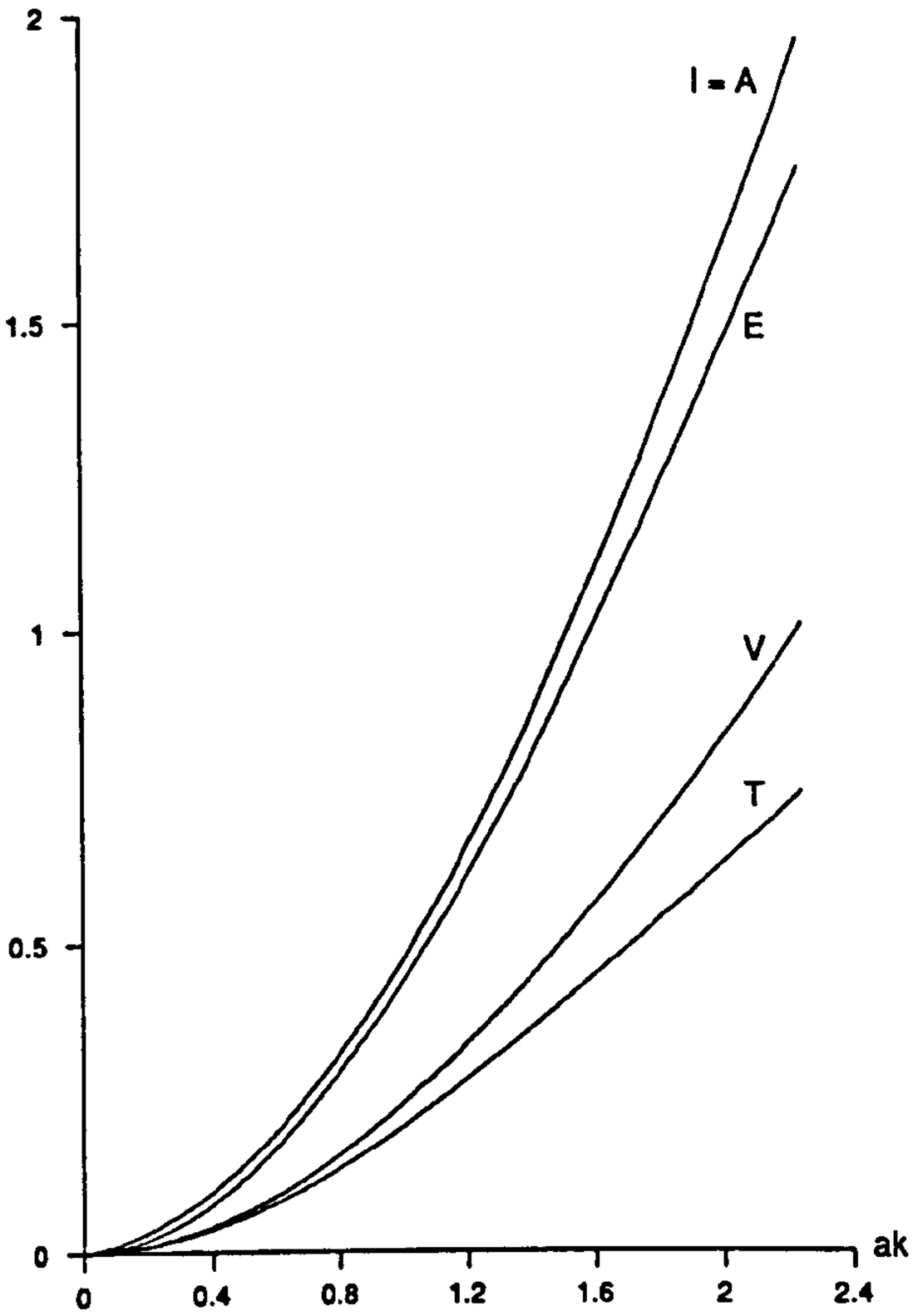

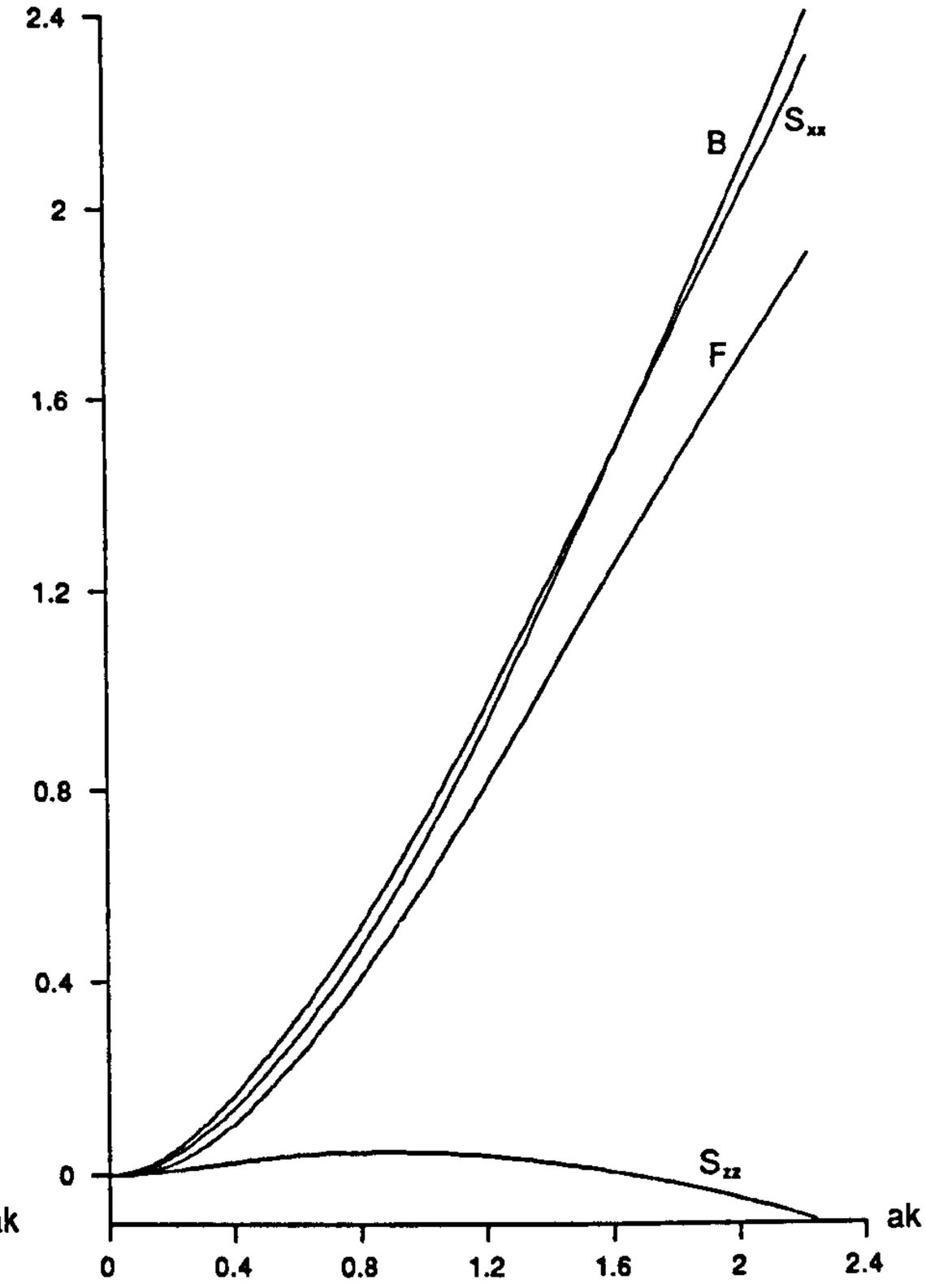

Figures 8.4

$\kappa = 0.25$

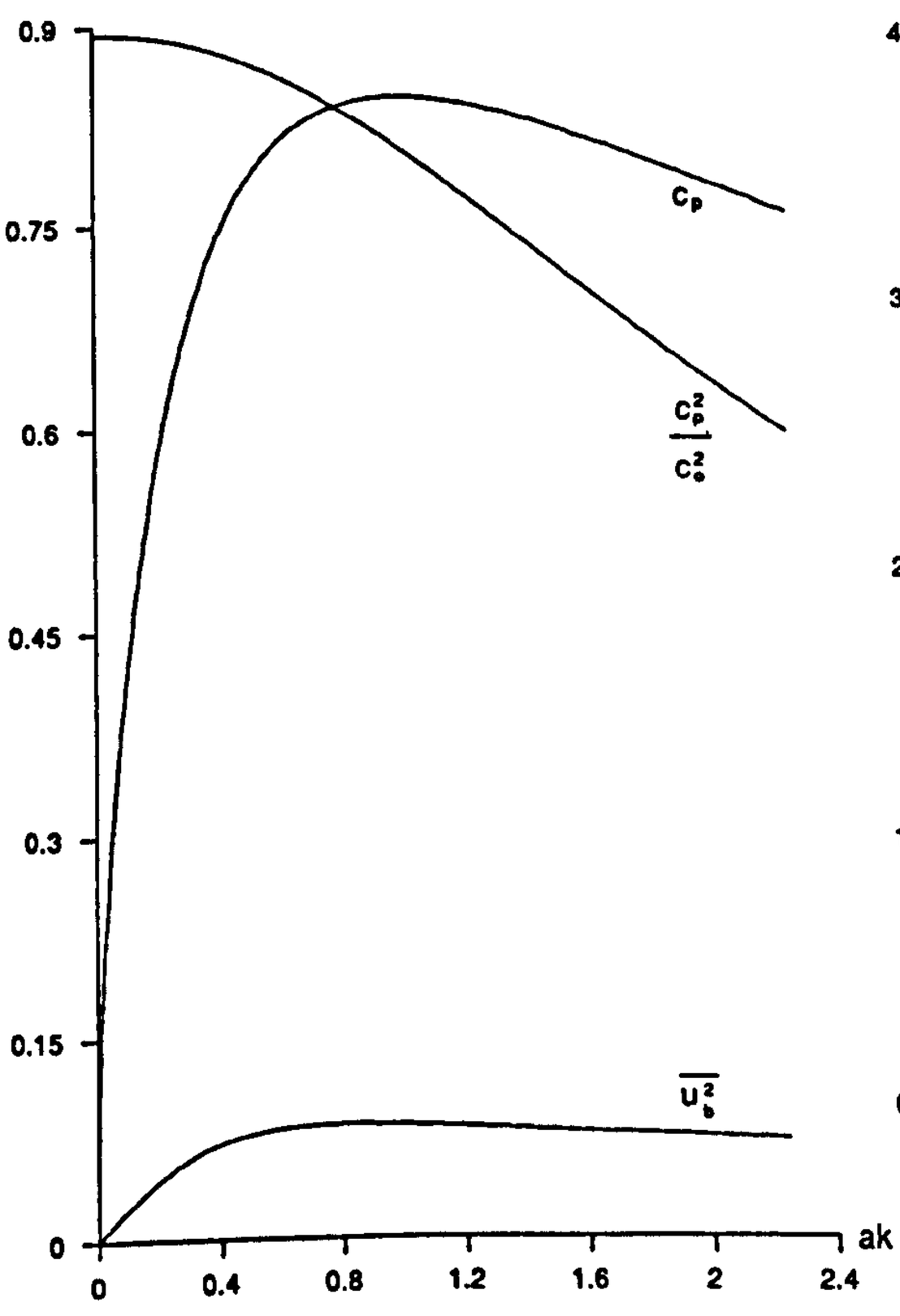

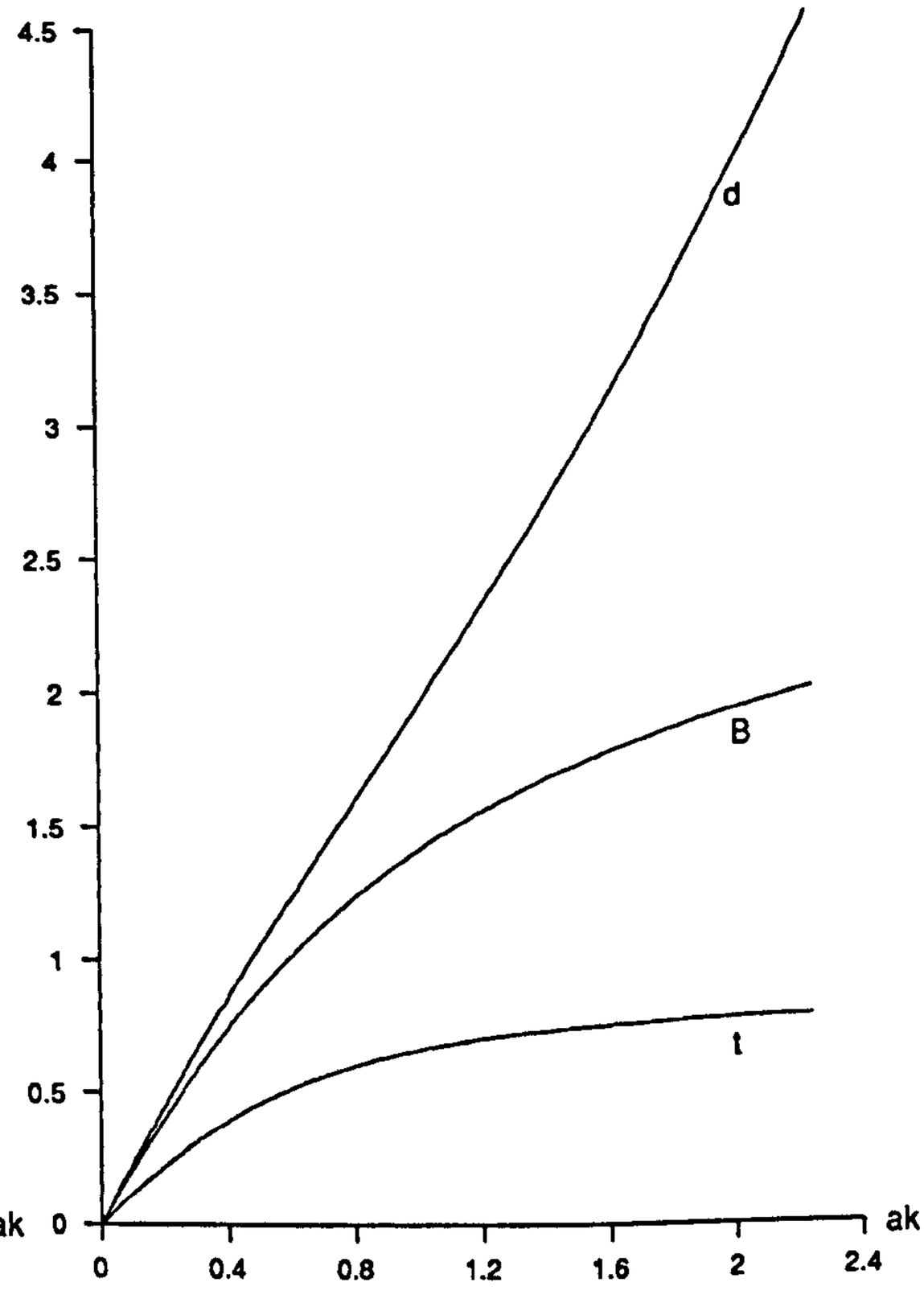

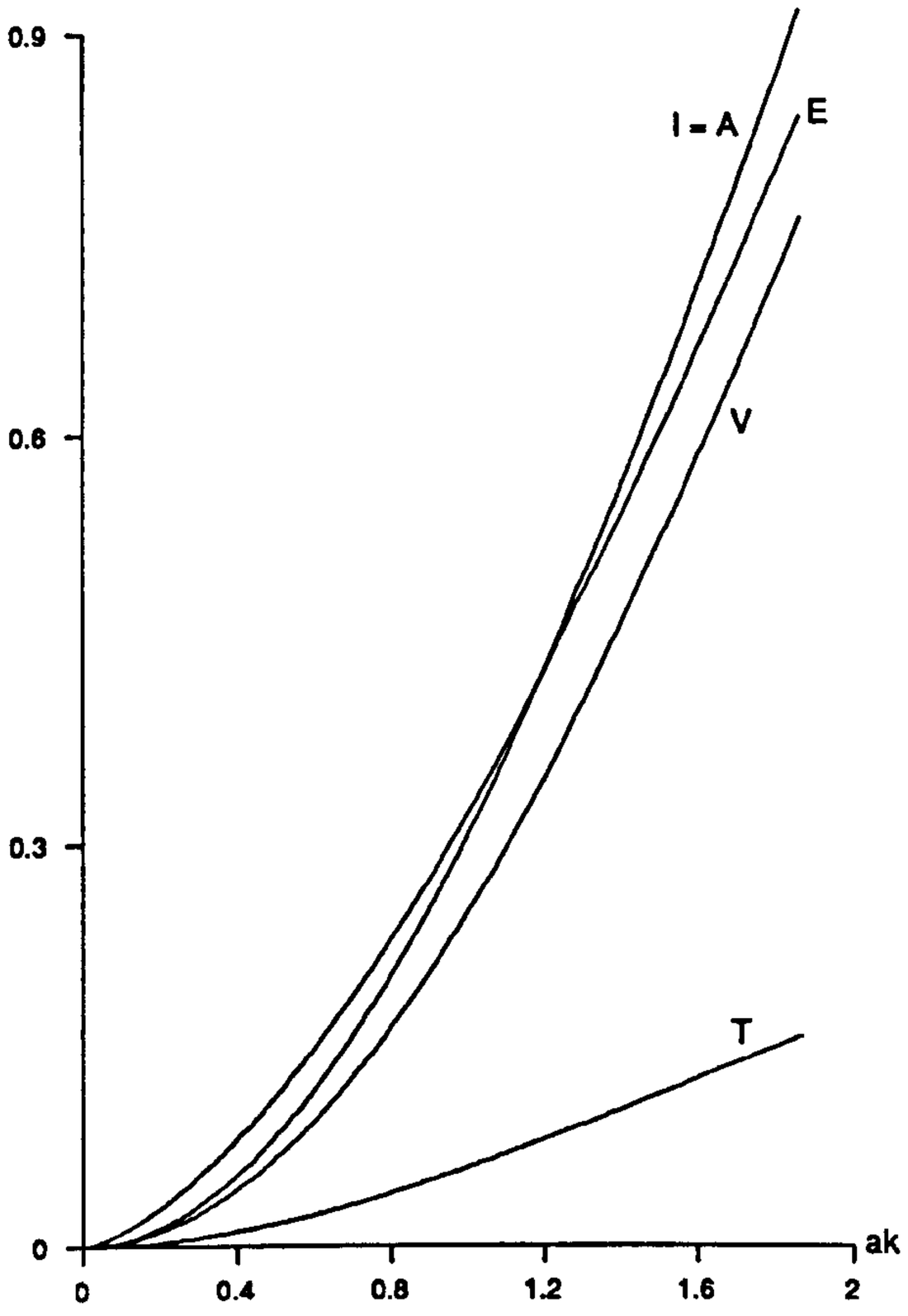

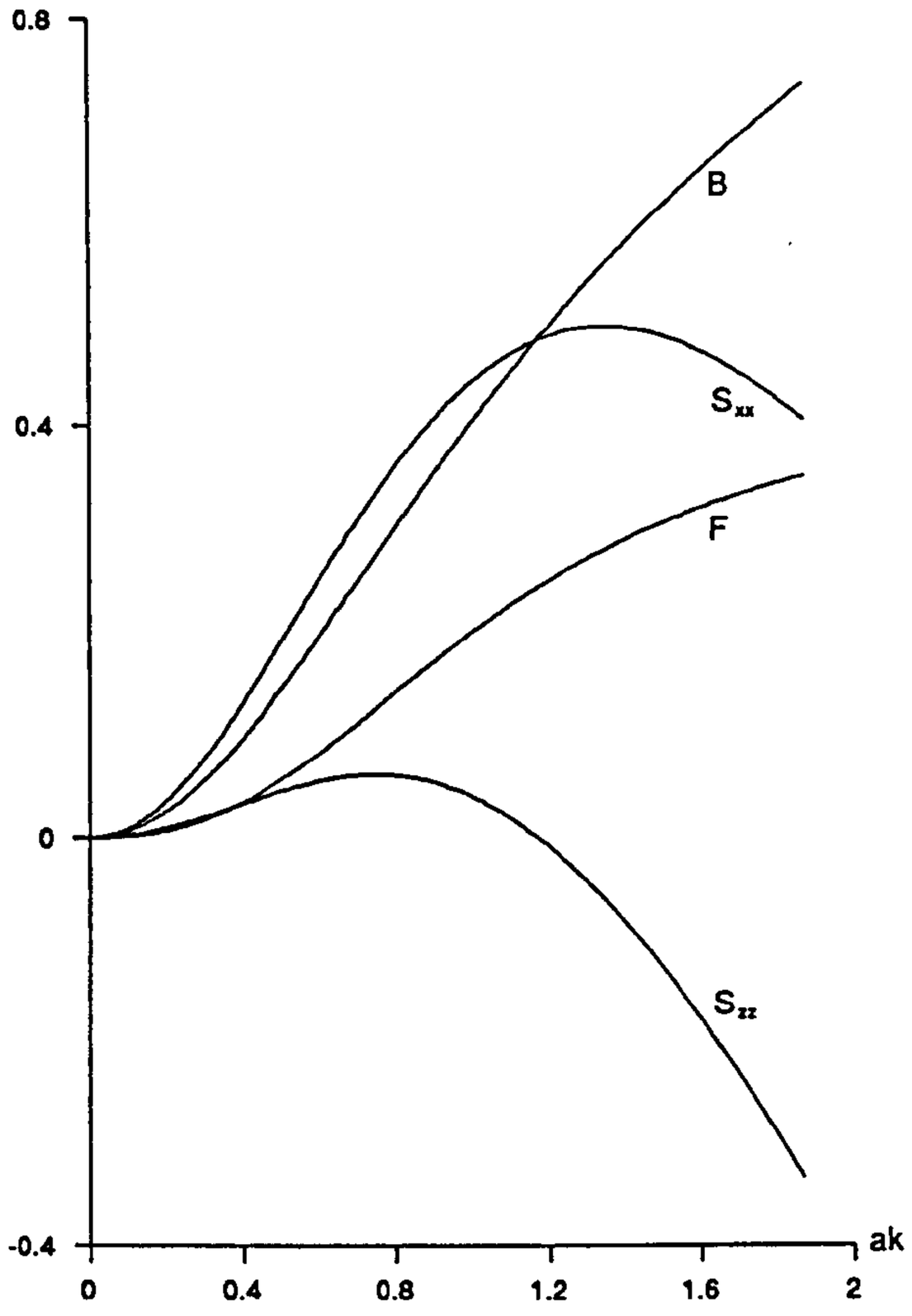

Figures 8.5

$\kappa = 0.75$

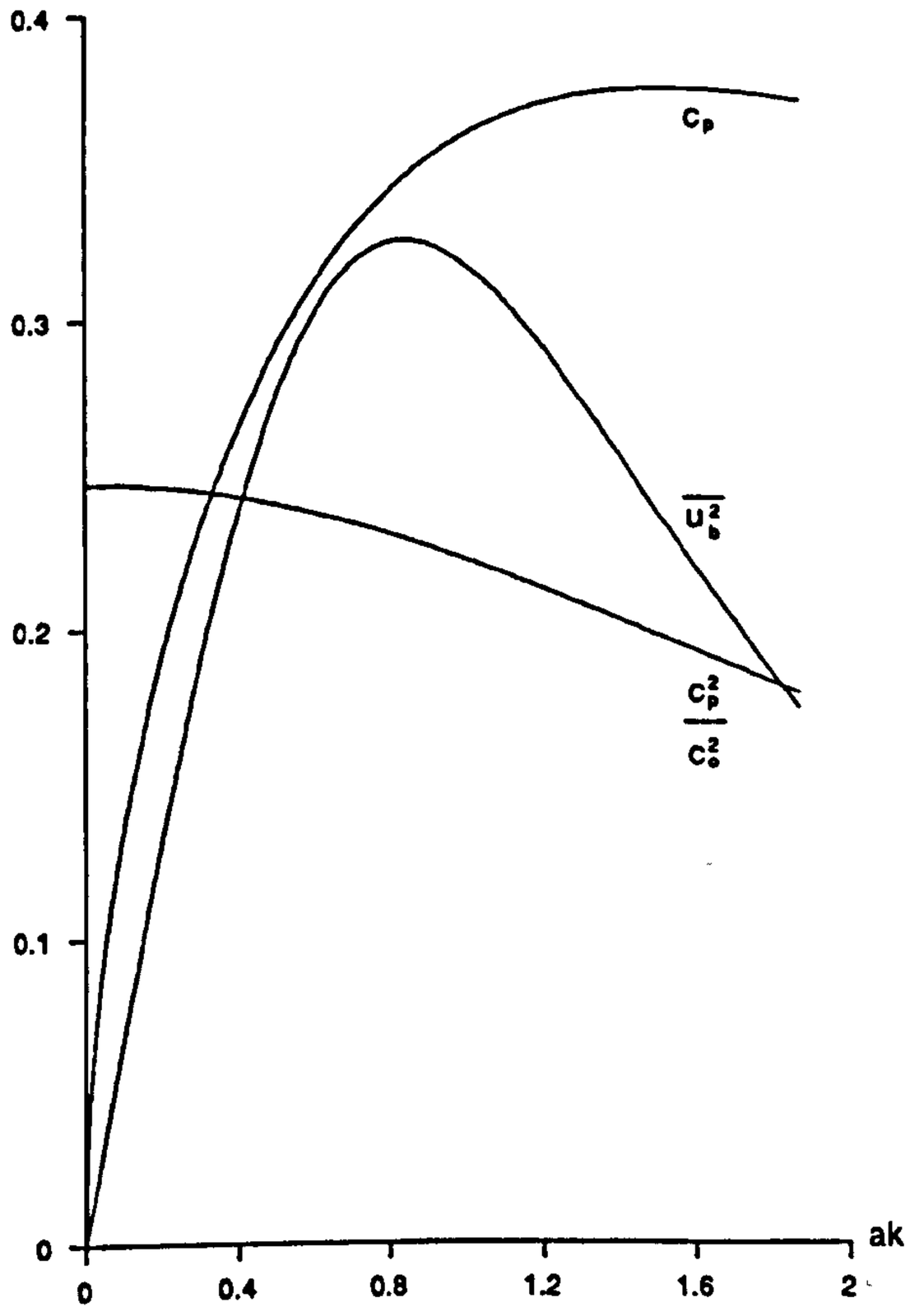

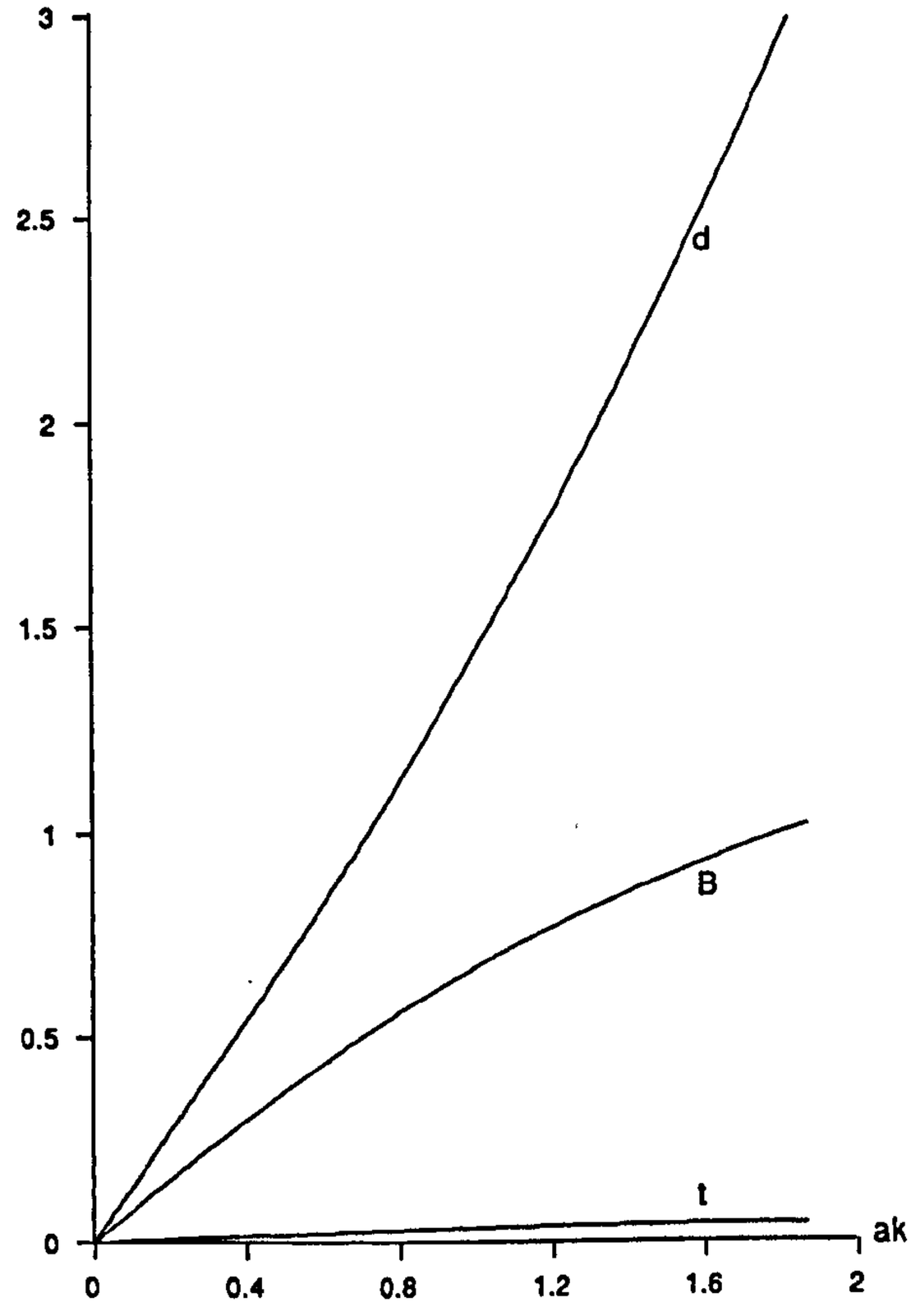

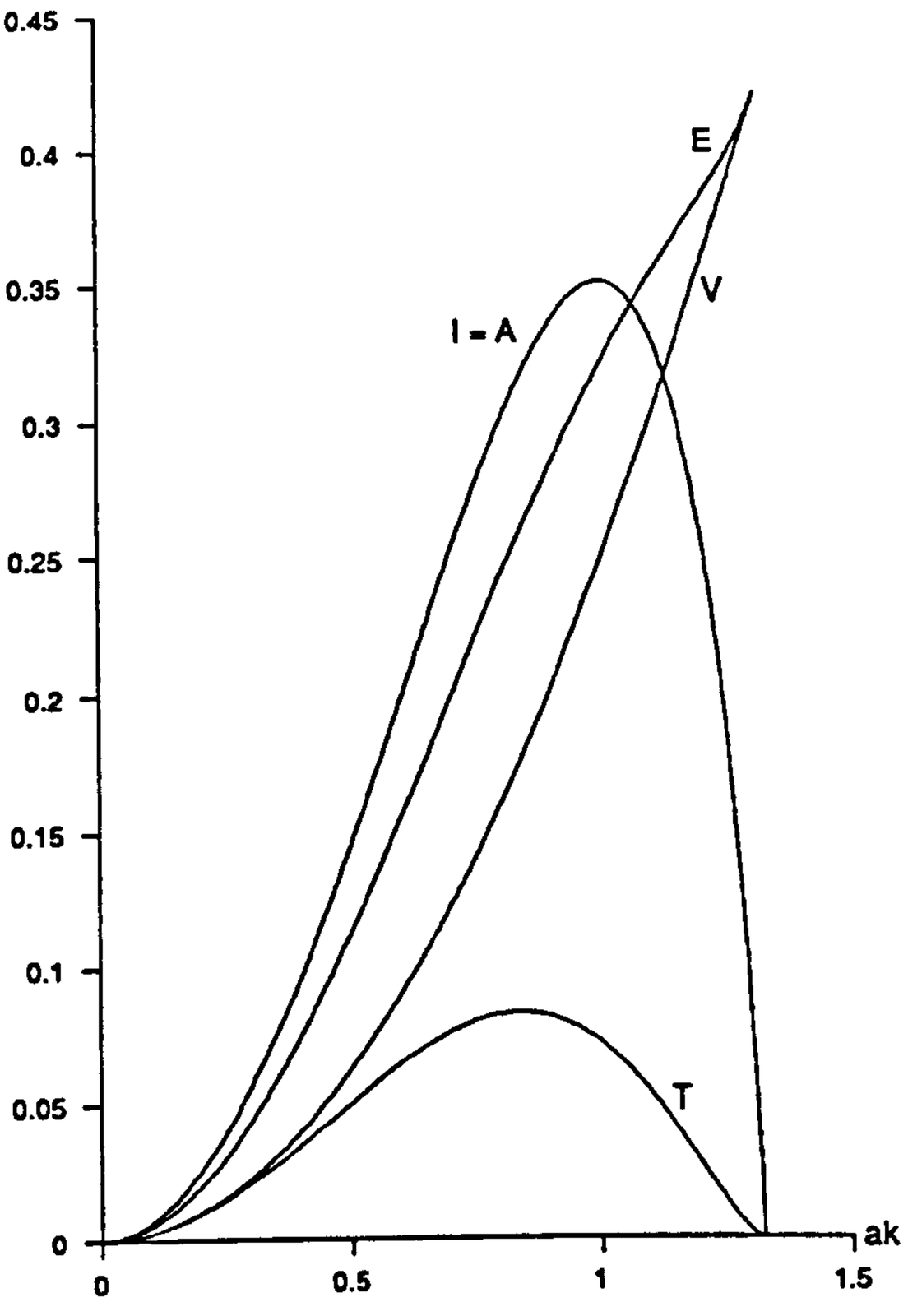

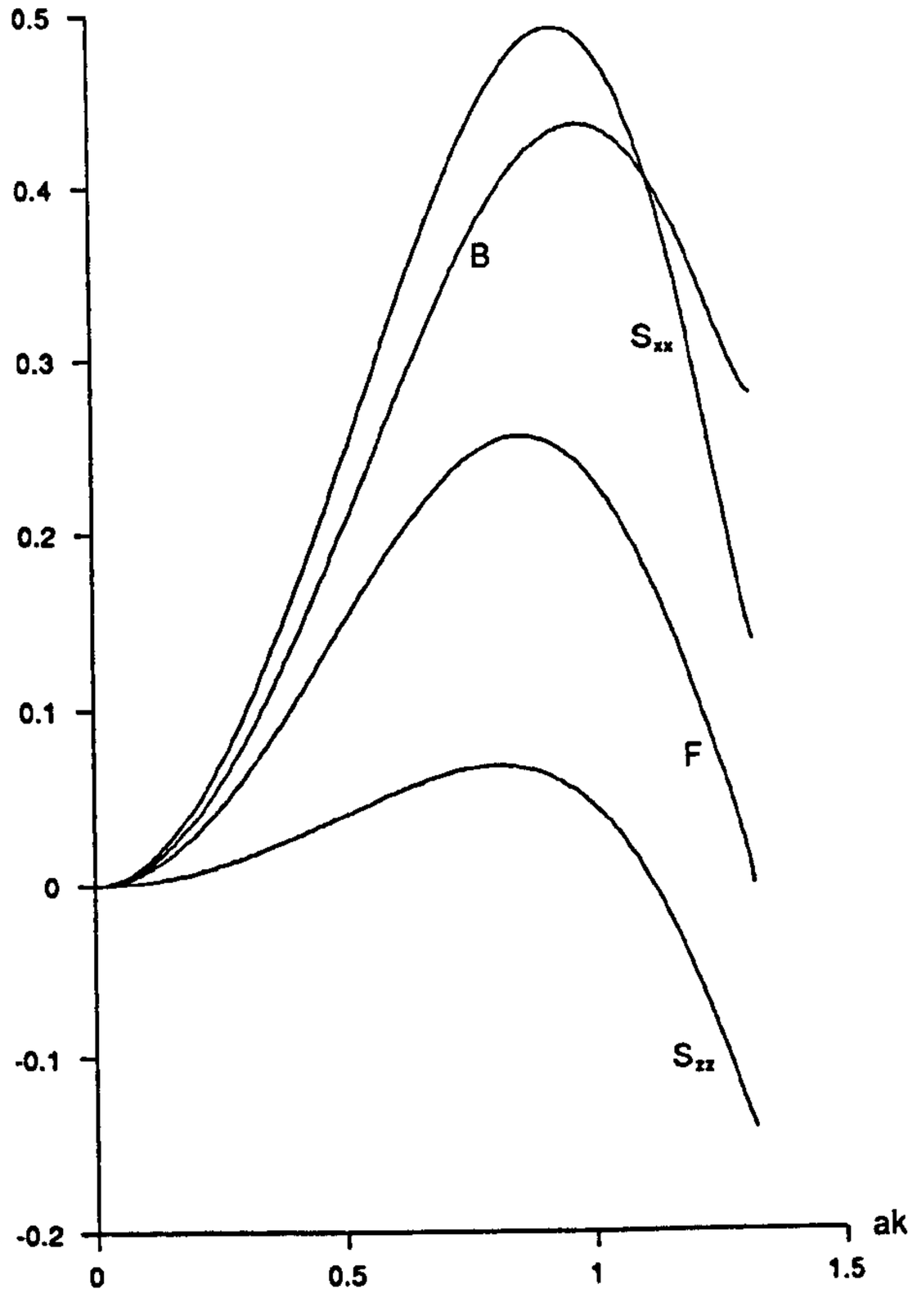

Figures 8.6

B = 0.7

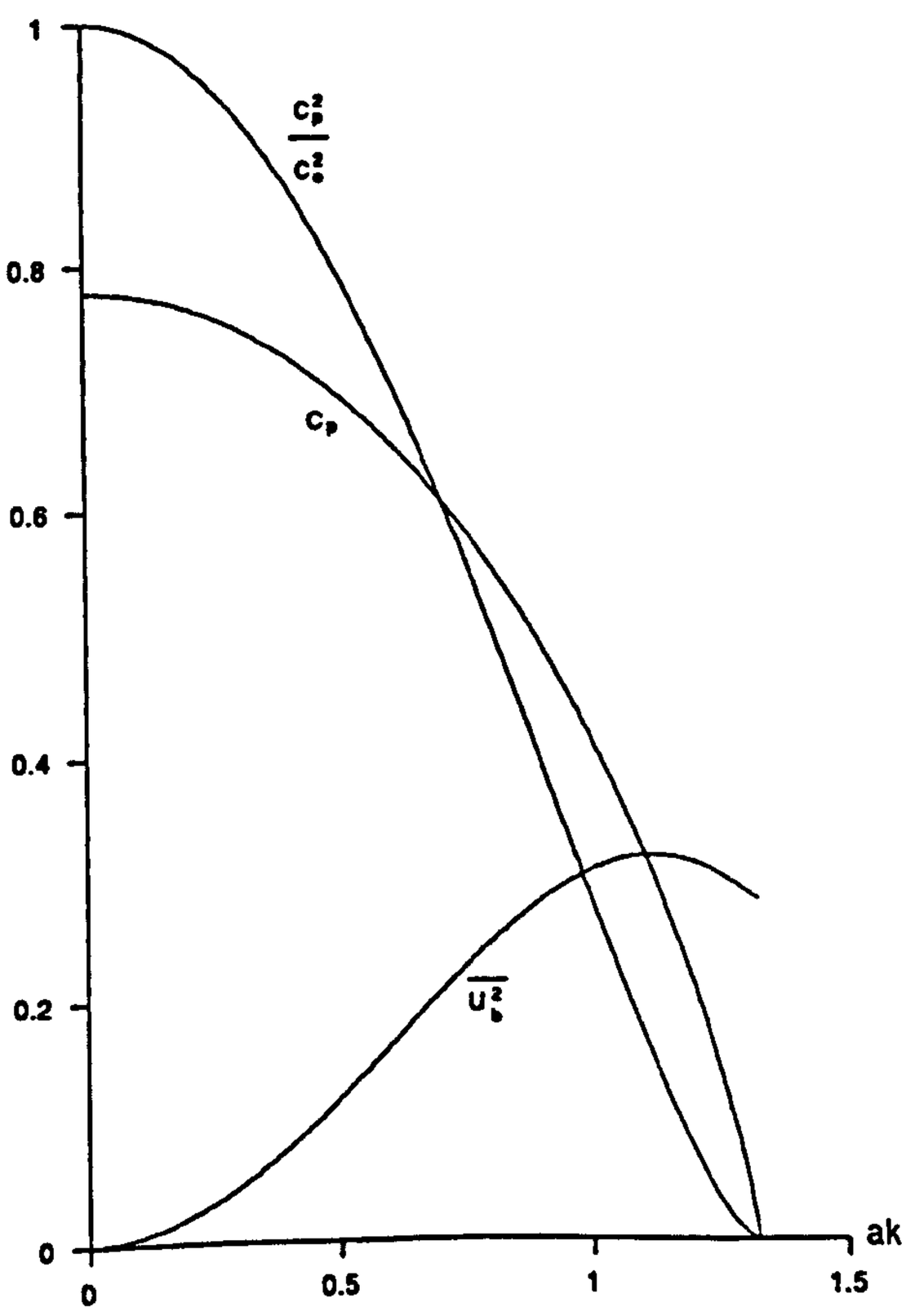

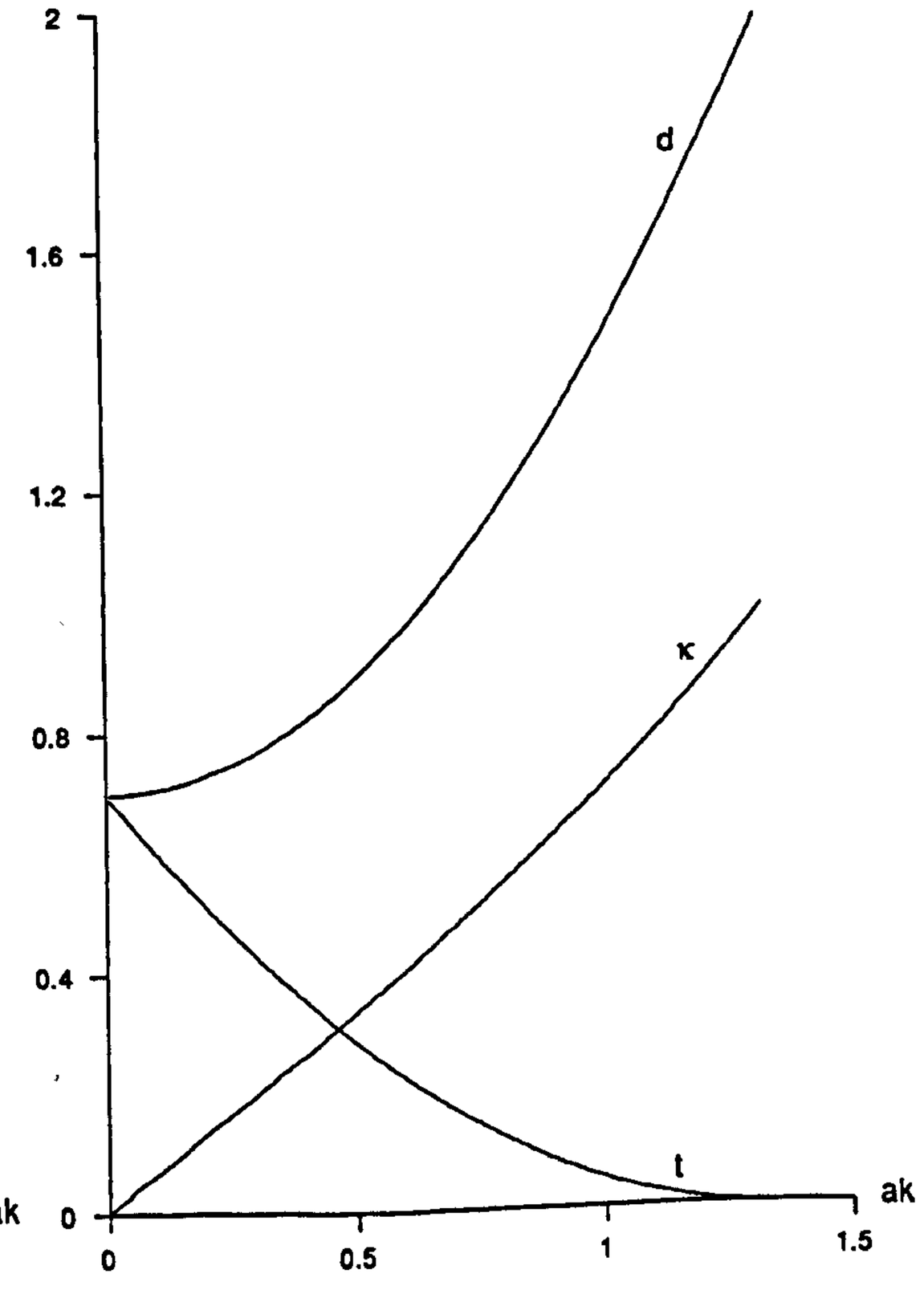

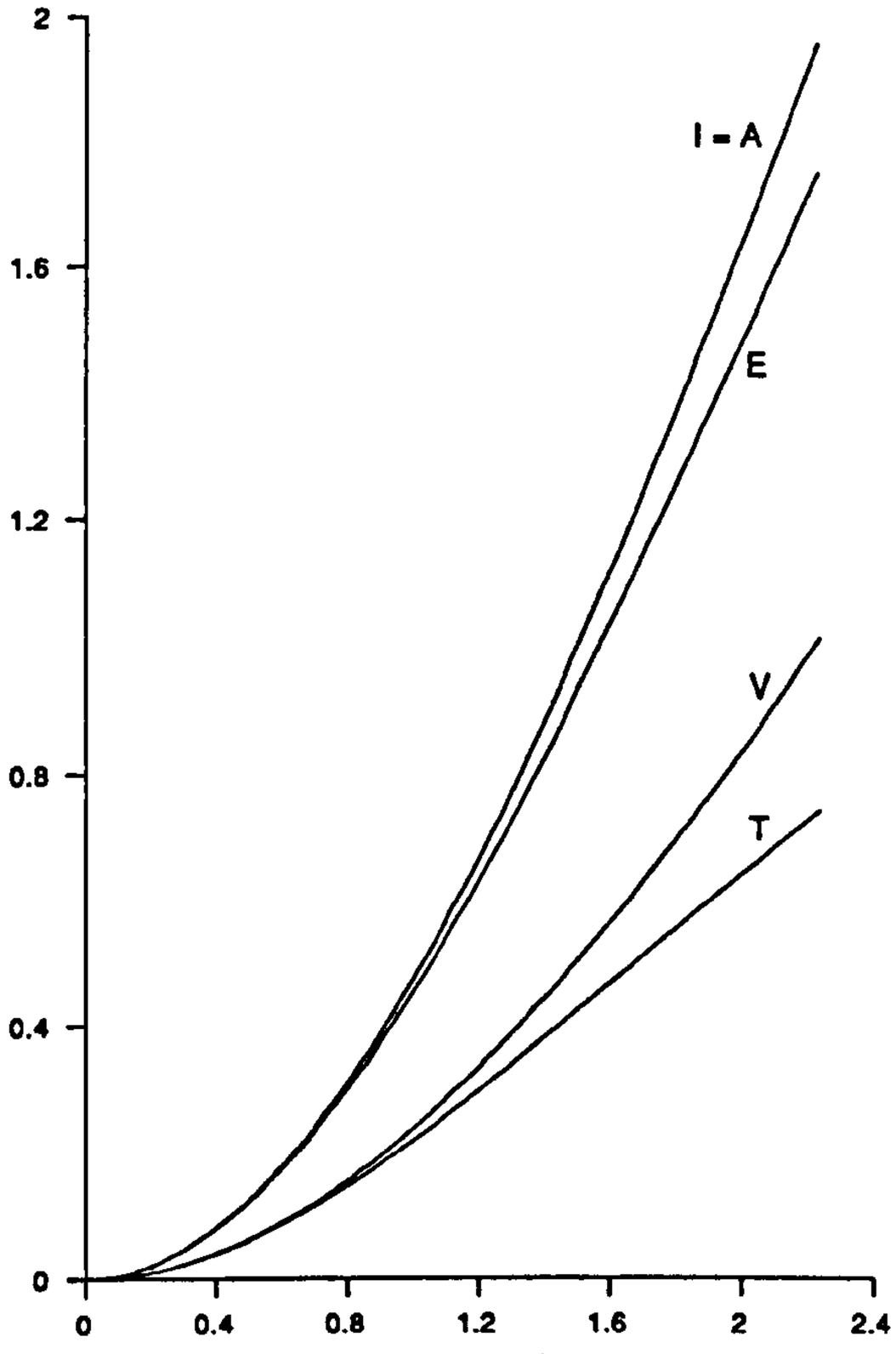

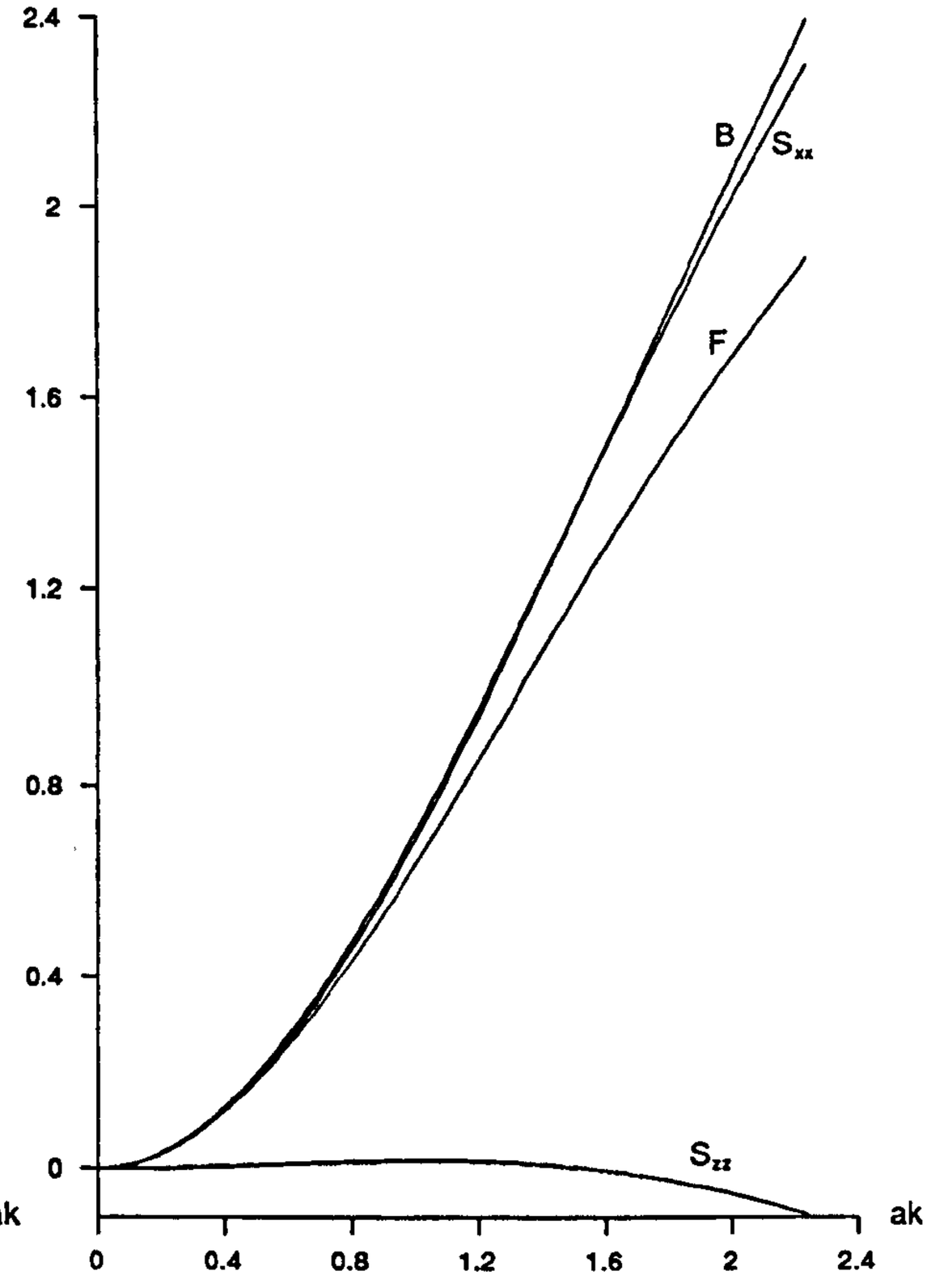

Figures 8.7

B = 2.0

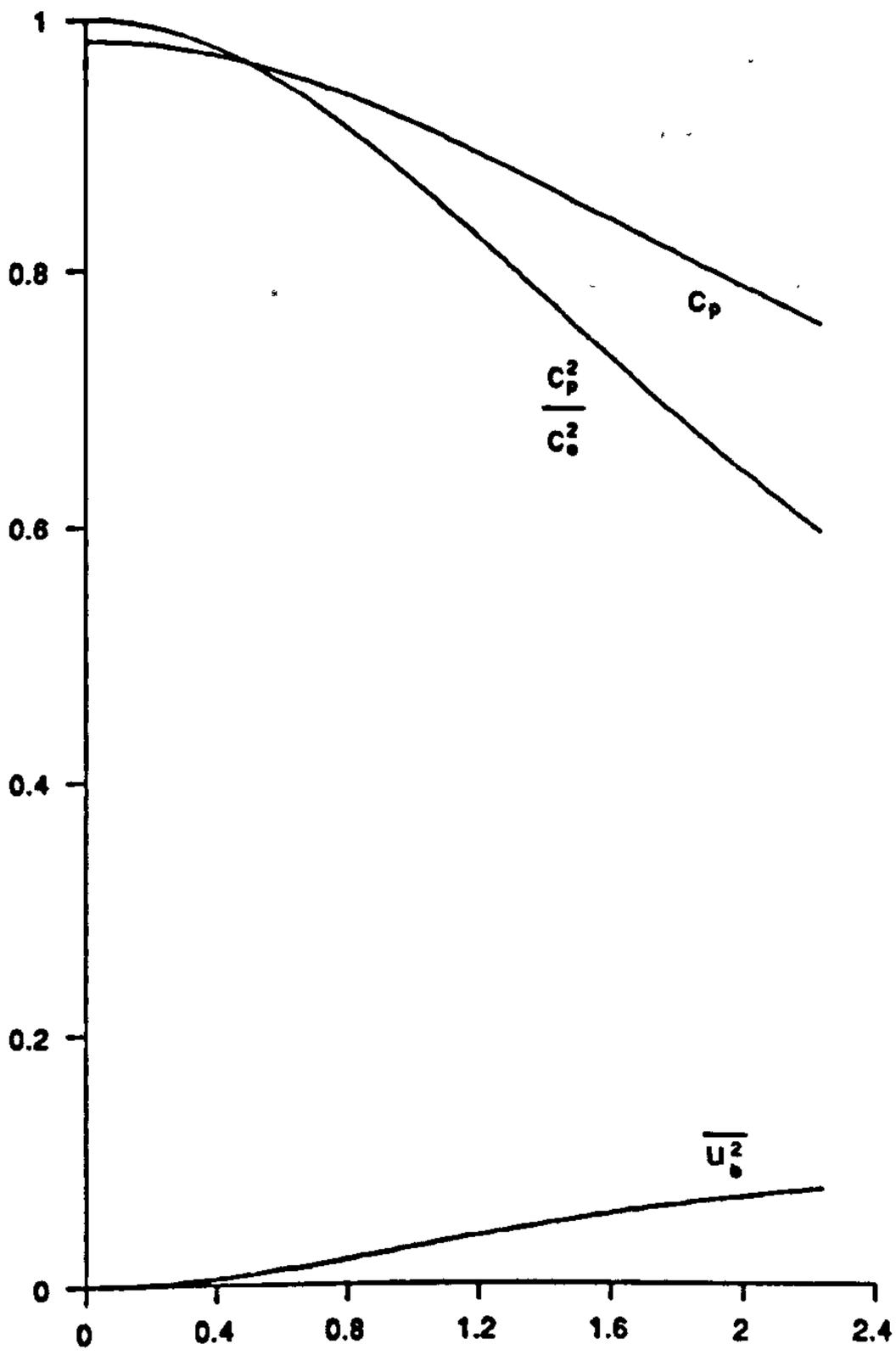

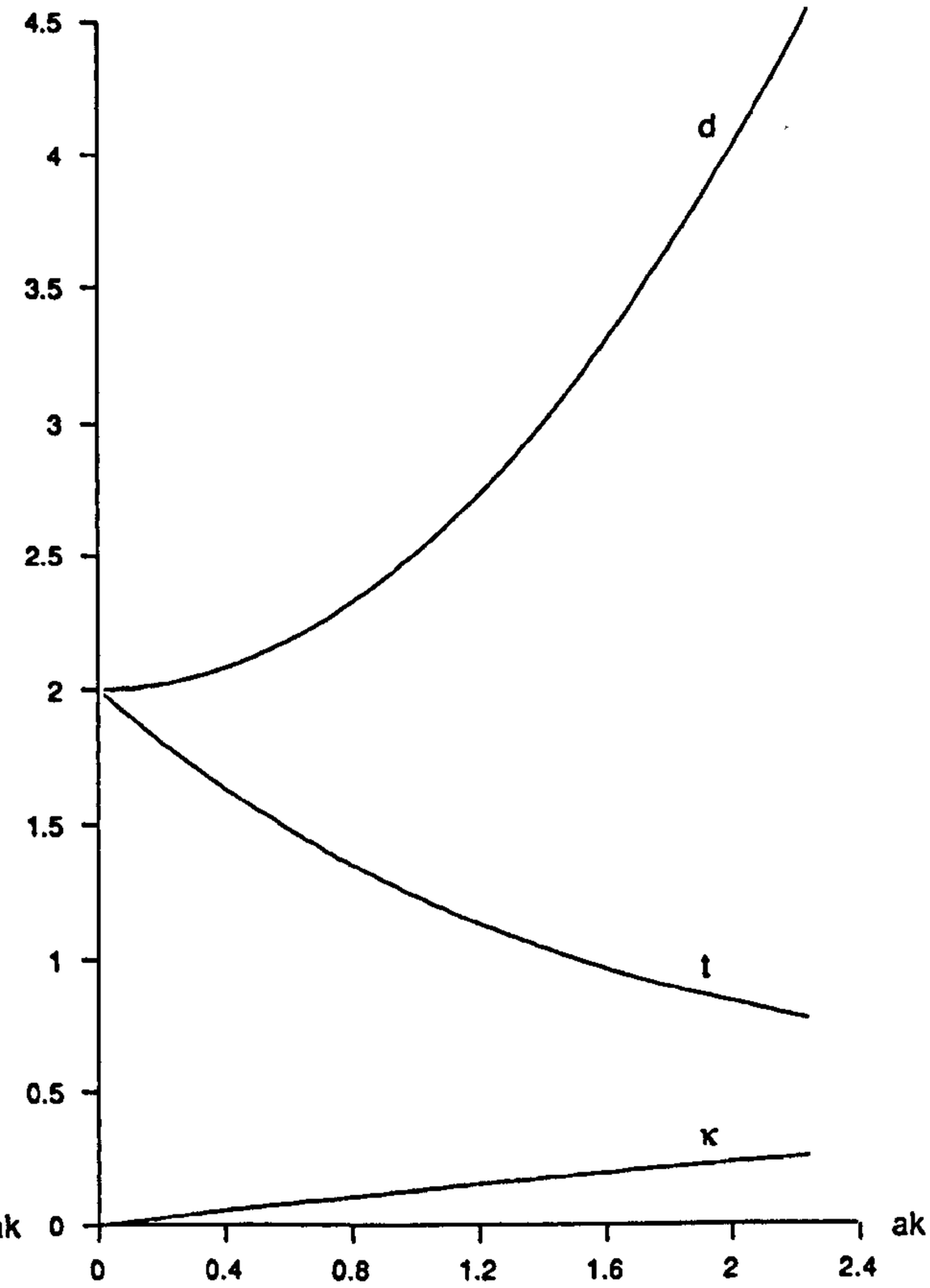

CHAPTER 9
THE LINEAR WAVE-CURRENT INTERACTION PROBLEM FOR CAPILLARY-GRAVITY WAVES ON FINITE DEPTH LIQUID

9.1 Introduction

It is now supposed that the depth of liquid is finite. Finite depth slowly-varying problems are far more complex than infinite depth slowly-varying problems. This is because variations in wave properties cause variations in the mainstream flow and the mean level of the liquid. One consequence of this is that only the wave-current interaction problem can be examined. The wave propagation problem can not be examined simply because the basic mainstream gravity flow can not be specified ab initio.

Here it is supposed that the waves have infinitesimal amplitudes and that both capillary and gravity forces effect the form of the waves. However, our interests are on those waves dominated by capillarity. This chapter is, thus, the finite depth version of chapter 3. Much of the analysis in this chapter, for example the possible waves, is based upon that of chapter 3.

Some general features of Whitham's equations, applicable to both linear and nonlinear waves, are discussed in section 9.2. The possible waves are analysed in section 9.3. Section 9.4 considers the general equations for the finite depth slowly-varying wave-current interaction problem. Results for the cases of stationary and Doppler shifted waves are presented and discussed in sections 9.5 and 9.6 respectively.

9.2 The Influence of Finite Depths

This section discusses some general features of Whitham's equations as presented in § 2.4. This discussion is included at this stage, and not in chapter 2, because it is more directly relevant to the work of this and the subsequent chapter and gives the reader a better appreciation of the mathematical method of solution used.

As in chapter 2, it is supposed that variations of wave parameters and mainstream flow are slowly-varying and that there is zero wave energy dissipation. From definition (2.4.9) of the Bernoulli "constant" γ and expression (2.5.7) for the mean bottom velocity squared in terms of the averaged Lagrangian $\mathcal{L}^w$ it is seen that

$$\gamma = \frac{1}{2}\,(U_i^2 + \overline{u_i^2}) + gb \ . \qquad (9.2.1)$$

For general nonlinear problems two of the three unknowns d, b and h are independent. For our purposes d and b (h) are the two independent parameters so that h = d - b (b = d - h) is the dependent parameter. The presence of two more unknowns requires two more equations to form a closed solvable system. These are the mass conservation equation (2.4.5) and the consistency conservation relation (2.3.5) together with the definition (9.2.1) of γ. Note that an alternative to the consistency conservation relation (2.3.5) is the momentum conservation equation (2.2.2, 5) in which case the definition (9.2.1) of γ is not needed.

If steady variations are considered then the consistency conservation relation (2.3.5) implies that γ, like ω, is constant and so is chosen ab initio. Under such circumstances the definition (9.2.1) of γ can be regarded as specifying variations of b once variations of all other flow properties are known. Thus, d can be regarded as the single unknown present as a result of finite depths. The mass conservation equation (2.4.5) is then the single equation needed in order to form a closed solvable system.

Also for steady variations, the actual value assigned to γ is qualitatively unimportant. From definition (9.2.1) of γ it is seen that γ acts like a translation factor for b since a translation $z \longrightarrow z - \gamma/g$ results in a translation of $b \longrightarrow b + \gamma/g$ so that definition (9.2.1) of γ gives

$$0 = \frac{1}{2}\,(U_i^2 + \overline{u_i^2}) + gb \ . \qquad (9.2.2)$$

Expression (9.2.2) is independent of γ so that such translations have no qualitative effects. Note that if flow properties vary with time then $\gamma = \gamma(x_i,t)$ so that the required translation of z varies with both position and time and the qualitative independence of γ is not true.

For infinitesimal waves the averaged Lagrangian $\mathcal{L}^w$ is of order a^2. Thus, it is seen from the expressions (2.4.7, 2.5.2 - 2.5.6) that all the mean wave properties, except d, are order a^2. It follows that the mean bottom velocity squared term in the definition (9.2.1) of γ and the $\mathcal{L}^w$ term in the mass conservation equation (2.4.5) are negligible to the order of linear theory. Consequently, these equations take the forms

$$\gamma = \frac{1}{2} U_i^2 + gb \quad \text{and} \quad \frac{\partial}{\partial t}(\rho b) + \frac{\partial}{\partial x_i}(\rho U d) = 0 \qquad (9.2.3)$$

respectively. Therefore, since the definition of γ here is exactly the same as for infinite depths, given by expression (2.6.6), b is independent of the wave motion for the case of linear waves on liquid of finite depths.

If the flow field is steady the mass conservation equation (2.7.2, 9.2.3) becomes

$$\rho d U_i = - m_i \ . \qquad (9.2.4)$$

It is, therefore, seen that steady finite depth problems generally have one more parameter vector m_i and one more unknown d than the infinite depth problem. This means that the general complexity of problems increases by one dimension the consequences of which can be dramatic.

All the above features are very important and must be kept in mind when reading this and the subsequent chapter.

9.3 The Possible Waves

A uniform plane-wave of infinitesimal amplitude propagating over still liquid of finite mean depth d with vertical displacement η and velocity potential ϕ given by

$$\eta = a \cos (kx - \sigma t) , \quad \phi = ac \frac{\cosh k(z + h)}{\sinh kd} \sin (kx - \sigma t) \qquad (9.3.1)$$

has dispersion relation and group velocity, the velocity of energy propagation,

$$\sigma^2 = (gk + sk^3) \tanh kd , \quad c_g = \frac{1}{2} c \left[\frac{g + 3sk^3}{g + sk^3} + \frac{2kd}{\tanh kd} \right] . \qquad (9.3.2)$$

Note that these expressions show that both c and $c_g \longrightarrow (gd)^{\frac{1}{2}}$ as $k \longrightarrow 0$. If the mean depth d is infinite then both c and $c_g \longrightarrow \infty$ as $k \longrightarrow 0$ as is shown in figure 3.1.

Figure 9.1 shows variations of c and c_g with k for water depths d = 10 mm, 5 mm and d = 1 mm. It is seen that for $d \gtrsim 5$ mm both c and c_g have local minima at some finite non-zero k but for $d \lesssim 5$ mm both c and c_g only have global minima, given by $(gd)^{\frac{1}{2}}$, at k = 0. Note that for $d \simeq 5$ mm waves are non-dispersive for wavenumbers less than $k \simeq 300\ m^{-1}$, i.e. wavelengths greater than $\lambda \simeq 20$ mm. This depth of 5 mm is usually referred to as the "ripple tank depth" since it is useful in simulating the effects of non-dispersive wave systems such as sound or light.

In § 3.2 the Doppler relation (2.3.1) and the dispersion relation (3.2.2) for waves on infinite depths of liquid are combined and all the possible waves, for a constant mainstream flow U, are found and discussed. A similar analysis is performed in this section for the case of finite depths. All the possible waves for a constant mainstream flow U and a constant mean depth d are found and discussed. Our usual convention of $k \geq 0$ and $U \leq 0$, with $\sigma \geq 0$ for stationary waves, is used. Figure 9.2 shows the variation of frequency σ with wavenumber k as given by the dispersion relation (9.3.2) for d = 10 mm, 5 mm and 1 mm.

Firstly consider the case of stationary waves where the total frequency ω is zero. The Doppler relation takes the form (3.2.4) of $\sigma = - kU$ or $c = - U$. The dispersion relation (9.3.2) implies that there are two possible waves CG and GC if $d \gtrsim 5$ mm and only one possible wave CG if $d \lesssim 5$ mm. This is clearly seen from examination of figures 9.1, 2. As for infinite depths waves only exist when $- U \geq c_{min}$. If $d \gtrsim 5$ mm then $c_{min} < (gd)^{\frac{1}{2}}$ and wave GC exists for $c_{min} \leq - U \leq (gd)^{\frac{1}{2}}$.

If $d \lesssim 5$ mm then $c_{min} = (gd)^{\frac{1}{2}}$, wave GC does not exist and wave CG exists for $-U \geq (gd)^{\frac{1}{2}}$. The directions of travel, etc., of the waves are exactly the same as their infinite depth counterparts. Note that if d is infinite then wave GC exists for all $-U \geq c_{min}$ as expected.

By discussing the transition of the stationary waves CG and GC as the magnitude of ω increases the general case is interpreted. If the stationary wave GC can exist then the analysis is exactly the same as that for infinite depths so that there are six possible waves. However, if the stationary wave GC can not exist then the transition results in only four possible waves. The waves GC+ and G+ do not exist. The general properties of waves, when they exist, are the same as their infinite depth counterparts and are listed in table 3.1.

If the stationary wave GC can exist then there is one possible stationary wave caustic, the CG/GC caustic, and three possible Doppler shifted wave caustics, the GC+/G+, CG+/GC+ and CG-/GC- caustics. However, if the stationary wave GC can not exist then there are no possible stationary wave caustics and only one possible Doppler shifted wave caustic, the CG-/GC- caustic.

Two interesting special cases are those of pure gravity and pure capillary waves. For stationary pure gravity waves the only possible wave is wave GC which will exist for all $-U \leq (gd)^{\frac{1}{2}}$. The stationary wave CG does not exist and there are no possible caustics. For Doppler shifted pure gravity waves the only possible waves are waves G(+,-) and GC(+,-) and the only possible caustic is the GC+/G+ caustic. For stationary pure capillary waves the only possible wave is the wave CG which exists for all U. The stationary wave GC does not exist and there are no possible caustics. For Doppler shifted pure capillary waves the only possible waves are waves CG(+,-), GC- and G- and the only possible caustic is the CG-/GC- caustic. The Doppler shifted pure gravity or pure capillary waves cases are qualitatively similar in their analysis to the corresponding infinite depth cases.

9.4 The Equations

The linear interaction problem is now examined. The mainstream flow and the wave parameters are all assumed to be steadily slowly-varying. The unknowns for the problem are σ, k, a and d. The equations used to find variations of these unknowns are the Doppler relation (2.3.1), the dispersion relation (9.3.1), the wave-action conservation equation (2.7.5) and the mass conservation equation (9.2.4).

The mass conservation equation (9.2.4) states that ρUd = - m so that our convention of $U \leq 0$ means that $m > 0$ since $d \geq 0$. Also, it is seen that a large (small) magnitude for the mainstream flow U means a small (large) magnitude of depth d. Note that $m = 0$ is not considered simply because it does not correspond to realistic flow fields.

The variation of k is given by using the Doppler relation (2.3.1), the dispersion relation (9.3.1) and the mass conservation equation (9.2.4). These give

$$s \tanh \frac{mk}{\rho U} k^3 - U^2 k^2 + \left[2\omega U + g \tanh \frac{mk}{\rho U}\right] k - \omega^2 = 0 . \quad (9.4.1)$$

For particular values of ω and m this equation is solved by varying U over a given range and solving for k. Note that this equation is singular when $U = 0$. However, from the mass conservation equation (9.2.4) it is seen that $U = 0$ implies that $d = \infty$ so solutions for $U = 0$ are found from the corresponding infinite depth equation (3.3.2).

Once equation (9.4.1) is solved for variations of k with U variations of σ are found using the Doppler relation (2.3.1). Variations of d are found from the mass conservation equation (9.2.4). Note that d is independent of ω. Variations of b are found using expression (9.2.3) with $\gamma = 0$, i.e.

$$b = - \frac{U^2}{2g} \quad (9.4.2)$$

with h given by $h = d - b$. Note that b is independent of both ω and m.

The variation of a, or ak, with U is given by the wave-action conservation equation (2.7.5). Expressions (3.3.3, 4) are true for finite depths as well as infinite depths so that the wave-action conservation equation takes the form (3.3.5). It is the expressions for the wave energy density $\mathcal{E}$ and the group velocity $C_g = U + c_g$ which are different. Expression (9.3.2) gives the group velocity c_g. The wave

energy density $\mathcal{E}$ is given by

$$\mathcal{E} = \tfrac{1}{2}\,\rho(g + sk^2)\,a^2 \qquad (9.4.3)$$

which can be derived in the same way as the corresponding infinite depth expression. Thus, equation (3.3.5) gives

$$a = \left[\frac{2\sigma}{\rho(g + sk^2)C_g}\,b\right]^{\frac{1}{2}} . \qquad (9.4.4)$$

Note that, as for infinite depths, the magnitude of b is qualitatively unimportant so that ω and m are the only parameters of the interaction problem. Also note that if the limit $d \longrightarrow \infty$ is taken, with U finite, then the mass conservation equation (9.2.4) implies that $m \longrightarrow \infty$ which implies that equations (9.4.1, 4) give equations (3.3.2, 6) respectively as would be expected.

Equation (9.3.2) is a transcendental equation whose solutions are found numerically using a standard solver for such equations (NAG LIB C05NBF). Such solvers require an initial estimate from which the solution is found. It turns out that the initial estimate, for a particular initial current U, is adequately given by the infinite depth solutions of chapter 3. As U is incremented a wave solution is tracked by using the solver but with the initial estimate given by the previous solution point.

9.5 Stationary Waves

The case of stationary waves is considered first. As usual, dimensional units are used and the liquid is water with density ρ = 1000 kg m^{-3} and surface tension τ = 0.0742 kg s^{-2}. Equation (9.4.1) becomes

$$s \tanh \frac{mk}{\rho U} k^2 - U^2 k + g \tanh \frac{mk}{\rho U} = 0 \qquad (9.5.1)$$

and since σ = - kU equation (9.4.4) becomes

$$a = \left[- \frac{2kU}{\rho(g + sk^2)C_g} b \right]^{\frac{1}{2}} . \qquad (9.5.2)$$

The mass conservation equation (9.2.4) aids in providing a lower bound of U for the existence of waves GC. It is known that waves GC exists if $d > d_c \simeq 5$ mm so that they exist if $U > - m/\rho d_c$ using the mass conservation equation (9.2.4). Now, from the possible waves analysis of § 9.3 it is also known that if both waves CG and GC (only waves CG) exist then waves GC (CG) cease to exist when $- U = (gd)^{\frac{1}{2}}$ or $U = (- gm/\rho)^{\frac{1}{3}}$ using the mass conservation equation (9.2.4). It follows that if $- m/\rho d_c \lesssim (- gm/\rho)^{\frac{1}{3}}$ then waves GC must exist otherwise only waves CG exist. Thus, waves GC exists if $m \gtrsim \rho(gd_c^3)^{\frac{1}{2}} = 1.11$ kg m^{-1} s^{-1}.

Results are shown in figures 9.3 for m = 1 and 3 kg m^{-1} s^{-1}. These show variations of wavenumber k and steepness ak with current U. For m = 1 kg m^{-1} s^{-1} only waves CG exist and there is no caustic as expected. For m = 3 kg m^{-1} s^{-1} both waves CG and GC exist and so does the CG/GC caustic as also expected. For m = 1 and 3 kg m^{-1} s^{-1} waves CG and GC respectively cease to exist when $U = (- gm/\rho)^{\frac{1}{3}}$ with zero k and ak and finite d.

For infinite depths variations of k with U, as shown in figure 3.6a, are exactly the same as variation of k with - c, as shown in figure 3.1, for the stationary waves case. No analogous feature exists here simply because d varies with U. However, the variations of k with U for m = 1 and 3 kg m^{-1} s^{-1} are qualitatively similar to those of k with - c for d = 1 mm and 10 mm respectively as shown in figure 9.1.

Our primary interest is that of pure capillary waves where only waves CG exist. This is the case when $m \lesssim 1.11$ kg m^{-1} s^{-1} so that the qualitative effects of gravity are unimportant for such m unless k is small, $k < 250$ m^{-1} say. Moreover, small m corresponds to small d so that the influence of the bed increases with decreasing m.

A dimensionless parameter comparing the effects of surface tension forces with the inertia of the mainstream motion is given from terms in the energy conservation equation. The energy conservation equation (2.2.3) has wave and mainstream terms $U_1\mathcal{E}$ and $\frac{1}{2}U_1\rho dU_j^2$ respectively so, for one-dimensional flows, the dimensionless parameter is

$$\frac{\mathcal{E}}{\frac{1}{2}\rho dU^2} = \frac{\tau(ak)^2}{\rho dU^2} \qquad (9.5.3)$$

for infinitesimal waves. The mass conservation equation (9.2.4) gives

$$\frac{\tau(ak)^2}{\rho dU^2} = \frac{\tau(ak)^2}{m|U|} \ . \qquad (9.5.4)$$

For thin film flows it is required that this parameter be "large", i.e.

$$\frac{\tau(ak)^2}{m|U|} > 1 \quad \Longrightarrow \quad m < \tau \qquad (9.5.5)$$

taking both $|U|$ and ak to be 1, say.

Now, results for flows with $m \lesssim 1.11$ kg m^{-1} s^{-1} all have wavenumber and steepness variations qualitatively the same as $m = 1$ kg m^{-1} s^{-1}. Thus, flows with $m < \tau$ all qualitatively resemble that of $m = 1$ kg m^{-1} s^{-1} and are not pursued. Note that the value of $U = (-gm/\rho)^{\frac{1}{3}}$ at which k and ak are zero becomes closer to zero as m decreases and is identically zero for pure gravity waves.

It is concluded that the effects of gravity are unimportant when $m \lesssim 1.11$ kg m^{-1} s^{-1} and that thin film flows have $m < \tau$.

9.6 The Doppler Shifted Waves

The case of Doppler shifted waves in now considered. As usual capillary units are used. The parameters for the problem are ω_1, g_1 and b_1, defined in § 3.5, and m_1 given by

$$m_1 = \frac{(s|\omega|)^{\frac{1}{3}}}{\tau} m \ . \qquad (9.6.1)$$

Again, the qualitative characteristics of amplitude variations are unaffected by the magnitude of b_1 for linear waves so that b_1 is taken to be equal to ± 1. The method of solution for the equations is as outlined in § 9.4.

Results are shown in figures 9.4, 5 for $|\omega| = 5$ rad s^{-1} and figures 9.6, 7 for $|\omega| = 100$ rad s^{-1}, i.e. $g_1 = 27.30$ and 0.5030, respectively. These show variations of wavenumber k_1 and steepness ak with current U_1. Two values of mass flux m_1, namely $m_1 = 1$ and 3, are considered. For $|\omega| = 5$ rad s^{-1} there are four waves and one caustic when $m_1 = 1$ and six waves and three caustics when $m_1 = 3$. For $|\omega| = 100$ rad s^{-1} there are four waves and one caustic for both values of m_1.

From the possible waves analysis of § 9.3 it is known that waves G+ and GC+ can only exist if the stationary waves GC exist. Note that, as for the infinite depth case, these waves may, or may not, exist depending on the actual value of ω because this effects the position of the Doppler relation lines on the (k,σ)-plane shown in figure 9.2. Waves GC exist when $m \geq 1.11$ kg m^{-1} s^{-1} so that, using the definition (9.6.3) for m_1, the waves G+ and GC+ can exist when $m_1 \geq 0.63 |\omega|^{\frac{1}{3}}$. So for $|\omega| = 5$ and 100 rad s^{-1} it is required that $m_1 \geq 1.07$ and $m_1 \geq 2.91$ respectively. Thus, for $m_1 = 1$ there are four possible waves and for $m_1 = 3$ there are six possible waves. However, only four of the six possible waves exist when $|\omega| = 100$ rad s^{-1} and $m_1 = 3$ because of the large value of ω as is the case for infinite depths.

Also, for infinite depths all six possible waves and all three possible caustics exist when $|\omega| = 5$ rad s^{-1} and only four of the six possible waves and one of the three possible caustics exist when $|\omega| = 100$ rad s^{-1} as seen form figures 3.12, 13 respectively. However, it is noted in § 9.4 that the infinite depth case is obtained by taking m, or m_1, to infinity whilst keeping U, or U_1, finite. Consequently, for $|\omega| = 5$ rad s^{-1} the case $m_1 = 3$ qualitatively resembles the infinite depth case whereas the case $m_1 = 1$ does not.

Now, different values of ω give different qualitative results because of the presence of gravity. This is not the case for pure capillary waves where the parameter g_1 is always zero. However, the effects of gravity are qualitatively unimportant only when waves G+ and GC+ do not exist. This is the case if $m_1 \lesssim 0.63\ |\omega|^{\frac{1}{3}}$. Thus, if it is required that gravity be unimportant when $m_1 = 1$ and 3 then it is required that $|\omega| \gtrsim 108\ s^{-1}$.

It is concluded that flows with "small" m_1 will correspond to thin films. These are not considered here but are examined more closely in chapter 10 since flows with "small" m_1 have negligible gravity effects. Flows with "large" m_1 will have negligible gravity effects if $|\omega|$ is "large".

CAPTIONS FOR FIGURES

Figure 9.1: The variation of phase velocity c (continuous lines) and group velocity c_g (dashed lines) with wavenumber k for water depths of 10 mm, 5 mm and 1 mm.

Figure 9.2: The general variation of frequency σ with wavenumber k as given by the Doppler and dispersion relations for water depths of 10 mm, 5 mm and 1 mm.

Figure 9.3: The variation of (a) wavenumber k and (b) steepness ak with current U for stationary waves with mass fluxes m = 1 and 3 kg m^{-1} s^{-1}.

Figure 9.4: The variation of (a) wavenumber k_1 and (b) steepness ak with current U_1 for $|\omega|$ = 5 rad s^{-1} with mass fluxes m_1 = 1 and 3.

Figure 9.5: The variation of (a) wavenumber k_1 and (b) steepness ak with current U_1 for $|\omega|$ = 100 rad s^{-1} with mass fluxes m_1 = 1 and 3.

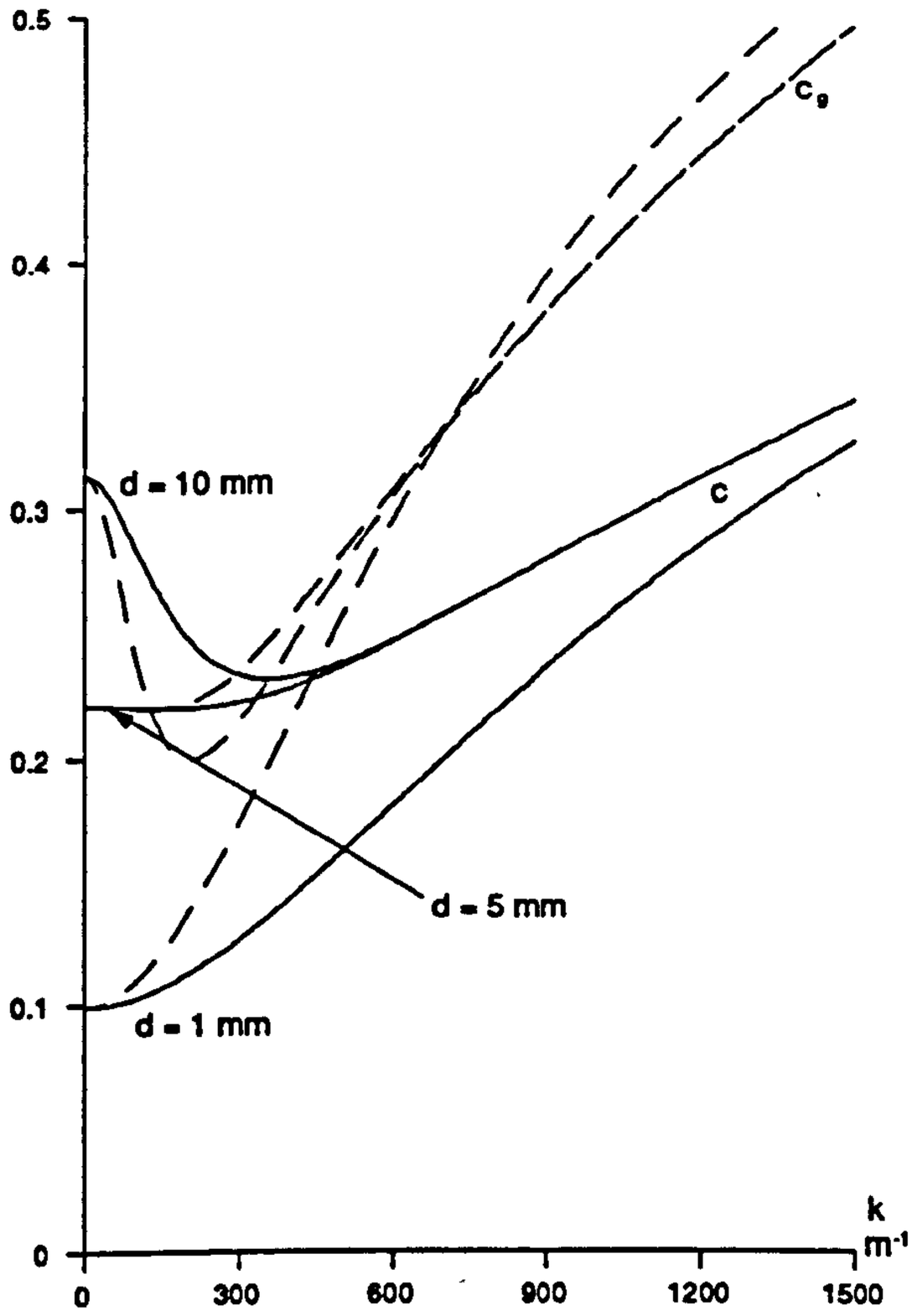

Figure 9.1

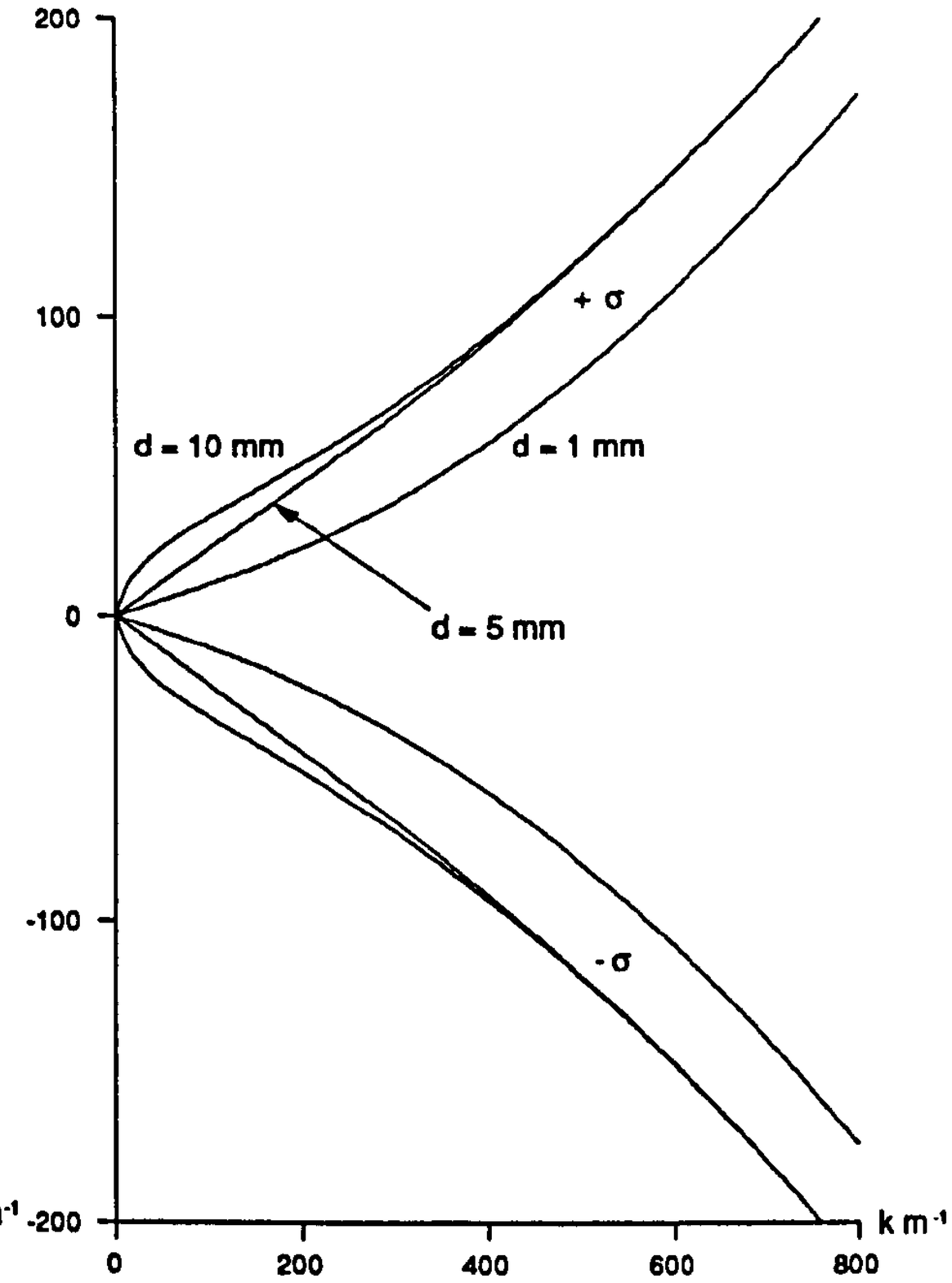

Figure 9.2

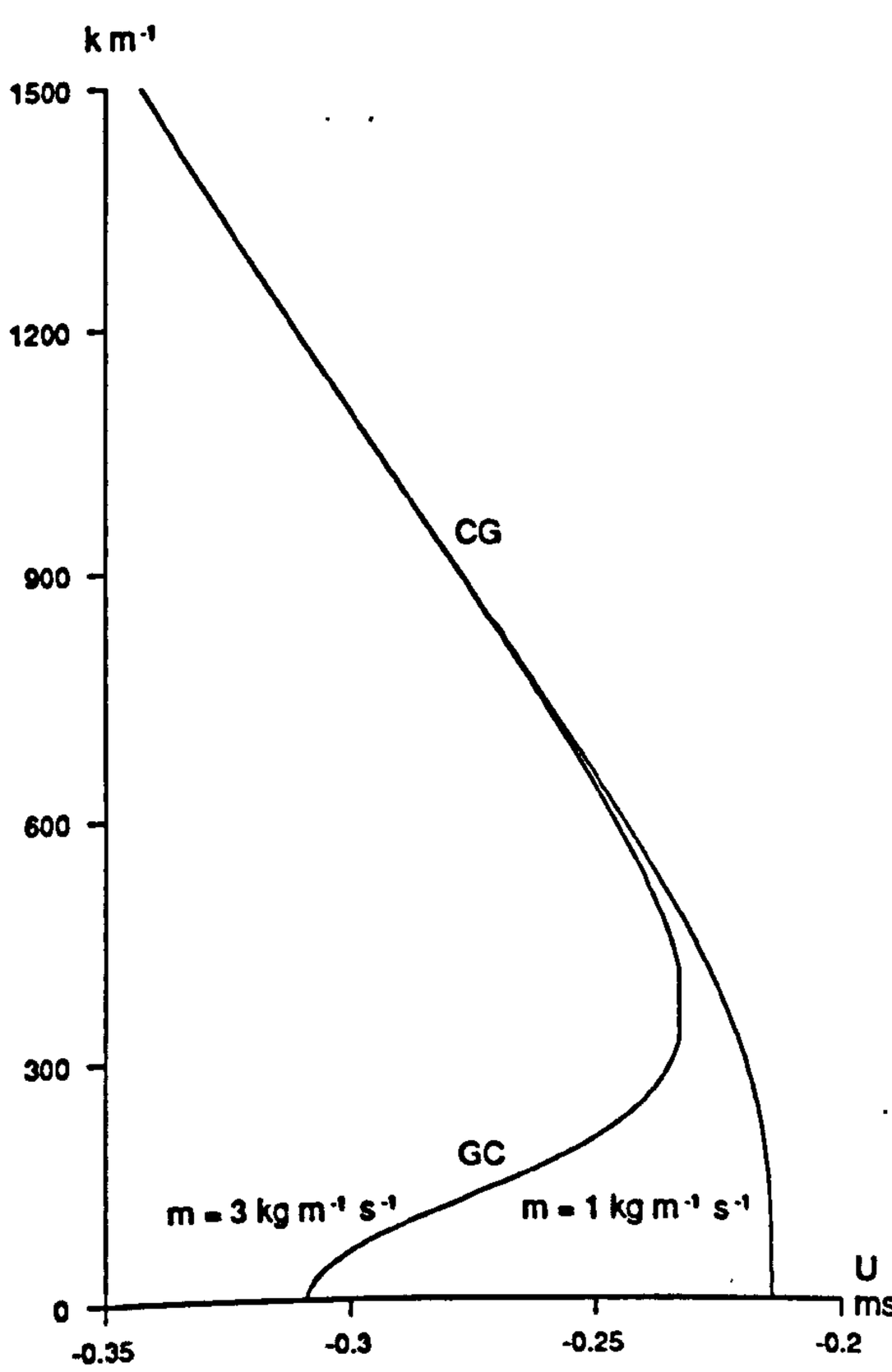

Figure 9.3a

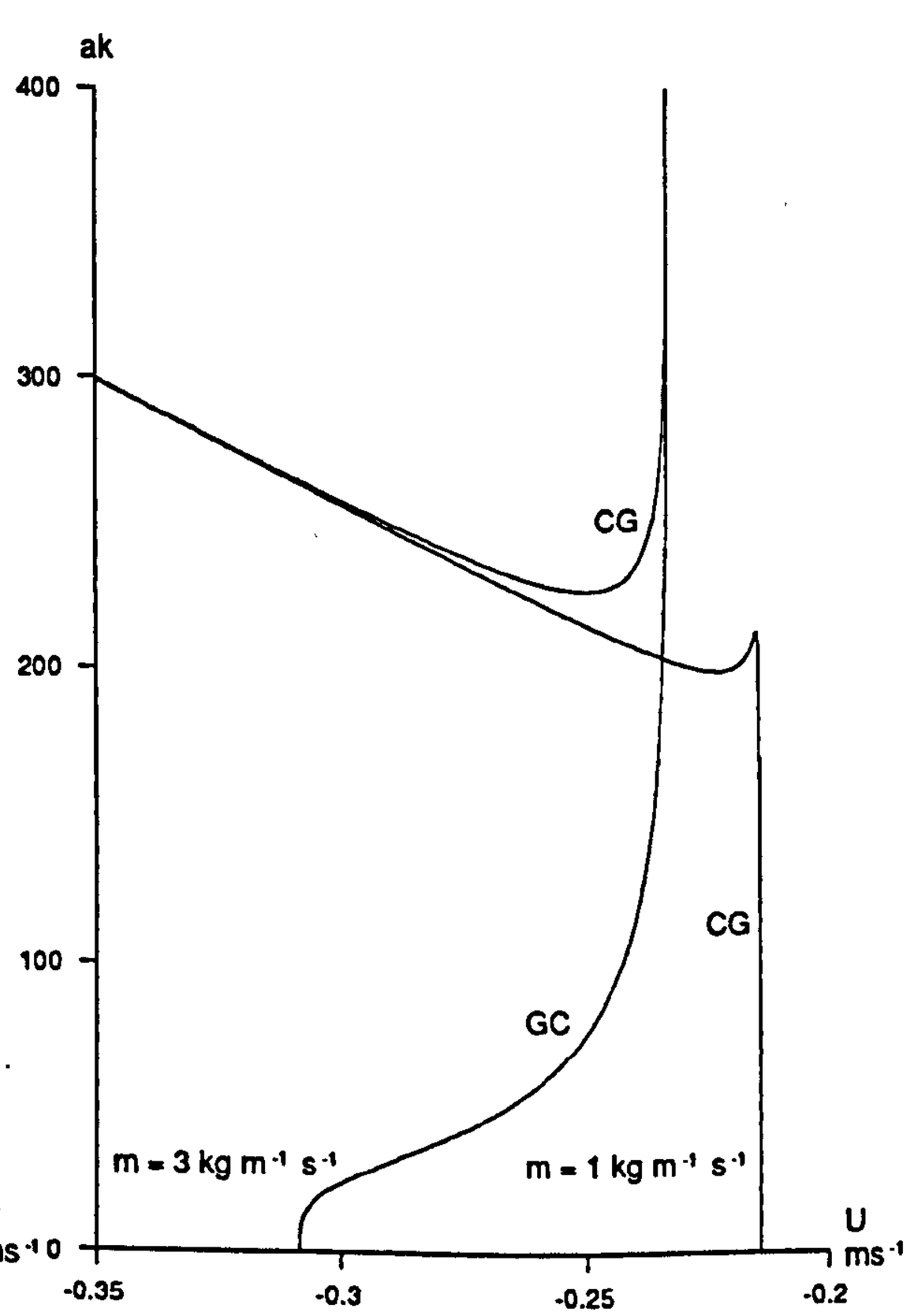

Figure 9.3b

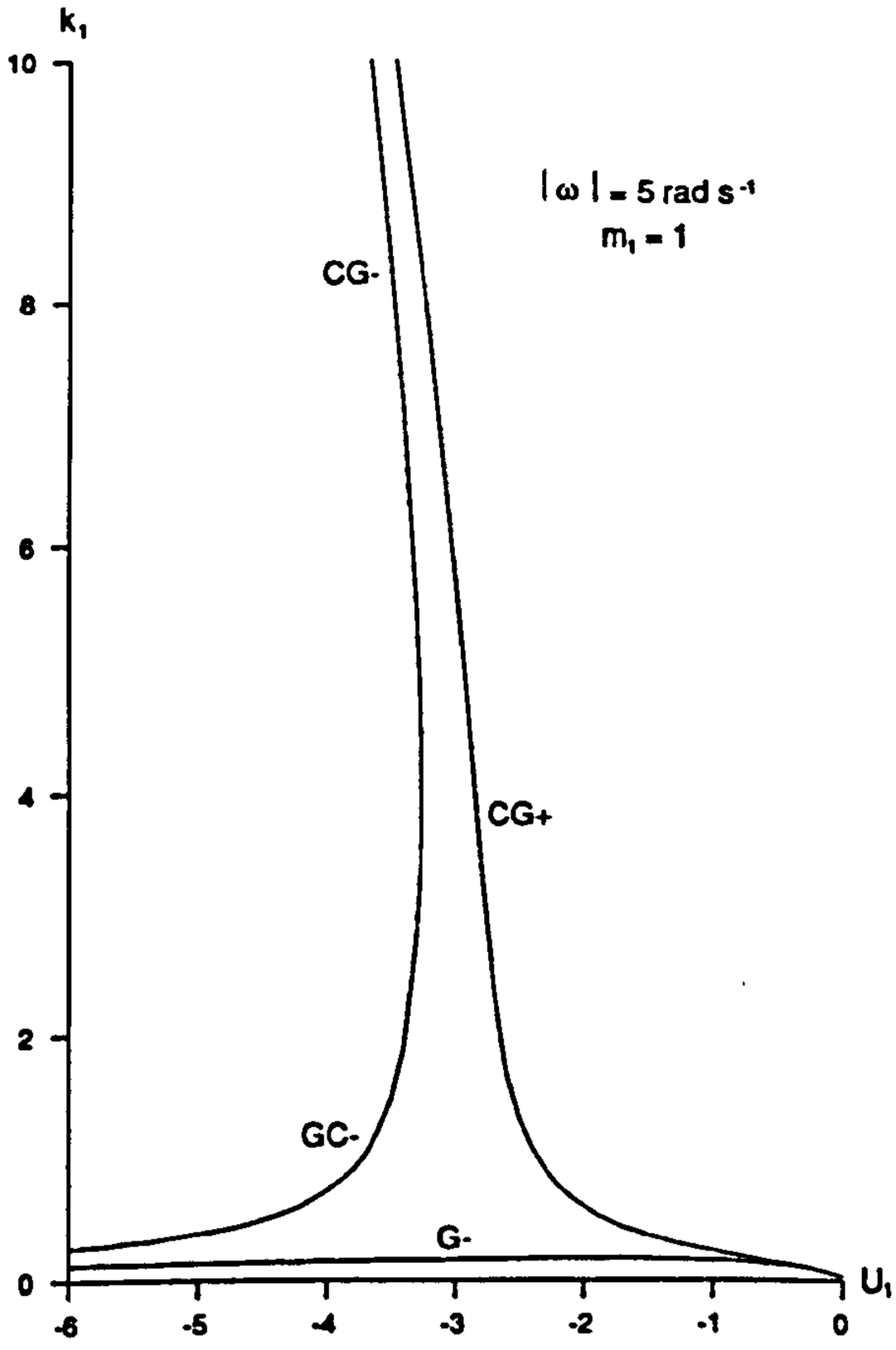

Figure 9.4a

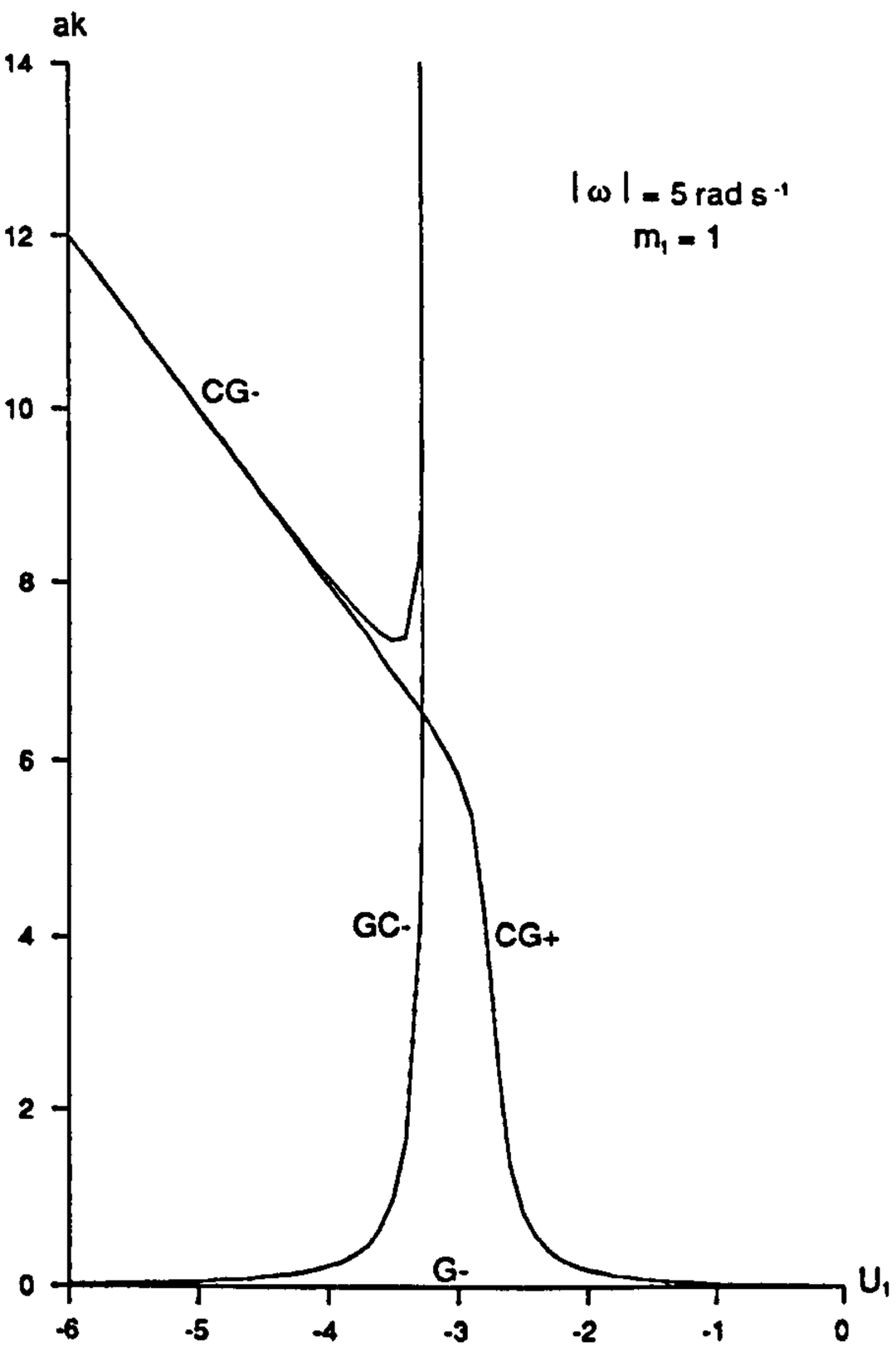

Figure 9.4b

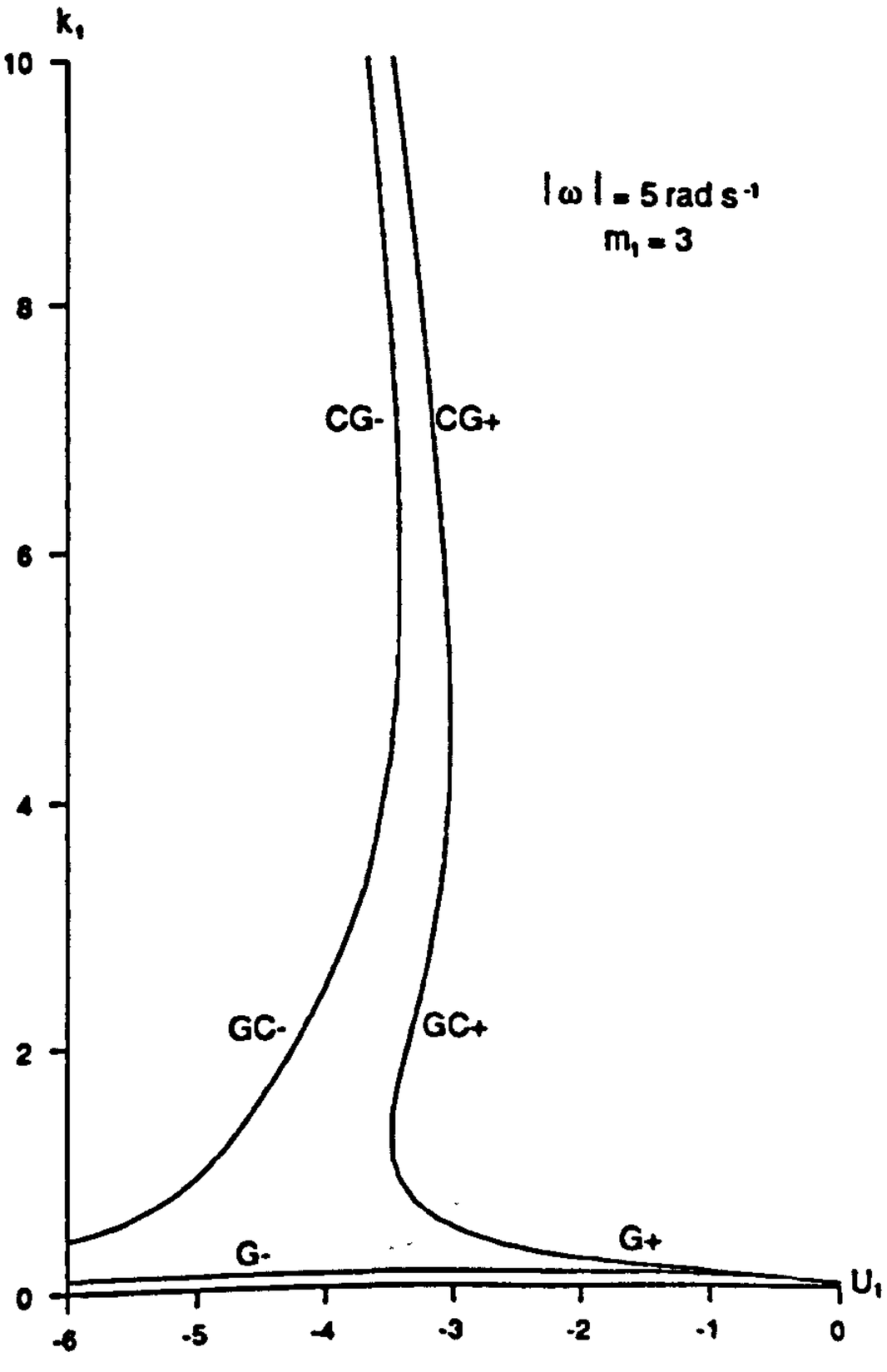

Figure 9.5a

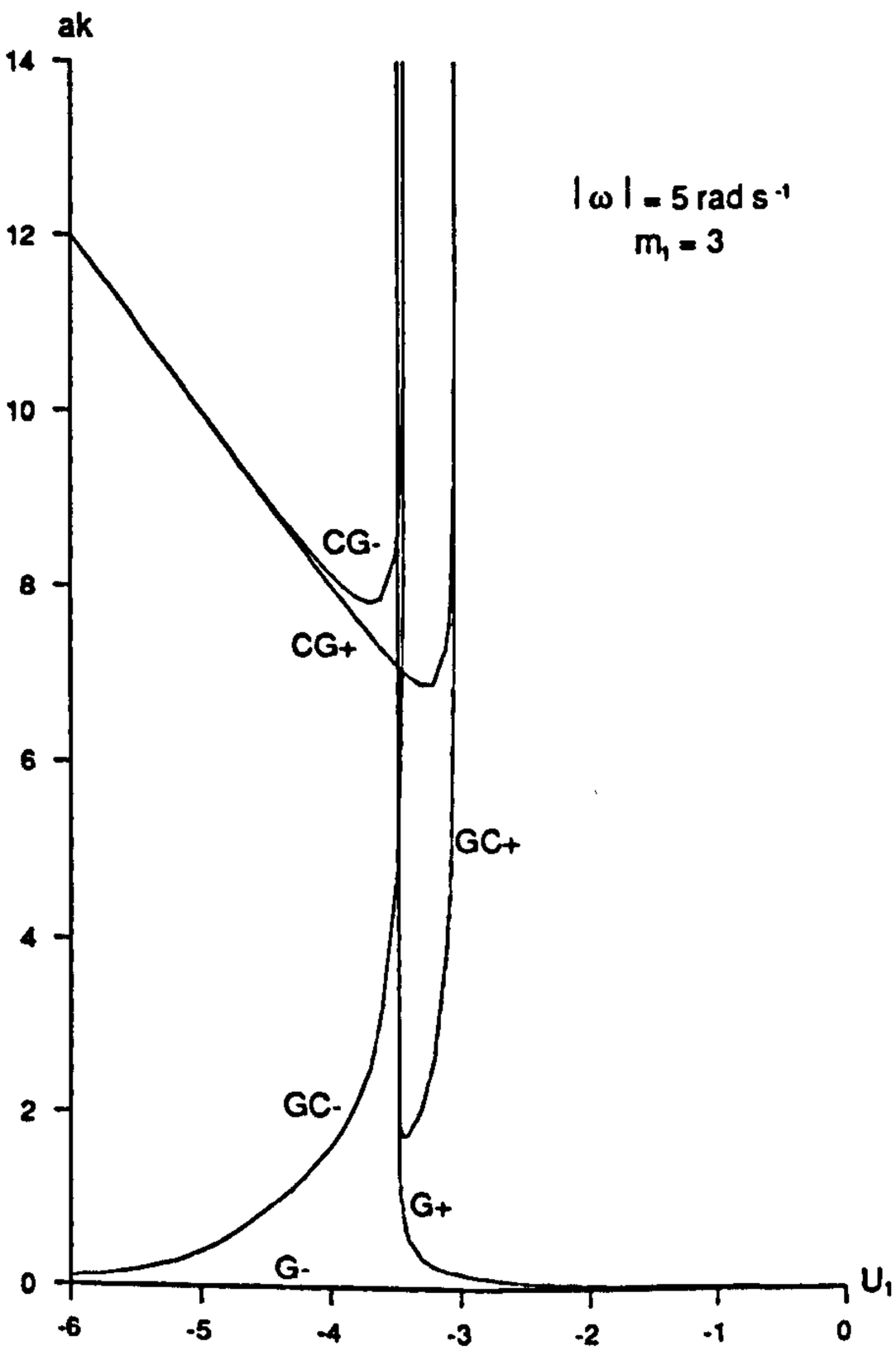

Figure 9.5b

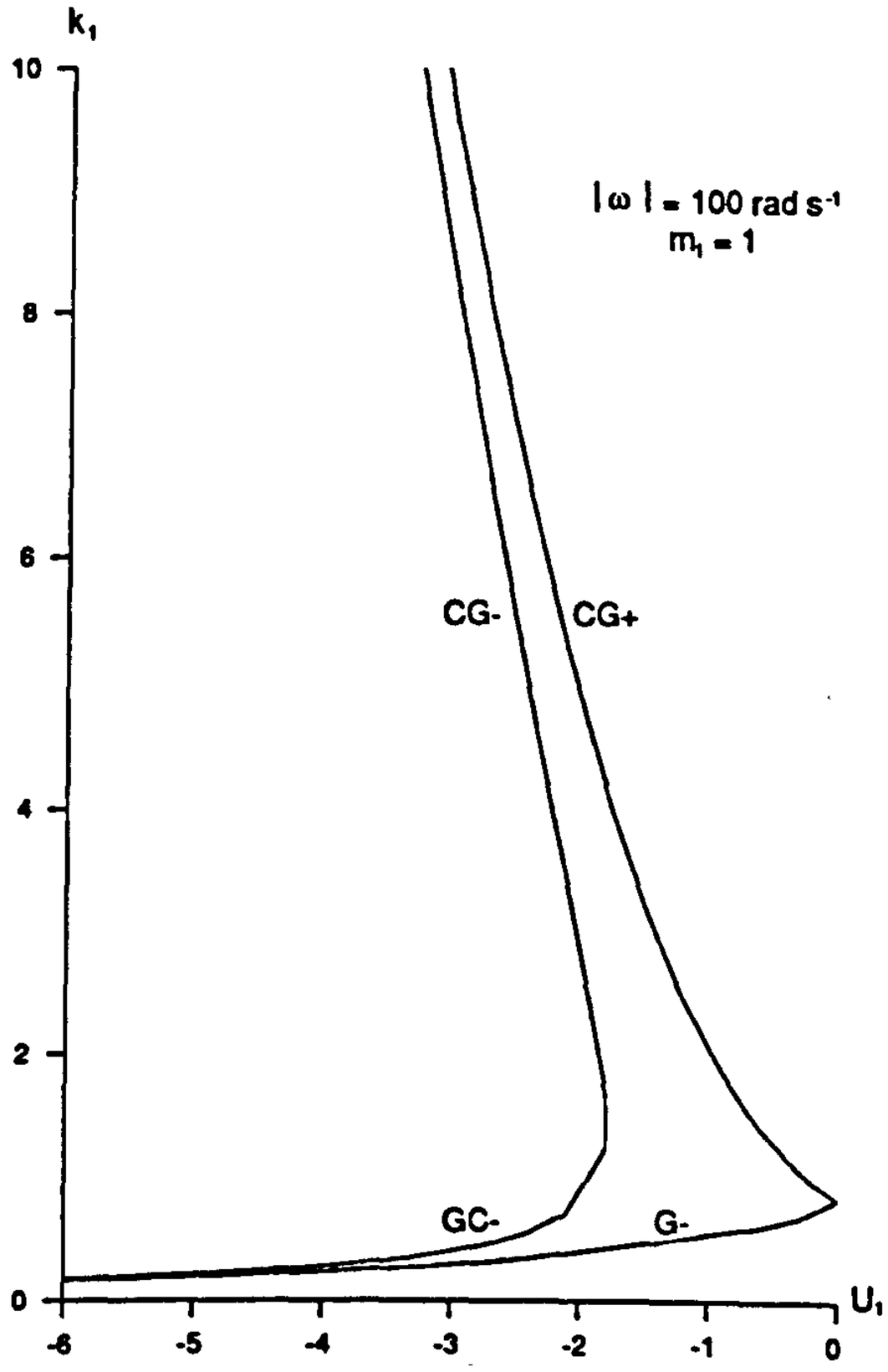

Figure 9.6a

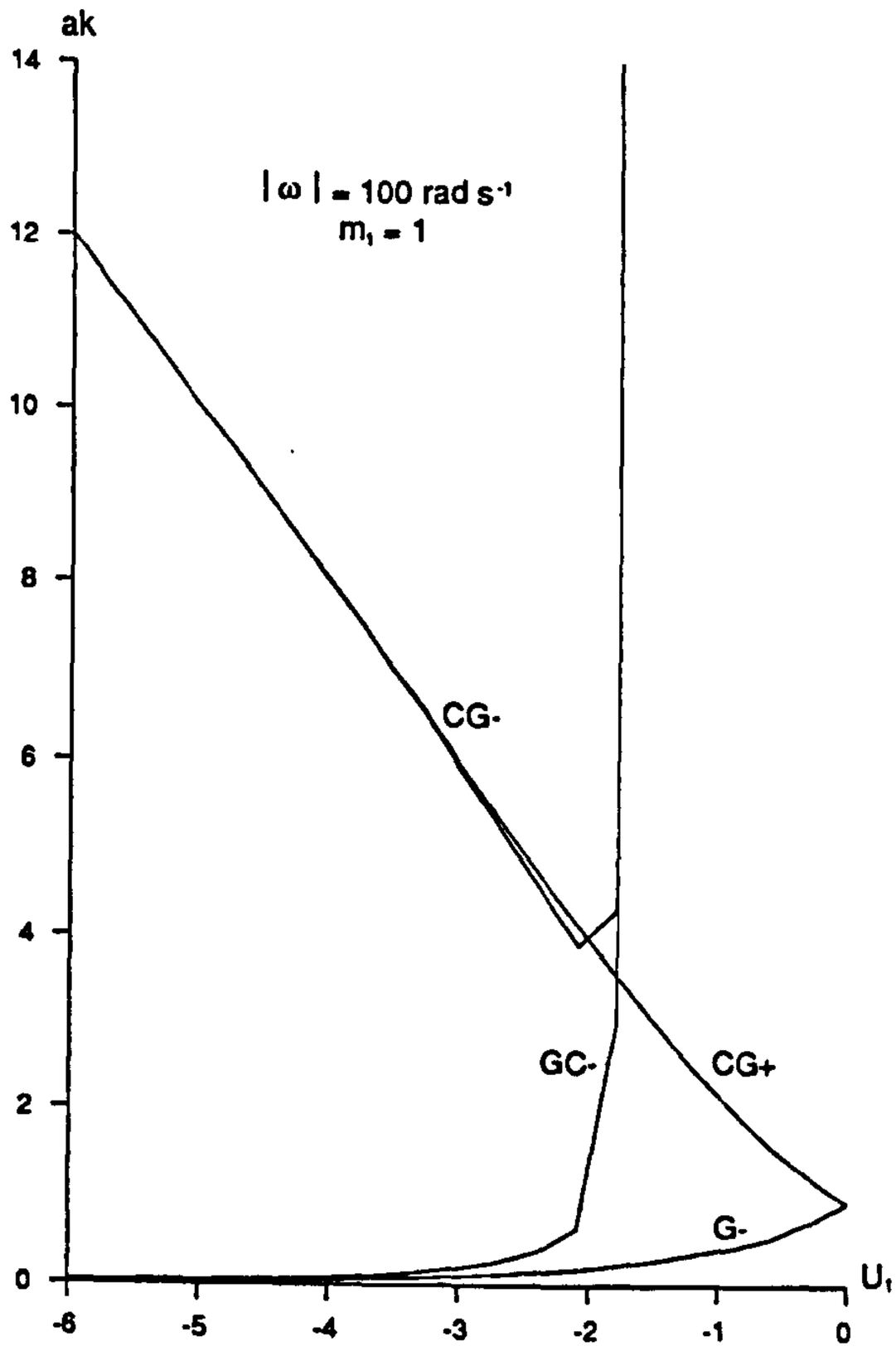

Figure 9.6b

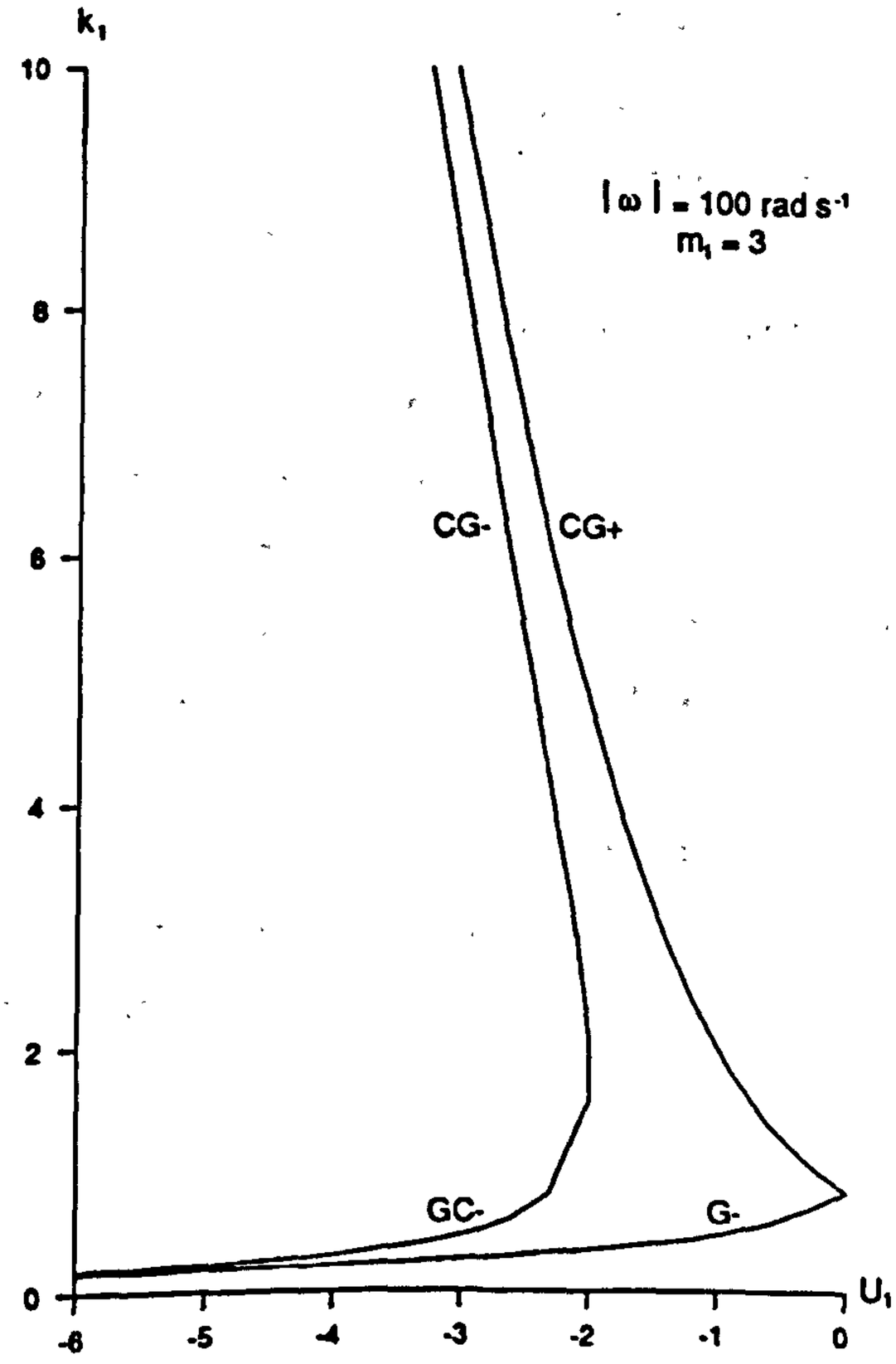

Figure 9.7a

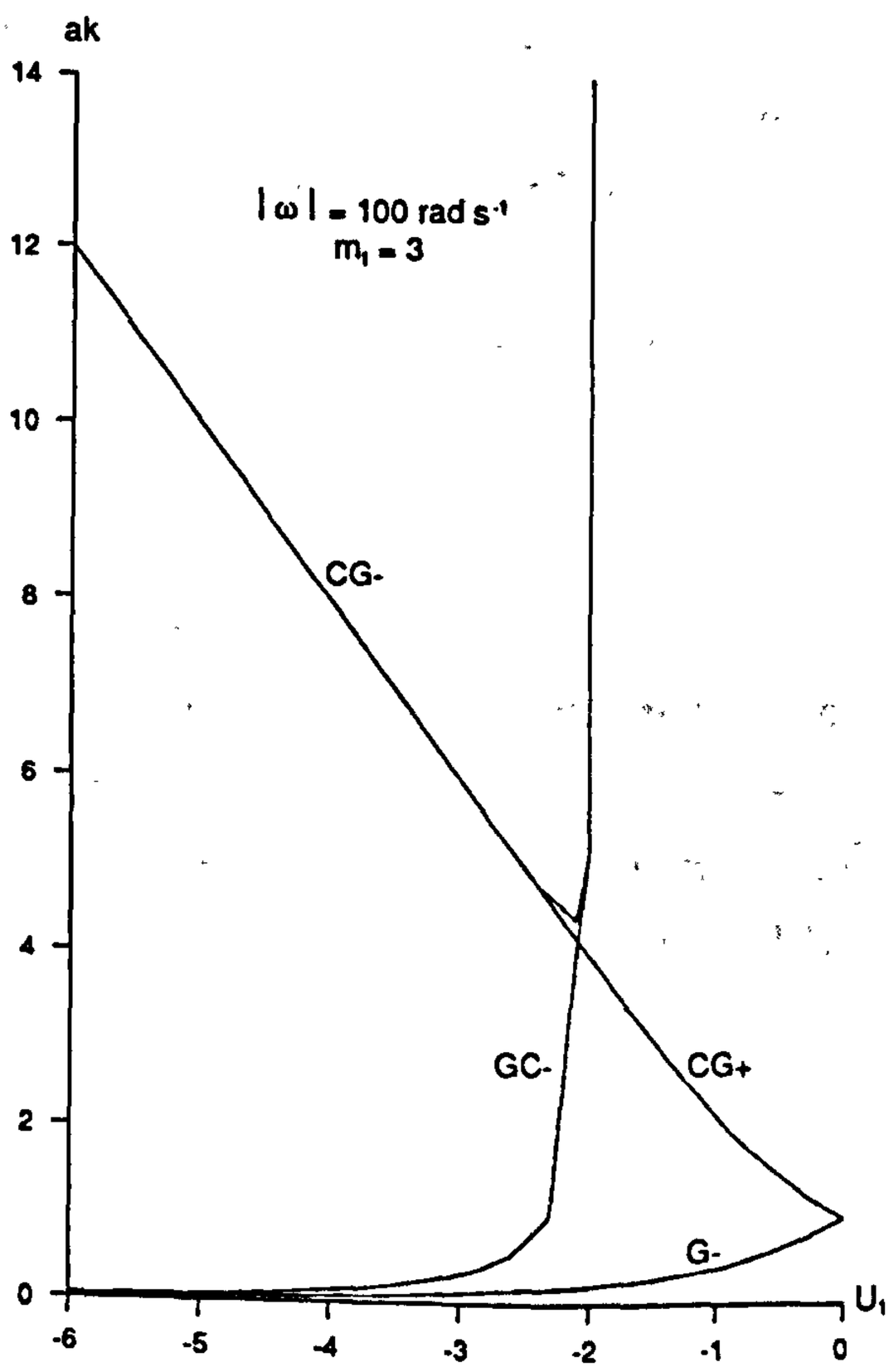

Figure 9.7b

CHAPTER 10
THE NONLINEAR WAVE-CURRENT INTERACTION PROBLEM FOR PURE CAPILLARY WAVES ON FINITE DEPTH LIQUID

10.1 Introduction

In this chapter the wave-current interaction problem is further examined for the case of finite amplitude pure capillary waves. This chapter is, thus, the finite depth version of chapter 4. The symmetric waves solution of Kinnersley (1976) is used. It is shown in chapter 8 that such waves have a variety of behaviour differing from the infinite depth Crapper waves. For instance, these waves can reach a zero trough depth singularity as well as the maximum steepness enclosed bubble singularity. Moreover, the mean properties of these waves experience considerable qualitative changes as the depth of the liquid decreases towards the thin films range.

Our aim is primarily to examine waves which occur far downstream on thin film flows. Previous work on thin film flows, for example Brauner and Moalem-Maron (1983) or as described in section 1.1, uses completely different methods to the slowly-varying approach used here. Our approach gives interesting general finite depth solutions as well as thin film solutions. Our literature searches have not revealed any previous work on the nonlinear finite depth (or thin film) slowly-varying problem. The simplest case to examine is that of stationary waves. This case is considered in detail in order to aid in the general analysis of the phenomena found.

This work is of an exploratory nature and involves the accumulation of several interesting mathematical concepts and ideas. Section 10.2 reintroduces Kinnersley symmetric waves solution and corresponding mean wave properties. All the possible waves are discussed in section 10.3. In section 10.4 the equations for the slowly-varying problem are developed and discussed. Section 10.5 discusses the numerical method of solution. The concept of windows is analysed in section 10.6 along with the limiting "maximum steepness curves". The cases of stationary and Doppler shifted waves are examined in sections 10.8 and 10.9 respectively.

10.2 Wave Parameters and Mean Wave Properties

Exact solutions for progressive pure capillary waves of arbitrary amplitude over finite depths of liquid are found by Kinnersley (1976). For problems in which a bed is present the symmetric (case Ib of Kinnersley) wave solution must be considered. The solution for such waves, as detailed in chapter 8, has origin $z = 0$ on the centreline or bed so that depth h is zero and mean level b is equal to mean depth d. For the purposes of the slowly-varying problems this is not a convenient situation since depth h will vary. Consequently, the origin $z = 0$ is transformed, in the z direction, to an arbitrary position so that depth h is non-zero and mean level b is not equal to mean depth d. Therefore, expression (8.4.13) gives the mean depth d and not the mean level b.

In chapter 8 expressions for wave parameters and mean wave properties are given in terms of the three parameters κ, B and c. It proves convenient to express all wave parameters and mean properties in the form of some function of κ and B multiplied by some integer power of c. From chapter 8

$$T = T(B,\kappa) \ , \quad V = V(B,\kappa) \ , \tag{10.2.1}$$

$$d = F_1(B,\kappa)\ \frac{1}{c^2} \quad \text{and} \quad \overline{u_h^2} = F_2(B,\kappa)\ c^2 \tag{10.2.2}$$

where
$$F_1(B,\kappa) = \frac{s\beta}{2\kappa'^2\theta}\ (2\theta\epsilon + \kappa'^2\beta I_3) \tag{10.2.3}$$

and
$$F_2(B,\kappa) = \frac{\kappa'^4K^2}{\theta^2} + \frac{\kappa'^6}{4\theta^2}\ (\theta I_4 - 2KI_5) \ . \tag{10.2.4}$$

Also
$$k = F_3(B,\kappa)\ c^2 \ , \quad a = F_4(B,\kappa)\ \frac{1}{c^2} \ , \tag{10.2.5}$$

$$t = F_5(B,\kappa)\ \frac{1}{c^2} \quad \text{and} \quad c_p = F_6(\kappa)\ c \tag{10.2.6}$$

where
$$F_3(B,\kappa) = \frac{\tau}{2s\theta}\ \text{ns B dc B} \ , \quad F_4(B,\kappa) = 2s\kappa\ \text{sn B sd B} \tag{10.2.7}$$

$$F_5(B,\kappa) = s\ \text{sn B cd B}\ [(1 + \kappa^2)B - 2E(B) + 2\ \text{sc B(dn B} - \kappa)] \tag{10.2.8}$$

$$F_6(\kappa) = \frac{\kappa'^2K}{\theta} \ . \tag{10.2.9}$$

The crest height H, i.e. the distance of capillary wave crests from the bed, is given from the symmetric waves solution (8.2.2) as $H = z(0,+B)$. It is more easily given as

$$H = t + 2a = (F_5 + 2F_4)\,\frac{1}{c^2}\ . \qquad (10.2.10)$$

Note that

$$\sigma = F_3(B,\kappa)\ F_6(\kappa)\ c^3 \qquad (10.2.11)$$

and that T, V and F_i, where i = 1,2...6, are always positive. Also note that wave steepness $ak = F_3F_4$ and the dimensionless parameter $kt = F_3F_5$ are independent of the velocity variable c.

Substitution of the above expressions for symmetric waves into expressions (2.5.7, 11, 12) for the wave momentum $\mathcal{I}$, the wave-action density $\mathcal{A}$ and the wave-action flux $\mathcal{B}$ in terms of the four basic mean wave properties give

$$\mathcal{I} = \frac{2T}{F_6}\,\frac{1}{c}\ , \quad \mathcal{A} = \frac{2T}{F_3F_6}\,\frac{1}{c^3} \quad \text{and} \quad \mathcal{B} = (6T + \rho F_1F_2)\,\frac{1}{2F_3}\,\frac{1}{c^2} \qquad (10.2.12)$$

as expressions for $\mathcal{I}$, $\mathcal{A}$ and $\mathcal{B}$ in terms of κ, B and c.

Note that as for infinite depth theory there are several possible definitions for the generalised group velocity c_g. However, no detailed discussion is undertaken here. The group velocity c_g for finite amplitude pure capillary waves is again defined as

$$c_g = \frac{\mathcal{B}}{\mathcal{A}} = (6T + \rho F_1F_2)\,\frac{F_6}{4T}\,c = \left[\frac{3}{2} + \frac{\rho F_1F_2}{4T}\right] c_p\ . \qquad (10.2.13)$$

This expression consists of two terms. The first term corresponds to the generalised group velocity for pure capillary waves, linear or nonlinear, on liquid of infinite depth. The second term is the additional term appearing because the depth of liquid is finite. It is remarked in Longuet-Higgins (1975) that the mean depth times the mean bottom velocity squared, i.e F_1F_2, tends to zero as the depth of liquid tends to infinity. So this expression gives the correct limit as the mean depth d tends to infinity.

10.3 The Possible Waves

Recall from chapter 9 that for linear pure capillary waves there is one possible stationary wave, namely wave CG, and there are four possible Doppler shifted waves, namely CG(+,-), GC- and G-. Also, for stationary waves there are no possible caustics and for Doppler shifted waves there is one possible caustic, namely the CG-/GC- caustic. For nonlinear pure capillary waves analytic and physical continuation imply that the same waves can still exist as is the case for infinite depths. However, this is not so easily seen as it is for infinite depths in § 4.2. Thus, a simple analysis is performed in this section to show that this is actually the case. The analysis also allows the parameter c to be related to the waves in both magnitude and sign. This proves to be useful later when solutions are sought.

To do this both the Doppler and dispersion relations, in terms of κ, B and c, are examined. It is supposed that the parameters κ and B take fixed values in the (κ,B)-plane shown in figure 8.1 given by the highest waves criterion of § 8.3. This is equivalent to considering fixed values of mean depth d and amplitude a since, in most instances, κ and B are interpreted as depth and amplitude parameters respectively (see § 8.2).

Using the expression (10.2.5) for wavenumber k the Doppler relation (2.3.1) gives

$$\sigma = \omega - F_3 U c^2 \qquad (10.3.1)$$

as one expression for frequency σ in terms of κ, B and c. A second expression for frequency σ in terms of κ, B and c is given by the "dispersion relation" (10.2.11) which states that $\sigma = F_3F_6c^3$. Note that this expression implies that sgn σ = sgn c.

Figure 10.1 gives a sketch of the possible ways in which the Doppler relation (10.3.1) can intersect the dispersion relation $\sigma = F_3F_6c^3$ in the (c,σ)-plane for fixed values of κ, B and U. This is used, in a similar manner to the (k,σ)-plane sketches in chapter 3, to show all the possible waves. The analysis in the rest of this section refers to this figure. Note that only a sketch is given simply because it is the qualitative characteristics which are required.

Recall that our convention requires that $k \geq 0$ and $U \leq 0$ with $\sigma > 0$ for stationary waves. Thus, for stationary waves $\sigma = F_3F_6c^3$ implies that the parameter $c \geq 0$. Also, for any $U \neq 0$ and c "small" - $F_3Uc^2 > F_3F_6c^3$ and for any $U \neq 0$ and c "large" - $F_3Uc^2 < F_3F_6c^3$ so a sketch of the (c,σ)-plane reveals that there is always one and only one wave

present. This wave must be the stationary wave CG.

For Doppler shifted waves consider the cases $\omega > 0$ and $\omega < 0$ separately. Firstly consider the case $\omega > 0$. For any U and $c \leq 0$ $\omega - F_3Uc^2 > F_3F_6c^3$ so that there are no waves. Also, for any U and c "small" and positive $\omega - F_3Uc^2 > F_3F_6c^3$ and for any U and c "large" and positive $\omega - F_3Uc^2 < F_3F_6c^3$ so a sketch of the (c,σ)-plane reveals that there is always one and only one wave present and it has $c > 0$. Thus, since this wave has both $\omega > 0$ and $c > 0$ this wave must be wave CG+. Note that, as for infinite depths, waves CG+ seems to be qualitatively similar to the stationary waves CG.

Now consider the case $\omega < 0$. Suppose that $c \leq 0$. For any U and $|c|$ "small" $\omega - F_3Uc^2 < F_3F_6c^3$ and for any U and $|c|$ "large" $\omega - F_3Uc^2 > F_3F_6c^3$ so a sketch of the (c,σ)-plane reveals that there is always one and only one wave present and it has $c < 0$. Thus, since both $\omega < 0$ and $c < 0$ this wave must be wave G-. Now suppose that $c \geq 0$. For any U and c both "small" and "large" $\omega - F_3Uc^2 < F_3F_6c^3$. There may, or may not, be a range of c over which $\omega - F_3Uc^2 > F_3F_6c^3$. This depends on the specific values chosen for U and ω. If such a range exists then a sketch of the (c,σ)-plane reveals that two waves exist both having $c > 0$. If no such range exists then a sketch of the (c,σ)-plane reveals that no waves exist. If these waves exist then, since $\omega < 0$ and $c > 0$, they must be the waves CG- and GC-.

The magnitude of c is directly proportional to the magnitude of σ since $\sigma = F_3F_6c^3$. Thus, it is concluded that the one possible stationary waves CG have $c \geq 0$. The possible Doppler shifted waves G- have $c < 0$ and the three possible Doppler shifted waves CG(+,-) and GC- have $c > 0$ with the magnitude of c having the distinct order

$$CG+ > CG- > GC- > G- \quad . \tag{10.3.2}$$

The signs of c and the ordering of the magnitude of c are useful for identifying specific wave solutions when they are found in terms of the parameters κ, B and c as is the case below.

10.4 The Equations

The nonlinear interaction problem is now examined. Our aim is to derive equations for the interaction problem in terms of the three parameters κ, B and c and subsequently solve these equations to find variations of these three parameters. The general equations used are those described in § 9.4 for the linear capillary-gravity wave-current interaction problem.

The dispersion relation for the waves is implicitly contained within the expressions for σ, k, a, d and t in § 10.2. Substituting expressions (10.2.5, 11) for k and σ respectively into the Doppler relation (2.3.1) gives

$$\omega = F_3 F_6 c^3 + F_3 c^2 U \qquad (10.4.1)$$

or

$$U = \frac{\omega}{F_3}\,\frac{1}{c^2} - F_6\, c \qquad (10.4.2)$$

which is an expression for U in terms of κ, B and c.

The equations for the interaction problem are found by substituting appropriate expressions given above into the mass conservation equation (2.7.2) and the wave-action conservation equation (2.7.5). The mass conservation equation (2.7.2) gives

$$m\, c^4 - (\rho F_1 F_6^2 - 2T)\,\frac{1}{F_6}\, c^3 + \frac{\rho\omega F_2}{F_3} = 0 \qquad (10.4.3)$$

and the wave-action conservation equation (2.7.5) gives

$$b\, c^5 - (2T + \rho F_1 F_2)\,\frac{1}{2F_3}\, c^3 - \frac{2\omega T}{F_3^2 F_6} = 0\ . \qquad (10.4.4)$$

The special case of zero total wave-action flux b needs separate consideration. Direct substitution of $b = 0$ leads to slight simplification of the equations but since the equations still involve elliptic functions and elliptic integrals their method of solution is exactly the same as the general case. It is expected that two independent solutions will arise, one corresponding to linear pure capillary waves and the other corresponding to stopped waves. The equations for the linear case are derived by taking the limit $\kappa \longrightarrow 0$ of equations (10.4.3, 4). This is examined below in § 10.7. As for the infinite depth case the equations for the stopped waves are given by dividing out the linear equations from the nonlinear equations (10.4.3, 4). Unfortunately, this is not explicitly possible so that the

equations for the stopped waves are contained within the nonlinear equations (10.4.3, 4) with $b = 0$. The stopped waves are also discussed further below in § 10.7.

Once a solution curve is found in terms of the parameters κ, B and c the variation of wave and mainstream flow parameters such as σ, k, a, d, t, H and U are all found using the appropriate expressions given above. Variations of the mean level b are determined using expression (9.2.2) since γ is taken to be zero, i.e.

$$b = -\frac{1}{2g}\left[\frac{\omega^2}{F_3^2}\frac{1}{c^4} - \frac{2\omega F_6}{F_3}\frac{1}{c} + (F_6^2 + F_2)\,c^2\right] \qquad (10.4.5)$$

with depth $h = d - b$. Note that the acceleration due to gravity g is present in this expression even though the waves are pure capillary waves. This is because the mean level b can be regarded as a property of the mainstream flow which, in the absence of waves, satisfies the shallow water equations (2.6.2). In essence, the mainstream flow is a gravity dominated flow and has zero surface tension so that g appears in an expression for the mean level b.

Wave solutions in the space of κ, B and c with equally distributed numerical solution points will often result in unequally spaced values of wave parameters such as σ, k, a, d, t, H and U. This is due to the nonlinear nature of evaluation of these wave parameters.

The method of derivation, as outlined in § 4.4 for the interaction problem on infinite depth liquid, involves the elimination of U from the equations. For infinite depths one equation (4.4.24) is derived involving two unknowns k and D. The unknown D is then varied over its range and the equation is solved. Here there are two equations (10.4.3, 4) involving three unknowns κ, B and c. These equations are solved by varying one of the three parameters, either κ or B, over its range and finding simultaneous solutions of the two equations for the remaining two parameters.

The range for κ is $0 \le \kappa \le 1$ with $0 \le B \le B_{max}(\kappa)$ and the range for B is $0 \le B \le \infty$ with $0 \le \kappa \le \kappa_{max}(B) \le 1$. The values of $B_{max}(\kappa)$ or $\kappa_{max}(B)$ are given from the results of § 8.3 for highest waves. In essence, solution curves in the (κ,B)-plane are required to remain within the area bounded by the curves $\kappa = 0$, $\kappa = 1$, $B = 0$ and $B = B_{max}(\kappa)$ or, equivalently, $\kappa = \kappa_{max}(B)$ as shown in figure 8.1.

One consequence of the increase in the "dimensionality" of the interaction problem from the infinite depth value of two to the finite depth value of three is that all the equations derived, either for the linear or nonlinear case, are transcendental equations rather than

polynomials so numerical solution of the equations becomes much more difficult. Another consequence is as follows. For fixed ω and different b solution curves for the infinite depth problem can not intersect. This is because an intersection of two, or more, solution curves would imply that the values of k and D at the intersection are the same so that the values of b would have be the same which is a contradiction. The same is true for the finite depth problem when solution curves are shown in a three dimensional space, for instance the space of κ, B and c. However, if solution curves are projected onto a two dimensional space then they may appear to cross.

10.5 Numerical Solution of the Equations

Equations (10.4.3, 4) are transcendental equations and are solved numerically using the standard solver NAG LIB C05NBF. Thus, for particular values of ω, m and b the parameter κ, or B, is fixed to some initial value and simultaneous solutions of (10.4.3, 4) for B, or κ, and c are sought. For this nonlinear interaction problem the initial estimate for the solver needs to be relatively close to the solution.

Once the initial solution point is found the parameter κ, or B, is incremented and the solver used, with initial estimate as the previous solution point, to find solutions for B, or κ, and c. Solutions are tracked in this manner until they reach one of the limiting "borders" of (κ,B)-plane, as shown in figure 8.1 and as described above where the ranges of κ or B are considered, or until they reach B = 10. The reason for the latter condition is that once B is so "large" the range for κ is so small, of the order 10^{-6}, that the numerical solver (NAG LIB C05NBF) finds it virtually impossible to continue tracking the solutions. Also, as $\kappa \longrightarrow 0$ and $B \longrightarrow \infty$ the linear expression for d (appendix E), shows that $d \longrightarrow \infty$ so that $B \geq 10$ corresponds to infinite depth solutions.

Four methods are used for choosing the initial estimates. Some of these are discussed in more detail in sections below but are briefly outlined here. One method is to consider the linear-limit $\kappa \longrightarrow 0$ and use the equations derived for this limit to give an initial estimate. This is only useful when the nonlinear solutions tend towards the linear solutions in some instance. This method works for three of the four possible waves, namely waves CG(+,-) and G-.

A second method is to find windows corresponding to the four possible waves. These are used to give initial estimates for the parameters B, or κ, and c for particular ω, m and b. This method works well for waves CG- when they do not tend towards the linear solutions in

any instance. However, it is mostly used for waves GC-.

A third method is to use the highest waves results of § 8.3 to find those regions in parameter space of ω, m and b for which solutions reach maximum steepness. These then give initial estimates for the parameters B, or κ, and c for particular ω, m and b. Note that the initial point must be situated on the highest waves curve of figure 8.1. This method obviously works well for those waves which reach breaking point. It is used for waves CG- and sometimes waves GC-.

The fourth method is to make estimates based on experience. The above analysis relating the parameter c to the waves is useful here. This method works successfully after some feel is gained for the general behaviour of solution curves and is most used for waves GC-.

10.6 "Windows" and Highest Waves

The question of existence of windows is now examined for finite depths. Suppose that ω and m are fixed. Choose a particular value of κ, or B. The windows for the four waves for this κ, or B, are found by varying B, or κ, over its range $0 \leq B \leq B_{max}(\kappa)$, or $0 \leq \kappa \leq \kappa_{max}(B) \leq 1$, and solving the polynomial (10.4.3) for corresponding ranges of c. Once these windows are found these values of κ, B and c are substituted into equation (10.4.4) to find corresponding ranges of b. An alternative method of finding windows is to reverse the roles of m and b and also equations (10.4.3, 4). Thus, equation (10.4.4) gives the windows for a fixed b and equation (10.4.3) gives the corresponding ranges of m. These two methods are referred to as the "m-fixed" and "b-fixed" methods respectively.

Either of these methods can be used to give initial estimates for the numerical solver. Suppose that particular values of ω, m and b and initial κ, or B, are chosen. Find the windows corresponding to this κ, or B, using either of the m-fixed or b-fixed methods. Then examine the ranges of b or m corresponding to these windows and find those points, if such points exist, at which b or m as given by these ranges is approximately equal to the particular b or m of interest. The closest of these points are then used as initial estimate for the solver.

In § 8.3 the highest waves criterion is explicitly solved for the symmetric (case Ib of Kinnersley) waves. The variation of B_{max} with κ, or κ_{max} with B, resulting from this criterion is shown in figure 8.1. It is noted that the highest waves solution is independent of c. However, for particular values for ω and m or b solutions for c corresponding to the highest waves are found by substituting the highest wave solutions

for κ and B into equations (10.4.3) or (10.4.4) respectively. The solutions for κ, B and c corresponding to the highest waves can then be used to find the values of wave and mainstream flow parameters, such as k, σ, ak, d, b, h, t, H, c_p, c_g and U, on the highest waves using the appropriate expressions given earlier.

Also, these solutions for κ, B and c can be substituted into equations (10.4.4) or (10.4.3) to find corresponding ranges for b or m. These can be used to give initial estimates for the numerical solver in the same manner as for the windows analysis when the initial point has κ and B on the highest waves curve of figure 8.1. Note that these κ, B and c are not solutions of the slowly varying interaction problem. They are one of the limits of solutions.

10.7 The Linear-Limit Equations

Here the linear-limit $\kappa \longrightarrow 0$ of equations (10.4.3, 4) is found. These linear equations are used to give initial estimates for the numerical solver. Comparison of general expressions (10.2.2, 5, 6) with the corresponding linear-limit expressions (appendix E) and use of linear-limit expression for the parameter A in terms of B (appendix E) gives the linear-limits of F_1, F_2, F_3 and F_6 as

$$F_1 \longrightarrow sB \tanh B \ , \quad F_2 \longrightarrow 2\kappa^2 \ , \tag{10.7.1}$$

$$F_3 \longrightarrow \frac{1}{s} \coth B \quad \text{and} \quad F_6 \longrightarrow 1 \ . \tag{10.7.2}$$

Substitution of these linear-limit expressions and the linear-limit expression for the kinetic energy density T (appendix E) into the general nonlinear equations (10.4.3, 4) gives the equations

$$m\,c^4 - sB \tanh B\, c^3 + s^2 \omega B \tanh^2 B = 0 \ . \tag{10.7.3}$$

$$b\,c^5 - \kappa^2 \tanh B\,(\sinh^2 B + B \tanh B)\,c^3 - 2\kappa^2 \sinh^2 B \tanh^2 B = 0 \tag{10.7.4}$$

respectively where only the leading order terms in equation (10.4.3) are retained.

In a nonlinear sense linear waves have zero b. Substitution of $b = 0$ into the linear equation (10.7.4) gives the expected result $\kappa = 0$. Thus, for the nonlinear interaction problem the linear equation (10.7.3) is solved to give the variation of B and c with $\kappa = 0$. These can then be substituted into the linear-limit expressions to find corresponding

variations of wave and mainstream flow parameters. Note that $\kappa = 0$ implies amplitude a = 0 and vice versa as expected.

As mentioned in § 10.5 the linear equations (10.7.3, 4) are useful for finding initial estimates for the numerical solver (NAG LIB C05NBF) used to solve the general nonlinear equations (10.4.3, 4) if the nonlinear solutions tend towards the linear solutions in some instance.

There are two cases to consider. These are stopped waves and general nonlinear waves. It is known that the stopped waves solution joins the linear solution at the linear caustic. Thus, once the linear solution is found from equation (10.7.3) the values of B and c at the caustic are found. These values are then used as the initial estimates and the nonlinear equations (10.4.3, 4) with $b = 0$ solved for some small fixed initial κ, $\kappa = 10^{-6}$ say, to find an initial solution point for the stopped waves. It is found that subsequently incrementing κ towards $\kappa = 1$ is the best method of finding the stopped waves solution.

For general nonlinear waves this method of generating initial estimates is only useful when the parameter B is fixed and simultaneous solutions of the nonlinear equations (10.4.3, 4) for κ and c are sought. Suppose that B is fixed to some initial value. This initial value is usually taken as B = 10 because at such a large value of B the range $0 \leq \kappa \leq \kappa_{max}(B)$ is small and corresponds to linear or near-linear values of κ. Note that near-linear values of κ are acceptable because it is only an initial estimate that is required. The linear equation (10.7.3) is then solved for c. These c and the initial B are then substituted into the linear equation (10.7.4) and values of κ found. If the value of κ is in the range $0 \leq \kappa \leq k_{max}(B)$ then these values of κ, B and c are used as initial estimates. Subsequently incrementing B in a decreasing direction is then employed to find general nonlinear solutions.

At the end of § 8.4 it is mentioned that the simplest way of checking the general expressions derived in that section is to show that the linear-limit of the expressions gives the correct results. A similar analysis is performed in appendix F. The linear mass conservation equation (9.2.4) and the wave-action conservation equation (2.7.5) are used to directly derive the linear interaction problem equations in terms of the parameters κ, B and c using the same method as in § 10.4. It is found that these equations are the same as the linear-limit equations (10.7.3, 4). This demonstrates the consistency of the algebra and equations derived above.

10.8 Stationary Waves

The case of stationary waves is considered first so that, as usual, dimensional units are used. For this case the equations of § 10.4 and § 10.7 considerably simplify as do the expressions of § 10.2. The linear equation (10.7.3) gives

$$c = \frac{S}{m} B \tanh B \qquad (10.8.1)$$

whilst the nonlinear equations (10.4.3, 4) give

$$c = \frac{1}{m} (\rho F_1 F_6^2 - 2T) \frac{1}{F_6} \quad \text{and} \quad c^2 = \frac{1}{b} (2T + \rho F_1 F_2) \frac{1}{2F_3} \qquad (10.8.2)$$

or

$$m^2 F_6^2 (2T + \rho F_1 F_2) - b\, 2F_3 (\rho F_1 F_6^2 - 2T)^2 = 0 \qquad (10.8.3)$$

on elimination of c. The linear equation (10.8.1) shows that

$$c \longrightarrow 0 \qquad \text{as } B \longrightarrow 0 \qquad (10.8.4)$$

$$c \longrightarrow \frac{S}{m} B \qquad \text{as } B \longrightarrow \infty \, . \qquad (10.8.5)$$

For given m and b the single equation (10.8.3) is solved to find solutions for B, or κ, for given values of κ, or B. These solutions are then substituted into the first of equations (10.8.2) to find the corresponding values of c. The second of equations (10.8.2) can also be used recalling that, by our convention, $c > 0$ for waves CG.

The above equations show that $m > 0$ and $b > 0$. Also, there is only one c corresponding to each κ and B so that there is only one possible window with one corresponding range for b or m. This is as expected for waves CG.

The simple form of the above equations allows for the following "transformation concept". Suppose that $m = m_a$, or $b = b_a$, is fixed and that solutions, in terms of the parameters κ, B and c, have been found for different b, or m. Then solutions for another fixed $m = m_b$, or $b = b_b$, and different b, or m, are most easily found using the transformation

$$b \longrightarrow \frac{m_b^2}{m_a^2} b \quad \text{and} \quad c \longrightarrow \frac{m_a}{m_b} c \, , \qquad (10.8.6)$$

or

$$m \longrightarrow \left[\frac{b_b}{b_a}\right]^{\frac{1}{2}} m \quad \text{and} \quad c \longrightarrow \left[\frac{b_a}{b_b}\right]^{\frac{1}{2}} c \, . \qquad (10.8.7)$$

Thus once one solution set for a fixed m, or b, is found solutions sets for other m, or b, are easily found. No such transformation concept exists for Doppler shifted waves.

Generally for any ω, expressions for k, a, d, t and H (§ 10.2) are all proportional to either c^2 or $1/c^2$ - a single power of c. Recall that ak and kt are independent of c. Also, for the case of stationary waves expressions for U and b (§ 10.4) are proportional to c and c^2 respectively - generally for any ω they are a combination of terms proportional to differing powers of c. Therefore, it follows that the qualitative variations of k, a, d, t, H, b, ak and kt with U will be the same for all fixed m, or B. That is, without loss of qualitative generality, one particular fixed m, or B, will be sufficient to show a wave solution set.

However, the qualitative variations of h will differ for different fixed m, or B, since

$$h = d - b = F_1 \frac{1}{c^2} + \frac{1}{2g} (F_6^2 + F_2)\, c^2 \quad . \qquad (10.8.8)$$

This is a minor point since it is easiest to calculate h after d and b are calculated if different solution sets are sought.

Solution sets are presented for fixed m and various b. The value m = 1 kg m^{-1} s^{-1} is chosen without loss of qualitative generality. Results are shown in figures 10.2 for this m and various b. The linear wave solutions (long-dashed lines) and the maximum steepness curves (dash-dot-dash lines), derived as described in § 10.6, are also shown in order to aid interpretation.

Figures 10.2a, b show variations of B and c with κ. These show the trajectories of wave solutions through the space of κ, B and c. It is seen that wave solutions exist for any b. All wave solutions reach maximum steepness as B increases from zero, say. No wave solution reaches $\kappa = 1$ so that no wave solutions reach zero trough depth. For "large" values of b the maximum value of κ reached by wave solutions becomes close to one but never actually reaches one. Thus, trough depths become very small but never zero. Recall that in chapter 8 it is concluded that thin film flows have $\kappa > 0.45$ or $B < 1.45$. Stationary wave solutions enter this region only when b is large, i.e. $b \geq 0.01$ kg m^3 s^{-2}.

Figures 10.2c, d show variations of wavenumber k and steepness ak with current U as given by the trajectories in the space of κ, B and c. The qualitative variations are exactly the same as for the infinite depth case (figures 4.2) when b is small, i.e. $b \leq 0.001$ kg m^3 s^{-2}. When b is large, i.e. $b \geq 0.01$ kg m^3 s^{-2}, different behaviour does exist.

This is not easily seen in the present scale of the figures. However, this is unimportant (for this particular m) since these wave solutions have small wavenumbers, less than 250 m^{-1} say, and are, therefore, always influenced by gravity.

The highest waves steepness curve in figure 10.2d shows that for all $U \lesssim -0.2$ m s^{-1} the maximum steepness is constant and equal to approximately 2.3, the maximum steepness of pure capillary wave on infinite depth liquid. For $U \gtrsim -0.2$ m s^{-1} the highest waves steepness curve is monotonic decreasing with increasing U. It is, therefore, suspected that for $U \lesssim -0.2$ m s^{-1} waves are unaffected by the bed so the bed appears to be at infinity and that finite depth effects probably occur for $U \gtrsim -0.2$ m s^{-1}.

Figure 10.2e shows the variation of the dimensionless parameter kt with current U. Wave solutions with $b \geq 0.0001$ kg m^3 s^{-2} and $b \geq 0.001$ kg m^3 s^{-2} always have $kt < \pi$ and $kt < 0.3$ respectively. Also, for $U > -0.25$ m s^{-1} all wave solutions have $kt < \pi$. Thus, when $U > -0.25$ m s^{-1} all wave solutions are affected by the bed. Moreover, waves solutions with $b \geq 0.0001$ kg m^3 s^{-2} are always affected by the bed. Wave solutions with $b \geq 0.001$ kg m^3 s^{-2} correspond to thin film flows. However, as mentioned above, these thin film wave solutions have wavenumbers corresponding to gravity waves.

It is shown above that solution sets for other values of m will be qualitatively the same as for m = 1 kg m^{-1} s^{-1}. Quantitative differences will occur. Thus, if a different m is chosen then the wavenumbers of the above thin film flow solutions will be scaled to values corresponding to capillary waves. The transformation (10.8.6) together with the expression (10.2.5) for k give the scaling on wavenumbers. Also, from chapter 9 it is known that $m < \tau$ for thin film flows. It follows that m = 0.05 kg m^{-1} s^{-1} is an appropriate value.

Transformation of wave solutions for m = 1 kg m^{-1} s^{-1} to those for m = 0.05 kg m^{-1} s^{-1} is done by, see expression (10.8.6), taking $b \longrightarrow 2.5 \times 10^{-3}\, b$ and $c \longrightarrow 20\, c$. The trajectories of wave solutions through the space of κ, B and c are exactly the same as for m = 1 kg m^{-1} s^{-1} except that c is scaled by 20 and the value of b corresponding to each wave solution is scaled by 2.5×10^{-3}. All wave solutions for m = 0.05 (1.0) kg m^{-1} s^{-1} have $kt < 0.3$ when $b \geq 2.5 \times 10^{-6}$ (0.001) kg m^3 s^{-2} and, thus, correspond to thin film flows.

Figures 10.3a, b show variations of wavenumber k and steepness ak with current U. When b is small, i.e. $b \leq 2.5 \times 10^{-6}$ kg m^3 s^{-2}, wavenumber k monotonically increases as current U decreases from zero, say, until maximum steepness is reached. However, the wavenumbers of

such wave solutions are very high near maximum steepness so that dissipation will have a strong effect. Thus, these wave solutions are not considered further. When b is large, i.e. $b \geq 2.5 \times 10^{-5}$ kg m^3 s^{-2}, wave solutions have a vertical tangent in the (U,k) and (U,ak)-planes. As the current U is decreased from zero, say, each wave solution ceases to exist when a critical velocity, i.e. the velocity at the vertical tangent, is reached and at that velocity the wave solution has neither zero trough depth nor maximum steepness. The only possible conclusion is that each wave solution itself consists of two branches.

One branch reaches maximum steepness "singularity" as U increases from the critical velocity. It is, therefore, called the "thin films singular branch" or simply the "TS-branch". The second branch has lower wavenumbers and steepnesses than the TS-branch. It asymptotes the linear (U,k) and (U,ak) curves for small b and small U, i.e. $b \leq 2.5 \times 10^{-6}$ kg m^{-1}s^{-1}, as U increases from the critical velocity. It never reaches maximum steepness and so remain "regular". Thus, it is called the "thin films regular branch" or simply the "TR-branch".

Wave solutions with large b, i.e. $b \geq 2.5 \times 10^{-4}$ kg m^3 s^{-2}, have wavenumbers which correspond to gravity waves. However, if m is chosen to be smaller than 0.05 kg m^{-1} s^{-1} then these wave solutions would be scaled to have wavenumbers corresponding to capillary waves. Thus, thin film flows, m < τ, always have this two branch characteristic.

Figures 10.3c - g show variations of mean depth d, trough depth t, crest height H, mean level b and depth h with current U. These show that for the TS-branch (TR-branch) the mean depth d, trough depth t and crest height H remain very small (tend to infinity as current U tends to zero from the critical velocity). Indeed, the trough depths near the critical velocity for both branches can not be seen by the naked eye. Figures 10.3f, g aid in forming a visualisation of the actual flow field. The mean level b is always negative simply because the mean Bernoulli constant γ is chosen to be zero. This means that the origin z = 0 is always above the mean level of the waves. The TR-branch has a minimum depth h at some finite non-zero U and has depth h tending to infinity as U increases to zero from the critical velocity.

Schematic diagrams, i.e. figures showing the relative variations of depth h, trough depth t, mean level b and crest height H, for the flow of some of the wave solutions are given. In essence, these involve showing the variations of - h, - h + t, b and - h + H with U. Figures 10.3h, i are schematic diagrams for $b = 2.5 \times 10^{-6}$ and 2.5×10^{-5} kg m^3 s^{-2} respectively. The monotonic decreasing trend in figure 10.3h is qualitatively typical of all wave solutions with

small b, i.e. $b \leq 2.5 \times 10^{-6}$ kg m^3 s^{-2}, through the velocity range (not near zero) for which they exist. The linearity in this figure is due to the nonlinear transformation of equally spaced point in the space of κ, B and c resulting in unequally spaced values of wave parameters. Recall that both these b represent thin film flows.

It is concluded that wave solutions corresponding to stationary waves CG for large m_i, i.e. $m \geq 0.5$ kg m^{-1} s^{-1} say, and any b will always be unaffected by the bed. All wave solutions will behave in the same manner as those for the infinite depth case already studied. Waves CG will experience finite depth and thin film effects if m is small - $m < 0.2$ for thin film effects. Thin film wave solutions with "large" b consist of two branches, the TS and TR-branches, which join at a critical velocity.

At present it is unclear how the transition from the TR-branches to the TS-branches occurs. The actual propagation of waves must involve the wave generation. For a given wave-action flux b waves can only be generated at velocities greater than the critical velocity. If waves the propagate towards the critical velocity it is unclear what happens to the waves when they reach the critical velocity.

However, the general validity of such inviscid wave solutions is dubious. Both physical observations and the infinite depth theory in the first part of this thesis imply that stationary waves CG are strongly affected by wave energy dissipation. It would be expected for dissipative wave solutions to experience a general decrease in total wave-action flux. Consequently, solution curves would effectively pass through a set of inviscid solutions with decreasing b. This would probably remove the presence of these critical velocity positions.

For the infinite depth case the qualitative characteristic of waves CG+ are the same as those of stationary waves CG. Also, waves CG+ have wavenumbers which correspond to pure capillary waves when ω is large. This feature may also possibly exist for finite depths of liquid. A detailed examination of this possibility is undertaken in § 10.9.

10.9 The Doppler Shifted Waves

The case of Doppler shifted waves is now considered so that dimensionless capillary units are used. Note that F_2 and F_6 will remain as they are simply because they themselves are dimensionless. It is seen that there are three parameters for the problem, namely ω_1, m_1 and b_1. The parameters ω_1 and b_1 are defined in § 3.5 and the parameter m_1 is defined by expression (9.6.1). From the linear equation (10.7.4) it is seen that

$$c_1 \longrightarrow 0 \qquad \text{as } B \longrightarrow 0 \qquad (10.9.1)$$

and

$$c_1 \longrightarrow \omega_1 \quad \text{or} \quad c_1 \longrightarrow \frac{B}{m_1} \quad \text{as } B \longrightarrow \infty \,. \qquad (10.9.2)$$

Wave solutions are sought for fixed positive values of total mass flux m_1 and various values of total wave-action flux b_1. It proves interesting to investigate the number of solutions that equations (10.7.3, 10.4.3) possess for fixed m_1. This number is directly related to the number of possible windows. Both these equations are quartics in c_1 so that for fixed values of κ and B there are either four, two or no real roots for c_1. Note that three or one real roots for c_1 are also possible in exceptional circumstances. The cases $\omega > 0$ and $\omega < 0$ are considered separately.

Firstly consider the case $\omega > 0$, i.e. $\omega_1 = +1$, with m_1 taking a fixed positive value. For a fixed value of B the linear equation (10.7.3) always has either two or no real roots for c_1. There are always two positive roots as $B \longrightarrow \infty$, one with a $c_1 \longrightarrow \infty$ and the other with $c_1 \longrightarrow 1$. These correspond to $U_1 \longrightarrow -\infty$ and $U_1 \longrightarrow 0$ respectively. As B decreases from infinity the two roots coalesce at some finite value of B with finite positive c_1. This corresponds to some finite negative value of U_1. Thus, the two roots for c correspond to one linear wave limit. This must be the linear-limit of wave CG+.

For fixed values of κ and B the nonlinear equation (10.4.3) also always has either two or no real roots for c_1. There are always two positive roots for c_1 when κ is small and B is large, i.e. for $0 < \kappa < \kappa_c$ and $B > B_c$ say, and no roots for c_1 when κ is large or B is small, i.e. for $\kappa_c < \kappa < 1$ or $0 < B < B_c$ say. The values of κ_c and B_c decrease and increase respectively with increasing m_1. Thus, there are either two or no nonlinear wave trajectories passing through every point of the (κ,B)-plane. These two trajectories must correspond to waves CG+ with different values of b_1. Note that this implies that for fixed m_1 and κ or B there are either two or no windows with either two or no

corresponding ranges for b_1. Both these windows must corresponding to waves CG+ when they exist.

Now consider the case $\omega < 0$, i.e. $\omega_1 = -1$, with m_1 taking a fixed positive value. For any fixed value of B the linear equation (10.7.3) always has two real roots for c_1. One root has $c_1 < 0$ and the other has $c_1 > 0$ and as $B \longrightarrow \infty$ these roots have $c_1 \longrightarrow -1$ and $c_1 \longrightarrow \infty$ respectively. As $B \longrightarrow 0$ both roots have $c_1 \longrightarrow 0$. The root with $c_1 < 0$ corresponds to the linear-limit of waves G- and the root with $c_1 > 0$ corresponds to the linear-limits of both waves CG- and GC- and, thus, the CG-/GC- caustic.

For any fixed values of κ and B the nonlinear equation (10.4.3) also always has two real roots for c_1. One root is positive and the other negative. Thus, there are two nonlinear wave trajectories passing through every point of the (κ,B)-plane. The one with negative c_1 corresponds to waves G- and the one with positive c_1 corresponds to either waves GC-, waves CG- or the stopped waves. This implies that the waves GC-, CG- and the stopped waves trajectories in the (κ,B)-plane can never cross. It follows that for fixed m_1 and κ or B there are always two windows, one with negative c_1 and the other with positive c_1, with two corresponding range for b_1. These correspond to waves G- and stopped waves, waves GC-, CG- respectively.

Thin film flows require small mass fluxes, i.e. $m < \tau$. Using expression (9.6.1) for m_1 in terms of m it is seen that $m < \tau$ implies $m_1 < (s|\omega|)^{\frac{1}{3}} = 0.25$ for $|\omega| = 200\ s^{-1}$ with s taking the value of water. However, on commencement of these investigations primary interest was focused on waves CG- and GC- because these waves encounter a caustic according to linear wave theory. It was found that small values of m_1 give waves invisible to the naked eye in the neighbourhood of the linear caustic (see below). Larger values of m_1 give waves visible to the naked eye.

Consequently, two cases are considered, namely $m_1 = 1$ and 3, in order to show the general effects of changes in total mass flux m_1. For gravity to have negligible effects $|\omega| > 108\ s^{-1}$ (see § 9.6). If $|\omega| = 200\ s^{-1}$, say, then $m_1 = 1$ and 3 imply that $m = 0.30$ and $0.91\ kg\ m^{-1}\ s^{-1}$ respectively. It is possible for these m_1 to correspond to $m < \tau$ but this would require extremely large frequencies $|\omega|$ which are unrealistic. In fact, these m_1 give solutions for waves G-, CG- and GC- which are affected by the bed on both a general finite depth basis and a thin films basis.

At the end of our investigations it is concluded that small values of m_1, $m_1 < 0.25$ say, should have been considered for waves CG+. This is obvious from what is said above but was not so obvious at the time of

these investigations were conducted. The process of finding wave solutions is very time consuming so that, unfortunately, no such investigation has been undertaken. Solutions of equations (10.7.3, 10.4.3, 4) are found separately for each of the waves CG+, G-, CG-, GC- and the stopped waves.

a. Waves CG+

Solutions for waves CG+ are found by taking $\omega_1 = +1$ and seeking wave solutions with $c_1 > 0$. Figures 10.4 show results for $m_1 = 1$. Figures 10.4a, b show variations of B and c_1 with κ. Wave solutions only exist in the region $0 < \kappa \lesssim 0.1$ and $B \gtrsim 2$, that is $\kappa_c \simeq 0.1$ and $B_c \simeq 2$ (see above discussion on number of possible solutions). Such small values of κ and large values of B imply that wave solutions will be mostly unaffected by the bed - there might be some finite depth effects. All wave solutions reach maximum steepness as B and c_1 increase. No wave solutions reach $\kappa = 1$ so that no wave solutions reach zero trough depth. Note that solutions curves for waves CG+ are in no way qualitatively similar to those for stationary waves CG in the space of κ, B and c_1.

Figures 10.4c, d show variations of wavenumber k_1 and steepness ak with current U_1. These show that wave solutions are, in fact, qualitatively similar to those of waves CG with "small" b and waves CG+ on liquid of infinite depth (figures 4.5). This is surprising considering the marked differences in wave solutions in the space of κ, B and c_1. This is due to the fact that calculations of k_1, ak and U_1 use a highly nonlinear transformation of the variables κ, B and c_1.

It is seen that $U_1 \longrightarrow 0$ as $\kappa \longrightarrow 0$, $B \longrightarrow \infty$ and $c_1 \longrightarrow 1$. Now, since solutions are numerically tracked to B = 10 waves solutions do not actually reach $U_1 = 0$. This is unimportant since the qualitative characteristics are clear and it is obvious that wave solutions would have finite non-zero values of wavenumber k_1 and steepness ak when $U_1 = 0$. Recall that waves CG+ can be regarded as an extension of waves G-, or vice versa, with opposite frequency ω_1 and equal wavenumbers k_1 and steepnesses ak when $U_1 = 0$. Moreover, as mentioned earlier, wave solutions for B > 10 definitely correspond to the infinite depth solutions already studied so that they are not of interest here.

The maximum steepness curve has steepness which is approximately constant at 2.3 for all currents U_1. There is no monotonic decreasing effect as U_1 increases towards zero as there is for the corresponding maximum steepness curve for stationary waves CG. This implies that kt is always greater than π so that waves CG+ never feel the effects of the bed.

Figure 10.4e shows the variations of parameter kt with current U_1. All wave solutions have kt > 0.3. Wave solutions with small b_1, i.e. $b_1 \leq 0.2$, have 1.7 < kt < π for a small range of currents U_1 and are, thus, affected by the bed over these currents. However, these bed effects show no qualitative changes in the variations of wavenumber k_1 or steepness ak with current U_1. Thus, these wave solutions are not considered further.

Figures 10.5 show results for $m_1 = 3$. Figures 10.5a, b show variations of B and c_1 with κ. These show that $\kappa_c \simeq 0.001$ and $B_c \simeq 6.5$. The qualitative variations of B and c_1 with κ are exactly the same as for $m_1 = 1$. This implies and, indeed, it has been shown numerically that the qualitative variations of wavenumber k_1, steepness ak, etc., are all the same as the case $m_1 = 1$ as would be expected since the bed will definitely have no effects on these wave solutions. Note that only two wave solutions are shown for $m_1 = 3$. This is because the tracking of wave solutions becomes very difficult when κ is of the order 10^{-3} and B so large, greater than 6 say.

It is concluded that wave solutions corresponding to waves CG+ for large m_1, i.e. $m_1 \geq 0.5$ say, and any b_1 will always be unaffected by the bed. All wave solutions will behave in the same manner as those for the infinite depth case already studied. Wave CG+ will experience finite depth and thin film effects if m_1 is small - $m_1 < 0.25$, say, for thin film effects. Wave solutions will have the same qualitative characteristics in the space of κ, B and c but will reach values of κ near one and "small" values of B. The general trend in previous chapters is that wave solutions for waves CG+ are qualitatively the same as those of stationary waves CG. Thus, it is expected that TS and TR-branches will exist for thin film flows with "large" b_1.

b. Waves G-

Now consider waves G- so that $\omega_1 = -1$ and wave solutions with $c_1 < 0$ are sought. These waves are not considered when the depth of the liquid is infinite because wavenumbers are so small that the effects of gravity become important. For the infinite depth problem a specific value for ω is chosen for the conversion of surface data of pure gravity waves to capillary units. No such choice on ω is needed here because no gravity flow is specified ab initio. Thus, if large values of ω are chosen the corresponding dimensional wavenumbers will always be those of pure capillary waves. In any case these prove interesting because they show finite depth and thin film effects.

It is found that wave solutions for $m_1 = 3$ are all qualitatively similar to those for $m_1 = 1$. There are some quantitative and maximum

steepness curve differences but these are not physically relevant. Results are shown in figures 10.6 for $m_1 = 1$. Figures 10.6a, b show variations of B and c_1 with κ. Wave solutions with small b_1, e.g. $b_1 \leq 0.2$, reach $\kappa = 1$ with $B < \pi/4$ as κ increases from zero so that such wave solutions reach a position where trough depth t_1 is zero. Wave solutions with large b_1, e.g. $b_1 \geq 0.6$, reach maximum steepness as κ increases from zero.

Figures 10.6c, d show variations of wavenumber k_1 and steepness ak with current U_1. All the wave solutions shown have a critical velocity position and, thus, consist of two branches. One branch reaches the singularities of either zero trough depth or maximum steepness as U_1 increases from the critical velocity and is, thus, an S-branch. The second branch has lower wavenumbers and steepnesses than the S-branch. It never reaches maximum steepness or zero trough depth and so remains "regular". It is, thus, called the "regular-branch" or "R-branch".

The R-branch has finite non-zero wavenumber k_1 and steepness ak when $U_1 = 0$. Moreover, $U_1 \longrightarrow 0$ for the R-branch as $\kappa \longrightarrow 0$, $c_1 \longrightarrow -1$ and $B \longrightarrow \infty$ so $U_1 = 0$ is not actually reached. As stated above waves G- can be regarded as an extension of waves CG+. Again, this is unimportant since wave solutions for $B > 10$ corresponds to the infinite depth solutions already studied so that they are not of interest here. This latter observation and the fact that wave solutions for waves CG+ with $B_1 > 1.45$, say, are unaffected by the bed imply that the R-branch will also be unaffected by the bed. Also, the critical velocity and, thus, the S-branch must be result of bed effects. If this is the case then the R-branches must be affected by the bed near the critical velocity.

Figures 10.6e shows the variations of parameter kt with current U_1. The S-branch always has $kt < 0.3$ and is, thus, a thin films branch or, simply, a TS-branch. The R-branch has $kt < 0.3$ near the critical velocity and generally has $kt < \pi$ except when current U is close to zero. This branch is, thus, generally a finite/infinite depth branch rather than a thin films branch. It is, thus, called the "finite/infinite depth regular branch" or the "FIR-branch".

The qualitative variations of trough depth t_1 with current U_1 are the same as those of parameter kt. Also, the qualitative variations of mean depth d_1, as shown in figure 10.6f, and crest height H_1 are the same. Schematic diagrams for the cases $b_1 = 0.2$, 0.6 are given in figures 10.6g, h. Recall that when $b_1 = 0.2$ and 0.6 the TS-branch reaches zero trough depth and maximum steepness respectively. Thus, figure 10.6g and h are typical of all wave solutions with $b_1 \leq 0.2$ and $b_1 \geq 0.6$ respectively. It is noted that in calculating the mean

level b_1 and, thus, the depth h_1 it becomes necessary to choose a specific value for dimensionless gravity g_1. Now, different g_1 give different quantitative variations but the same qualitative variations of b_1 and h_1. So, without loss of qualitative generality, g_1 is chosen to be one.

It has been shown numerically that the qualitative characteristics of wave solutions for all m_1 in the space of κ, B and c_1 are the same. That is, the $\omega < 0$ Doppler shifting causes the general characteristics of wave solutions for all m_1 to be the same. It is, therefore, concluded that wave solutions for waves G- will always consist of two branches - a TS-branch and a FIR-branch. It is, thus, shown that the $\omega < 0$ Doppler shifting of the stationary wave CG results in the existence of thin film and general finite depth flows for large mass fluxes m_1.

c. Waves CG-

Now consider waves CG- so that $\omega_1 = -1$ and wave solutions with "large" $c_1 > 0$ are sought. Results are shown in figures 10.7, 8 for $m_1 = 1, 3$ respectively. Figures 10.7a, b show variations of B and c_1 with κ. It is seen that there exists a nonlinear wave solution for $b_1 = 0$ - the stopped waves solution (short-dashed lines). It intersects the linear waves solution $\kappa = 0$ at the caustic and ceases to exist when $\kappa = 1$ and $B = 0$ where both the trough depth t_1 and amplitude a_1 are zero. It never intersects the maximum steepness curve so that the stopped waves never break. Generally, wave solutions only exist for $b_1 \leq 0.20$. Wave solutions for small b_1, i.e. $b_1 \leq 0.07$, reach maximum steepness at one end and zero trough depth at the other.

Wave solutions for large b_1, i.e. $b_1 \geq 0.08$, have two separate branches. One branch ($0.08 \leq b_1 \leq 0.15$) reaches maximum steepness at both ends. The other branch ($0.08 \leq b_1 \leq 0.2$) reaches zero trough depth at one end and either maximum steepness or again zero trough depth at the other. Thus, both these branches are S-branches. The behaviour of all wave solutions in the (κ, c_1)-plane is qualitatively the same as that in the (κ, B)-plane.

Figures 10.7c, d show variations of wavenumber k_1 and steepness ak with current U_1. The stopped waves solutions has a critical velocity position and so consists of two branches. This feature is not present for infinite depths and so must be a result of bed effects. Also, for infinite depths the stopped waves solution reaches maximum steepness (figures 4.6) which is not the case here. It is, therefore, suspected that both branches of the stopped waves solution will be affected by the bed.

Wave solutions with small b_1, i.e. $b_1 \leq 0.07$, have a critical velocity and, thus, also consist of two branches. One branch reaches maximum steepness whilst the other branch reaches zero trough depth as U_1 decreases from the critical velocity. Thus, both these branches are also S-branches. The two branches of wave solutions for large b_1, i.e. $b_1 \geq 0.08$, have no critical velocities. One branch has a minimum non-zero steepness at some finite current U_1.

The maximum steepness curve has a constant steepness of approximately 2.3 for $U_1 \leq -3$. This is not actually shown in the figure. So wave solutions in the region $U_1 < -3$ will probably be unaffected by the bed. Thus, wave solutions for any non-zero b_1 generally comprise of two S-branches. One branch exists only for $b_1 \leq 0.15$ whilst the other only for $b_1 \leq 0.20$.

Figures 10.7e shows the variation of parameter kt with current U_1. It is seen that one branch has very small (< 0.05) values of parameter kt and is, thus, a thin films branch or a TS-branch. The other branch has kt increasing as U_1 decreases from the critical velocity (if it exists). Nevertheless, it is found that $kt < \pi$ except when b_1 is small, i.e. $b_1 < 0.06$, so that this is mostly influenced by the bed. It is, thus, a FIS-branch. The actual trough depth t_1 for the TS-branch itself remains less than 0.03 and its general variations are qualitatively the same as those of the parameter kt.

Schematic diagrams for the cases $b_1 = 0.07$, 0.1 for the FIS-branch and $b_1 = 0.07$, 0.1, 0.2 (0.1 gives maximum steepness at one end whilst 0.2 gives zero trough depth at both ends) for the TS-branch are given in figures 10.7f, g and f, h, i respectively. A schematic diagram for the stopped waves branch is given in figure 10.7j. Note that the monotonic decreasing characteristic of depth - h_1, etc., as current U_1 decreases continues until trough depth t_1 is zero at $U_1 \simeq -78$. Also, the curves for $-h+t$, $-h+d$ and $-h+H$ meet at a single point corresponding to the linear caustic.

Figures 10.8a, b show variations of B and c with κ. These show that the stopped waves solution has two distinct branches. One branch intersects the linear waves solution $\kappa = 0$ at the caustic and reaches maximum steepness - clearly a FIS-branch. The other branch goes from the point $\kappa = 1$ and $B = 0$, where both the trough depth t_1 and steepness ak are zero, and reaches maximum steepness - clearly a TS-branch. Generally, all wave solutions also consist of two distinct branches. One is a FIS-branch whilst the other is a TS-branch. Again, the FIS-branch only exists for $b_1 \leq 0.15$. However, the TS-branch exists for $b_1 \leq 0.30$. Again, the behaviour of all wave solutions in the (κ, c_1)-plane are qualitatively the same as those in the (κ, B)-plane.

Figures 10.8c, d show variations of wavenumber k_1 and steepness ak with current U_1. The qualitative variations of wavenumber k_1 and steepness ak for the FIS-branch are exactly the same as those of infinite depth solutions (figures 4.6). Also, the maximum steepness curve has a constant steepness of approximately 2.3 for $U_1 \leq -1.6$. Thus, since the FIS-branch only exists for such currents, it is suspected that there are no bed effects on this branch.

Figures 10.8e show the variation of parameter kt with current U_1. The TS-branch has very small values of parameter kt - they can not be seen on the scale shown. The FIS-branch does have $kt < \pi$ over a small range of currents U_1 so that this is mostly uninfluenced by the bed. The actual trough depth t_1 for the TS-branch itself remains less than 0.0045 and its general variations are qualitatively the same as those of the parameter kt.

Schematic diagrams for the cases $b_1 = 0.1$ for the FIS-branch and $b_1 = 0.06$, 0.3; (0.06 gives maximum steepness at one end whilst 0.3 gives zero trough depth at both ends) for the TS-branch are given in figures 10.8f and g, h respectively. Schematic diagram for FIS and TS-stopped waves branches are given in figure 10.8i, j. Again, for the FIS-stopped waves branch, the curves for $-h+t$, $-h+d$ and $-h+H$ meet at a single point corresponding to the linear caustic position.

From figures 10.7a, 8a it is seen that the value of B at which the stopped waves solution meets the line $\kappa = 0$ (the caustic point) for the case $m_1 = 1$ is less than that for the case $m_1 = 3$. This is generally true: the B value at the caustic decreases with decreasing mass flux m_1. Thus, it is clear that small m_1, $m_1 < 0.25$ say, will give small B value at the caustic. Waves with small B values can not be seen by the naked eye. Nevertheless, it has been shown numerically that the qualitative variations of wave solutions for all m_1 in the space of κ, B and c_1 are the same as either $m_1 = 1$ or 3 when $\omega < 0$. Thus, $m_1 = 1$, 3 are enough to show the general behaviour of waves with such ω.

It is concluded that in general solutions for waves CG- consist of two branches - the TS and FIR-branches. For small m_1, i.e. $m_1 \leq 1$, and "small" b_1 both branches meet at a critical velocity. For small m_1, i.e. $m_1 \leq 1$, and "large" b_1 both the branches are disjoint as they are for large m_1, i.e. $m_1 \geq 3$, and any b_1. The FIR-branch stops feeling the effects of the bed as m_1 increases. In contrast, the TS-branch has decreasing trough depths as m_1 increases.

d. Waves GC-

Now consider waves GC- so that $\omega_1 = -1$ and wave solutions with "small" $c_1 > 0$ are sought. Results are shown in figures 10.9, 10 for $m_1 = 1, 3$ respectively. Figures 10.9a, b show variations of B and c with κ. Wave solutions are closed orbits which only exist for $b_1 \geq -0.12$. No wave solutions reach either maximum steepness or zero trough depth so that all wave solutions are "regular". The presence of closed orbits in the (κ,B) and (κ,c_1)-planes implies that wave solutions in all other planes will also be closed. Note that the maximum steepness curves are not shown.

Figures 10.9c, d show variations of wavenumber k_1 and steepness ak with current U_1. All wave solutions have two critical velocity positions as expected from closed solution curves. All wave solutions, thus, consist of two R-branches. Neither of these branches reach maximum steepness which is not the case for infinite depths (figures 4.6). It is, therefore, suspected that both branches will be affected by the bed.

Figures 10.9e shows the variation of parameter kt with current U_1. It is seen that all wave solutions have $kt < \pi$. One branch has $kt < 0.3$ for large b_1, i.e. $b_1 \leq -0.04$. The other branch always has $kt < 0.3$. Thus, the majority of wave solutions for both branches are thin film solutions. So, one branch is a TR-branch whilst the other is a FTR-branch. The qualitative characteristics of trough depth t_1 are the same as those of the parameter kt. Schematic diagrams for the case $b_1 = -0.04$ are given in figures 10.9f and represents both TR and FTR-branches.

Figures 10.10a, b show variations of B and c_1 with κ. It is seen that the most striking difference between wave solutions for $m_1 = 1$ and 3 is in their breaking properties. Wave solutions for $m_1 = 3$ (1) can (not) break. Whether solutions for a given m_1 can or can not break is most easily deduced by consideration of the relative positions of the stopped waves solution curve and the maximum steepness curve. If the stopped waves solution curve does (not) intersect the maximum steepness curve then waves GC- can (not) break as is the case for $m_1 = 3$ (1). This is most easily seen from figure 10.10a (10.9a).

Wave solutions for small b_1, i.e. $b_1 \geq -0.3$, reach maximum steepness at two positions and so are S-branches. Wave solutions for large b_1, i.e. $b_1 \leq 0.4$, are closed orbits which exist for $b_1 \geq -0.55$ and so are R-branches. These latter wave solutions are, therefore, similar to those for $m_1 = 1$. So it is seen that wave solutions can break but can not reach zero trough depth.

Figures 10.10c, d show variations of wavenumber k_1 and steepness ak with current U_1. These show that the stopped waves solution branches now have no critical velocity positions. All wave solutions for small b_1, i.e. $b_1 \geq -0.3$, have only one critical velocity whereas wave solutions for large b_1, i.e. $b_1 \leq -0.4$, have two critical velocities. Thus, all wave solutions consist of two branches. Both branches reach maximum steepness when b_1 is small, e.g. $b_1 \geq -0.3$, and neither branches reach maximum steepness when b_1 is large, i.e. $b_1 \leq -0.4$.

The maximum steepness curve has a maximum steepness of approximately 2.3 for $U_1 \lesssim -1.75$ and is monotonic decreasing with increasing U_1 for $U_1 \gtrsim -1.75$. Now, when all wave solutions, including the stopped waves solution, reach breaking they intersect the maximum steepness curve along the monotonic decreasing part. It would follow that the effects of the bed are felt by both branches. However, the qualitative variations of wavenumber k_1 for one of the branches when b_1 is small, i.e. $b_1 \geq -0.3$, is the same as for infinite depths (figures 4.6) in the vicinity of maximum steepness. So it seems that the effects of the bed are not felt qualitatively for this branch in this region.

Figures 10.10e show the variation of parameter kt with current U. It is seen that all wave solutions have $kt < \pi$. One branch has $kt < 0.3$ for large b_1, i.e. $b_1 \leq -0.3$. The other branch always has $kt < 0.3$. Thus, one branch is a TRS-branch whilst the other is a FRS-branch. The qualitative characteristics of trough depth t_1 are the same as those of the parameter kt. Schematic diagrams for the case $b_1 = -0.06$ are given in figures 10.10f and represents both branches.

Recalling that $m_1 = 1, 3$ are enough to show the general behaviour of waves GC- the following conclusions are made. General solutions for waves GC- consist of two branches. One is a T-branch whilst the other is a F-branch. For small m_1, i.e. $m_1 \leq 1$, the T and F-branches are actually TR and FTR-branches. For large m_1, i.e. $m_1 \geq 3$, the T and F-branches are actually TRS and FRS-branches. Thus, the occurrence of wave breaking increases as m_1 increases. Also, the effects of the bed become increasingly less important on the F-branch as m_1 increases.

10.10 Discussion

Inviscid theory shows that stationary waves CG have two branches of wave solutions when the bed has a strong influence on the flow. These occur for thin film flows with "large" wave-action fluxes. The two branches meet at a critical velocity. The Doppler shifted waves CG+ have only been investigated for "large" values of dimensionless mass flux m_1 for which wave solutions are the same as those for infinite depths of liquid discussed earlier in this thesis. The general trend of these waves is to exhibit the same qualitative behaviour as the stationary waves CG. It is, therefore, felt that these waves will also give two branches of wave solutions for thin film flows, i.e. flows in which m_1 is "small" - less than 0.25 say.

The Doppler shifted waves G-, CG- and GC- give two branches of wave solutions for any m_1. One branch is a thin films branch whilst the other branch is a finite/infinite depth branch. For waves G- and CG- the effect of the bed on the thin films (finite/infinite depth) branch increases (decreases) with increasing m_1. For waves GC- the thin films branch becomes a thin films/finite depth branch with increasing m_1. One branch always tends towards the infinite depth solutions as m_1 increases. Like the stationary waves CG, pairs of solutions branches for the Doppler shifted waves meet/originate at critical velocities.

The existence of these critical velocities is not yet understood. It is felt that detailed investigation of the actual flow field, perhaps along the lines of the schematic diagrams given above, may lead to explanations for such velocities. On the other hand the inviscid approximation is not entirely realistic. The addition of viscous effects on the flow would almost certainly result in a deeper understanding of the actual behaviour of such flows and lead to corresponding physical explanations. This is certainly the case in the first part of this thesis.

There are two leading order viscous effects. Firstly, the wave motion results in a oscillating Stokes type boundary layer at the bed. This boundary layer will either result in wave energy dissipation or perhaps even wave energy addition. Sarpkaya (1957) demonstrates that waves can be amplified as a result of the presence of a current and a bed. Secondly, the viscous shear from the bed results in a vorticity distribution through the flow. This vorticity distribution develops over a distance of many wavelengths and for a steady flow corresponds to a Poiseuille flow. This vorticity is likely to be most important in the "inviscid" effect of vorticity on the waves. Inviscid (constant) vorticity effects on steep, steady gravity waves on water of finite

depth are described by Teles da Silva and Peregrine (1988). These would probably only quantitatively change results shown here.

Many naturally occurring thin film flows have such viscous effects. For example, waves on an inclined plane. A kinematic wave model for such a flow is as follows. The continuity equation (2.2.1), with U = 0, gives

$$\rho \frac{\partial b}{\partial t} + \frac{\partial I}{\partial x} = 0 \quad \text{with} \quad I = \rho Q = \frac{\rho^2 g \cos \alpha}{3\mu} b^3 \qquad (10.10.1)$$

where d = b since h = 0, Q is the volume flux of liquid across a plane normal to the flow (per unit width) and α is the angle between the inclined plane and the vertical (see Batchelor, expression 4.2.13, note that his h equals our b). This gives

$$\frac{\partial b}{\partial t} + \frac{\rho^2 g \cos \alpha}{\mu} b^2 \frac{\partial b}{\partial x} = 0 \ . \qquad (10.10.2)$$

Solutions are readily found using the method of characteristics (see Whitham 1974 for general solution method). These show that the forward facing slopes of waves continually steepen. This steepening implies that the simple kinematic approximation fails. The corresponding example in turbulent flow gives roll waves.

For thin enough films the structure of steep wavefronts becomes dominated by capillary action. Also, when viewed from a reference frame moving with the waves, the bulk of liquid prior to the steep leading edges is stationary . If no wave breaking occurs then it is observed that this stagnant liquid causes the generation of a train of capillary waves in front of the gravity driven kinematic waves. Frequently, the first of the waves generated has a trough very close to, if not quite touching, the bed. Note that this implies that there is little motion present in the bulk of the liquid of this wave as is the case for Kinnersley's symmetric waves with κ near one - most of the motion occurs near wave troughs. These capillary waves experience "global (large) scale" wave energy dissipation. Thus, it may be possible to model the flow of these capillary roll waves using the slowly-varying approximation and Kinnersley's symmetric waves solution. The whole flow could then be modelled by "locally" matching, i.e. on the scale of a quarter of a wavelength say, the slowly-varying capillary wave flow with a hydrostatic gravity-capillary profile. Perhaps this could be related to the deep water gravity-capillary solitary wave solution described by Longuet-Higgins (1989).

The inclusion of energy dissipation (addition) or vorticity effects is not a trivial task. The modelling of such viscous effects is a major project in its own right. It is easier to consider the flow in a sheet of liquid as given, for example, by a vertically falling thin sheet. The effects of dissipation on such a flow are given in the same way as in chapter 5 for infinite depth liquids. Thus, the dissipation term $\mathcal{D}$ is given using expression (5.2.5). For Kinnersley's symmetric waves the expressions in chapter 8 give

$$\mathcal{D} = - \frac{\mu}{\lambda} c^2 \int_0^{4K} \frac{\partial}{\partial \psi} (q^2) \Big|_{\psi=B} d\phi \ , \qquad (10.10.3)$$

but since $$\frac{\partial q}{\partial \psi} = \frac{1}{2A} (1 - q^2) \quad \text{and} \quad q = \frac{1 - \alpha \ cd \ \phi}{1 + \alpha \ cd \ \phi} \qquad (10.10.4)$$

it follows that $$\mathcal{D} = \frac{\mu \kappa'^2 \alpha c^4}{s\theta} I_6 \qquad (10.10.5)$$

where $$I_6 = \int_0^{4K} \frac{cd \ \phi \ (\alpha \ cd \ \phi - 1)}{(\alpha \ cd \ \phi + 1)^3} d\phi \ . \qquad (10.10.6)$$

The addition of such dissipation and parallel acceleration ($g_p = g$, $g_v = 0$ if x-axis is downward and z-axis horizontally rightwards) effects to the slowly-varying equations of chapter 2 are described in chapter 7. It is seen that either the modified averaged equations or Whitham's equations must be used. These require the calculation of the mean rate of momentum transfer Σ given by expression (7.4.1) or, more appropriately, (7.4.13). It is not a difficult task to derive this term for Kinnersley's symmetric waves. The term itself is rather long and consists of a sum of terms involving many different integrals, similar in form to those already encountered, and so is not given here.

The presence of three unknowns, namely κ, B and c, requires the use of three equations - the mass, momentum and energy conservation equations say. Three ordinary differential equations have been derived from these equations for the steady-state problem. The algebra involved in deriving these is very long and tedious. This is essentially because the derivatives of elliptic functions, integrals and mean wave properties causes the appearance of many long and complex expressions involving a large quantity of integrals of the type $I_1 - I_6$. Note that the mass flux $\rho U d + I$ is still constant but is best expressed in the form of a differential equation. The equations are not presented here.

An attempt has been made to solve these equations using several standard solvers from the NAG library of routines. However, although integration was achieved, no sensible solutions were obtained. This maybe due to "bugs" present in the program or to the complex nature of

terms involved in the equations. To overcome this latter feature of the problem it may be better to devise an integrating scheme designed specifically for these equations rather than use a standard solver. This dissipative study was abandoned for lack of time. Results to this problem would hopefully lead to further understanding.

CAPTIONS FOR FIGURES

Figure 10.1: Diagram illustrating the possible existence of stationary waves CG and Doppler shifted waves CG(+,-), GC- and G-.

Figure 10.2: The variation of parameters (a) B and (b) c with κ; and (c) wavenumber k, (d) steepness ak and (e) parameter kt with current U for stationary waves with mass flux m = 1 kg m^{-1} s^{-1}; various wave-action fluxes b as shown.

Figure 10.3: The variation of (a) wavenumber k, (b) steepness ak, (c) mean depth d, (d) trough depth t, (e) crest height H, (f) mean level b and (g) depth h with current U for stationary waves with mass flux m = 0.05 kg m^{-1} s^{-1}; various wave-action fluxes b as shown. The variations of parameters B and c with κ are given by figures 10.2a, b with c and wave-action flux b scaled by 20 and 2.5 x 10^{-3} respectively.

Also, the schematic diagrams for stationary waves with mass flux m = 0.05 kg m^{-1} s^{-1} and wave-action fluxes b equal to (h) 2.5 x 10^{-6} and (i) 2.5 x 10^{--5} kg m^3 s^{-2}.

Figure 10.4: The variation of parameters (a) B and (b) c_1 with κ; and (c) wavenumber k_1, (d) steepness ak and (e) parameter kt with current U_1 for waves CG+ with mass flux m_1 = 1; various wave-action fluxes b_1 as shown.

Figure 10.5: The variation of parameters (a) B and (b) c_1 with κ for waves CG+ with mass flux m_1 = 3; various wave-action fluxes b_1 as shown.

Figure 10.6: The variation of parameters (a) B and (b) c_1 with κ; and (c) wavenumber k_1, (d) steepness ak, (e) parameter kt and (f) mean depth d_1 with current U_1 for waves G- with mass flux m_1 = 1; various wave-action fluxes b_1 as shown.

Also, the schematic diagrams for waves G- with mass flux m_1 = 1 and wave-action fluxes b_1 equal to (g) 0.2 and (h) 0.6.

Figure 10.7: The variation of parameters (a) B and (b) c_1 with κ; and (c) wavenumber k_1, (d) steepness ak and (e) parameter kt with current U_1 for waves CG- with mass flux m_1 = 1; various wave-action fluxes b_1 as shown.

Also, the schematic diagrams for waves CG- with mass flux m_1 = 1 and wave-action fluxes b_1 equal to (f) 0.07, (g,h) 0.1, (i) 0.2 and (j) 0.

Figure 10.8: The variation of parameters (a) B and (b) c_1 with κ; and (c) wavenumber k_1, (d) steepness ak and (e) parameter kt with current U_1 for waves CG- with mass flux m_1 = 3; various wave-action fluxes b_1 as shown.

Also, the schematic diagrams for waves CG- with mass flux m_1 = 3 and wave-action fluxes b_1 equal to (f) 0.1, (g) 0.06, (h) 0.3 and (i,j) 0.

Figure 10.9: The variation of parameters (a) B and (b) c_1 with κ; and (c) wavenumber k_1, (d) steepness ak and (e) parameter kt with current U_1 for waves GC- with mass flux m_1 = 1; various wave-action fluxes b_1 as shown.

Also, the schematic diagrams for waves GC- with mass flux m_1 = 1 and wave-action flux b_1 equal to (f) - 0.04.

Figure 10.10: The variation of parameters (a) B and (b) c_1 with κ; and (c) wavenumber k_1, (d) steepness ak and (e) parameter kt with current U_1 for waves GC- with mass flux $m_1 = 3$; various wave-action fluxes b_1 as shown.

Also, the schematic diagrams for waves GC- with mass flux $m_1 = 3$ and wave-action flux b_1 equal to (f) - 0.06.

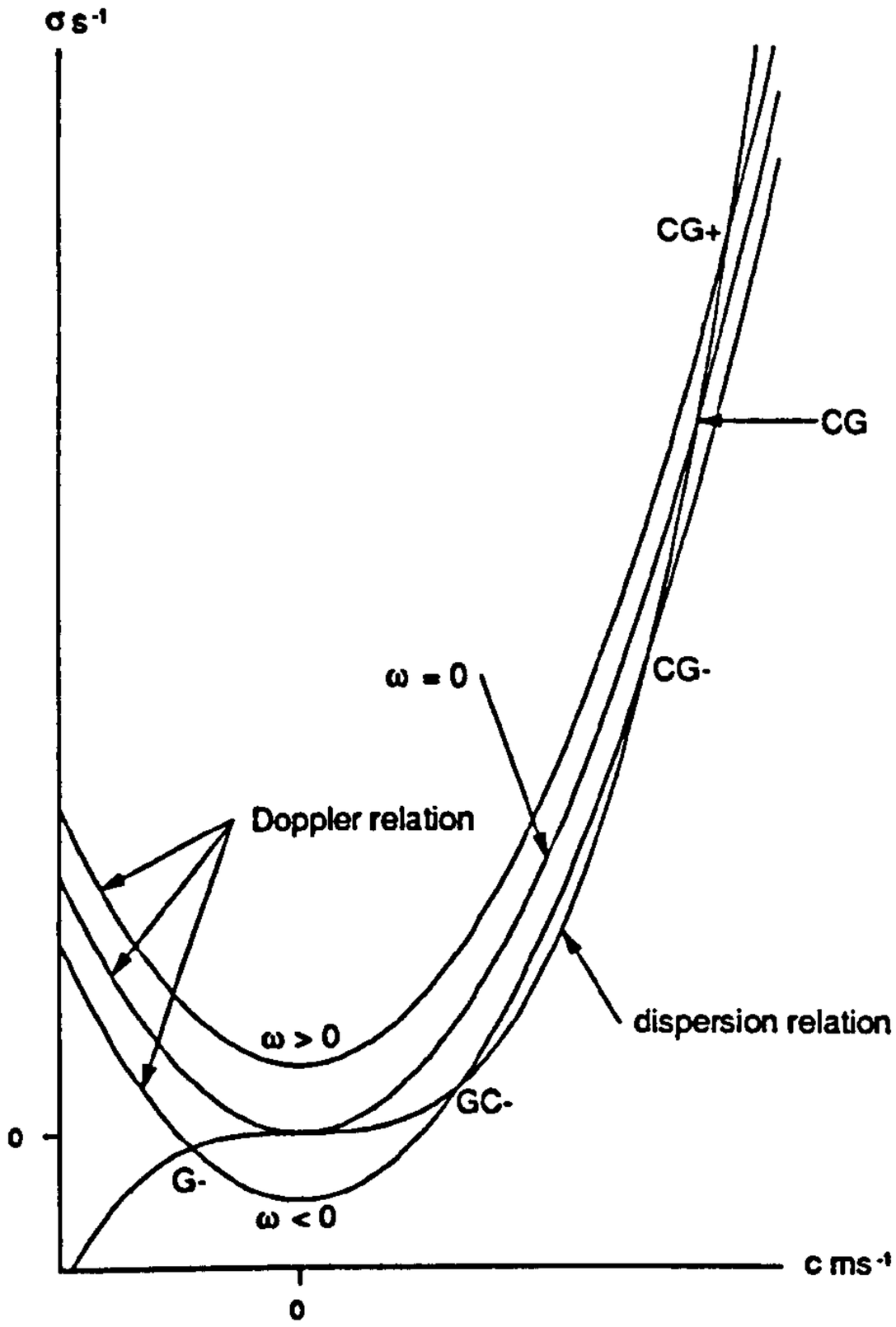

Figure 10.1

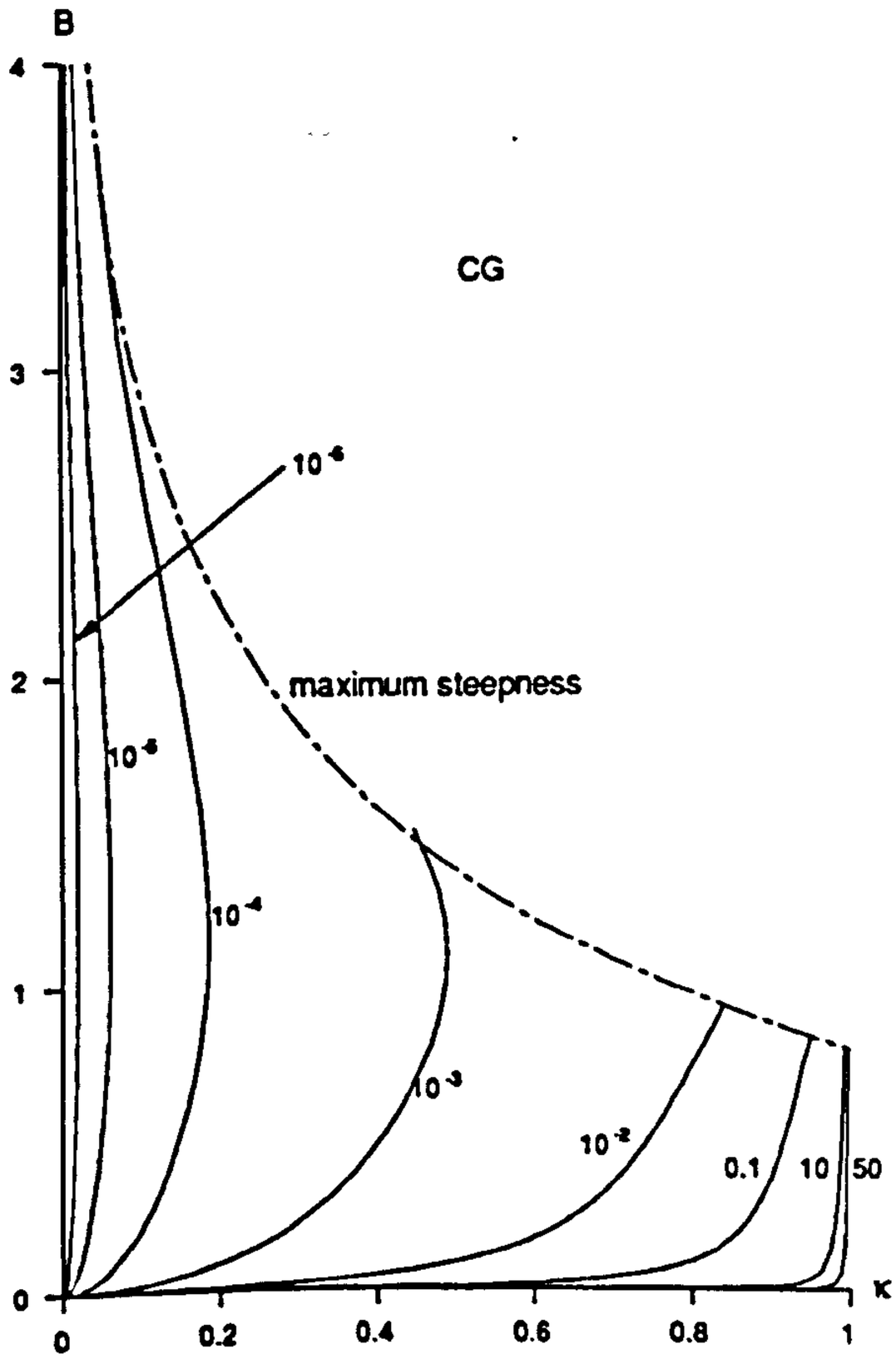

Figure 10.2a

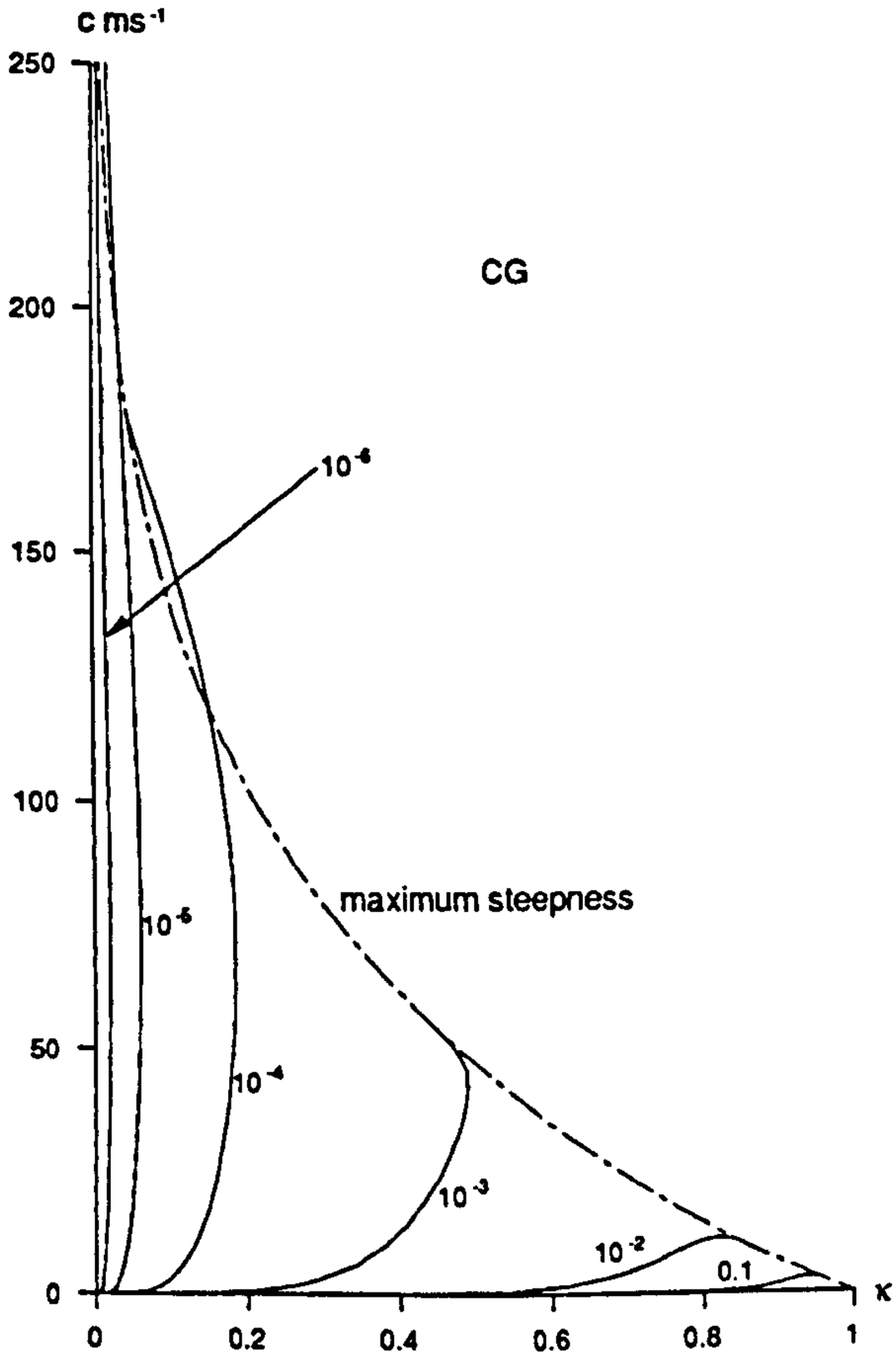

Figure 10.2b

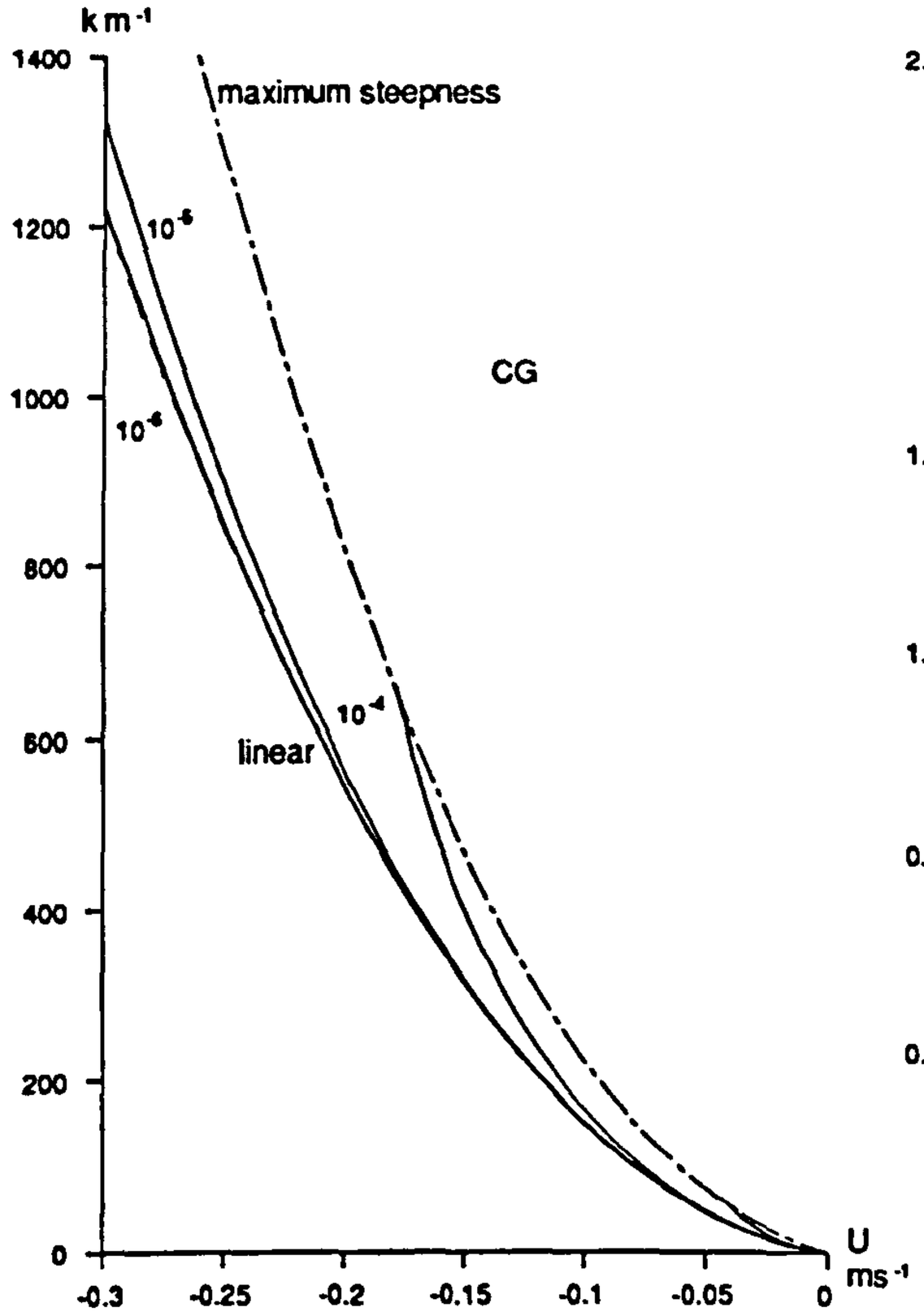

Figure 10.2c

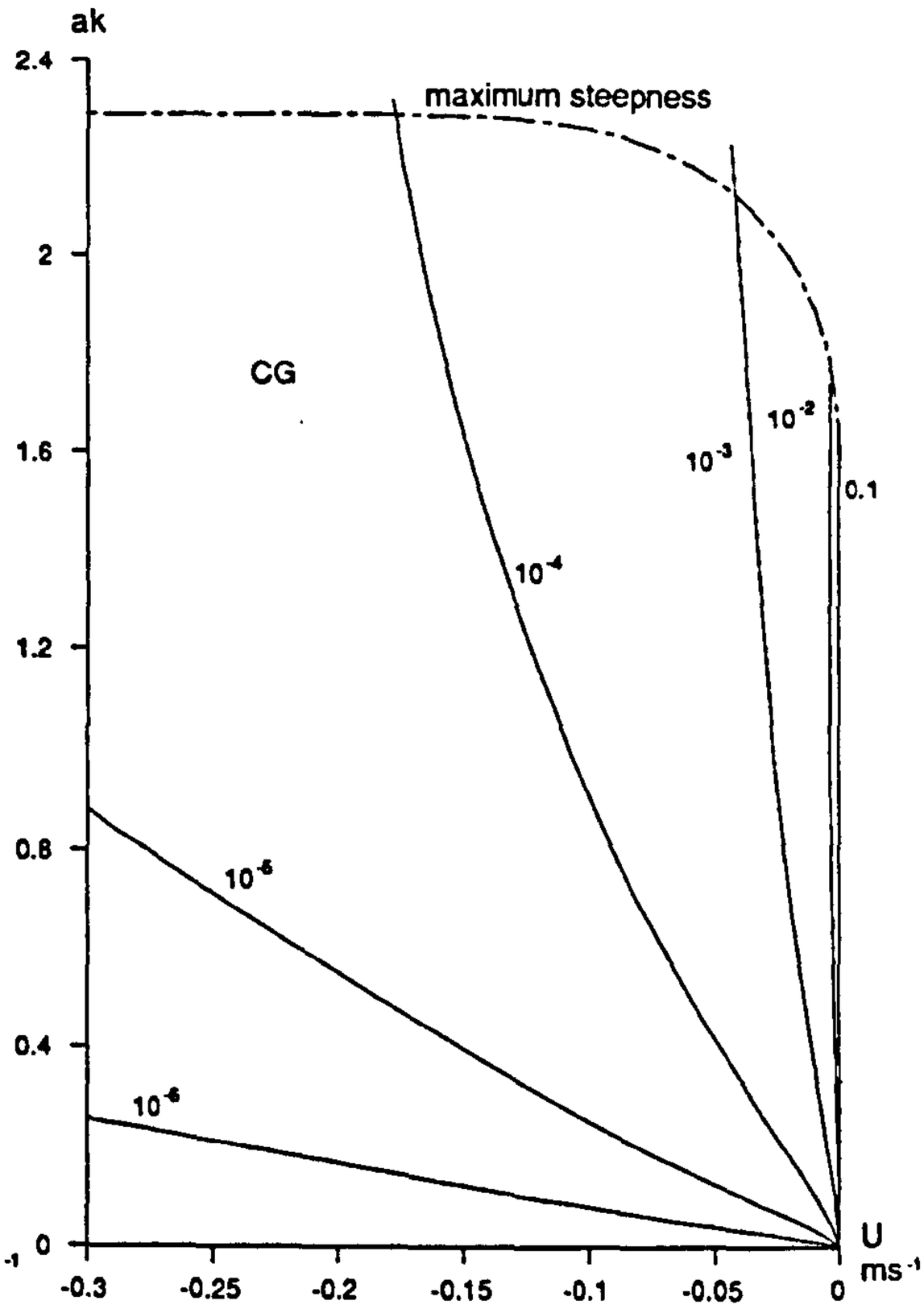

Figure 10.2d

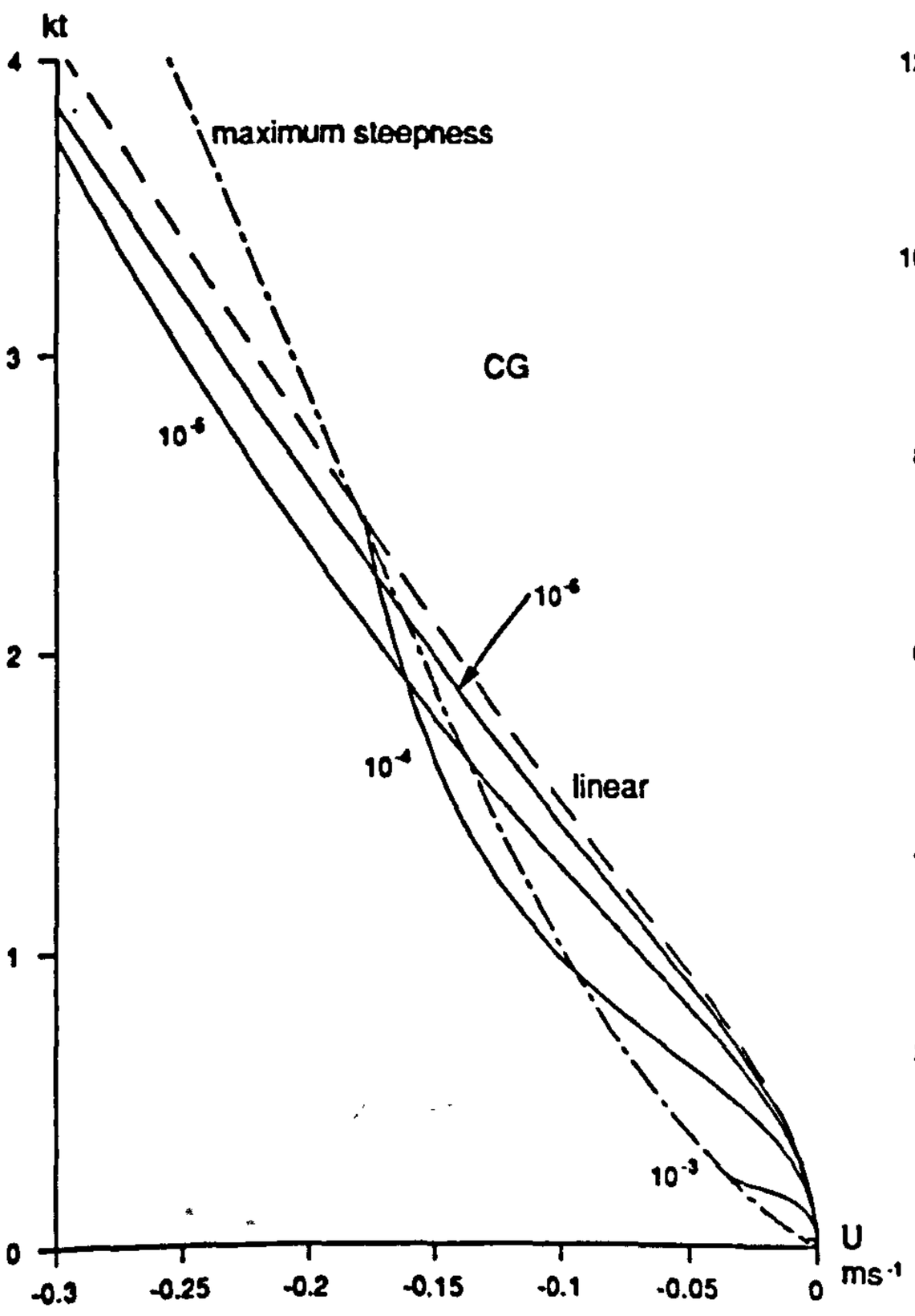

Figure 10.2e

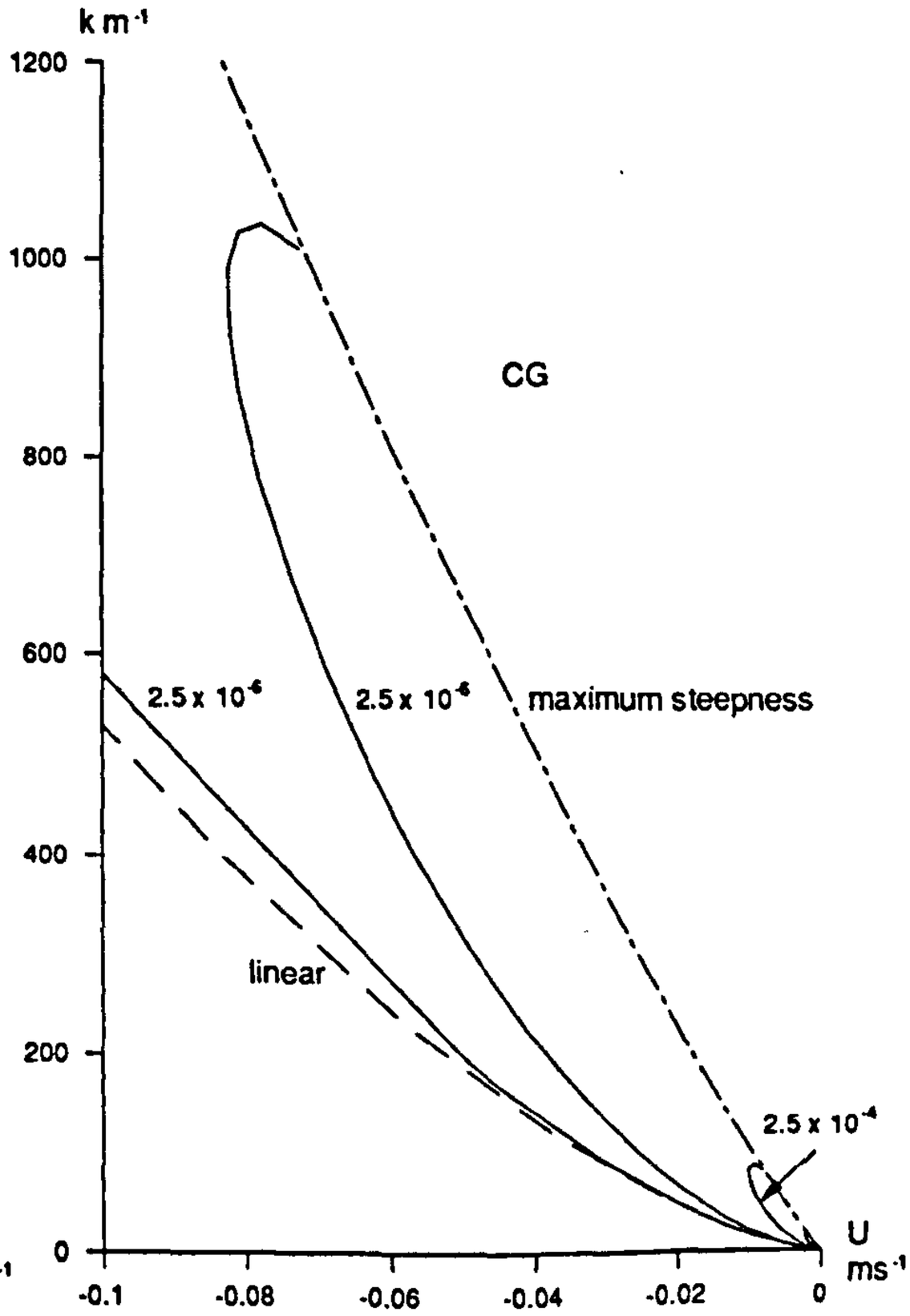

Figure 10.3a

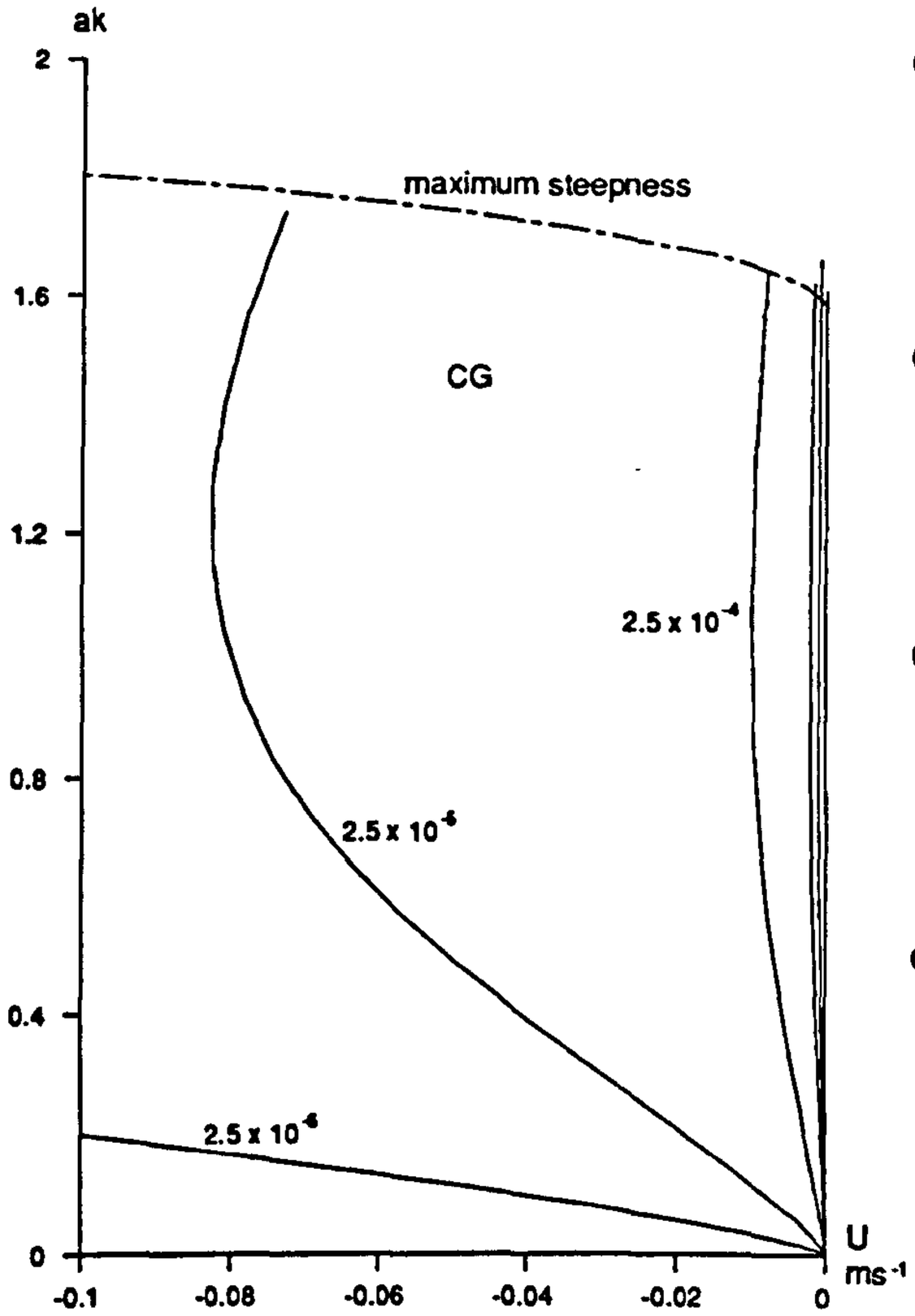

Figure 10.3b

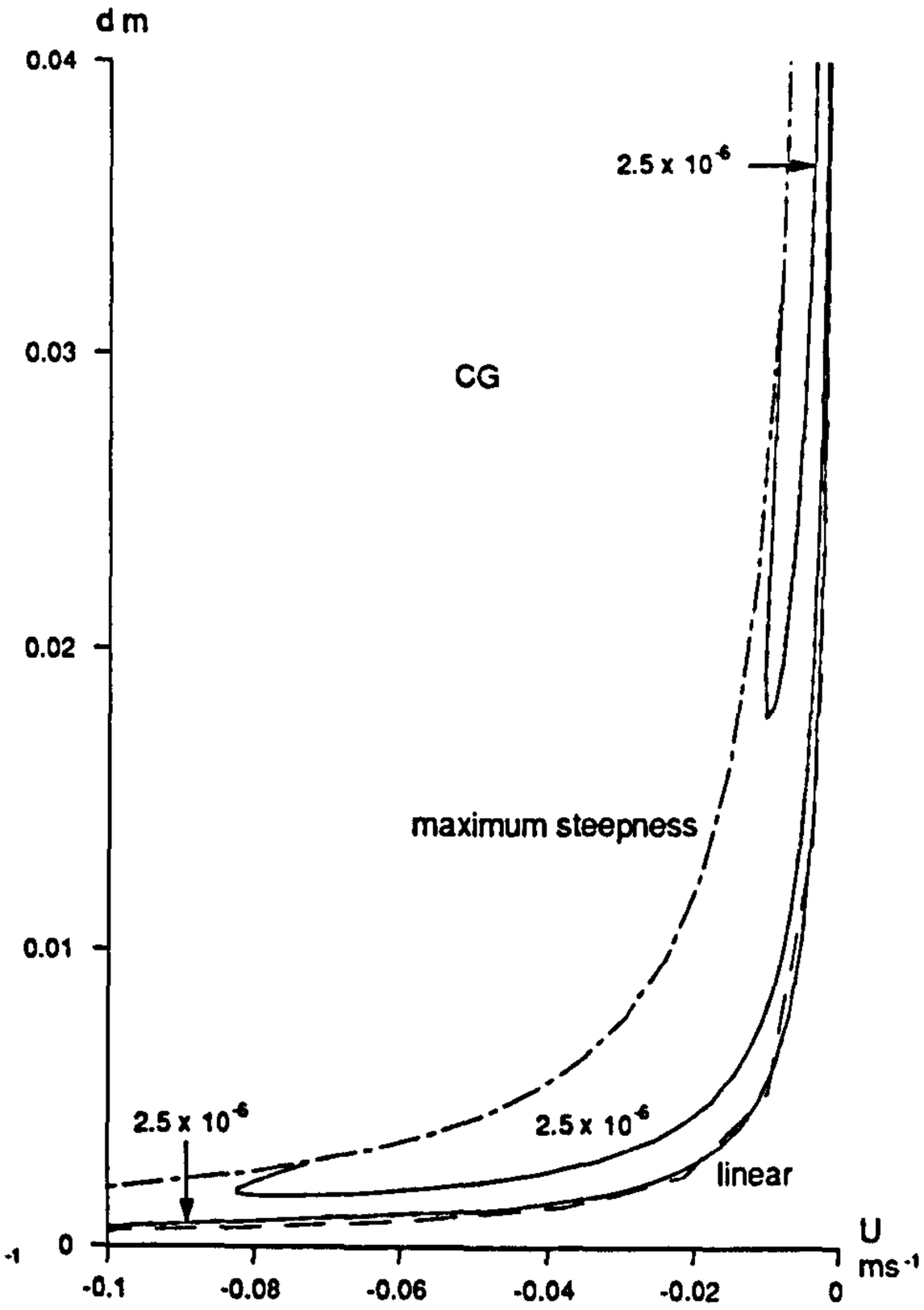

Figure 10.3c

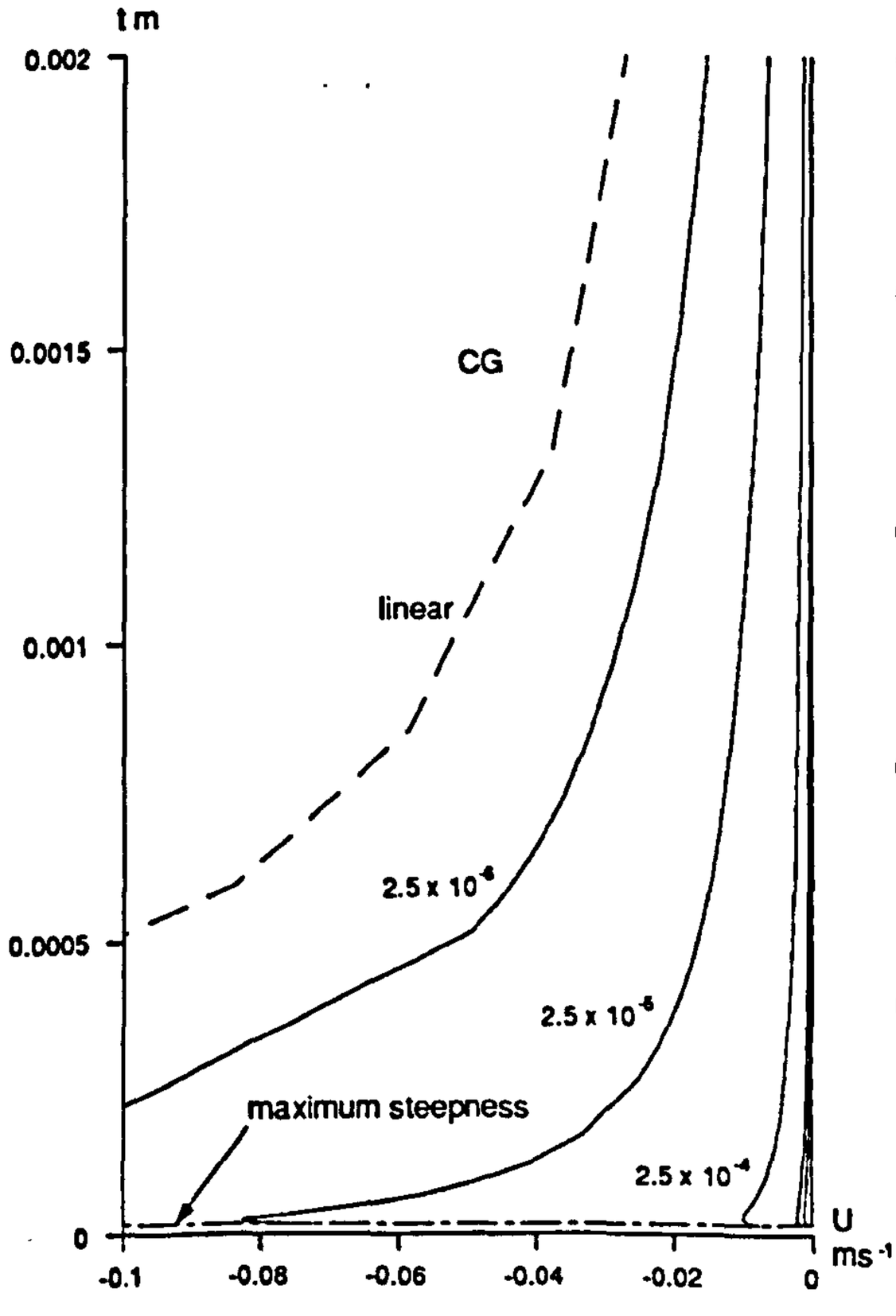

Figure 10.3d

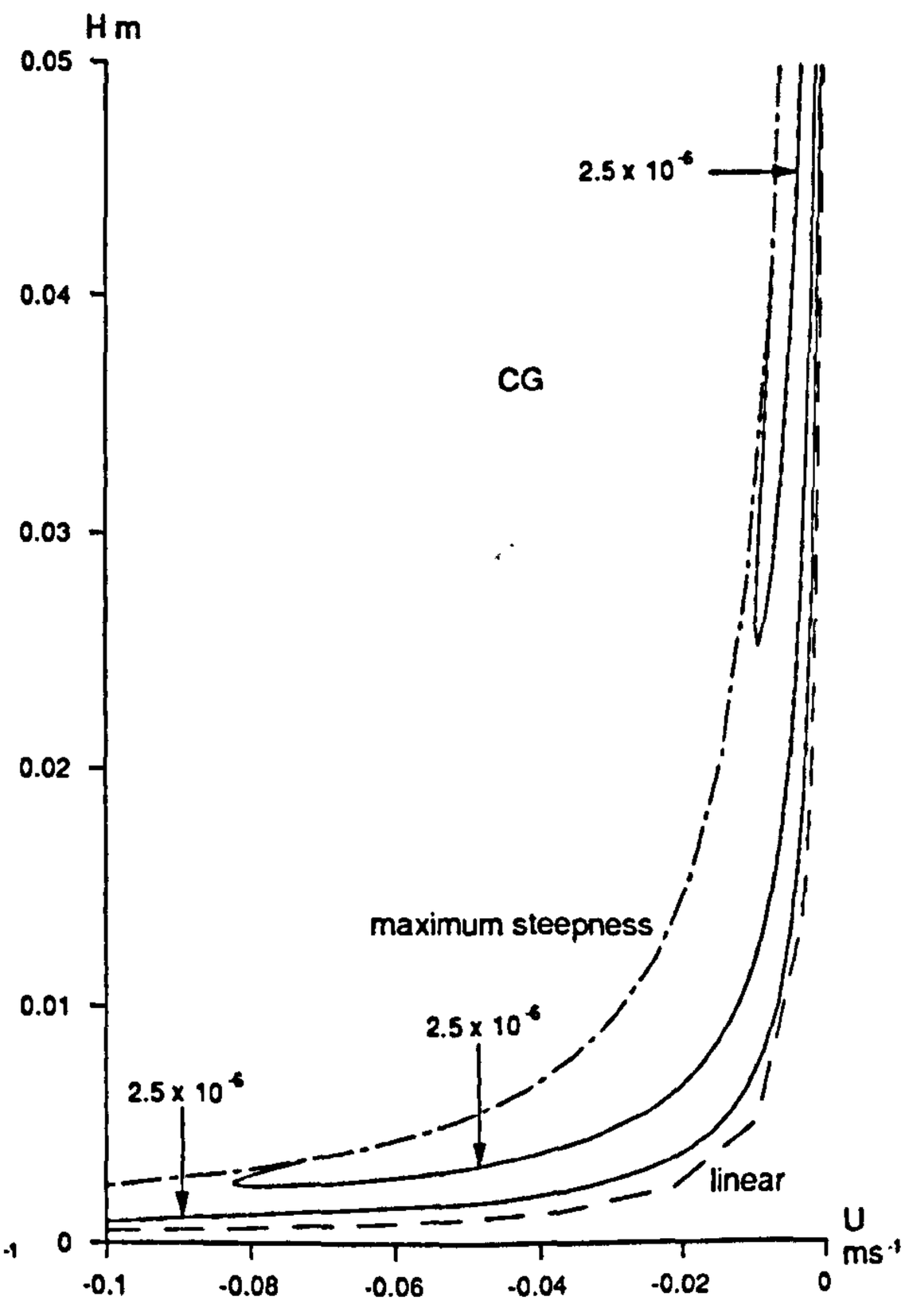

Figure 10.3e

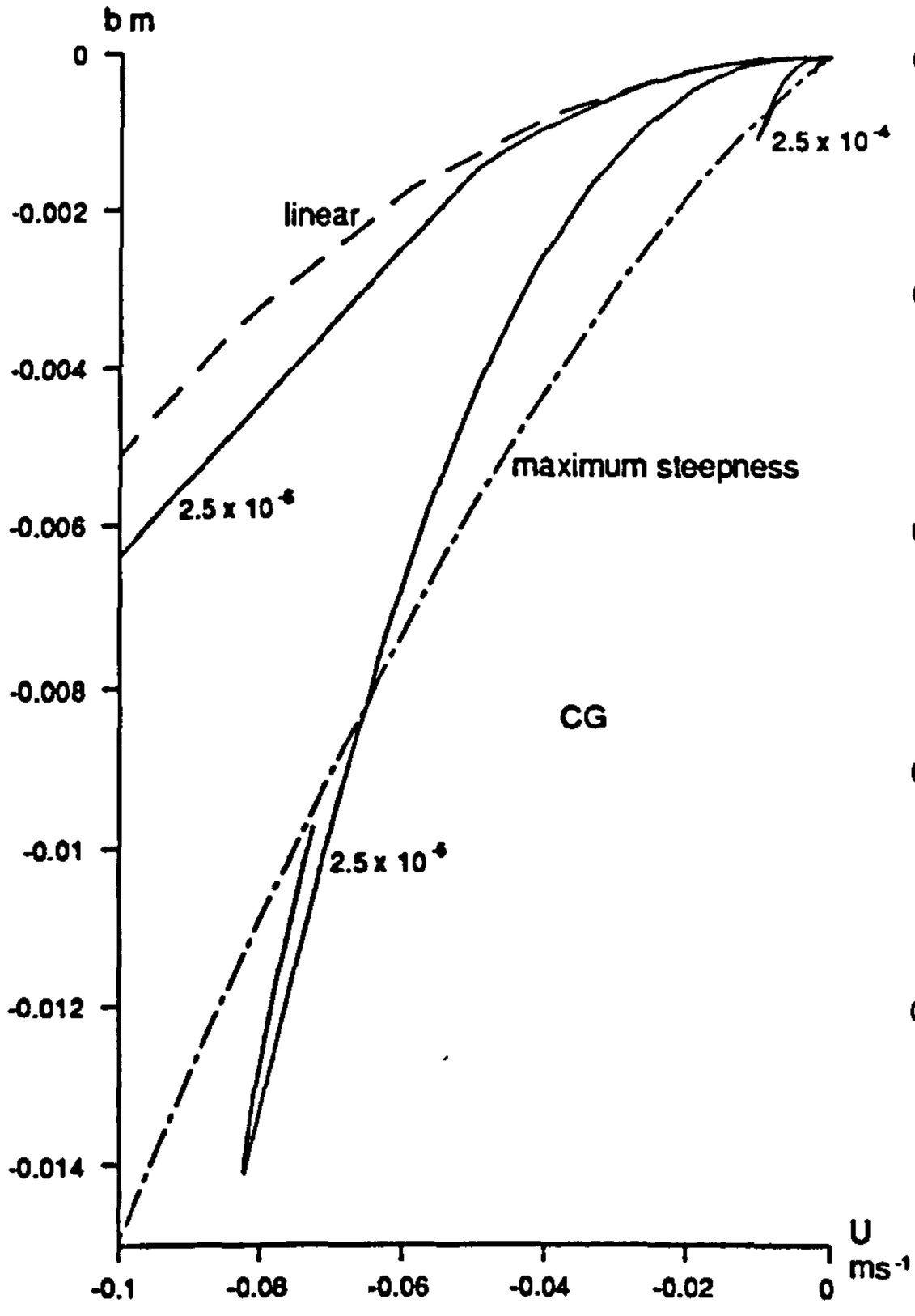

Figure 10.3f

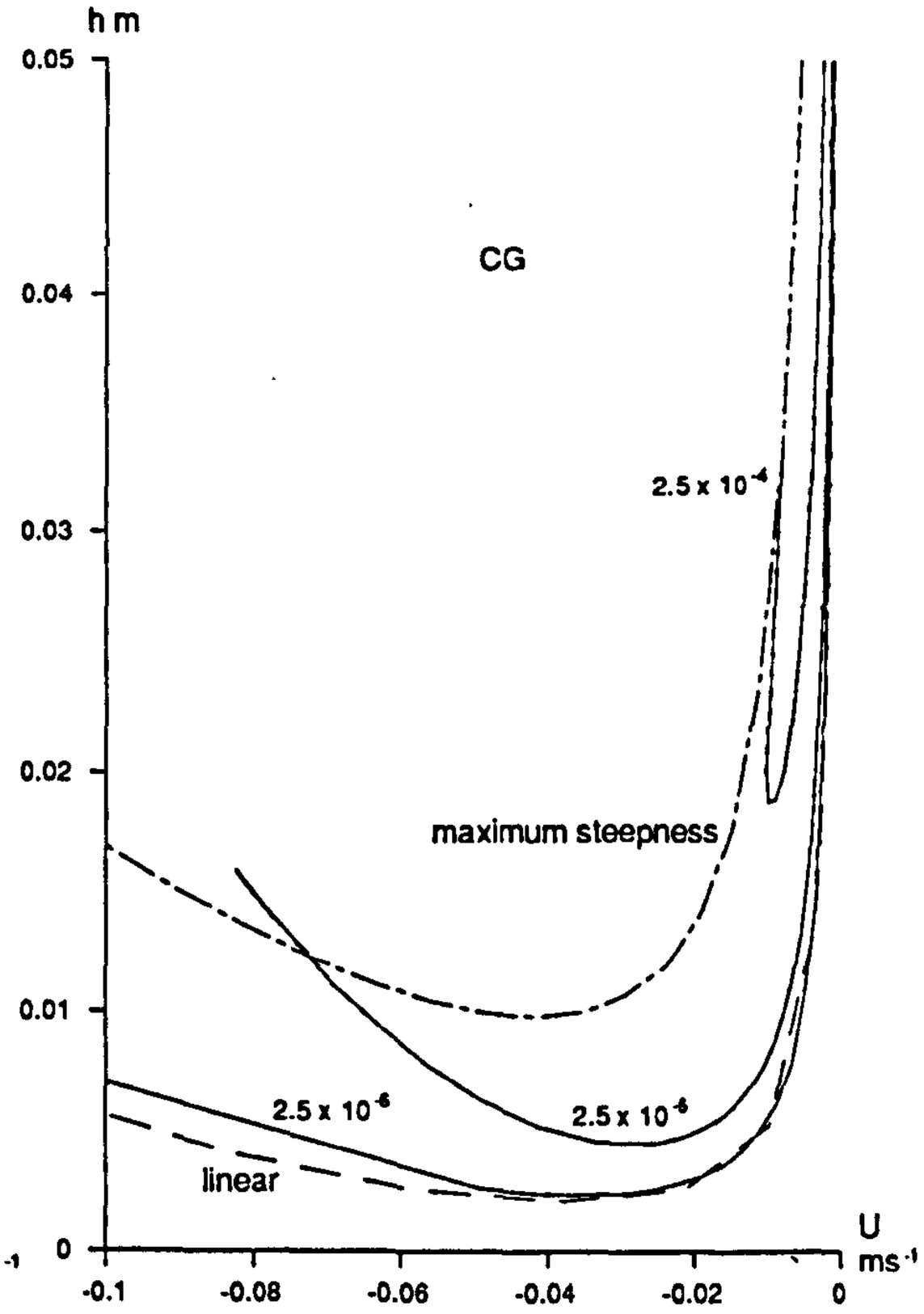

Figure 10.3g

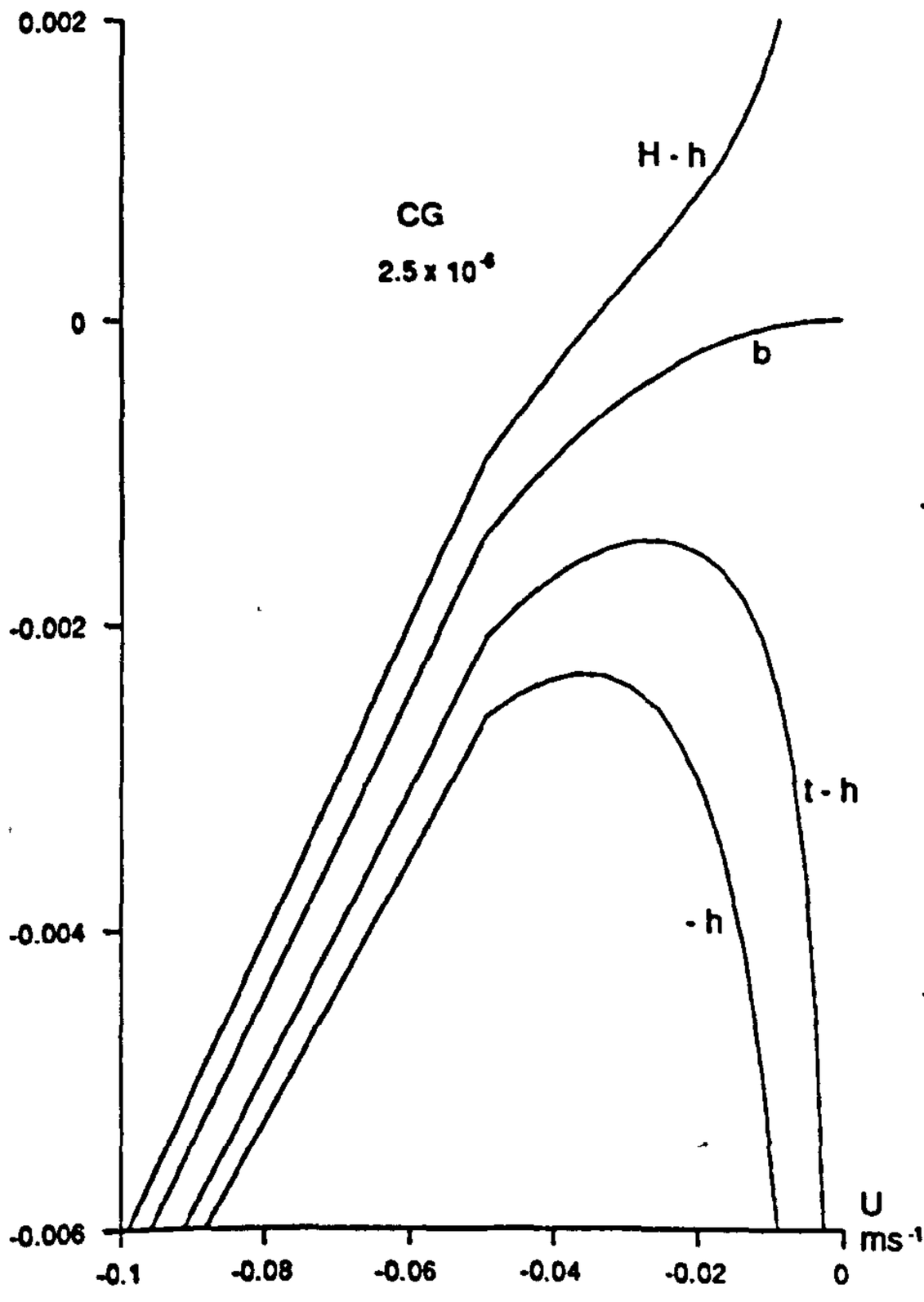

Figure 10.3h

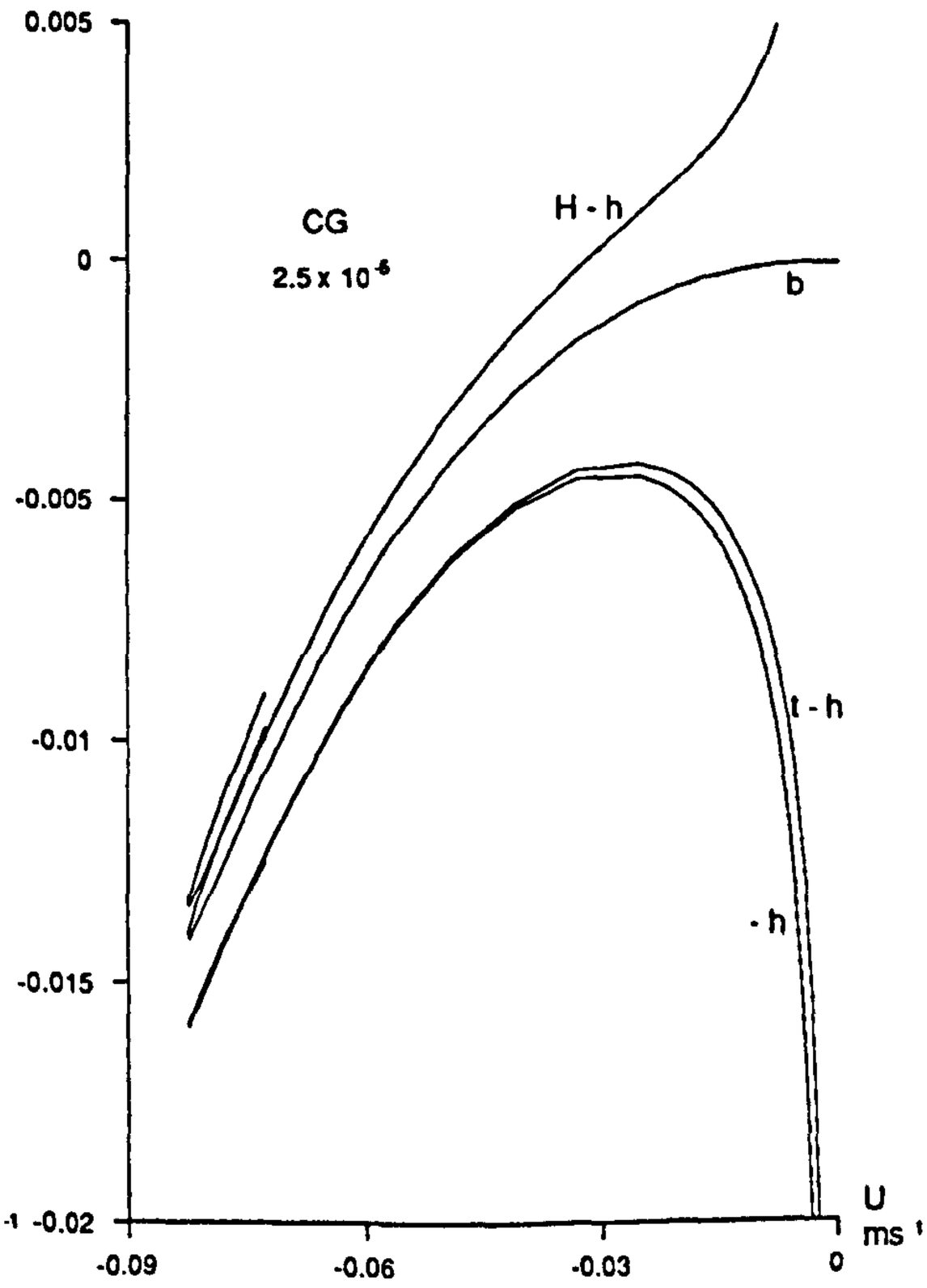

Figure 10.3i

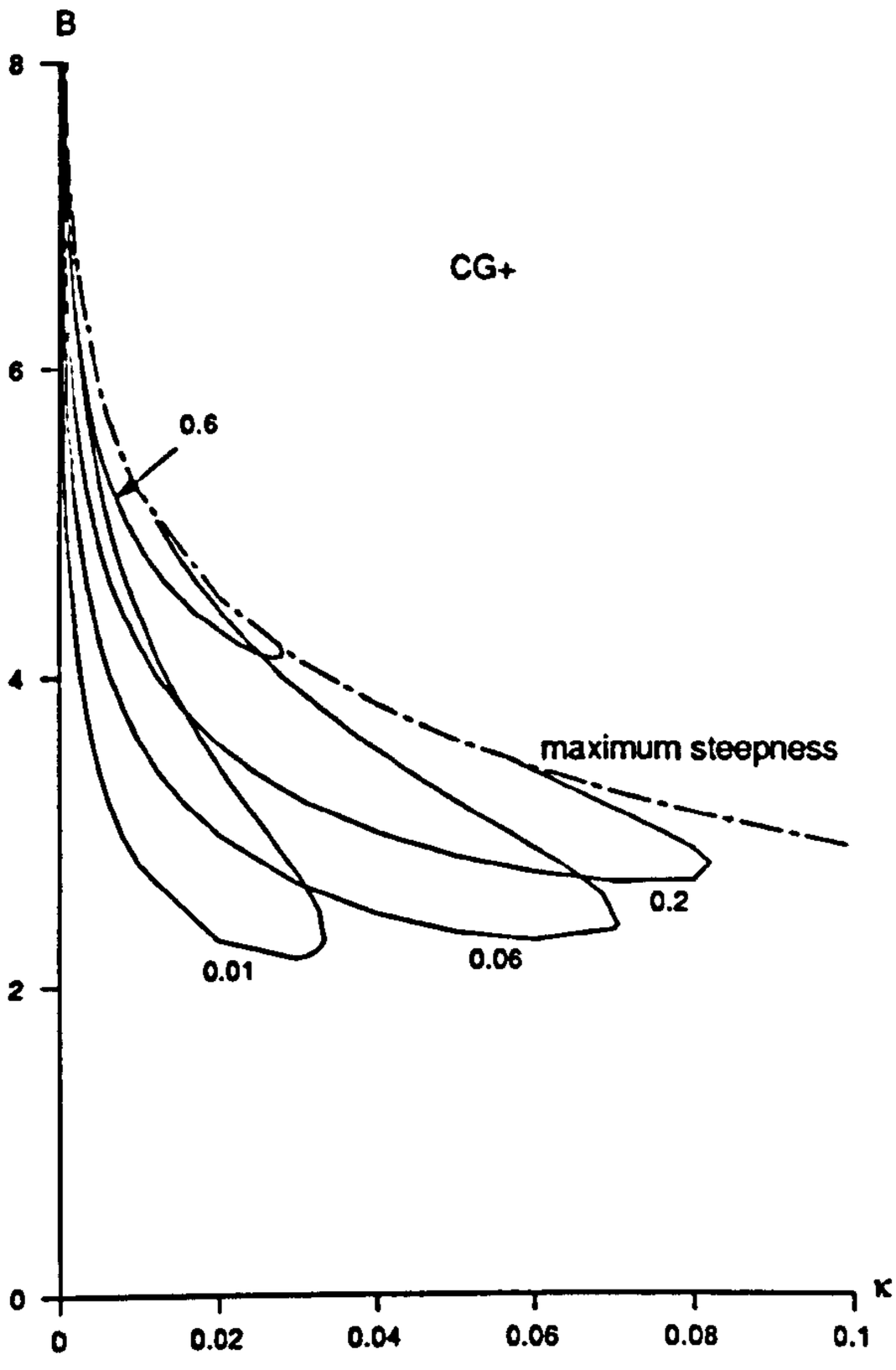

Figure 10.4a

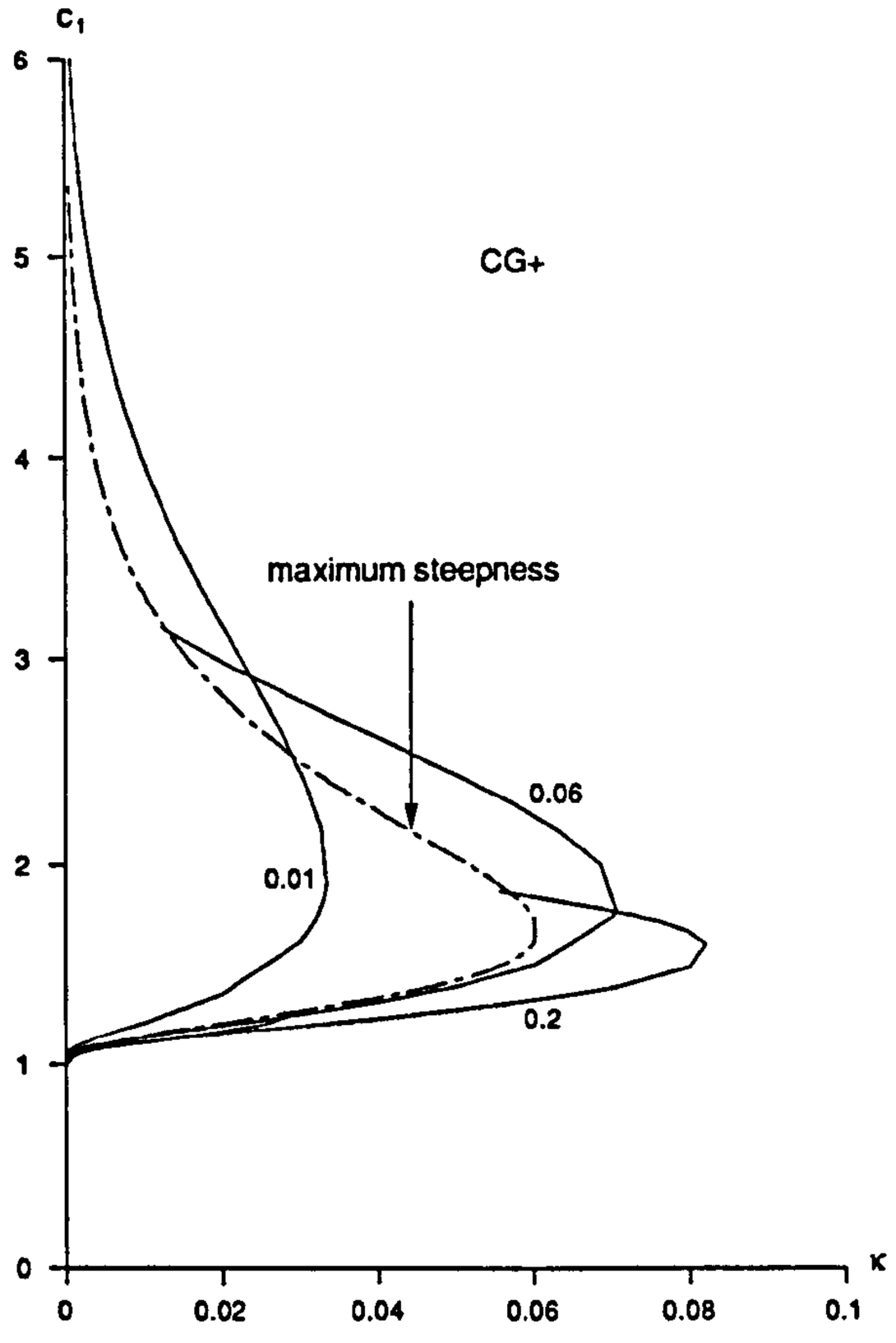

Figure 10.4b

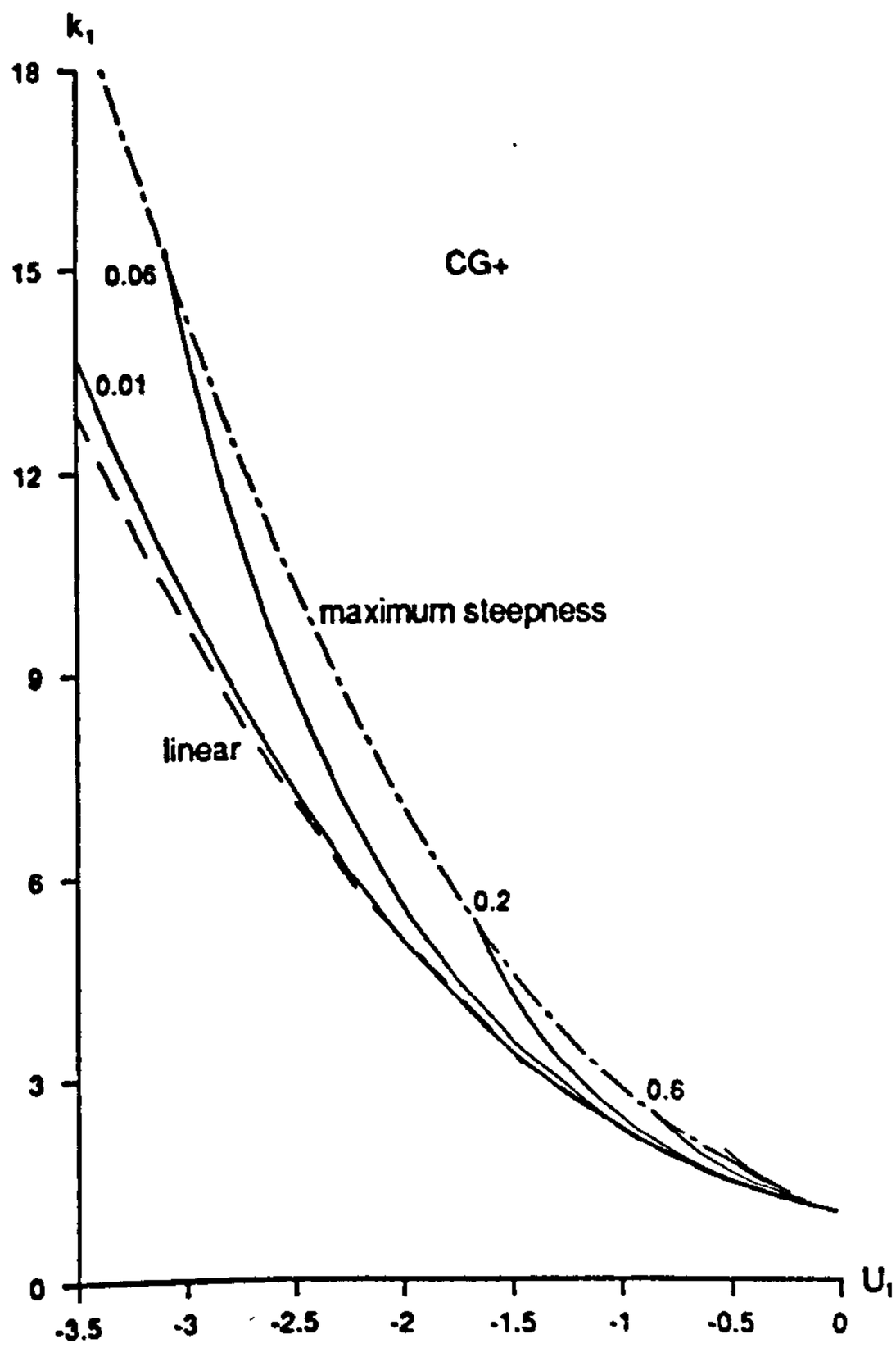

Figure 10.4c

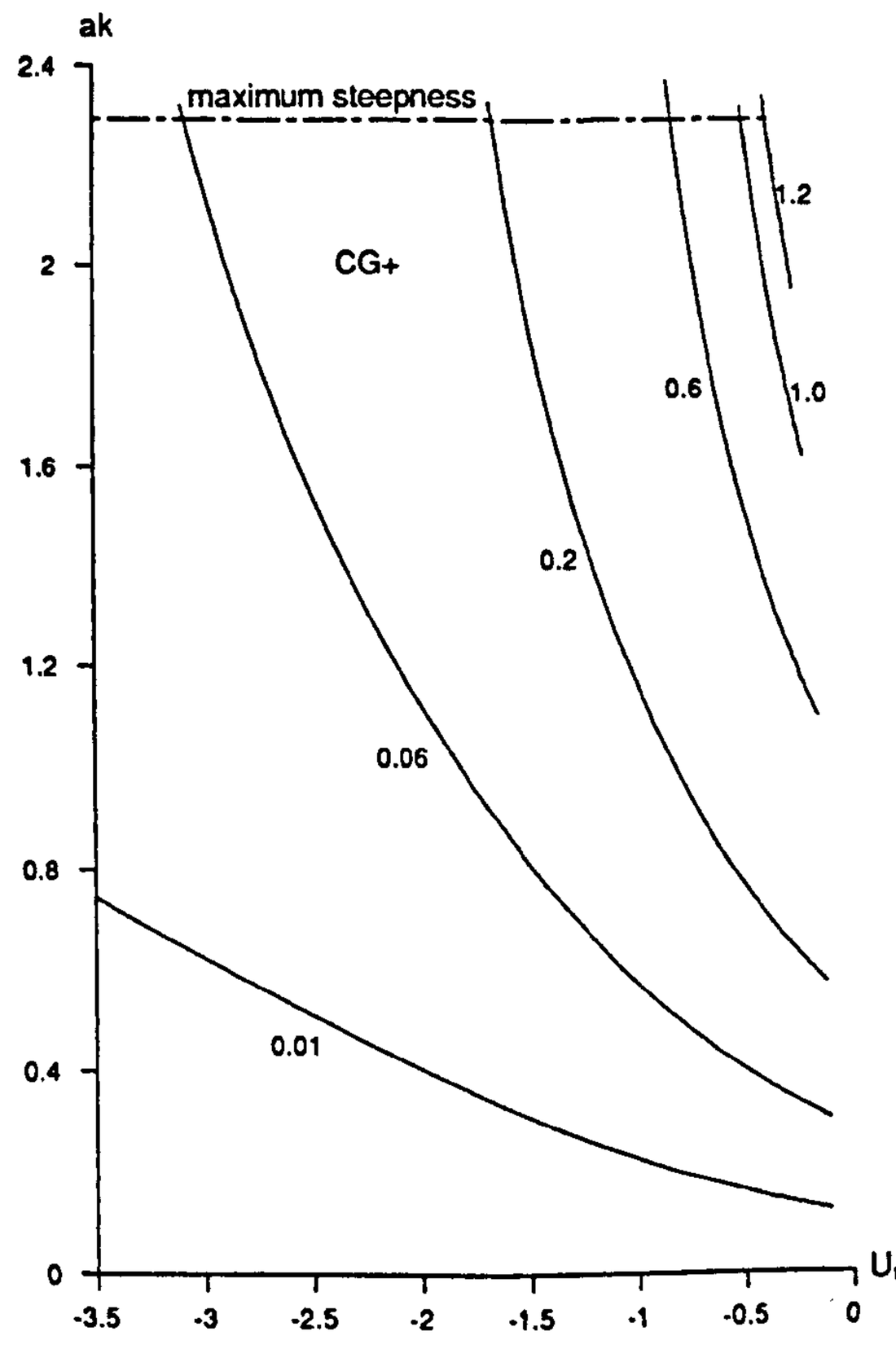

Figure 10.4d

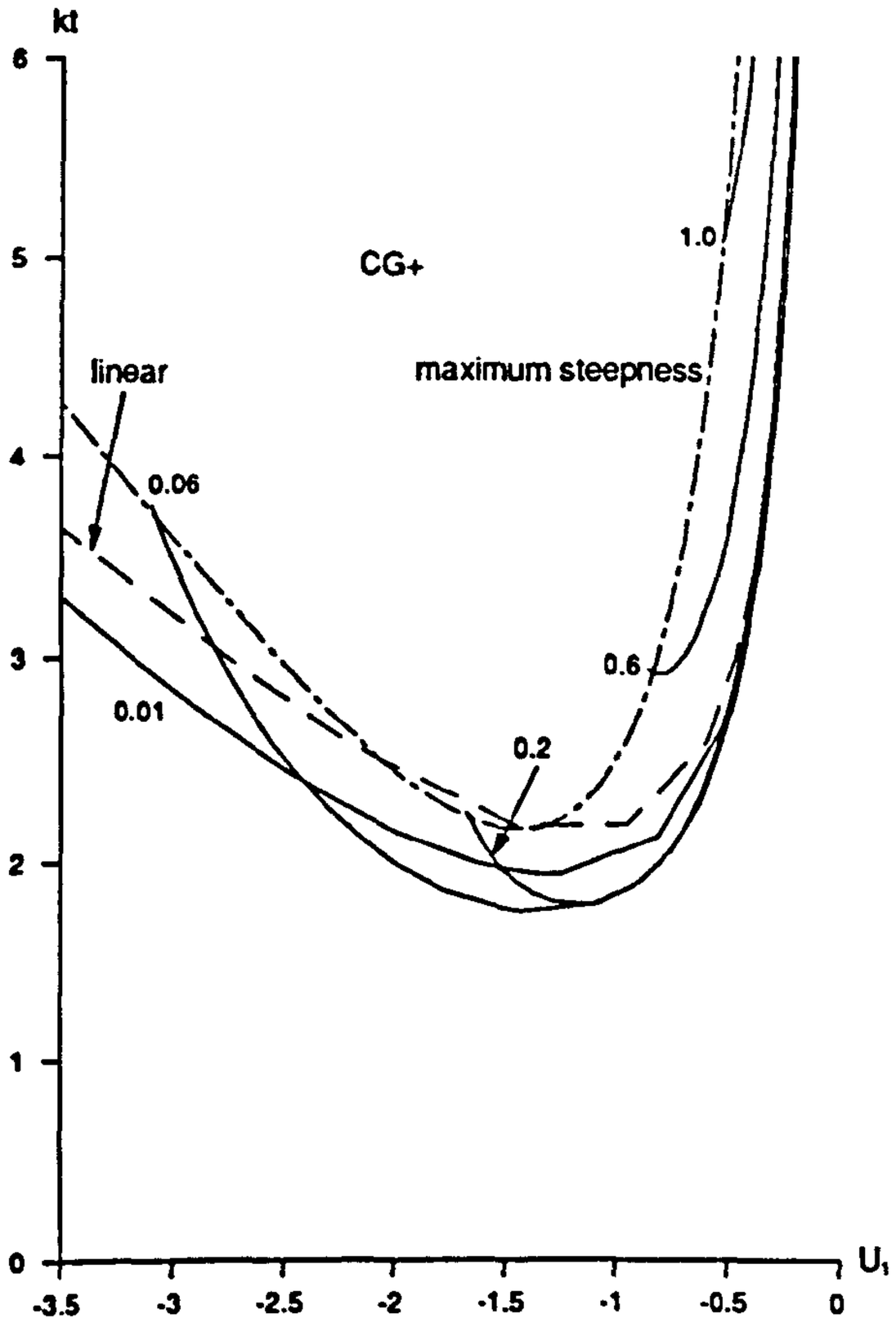

Figure 10.4e

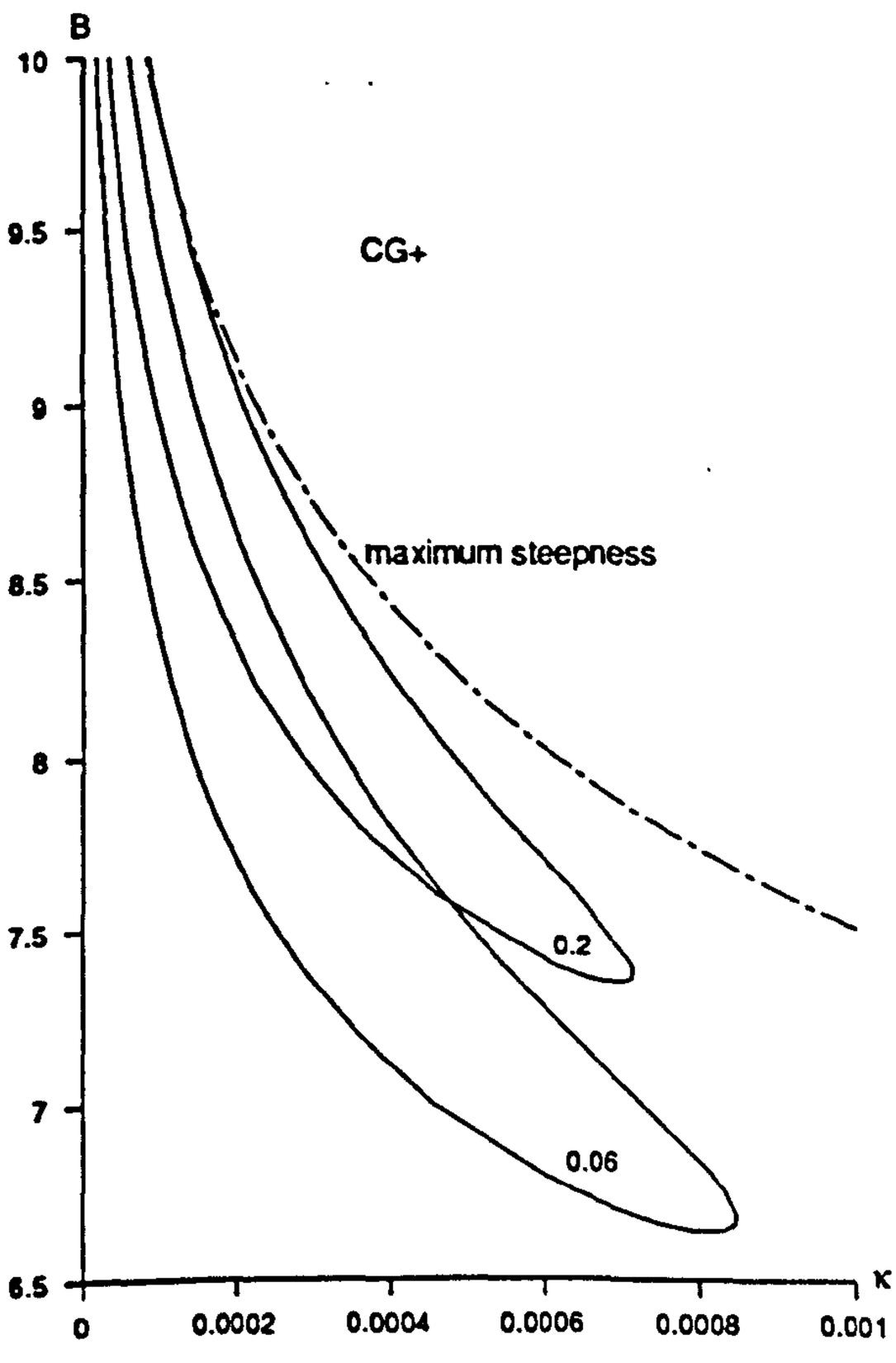

Figure 10.5a

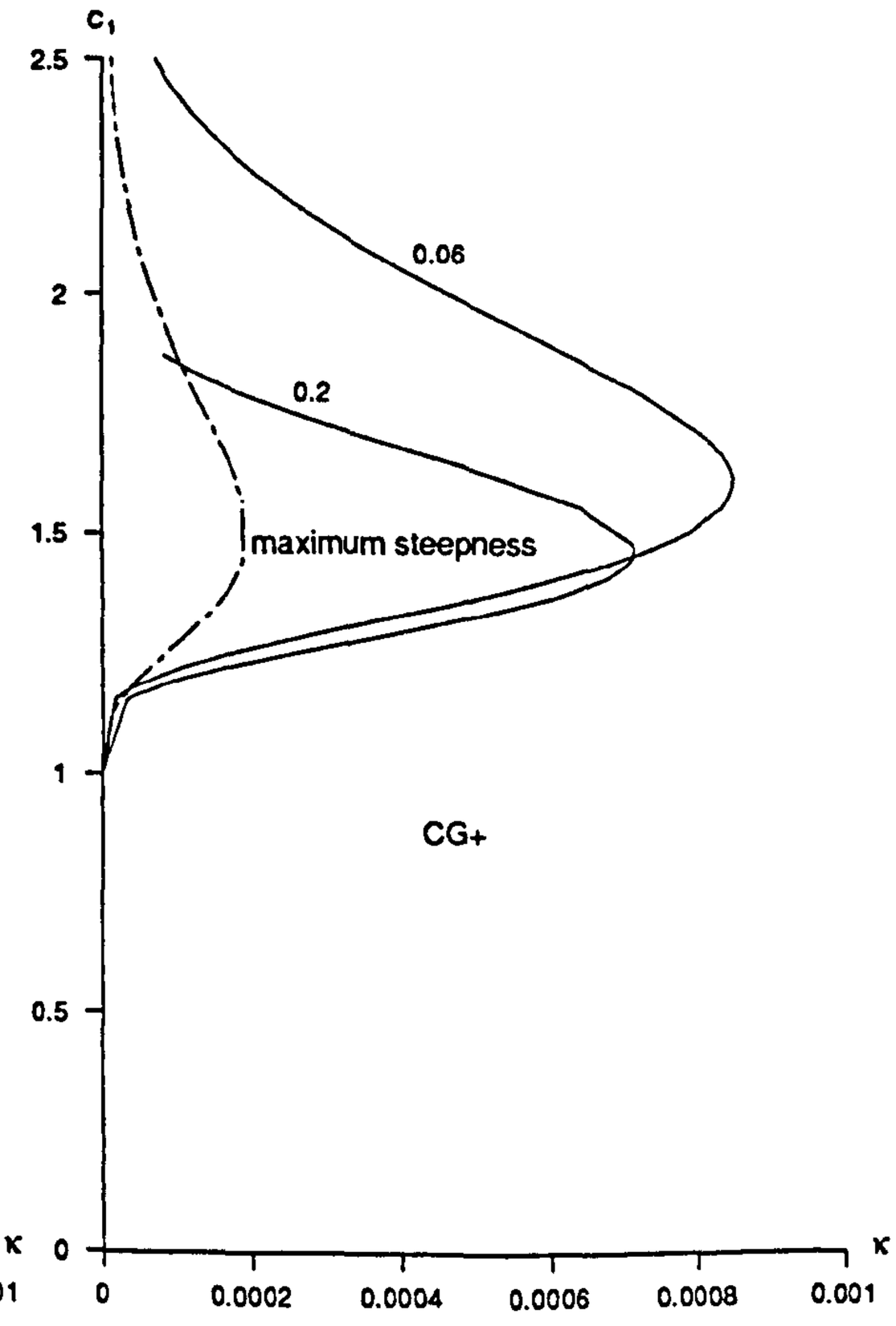

Figure 10.5b

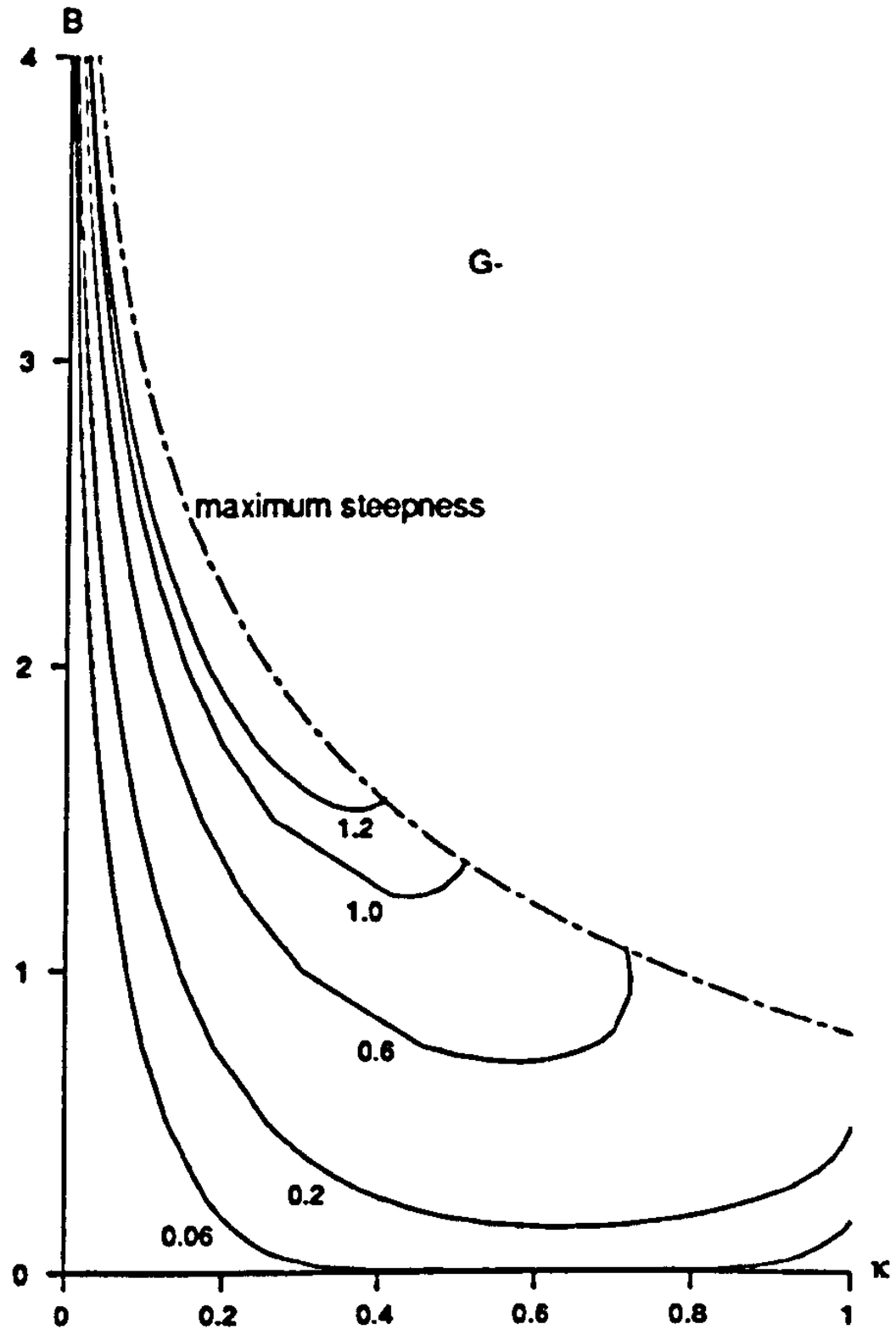

Figure 10.6a

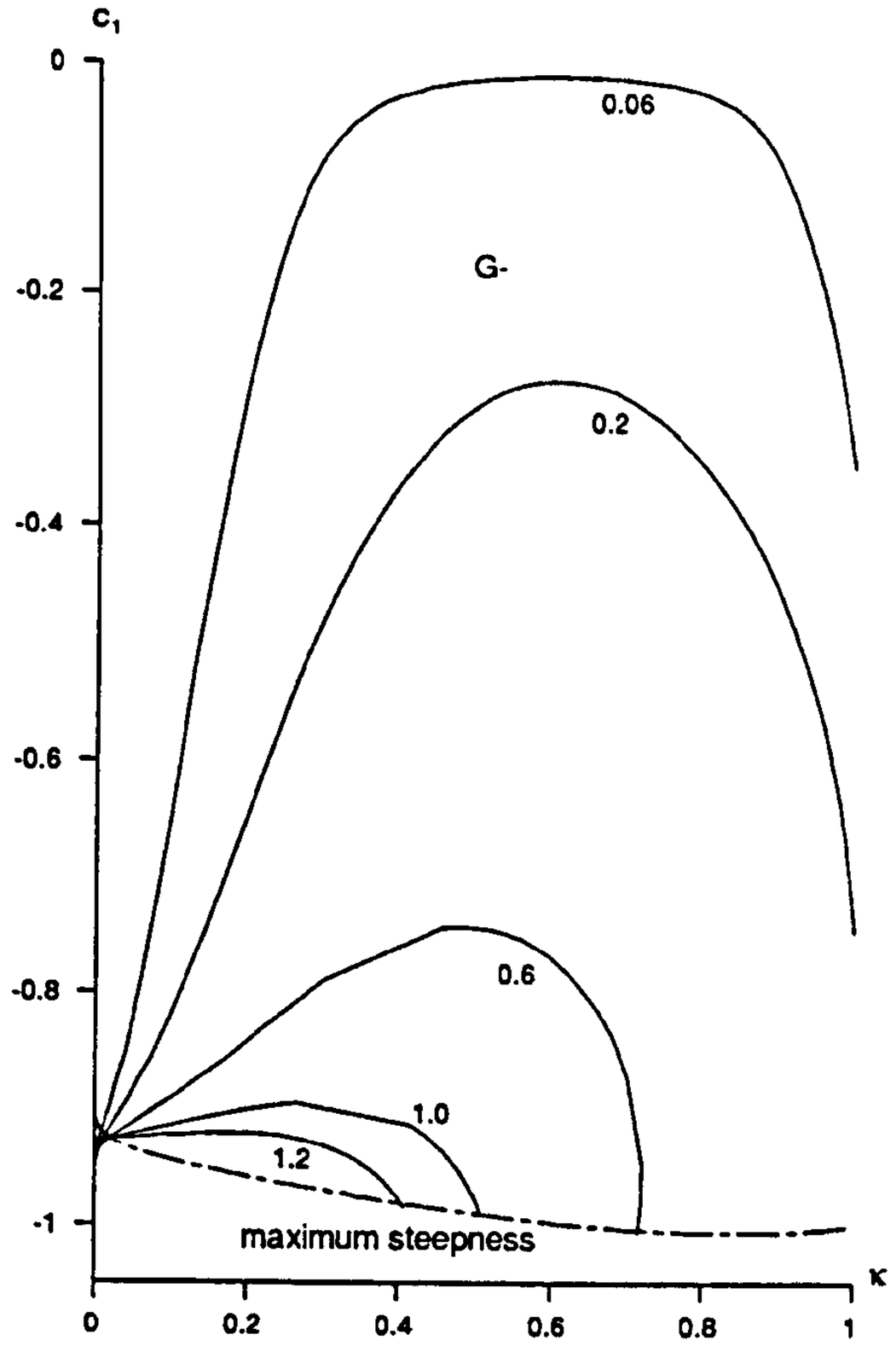

Figure 10.6b

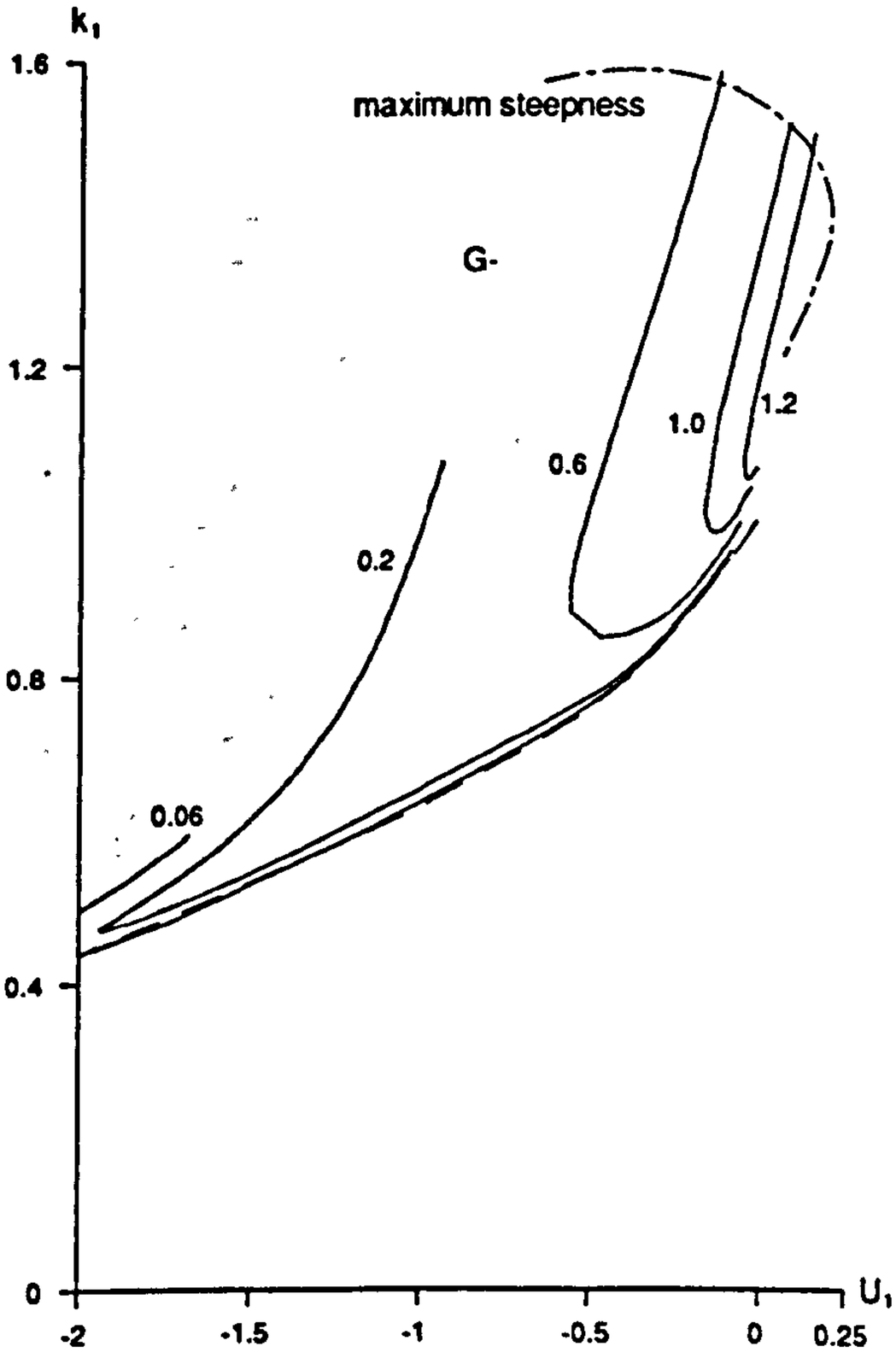

Figure 10.6c

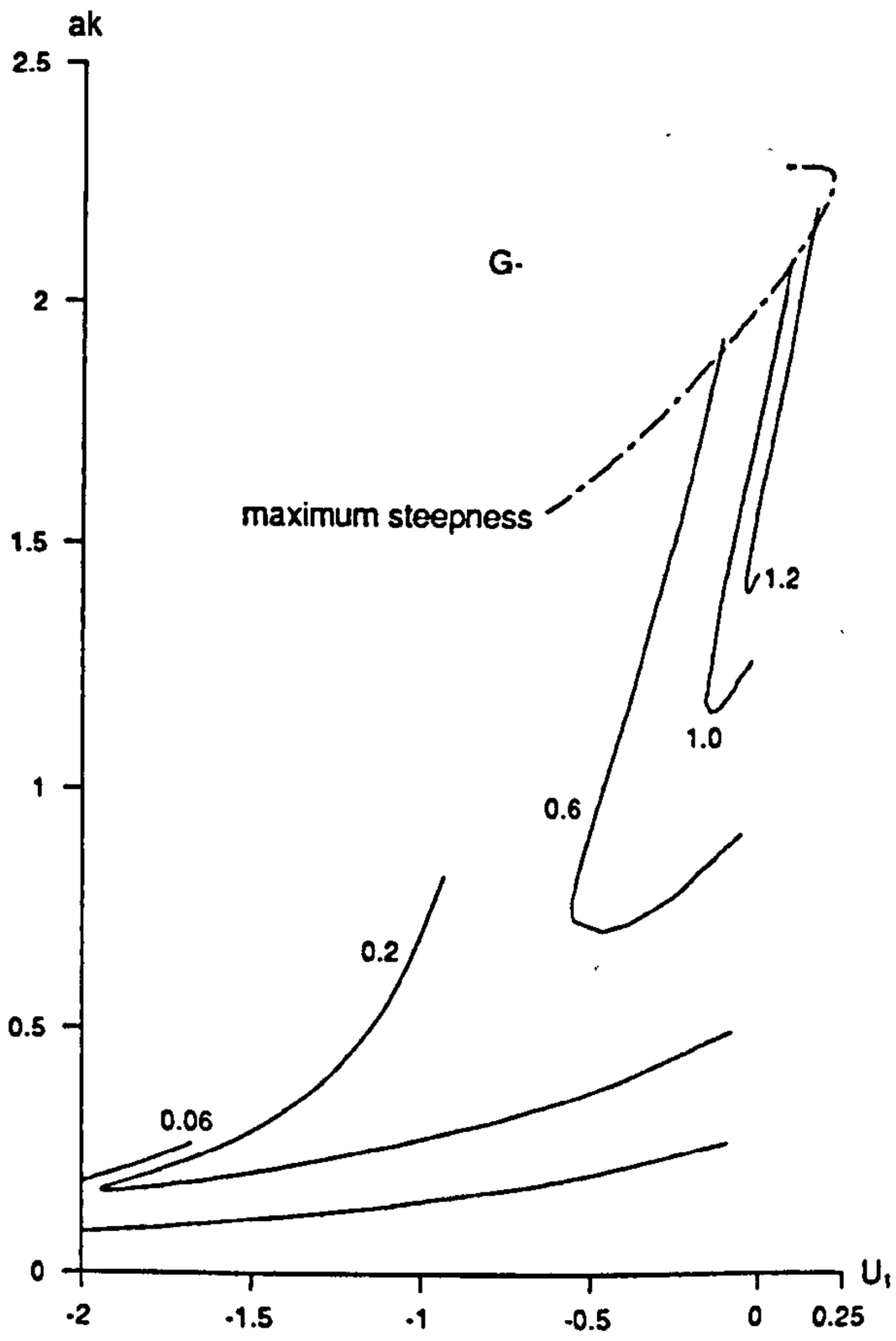

Figure 10.6d

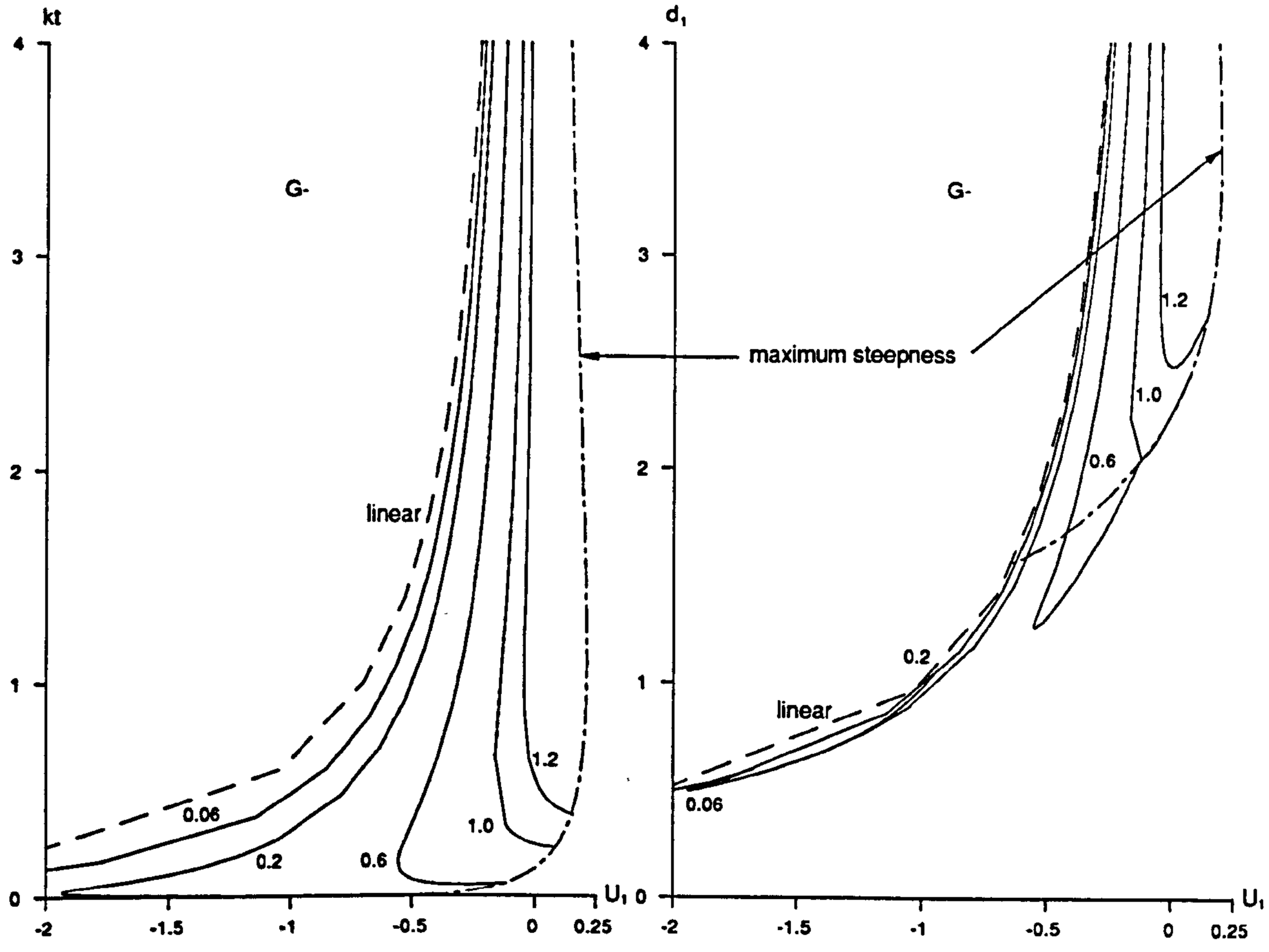

Figure 10.6e

Figure 10.6f

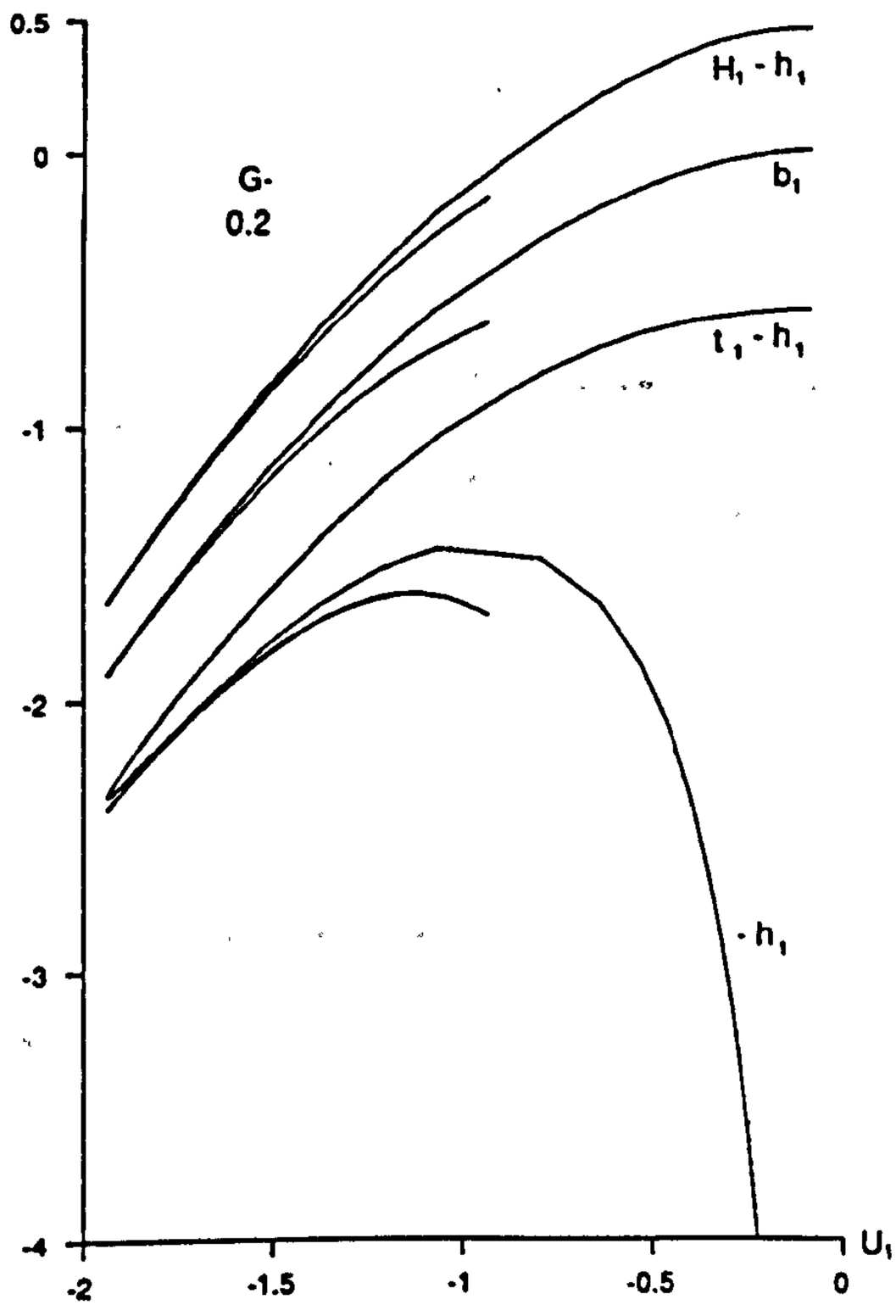

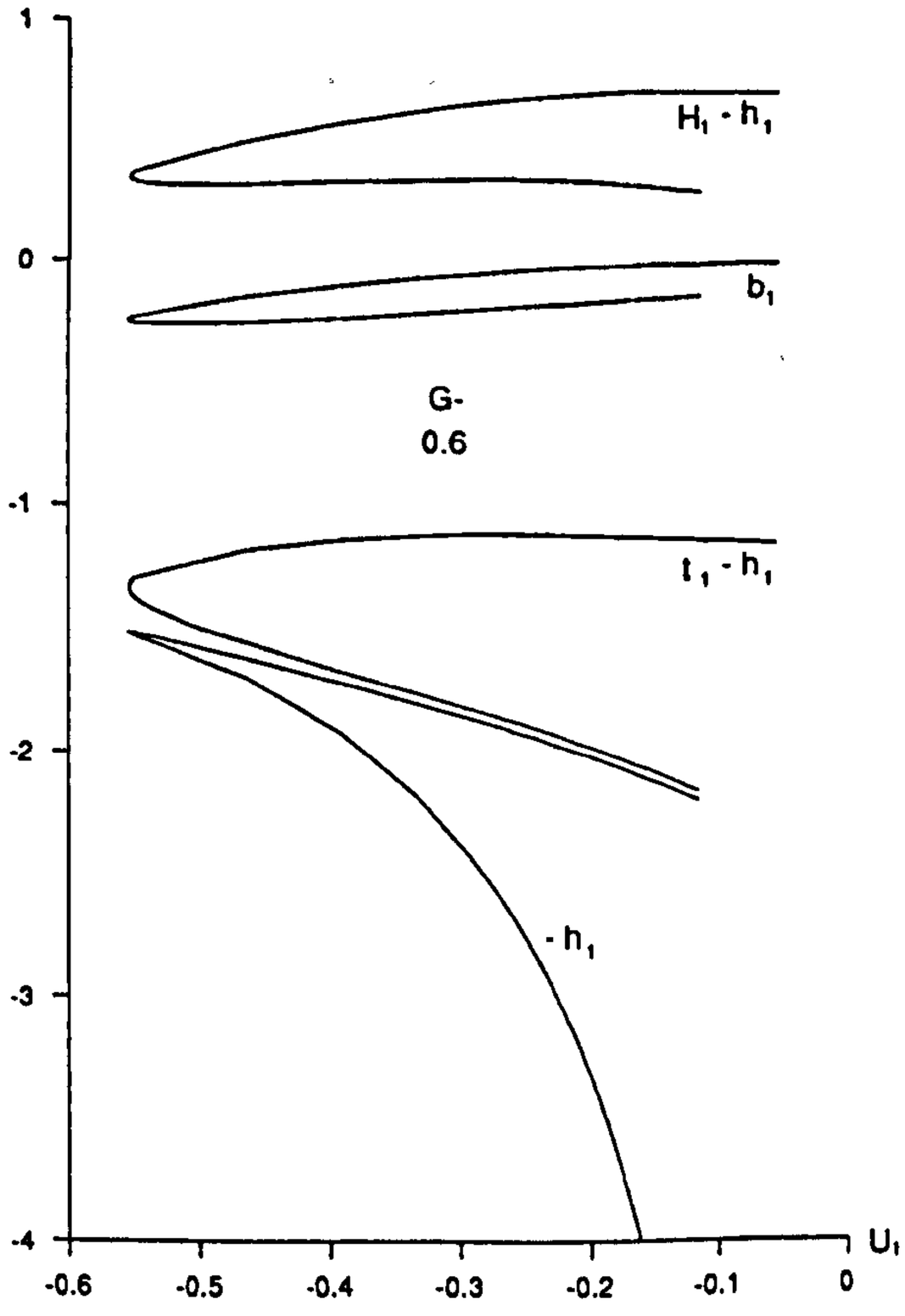

Figure 10.6g

Figure 10.6h

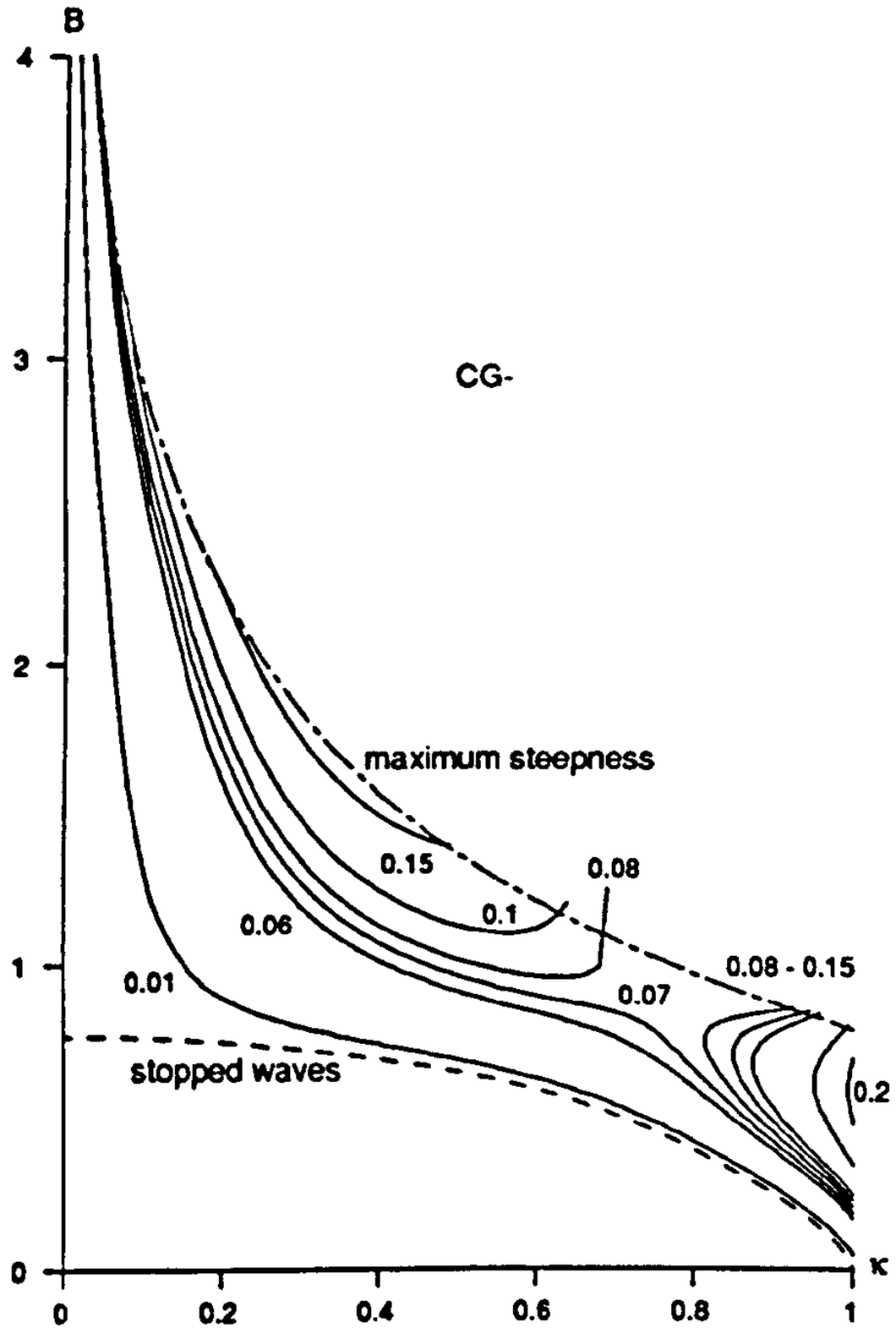

Figure 10.7a

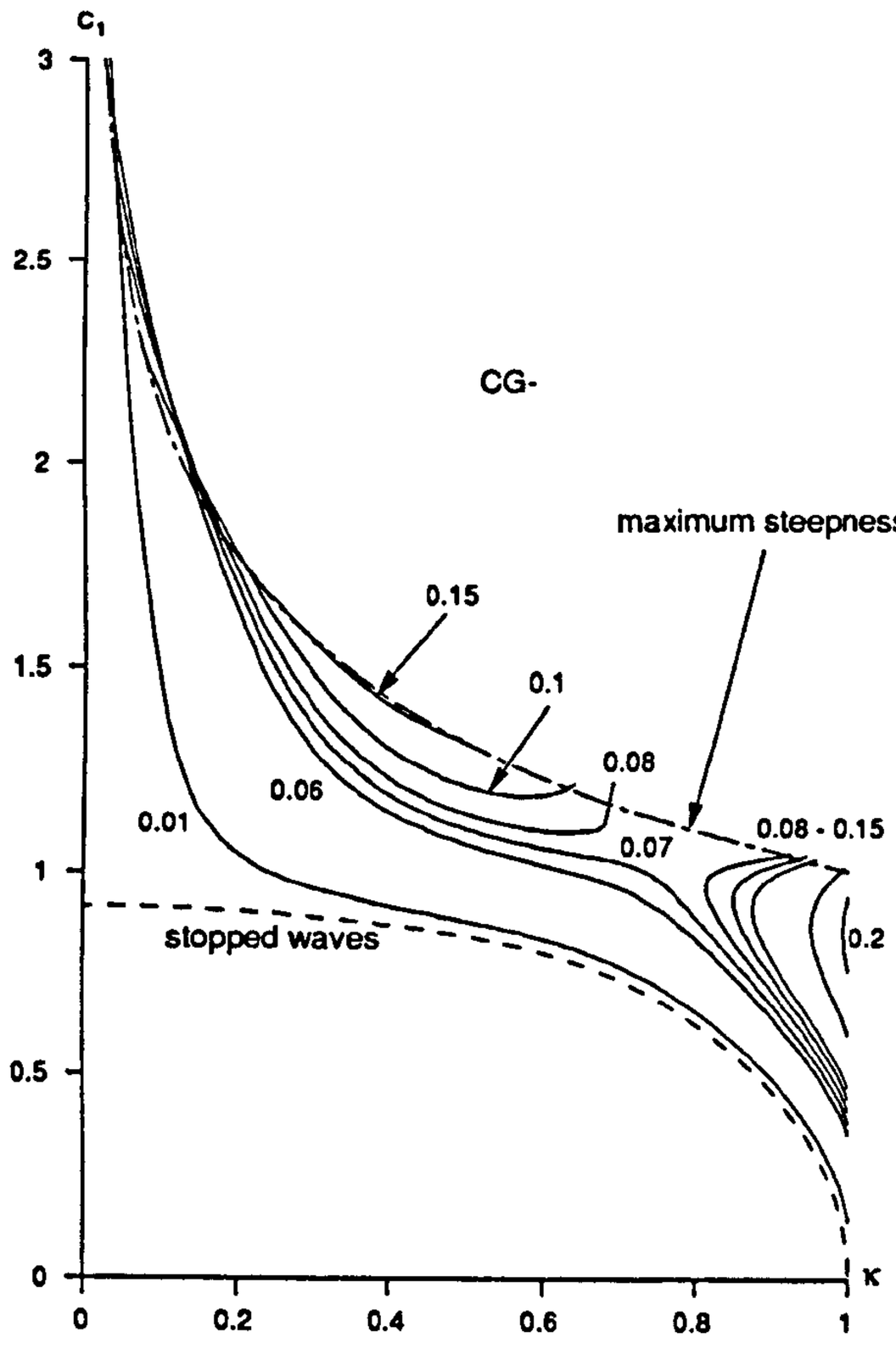

Figure 10.7b

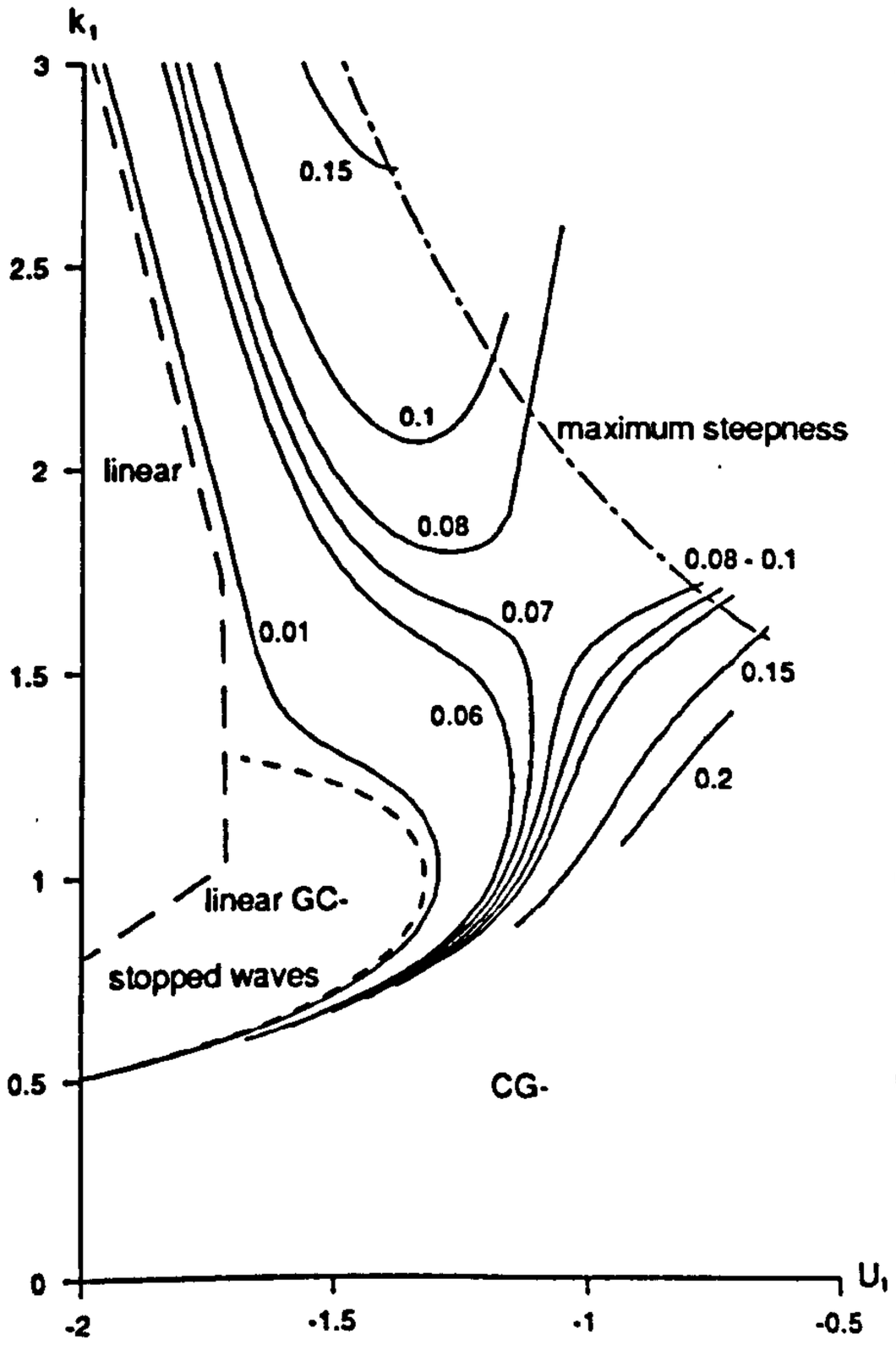

Figure 10.7c

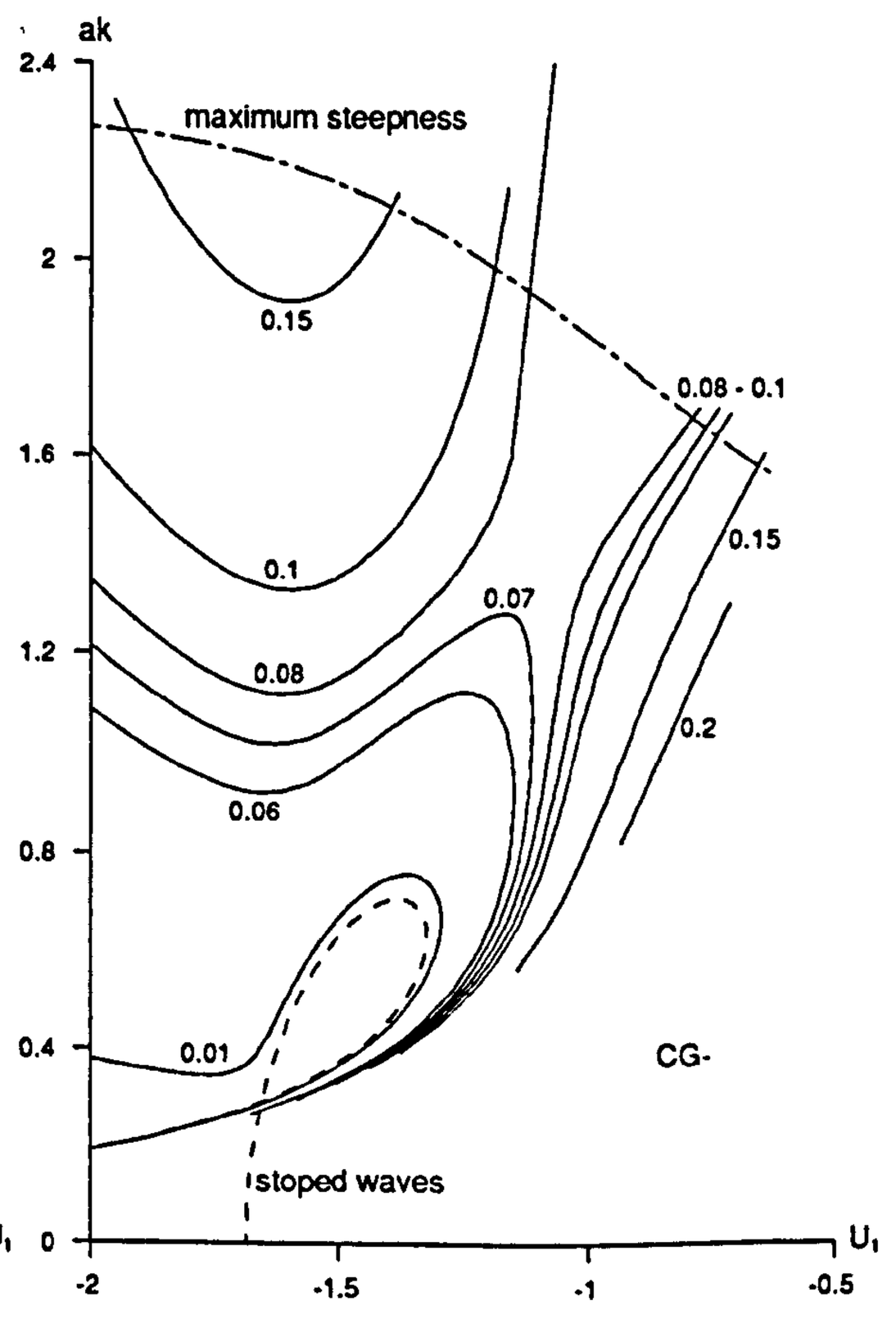

Figure 10.7d

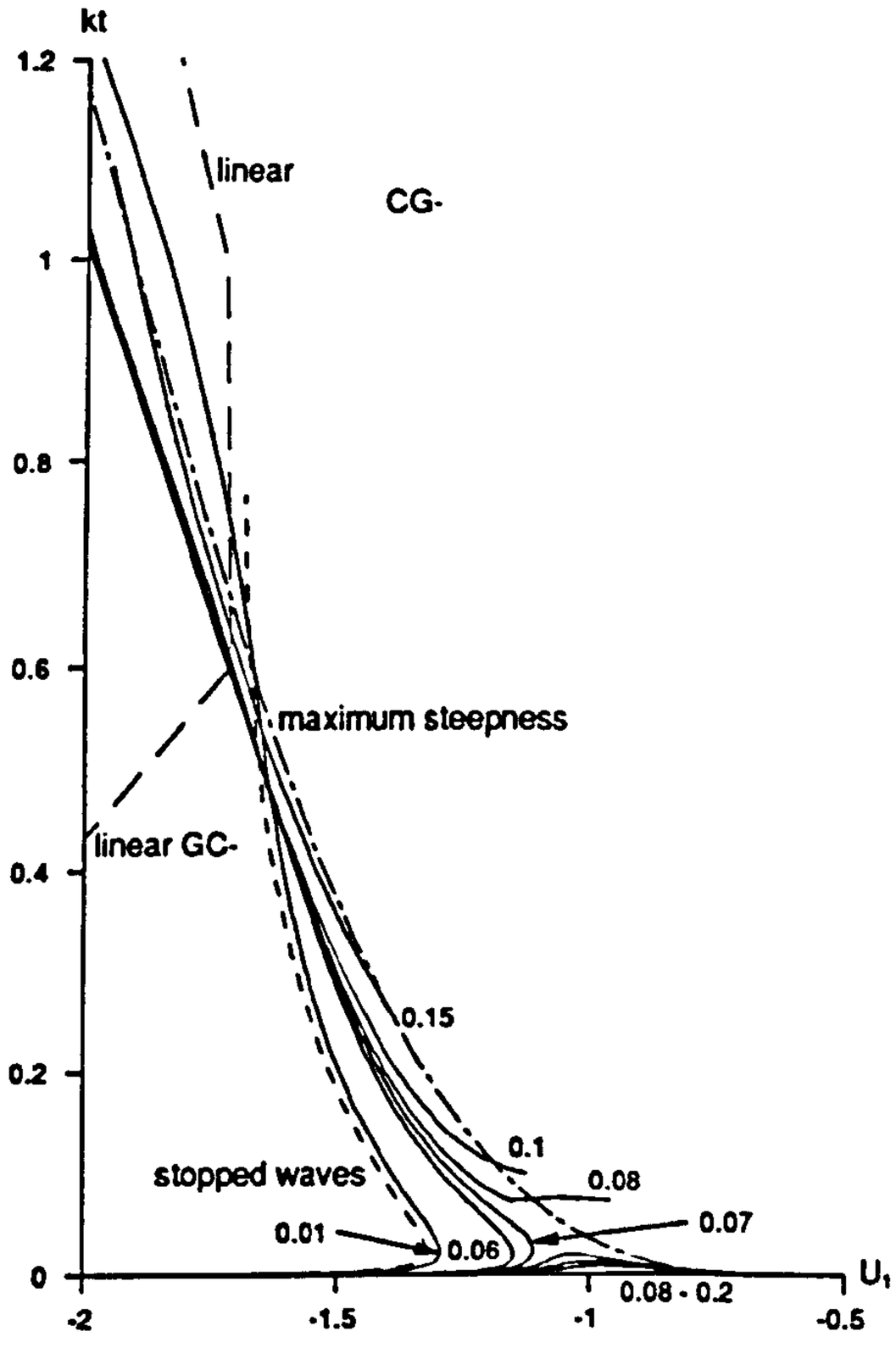

Figure 10.7e

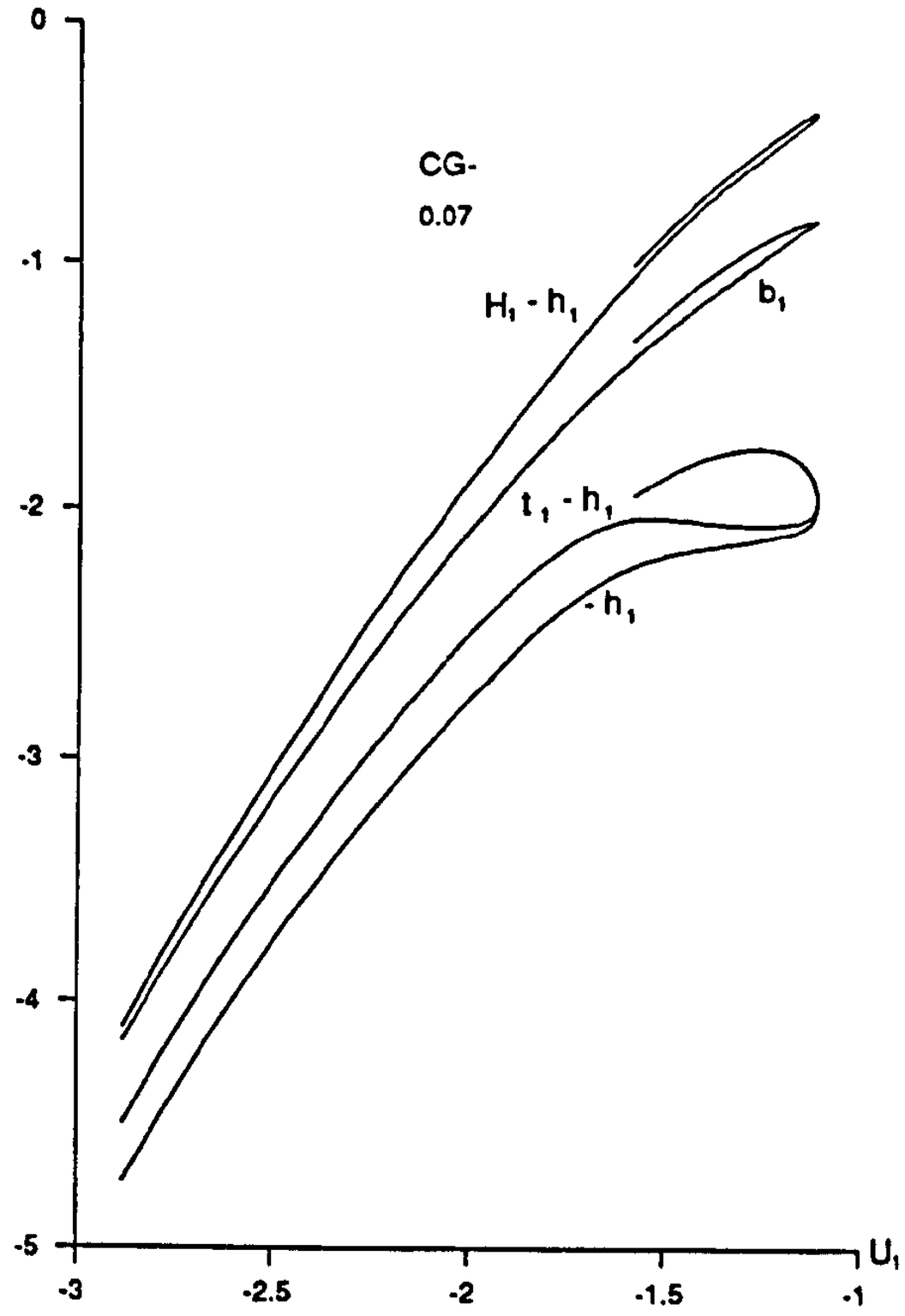

Figure 10.7f

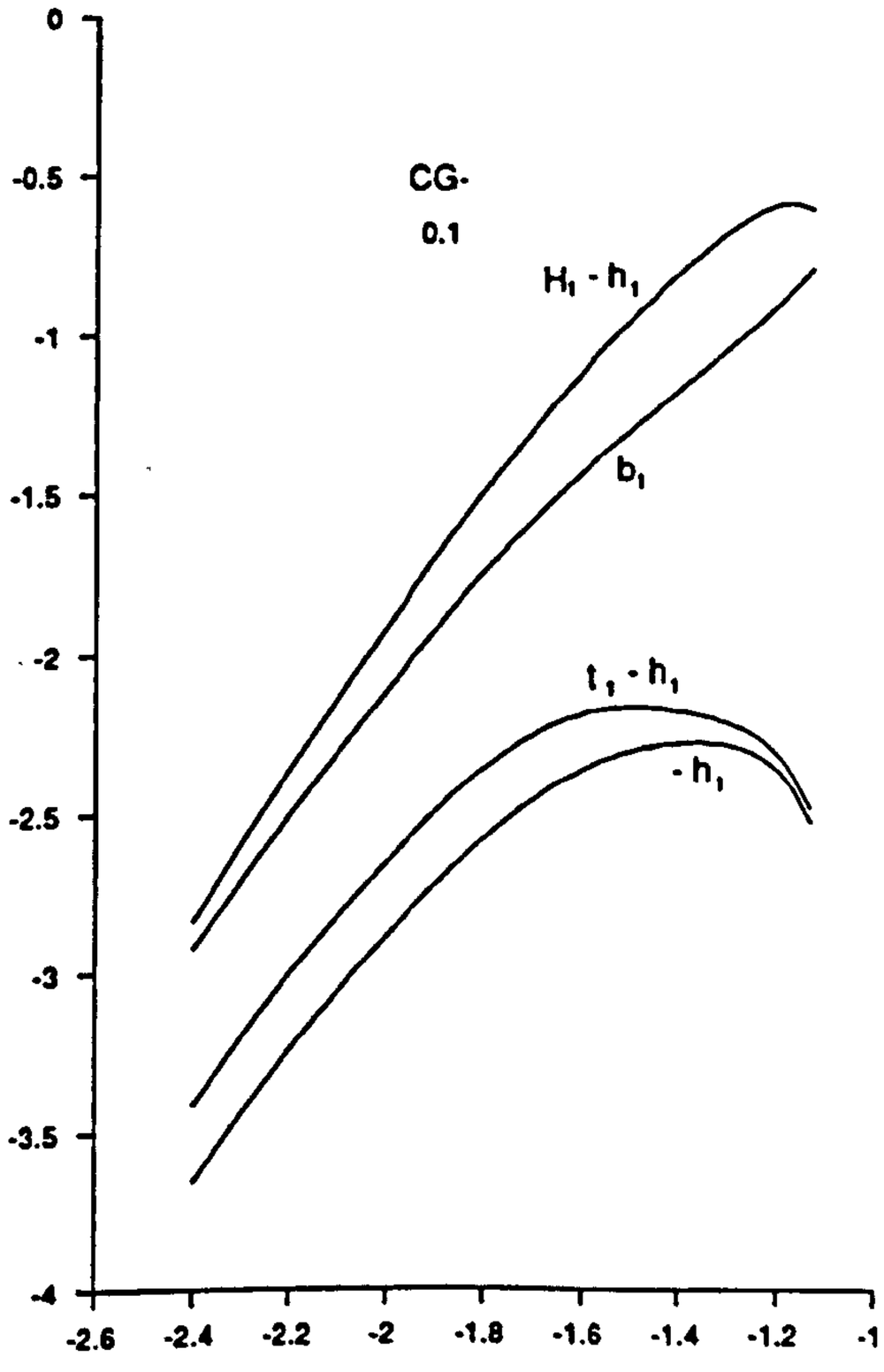

Figure 10.7g

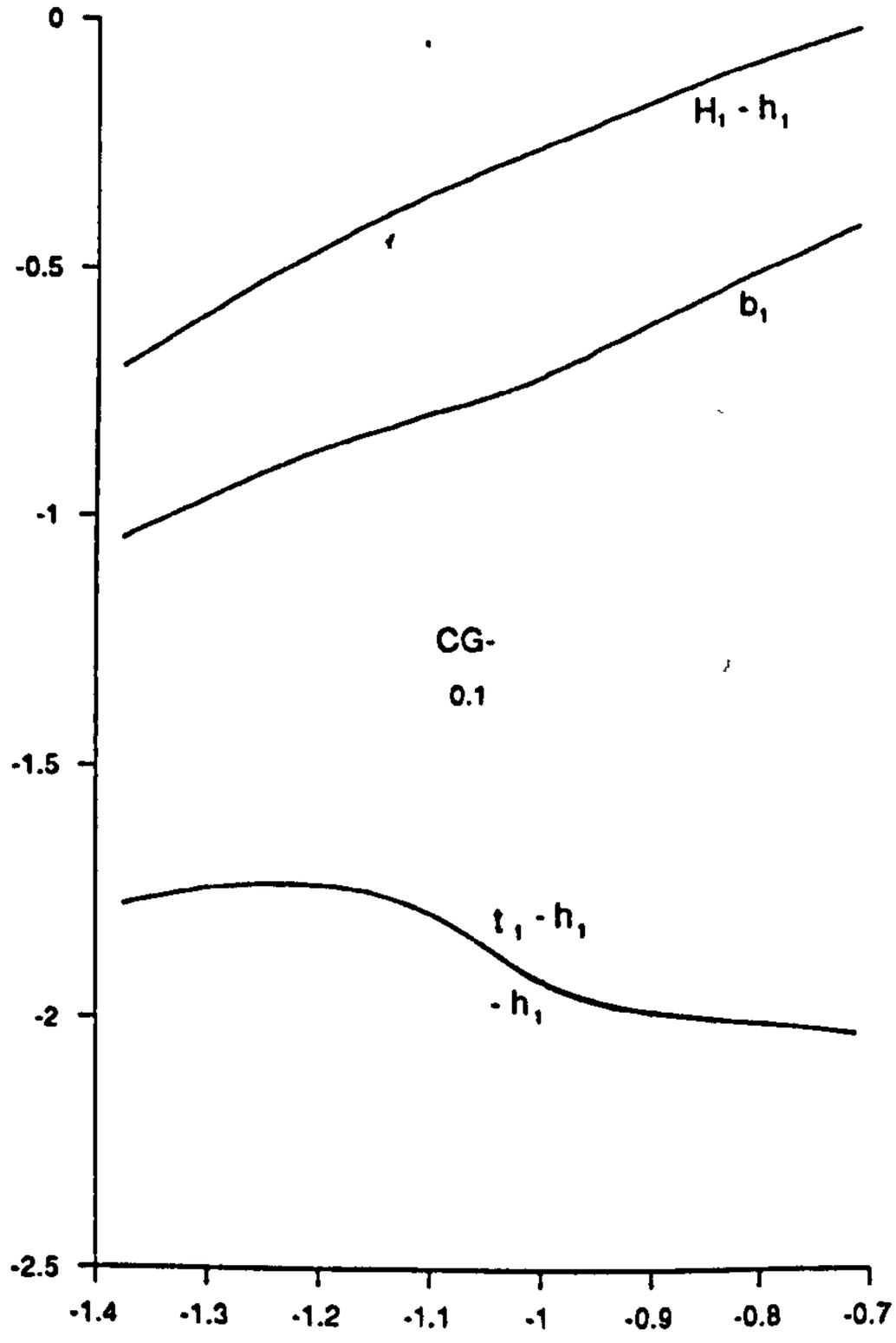

Figure 10.7h

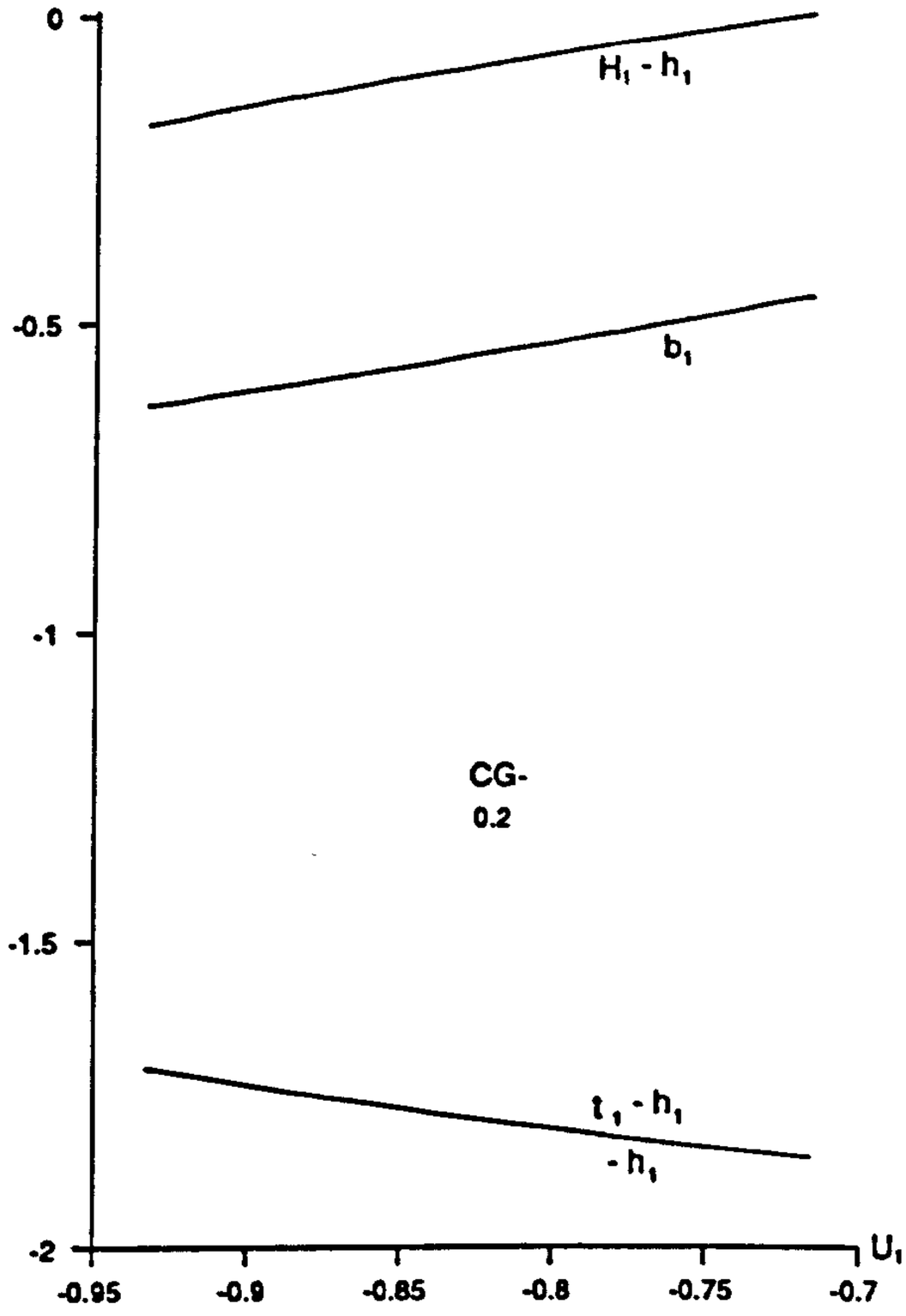

Figure 10.7i

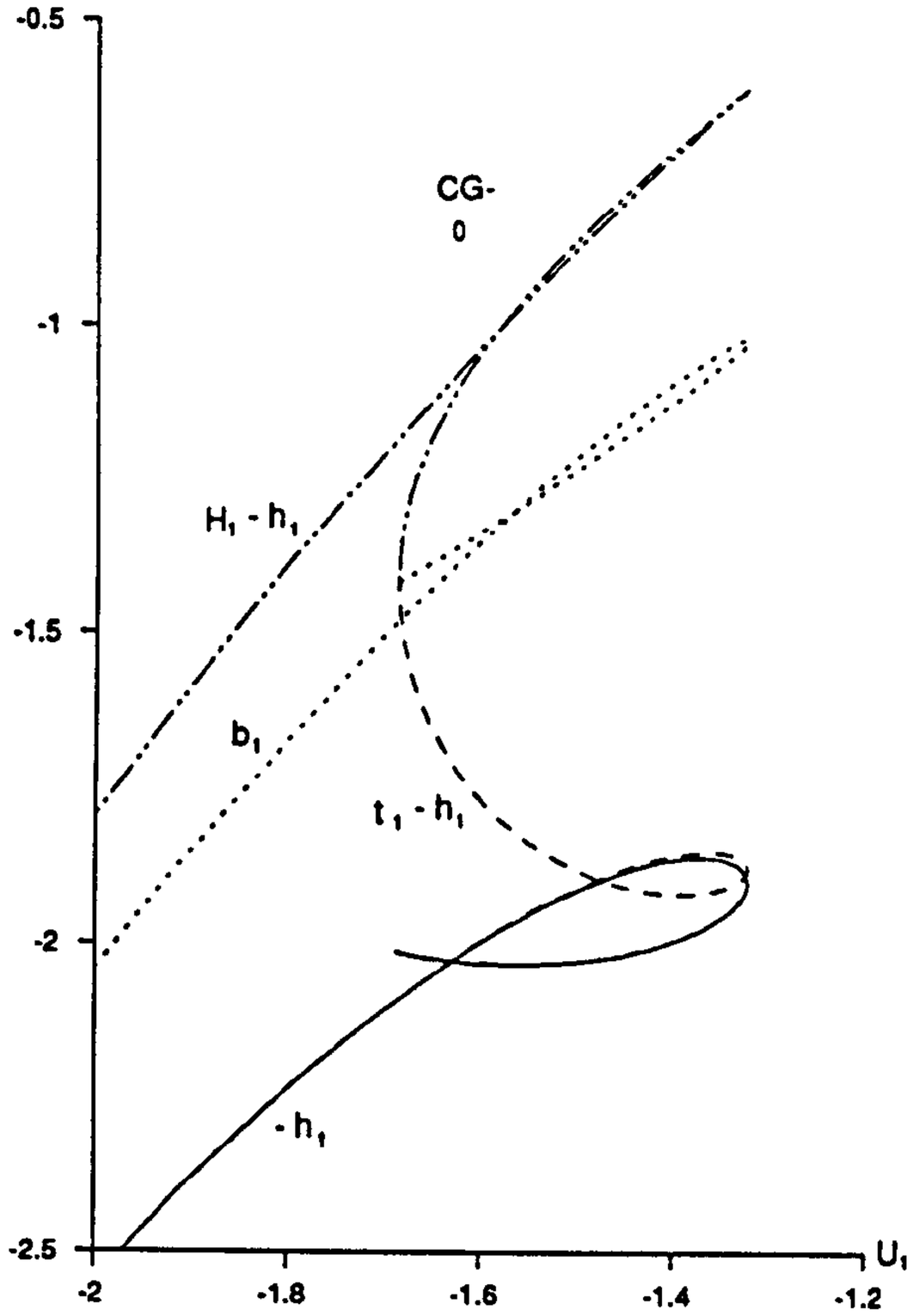

Figure 10.7j

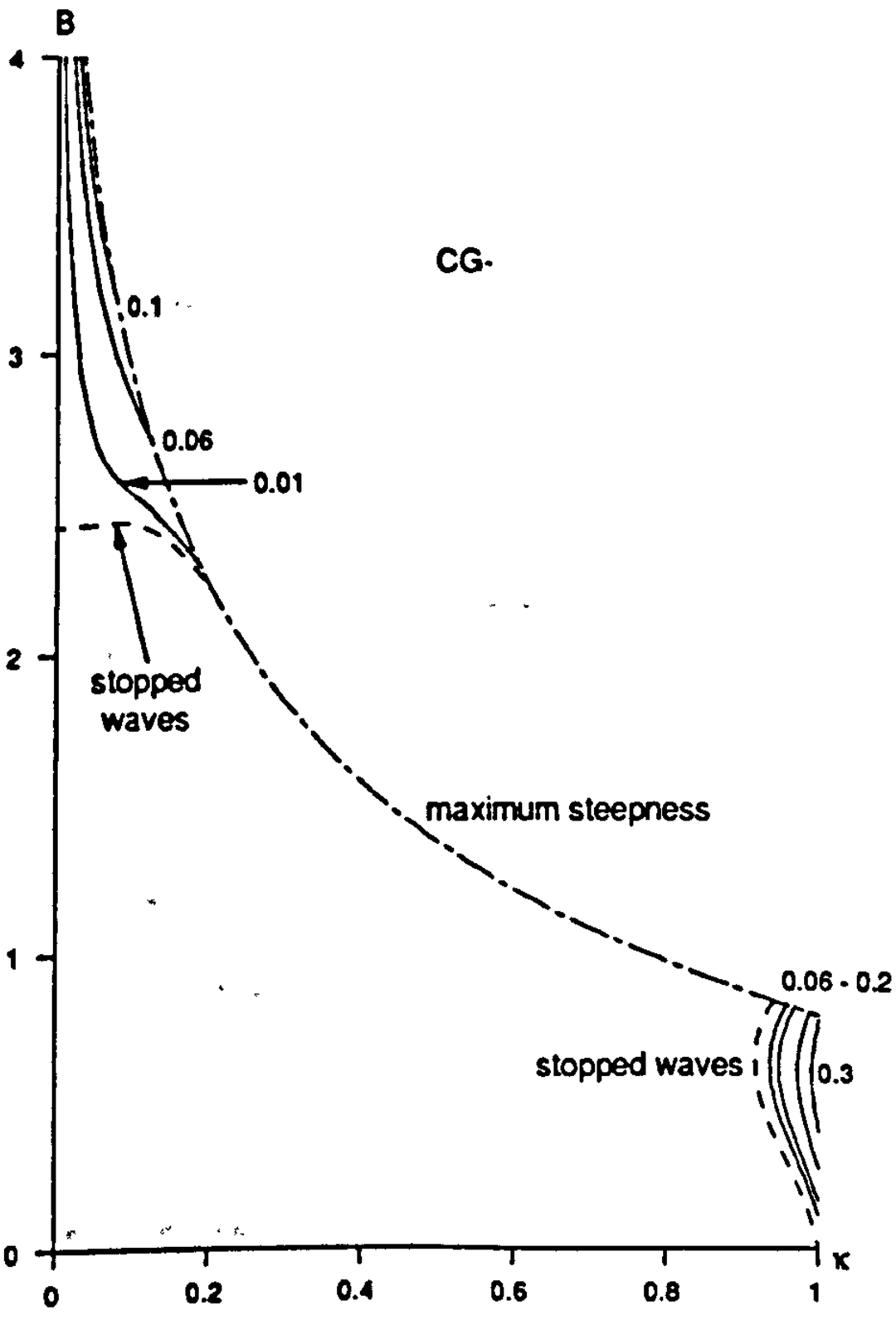

Figure 10.8a

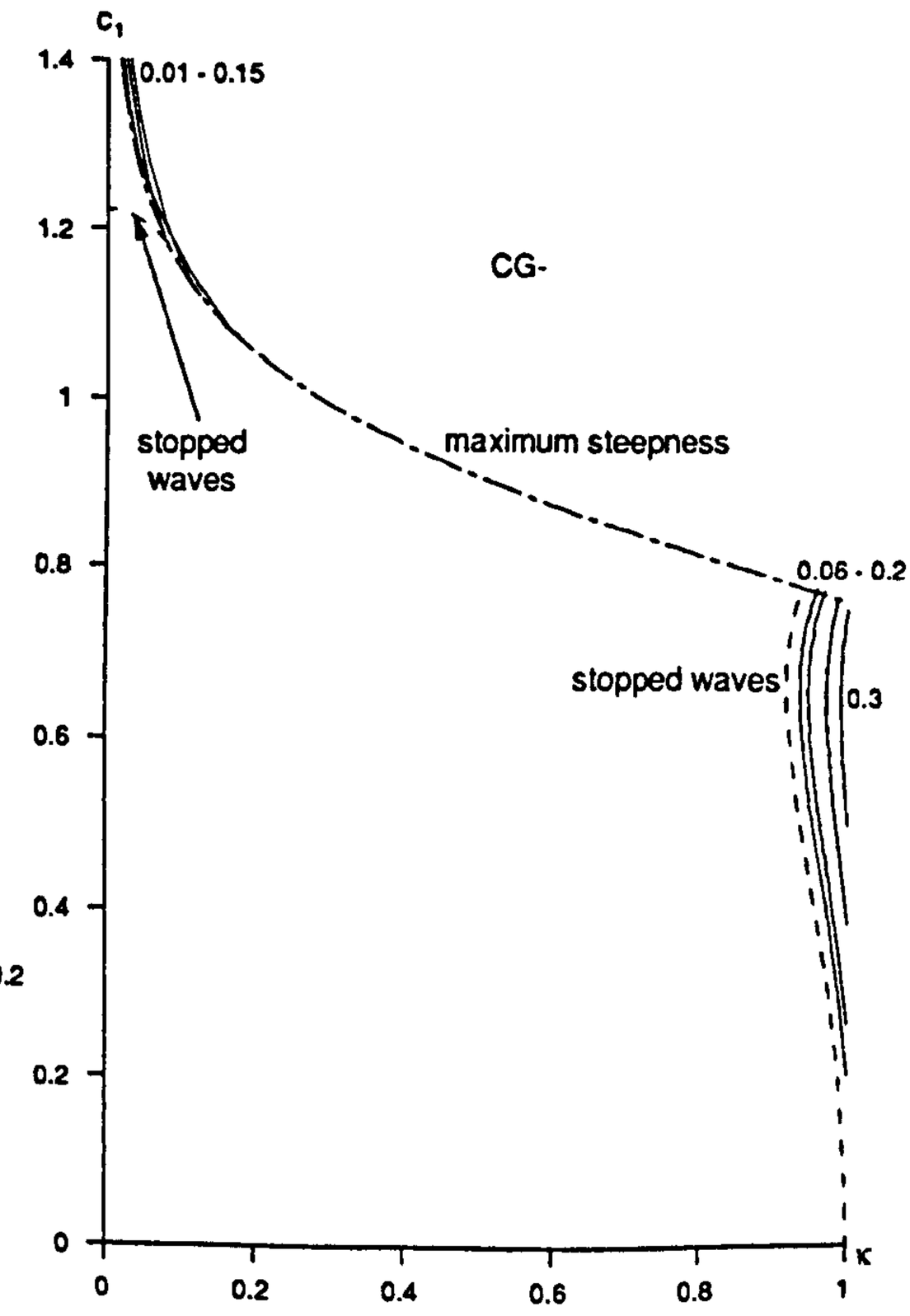

Figure 10.8b

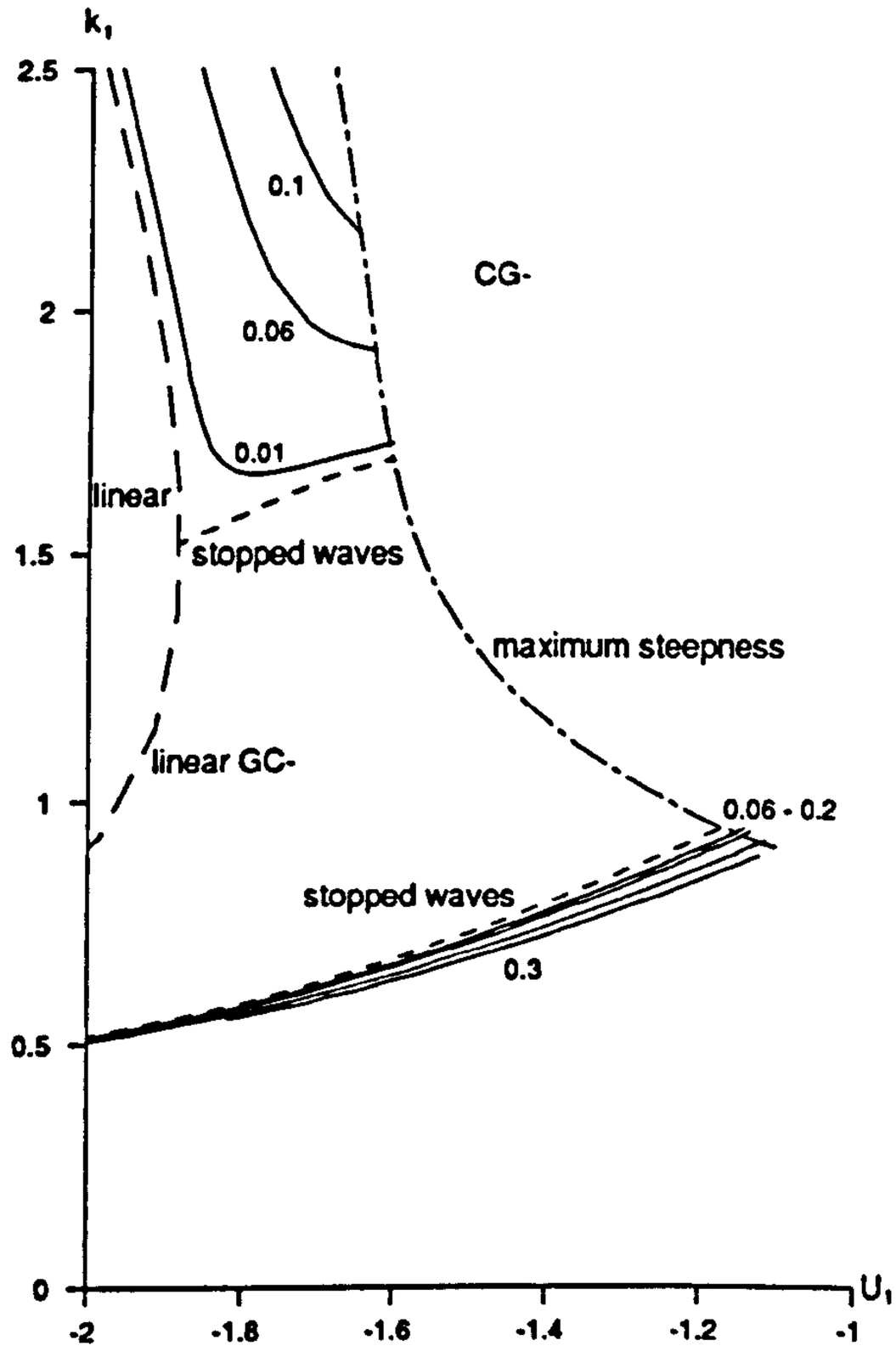

Figure 10.8c

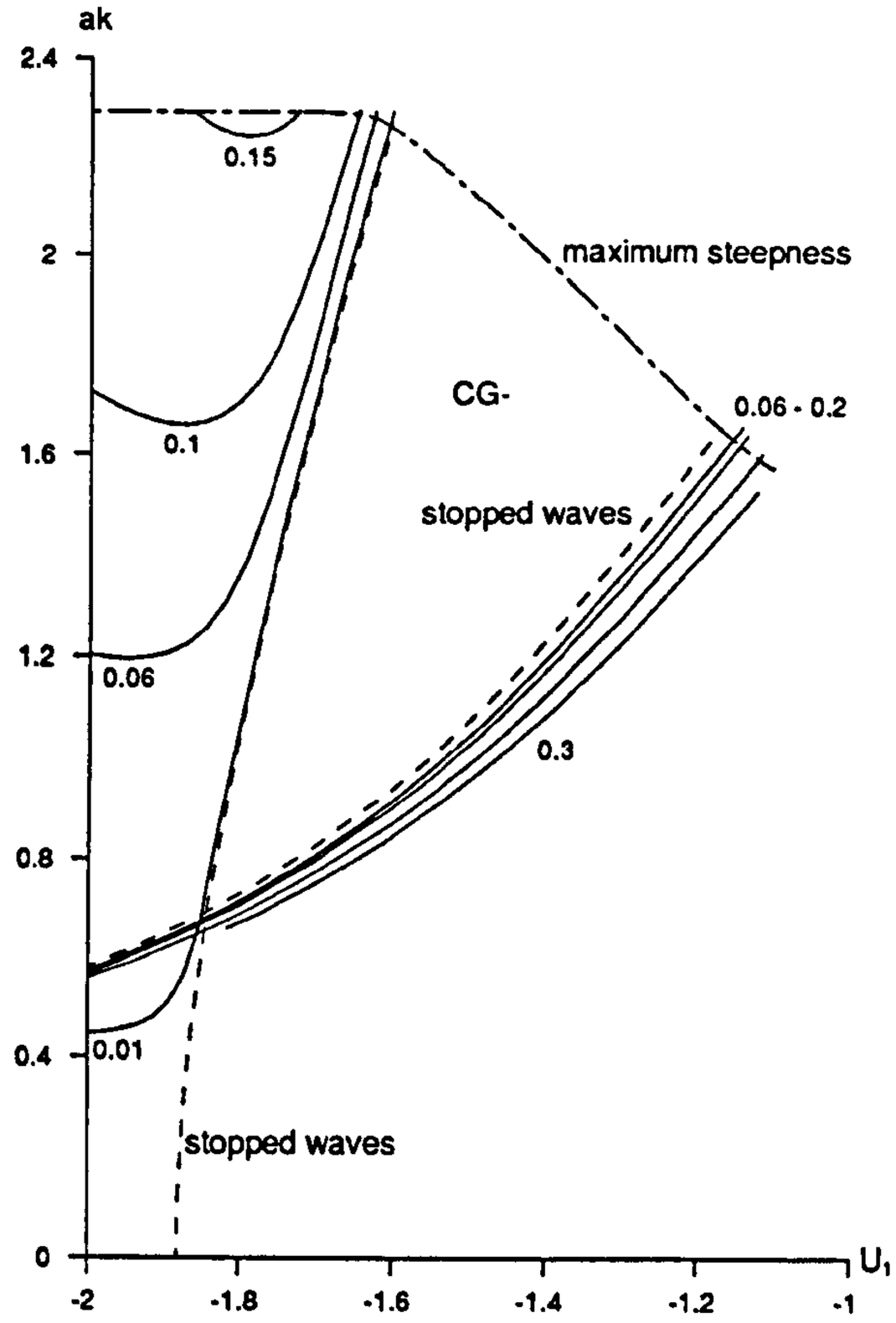

Figure 10.8d

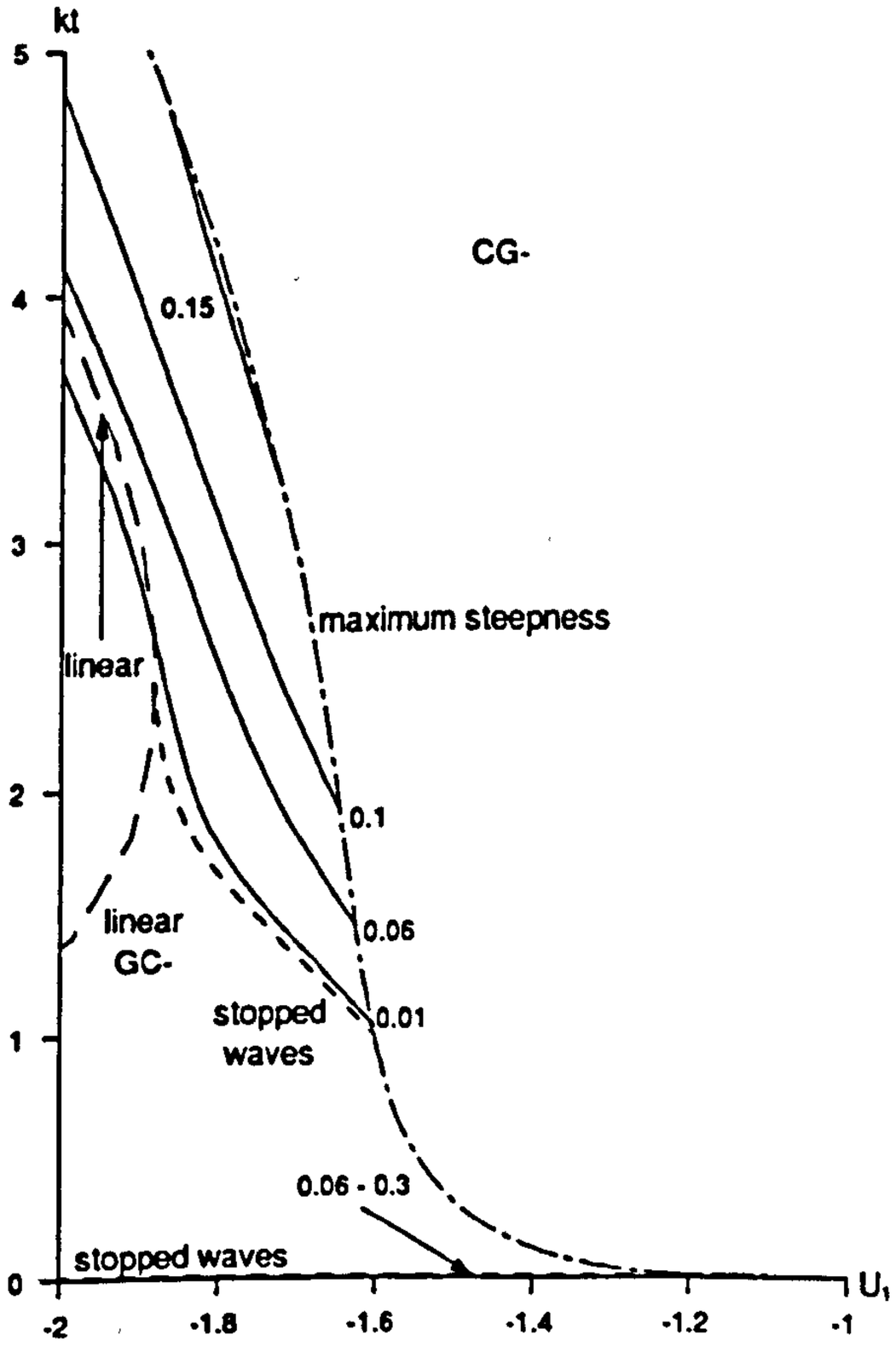

Figure 10.8e

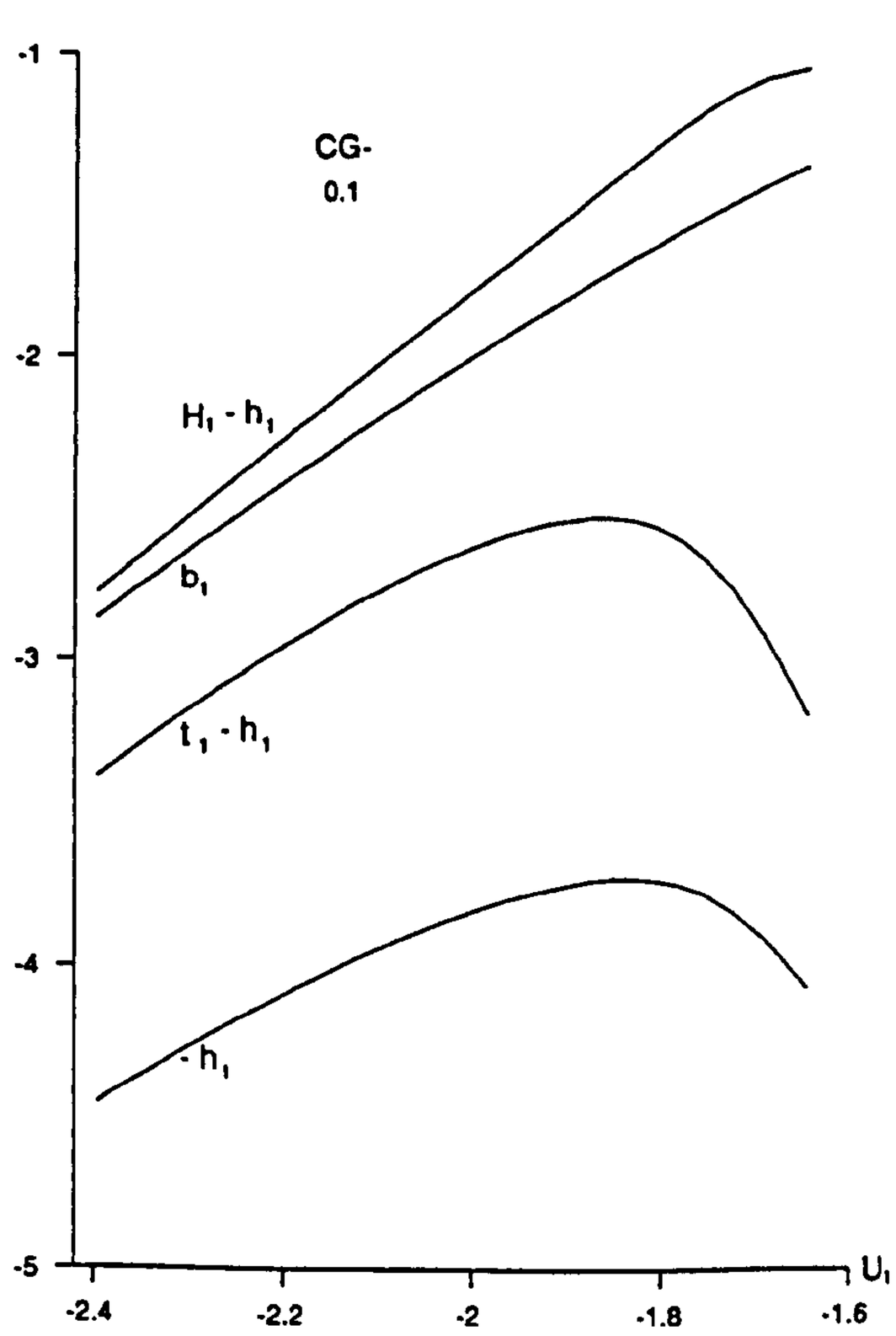

Figure 10.8f

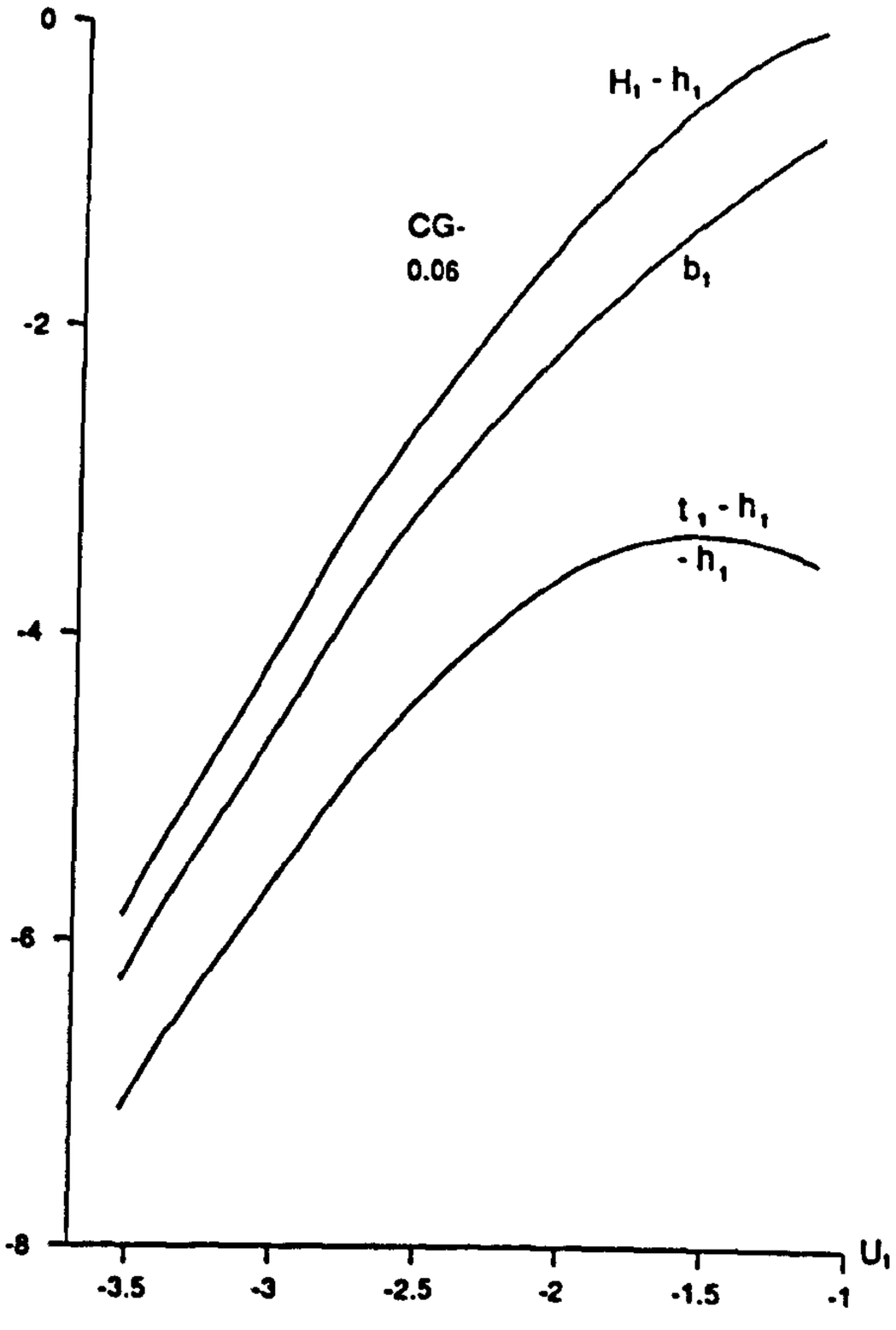

Figure 10.8g

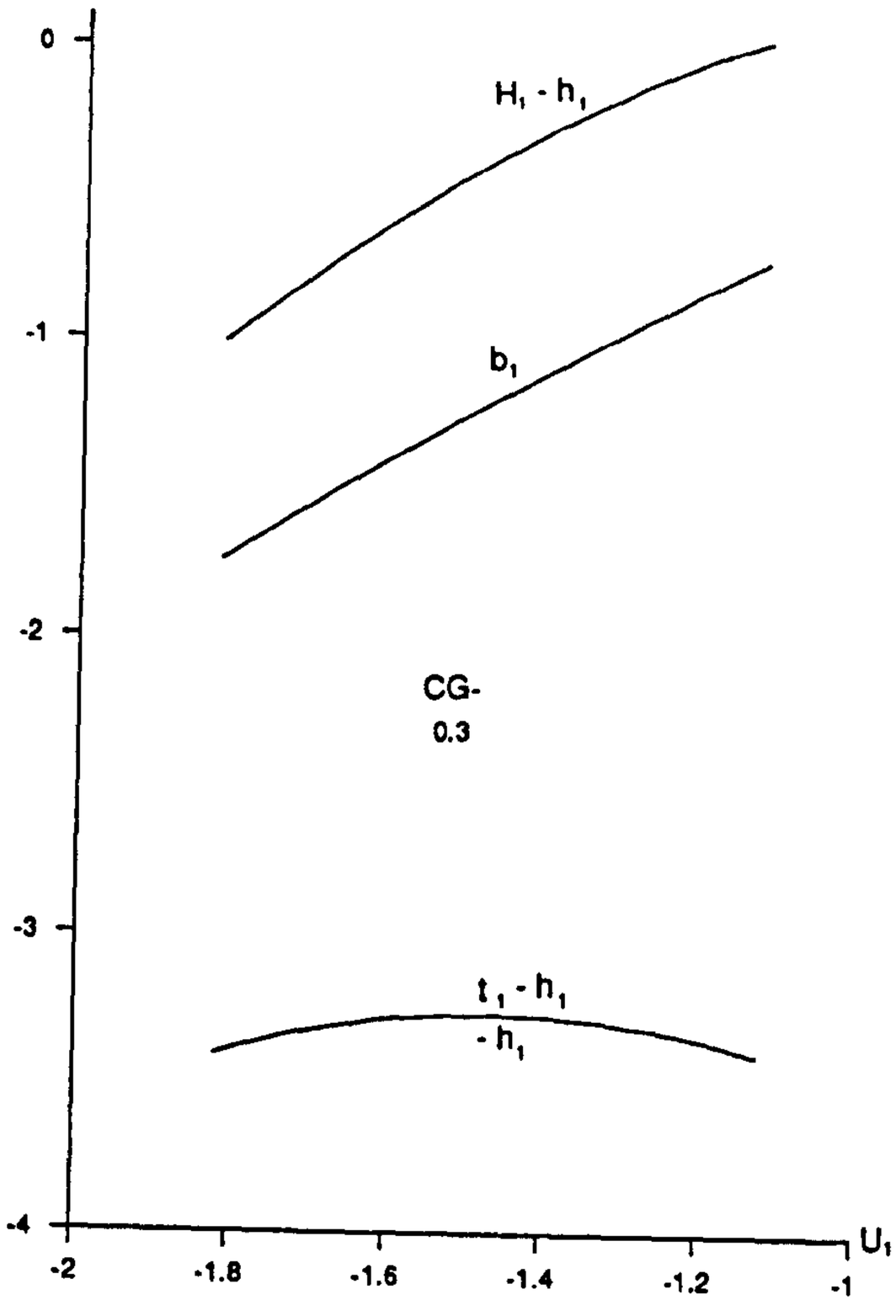

Figure 10.8h

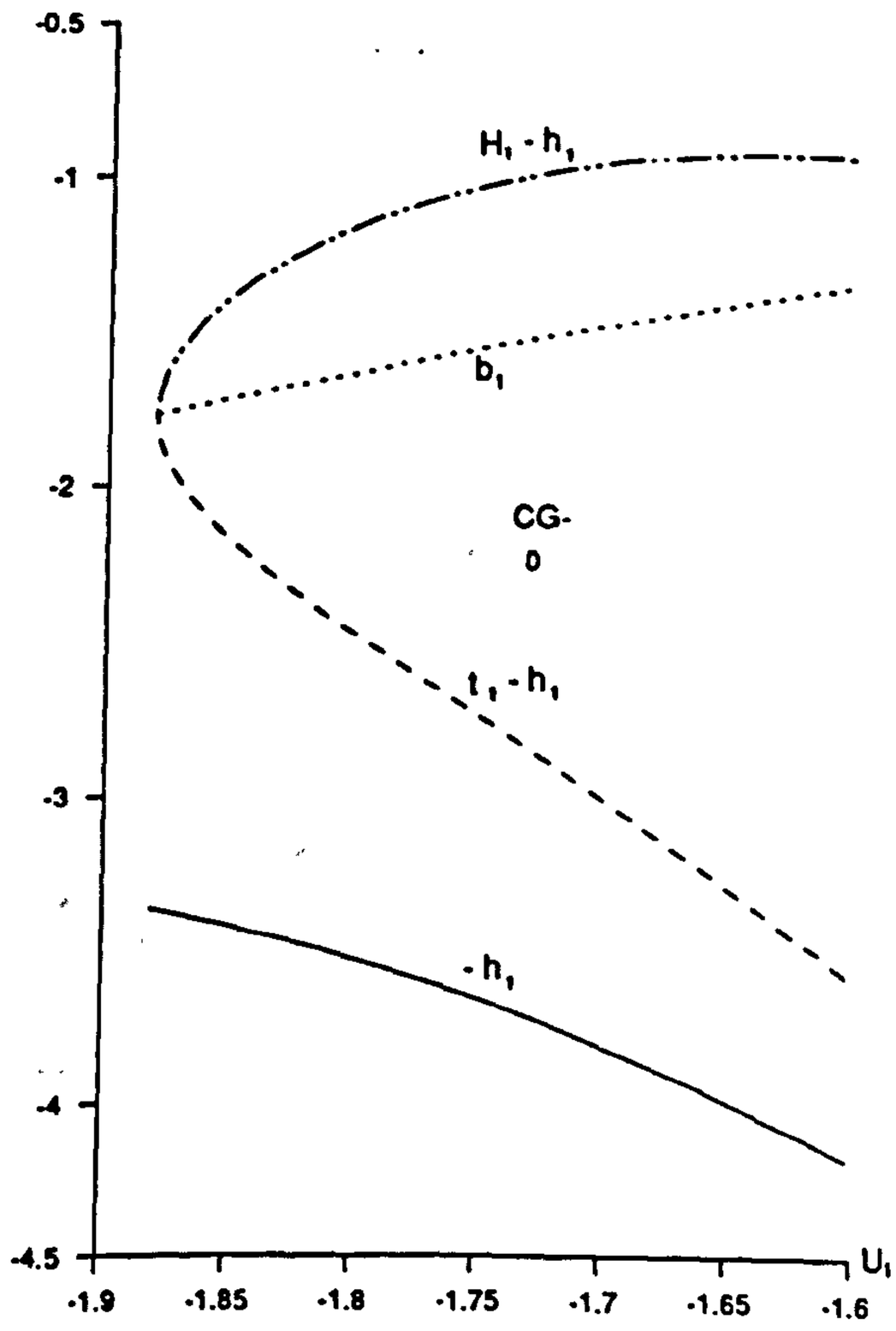

Figure 10.8i

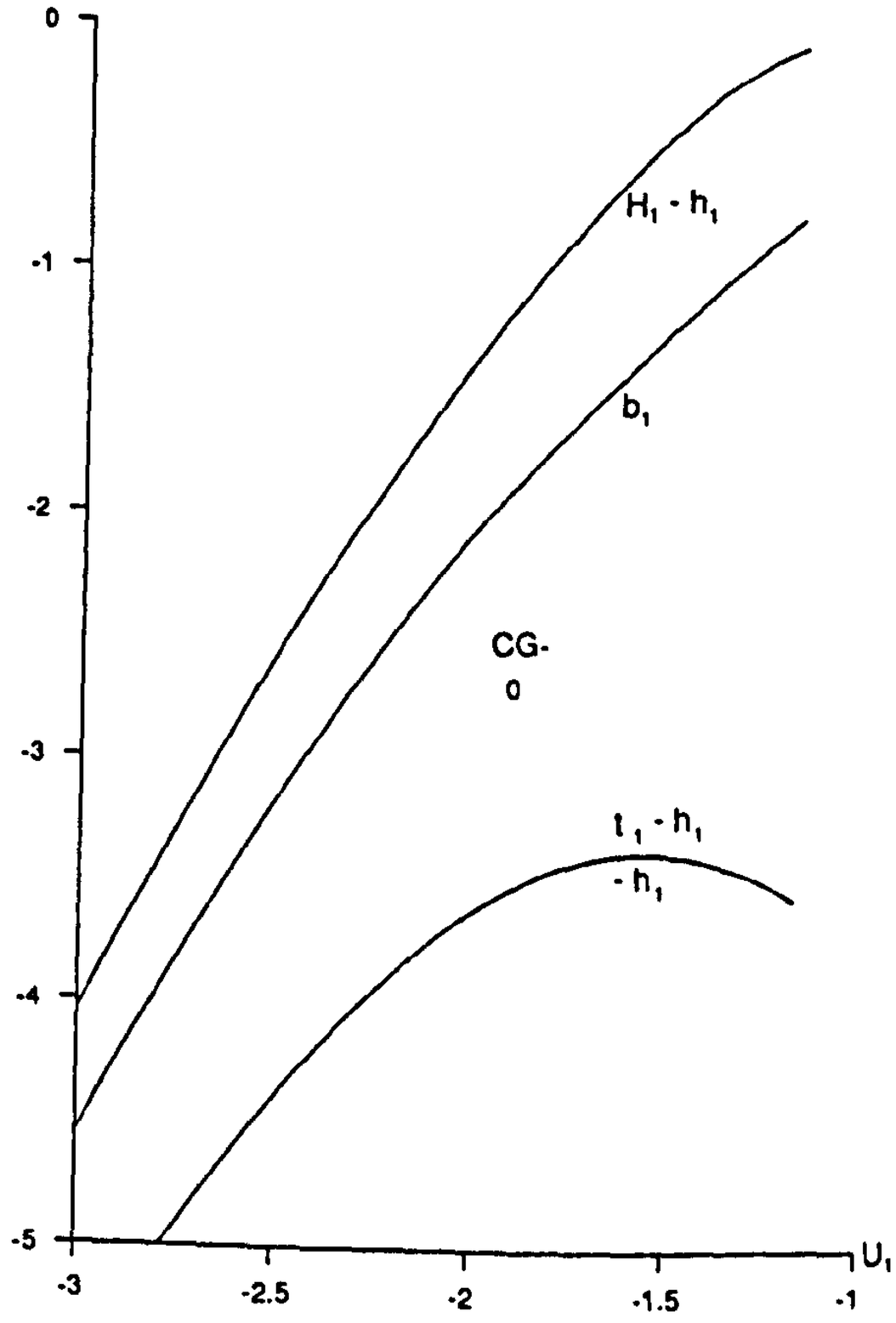

Figure 10.8j

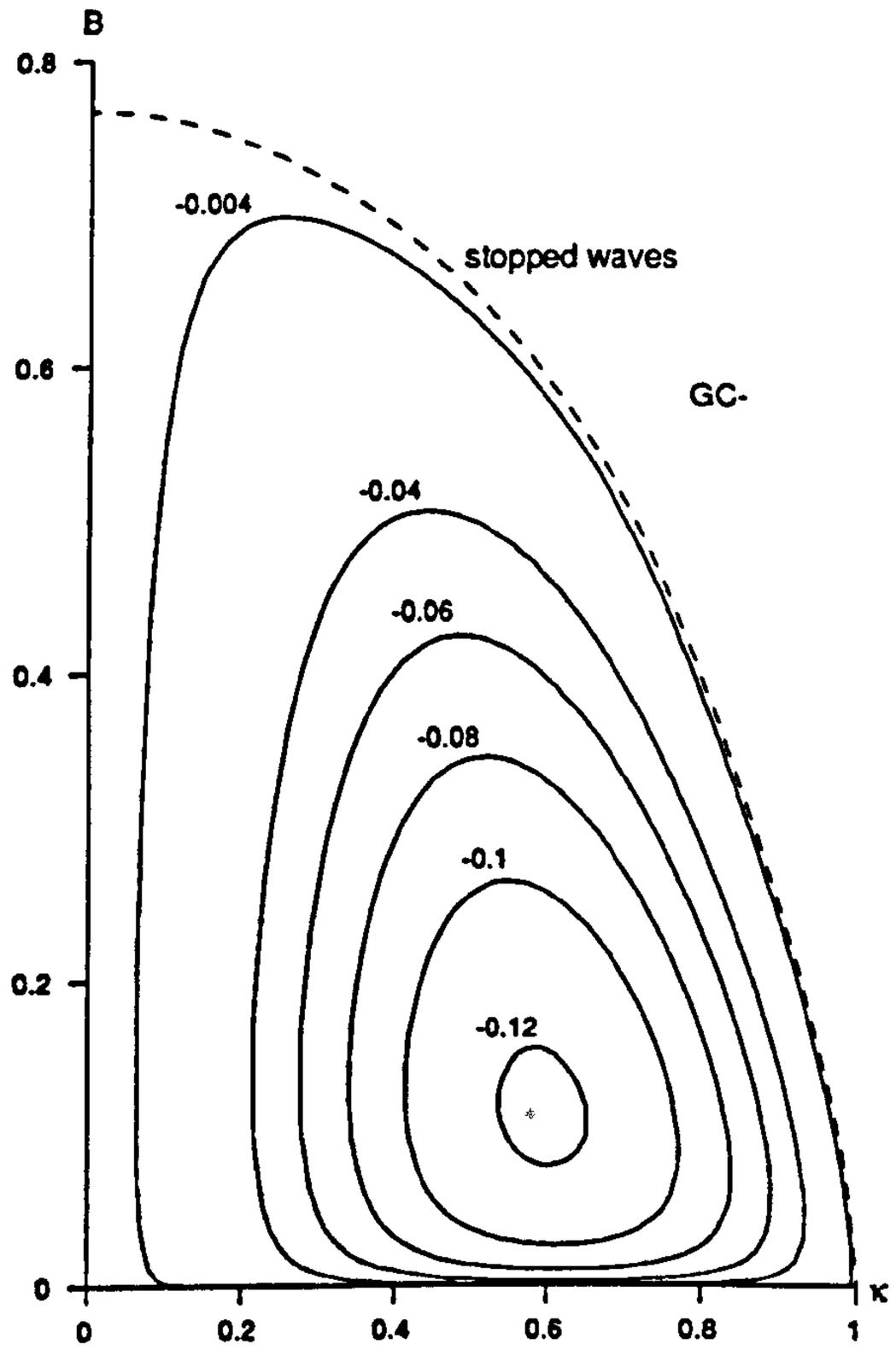

Figure 10.9a

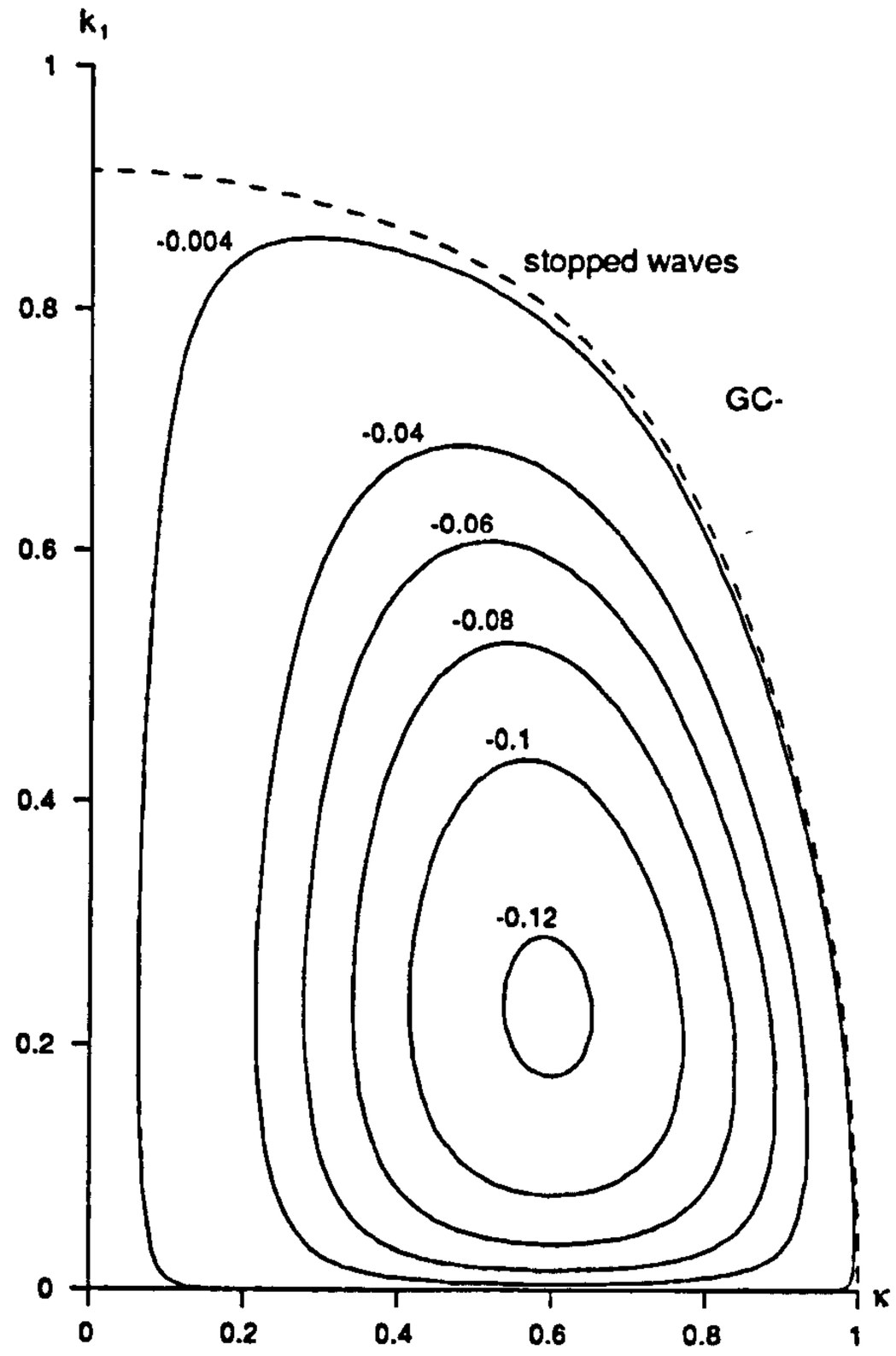

Figure 10.9b

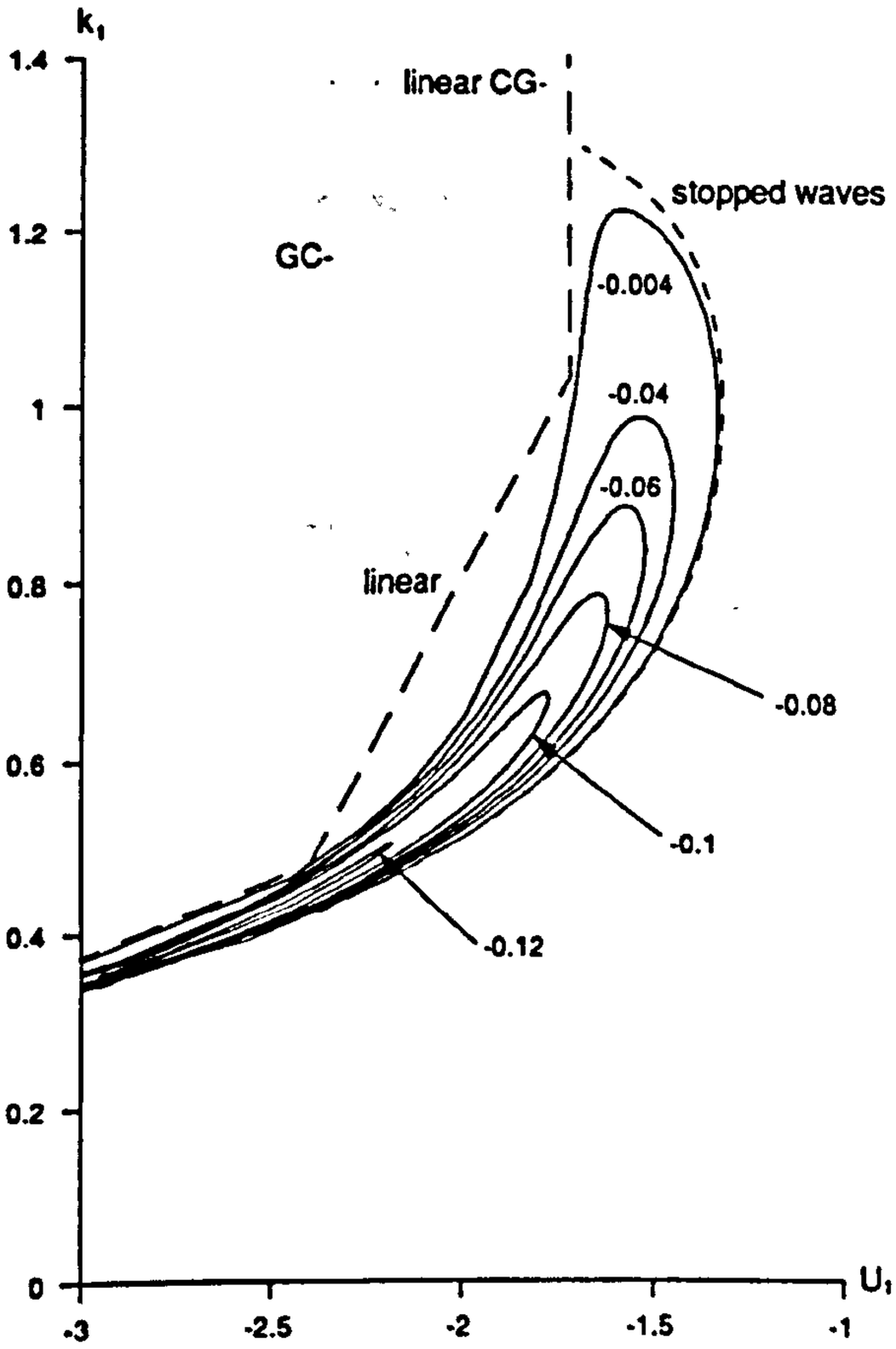

Figure 10.9c

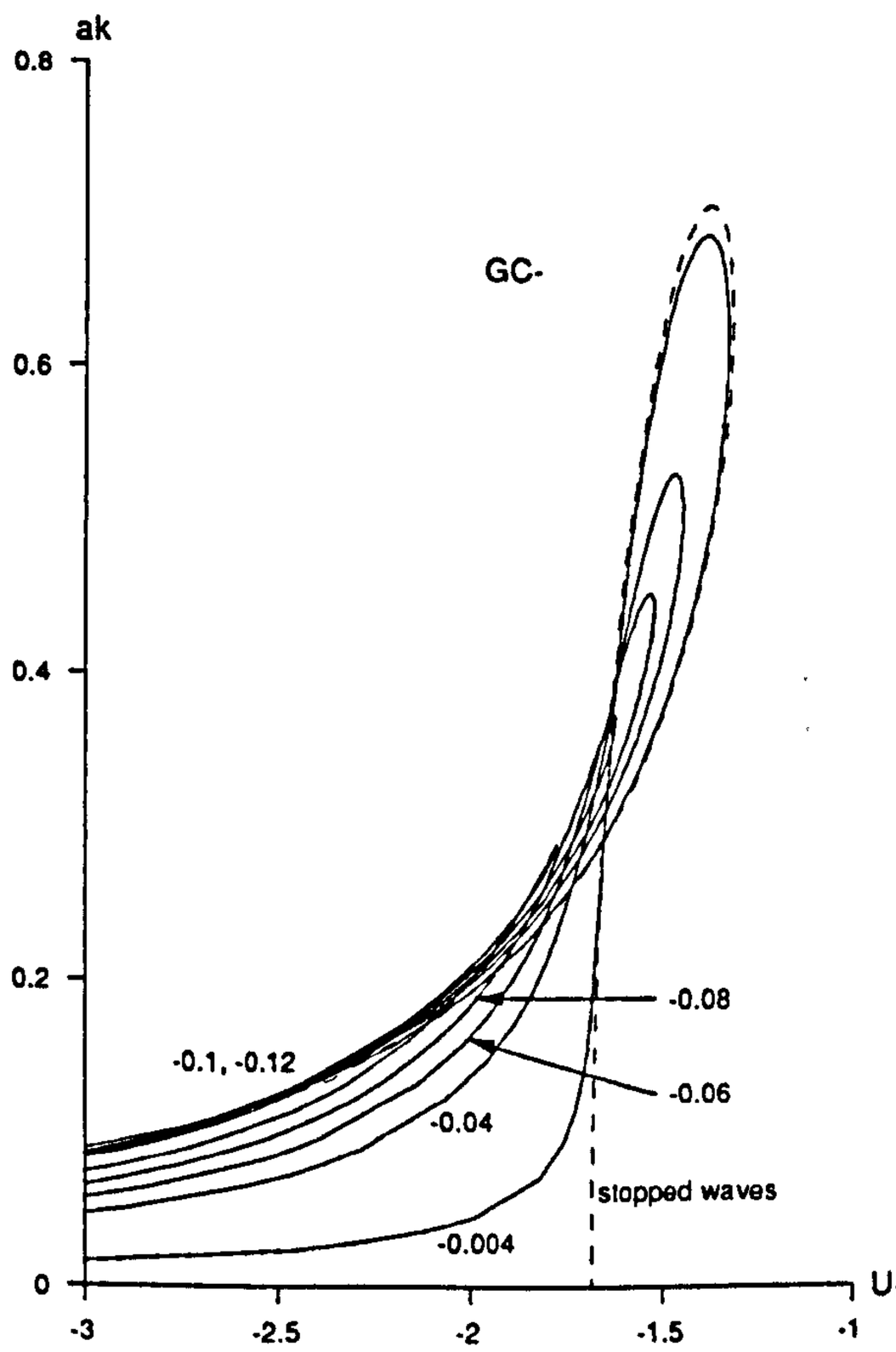

Figure 10.9d

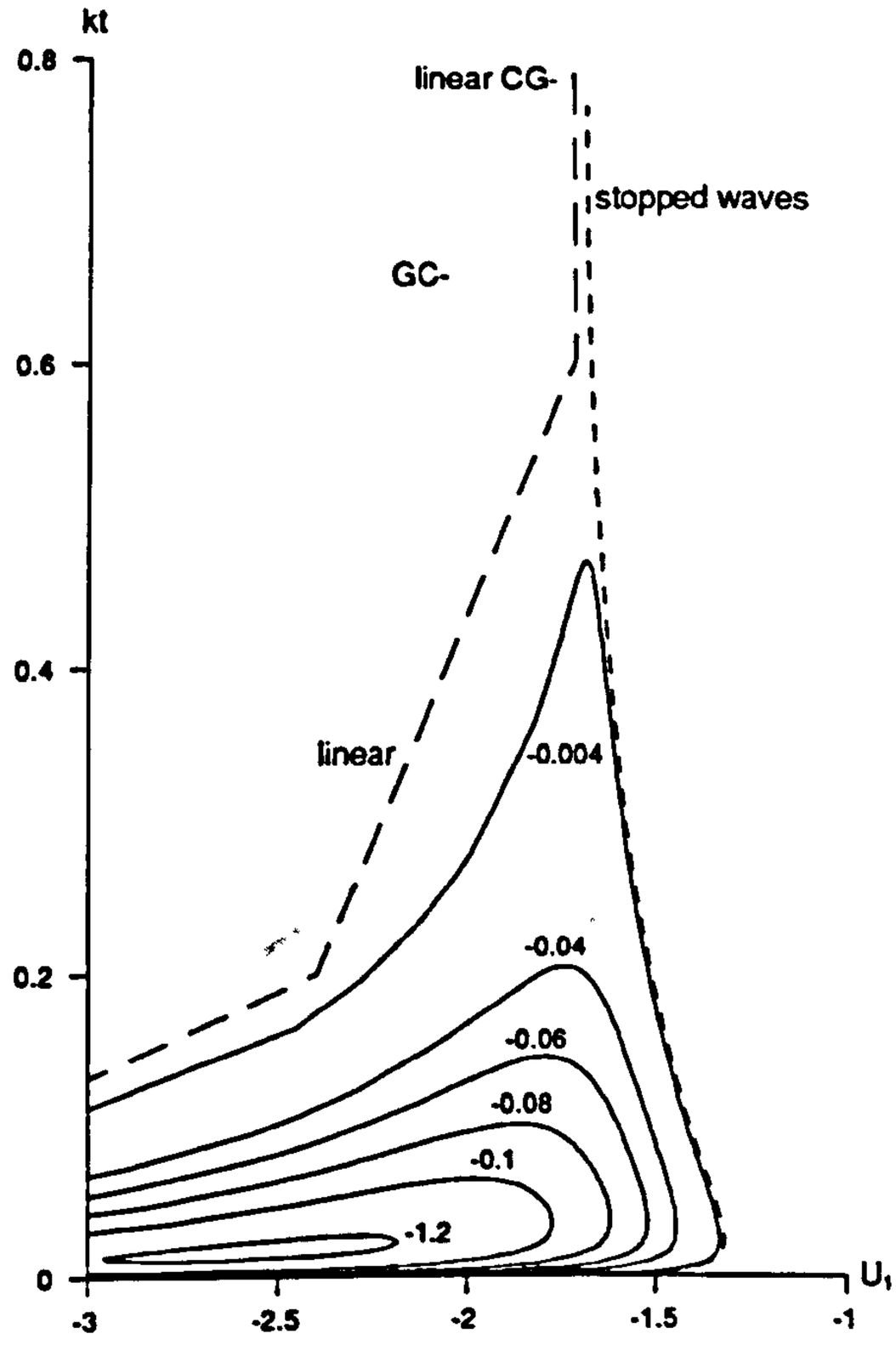

Figure 10.9e

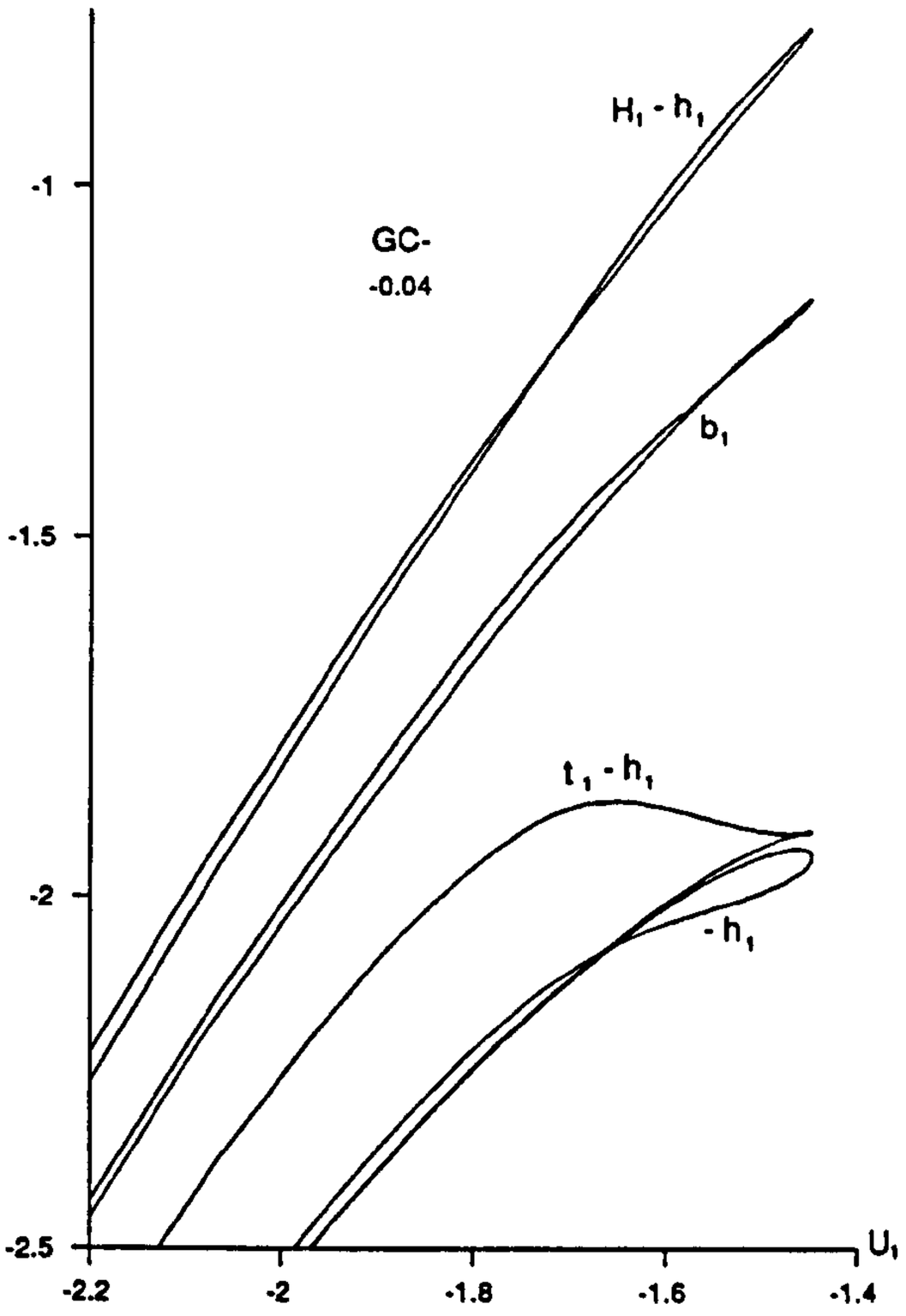

Figure 10.9f

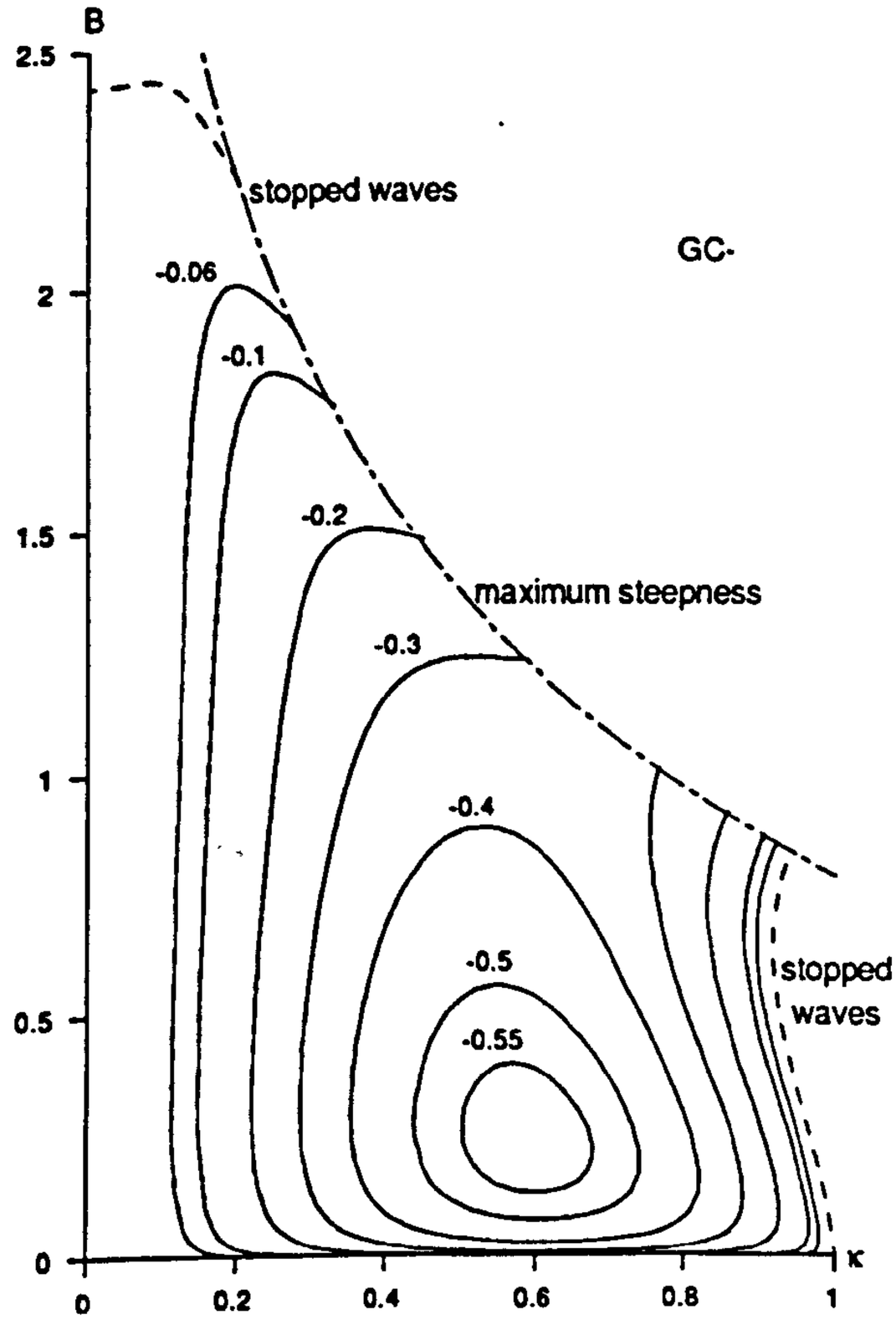

Figure 10.10a

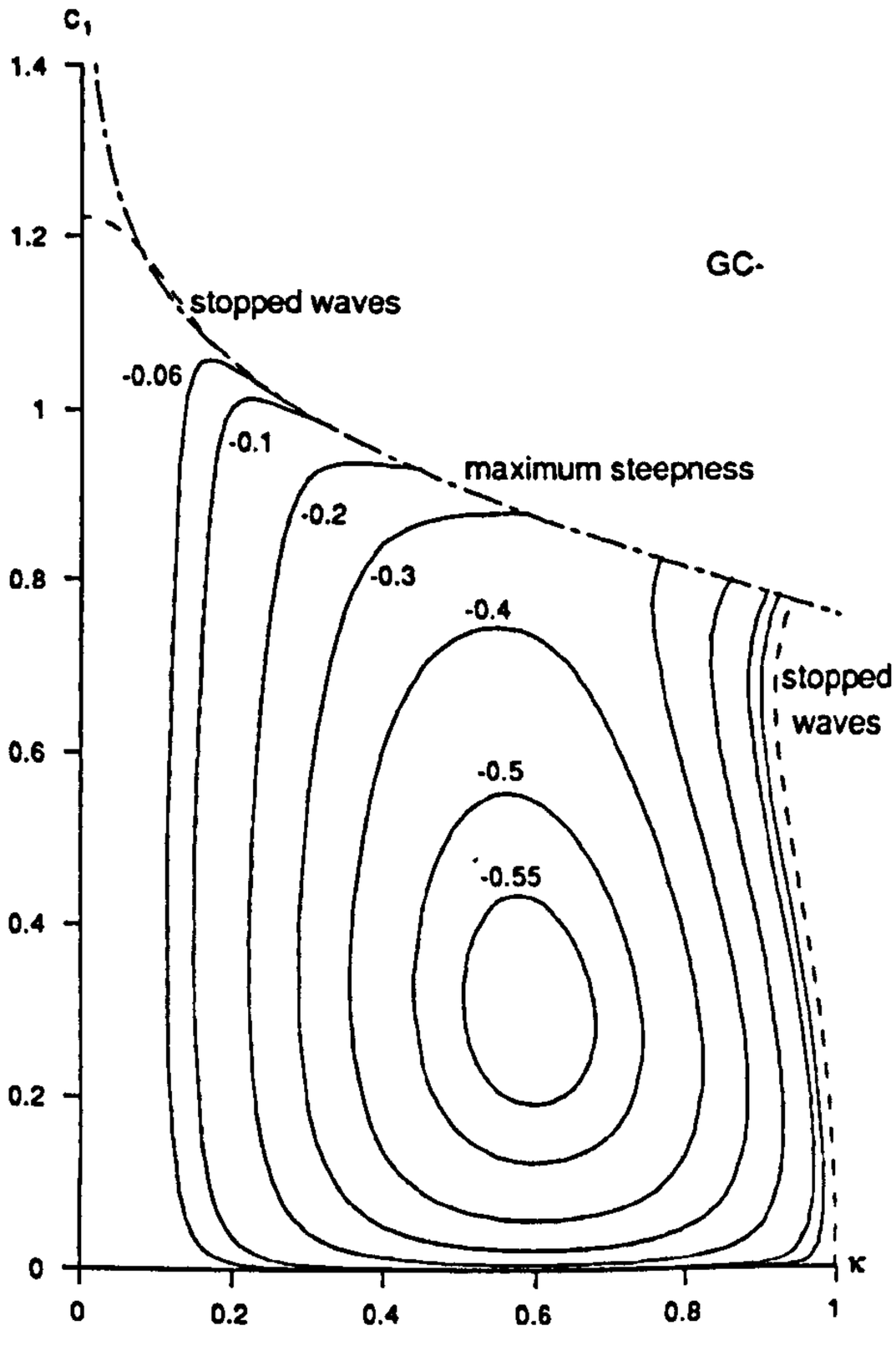

Figure 10.10b

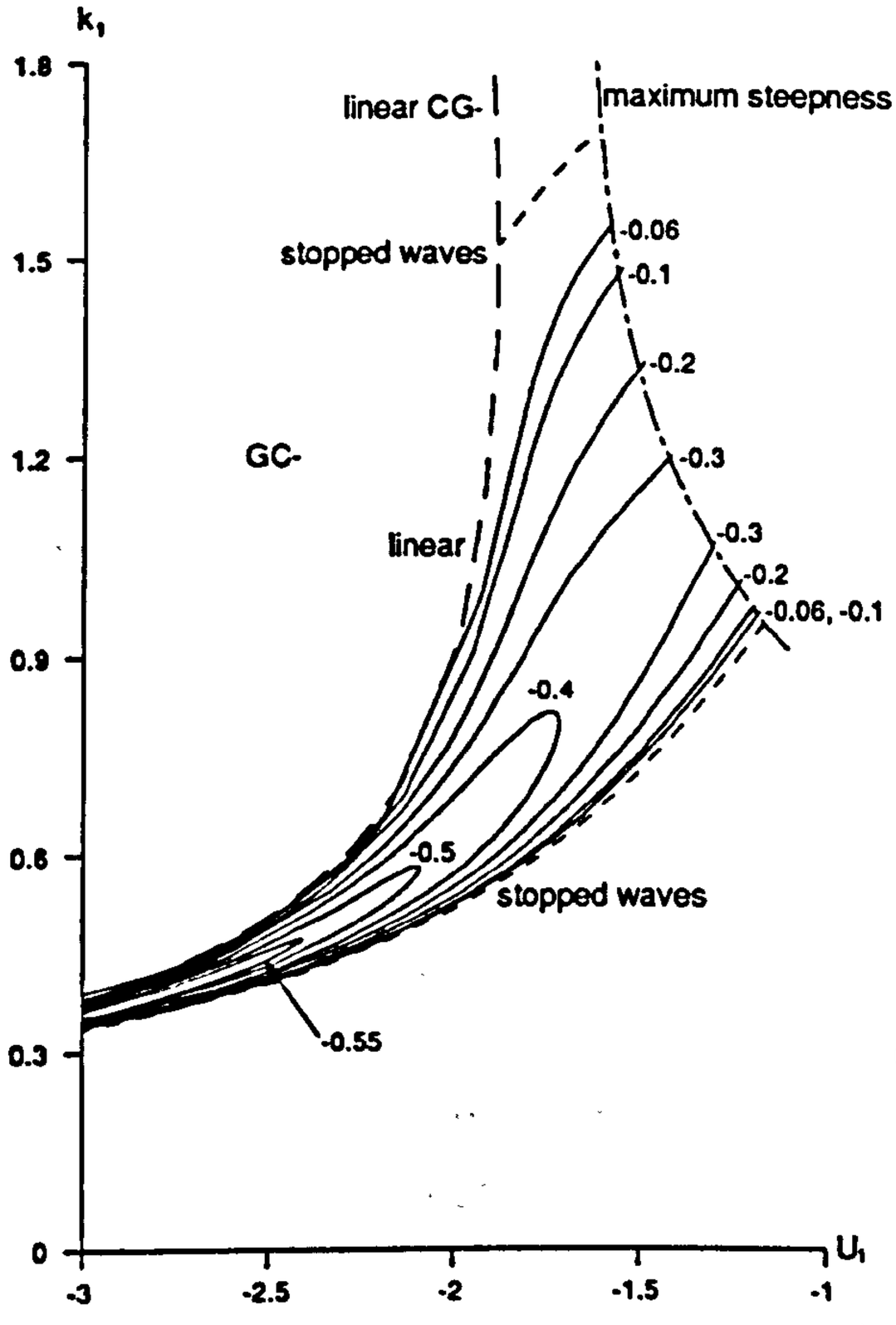

Figure 10.10c

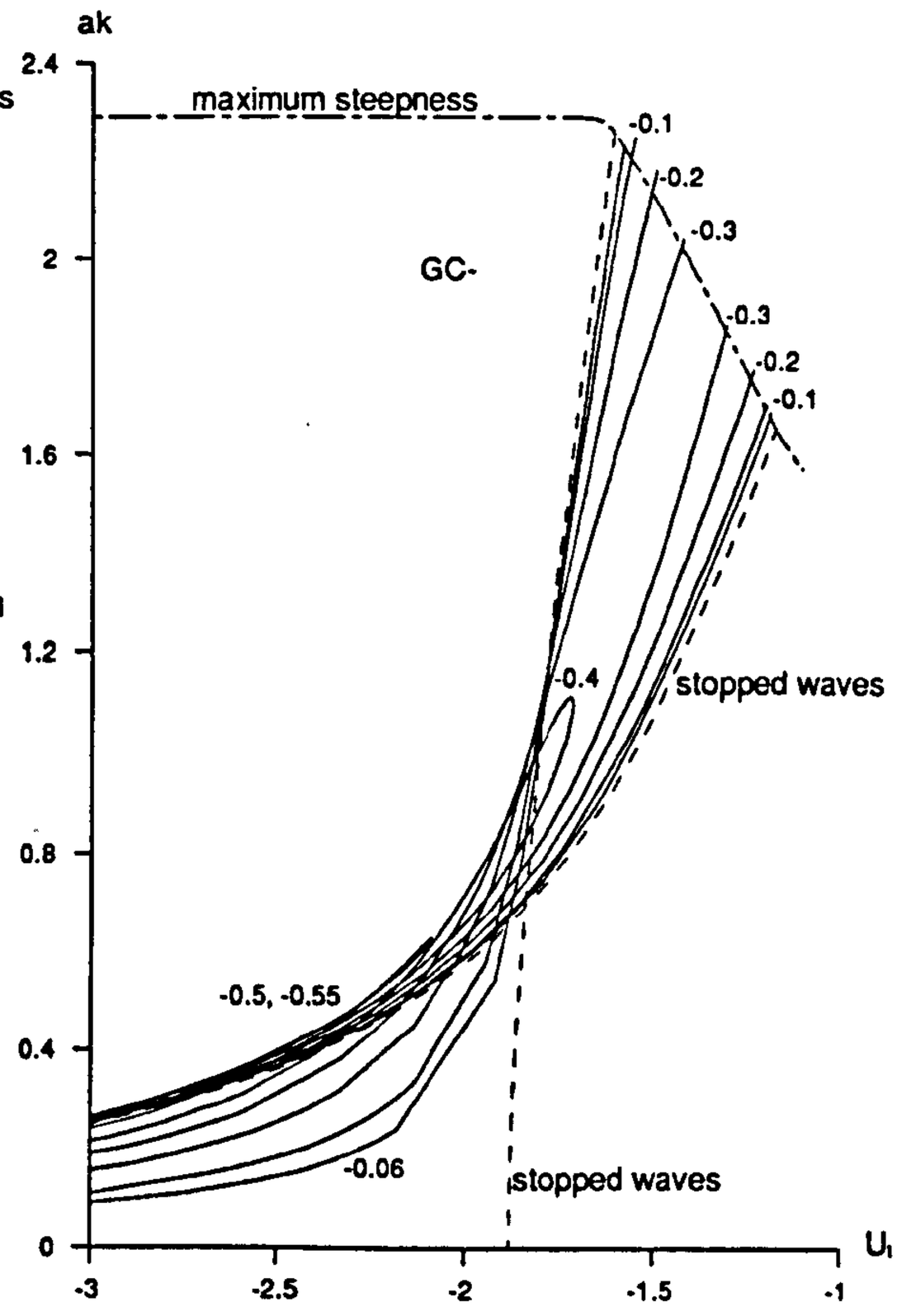

Figure 10.10d

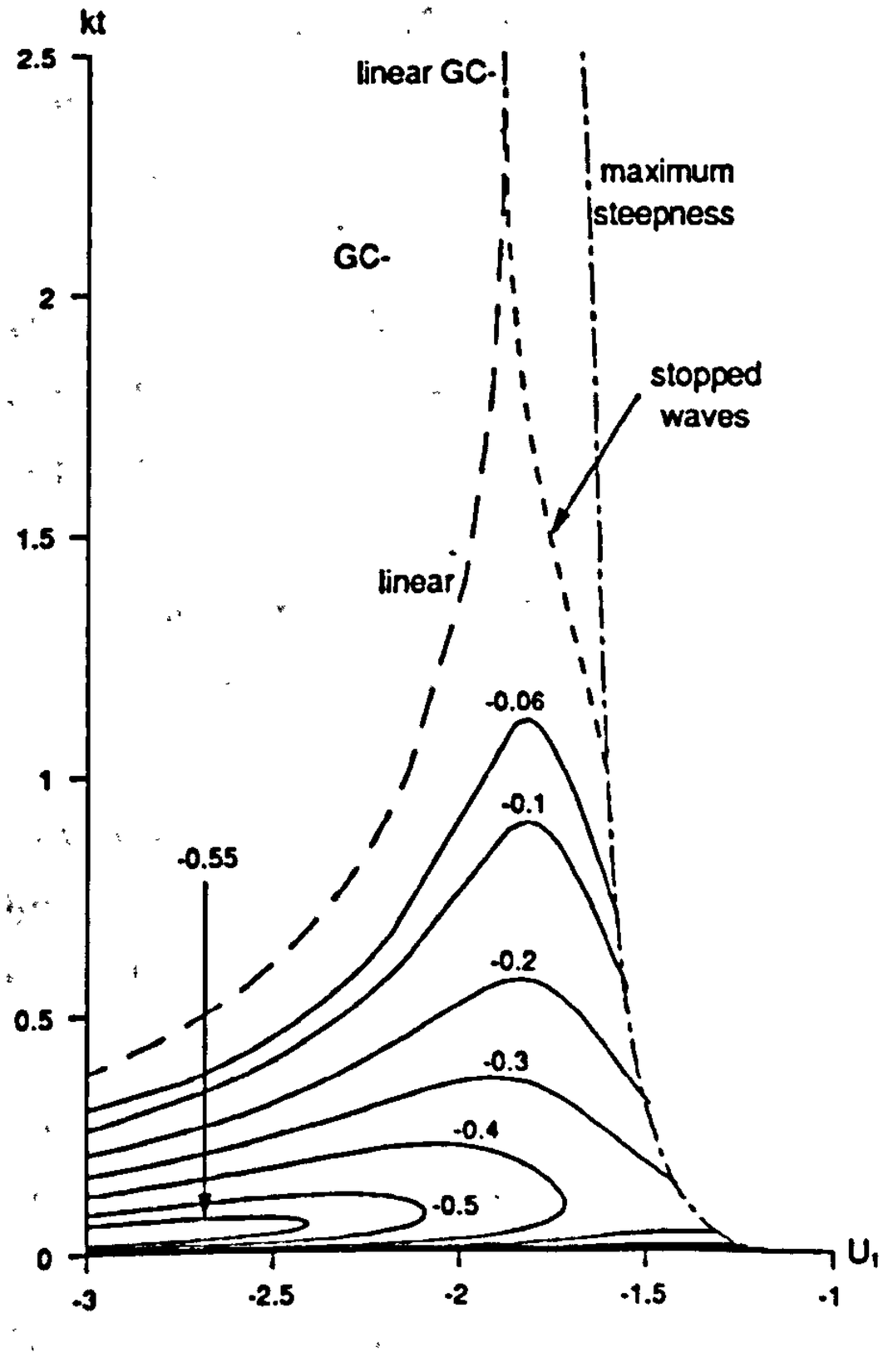

Figure 10.10e

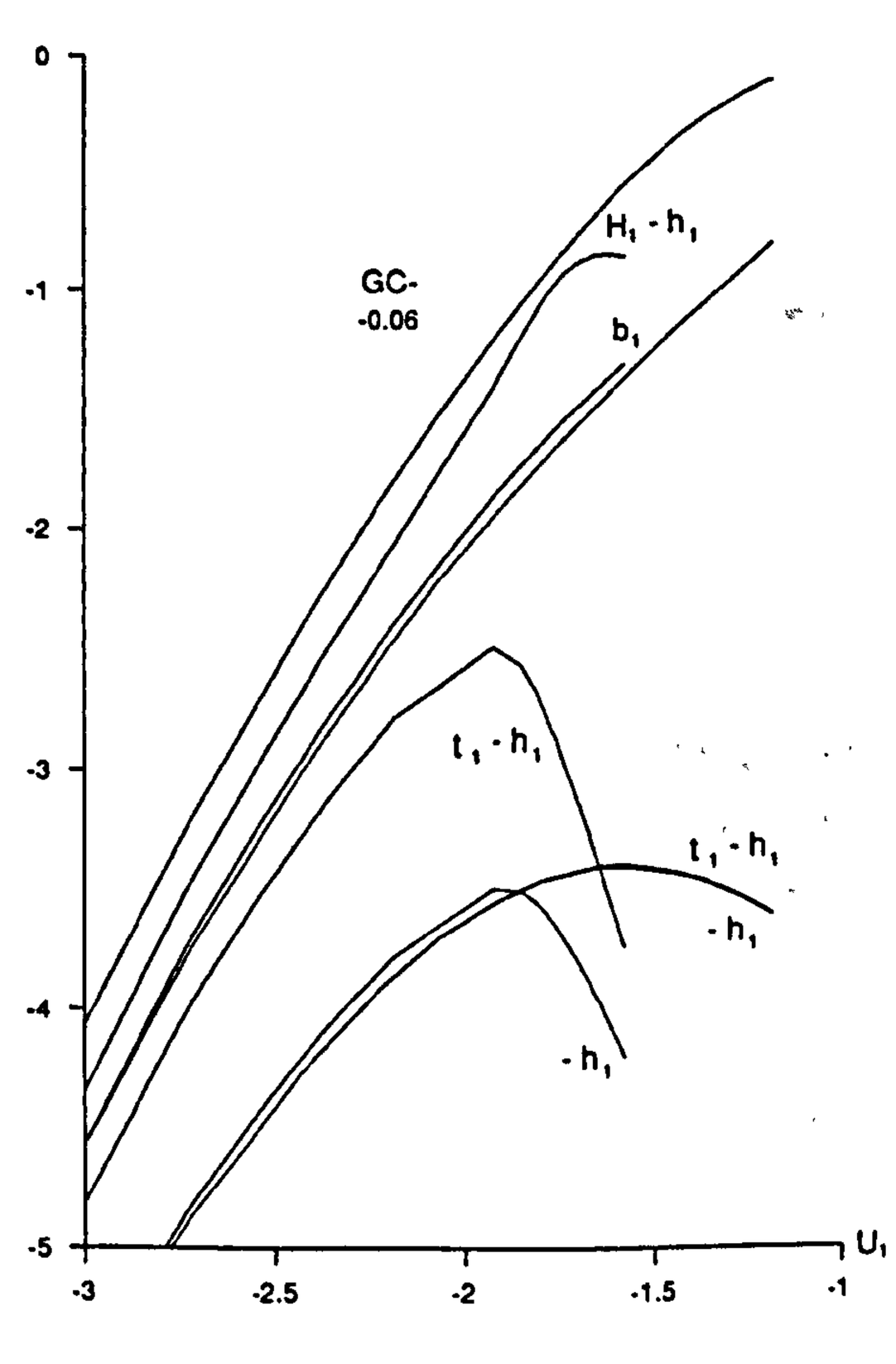

Figure 10.10f

EPILOGUE

This thesis consists of two parts. The first part considers "short" waves either interacting with a slowly-varying mainstream flow or propagating on the surface of pure gravity waves on liquid of infinite depth. The second part considers "short" waves interacting with a slowly-varying mainstream flow on liquid of finite depth. In either part it is supposed that the waves are dominated by surface tension.

In the first part it is shown that the neglect of gravity effects on the "short" waves is justifiable for flows on many "typical" gravity waves. The inviscid theory permits calculation of those gravity waves on which capillary wave breaking occurs. However, the dissipative theory shows that only waves GC-, which propagate up the forward faces of pure gravity waves, can break. If these waves do not break then they may actually persist for long periods of time or, alternatively, they may undergo wave reflection, transmission or even a combination of both. Usually waves CG and CG(+,-), which propagate up the backward faces of pure gravity waves, rapidly dissipate. On rare occasions waves CG- may possibly persist for long periods of time. This explains why capillary waves are generally seen on the forward faces of gravity wavetrains. It is very difficult to make quantitative observations of capillary waves on the surface of gravity waves. Thus, a quantitative confirmation of results is not undertaken.

The second part of this thesis is less complete. A detailed account is given of the interaction of all possible finite-amplitude capillary waves with a shallow water gravity driven mainstream flow. Infinitesimal wave theory always shows the existence of one branch of wave solution for each of the possible waves. However, finite-amplitude theory shows that generally finite depth influenced flows give two branches of wave solution for each of the possible waves. In some cases, for example the thin films stationary waves case, the two branches join at a singularity in the form of a vertical tangent velocity position. In other cases, for example waves CG- with "large" dimensionless mass flux m_1, the two branches of wave solutions are completely disjoint - one representing a thin films flow and the other a finite/infinite depth flow.

Interpreting wave solutions, especially the existence of critical velocity positions, is a difficult task. Possible reasons for such velocity positions may be found upon further examination of details of the flow field. For instance, the schematic diagrams given may lead to further understanding. It is seen from the introductory section 1.2 on wave-currents interactions and the first part of this thesis that the

behaviour of some waves, here waves CG- and GC-, is more clearly interpreted once the stopped waves solution or, in this case, solutions are clearly interpreted.

The second part of this thesis forms the foundation for further study in several different directions leading to explanations of observed naturally occurring phenomena. These are discussed at the end of chapter 10 and involve the inclusion of, for example, wave energy dissipation and vorticity effects.

APPENDIX A
Integral Definitions of Mean Wave Properties

Some integral definitions of mean properties of the wave motion are given here. The wave momentum vector $\mathcal{I}_i$ is defined as

$$\mathcal{I}_i = \rho \overline{\int_{-h}^{\eta} u_i \, dz} \tag{A1}$$

and is equal to the mass flux in the i-direction due to the waves. An overbar denotes the average over the waves.

The radiation stress $\mathcal{S}^{g}_{ij}$ for pure gravity waves is defined as

$$\mathcal{S}^{g}_{ij} = \overline{\int_{-h}^{\eta} (\rho u_i u_j + p\delta_{ij}) \, dz} - \frac{1}{2} \rho g d^2 \, \delta_{ij} \tag{A2}$$

where p is the pressure. The radiation stress $\mathcal{S}^{\tau}_{ij}$ for pure capillary waves is defined as

$$\mathcal{S}^{\tau}_{ij} = \tau \left\{ \overline{\frac{\frac{\partial \eta}{\partial x_i}\frac{\partial \eta}{\partial x_j}}{\left[1 + \left[\frac{\partial \eta}{\partial x_k}\right]^2\right]^{\frac{1}{2}}}} - \overline{\left\{\left[1 + \left[\frac{\partial \eta}{\partial x_k}\right]^2\right]^{\frac{1}{2}} - 1\right\} \delta_{ij}} \right\} . \tag{A3}$$

where τ is the surface tension of the liquid. The total radiation stress $\mathcal{S}_{ij}$ is then given by

$$\mathcal{S}_{ij} = \mathcal{S}^{g}_{ij} + \mathcal{S}^{\tau}_{ij} \tag{A4}$$

and represents the excess momentum flux due to the waves. This is a tensor since the square root in each term is invariant under rotation of axes.

The energy density $\mathcal{E}^{g}$ for pure gravity waves is defined as

$$\mathcal{E}^{g} = \frac{1}{2} \rho \overline{\int_{-h}^{\eta} (u_i u_j + w^2) \, dz} + \frac{1}{2} \rho g \, (\overline{\eta^2} - b^2) \, . \tag{A5}$$

The potential energy density $\mathcal{E}^{\tau}$ for pure capillary waves is defined as

$$\mathcal{E}^{\tau} = \tau \overline{\left\{\left[1 + \left[\frac{\partial \eta}{\partial x_k}\right]^2\right]^{\frac{1}{2}} - 1\right\}} \, . \tag{A6}$$

The total energy density $\mathcal{E}$ is then given by

$$\mathcal{E} = \mathcal{E}^{g} + \mathcal{E}^{\tau} \quad . \tag{A7}$$

The energy flux vector $\mathcal{F}_i^g$ for pure gravity waves is defined as

$$\mathcal{F}_i^g = \overline{\int_{-h}^{\eta} u_i \left[\frac{1}{2}\rho\,(u_i u_i + w^2) + p + \rho g\,(z - b)\right] dz} \quad . \tag{A8}$$

The energy flux vector $\mathcal{F}_i^I$ for pure capillary waves is defined as

$$\mathcal{F}_i^I = \tau \overline{\frac{\partial \eta}{\partial x_i}\left[w - u_j \frac{\partial \eta}{\partial x_j}\right]_\eta \left[1 + \left[\frac{\partial \eta}{\partial x_k}\right]^2\right]^{-\frac{1}{2}}} \quad . \tag{A9}$$

where the subscript η denotes evaluation at $z = \eta$, i.e. at the surface of the liquid. The total energy flux vector $\mathcal{F}_i$ is then given by

$$\mathcal{F}_i = \mathcal{F}_i^g + \mathcal{F}_i^I \quad . \tag{A10}$$

The kinetic energy density T is defined by

$$T = \frac{1}{2}\rho \int_{-h}^{\eta} \left[\left[\frac{\partial \phi}{\partial x_i}\right]^2 + \left[\frac{\partial \phi}{\partial z}\right]^2\right] dz \quad . \tag{A11}$$

The potential energy density V^g for pure gravity waves is defined by

$$V^g = \frac{1}{2}\rho g(\overline{\eta^2} - b^2) \quad . \tag{A12}$$

The potential energy density V^τ for pure capillary waves is defined as

$$V^\tau = \tau \overline{\left\{\left[1 + \left[\frac{\partial \eta}{\partial x_i}\right]^2\right]^{\frac{1}{2}} - 1\right\}} = \mathcal{E}^\tau \quad . \tag{A13}$$

The total potential energy density V is then given by

$$V = V^g + V^\tau \quad . \tag{A14}$$

Note that

$$\mathcal{E}^\tau = V^\tau \tag{A15}$$

and that

$$\mathcal{E} = T + V \quad . \tag{A16}$$

APPENDIX B

Whitham's Averaged Lagrangian Method

The averaged Lagrangian method of Whitham (1965, 1967, 1974) and the equations derived are outlined here. Whitham proposes that once a Lagrangian L is found for a specific wave problem an averaged Lagrangian $\mathcal{L}$ is found by substituting the plane-wave solution into the Lagrangian L and averaging over the waves. Then, for slowly-varying wavetrains, the equations for the wave parameters are found by use of the averaged variational principle

$$\delta \iint \mathcal{L}\, dx_i dt = 0 \ . \tag{B1}$$

The appropriate form for the Lagrangian L is found by taking the form suggested by Luke (1967) for pure gravity waves and adding on a surface tension term. Thus,

$$L = -\rho \int_{-h}^{\eta} \left\{ \frac{\partial \Phi}{\partial t} + \frac{1}{2}\left[\left[\frac{\partial \Phi}{\partial x_i} \right]^2 + \left[\frac{\partial \Phi}{\partial z} \right]^2 \right] + gz \right\} dz - \tau \left\{ \left[1 + \left[\frac{\partial \eta}{\partial x_i} \right]^2 \right]^{\frac{1}{2}} - 1 \right\}$$

where Φ is the velocity potential function.

The most generalised form of the velocity potential Φ for uniform wavetrains is given by

$$\Phi = \psi + \phi(\chi, z) \tag{B2}$$

with

$$\eta = b + \eta(\chi) \tag{B3}$$

where ϕ is the velocity potential for the wave motion alone. Substituting into L and averaging over the waves gives

$$\mathcal{L} = -\rho d\left[\frac{\partial \psi}{\partial t} + \frac{1}{2}\left[\frac{\partial \psi}{\partial x_i} \right]^2 \right] - \rho \overline{\int_{-h}^{\eta} \left[\frac{\partial \phi}{\partial t} + \frac{\partial \psi}{\partial x_i} \frac{\partial \phi}{\partial x_i} \right] dz}$$

$$- \frac{1}{2} \rho \overline{\int_{-h}^{\eta} \left[\left[\frac{\partial \phi}{\partial x_i} \right]^2 + \left[\frac{\partial \phi}{\partial z} \right]^2 \right] dz} - \frac{1}{2} \rho g(\overline{\eta^2} - h^2) - \tau \overline{\left\{ \left[1 + \left[\frac{\partial \eta}{\partial x_i} \right]^2 \right]^{\frac{1}{2}} - 1 \right\}} \ .$$

By definition of the velocity potential ϕ

$$u_i = \frac{\partial \phi}{\partial x_i} , \quad w = \frac{\partial \phi}{\partial z} \tag{B4}$$

so
$$\frac{1}{2} \rho \overline{\int_{-h}^{\eta} \left[\left[\frac{\partial \phi}{\partial x_i} \right]^2 + \left[\frac{\partial \phi}{\partial z} \right]^2 \right] dz} = T . \tag{B5}$$

Also note that (appendix A)

$$\frac{1}{2} \rho g(\overline{\eta^2} - b^2) + \tau \overline{\left\{ \left[1 + \left[\frac{\partial \eta}{\partial x_i} \right]^2 \right]^{\frac{1}{2}} - 1 \right\}} = V . \tag{B6}$$

Thus, using the definition (2.3.3) of the pseudo-phase,

$$\mathcal{L} = \rho d \left[\gamma - \frac{1}{2} U_i^2 \right] - \frac{1}{2} \rho g(b^2 - h^2) - T - V - \rho \overline{\int_{-h}^{\eta} \left[\frac{\partial \phi}{\partial t} + U_i \frac{\partial \phi}{\partial x_i} \right] dz}$$

and since, using definition (2.3.2) for the phase,

$$\frac{\partial \phi}{\partial t} = \frac{\partial \phi}{\partial \chi} \frac{\partial \chi}{\partial t} = - \omega \frac{\partial \phi}{\partial \chi} , \quad \frac{\partial \phi}{\partial x_i} = \frac{\partial \phi}{\partial \chi} \frac{\partial \chi}{\partial x_i} = - k_i \frac{\partial \phi}{\partial \chi} \tag{B7}$$

it follows, using the Doppler relation (2.3.1), that

$$\frac{\partial \phi}{\partial t} + U_i \frac{\partial \phi}{\partial x_i} = (- \omega + k_i U_i) \frac{\partial \phi}{\partial \chi} = - \sigma \frac{\partial \phi}{\partial \chi} \tag{B8}$$

but, by definition, $\quad c_i = \frac{\sigma}{k^2} k_i \quad \Longrightarrow \quad c_i k_i = \sigma , \tag{B9}$

where c_i is the phase velocity vector of the wave motion alone, so that

$$\sigma \frac{\partial \phi}{\partial \chi} = c_i k_i \frac{\partial \phi}{\partial \chi} = c_i \frac{\partial \phi}{\partial x_i} = c_i u_i \tag{B10}$$

after use of (B7) and (B4). Thus, since

$$\rho \overline{\int_{-h}^{\eta} c_i u_i \, dz} = c_i \mathcal{I}_i \tag{B11}$$

the averaged Lagrangian $\mathcal{L}$ is given by

$$\mathcal{L} = \rho d \left[\gamma - \frac{1}{2} U_i^2 \right] - \frac{1}{2} \rho g(b^2 - h^2) + c_i \mathcal{I}_i - T - V . \tag{B12}$$

From Longuet-Higgins (1975 § 2) it is easily seen that the generalisation of the Levi-Civita relation is

$$2T = c_i \mathcal{I}_i \tag{B13}$$

so that $$\mathcal{L} = \rho d\left[\gamma - \frac{1}{2} U_i^2\right] - \frac{1}{2} \rho g(b^2 - h^2) + T - V \tag{B14}$$

Let $$\mathcal{L}^w = T - V \ , \tag{B15}$$

where w denotes that this is a property of the wave motion alone, then

$$\mathcal{L}^w = \mathcal{L}^w(\sigma, k, a, d) \tag{B16}$$

so, using the Doppler relation (2.3.1),

$$\mathcal{L}^w = \mathcal{L}^w(\omega - k_i U_i, k, a, d) \ , \tag{B17}$$

where a is the amplitude of the waves. For differentiations in Whitham's averaged variational principle the form (B17), with ω rather than σ, must be used.

The Euler equations corresponding to the variational principle (B1) lead to the following four equations:

$$\frac{\partial \mathcal{L}}{\partial a} = 0 \ , \quad \frac{\partial \mathcal{L}}{\partial b} = 0 \ , \tag{B18}$$

$$\frac{\partial}{\partial t}\left[\frac{\partial \mathcal{L}}{\partial \gamma}\right] - \frac{\partial}{\partial x_i}\left[\frac{\partial \mathcal{L}}{\partial U_i}\right] = 0 \ , \quad \frac{\partial}{\partial t}\left[\frac{\partial \mathcal{L}}{\partial \omega}\right] - \frac{\partial}{\partial x_i}\left[\frac{\partial \mathcal{L}}{\partial k_i}\right] = 0 \ . \tag{B19}$$

Substitution of expression (B14) into these equation gives the four equations (2.4.3 - 2.4.6) in terms of $\mathcal{L}^w$.

APPENDIX C

Relations between terms in the Averaged Equations and Whitham's Equations of Motion

In this appendix two general equations are derived. No equations or relations are to be used except the Doppler relation (2.3.1), the consistency relations (2.3.4) between the wavenumber vector k_i and the total wave frequency ω and the dispersion relation in the basic form (2.4.3) in terms of $\mathcal{L}^w$. The method of Crapper (1979) § 3 is followed.

Consider the equation

$$\frac{\partial \mathcal{L}^w}{\partial x_i} = \frac{\partial \mathcal{L}^w}{\partial \sigma}\,\frac{\partial \sigma}{\partial x_i} + \frac{\partial \mathcal{L}^w}{\partial k}\,\frac{\partial k}{\partial x_i} + \frac{\partial \mathcal{L}^w}{\partial d}\,\frac{\partial d}{\partial x_i} + \frac{\partial \mathcal{L}^w}{\partial a}\,\frac{\partial a}{\partial x_i}\ . \tag{C1}$$

The Doppler relation (2.3.1) gives

$$\frac{\partial \sigma}{\partial x_i} = \frac{\partial \omega}{\partial x_i} - U_j\,\frac{\partial k_j}{\partial x_i} - k_j\,\frac{\partial U_j}{\partial x_i} \tag{C2}$$

so

$$\frac{\partial \mathcal{L}^w}{\partial x_j}\,\delta_{ij} = -\,\frac{\partial \mathcal{L}^w}{\partial \sigma}\left[\frac{\partial k_i}{\partial t} + U_j\,\frac{\partial k_i}{\partial x_j} + k_j\,\frac{\partial U_j}{\partial x_i}\right] + \frac{\partial \mathcal{L}^w}{\partial k}\,\frac{\partial k}{\partial x_i} + \frac{\partial \mathcal{L}^w}{\partial d}\,\frac{\partial d}{\partial x_i} \tag{C3}$$

where the consistency relations (2.3.4) are used in (C2) and the dispersion relation is used in (C1). Adding

$$k_i\left[\frac{\partial}{\partial t}\left[\frac{\partial \mathcal{L}^w}{\partial \sigma}\right] + \frac{\partial}{\partial x_j}\left[U_j\,\frac{\partial \mathcal{L}^w}{\partial \sigma} - \frac{k_j}{k}\,\frac{\partial \mathcal{L}^w}{\partial k}\right]\right] \tag{C4}$$

to both sides of (C3) gives

$$\frac{\partial k_i}{\partial t}\,\frac{\partial \mathcal{L}^w}{\partial \sigma} + k_i\,\frac{\partial}{\partial t}\left[\frac{\partial \mathcal{L}^w}{\partial \sigma}\right] + U_j\,\frac{\partial k_i}{\partial x_j}\,\frac{\partial \mathcal{L}^w}{\partial \sigma} - \frac{\partial k}{\partial x_i}\,\frac{\partial \mathcal{L}^w}{\partial k} + \frac{\partial \mathcal{L}^w}{\partial x_j}\,\delta_{ij}$$

$$+ k_i\,\frac{\partial}{\partial x_j}\left[U_j\,\frac{\partial \mathcal{L}^w}{\partial \sigma} - \frac{k_j}{k}\,\frac{\partial \mathcal{L}^w}{\partial k}\right] + k_j\,\frac{\partial \mathcal{L}^w}{\partial \sigma}\,\frac{\partial U_j}{\partial x_i} - \frac{\partial \mathcal{L}^w}{\partial d}\,\frac{\partial d}{\partial x_i} =$$

$$k_i\left[\frac{\partial}{\partial t}\left[\frac{\partial \mathcal{L}^w}{\partial \sigma}\right] + \frac{\partial}{\partial x_j}\left[U_j\,\frac{\partial \mathcal{L}^w}{\partial \sigma} - \frac{k_j}{k}\,\frac{\partial \mathcal{L}^w}{\partial k}\right]\right]\ . \tag{C5}$$

Now

$$\frac{\partial k}{\partial x_i} = \frac{k_j}{k}\,\frac{\partial k_j}{\partial x_i} = \frac{k_j}{k}\,\frac{\partial k_i}{\partial x_j}\ , \tag{C6}$$

using the consistency relations (2.3.4), so that (C5) gives

$$\frac{\partial}{\partial t}\left[k_i \frac{\partial \mathcal{L}^w}{\partial \sigma}\right] + \frac{\partial}{\partial x_j}\left[U_j k_i \frac{\partial \mathcal{L}^w}{\partial \sigma} - \frac{k_i k_j}{k} \frac{\partial \mathcal{L}^w}{\partial k} + \mathcal{L}^w \delta_{ij}\right] + k_j \frac{\partial \mathcal{L}^w}{\partial \sigma} \frac{\partial U_j}{\partial x_i} - \frac{\partial \mathcal{L}^w}{\partial d} \frac{\partial d}{\partial x_i}$$

$$= k_i\left[\frac{\partial}{\partial t}\left[\frac{\partial \mathcal{L}^w}{\partial \sigma}\right] + \frac{\partial}{\partial x_j}\left[U_j \frac{\partial \mathcal{L}^w}{\partial \sigma} - \frac{k_j}{k} \frac{\partial \mathcal{L}^w}{\partial k}\right]\right] . \qquad (C7)$$

But $$- \frac{\partial \mathcal{L}^w}{\partial d} \frac{\partial d}{\partial x_i} = \frac{\partial}{\partial x_j}\left[- d \frac{\partial \mathcal{L}^w}{\partial d} \delta_{ij}\right] + d \frac{\partial}{\partial x_i}\frac{\partial \mathcal{L}^w}{\partial d} , \qquad (C8)$$

so $$\frac{\partial}{\partial t}\left[k_i \frac{\partial \mathcal{L}^w}{\partial \sigma}\right] + \frac{\partial}{\partial x_j}\left[U_j k_i \frac{\partial \mathcal{L}^w}{\partial \sigma} + \mathcal{L}^w \delta_{ij} - \frac{k_i k_j}{k} \frac{\partial \mathcal{L}^w}{\partial k} - d \frac{\partial \mathcal{L}^w}{\partial d} \delta_{ij}\right]$$

$$+ k_j \frac{\partial \mathcal{L}^w}{\partial \sigma} \frac{\partial U_j}{\partial x_i} + d \frac{\partial}{\partial x_i}\frac{\partial \mathcal{L}^w}{\partial d} = k_i\left[\frac{\partial}{\partial t}\left[\frac{\partial \mathcal{L}^w}{\partial \sigma}\right]\right.$$

$$\left. + \frac{\partial}{\partial x_j}\left[U_j \frac{\partial \mathcal{L}^w}{\partial \sigma} - \frac{k_j}{k} \frac{\partial \mathcal{L}^w}{\partial k}\right]\right] , \qquad (C9)$$

which, after use of definitions (2.4.7) and (2.5.2, 3) for the mean wave properties in terms of $\mathcal{L}^w$, gives

$$\frac{\partial I_i}{\partial t} + \frac{\partial}{\partial x_j}(U_j I_i + S_{ij}) + I_j \frac{\partial U_i}{\partial x_j} + d \frac{\partial}{\partial x_i}\frac{\partial \mathcal{L}^w}{\partial d} = k_i\left[\frac{\partial \mathcal{A}}{\partial t} + \frac{\partial}{\partial x_j}(U_j \mathcal{A} + B_j)\right]$$

$$+ I_j\left[\frac{\partial U_i}{\partial x_j} - \frac{\partial U_j}{\partial x_i}\right] . \qquad (C10)$$

This is the first of the required equations. To find the second consider

$$\frac{\partial \mathcal{L}^w}{\partial t} = \frac{\partial \mathcal{L}^w}{\partial \sigma} \frac{\partial \sigma}{\partial t} + \frac{\partial \mathcal{L}^w}{\partial k} \frac{\partial k}{\partial t} + \frac{\partial \mathcal{L}^w}{\partial d} \frac{\partial d}{\partial t} + \frac{\partial \mathcal{L}^w}{\partial a} \frac{\partial a}{\partial t} . \qquad (C11)$$

Now $$\frac{\partial d}{\partial t} = \frac{\partial b}{\partial t} \quad \text{and} \quad \frac{\partial k}{\partial t} = \frac{k_i}{k} \frac{\partial k_i}{\partial t} \qquad (C12)$$

so, using dispersion relation (2.4.3), (C11) gives

$$\frac{\partial}{\partial t}\left[\sigma \frac{\partial \mathcal{L}^w}{\partial \sigma} - \mathcal{L}^w\right] = \sigma \frac{\partial}{\partial t}\left[\frac{\partial \mathcal{L}^w}{\partial \sigma}\right] - \frac{\partial k_i}{\partial t} \frac{k_i}{k} \frac{\partial \mathcal{L}^w}{\partial k} - \frac{\partial \mathcal{L}^w}{\partial d} \frac{\partial b}{\partial t} . \qquad (C13)$$

Also $$\frac{\partial}{\partial x_i}\left[U_i\left[\sigma \frac{\partial \mathcal{L}^w}{\partial \sigma} - \mathcal{L}^w\right] - \sigma \frac{k_i}{k} \frac{\partial \mathcal{L}^w}{\partial k}\right] = \sigma \frac{\partial}{\partial x_i}\left[U_i \frac{\partial \mathcal{L}^w}{\partial \sigma} - \frac{k_i}{k} \frac{\partial \mathcal{L}^w}{\partial k}\right]$$

$$+ \frac{\partial \sigma}{\partial x_i}\left[U_i \frac{\partial \mathcal{L}^w}{\partial \sigma} - \frac{k_i}{k} \frac{\partial \mathcal{L}^w}{\partial k}\right] - \frac{\partial}{\partial x_i}(U_i \mathcal{L}^w) \qquad (C14)$$

so $$\frac{\partial}{\partial t}\left[\sigma\frac{\partial \mathcal{L}^w}{\partial \sigma} - \mathcal{L}^w\right] + \frac{\partial}{\partial x_i}\left[U_i\left[\sigma\frac{\partial \mathcal{L}^w}{\partial \sigma} - \mathcal{L}^w\right] - \sigma\frac{k_i}{k}\frac{\partial \mathcal{L}^w}{\partial k}\right] =$$

$$\sigma\left[\frac{\partial}{\partial t}\left[\frac{\partial \mathcal{L}^w}{\partial \sigma}\right] + \frac{\partial}{\partial x_i}\left[U_i\frac{\partial \mathcal{L}^w}{\partial \sigma} - \frac{k_i}{k}\frac{\partial \mathcal{L}^w}{\partial k}\right]\right] + \frac{\partial \sigma}{\partial x_i}\left[U_i\frac{\partial \mathcal{L}^w}{\partial \sigma} - \frac{k_i}{k}\frac{\partial \mathcal{L}^w}{\partial k}\right]$$

$$- \frac{\partial}{\partial x_i}(U_i\mathcal{L}^w) - \frac{\partial k_i}{\partial t}\frac{k_i}{k}\frac{\partial \mathcal{L}^w}{\partial k} - \frac{\partial \mathcal{L}^w}{\partial d}\frac{\partial b}{\partial t}\,. \qquad (C15)$$

The dispersion relation (2.4.3) and expressions (C1, 6) give

$$\frac{\partial \mathcal{L}^w}{\partial x_i} = \frac{\partial \mathcal{L}^w}{\partial \sigma}\frac{\partial \sigma}{\partial x_i} + \frac{\partial \mathcal{L}^w}{\partial k}\frac{k_j}{k}\frac{\partial k_j}{\partial x_i} + \frac{\partial \mathcal{L}^w}{\partial d}\frac{\partial d}{\partial x_i} \qquad (C16)$$

so $$\frac{\partial \sigma}{\partial x_i}\left[U_i\frac{\partial \mathcal{L}^w}{\partial \sigma} - \frac{k_i}{k}\frac{\partial \mathcal{L}^w}{\partial k}\right] - \frac{\partial}{\partial x_i}(U_i\mathcal{L}^w) - \frac{\partial k_i}{\partial t}\frac{k_i}{k}\frac{\partial \mathcal{L}^w}{\partial k} - \frac{\partial \mathcal{L}^w}{\partial d}\frac{\partial b}{\partial t} =$$

$$- \frac{\partial \sigma}{\partial x_i}\frac{k_i}{k}\frac{\partial \mathcal{L}^w}{\partial k} - U_i\frac{k_j}{k}\frac{\partial k_j}{\partial x_i}\frac{\partial \mathcal{L}^w}{\partial k} - \frac{\partial k_i}{\partial t}\frac{k_i}{k}\frac{\partial \mathcal{L}^w}{\partial k}$$

$$- \mathcal{L}^w\frac{\partial U_i}{\partial x_i} - \frac{\partial \mathcal{L}^w}{\partial d}\frac{\partial b}{\partial t} - U_i\frac{\partial \mathcal{L}^w}{\partial d}\frac{\partial d}{\partial x_i}\,. \qquad (C17)$$

The consistency relation (2.3.4) and the expression (C2) give

$$\frac{\partial \sigma}{\partial x_i} = -\frac{\partial k_i}{\partial t} - U_j\frac{\partial k_i}{\partial x_j} - k_j\frac{\partial U_j}{\partial x_i}\,. \qquad (C18)$$

So, after substitution of (C18) into (C17), expression (C15) gives

$$\frac{\partial}{\partial t}\left[\sigma\frac{\partial \mathcal{L}^w}{\partial \sigma} - \mathcal{L}^w\right] + \frac{\partial}{\partial x_i}\left[U_i\left[\sigma\frac{\partial \mathcal{L}^w}{\partial \sigma} - \mathcal{L}^w\right] - \sigma\frac{k_i}{k}\frac{\partial \mathcal{L}^w}{\partial k}\right] =$$

$$\sigma\left[\frac{\partial}{\partial t}\left[\frac{\partial \mathcal{L}^w}{\partial \sigma}\right] + \frac{\partial}{\partial x_i}\left[U_i\frac{\partial \mathcal{L}^w}{\partial \sigma} - \frac{k_i}{k}\frac{\partial \mathcal{L}^w}{\partial k}\right]\right] + \frac{k_i k_j}{k}\frac{\partial \mathcal{L}^w}{\partial k}\frac{\partial U_j}{\partial x_i}$$

$$- \mathcal{L}^w\frac{\partial U_i}{\partial x_i} - \frac{\partial \mathcal{L}^w}{\partial d}\frac{\partial b}{\partial t} - U_i\frac{\partial \mathcal{L}^w}{\partial d}\frac{\partial d}{\partial x_i} \qquad (C19)$$

or $$\frac{\partial}{\partial t}\left[\sigma\frac{\partial \mathcal{L}^w}{\partial \sigma} - \mathcal{L}^w\right] + \frac{\partial}{\partial x_i}\left[U_i\left[\sigma\frac{\partial \mathcal{L}^w}{\partial \sigma} - \mathcal{L}^w\right] - \sigma\frac{k_i}{k}\frac{\partial \mathcal{L}^w}{\partial k} - \frac{1}{\rho}\frac{\partial \mathcal{L}^w}{\partial d}k_i\frac{\partial \mathcal{L}^w}{\partial \sigma}\right]$$

$$+ \left[\mathcal{L}^w\delta_{ij} - \frac{k_i k_j}{k}\frac{\partial \mathcal{L}^w}{\partial k} - d\frac{\partial \mathcal{L}^w}{\partial d}\delta_{ij}\right]\frac{\partial U_j}{\partial x_i} =$$

$$\sigma\left[\frac{\partial}{\partial t}\left[\frac{\partial \mathcal{L}^w}{\partial \sigma}\right] + \frac{\partial}{\partial x_i}\left[U_i\frac{\partial \mathcal{L}^w}{\partial \sigma} - \frac{k_i}{k}\frac{\partial \mathcal{L}^w}{\partial k}\right]\right]$$

$$- \frac{\partial \mathcal{L}^w}{\partial d}\frac{\partial b}{\partial t} - U_i\frac{\partial \mathcal{L}^w}{\partial d}\frac{\partial d}{\partial x_i} - d\frac{\partial \mathcal{L}^w}{\partial d}\frac{\partial U_i}{\partial x_i} - \frac{1}{\rho}\frac{\partial}{\partial x_i}\left[\frac{\partial \mathcal{L}^w}{\partial d}k_i\frac{\partial \mathcal{L}^w}{\partial \sigma}\right]\,. \qquad (C20)$$

But $$\frac{\partial \mathcal{L}^w}{\partial d}\frac{\partial b}{\partial t} + U_i\frac{\partial \mathcal{L}^w}{\partial d}\frac{\partial d}{\partial x_i} + d\frac{\partial \mathcal{L}^w}{\partial d}\frac{\partial U_i}{\partial x_i} + \frac{1}{\rho}\frac{\partial}{\partial x_i}\left[\frac{\partial \mathcal{L}^w}{\partial d}k_i\frac{\partial \mathcal{L}^w}{\partial \sigma}\right] =$$

$$\frac{\partial \mathcal{L}^w}{\partial d}\left[\frac{\partial b}{\partial t} + \frac{\partial}{\partial x_i}(dU_i) + \frac{1}{\rho}\frac{\partial}{\partial x_i}\left[k_i\frac{\partial \mathcal{L}^w}{\partial \sigma}\right]\right] + \frac{1}{\rho}k_i\frac{\partial \mathcal{L}^w}{\partial \sigma}\frac{\partial}{\partial x_i}\frac{\partial \mathcal{L}^w}{\partial d}\,,$$

so, using definitions (2.4.7) and (2.5.2, 3 ,6) for mean wave properties in terms of $\mathcal{L}^w$, expression (C20) gives

$$\frac{\partial \mathcal{E}}{\partial t} + \frac{\partial}{\partial x_i}(U_i \mathcal{E} + \mathcal{F}_i) + \mathcal{S}_{ij} \frac{\partial U_j}{\partial x_i} + \frac{1}{\rho} \mathcal{I}_i \frac{\partial}{\partial x_i} \frac{\partial \mathcal{L}^w}{\partial d} =$$

$$\frac{1}{2} \overline{u_h^2} \left[\rho \frac{\partial b}{\partial t} + \frac{\partial}{\partial x_i}(\rho d U_i + \mathcal{I}_i) \right] + \sigma \left[\frac{\partial \mathcal{A}}{\partial t} \frac{\partial}{\partial x_i}(U_i \mathcal{A} + B_i) \right] \qquad (C21)$$

which is the second of the required equations.

APPENDIX D

Expressions required for the calculation of Mean Wave Properties for Kinnersley's Symmetric Waves

In this appendix expressions are derived for the quantities

$$\frac{d\hat{x}}{d\phi}, \quad \frac{d\eta}{d\phi} \quad \text{and} \quad \left[\frac{d\hat{x}}{d\phi}\right]^2 + \left[\frac{d\eta}{d\phi}\right]^2 \qquad (D1)$$

for the case of symmetric waves since these are needed to find expressions for the four basic mean wave properties. Extensive use is made of formulae, involving elliptic functions, in Byrd and Friedman (1971).

Now, expressions (8.4.1, 2) give $\hat{x}$ and η. The latter clearly gives

$$\frac{d\eta}{d\phi} = \frac{s\beta}{c^2} \frac{1}{(1 - \alpha\, cd\, \phi)^2} [-2\alpha\beta\, sd\, \phi\, nd\, \phi] \qquad (D2)$$

whilst the former gives

$$\frac{d\hat{x}}{d\phi} = \frac{s\beta}{c^2} \left[1 + 2\kappa^2 sd^2\phi + 2\alpha \frac{d}{d\phi} \left[\frac{sd\, \phi\, nd\, \phi}{1 - \alpha\, cd\, \phi}\right]\right] . \qquad (D3)$$

Now
$$\frac{d}{d\phi} \left[\frac{sd\, \phi\, nd\, \phi}{1 - \alpha\, cd\, \phi}\right] = \frac{1}{(1 - \alpha\, cd\, \phi)^2} [cd\, \phi(nd^2\phi + \kappa^2 sd^2\phi)$$

$$- \alpha^2(nd^2\phi + \kappa^2 cd^2\phi sd^2\phi)] \qquad (D4)$$

so
$$\frac{d\hat{x}}{d\phi} = \frac{s\beta}{c^2} \frac{1}{(1 - \alpha\, cd\, \phi)^2} [(1 + 2\kappa^2 sd^2\phi) - \alpha^2(cd^2\phi + 2sd^2\phi)] \qquad (D5)$$

It follows that

$$\left[\frac{d\hat{x}}{d\phi}\right]^2 + \left[\frac{d\eta}{d\phi}\right]^2 = \frac{s^2\beta^2}{c^4}\,\frac{1}{(1 - \alpha\ \mathrm{cd}\ \phi)^4}\,\{[(1 + 2\kappa^2\mathrm{sd}^2\phi) - \alpha^2(\mathrm{cd}^2\phi + 2\ \mathrm{sd}^2\phi)]^2 + 4\alpha^2\beta^2\mathrm{sd}^2\phi\ \mathrm{nd}^2\phi\}\ . \qquad \text{(D6)}$$

Substituting $$\alpha^2\beta^2 = (\alpha^2 - \kappa^2)(1 - \alpha^2) \qquad \text{(D7)}$$

into expression (D6) and collecting terms of the same order in α gives

$$\left[\frac{d\hat{x}}{d\phi}\right]^2 + \left[\frac{d\eta}{d\phi}\right]^2 = = \frac{s^2\beta^2}{c^4}\,\frac{(1 - \alpha^2\mathrm{cd}^2\phi)^2}{(1 - \alpha\ \mathrm{cd}\ \phi)^4}\ . \qquad \text{(D8)}$$

APPENDIX E
The Linear-Limit $\kappa \longrightarrow 0$

It is mentioned in § 8.2 that the limit $\kappa \longrightarrow 0$ represents the linear-limit. This limit is now considered in detail so that the general expressions derived for the mean properties above are shown to be correct in this limit and so the algebraic manipulations of § 8.4 are verified as being correct. If such an analysis is not undertaken then the validity of the expressions derived in § 8.4 would be dubious.

As the modulus $\kappa \longrightarrow 0$ the complementary modulus $\kappa' \longrightarrow 1$. All the limiting expressions for elliptic functions and elliptic integrals used above can be found, after a little manipulation in some cases, using formulae in Byrd and Friedman (1971). These are shown in appendix G.

Directly taking the limit $\kappa \longrightarrow 0$, using appendix G, in the solution (8.2.1, 2) for symmetric (case Ib) waves neglecting terms of order κ^2 and above gives,

$$x = -\frac{S}{c^2A}\,(\phi + 2\kappa\ \sin\phi\ \cosh\psi + 2\kappa^2\ \cosh^2\psi\ \sin\phi\ \cos\phi) \qquad \text{(E1)}$$

$$\text{and} \quad z = -\frac{S}{c^2A}\,(\psi - 2\kappa\ \cos\phi\ \sinh\psi - 2\kappa^2\ \sinh\psi\ \cosh\psi\ \cos^2\phi)\ . \qquad \text{(E2)}$$

Also, taking the limit $\kappa \longrightarrow 0$, again using appendix G, on expressions (8.2.3 - 8.2.10) and retaining the leading order term only gives

$$1 = - A \tanh B \ , \tag{E3}$$

$$\lambda = - \frac{2\pi S}{C^2 A} \ , \quad a = - \frac{2S\kappa}{C^2 A} \sinh B \ , \tag{E4}$$

$$t = - \frac{S}{C^2 A} B \quad \text{and} \quad c_p = c \ . \tag{E5}$$

Note that the only place at which κ occurs in expressions (E4, 5) is in the expression for the amplitude a so that as $\kappa \longrightarrow 0$ the function of κ is to behave as an amplitude parameter. In this limit B and c behave like depth and velocity parameters with A as a wavelength parameter as for the general case.

Substituting $\phi = + B$ into expression (E2) and averaging over the waves gives

$$d = b = - \frac{S}{C^2 A} B = \frac{S}{C^2} B \tanh B \ . \tag{E6}$$

It immediately follows that the total depth d is equal to the trough depth t in the linear-limit. The above expressions (E3 - E5), thus, give

$$c^2 = sk \tanh kd \tag{E7}$$

where k is the wavenumber of the waves. This is the linear dispersion relation for pure capillary waves on liquid of finite depth. This shows that expressions (E1 - E5) are the correct equations for the linear-limit.

The kinetic and potential energy densities of linear pure capillary waves are given by

$$T = V = \frac{\tau}{4} k^2 a^2 \tag{E8}$$

and the mean bottom velocity squared is given by

$$\overline{u_h^2} = \frac{1}{2} k^2 a^2 c^2 \operatorname{cosech}^2 kd \ . \tag{E9}$$

These can be found in any elementary textbook on water waves or can, alternatively, be found from first principles using the

expressions (E1 - E7).

The general expression for the mean properties of the wave motion are given in terms of the parameter κ, B and c. Therefore, the limits of these expressions will also be in terms of κ, B and c. The above expressions are given in these variables using expressions (E3 - E5). These are

$$T = V = \tau\kappa^2 \sinh^2 B \quad \text{and} \quad \overline{u_h^2} = 2\kappa^2 c^2 \ . \tag{E10}$$

In order to find limits of the general expressions for the mean properties of the wave motion the limits of the integrals I_1 - I_5 are found first. Terms to order κ^3 and above are neglected in the evaluation. Expressions for the limits of these integrals are found in appendix H. It is shown that

$$I_1 \longrightarrow 2\pi + \kappa^2 \frac{\pi}{2} (1 + 2 \cosh^2 B) \ , \tag{E11}$$

$$I_2 \longrightarrow \pi + \kappa^2 \frac{3\pi}{2} \cosh^2 B \ , \tag{E12}$$

$$I_3 \longrightarrow 2\pi + \kappa^2 \frac{\pi}{2} (5 + 6 \cosh^2 B) \ , \tag{E13}$$

$$I_4 \longrightarrow 2\pi + \kappa^2 \frac{\pi}{2} (29 - 16 \cosh B) \tag{E14}$$

and

$$I_5 \longrightarrow 2\pi + \kappa^2 \frac{\pi}{2} (13 - 8 \cosh B) \ . \tag{E15}$$

The limits of α, β, ϵ and θ are also required. These can all be deduced with little difficulty from those limits given in appendix G. As for the integrals I_1 - I_5 terms of order κ^3 and above are neglected. It is found that

$$\alpha \longrightarrow \kappa \cosh B \ , \tag{E16}$$

$$\beta \longrightarrow \tanh B$$

$$- \frac{\kappa^2}{2} \operatorname{sech}^2 B \ [\sinh B \cosh B \ (2 \sinh^2 B + 3) + B] \ , \tag{E17}$$

$$\epsilon \longrightarrow B - 2 \tanh B + \kappa^2 \tanh B \ (1 - B \tanh B) \tag{E18}$$

and

$$\theta \longrightarrow \frac{\pi}{2} \left[1 + \frac{\kappa^2}{4}\right] \ . \tag{E19}$$

Substituting these limits into the general expressions for the mean properties of the wave motion found in § 8.4 and retaining only the leading order terms gives

$$d = b \longrightarrow \frac{S}{C^2} B \tanh B \ , \tag{E20}$$

$$T \longrightarrow \kappa^2 \tau \sinh^2 B \ , \tag{E21}$$

$$V \longrightarrow \kappa^2 \tau \sinh^2 B \tag{E22}$$

and

$$\overline{u_h^2} \longrightarrow \kappa^2 2c^2 \ . \tag{E23}$$

These agree with the direct linear expressions (E9, 10).

APPENDIX F
The Linear Interaction Problem Equations

The linear mass conservation equation (9.2.4) and the wave-action conservation equation (2.7.5) are used to directly derive the linear interaction problem equations in terms of the parameters κ, B and c using the same method as in § 10.4.

Substitution of the linear-limit expressions of appendix E into the Doppler relation (2.3.1) gives

$$U = s\omega \tanh B \frac{1}{C^2} - c \tag{F1}$$

which is an expression for U in terms of B and c.

Also, substitution of the linear-limit expressions of appendix E into expressions (2.5.12, 13) for $\mathcal{A}$ and $\mathcal{B}$ in terms of the four basic mean wave properties gives

$$\mathcal{A} = 2\tau s\kappa^2 \sinh^2 B \tanh B \frac{1}{C^3} \ , \tag{F2}$$

$$\mathcal{B} = \tau s\kappa^2 \tanh B \ (3 \sinh^2 B + B \tanh B) \frac{1}{C^2} \tag{F3}$$

as expressions for $\mathcal{A}$ and $\mathcal{B}$ in terms of κ, B and c. Note that both these expressions are of order κ^2 so that, using the analysis of appendix E, they are both of order a^2 as is expected.

Substitution of expression (F1) for U into the linear mass conservation equation (9.2.4) and use of the linear-limit expression

for d, given in appendix E, gives equation (10.7.3). Also, substitution of the above linear-limit expressions into the wave-action conservation equation (2.7.5) gives equation (10.7.4).

A linear analysis of the wave-current interaction problem, as in chapter 9, is given in as follows. The linear equation (10.7.3) is solved for fixed ω and m by varying B over a given range and solving for c using a standard polynomial solver (NAG LIB C02AEF). Substitution of this solution into the linear equation (10.7.4) then gives the variation of κ. Note that the magnitude of b is taken as one since this is sufficient for linear theory so that κ may possibly be less than zero or greater than one. Substitution of the solution for κ, B and c into the linear-limit expressions of appendix E and expression (F1) give the variations of wave and mainstream flow parameters. It is found that the solutions of the linear equations (10.7.3, 4) are exactly the same as those of the linear equations (9.4.1, 4) with g equal to zero. This again confirms the validity of the equations.

APPENDIX G
The Limits of Elliptic Functions and Integrals as the modulus $\kappa \longrightarrow 0$

The limits of elliptic functions, complete elliptic integrals and incomplete elliptic integrals are given as the modulus $\kappa \longrightarrow 0$ or complementary modulus $\kappa' \longrightarrow 1$. The majority of limits are taken directly from Byrd and Friedman (1971) but some require a little algebra.

Firstly, the elliptic functions are considered. Recall that all functions of ϕ have modulus κ and all functions of ψ have modulus κ'. As $\kappa \longrightarrow 0$

$$\mathrm{sn}\ \phi \longrightarrow \sin\phi - \frac{\kappa^2}{4}\cos\phi(\phi - \sin\phi\cos\phi) \qquad \text{(G1)}$$

$$\mathrm{cn}\ \phi \longrightarrow \cos\phi + \frac{\kappa^2}{4}\sin\phi(\phi - \sin\phi\cos\phi) \qquad \text{(G2)}$$

and

$$\mathrm{dn}\ \phi \longrightarrow 1 - \frac{\kappa^2}{2}\sin^2\phi\ . \qquad \text{(G3)}$$

It follows that

$$\mathrm{sd}\ \phi \longrightarrow \sin\phi - \frac{\kappa^2}{4}(\phi\cos\phi - \sin\phi\cos^2\phi + 2\sin^3\phi) \qquad \text{(G4)}$$

and

$$\mathrm{cd}\ \phi \longrightarrow \cos\phi + \frac{\kappa^2}{4}\sin\phi(\phi + \sin\phi\cos\phi) \qquad \text{(G5)}$$

so

$$\mathrm{sd}^2\phi \longrightarrow \sin^2\phi - \frac{\kappa^2}{2}(\phi\cos\phi - \sin\phi\cos^2\phi + 2\sin^3\phi) \qquad \text{(G6)}$$

and

$$\mathrm{cd}^2\phi \longrightarrow \cos^2\phi + \frac{\kappa^2}{2}\sin\phi(\phi + \sin\phi\cos\phi)\ . \qquad \text{(G7)}$$

As $\kappa' \longrightarrow 1$

$$\mathrm{sn}\ \psi \longrightarrow \tanh\psi + \frac{\kappa^2}{4}\,\mathrm{sech}^2\psi(\sinh\psi\cosh\psi - \psi) \qquad \text{(G8)}$$

$$\mathrm{cn}\ \psi \longrightarrow \mathrm{sech}\ \psi - \frac{\kappa^2}{4}\,\tanh\psi\,\mathrm{sech}\ \psi(\sinh\psi\cosh\psi - \psi) \qquad \text{(G9)}$$

and

$$\mathrm{dn}\ \psi \longrightarrow \mathrm{sech}\ \psi + \frac{\kappa^2}{4}\tanh\psi\,\mathrm{sech}\ \psi(\sinh\psi\cosh\psi + \psi)\ . \qquad \text{(G10)}$$

Also, as $\kappa \longrightarrow 0$

$$K(\kappa) \longrightarrow \frac{\pi}{2}\left[1 + \frac{\kappa^2}{4}\right] \quad \text{and} \quad E(\kappa) \longrightarrow \frac{\pi}{2}\left[1 - \frac{\kappa^2}{4}\right]\ . \qquad \text{(G11)}$$

The limit of $E(\phi)$ and $E(\psi)$ as $\kappa \longrightarrow 0$ are found using

$$\frac{d}{du}\,E(u) = \mathrm{dn}^2u\ . \qquad \text{(G12)}$$

Thus, using expressions (G3, 10),

$$\frac{d}{du}\,E(\phi) \longrightarrow 1 - \kappa^2\sin^2\phi \qquad \text{(G13)}$$

and

$$\frac{d}{du}\,E(\psi) \longrightarrow \mathrm{sech}^2\psi + \frac{\kappa^2}{2}\tanh\psi\,\mathrm{sech}^2\psi(\sinh\psi\cosh\psi + \psi) \qquad \text{(G14)}$$

so that

$$E(\phi) \longrightarrow \phi - \frac{\kappa^2}{2}(\phi - \sin\phi\cos\phi) \qquad \text{(G15)}$$

and

$$E(\psi) \longrightarrow \tanh\psi + \frac{\kappa^2}{2}(\psi - \tanh\psi + \psi\tanh^2\psi)\ . \qquad \text{(G16)}$$

APPENDIX H

The Linear-Limits of Integrals I_1 to I_5

The limits of I_1 - I_5 as $\kappa \longrightarrow 0$ are found up to and including terms of order κ^2. Expressions in appendix G are used to find the limits of the integrand and integral limits. Firstly, consider

$$I_1 = \int_0^{4K} \frac{1}{1 - \alpha \text{ cd } \phi} \, d\phi \ . \tag{H1}$$

From appendix G $$\alpha \text{ cd } \phi \longrightarrow \kappa \cosh B \cos \phi \tag{H2}$$

so $$\frac{1}{1 - \alpha \text{ cd } \phi} \longrightarrow 1 + \kappa \cosh B \cos \phi + \kappa^2 \cosh^2 B \cos^2 \phi \ . \tag{H3}$$

Therefore $$I_1 \longrightarrow \int_0^{\pi} (1 + \kappa \cosh B \cos \phi + \kappa^2 \cosh^2 B \cos^2 \phi) \, d\phi \tag{H4}$$

where $$4K \longrightarrow \gamma = 2\pi\left[1 + \frac{\kappa^2}{4}\right] \ . \tag{H5}$$

It follow that $$I_1 \longrightarrow 2\pi + \kappa^2 \frac{\pi}{2} (1 + 2 \cosh^2 B) \ . \tag{H6}$$

Also $$I_2 = \int_0^{4K} \frac{\text{sd}^2 \phi}{(1 - \alpha \text{ cd } \phi)^2} \, d\phi \ . \tag{H7}$$

Expression (H3) gives

$$\frac{1}{(1 - \alpha \text{ cd } \phi)^2} \longrightarrow 1 + \kappa \ 2 \cosh B \cos \phi + \kappa^2 \ 3 \cosh^2 B \cos^2 \phi \tag{H8}$$

whilst the limit of $\text{sd}^2 \phi$ is given by expression (G6). So

$$I_2 \longrightarrow \int_0^{\pi} \left[\sin^2 \phi + \kappa \ 2 \cosh B \sin^2 \phi \cos \phi + \frac{\kappa^2}{2} (6 \cosh^2 B \sin^2 \phi \cos^2 \phi \right.$$
$$\left. - \phi \cos \phi - \sin \phi \cos^2 \phi + 2 \sin^3 \phi)\right] d\phi \ . \tag{H9}$$

It follows that $$I_2 \longrightarrow \pi + \kappa^2 \frac{3\pi}{2} \cosh^2 B \ . \tag{H10}$$

Also $$I_3 = \int_0^{4k} \frac{(1 + 2\kappa^2 \text{sd}^2 \phi) - \alpha^2 (\text{cd}^2 \phi + 2 \text{ sd}^2 \phi)}{(1 - \alpha \text{ cd } \phi)^3} \, d\phi \tag{H11}$$

Again use of expression (H3) and appendix G leads to

$$I_3 \longrightarrow \int_0^{\pi} \{1 + \kappa\, 3 \cos B \cos\phi + \kappa^2 [\cosh^2 B\, (2 + 7\cos^2\phi) + 2\sin^2\phi]\}\, d\phi \,. \tag{H12}$$

It follows that $$I_3 \longrightarrow 2\pi + \kappa^2 \frac{\pi}{2} (5 + 6\cosh^2 B) \,. \tag{H13}$$

The remaining two integrals are given by

$$I_4 = \int_0^{4k} \frac{1}{dn^4\phi (1 + \kappa\, cd\ \phi)^4} \frac{(1 + 2\kappa^2 sd^2\phi) - \alpha^2 (cd^2\phi + 2\ sd^2\phi)}{(1 - \alpha\, cd\ \phi)^2}\, d\phi \,,$$

$$I_5 = \int_0^{4k} \frac{1}{dn^2\phi (1 + \kappa\, cd\ \phi)^2} \frac{(1 + 2\kappa^2 sd^2\phi) - \alpha^2 (cd^2\phi + 2\ sd^2\phi)}{(1 - \alpha\, cd\ \phi)^2}\, d\phi$$

which on use of expression (H3) and appendix G give

$$I_4 \longrightarrow \int_0^{\pi} \{1 + \kappa\, 2(\cosh B - 2)\cos\phi + \kappa^2\, 2[(\cosh^2 B - 4\cosh B + 5) - (2\cosh^2 B - 4\cosh B + 3)\sin^2\phi]\}\, d\phi \tag{H14}$$

$$I_5 \longrightarrow \int_0^{\pi} \{1 + \kappa\, 2(\cosh B - 1)\cos\phi + \kappa^2 [(2\cosh^2 B - 4\cosh B + 3) - (4\cosh^2 B - 4\cosh B)\sin^2\phi]\}\, d\phi \,. \tag{H15}$$

It follows that $$I_4 \longrightarrow 2\pi + \kappa^2 \frac{\pi}{2} (29 - 16\cosh B) \tag{H16}$$

and $$I_5 \longrightarrow 2\pi + \kappa^2 \frac{\pi}{2} (13 - 8\cosh B) \,. \tag{H17}$$

REFERENCES

Abramowitz, M., and Stegun, I.A., 1965, *Handbook of mathematical functions*, Washington: National Bureau of Standards.

Banner, M.L. and Phillips, O.M., 1974, On the incipient breaking of small scale waves, *J. Fluid Mech.*, 65, 647.

Benney, D.J., 1977, A general theory for interactions between short and long waves, *Studies in Appl. Math.*, 56, 81.

Brauner, N., and Moalem-Maron, D., 1982, Characteristics of inclined thin films, waviness and the associated mass transfer, *Int. J. Heat and Mass Transfer*, 25, 99.

Brauner, N., Moalem-Maron, D., 1985, Modelling of wavy flow in inclined thin films, *Chem. Eng. Sci.*, 38, 775.

Bretherton, F.P., and Garrett, C.J.R., 1968, Wavetrains in inhomogeneous media, *Proc. Roy. Soc. Lond. (A)*, 302, 529.

Byrd, P.F., and Friedman, M.D., 1971, *Handbook of elliptic integrals for engineers and scientists*, Springer-Verlag, New York, Heidelberg and Berlin.

Chang, J.H., Wagner, R.N., and Yuen, H.C., 1978, Measurement of high frequency capillary waves on steep gravity waves, *J. Fluid Mech.*, 86, 401.

Christoffersen, J.B., and Jonsson, I.G., 1980, A note on wave action conservation in a dissipative current wave motion, *Appl. Ocean Res.*, 2, 179.

Cokelet, E.D., 1977, Steep gravity waves in water of arbitrary uniform depth, *Phil. Trans. Roy. Soc. Lond. A*, 286, 183.

Cox, C.S., 1958, Measurements of slopes of high frequency wind waves, *J. Marine Res.*, 16, 199.

Crapper, G.D., 1957, An exact solution for progressive capillary waves of arbitrary amplitude, *J. Fluid Mech.*, 2, 532.

Crapper, G.D., 1970, Nonlinear capillary waves generated by steep gravity waves, *J. Fluid Mech.*, 40, 149.

Crapper, G.D., 1972, Nonlinear gravity waves on steady non-uniform currents, *J. Fluid Mech.*, 52, 713.

Crapper, G.D., 1979, Energy and momentum integrals for progressive capillary-gravity waves, *J. Fluid Mech.*, 94, 13.

Dukler, A.E., 1972, Characterisation, effects and modelling of wavy gas-liquid interface, *Prog. Heat and Mass Transfer*, 6, 207.

Ferguson, W., Saffman, R., and Yuen, H.C., 1978, A model equation to study the effects of nonlinearity, surface tension and viscosity in water waves, *Studies in Appl. Math.*, 58, 165.

Hasselmann, K., 1971, On the mass and momentum transfer between short gravity waves and larger-scale motions, *J. Fluid Mech.*, 50, 189.

Hayes, W.D., 1973, Group velocity and nonlinear dispersive wave propagation, *Proc. Roy. Soc. Lond. A*, 332, 199.

Hogan, S.J., 1979, Some effects of surface tension on steep water waves, *J. Fluid Mech.*, 91, 417.

Hogan, S.J., 1980, Some effects of surface tension on steep water waves. Part 2, *J. Fluid Mech.*, 110, 417.

Hogan, S.J., 1981, Some effects of surface tension on steep water waves. Part 3, *J. Fluid Mech.*, 96, 417.

Hogan, S.J., 1984, Particle trajectories in nonlinear capillary waves, *J. Fluid Mech.*, 143, 243.

Hogan, S.J., 1985, Particle trajectories in nonlinear gravity-capillary waves, *J. Fluid Mech.*, 151, 105.

Hogan, S.J., 1985, The fourth-order evolution equation for deep-water gravity-capillary waves, *Proc. Roy. Soc. Lond. A*, 402, 359.

Hogan, S.J., 1986, Highest waves, phase speeds and particle trajectories of nonlinear capillary waves on sheets of fluid, *J. Fluid Mech.*, 172, 547.

Holliday, D., 1973, Nonlinear gravity-capillary surface waves in a slowly varying current, *J. Fluid Mech.*, 57, 797.

Ince, E.L., 1944, *Ordinary differential equations*, New York: Dover.

Isobe, M, and Kraus, N.C., 1983, Derivation of a third order Stokes wave theory, *Hydrolics Lab. Report YNU-HY-83-1, Dept. of Civil Eng., Yokohoma National Univ.,*.

Kinnersley, W, 1976, Exact large amplitude capillary waves on sheets of fluid, *J. Fluid Mech.*, 77, 229.

Kinsman, B., 1965, *Wind waves - their generation and propagation on the ocean surface*, Prentice-Hall, Inc., Englewood Cliffs, New Jersey. Reprinted: 1984, New York: Dover.

Lamb, H., 1932, *Hydrodynamics*, Cambridge University Press, London and New York:

Lighthill, M.J., 1965, Contributions to the theory of waves in nonlinear dispersive systems, *J. Inst. Math. Appl.*, 1, 269.

Lighthill, M.J., 1967, Special cases treated by the Whitham theory, *Proc. Roy. Soc. Lond. A*, 299, 28.

Longuet-Higgins, M.S., 1963, The generation of capillary waves by steep gravity waves, *J. Fluid Mech.*, 16, 138.

Longuet-Higgins, M.S., 1975, Integral properties of periodic gravity waves of finite-amplitude, *Proc. Roy. Soc. Lond. A*, 342, 157.

Longuet-Higgins, M.S., 1987, The propagation of short surface waves on longer gravity waves, *J. Fluid. Mech.*, 177, 293.

Longuet-Higgins, M.S., 1988, Limiting forms of capillary-gravity waves, *J. Fluid. Mech.*, 194, 351.

Longuet-Higgins, M.S., 1989, Capillary-gravity waves of a solitary type on deep water, *J. Fluid. Mech.*, 200, 451.

Longuet-Higgins, M.S., and Stewart, R.W., 1964, Radiation stress in water waves, a physical discussion with application, *Deep Sea Res.*, 1, 529.

Luke, J.C., 1967, A variational principle for a fluid with a free surface, *J. Fluid Mech.*, 27, 395.

Mallory, J.K., 1974, Abnormal waves on the south east coast of South Africa, *Int. Hydrog. Rev.*, 51, 99.

Marchant, T.R., and Roberts, A.J., 1988, A variational approach to the problem of deep water waves forming a circular caustic, *J. Fluid. Mech.*, 194, 581.

McGoldrick, L.F., 1965, Resonant interactions among capillary-gravity waves, *J. Fluid. Mech.*, 21, 305.

McGoldrick, L.F., 1972, On the rippling of small waves: a harmonic nonlinear nearly resonant interaction. *J. Fluid Mech.*, 52, 725.

Miles, J.W., 1978, On the second Painlevé transcendent, *Proc. Roy. Soc. Lond. A*, 361, 277.

Miles, J.W., 1980, The second Painlevé transcendent: a nonlinear Airy function, *Mechanics Today: Pergamon Press*, 5, 297.

Moalem-Maron, D., Brauner, N., and Dukler, A., 1985, Interfacial structure of thin falling films: piecewise modelling of the waves, *Physico Che. Hyd.*, 6, 87.

Munk, W.H., 1955, High frequency spectrum of ocean waves, *J. Marine Res.*, 14, 302.

Peregrine, D.H., 1972, River currents and trains of waves, *Bull. Inst. Math. Its Appl.*, 8, 326.

Peregrine, D.H., 1976, Interaction of water waves and currents, *Adv. App. Mech.*, 16, 9.

Peregrine, D.H., 1981, Refraction of finite-amplitude water waves: deep water waves approaching circular caustics, *J. Fluid Mech.*, 109, 63.

Peregrine, D.H., 1983, Wave jumps and caustics in the propagation of finite-amplitude water waves, *J. Fluid Mech.*, 136, 425.

Peregrine, D.H., and Ryrie, S., 1983, Anomalous refraction and conjugate solutions of finite-amplitude water waves, *J. Fluid Mech.*, 134, 91.

Peregrine, D.H., and Smith, R., 1979, Nonlinear effects upon waves near caustics, *Philos. Trans. Roy. Soc. Lond. A*, 292, 341.

Peregrine, D.H., and Thomas, G.P., 1979, Finite-amplitude deep water waves on currents, *Philos. Trans. Roy. Soc. Lond. A*, 292, 371.

Phillips, O.M., 1966, *The Dynamics of the Upper Ocean*, Cambridge University Press, London and New York.

Rosales, R., 1978, The similarity solution for the Korteweg-de Vries equation and the related Painlelé transcendent, *Proc. Roy. Soc. Lond. A*, 361, 265.

Russell, J.S., 1838 and 1845, Report on the Committee on Waves, *British Assoc. Reports*, 6, 417, 13, 311.

Ryrie, S., and Peregrine, D.H., 1982, Refraction of finite-amplitude water waves obliquely incident on a uniform beach, *J. Fluid Mech.*, 115, 91.

Sarpkaya, T., 1957, Oscillatory gravity waves in flowing water, *Trans. Amer. Soc. Civil Eng.*, 122, 564.

Schooley, A.H., 1958, Profiles of wind-created water waves in the capillary-gravity transition region, *J. Marine Res.*, 16, 101.

Schooley, A.H., 1960, Double, triple, and higher-order dimples in the profiles of wind-generated water waves in the capillary-gravity transition region, *J. Geo. Res.*, 65, 4075.

Schwartz, L.W., 1974, Computer, extensions and analytic continuation of Stokes' expansion for gravity waves, *J. Fluid Mech.*, 62, 553.

Smith, R., 1976, Giant waves, *J. Fluid Mech.*, 77, 417.

Stiassnie, M., and Peregrine, D.H., 1979, On the averaged equations for finite amplitude water waves, *J. Fluid Mech.*, 94, 401.

Stokes, G.G., 1847, On the theory of oscillatory waves, *Trans. Cambridge Phil. Soc.*, 8, 44 (1880, *Mathematical and Physical Papers*, 1, 197).

Taylor, G.I, 1959, The dynamics of thin sheets of fluid II. Waves on fluid sheets. *Proc. Roy. Soc. Lond. A*, 253, 296.

Teles da Silva, A.F. and Peregrine, D.H., 1988, Steep, steady, surface waves on water of finite depth with constant vorticity, *J. Fluid Mech.*, 195, 281.

Whitham, G.B., 1965a, Nonlinear dispersive waves, *Proc. Roy. Soc. Lond. A*, 283, 238.

Whitham, G.B., 1965b, A general approach to linear and non-linear dispersive waves using a Lagrangian, *J. Fluid Mech.*, 22, 273.

Whitham, G.B., 1967a, Variational methods and applications to water waves, *Proc. Roy. Soc. Lond. A*, 299, 6.

Whitham, G.B., 1967b, Nonlinear dispersion of water waves, *J. Fluid Mech.*, 27, 399.

Whitham, G.B., 1970, Two-timing, variational principles and waves, *J. Fluid Mech.*, 44, 373.

Whitham. G.B., 1974, *Linear and non-linear Waves*, Wiley, Interscience.

Wilton, J.R., On ripples, *Phil. Mag. S. 6*, 29, 173.

Yue, D.K.P., and Mei, C.C., 1980, Forward diffraction of Stokes waves by a thin wedge, *J. Fluid Mech.*, 99, 33.